2 / 2

FIG. 4.

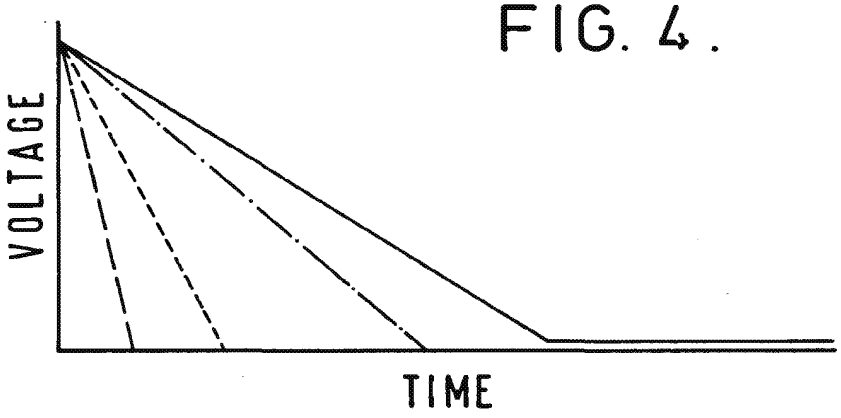
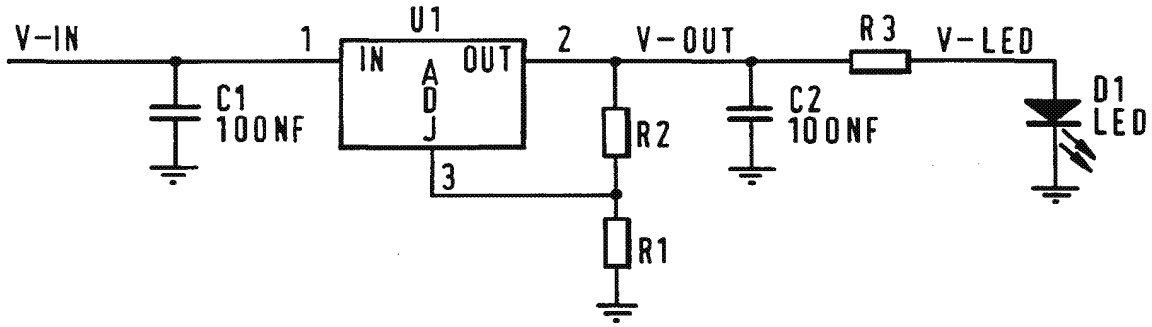

VOLTAGE
TIME

FIG. 5.


V-IN
1
U1
IN
ADJ
OUT
2
V-OUT
R3
V-LED
C1
100NF
R2
C2
100NF
D1
LED
3
R1

INTERNATIONAL SEARCH REPORT

International Application No PCT/GB 93/01356

I. CLASSIFICATION OF SUBJECT MATTER (if several classification symbols apply, indicate all)[6]

According to International Patent Classification (IPC) or to both National Classification and IPC

Int.Cl. 5 G01J1/46

II. FIELDS SEARCHED

Minimum Documentation Searched[7]

Classification System	Classification Symbols
Int.Cl. 5	G01J ; G01N

Documentation Searched other than Minimum Documentation to the Extent that such Documents are Included in the Fields Searched[8]

III. DOCUMENTS CONSIDERED TO BE RELEVANT[9]

Category °	Citation of Document,[11] with indication, where appropriate, of the relevant passages[12]	Relevant to Claim No.[13]
Y	PATENT ABSTRACTS OF JAPAN vol. 14, no. 415 (P-1102)17 September 1990 & JP,A,02 159 527 (OLYMPUS OPTICAL) 19 June 1990 see abstract ---	1,5-8
Y	DE,A,3 131 546 (HENGST) 17 March 1983 see page 6, line 1 - line 10 see page 8, last paragraph see page 7, paragraph 2 see page 9, line 4 - line 14 see page 9, last paragraph see figures 1,4 --- -/--	1,5-8

° Special categories of cited documents :[10]

"A" document defining the general state of the art which is not considered to be of particular relevance

"E" earlier document but published on or after the international filing date

"L" document which may throw doubts on priority claim(s) or which is cited to establish the publication date of another citation or other special reason (as specified)

"O" document referring to an oral disclosure, use, exhibition or other means

"P" document published prior to the international filing date but later than the priority date claimed

"T" later document published after the international filing date or priority date and not in conflict with the application but cited to understand the principle or theory underlying the invention

"X" document of particular relevance; the claimed invention cannot be considered novel or cannot be considered to involve an inventive step

"Y" document of particular relevance; the claimed invention cannot be considered to involve an inventive step when the document is combined with one or more other such documents, such combination being obvious to a person skilled in the art.

"&" document member of the same patent family

IV. CERTIFICATION

Date of the Actual Completion of the International Search	Date of Mailing of this International Search Report
06 OCTOBER 1993	15. 10. 93
International Searching Authority	**Signature of Authorized Officer**
EUROPEAN PATENT OFFICE	THOMAS R.M.

Form PCT/ISA/210 (second sheet) (January 1985)

SPECTRAL 0000508

ANNEX TO THE INTERNATIONAL SEARCH REPORT

SPECTRAL_0000509

III. DOCUMENTS CONSIDERED TO BE RELEVANT (CONTINUED FROM THE SECOND SHEET)

Category °	Citation of Document, with indication, where appropriate, of the relevant passages	Relevant to Claim No.
A	US,A,4 249 169 (MALINKOWSKI) 3 February 1981 see abstract see column 2, line 20 - line 30 see column 2, line 53 - line 61 see column 2, line 65 - column 3, line 2 see figure 1	1-4,8,9
A	PATENT ABSTRACTS OF JAPAN vol. 13, no. 38 (E-709)27 January 1989 & JP,A,63 236 378 (HITACHI SEIKO) 3 October 1988 see abstract	1-4,8,9
A	US,A,3 879 137 (SAKA ZAKI) 22 April 1975 see column 3, line 43 - column 4, line 5 see column 4, line 37 - line 58 see figures 3,4	1,5,6,8

Example of Application

Luminescence imaging is only possible for glow-type luminescence because it would be almost impossible to dispense reagents into (intact) samples and take an image at the same time. Even so, the weak and chemical flash-type luminescence of the jellyfish photoprotein aequorin can be detected. Figure 6 shows aequorin expression in the brain of a transgenic fruit fly *Drosophila melanogaster* as an actual example for reporter gene analysis.

The macroscopic and microscopic imaging system NightOWL from EG&G Berthold[30] was used for this spatial detection of the luminescent label aequorin. Figure 6 presents an overlay of two images. First, a transilluminated image was acquired using a 20-msec exposure time. For this image, less sensitivity was required due to the illumination, but high resolution was required for maintaining good spatial resolution. Therefore, each pixel was read out separately. Second, a luminescent image was acquired. Here, camera parameters were set mainly for high sensitivity but less for spatial resolution: An exposure time of 3 min was chosen and groups of 5×5 pixels were connected together (pixel binning) to increase sensitivity. For comparison, the emitted aequorin luminescence was quantified to about 200 to 500 RLU per 15 sec using a LB 9507 luminometer from EG&G Berthold (Bad Wildbad, FRG) (J. D. Amstrong, personal communication).

[30] B. Möckel, J. Grand, and R. Ochs, *in* "Bioluminescence and Chemiluminescence" (J. W. Hastings, L. J. Kricka, and P. E. Stanley, eds.), p. 539. Wiley, Chicester, 1996.
[31] P. Rosay, S. A. Davies, Y. Yu, M. A. Sozen, K. Kaiser, and J. A. T. Dow, *J. Cell Sci.* **110,** 1683 (1997).
[32] M. Tettamanti, J. D. Amstrong, K. Endo, M. Y. Yang, K. Furukubo Tokunaga, K. Kaiser, and H. Reichert, *Dev. Genes Evol.* **207,** 242 (1997).
[33] M. Y. Yang, J. D. Amstrong, I. Vilinsky, N. J. Strausfeld, and K. Kaiser, *Neuron* **15,** 45 (1995).

[5] Absolute Calibration of Luminometers with Low-Level Light Standards

By DENNIS J. O'KANE and JOHN LEE

Relative light units are commonly reported in the measurement of bioluminescent and chemiluminescent reactions. The reason is that the calibration of the absolute photon sensitivity of the detector system entails overcoming severe technical problems. Absolute photon calibration is essential if one is to determine the absolute quantum yields of these reactions, important information required for elucidating the mechanisms of

Copyright © 2000 by Academic Press
All rights of reproduction in any form reserved.
METHODS IN ENZYMOLOGY, VOL. 305
0076-6879/00 $30.00

SPECTRAL_0000511

these reactions. At the present time, the exploding applications of luminescence measurements would seem to render a knowledge of the absolute values of the photon fluxes rather desirable, for example, for the comparison of methodologies or to quantify the performance of instrumentation.

The standard of photon flux is a blackbody radiation source which are maintained in many national standards laboratories. The National Institute of Standards and Technology in Gaithersburg, Maryland, for example, issues a standard tungsten lamp of radiance calibrated with reference to the standard blackbody, and such a lamp is employed in many photon calibration applications. A difficulty is that this lamp is many orders of magnitude too bright to be used directly for the calibration of a photomultiplier as normally employed in a luminometer. Calibration of the absolute photon sensitivity of a photomultiplier was achieved by precise attenuation of the output of a standard lamp, and the bioluminescence quantum yield of the firefly reaction and the chemiluminescence quantum yield of the luminol reaction were determined to satisfactory accuracy, about 25%.[1,2] The value of this experimental approach is that the quantum yields are directly traceable to the standard blackbody.

Another technical problem in luminometer calibration is that of detector geometry.[2] The preferred geometrical arrangement for a quantum yield measurement is that of point source geometry, i.e., the luminescing solution should be, say, in a 1-ml volume, at about 25 cm from the face of the detector, and in a suitably baffled holder. This last baffling is so that only light truly emanating in the direction of the detector is allowed to pass, i.e., no reflections from the cuvette walls or light piping down the sides. These conditions are important on two counts. The first is that the size of light source viewed from the detector depends on the square of the refractive index of the reaction medium. Whereas bioluminescence reactions are carried out in aqueous medium, many chemiluminescence reactions are in organic solution. The detector as calibrated with the standard lamp sits in air, of course, so the refractive index correction is considerable. This correction has been verified experimentally.[2] Unfortunately, this simple refractive index-squared relationship only holds for the point source, and most luminometers have the reaction chamber quite close to the detector in order to maximize sensitivity. Under such a condition the correction becomes impossible to estimate directly. Therefore, the secondary calibration with reference to the luminol chemiluminescence reaction has a distinct advantage under this circumstance.

[1] H. H. Seliger and W. D. McElroy, *Arch. Biochem. Biophys.* **88,** 136 (1960).
[2] J. Lee and H. H. Seliger, *Photochem. Photobiol.* **4,** 1015 (1965).

SPECTRAL_0000512

The second problem with the nonpoint source and "close-up" arrangement is that detection is prone to variations in mixing. Many reactions are initiated by injection and, depending on the rate of mixing, the light emission may be uniform throughout the reaction volume, giving rise to considerable variation in distance from the detector face.

It is relevant to mention in this introductory section that the employment of a silicon photodiode as a detector obviates the requirement for absolute photon calibration as these photodiodes are "self-calibrating."[3] Photodiodes have the advantage of much more uniform wavelength dependence of the sensitivity than a photomultiplier and they are also unaffected by exposure to ambient light, in contrast to photomultipliers.[4] A photomultiplier-based luminometer must always be designed to strictly avoid exposing the detector to room light. The disadvantage of the photodiode is that the visible photon sensitivity is about 100 times less than a photomultiplier, although if the photodiode has a "close-up" geometry to the reaction chamber, the sensitivity is still enough for many luminescence applications. However, this geometry again entails calibration with reference to a standard chemiluminescence reaction.[5]

Luminol Chemiluminescence Standard

The absolute quantum yield from the luminol (3-aminophthalhydrazide) chemiluminescence reaction is 0.0124. This means that for each 100 molecules of luminol reacting, 1.24 photons on average are emitted within the spectral envelope, depending on the solvent. The same quantum yield is obtained for reactions in aqueous solution or in dimethyl sulfoxide (DMSO), although the conditions are very different.[2] The quantum yield translates to a value of 9.75×10^{14} photons from 1 ml of a luminol solution having an absorbance of unity at the maximum wavelength, 347 nm for aqueous solution at pH 11.5, and 359 nm in DMSO.[5]

The photon sensitivity of photomultiplier detectors used in most luminometers depends strongly on wavelength. Therefore, the detector signal from the luminol or any other chemiluminescence reaction will be a result of the overlap between the spectral emission distribution and the spectral response curve of the detector. For high accuracy, this response needs to be determined directly for the detector being employed, but this is not

[3] E. F. Zalewski, *in* "Optical Radiation Measurements" (K. D. Mielenz, ed.), Vol. 3, p. 89. Academic Press, New York, 1982.

[4] J. Lee, A. S. Wesley, J. F. Ferguson III, and H. H. Seliger, *in* "Bioluminescence in Progress" (F. H. Johnson and Y. Haneda, eds.), p. 35. Princeton Univ. Press, Princeton, NJ, 1966.

[5] I. B. C. Matheson, J. Lee, and E. F. Zalewski, *Proc. Soc. Photo-Opt. Instrum. Eng.* **489**, 380 (1984).

SPECTRAL_0000513

practical unless the laboratory is set up for photometric measurements. It is usually sufficient to accept the spectral response curve provided by the manufacturer, e.g., for a commonly used photomultiplier with S11 response, which has a maximum around 420 nm and falls to 50% by 550 nm. An advantage of the photodiode is that its spectral response is practically constant over the visible wavelength region.[6]

The emission maximum for the aqueous reaction is at 428 nm and for DMSO is at 486 nm. If the geometry of the emitter is a point source with respect to the detector, then the detector will view the DMSO reaction $(1.33/1.49)^2 = 80\%$ less efficiently than from the aqueous reaction, where the ratio is of the solvent refractive indices. For proximate geometry, this refractive index correction is closer to unity. For the detector arrangement commonly employed with luminometers, this correction is hard to calculate accurately for the reasons discussed above but can be estimated to be in the range 90–95%. It is the experience of this laboratory that the integrated signal measured from the DMSO reaction is about half that from the aqueous reaction.

The important property of the luminol calibration method, therefore, is that both detector geometry and spectral response for the reactions in the two solvents are different but the final result after taking these factors into account must be the same. This condition provides a vital cross-check on the reaction integrity. The accuracy of the spectral overlap and geometrical corrections also contribute, but to a lesser extent.[6]

Aqueous Luminol Chemiluminescence

High-purity 3-aminophthalhydrazide can be purchased from a number of commercial sources but nevertheless should be assayed for purity by its absorption spectrum: $\varepsilon(347\text{ nm}) = 7640\ M^{-1}\ \text{cm}^{-1}$. A solution containing 0.1 *M* potassium carbonate to maintain pH 11.5 is used for all reactants. It is recommended to make up a stock solution of the luminol to absorbance around 20, measured accurately by dilution.

The other reagents are H_2O_2 (30%, about 12 *M*) and a catalyst; heme proteins are usually employed, hemoglobin[5] or peroxidase[6] is recommended (indeed, fresh blood is quite superior). The protein concentration in the carbonate buffer should be such as to give a just perceptible brown color due to the heme absorption. If the catalyst concentration is kept dilute, then on addition to the reaction, the absorbance in the 420-nm region will not exceed, say, 0.02 cm^{-1} and the chemiluminescence emission intensity will not be attenuated.

[6] D. J. O'Kane, M. Ahmad, I. B. C. Matheson, and J. Lee, *Methods Enzymol.* **133B,** 109 (1986).

SPECTRAL_0000514

The amount of luminol used in the reaction should be adjusted to the response range of the luminometer. Typically one would take 0.9 ml of a luminol solution with A(347 nm) = 0.0001 and add 10 μl of freshly 1 : 1000 diluted H_2O_2. The amount of H_2O_2 used has to be determined by trial and error. The 30% concentration of the stock can be quite uncertain and a highly diluted solution of peroxide is unstable.

After taking appropriate precautions to ensure light tightness, chemiluminescence is initiated by rapid injection of the catalyst solution (0.05 ml) into the luminol sample. The emitted light intensity will rise quickly to a maximum, then should decay slowly over about 100 sec. If the light decays rapidly over only a few seconds, the amount of H_2O_2 added should be reduced (usually) to achieve the more slowly decaying condition. After the slow decay is nearly complete, several minutes of time usually, a second addition of catalyst should be made. This second addition will increase the total light measured typically by another 25%. A third addition may also be necessary, also with more H_2O_2 addition, until the operator is convinced that the luminol is completely exhausted. The maximum integrated intensity should be attained after only two or three additions. It should also be cautioned that a few percent of the total light may be generated on the first addition of the H_2O_2 before the addition of catalyst.

It is important to practice the reaction technique until the maximum total signal response is attained. It is our experience that in laboratories that have not had previous experience with this reaction, the operator may need many repetitions to achieve confidence in the procedure.

Dimethyl Sulfoxide Luminol Chemiluminescence

In this method it is important to keep the reaction mixture relatively anhydrous. High-purity and water-free DMSO is inexpensive, so we have always found it convenient to use a new unopened bottle of DMSO on each occasion the reaction is performed. The luminol stock solution can be made up and, for the reaction, diluted to the appropriate A(359) necessary to calibrate the luminometer on the desired scale. The only other reagent needed is a saturated solution of potassium *tert*-butoxide in dry *tert*-butanol. Because this solution freezes around 20°, it needs to be kept slightly above this temperature. It may have to be prepared every few hours due to the instability of the *tert*-butoxide.

To 1.0 ml of the luminol solution in DMSO is rapidly injected 0.02 ml of the potassium *tert*-butoxide/*tert*-butanol. The emission intensity should rise to a maximum in about 1 min, then decay to a negligible level in 10–15 min. A second injection could be tried but should not be necessary. Sometimes the basicity is not sufficient with only one injection. Too much

SPECTRAL_0000515

butoxide, however, is equivalent to the water contamination problem, slowing the reaction and decreasing the total light yield. If the reaction time is much slower than about 45 min, contamination by traces of water can be suspected and the total light emitted will be too low.

As pointed out earlier, the integrated signal from the DMSO reaction in a luminometer employing a photomultiplier should be about one-half that for the aqueous reaction for the same amount of luminol employed. After corrections, therefore, the quantum yield will be the same for aqueous and DMSO reactions. This provides a critical cross-check on the operator and reaction procedures.

Day-to-Day Calibrators

Although absolute photometer calibration is essential for research applications and for standardizing routine measurements, this approach is too tedious to implement on a daily basis. Instead, a secondary calibrator is used to monitor variation both in instrument response and in the chemiluminescence or bioluminescence system. Several different day-to-day calibrators have been utilized for these purposes. The most commonly used calibrators include radioactive liquid standards,[7] encapsulated phosphors with adsorbed radioactive compounds,[8,9] uranyl salts,[10,11] light-emitting diodes, and commercially available acridinium chemiluminescence calibrators (Quest Diagnostic Laboratories, San Juan Capistrano, CA). Each calibrator has advantages and disadvantages.

Radioactive Liquid Calibrators

These calibrators use soft β disintegration to excite fluorescence emission from scintillators in organic solvents. The major optical advantage of these calibrators is that they produce isotropic emissions. A disadvantage, however, is that the emission is structured and may not overlap significantly the bioluminescence or chemiluminescence emission of interest.[9] Two different approaches have been reported for developing liquid radioactive standards: the use of tritiated[7] and quenched ^{14}C-labeled compounds.[12]

[7] J. W. Hastings and G. Weber, *J. Opt. Soc. Am.* **53,** 1410 (1963).
[8] W. H. Biggley, E. Swift, R. J. Buchanan, and H. H. Seliger, *J. Gen. Physiol.* **54,** 95 (1969).
[9] D. J. O'Kane and J. Lee, *Photochem. Photobiol.* **52,** 723 (1990).
[10] G. D. Mendenhall and X. Hu, *J. Photochem. Photobiol A* **52,** 285 (1990).
[11] D. J. O'Kane and D. F. Smith, *in* "Bioluminescence and Chemiluminescence: Status Report" (A. Szalay, L. Kricka, and P. Stanley, eds.), p. 38. Wiley, Chichester, 1993.
[12] T. E. T. Oikari, I. A. Hemmil, and E. J. Soini, *in* "Analytical Applications of Bioluminescence and Chemiluminescence" (L. J. Kricka, P. E. Stanley, G. H. G. Thorpe, and T. P. Whitehead, eds.), p. 475. Academic Press, New York, 1984.

SPECTRAL_0000516

Tritiated calibrators have the advantage of producing single-photon emissions due to the low energy β^- particles. Because of the higher energy β^- particles, ^{14}C-liquid calibrators will generate multiphoton emissions that will not register correctly in all luminometers. Consequently, these calibrators should be quenched. The main disadvantage encountered with these standards is the decrease in emission output over time. The emission fall off from tritiated standards is predominantly attributable to the half-life of tritium (12.3 years; Table I). This decrease in emission can be corrected using standard tables and the time between initial and subsequent measurements. However, radiation damage appears to contribute to the decrease in the emission level from ^{14}C calibrators and this is more difficult to predict and correct over time.

Encapsulated Radioactive Phosphors Calibrators

Different radionuclides can be deposited on the surface of phosphor powders to generate radiophosphorescence emissions.[8,9] ^{14}C-bicarbonate is precipitated in a slurry of inorganic phosphor powder by $BaCl_2$ addition. The phosphor is then embedded in epoxy resin.[8] This procedure produces calibrators in a tube format that are stable for many years and that are useful in the range of intensities found in most chemiluminescence-emitting systems. The disadvantage is that it is difficult to prepare calibrators that emit at sufficiently high intensities to permit calibrating luminometers for use with bioluminescent organisms. Because the amount of light emitted by

TABLE I
CHARACTERISTICS OF RADIONUCLIDES POTENTIALLY SUITABLE FOR LIGHT STANDARDS

Radionuclide[a]	$t_{1/2}$ (years)	Mode of emission (Mev)		Specific activity (Ci/g) Theoretical[b]	Specific activity (Ci/g) Commercial
^{3}H	12.3	β^-	0.019	9688	9688
^{121m}Sn	55	β^- and γ	0.357	54	0.02
^{232}U	73.6	α and γ	5.41	21	NCA[c]
^{151}Sm	93 ± 8	β^- and γ	0.076	25	NCA
^{63}Ni	96	β^-	0.066	59	12
^{32}Si	104	β^-	0.227	107	NCA
^{14}C	5730	β^-	0.156	4.5	4.5

[a] Radionuclides arranged in increasing order of half-life. Half-life and maximum particle energy taken from NCRP Report 58 or from "The Handbook of Chemistry and Physics."
[b] Theoretical specific activity (Ci/g) = $kn/(3.7 \times 10^{10}$ dps), where k is the first-order radioactive decay constant (sec^{-1}) and n is the number of atoms per gram of radionuclide.
[c] Not available commercially.

SPECTRAL_0000517

these standards is proportional to the number of radioactive disintegrations, very large amounts of ^{14}C must be used to prepare high-intensity standards. Alternatively, radionuclides with shorter half-lives, a greater number of disintegrations per unit time, and potentially greater levels of emission may be useful for this purpose (Table I). The use of ^{63}Ni ($t_{1/2}$ = 96 years) is advantageous because it is available commercially at high specific activity, precipitates quantitatively as the insoluble alkaline carbonate, emits soft β radiation that does not produce measurable damage to the phosphors, and is inexpensive compared to ^{14}C-bicarbonate. Calibrators can be prepared in several formats using different phosphors that span wide spectral emission ranges that correspond closely to many bioluminescence and chemiluminescence emissions.[9] The radioactive phosphors may be embedded in plastics either by simply mixing the phosphor with the plastic or by a combined vacuum infiltration and centrifugal infiltration of a phosphor layer. The second procedure produces calibrators with greater emission intensities than those produced by mixing phosphor with plastic. The major advantage of these calibrators is that they are robust physically and the emission levels do not decay quickly over time (~1% per year initial loss). However, the calibrators are not necessarily isotropic, and this must be tested.

Uranyl Salt Calibrators

Uranyl salts emit low-intensity radioluminescence, as first noted by Becquerel.[13] In solution, emission is attributed predominantly to the ^{232}U daughter radionuclide generated in the ^{238}U decay series.[10] However, radioluminescence from solid uranyl salts appears to result from the decay of ^{238}U directly. Different uranyl salt forms emit different levels of radioluminescence, with acetate and nitrate salts producing the highest levels of radioluminescence. The degree of hydration of the uranyl salt affects the level of radioluminescence. Consequently, calibrators should be sealed in order to prevent dehydration and changes in environmental humidity from affecting the level of radioluminescence. In contrast to the radioactive phosphor calibrators described earlier, uranyl salt calibrators should preferably not be embedded in plastic. Over time, radiation damage from the high energy α-particles emitted from ^{238}U and radioactive daughter nuclides darkens the plastic, resulting in decreased radioluminescence over time. Calibration of a luminometer with a liquid uranyl nitrate standard and a

[13] H. Becqueral, *C.R. Acad. Sci.* **122,** 689 (1896).

SPECTRAL_0000518

solid uranyl acetate standard is shown in Fig. 1. The luminometer and calibrators were moved several times and resited in different laboratories during the period indicated. Caution is required when using uranyl salt calibrators with new luminometers. In certain applications, optical filters may be placed in the photomultiplier housing to reduce background chemiluminescence noise. These filters may absorb the radioluminescence as well and must be removed in order to calibrate with uranyl salts. Unlike the components of the other calibrators listed earlier, the amount of uranyl salt used in a calibrator (as much as 10 g) may pose a health hazard to personnel through dermal exposure or by inhalation if the calibrator is broken. A second disadvantage is that the disposal of uranyl salts is regulated by statute and must be disposed of properly.

Discussion

Little attention has as yet been given to absolute standardization of the various luminometers and bioluminescence and chemiluminescence assay systems in use commercially and for diagnostic procedures. The National Institute of Standards and Technology has initiated a program in the United States to develop an absolute, traceable calibration standard for luminometers. Unfortunately, this may not be entirely applicable for calibrating all bioluminescence and chemiluminescence reaction systems such as the firefly luciferase reaction. This is attributed to photocathode spectral sensitivity differences between photomultiplier tubes and dissimi-

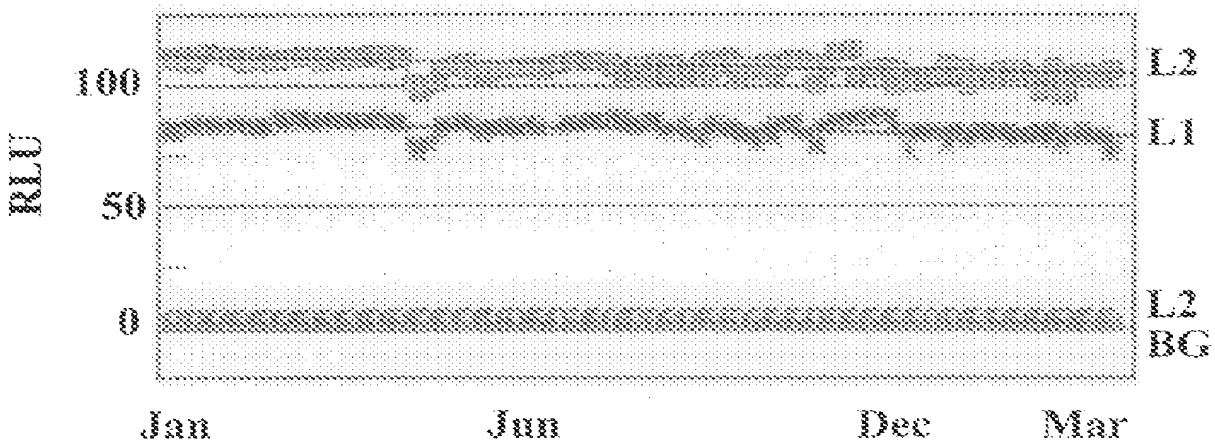


FIG. 1. Calibration of a luminometer with a liquid uranyl nitrate standard. A solid uranyl acetate standard is also shown.

SPECTRAL_0000519

larities between emission spectra of potential chemiluminescence calibrators and the oxyluciferin. Another area where much needs to be accomplished is in the area of low-level light imaging where calibration is still primitive.[14–16]

[14] D. J. O'Kane and J. E. Wampler, *Proc. Soc. Photo-Opt. Instr. Eng.* **1161,** 205 (1989).
[15] F. Berthold, K. Hafner, and D. DiPrato, *in* "Bioluminescence and Chemiluminescence: Fundamental and Applied Aspects" (A. K. Campbell, L. J. Kricka, and P. E. Stanley, eds.), p. 617. Wiley, Chichester, 1994.
[16] D. H. Leaback, *in* "Bioluminescence and Chemiluminescence: Molecular Reporting with Photons" (J. W. Hastings, L. J. Kricka, and P. E. Stanley, eds.), p. 545. Wiley, Chichester, 1997.

[6] Commercially Available Luminometers and Low-Level Light Imaging Devices

By PHILIP E. STANLEY

The study of bioluminescence (BL) and chemiluminescence (CL) and assays and techniques based on them usually requires the measurement of light output. Today, the life scientist uses a commercially available instrument because there are many from which to choose in the marketplace. This article discusses briefly some aspects of the various types of instruments and provides a list of many of the suppliers.

In Volume 133 of "Methods in Enzymology" the specifications of various types of luminometers are described in some detail.[1] In this volume, Berthold *et al.*[2] review this topic in light of today's technology, whereas Voss[3] describes the mode of action of detectors used in this instrumentation. Technical specifications of many other luminometers are given elsewhere.[4–12]

[1] P. E. Stanley, *Methods Enzymol.* **133,** 587.
[2] F. Berthold, K. Herick, and R. M. Siewe, *Methods Enzymol.* **305** [4] 2000 (this volume).
[3] K. J. Voss, *Methods Enzymol.* **305** [3] 2000 (this volume).
[4] P. E. Stanley, *in* "Clinical and Biochemical Luminescence" (L. J. Kricka and T. J. N. Carter, eds.), p. 219. Dekker, New York, 1982.
[5] P. E. Stanley, *J. Biolumin. Chemilumin.* **7,** 77 (1992).
[6] P. E. Stanley, *J. Biolumin. Chemilumin.* **7,** 157 (1992).
[7] P. E. Stanley, *J. Biolumin. Chemilumin.* **8,** 237 (1993).
[8] P. E. Stanley, *J. Biolumin. Chemilumin.* **9,** 51 (1994).
[9] P. E. Stanley, *J. Biolumin. Chemilumin.* **9,** 123 (1994).
[10] P. E. Stanley, *J. Biolumin. Chemilumin.* **11,** 175 (1996).
[11] P. E. Stanley, *J. Biolumin. Chemilumin.* **12,** 61 (1997).
[12] P. E. Stanley, *Luminescence* **14,** 215 (1999).

Copyright © 2000 by Academic Press
All rights of reproduction in any form reserved.
METHODS IN ENZYMOLOGY, VOL. 305
0076-6879/00 $30.00

SPECTRAL_0000520

ABSOLUTE RADIOMETRIC CALIBRATION OF DIGITAL IMAGING SYSTEMS

Steven W. Brown, Thomas C. Larason, Catherine Habauzit, George P. Eppeldauer,
Yoshihiro Ohno, and Keith R. Lykke
National Institute of Standards and Technology, Gaithersburg, MD 20899

ABSTRACT

We have developed a tunable laser-based facility for the absolute radiometric calibration of digital imaging systems such as CCD cameras, spectrographs, and microscopes. Several types of silicon-based digital imaging systems have been calibrated in this new facility, including a commercially available camera equipped with a removable photopic filter, a custom-designed digital microscope, and a CCD spectrograph. We present results of the CCD camera calibration in detail and discuss relevant aspects of the microscope and spectrograph calibrations. During the radiometric calibration, the pixel-to-pixel uniformity, linearity, and absolute spectral responsivity of each system were determined over the visible spectral range (400 nm to 800 nm). Each of these aspects of the CCD camera calibration will be presented, along with a discussion of the measurement uncertainties.

Keywords: calibration, CCD, digital camera, radiometry

1. INTRODUCTION

Improvements in the operation and performance of Digital Imaging Systems (DIS's) have led to an explosion in the use of these systems in a variety of scientific, medical, and industrial imaging applications. In many of these new applications, it is important that the spectral characteristics of the imaging system as well as its spatial (geometric) properties be well characterized and its photometric, radiometric, or colorimetric performance known. This has resulted in increased demand for characterization and calibration methodologies that are traceable to common standards.

By knowing the spectral responsivity of a DIS, one can accurately predict its performance under differing operating conditions. Currently, these systems can be calibrated with relative combined standard uncertainties of approximately 5 % to 10 %. In many cases, DIS's are calibrated against broad-band incandescent sources – such as Illuminant A – and subsequently measure sources with very different spectral power distributions. In this case, the measurement uncertainties are not well known in general, and can be much larger than expected.

2. DESCRIPTION OF THE SIRCUS FACILITY

We have developed a facility at the National Institute of Standards and Technology (NIST) for Spectral Irradiance and Radiance Responsivity Calibrations using Uniform Sources (SIRCUS) to calibrate DIS's. In this facility — shown in Fig 1 — lasers are directed into an integrating sphere to produce a monochromatic, Lambertian source for irradiance and radiance responsivity calibrations. This integrating sphere source (ISS) has been used to calibrate the spectral radiance and irradiance responsivity of a variety of detectors and imaging systems [1]. The two critical cornerstones of the facility are broadly tunable continuous-wave (cw) laser sources and reference standard detectors that are well-characterized and calibrated with low uncertainties to determine the radiance of the ISS with low uncertainty.

A variety of lasers are used to provide continuous coverage over the spectral range from 370 nm to 1000 nm. A Ti:sapphire laser provides tunable coverage from 690 nm to 1000 nm, frequency-doubling enables tunability from 370 nm to 450 nm. Discrete lasers were used for the spectral range from 450 nm to 550 nm and dye lasers are used to cover the spectral region from 550 nm to 700 nm. Currently, dye lasers are used to cover the spectral range from 415 nm to 700 nm.

Reference standard detectors with spectral power responsivities directly traceable to the NIST primary standard equipped with precision apertures were used to determine the sphere radiance [2]. These trap detectors are calibrated for spectral power responsivity directly against a cryogenic radiometer over the spectral range from 405 nm to 920 nm [3]. From the power responsivity and the aperture area, the irradiance responsivity of the trap detector is determined. By measuring the distance between the sphere exit port and the trap detector entrance aperture and the area of the ISS exit port, the radiance of

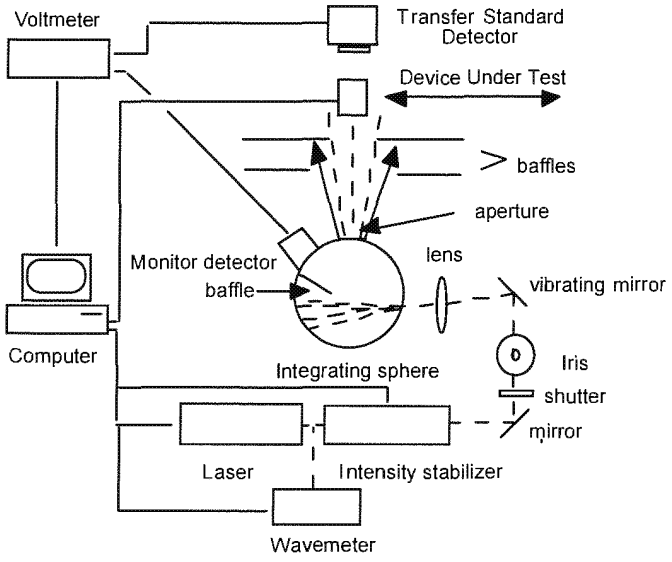


Fig. 1. Schematic diagram of the SIRCUS facility.

the ISS was determined with a relative combined standard uncertainty of 0.1 % [4, 5]. A silicon monitor detector mounted on the wall of the ISS was used to correct for small power fluctuations in the laser between measurements with the reference standard detector and the DIS.

3. CALIBRATION RESULTS

In general, the absolute spectral responsivity (ASR) of an instrument, $R(\lambda)$, relates the signal measured by a detector, S, to the spectral radiance of the source being measured, $L(\lambda)$:

$$S = \int R(\lambda)L(\lambda)d\lambda . \qquad (1)$$

The integration is over the full spectral bandwidth of the source. A DIS can be considered to be comprised of i by j independent detectors, with an individual measurement equation for each detector, or pixel, in the array. Each pixel in the array will also image a different area of the ISS, and in general:

$$S_{i,j} = \int R_{i,j}(\lambda)L_{i,j}(\lambda)d\lambda , \qquad (2)$$

with i defining the column position and j equal to the corresponding row in the array. $L_{i,j}(\lambda)$ refers to the radiance of the spatial region of the sphere exit port imaged onto pixel i, j. Note that for uniform sources, we can eliminate the spatial dependence on radiance: $L_{i,j}(\lambda) \sim L(\lambda)$.

Because we are using narrow-band laser sources (with a bandwidth of approximately 10 MHz, or 0.00001 nm), $L(\lambda)$ can be approximated by a delta function, $L(\lambda)=L(\lambda_o)\delta(\lambda - \lambda_o)$, and Eq. 2 can be rewritten as,

$$S_{i,j} = R_{i,j}(\lambda_o)L(\lambda_o) . \qquad (3)$$

Knowing the source radiance $L(\lambda_o)$ and measuring the CCD signal $S(\lambda_o)$, we obtain a direct measurement of the desired quantity $R_{i,j}(\lambda_o)$:

$$R_{i,j}(\lambda_o) = S_{i,j} / L(\lambda_o) . \qquad (4)$$

By tuning the wavelength of the calibration source, we directly obtain the absolute spectral responsivity of each element in the DIS.

To complete the radiometric calibration of an instrument, other factors need to be considered as well, including the linearity of the response and the exposure time correction.

3.1. Camera Calibration

We calibrated an 8-bit silicon-based CCD camera with 640 x 480 pixels equipped with a 35 mm focal length lens and a removable photopic filter. The instrument field-of-view under normal operating conditions is 13.5°. It comes equipped with 8 user-selectable shutter speeds, enabling measurements of luminance levels as low as 0.34 cd/m^2. It has a short-term repeatability of 0.4 %, and is calibrated by the manufacturer against Illuminant A with a stated relative combined standard uncertainty (k=1) of 4 %. The camera pixel-to-pixel response uniformity, linearity, and absolute responsivity — both with and without the photopic V(λ) filter on the front of the camera — were determined.

We used a 20 cm diameter Spectralon-coated integrating sphere with a 5.34 cm diameter exit port to calibrate the CCD camera. Typical power levels of radiation introduced into the ISS range from a few mW to a few hundred mW, depending on the laser used, giving a source radiance in the range from 1 x 10^{-7} W/mm^2/sr to 1 x 10^{-4} W/mm^2/sr. Prior to determining the responsivity of the CCD camera, the monitor detector was calibrated against the reference standard detector over the

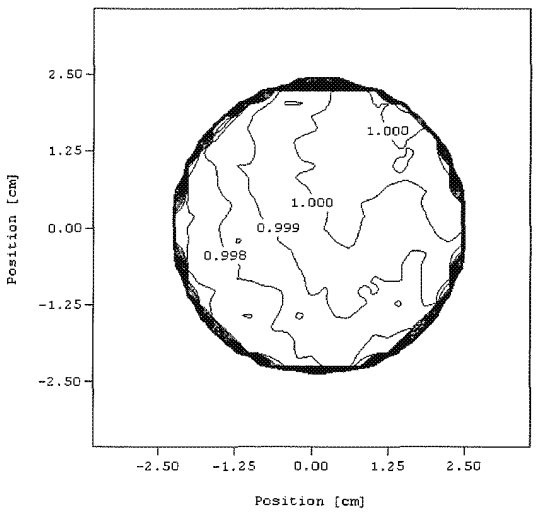


Fig. 2. ISS exit port radiance uniformity with 532 nm excitation.

wavelength range of interest. The calibration related the monitor detector signal to the ISS radiance. The CCD camera was then aligned in front of the ISS and its radiance responsivity determined. During the camera calibration, the sphere radiance was determined at a particular wavelength by measuring the monitor detector signal.

We measured the uniformity of the ISS at 488 nm, 532 nm, and 633 nm using a temperature-stabilized Si radiometer with a narrow field of view mounted on a computer controlled two-axis (XY) translation stage. The stage was stepped in 2 mm increments over a 6 cm by 6 cm square area (an area larger than the area of the sphere exit port). The radiometer signal, normalized by the sphere monitor photodiode signal, was recorded at each position. Results are shown in Fig. 2 for the relative radiance over the ISS exit port at 532 nm; the 633 nm and 488 nm results were similar. As shown in the figure, the radiance from upper right quadrant of the sphere is slightly larger than the radiance from the rest of the sphere. We therefore allow $L_{i,j}(\lambda) \approx L(\lambda)$, with an added relative standard uncertainty of 0.25 %.

We then positioned the camera in front of the ISS exit port. Using a target grid centered on the ISS exit port, we positioned the camera to image the central 4 cm by 3 cm region of the sphere exit port. Prior to determining the absolute responsivity of the CCD, it is necessary to measure and correct for any non-linearity in the response of the camera. We therefore measured the response of the CCD array, averaged over the central 50 by 50 pixels, as the sphere radiance was changed. The measurements involved changing the intensity of the laser light entering the ISS (by adjusting the throughput of a laser power controller) and comparing the radiance of the sphere measured by the CCD with the known ISS radiance determined by the calibrated monitor photodiode. The 8-bit camera has a maximum digital number (DN) of 255, corresponding to a 90 % of the CCD full-well capacity; data were taken with the same CCD exposure time (2 ms) over a radiance range giving count levels varying from approximately 10 DN to 240 DN. The resultant data are plotted in Fig. 3 as the ratio of the CCD signal to the sphere radiance versus the CCD signal (DN). If the CCD response were linear, the ratio of the CCD signal to the ISS radiance would remain constant as a function of CCD count level. However, the ratio increased sharply as the CCD camera signal increased from 10 DN to 100 DN. Above 100 DN, the ratio continued to rise slightly, increasing from a value of approximately 60 at 100 DN to a value of approximately 63 at 230 DN. In determining the absolute radiance responsivity of the CCD, we normalized individual data sets to the high-count level, with the individual scaling factors determined by the results shown in Fig. 3.

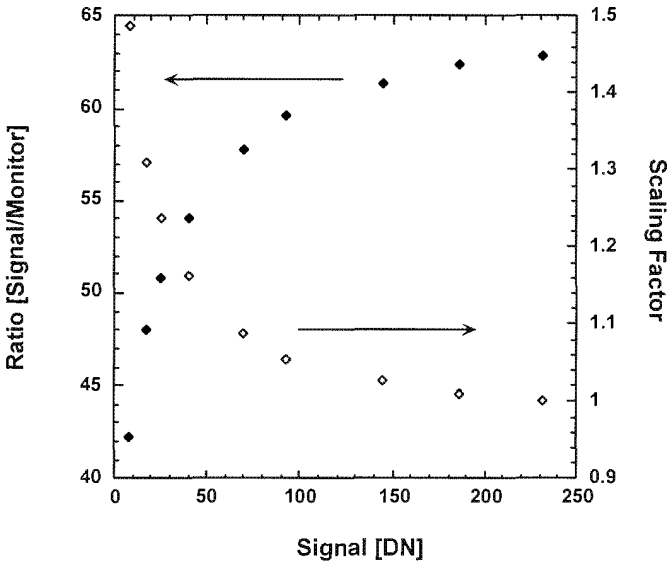


Fig. 3. Non-linear response of the CCD camera and the resultant scaling factors used in the absolute responsivity calibration.

Note that we only calibrated the linearity of the CCD using a shutter setting corresponding to an exposure time of 2 ms. It is difficult to distinguish between a non-linearity in the CCD response, and a variability in the camera readout offset value. For example, we

SPECTRAL_0000523

performed a correction to the response of the CCD by changing the offset level by 7 DN. Applying this simple correction to the data in Fig. 3, the response of the CCD camera was linear to within 1 % over the range from 25 DN to 230 DN.

The CCD camera was then positioned in front of the ISS, and its spectral responsivity, in DN per second per unit radiance, was determined. During the calibration on SIRCUS, the laser was tuned to the wavelength of interest. The CCD camera measured the radiance from the ISS exit port and the radiance responsivity (DN/s/(W/cm^2/sr)) was calculated by dividing the CCD output signal, corrected for the exposure time, by the sphere radiance. During the calibration, images were acquired with several different exposure times. The CCD responsivity was measured for different exposure times at several wavelengths during the calibration. The CCD responsivity agreed to within 1 % for the different exposure times.

The pixel-to-pixel responsivity of the camera was uniform over the central 90 % of the array to within approximately 5 %, as shown in Fig. 4(a) for 580 nm excitation. With the photopic filter installed, the non-uniformity in the CCD responsivity increased to approximately 10 %, as shown in Fig. 4(b). All measurements were performed under the same conditions. The data were not corrected for the non-uniformity of the ISS radiance because it was negligible compared with the non-uniformity of the pixel-to-pixel responsivity of the CCD.

To determine the ASR, we averaged the response of the central 50 by 50 pixels over the wavelength range from 400 nm to 800 nm. At the time of the calibration, we did not have continuously tunable lasers for the spectral range from 450 nm to 550 nm. To fill in this spectral region, we calculated the relative responsivity using the output from a lamp-monochromator source (4 nm bandwidth) [6], and determined the absolute responsivity by comparison with results obtained on SIRCUS. For this part of the calibration, relay optics were used to create a parallel 2.5 cm diameter beam. The radiation, under-filling the CCD field-of-view, was imaged onto a small region in the center of the CCD array. During the calibration, the radiant power in the beam was measured at each wavelength using reference detectors and an image subsequently acquired by the CCD. A 35 by 35 pixel area on the CCD was selected to give an averaged response. The data were subsequently corrected for the nonlinear response of the CCD and normalized to the radiant power in the beam, giving a relative responsivity of the CCD. To determine the absolute responsivity of the camera, the data were normalized to the SIRCUS results near 580 nm. Results are shown in Fig. 5 for the camera (a) with and (b) without the photopic filter attached.

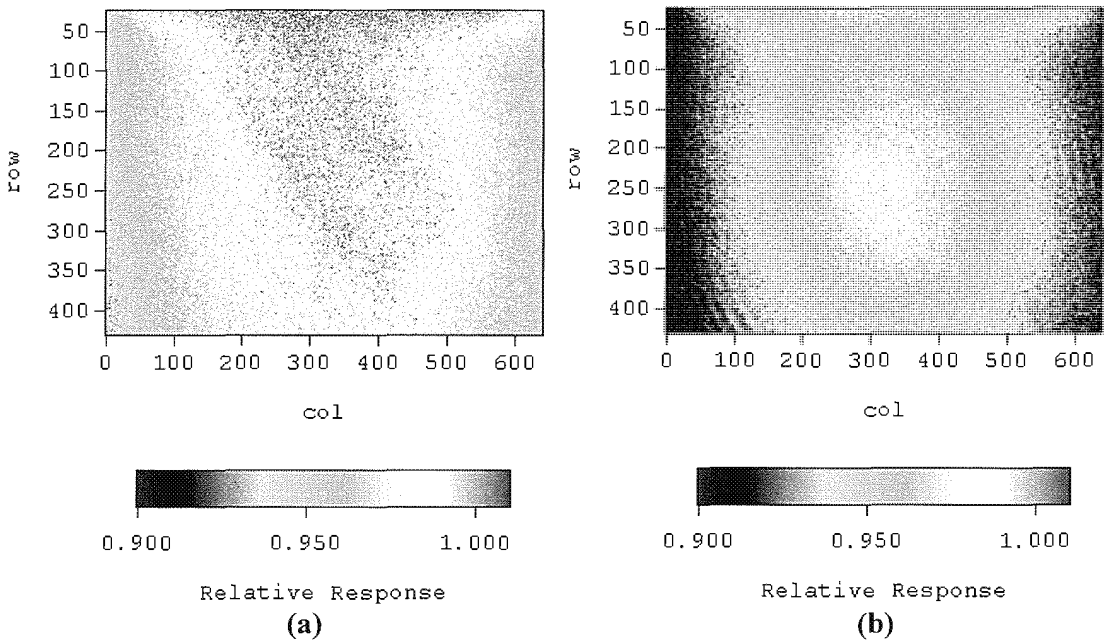


Fig. 4. Pixel-to-pixel uniformity (a)without and (b) with the photopic filter installed.

SPECTRAL_0000524

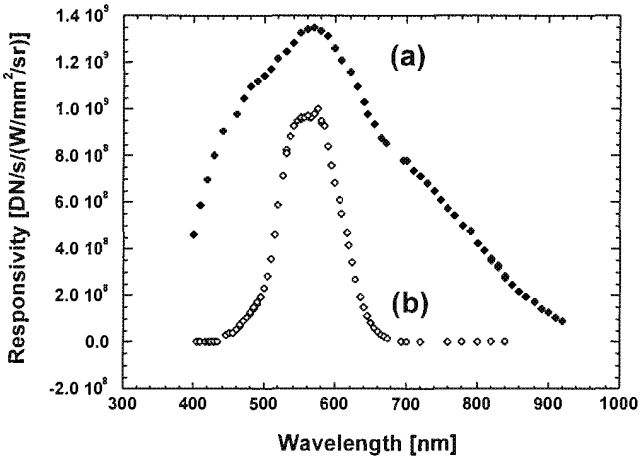


Fig. 5. CCD camera ASR (a) without and (b) with the photopic filter installed.

3.2. Uncertainty of camera radiance responsivity

Each component in the calibration chain contributes to the overall uncertainty in the radiance responsivity calibration. We estimated the contributions of all known components to the combined standard uncertainty in the CCD radiance responsivity calibration on SIRCUS. These contributions are listed in Table 1. We estimate that the relative combined standard uncertainty in the sphere radiance is 0.1 %, the uncertainty in the non-linear correction to the responsivity to be 1 %; the uncertainty in the exposure time correction to be 0.5 %; and the reproducibility, including short-term repeatability, alignment and focus, to be approximately 2 %. Taking the root-sum-square of the individual components, the relative combined standard uncertainty in the CCD radiance responsivity calibration is 2.3 % (coverage factor k=1). For imaging applications, there will be an additional uncertainty of approximately 1 % from the non-uniformity of the CCD.

Table 1. Relative combined standard uncertainty of the CCD radiance responsivity calibration on SIRCUS.

Component	Uncertainty [%]
Sphere Radiance (Monitor detector calibration)	0.1
Sphere Radiance Non-uniformity	0.25
CCD Non-linearity	1
Exposure time correction	0.5
Reproducibility	2
Relative Combined Std. Uncertainty	2.3

The radiant power distribution in the beam from the monochromator was highly non-uniform, leading to increased uncertainty in the calibration of the CCD, both because of the increased uncertainty in the reproducibility of the measurements, and also because of the increased uncertainty in the non-linearity correction of the averaged response. There was an additional uncertainty in the normalization of the response to the measurements on SIRCUS. Consequently, measurements using the lamp-monochromator had a relative combined standard uncertainty of approximately 4 %.

For measurements of photometric quantities, a source spectral radiance distribution is weighted by the $V(\lambda)$ function [7]. The photometric uncertainty is different than the above discussed radiometric responsivity measurement uncertainty and depends on how closely the response of the camera with the photopic filter approximates the $V(\lambda)$ function. For poor matches, the photometric uncertainty can be large and will depend on the source spectral distribution. There will be an additional uncertainty for imaging applications from the larger non-uniformity in the pixel-to-pixel response.

3.3 Microscope Calibration

The microscope consists of an objective lens and a 1024 by 1024 pixel cooled CCD array. It is used to determine x-ray phosphor efficiencies from scintillator crystals [8]. Imaging a scintillation region on a crystal is extremely advantageous because the radiation from scintillators is Lambertian and viewing the source distribution enables the determination of radiometric quantities with lower uncertainties. We measured the linearity, exposure time correction, pixel to pixel uniformity and the absolute spectral radiance responsivity of the microscope on SIRCUS. For these measurements, we used a 5 cm diameter ISS with a 2 mm aperture. The microscope, equipped with a 10X objective, was positioned in front of the ISS. Each pixel imaged the same region of the back wall of the ISS, resulting in minimal additional uncertainty in the calibration from any potential non-uniformity in the sphere exitance.

The CCD array had a 12-bit A/D converter, with 4095 DN corresponding to 90 % of the CCD full-well capacity. We first determined the exposure time and the non-linearity corrections in the response of the microscope; results are shown in Figs. 6 and 7, respectively. The exposure time correction was negligible for exposure times greater that 500 ms. For shorter exposure times, a correction — as large as 100 % for 10 ms exposure times — had to be applied. In many of these systems, there is a delay in opening and closing the shutter, leading to an exposure time that is slightly different than the nominal value. For this instrument, adding 10 ms to the nominal exposure time reduced the correction to the 5 % level for the shortest exposure times. The system response was linear for count rates larger than 100 DN. Offset variations and uncertainty in the determination of the background signal could contribute to the non-linear behavior at the smaller count rates. During the absolute radiometric calibration, the count rates were kept larger than 1000 DN and the exposure time was kept constant at 100 ms. This is easy to accomplish using a laser-based ISS; we merely adjust the power into the ISS at a given wavelength to achieve these goals.

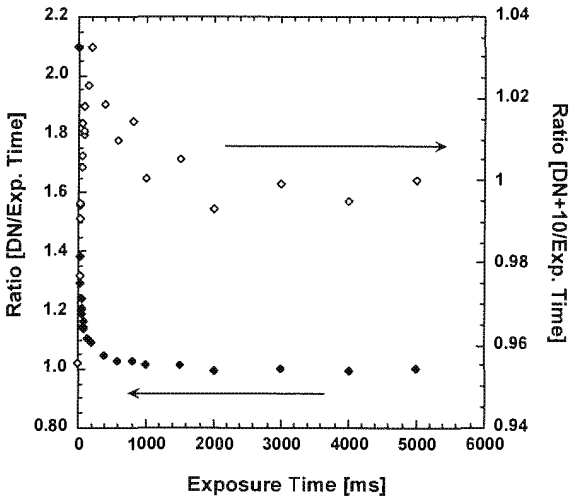


Fig. 6. Digital microscope exposure time correction.

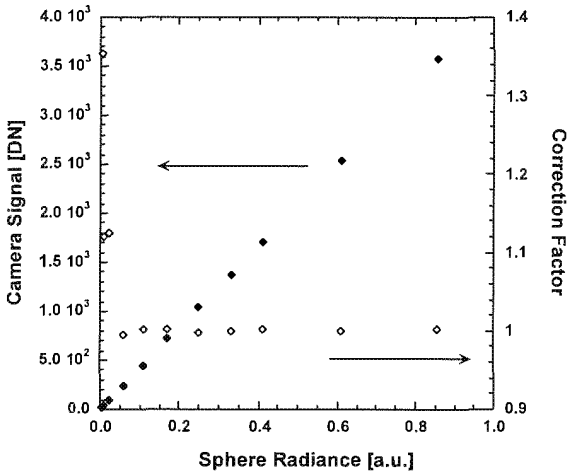


Fig. 7. Microscope response linearity.

The microscope response was uniform to with 0.2 % over the central 90 % of the CCD array; the ASR, averaged over the central 25 by 25 pixels, is shown in Fig. 8. Because of the smaller non-linear correction, the better pixel to pixel uniformity and the 12 bit digitization, we estimate the relative combined standard uncertainty in the microscope ASR measurement to be approximately 1 %.

3.4 Spectrograph Calibration

Spectrographs are typically calibrated for spectral radiance responsivity against broad-band sources such as lamp-illuminated integrating sphere sources (ISSs) and plaques. Stray light, wavelength errors, and lack of knowledge of the single pixel relative responsivity all give rise to increased uncertainties in the calibration and subsequent operation of these instruments. Many of these sources of calibration error can be greatly reduced or eliminated using tunable, monochromatic laser sources in place of conventional broad-band sources.

SPECTRAL_0000526

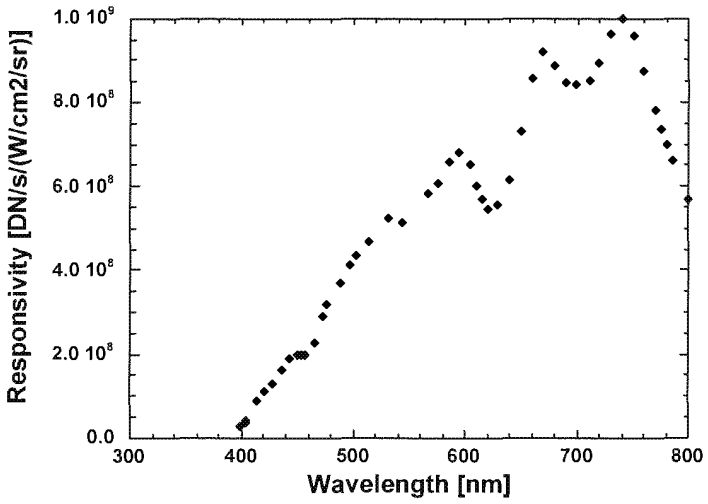


Fig. 8. ASR of digital microscope.

A dual-spectrograph radiometer was calibrated on SIRCUS for radiance responsivity over the spectral range from 400 nm to 850 nm. Details of the calibration are described elsewhere [4, 5]. In this instrument, radiation enters the spectrograph through an entrance slit, is dispersed using a grating, and imaged onto the CCD array using a mirror, as shown in Fig. 9. For excitation using monochromatic radiation, the image formed is a line reflecting the image of the entrance slit on the CCD (Fig. 10). Note that the image is spread out over several pixels in the horizontal (dispersion) direction, is not centered vertically on the CCD array, and shows a pronounced curvature (Fig. 11). By tuning the excitation wavelength, the image moves across the array and each pixel's ASR can be determined. In this work, we measured the responsivity of the averaged central 100 pixels in each column. Eq. 4 was modified to:

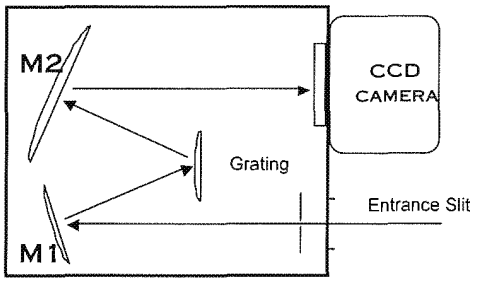


Fig. 9. Spectrograph optical layout.

$$R_i(\lambda_o) = S_i / L(\lambda_o), \qquad (5)$$

where i now refers to the particular column in the array. In Fig. 12, we show the absolute spectral responsivity, $R_i(\lambda)$, for columns 243 – 247 over the wavelength range from 735 nm to 750 nm. We measured a 0.8 nm separation between the maximum responsivity of adjacent pixels and nominal single pixel bandwidth of 2 nm. The curvature in the spectrograph image, Fig. 11 gave rise to the pronounced shoulder observed to shorter wavelength in the ASR. This shoulder in the single pixel ASR was attributed to the CCD not being located at the spectrograph image plane. We estimate the relative combined standard uncertainty in the calibration to be approximately 3 %. Note that the determination of each pixel's ASR is difficult to obtain using any technique other than the tunable-laser-based ISS approach developed on SIRCUS.

4. SUMMARY

We have developed a flexible, detector-based calibration facility using tunable laser sources and high accuracy reference standard detectors for the irradiance and radiance responsivity calibration of digital imaging systems. We have calibrated a number of instruments on this facility, and presented results for a digital camera, a digital microscope and a digital spectrograph. This approach has several advantages over conventional calibration techniques using broad-band sources, including uniform, monochromatic irradiance and radiance sources; lower wavelength uncertainty; no stray light contribution

to the signal; and the ability to determine each pixel's responsivity. Using this approach, uncertainties in the radiometric calibration of DIS's can be reduced by a factor of 2 or greater over conventional calibration techniques.

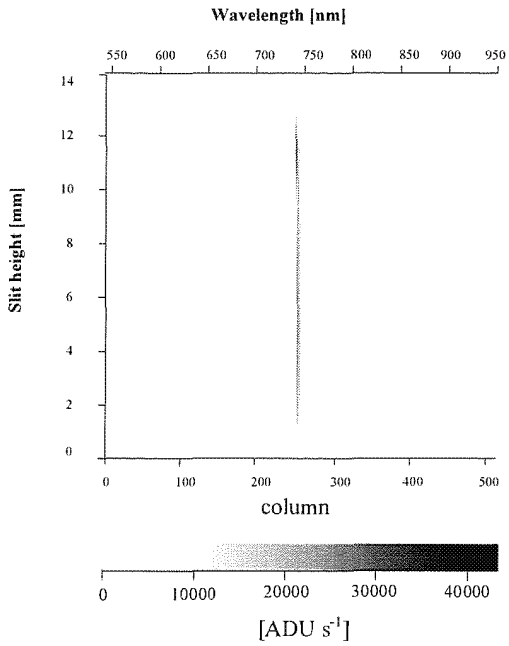


Fig. 10. Spectrograph image of ISS with 745 nm excitation.

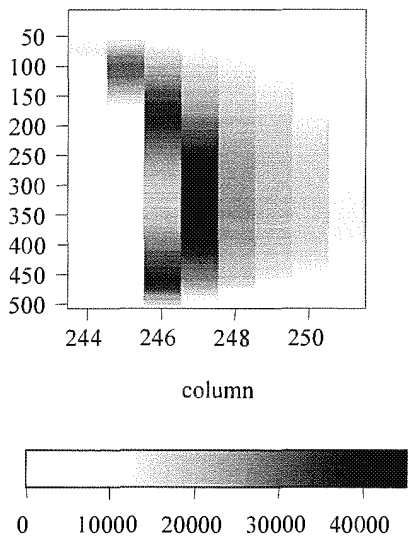


Fig. 11. Expanded view of spectrograph image of ISS with 745 nm excitation.

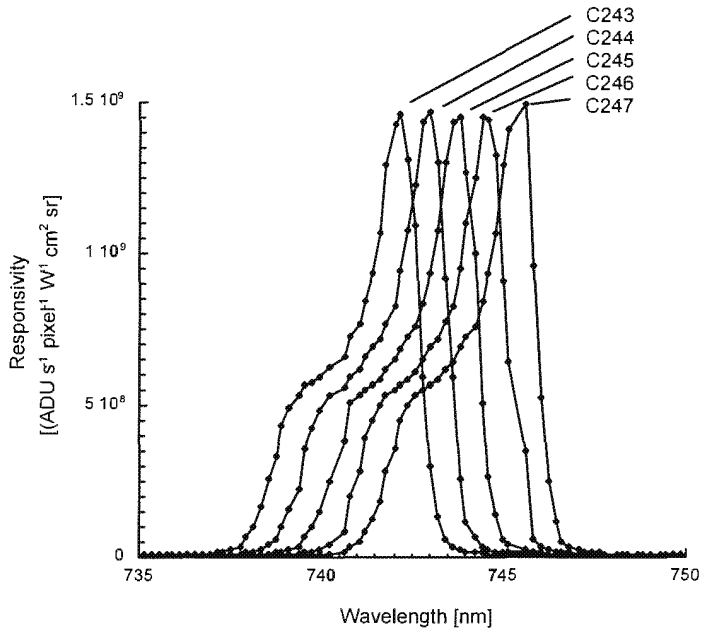


Fig. 12. Absolute spectral responsivity of columns 243 to 247.

SPECTRAL_0000528

5. ACKNOWLEDGMENTS

We would like to thank Carol Johnson for useful discussions and acknowledge support for this work by the U. S. Air Force Metrology under contract numbers 97-421 and 98-439.

6. REFERENCES

1 S. W. Brown, G. P. Eppeldauer, and K. R. Lykke, "NIST facility for spectral irradiance and radiance responsivity calibrations with uniform sources," *Metrologia* 37, 579-582 (2000).
2 G.P. Eppeldauer and D.C. Lynch, "Opto-mechanical and electronic design of a tunnel-trap Si-radiometer," *J. Res. Natl. Inst. Stand. Technol.* (in press).
3 T. R. Gentile, J. M. Houston, J. E. Hardis, C. L. Cromer, and A. C. Parr, "National Institute of Standards and Technology high accuracy cryogenic radiometer," *Appl. Opt*, 35, 1056-1068 (1996).
4 C. Habauzit, *et al.*, "Radiometric characterization and absolute calibration of the Marine Optical System (MOS) bench unit," *J. Atmos. and Ocean. Technol.*, to be submitted.
5 S. W. Brown, C. Habauzit, B. C. Johnson, and K. R. Lykke, "Tunable-laser-based calibration of a digital spectrograph," *Appl. Opt.*, to be submitted.
6 T. C. Larason, S. S. Bruce, and A. C. Parr, Spectroradiometric Detector Measurements, Natl. Inst. Stand. Technol. Spec. Publ. 250-41, U. S. Government Printing Office, Washington, DC, 1998.
7 Yoshihiro Ohno, Photometric Calibrations, Natl. Inst. Stand. Technol. Spec. Publ. 250-37, U. S. Government Printing Office, Washington, DC, 1997.
8 Steven Grantham, NIST, personal communication.

AUAOMATED CALIBRATION OF A ZOOM LENS CCD IMAGE SYSTEM FOR VIDEOGRAMMETRY

DongBin Chen, YiDong Huang
Research Student, Senior Lecturer
School of Surveying, University of East London, Longbridge Road
Dagenham, Essex RM8 2AS, The United Kingdom
Tel +44 208 2232522, +44 208 2236250 Fax +44 208 2233618
d.chen@uel.ac.uk, Y.Huang@uel.ac.uk

KEY WORDS: Calibration, CCD camera, Image processing, Videotheodolite, Photogrammetry

ABSTRACT

This paper presents the automated calibration method and the calibration results of the off-the-shelf zoom lens CCD block camera. The CCD camera interior and exterior parameters with respect to the total-station were determined at every step of the focal length settings. The repeatability of the calibrated parameters against zooming action was assessed at five steps of the focal length settings. Both the accuracy and the repeatability for the automated calibration were analyzed.

1 INSTODUCTION

Zoom lenses have many desirable features but appear to be geometrically unstable and difficult to calibrate. It is common knowledge that the zooming camera parameters change with zoom position. The calibration needs to be performed at various focal settings within the zoom range. If the zoom lenses are used in a measurement application at the setting from which the calibrations had been carried out, the camera parameters need to be derived from the calibrated values.

The problem with the use of zoom lenses is the identification of calibration parameters at every used focal setting. For any vision system, geometric distortions caused by system electronics, focal plane construction, and imperfect lenses, lead to a less than perfect two-dimensional representation. In order to achieve precise three-dimensional positioning of objects, it is necessary to calibrate the vision system and correct for the effects of the above mentioned distortions. Changing the focal length alters the interior geometry of the camera, and consequently changes the magnitude of virtually all of interior orientation parameters.

Calibration of zoom lenses at every used focal length by manual processes is complicated and very time consuming. An auto-calibration method needs to be developed for calibrating zoom lenses for photogrammetric applications. The paper presents an auto-calibration routine for zoom lenses that has been developed from the camera-on-theodolite method by Huang and Harley. The results of auto-calibration using the Sony EVI-371 were presented. The repeatability of auto-calibration results was tested on numerous focal lengths to check the stability of the camera against zoom. The warm-up effect of imaging system was also assessed.

2 THE SYSTEM REQUIREMENTS

The system is comprised of the videotheodolite, an image grabber and a desktop computer. This videotheodolite is set at a number of stations during the research. At each station, the theodolite controlled by the desktop computer can precisely rotate at every angular step for the CCD camera to capture images to cover the designed target. The theodolite angular readings were recorded on capturing of each image to calculate the central position and bias error of the designed target in the image.

The CCD camera of the system is the Sony EVI-371D. It is a 1/3inch CCD image sensor with the 752(H) x 582(V) sensing area and its cell size is 6.35(H) x 7.4(V) microns. The zoom lens has the focal length from 5.4mm to 64.8mm, auto focus and 12 X zoom lens. For this calibration, the focus was fixed at a certain distance and the iris was fixed for the solid exposure.

The frame grabber used for this system is the MRT PCMCIA I imaging card. This card can be directly used with a portable computer or with a desktop computer via an adapter. It digitizes both fields of the composite video input and

generates a digital image of 508(H) x 480(V) pixels. Only the luminance signal, which is quantified into 8 bits, was used for processing.

In fact, the theodolite chosen for this system is the Geodimeter System 600, which is a total station and includes the features of the servo-assisted drive, the numeric keyboard, the tracklight and the RS-232C communication. By sending the appropriate commands from the computer, the computer controlled the rotating angle of the total station and the data of the angles of the total station are transferred between the total station and the computer. Therefore, the computer can precisely and quickly control the rotating angles of the videotheodolite.

3 CALIBRATION METHOD AND ITS AUTO-PROCEDURE

In the camera-on-theodolite calibration method, two targets were used and kept the suitable depth of field between them. The telescope of the theodolite was rotated to 25 positions so that the image of each target was captured. There were 25 different positions that cover every part of the image frame. For each image telescope position, the horizontal and vertical angle readings were recorded when every image was captured. The corresponding 25 sets of three dimensional co-ordinates of the targets with the respect to the rotating telescope system were calculated by the following equations:

$$\begin{bmatrix} X \\ Y \\ Z \end{bmatrix} = D \begin{bmatrix} -\cos \nu_0 \sin (h-h_0) \\ \sin \nu \sin \nu_0 + \cos \nu \cos \nu_0 \cos(h-h_0) \\ \cos \nu \sin \nu_0 - \sin \nu \cos \nu_0 \cos(h-h_0) \end{bmatrix}$$

In the equations, D is the distance between the target and the theodolite; h_0 and ν_0 are the horizontal and vertical readings while the theodolite is initially sighting at the target; h and ν are the readings with the captured image. With these corresponding 2D and 3D co-ordinates for 50 points (both targets), the analytical space resection with lens distortion models was performed to determine the interior and exterior parameters. The exterior parameters are the camera to theodolite parameters. For the detail of the camera-on-theodolite calibration method, see the Huang' s previous paper.

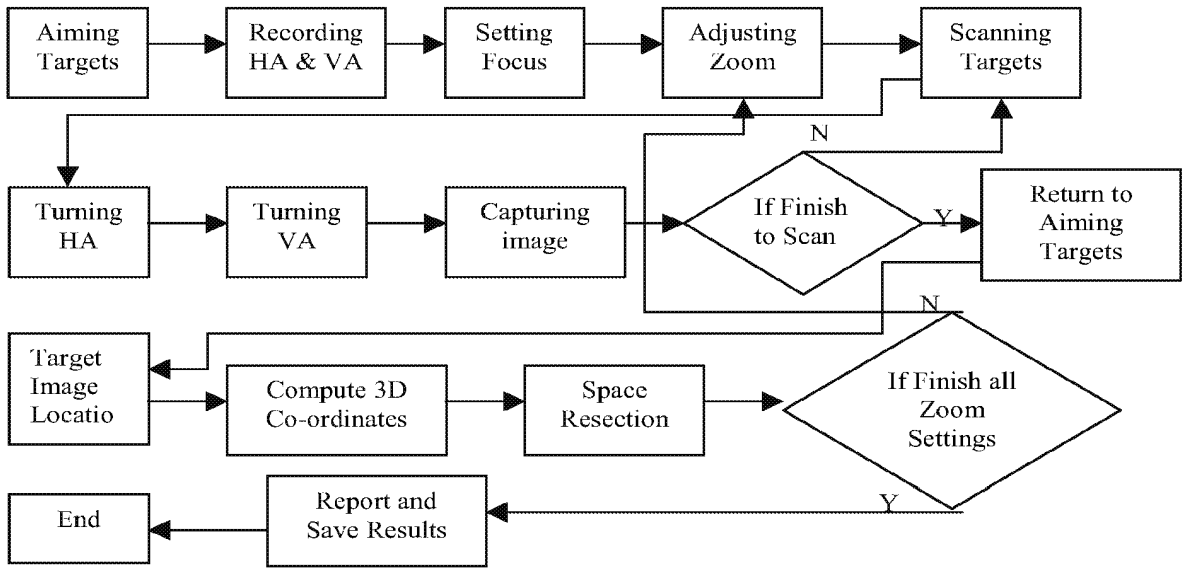


Figure 1. The diagram of auto-calibration procedure

According to this calibration method, the procedure of auto-calibration is shown as the figure 1. The auto-calibration is designed to cover every zoom setting. At every zoom setting, 25 images are captured in 5 X 5 rectangular locations within its field of view so that the targets can cover every part of the zoom lens in 25 images. Besides the camera-on-theodolite parameters, the program can also automatically determine the calibrated interior camera parameters that are the principle point, the principle distance, the affine parameters, three radial lens parameters and two tangential lens parameters at each focal setting.

4 DISTORTION MODEL

The calibrated parameters include the camera exterior orientation parameters with respect to the telescope of the theodolite, the camera interior orientation parameters, and the parameters in the error function model are shown below:

$$\delta x = A*y + x(k_1r^2 + k_2r^4 + k_3r^6) + p_1(r^2 +2x^2) +p_2(2xy)$$
$$\delta y = B*y + y(k_1r^2 + k_2r^4 + k_3r^6) + p_1(2xy) +p_2(r2 +2y^2)$$

Here, A and B are the affine deformation parameters. The ks are the radial lens distortion parameters and the ps are the decentring lens distortion parameters (Brown 1971).

5 WARM-UP EFFECT AND STABILITY TEST

The CCD camera and a target were fitted on two stable pillars. A series of images were automatically captured of the target at a five minutes interval after switch-on. The x and y co-ordinates of captured images were graphed against time as in Fig.2 and Fig. 3. The Fig.2 and the Fig.3 show that the warm-up period is about 4 hours and after 2 hours the x (lines) and y (samples) stayed stable to between 0.01 and 0.02 pixel respectively. In order to minimise the warm-up effect, The CCD camera was always switched on at least two hours before the experiments.

6 AUTO-CALIBRATION RESULTS

The auto-calibration experiments were carried out at twelve identifiable focal length settings. The focal length settings from 5.4mm to 64.8mm were divided into twelve settings. The calibrated values and the root mean squared residuals (RMS) for image co-ordinates are shown in the Table 1 where the symbols are defined as the following:

X_0, Y_0, Z_0	telescope co-ordinates of the camera perspective centre;
x_0,y_0	image co-ordinates of the principle point;
C	principle distance;
A,B	affine deformation parameters;
K_1,K_2,K_3	the radial lens distortion parameters;
P_1,P_2	the tangential distortion parameters;
ω	rotation for the X axis;
ϕ	rotation for the Y axis;
κ	rotation for the Z axis;
RMSx	the root mean squared residuals of image samples for target center;
RMSy	the root mean squared residuals of image lines for target center;
RMSc	the root mean squared residuals for target center;

Table 1. Auto-calibration Results

	Focal Settings (mm)					
Parameters	5.4	6.6	7.7	9.4	11.6	14.5
X_0	-1.098	-0.59	1.525	-0.631	-25.954	-944.666
Y_0	30.84	32.04	33.14	34.84	39.966	39.94
Z_0	59.099	58.656	62.645	62.45	49.282	-228.027
ϕ	-1.69812	4.66964	1.5049	2.09242	1.63453	-1.24384
ω	1.55673	1.55904	1.58827	1.58111	1.62226	1.37764
κ	0.12343	-6.24466	-3.07934	-3.66765	-3.21029	-0.33057
C	919.673	1069.289	1223.358	1503.718	1847.431	2200.899
x_0	265.3164	267.1964	266.2999	276.0205	281.0262	520.4202
y_0	247.0998	249.8458	244.162	255.7668	172.4327	-471.451
K_1	4.24E-12	2.27E-12	1.16E-12	1.70E-12	-1.08E-12	4.34E-13
K_2	-4.59E-21	-1.04E-21	4.94E-22	-1.78E-21	3.26E-21	7.25E-24
K_3	3.98E-30	4.36E-31	-6.85E-31	8.71E-31	-1.82E-30	-2.79E-34
P_1	-1.63E-09	-1.29E-09	-1.96E-09	-8.34E-10	1.27E-09	1.18E-09
P_2	-9.84E-10	-4.24E-10	4.35E-11	-2.91E-09	-7.52E-10	-4.16E-09
A	2.82E-06	1.26E-06	9.53E-06	4.09E-06	4.75E-06	4.63E-05

B	-1.78E-05	-1.45E-05	-1.90E-05	-2.61E-05	-8.63E-06	-1.15E-04
RMSx	0.057	0.092	0.052	0.100	0.139	0.122
RMSy	0.127	0.116	0.121	0.167	0.151	0.180
RMSc	0.098	0.105	0.093	0.138	0.145	0.154

	Focal	Settings	(mm)			
parameters	18.4	24.5	32.7	44.2	59.7	64.8
X_0	5.282	1.914	1.173	1.006	-6.069	-582.122
Y_0	43.84	45.74	51.99	58.19	69.72	89.94
Z_0	48.626	48.455	1037.541	45.794	47.46	224.997
ϕ	1.23139	-0.71444	-0.18639	0.83815	1.09493	-6.63511
ω	1.53806	1.52006	1.66582	1.59435	1.58543	1.56287
κ	-2.80636	-0.85959	-1.39357	-2.41422	-2.66987	5.06003
C	2970.936	3011.576	3754.129	5659.798	7663.076	10480.06
x_0	312.6916	396.7678	-330.0771	211.2441	262.3246	338.7931
y_0	385.2845	193.8781	377.5177	232.8796	258.5213	119.4646
K_1	4.09E-12	-6.39E-14	7.91E-13	8.79E-12	6.43E-12	4.57E-13
K_2	-1.05E-20	5.05E-22	3.01E-23	-1.97E-20	-1.24E-20	-5.26E-22
K_3	7.36E-30	-1.78E-31	-2.66E-33	1.37E-29	7.75E-30	1.62E-31
P_1	6.74E-10	2.80E-10	-4.44E-08	0	0	-6.25E-10
P_2	-4.97E-10	-1.70E-10	4.53E-09	0	0	1.88E-10
A	-1.27E-05	9.54E-06	-1.10E-04	-1.22E-05	-1.38E-06	-2.92E-06
B	1.26E-05	-5.71E-06	-5.09E-04	8.75E-07	-3.93E-05	-1.01E-05
RMSx	0.161	0.166	0.113	0.112	0.168	0.082
RMSy	0.177	0.177	0.231	0.195	0.126	0.090
RMSc	0.169	0.171	0.182	0.159	0.148	0.094

In the auto-calibration experiment, the auto-calibration accuracy was between 0.093 pixels and 0.182 pixels. The auto-calibration accuracy in the line direction was from 0.052 pixels to 0.168 pixels. That in the sample direction was from 0.090 pixels to 0.231 pixels. The line direction had higher accuracy of measurement than the sample direction because the sample direction of CCD camera has the random jitters. Fig. 4 shows the distributions of measurement accuracy for all of the calibrated focal settings. There was a high reliability of calibration when the measurement accuracy was high. Generally, the shorter focal length led to the higher accuracy of calibration.

7 REPEATABILITY OF CALIBRATED VALUES

It was expected that the calibrated parameter values of each focal setting retained certain accuracy when the lens returned to the focal setting after zooming in or out. In order to assess this repeatability, the auto-calibration was repeated at some of the calibrated focal settings after sufficient zoom actions. The focusing was fixed at the same distance as the last calibration. The calibrated values for the repetitions are shown in the table 2. Table 3 gives the RMS errors between the detected target image centers and the their corresponding image positions computed from 3D co-ordinates using the calibrated orientation parameter values determined at the first round. Fig. 5 shows the comparison of the measurement accuracy for the target centers in the same focal settings between the calibration values and the reference-calibration values. The repeated focal settings show an ideal consistence of measurement accuracy when the lens is in the wide field of view. When the lens is in the narrow field of view, the RMS values have a large bias because there is a relatively large uncertainty in both calibration and measurement of the lens.

Table 2. Repeated Auto-calibration Results

	Repeat	focal	Settings		
parameters	5.4	6.6	18.4	59.7	64.8
X_0	-1.178	-1.711	5.657	-6.339	-583.493
Y_0	28.366	34.966	46.766	72.566	92.866
Z_0	59.018	58.594	47.619	48.66	225.334
ϕ	1.50528	1.26022	1.91549	1.19263	1.01683
ω	1.58514	1.58701	1.66597	1.5855	1.55539
κ	-3.08034	-2.83522	-3.48937	-2.76762	-2.59121

C	919.17	1068.741	2955.115	7675.3	10319.68
x_0	266.2204	262.6462	377.4435	272.3104	343.9194
y_0	246.6523	245.5286	28.5754	253.7907	284.6795
K_1	2.81E-12	2.19E-12	-2.54E-13	9.47E-12	-6.53E-12
K_2	3.61E-22	-5.71E-22	5.54E-22	-2.09E-20	1.02E-20
K_3	-7.52E-31	-3.68E-32	-1.20E-31	1.43E-29	-5.07E-30
P_1	-2.13E-09	-1.08E-09	0	0	-6.13E-09
P_2	-1.21E-09	-2.91E-10	0	0	9.91E-09
A	-1.01E-07	-2.09E-06	2.20E-05	-3.28E-05	6.33E-06
B	-2.39E-05	-2.08E-05	-3.32E-05	-4.47E-05	3.96E-05
RMSx	0.069	0.086	0.135	0.168	0.087
RMSy	0.129	0.109	0.202	0.105	0.282
RMSc	0.103	0.099	0.172	0.140	0.208

Table 3. The RMS values of the accuracy of target center for reference-calibration parameters

	repeated	focal	settings	
	5.4	6.6	18.4	59.7	64.8
RMSx	0.185	0.152	0.292	0.527	0.25
RMSy	0.227	0.177	0.294	0.526	1.071
RMSc	0.207	0.165	0.293	0.526	0.777

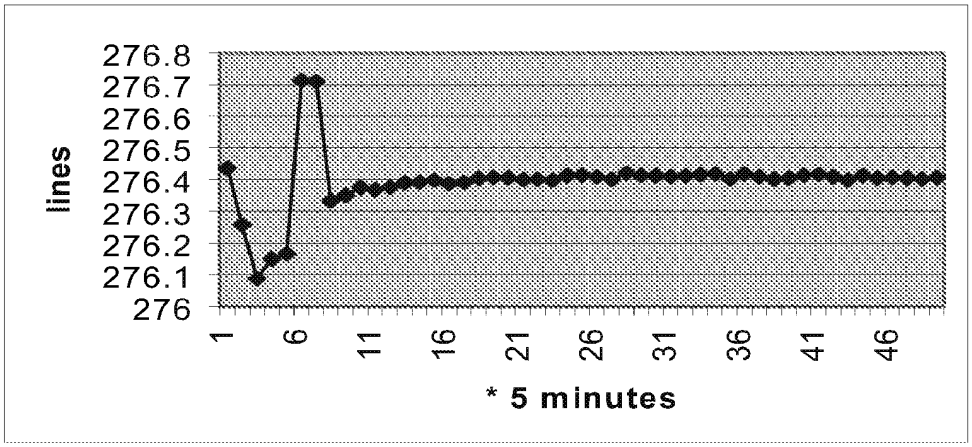


Figure 2. Lines of Warm-up effect

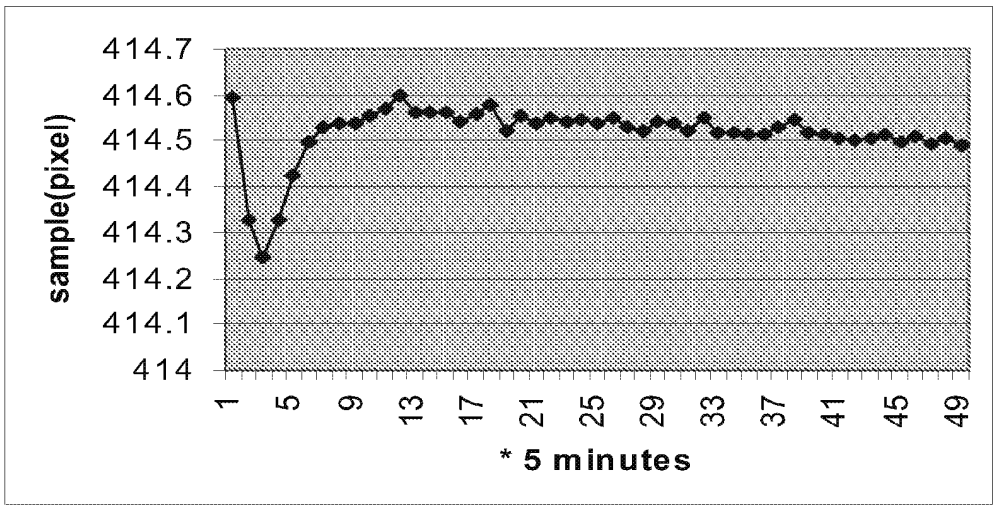


Figure 3. Samples of Warm-up Effect

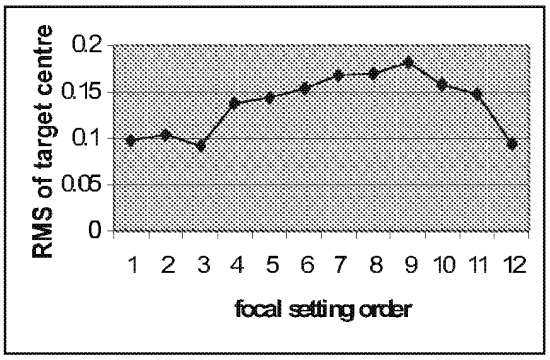


Figure 4. The distributions for the accuracy target center

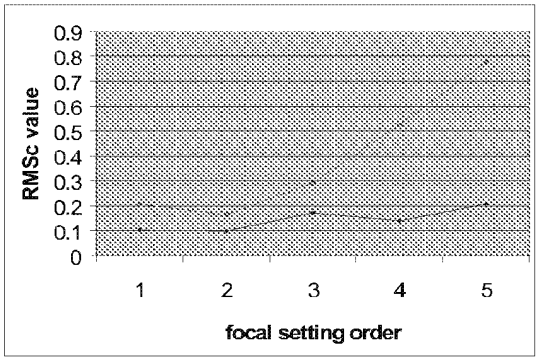


Figure 5. The comparison of two time distributions of for the accuracy of target center

8 CONCLUSIONS

The results of this research prove that automatic calibration of a motorized video-theodolite equipped with a zoom lens is possible and effective using the method and routine proposed. The camera-on-theodolite method demonstrated once again its benefits for frequent camera calibration and video-theodolite calibration. The repeatability of the calibrated zoom camera system against zooming ranges from 0.2 to 0.8 pixel, with the better result at the wide field angles. This accuracy for zoom camera can satisfy many surveying applications, especially when considering the very small angle subtended by a pixel at zoom-in settings.

REFERENCES

Huang, Y.D. & Harley, I.1990, CCD camera calibration without a control field, International Archives of Photogrammetry and Remote Sensing, Zurich, Vol. 28, Part 5/2, pp. 1028-34.

Wiley, A.G. & Wong, K.W., 1990, Metric aspects of zoom vision. International Archives of Photogrammetry and Remote Sensing, Zurich, Vol. 28, Part 5/1, pp.112-118.

Wiley, A.G. & Wong, K.W., 1995. Geometric calibration of zoom lenses for computer vision metrology. Photogrammetric Engineering and Remote Sensing, Vol. 61, No. 1, pp.69-74.

Bioluminescence and Chemiluminescence

Fundamentals and Applied Aspects

Proceedings of the 8th International Symposium on Bioluminescence and Chemiluminescence, Cambridge, September 1994

Edited by

A K Campbell, L J Kricka and P E Stanley

S. 617 – 620

JOHN WILEY & SONS
Chichester · New York · Brisbane · Toronto · Singapore

536

SPECTRAL_0000536

AN IMAGING SYSTEM FOR BIO- AND CHEMILUMINESCENCE, FLUORESCENCE, AND RADIOACTIVITY

Berthold, F.[1] , *Hafner, K.*[2] , *DiPrato, D.*[3]

[1] *EG&G Berthold, D-75323 Bad Wildbad, Germany*

[2] *EG&G Berthold, D-75323 Bad Wildbad, Germany*

[3] *EG&G Princeton Applied Research, Trenton NJ 08618, USA*

Introduction

Optoelectonic imaging is the most recent technology to find use in bioluminescence and chemiluminescence (BCL), made possible both by new detector technology and the availability of increased computer power at moderate cost.

It is convenient to distinguish between micro- and macroimaging. In microimaging, the image is captured and processed directly from a microscope; thus, aiming essentially at cells and tissue. Macroimaging, on the other hand, applies to objects like thin-layer-chromatograms, gels, blots, macroscopic tissue-sections, petri dishes or other planar samples.

Basically, a BCL macroimager (fig. 1) consists of a low level light detector mounted inside a light-tight box, with a door for sample access sample support, a lens imaging the sample onto the detector surface, detector electronics, and a computer for storing, analyzing and displaying data.

Detector technology which can be applied to luminescence imaging include slow-scan cooled CCD cameras, intensified CCD cameras (1. Jones et al., 1991; 2. Hooper and Ansorge, 1991), and vidicon tube cameras with intensifier (3. Bräuer et al., 1993).

The relative merits of different detectors have been discussed repeatedly (4. Ansorge et.al., 1991; 5. Wick et al., 1993). In our view, it has not been proven that any particular type of detector is superior to others. However there are considerable performance differences within each class of detectors.

System description

We use a slow-scan CCD camera (model 1530P-512MPP, EG&G Princeton Applied Research, Trenton NJ) with a 512 x 512 pixel structure in MPP multi-pinned-phase technology, which is characterized by extremely low thermal noise. In a CCD, electron-hole pairs are generated by the impinging photons, and the electrons are accumulated at the pixels closest to their origin. After the exposure electron charges are read out pixel by pixel, and stored. The resulting pattern represents the image.

CCD's have quantum efficiencies of up to 40 %, for optional backside-thinned versions even up to 80 %. The spectral response is very different from that of a bialkali photocathode, and extends from about 400 to 1100 nm, with a broad maximum from 500 to 900 nm. Sensitivity can be extended down to 200 nm by using an UV-enhanced version.

There are two main sources of background: dark current or thermal background, and read-out noise. Thermal noise is the spontaneous (not photon-induced) release of electrons which can be overcome by cooling either cryogenically or through Peltier elements. Since the use of liquid nitrogen may not be convenient in many laboratories, we used Peltier cooling with secondary liquid circulation. This allows cooling down to -80 °C, where thermal background is only about 7 electrons/pixel/hour for scientific grade CCD's with $(19\mu m)^2$ pixels.

This means that the detector is virtually free of thermal noise for exposure times below 30 minutes. The other source of noise is generated by the read-out process itself, and amounts to about 5 electrons.

SPECTRAL_0000537

As indicated in Fig. 1, the sample is placed onto a support (1), with options for temperature control and XY transport. A camera lens with f '= 25 mm, K= 0,95 (2) images the samples onto the CCD chip (3) being part of the camera (4), also including the Peltier elements and low noise input electronics.

To allow fluorescence imaging, different fluorescent light sources (5) can be installed together with suitable emission and measurement filters. White light sources (6) are used to generate standard epiluminescence images, which can be overlaid with luminescence or radioactivity images, and also useful for focusing. Image capture, display, and processing is effected using a PC with HIDRIS software (EG&G Princeton Applied Research, Trenton NJ).

The vertical position of both the CCD camera and the lens can be adjusted independently, to bring sample areas between 5x5 and 20x20 cm into full view of the detector area, and allowing autofocussing.

For radioactivity imaging, thin scintillator sheets are positioned on top of the samples. For optimum sensitivity and resolution, especially for high-energy beta-emitters like ^{32}P, the scintillator has to have high density and a high scintillation efficiency. These requirements are met, e.g., by Zn Cd S(Ag) (4.4 g/cm^3 ,efficiency about 50 photons/keV) and $Gd_2 O_2 S(Tb)$ (7,5 g/ cm^3 ,efficiency about 33 photons/keV).

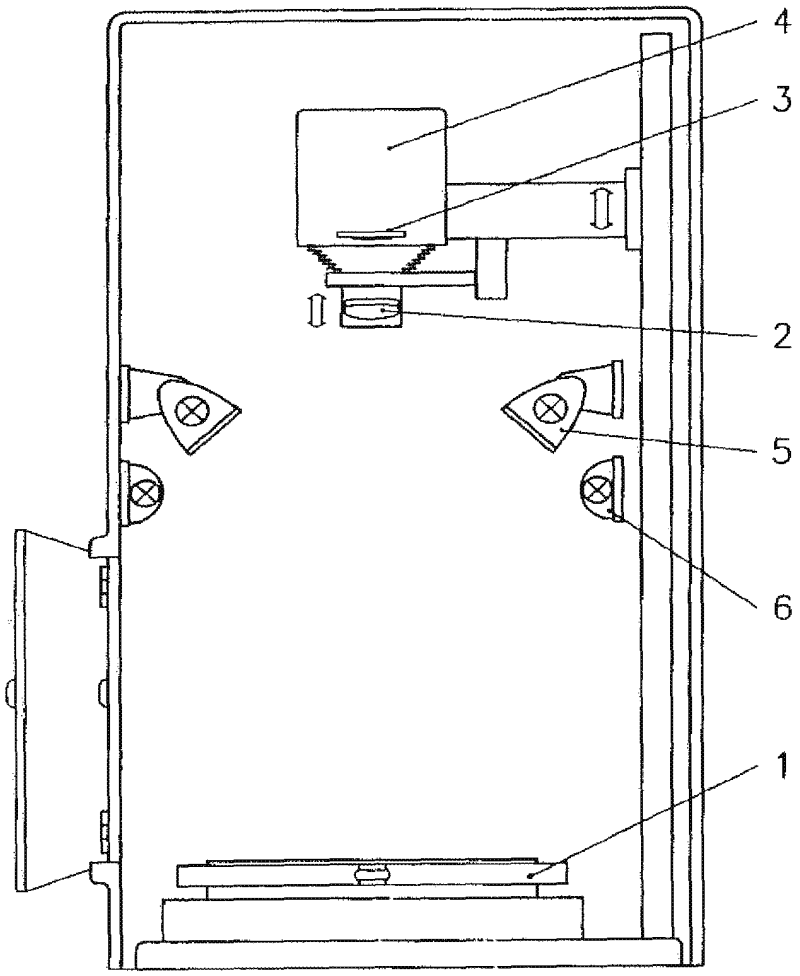


Figure 1. Schematic of a low-level light imager.
1. sample support 2. lens 3. CCD ship 4. fluorescent light source
5. white light source

SPECTRAL_0000538

Results

Sensitivity was determined using the following method:

1. Take a statistically significant number (≧ 20) of background measurements (with all reagents, but zero analyte concentration).
2. Measure a known amount of analyte in the midrange, e.g. 100 to 1000 times above background.
3. Calculate sensitivity using the formula $$S = \frac{A \cdot 3\sigma(BG)}{S(A) - \overline{BG}}$$

where
- S: sensitivity
- A: amount of analyte used for calibration
- S(A): result for measurement of A (in counts, cps, relative light units, or any other unit)
- $\overline{BG}$ mean value for background measurement (same unit as S(A))
- σ standard variation of background measurement

For luminescence imaging, we measured the sensitivity in the Promega luciferase assay system. Sensitivity was determined to be 300 fg luciferase.

For comparison, we determined the sensitivity of the LB 96 P microplate luminometer to be 1.4 fg luciferase using the same method and calculation.

Fig. 2 shows the image for a ^{32}P-labelled southern blot measured with a Gd_2O_2S(Tb) scintillator at 2 min exposure time. The weakest spot in this sample contained about 2500 dpm of ^{32}P. The same sample measured with a multi-wire proportional chamber and a phospor imager showed very similar results.

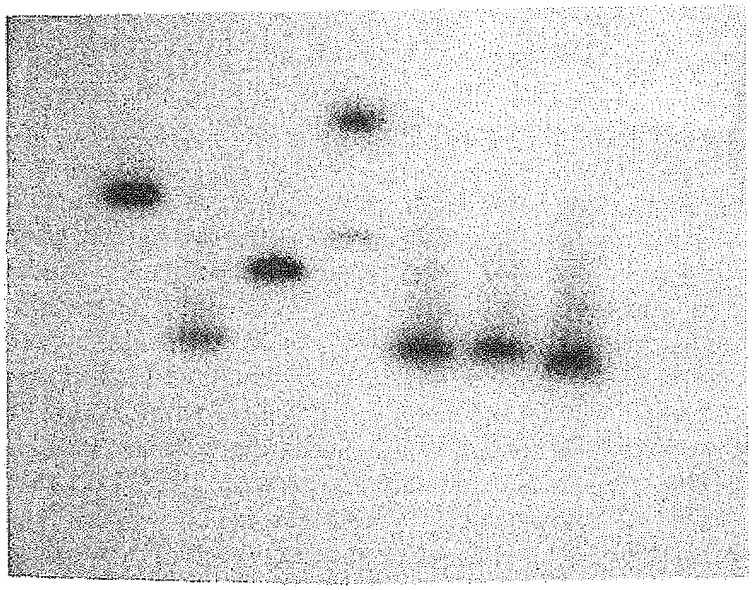


Figure 2. Image of a southern blot, ^{32}P labelled, with Gd_2O_2S(Tb) scintillator

SPECTRAL_0000539

Discussion:

Since the multi-lable imager is designed around low level light measuring technology, it is optimized for BCL imaging. For fluorescence, less sensitive detectors could be used.

While the sensitivity for microplate evaluation is high, this should be considered as an optional, and not the principle use for an imaging system. Contrary to a microplate luminometer, imaging systems allow measurement of glow kinetics only. Flash kinetics would require simultaneous reagent dispensing and measurement, which is hardly feasible for an imaging system.

For radioactivity imaging, the sensitivity is surprisingly high, in view of the fact that less than only one in thousand photons emitted can reach the detector. We expect, that with further development, this could become a routine method for imaging of high energy beta particles.

References

1. Jones, P.L., Greenfield, I.M., Hooper, C.E., Ansorge R., and Stanley, M.A. (1991). Quantification of Levels of Mutant RAS Protein in Keratinocytes Transfected with Activated RAS Oncogenes. In „Bioluminescence & Chemiluminescence: Current Status" (P. Stanley and L. Kricka, eds.), John Wiley and Sons Ltd., Chicester, 175-178.
2. Hooper, C.E. and Ansorge, R.E. (1991. Quantitative Photon Imaging in the Life Sciences Using Intensified CCD Cameras. In „Bioluminescence & Chemiluminescence: Current Status" (P. Stanley and L. Kricka eds.), John Wiley and Sons Ltd., Chicester, 337-344.
3. Bräuer, R., Lübbe, B., Ochs, R., Helma, H., and Hoffmann, J. (1993). Measuring Luminescence with a Low Light-Level Imaging System Using Electronic Light Standards. In „Bioluminescence & Chemiluminescence: Current Status" (P. Stanley and L. Kricka, eds.), John Wiley and Sons Ltd., Chicester, 13-17.
4. Ansorge, R.E., Hooper, C.E., Neale, W.W., and Rushbrooke, J.G. (1991). Recent Developments in Low Light-Level Imaging System. In „Bioluminescence & Chemiluminescence: Current Status" (P. Stanley and L. Kricka, eds.), John Wiley and Sons Ltd., Chicester, 349-352.
5. Wick, R.A., Iglesias, G., and Oshiro, M. (1993). A comparison of Cooled CCD and Intensified CCD Detectors for Luminescence Imaging. In „Bioluminescence & Chemiluminescence: Current Status" (P. Stanley and L. Kricka, eds.), John Wiley and Sons Ltd., Chicester, 47-51.

© 1998 Nature Publishing Group http://www.nature.com/naturemedicine

Bioluminescent indicators in living mammals

PAMELA R. CONTAG[1,2], I. NICK OLOMU[2], DAVID K. STEVENSON[2] & CHRISTOPHER H. CONTAG[2]

[1]*Xenogen Corporation, P.O. Box 9497, Stanford, California 94309-9497, USA*

[2]*Department of Pediatrics, 300 Pasteur Drive, Stanford University School of Medicine, Stanford, California 94305-5119, USA*

Correspondence should be addressed to C.H.C.

e-mail: ccontag@cmgm.stanford.edu

The functional status of electronic devices such as video cassette recorders and televisions can be monitored by observing external indicator lights that have been built into these systems. These diagnostic lights may tell the observer a range of information from "power on" to the overall functional state of the device. A similar approach can now be used in animal models of human development and disease by building into these living systems biological light sources that report externally the inner workings of mammalian biology[1-3].

Background

There are many biological processes that can not be externally monitored with noninvasive imaging modalities such as magnetic resonance imaging (MRI), positron emission tomography (PET) or via x-rays (computerized tomography, CT), because key molecules in these processes are not distinguishable even in the presence of contrast dyes or radioactive tracers. Reporter genes with optical signatures (for example, fluorescence, color or bioluminescence) have been used in cell culture, in small organisms that are relatively transparent (*Drosophila*) or two-dimensional (plant leaves), and in *ex vivo* analyses after expression in larger animals. In such assays reporter genes are linked to genetic regulatory elements and can reveal spatial and temporal information about a variety of biological processes at the level of transcription.

The goal of real-time analysis of biological events in intact living mammals was recently realized in our laboratories[3]. Two key observations lead to the development of this technology. The first observation was that biological sources of light are sufficiently intense such that the light generated within a mammal can be detected externally[3]. The second observation was that substrate, either endogenous (bacterial) or exogenous (insect), could be made available to bioluminescent reporters in living mammals[1-3].

We have employed sensitive detection devices to visualize and quantify bioluminescent light by detecting photons that are transmitted through mammalian tissue from internal sources[3]. Several technical advances for imaging weak visible light sources using charged coupled device (CCD) cameras have emerged recently and include microchannel plate intensifiers, Peltier or liquid nitrogen cooling of the detector, and a combination where the intensifier, and not the CCD detector, is cooled. The goal of these technologies is to enhance signal-to-noise ratios by either reducing background (cooled) or increasing signal (intensified). These instruments have broad application in science and industry and are available from a variety of commercial sources. A Hamamatsu intensified CCD (ICCD, model C2400-32) has been used for monitoring infection and gene expression in living mammals in our laboratories.

There are many strengths of bioluminescence as a reporter in living animals. Foremost is the inherent low background of bioluminescent markers as compared with fluorescent or colorimetric reporters. This principle alone makes luciferase a superior *in vivo* reporter compared to fluorescent reporters where autofluorescence of tissue results in significant background, and already poor signal-to-noise ratios can further be reduced by photobleaching. Furthermore, the rate of luciferase enzyme turnover in the presence of substrate allows for real-time measurements as this reporter does not accumulate to the extent of other reporters in cells.

Consider, also, the advances made over the long history of luciferase as a reporter in biological systems that have provided much biochemical data on the luciferase enzyme reactions. The biochemistry, nucleic acid sequence and even the predicted three-dimensional structure of bacterial and firefly luciferase enzymes have been revealed through decades of study. Moreover, luciferases have been used widely as biological reporters in cell culture assays designed as correlates of *in vivo* functions, facilitating direct application to animal models. Bioluminescent technologies have advanced to the point where reporters with a range of emission colors are available, as are commercial kits for two-color assays in cell culture (Promega, Madison, WI). Throughout this long history most bioluminescent assays in animal cells have been performed on cell lysates and not in living systems; analyses can be now performed in living cells and animals.

Use of bioluminescence as a real-time reporter in living mammalian cell cultures has been described for assessment of gene expression[4], viral infection[5-7] and interaction between bacterial and mammalian cells (adherence and invasion[3,8]). *Ex vivo* luciferase assays have been used to assess levels of expression of the reporter in mammalian tissues[9,10], and to monitor tumor burden[11] and infection[12].

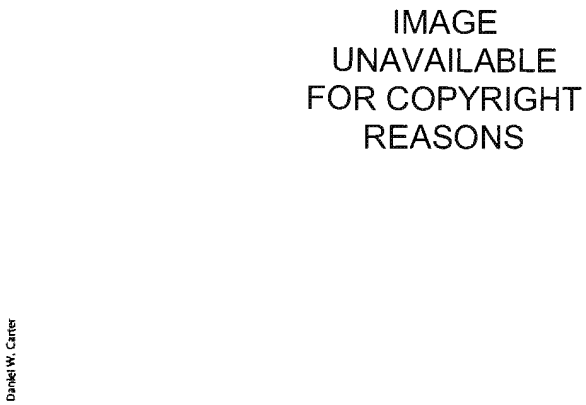
Following the use of bioluminescent assays in living cells, a logical next step in the development of bioluminescent technologies was its use in intact living animal models. This refinement holds great potential for increasing the depth of our understanding of normal physiology and pathophysiology of mammals by providing real-time access to complex processes that only occur in the context of the intact living system, and thus increasing the predictive value of animal models for human biology. Studying processes such as mammalian development, tumor progression and pathogenesis in living animals offers new opportunity for evaluating and developing novel therapeutics for human diseases.

Infectious disease

In vivo monitoring of luciferase was developed initially using a bacterial model in which a bacterial luciferase, and its ac-

SPECTRAL_0000541

© 1998 Nature Publishing Group http://www.nature.com/naturemedicine



Daniel W. Carter

In vivo monitoring of gene expression and infection. A diagrammatic representation of the camera set-up (left), and examples of actual data (right) are shown. A photographic lens (Nikkor 50 mm, f 1.2; Nikon, Japan) focuses light from the animal subject into the ICCD camera. Although light is emitted in 360°, only the light emitted from the animal that reaches the lens is diagrammed. Since the animal subject is in a light-tight box, grayscale reference images of subjects are generated with the door to the box slightly open in low room light. The door is closed and the gain on the intensifier turned to maximum for detection of the bioluminescent signal, which is presented as a pseudocolor image representing light intensity (red most and blue least intense). This pseudoimage is superimposed on the reference image for orientation. ***a***, External monitoring of bacterial pneumonia using *Salmonella* labeled with constitutive expression of the *P. luminescens lux* operon is demonstrated. Note the heart shadow in this image. For panels *b–d*, a Tg mouse in which the transgene consists of a portion of the HIV LTR fused to the coding sequences of firefly luciferase[13] was used to demonstrate that gene expression could be externally monitored[1]. ***b***, The viral promoter can be activated by the chemical DMSO and a Tg mouse where expression of the transgene is activated over half the skin surface with topical application of 100% DMSO is shown. ***c***, Optimization of transdermal substrate delivery is shown using the Tg mouse where expression was activated over the entire surface of the back (shaved previously) and concentrations of luciferin in DMSO (12.5–200 mM) were spotted in quadruplicate. Peak light emission was observed with 100 mM luciferin. ***d***, Developmental expression of the HIV LTR in neonatal LTR-*luc* Tg mouse where increased levels of luciferase expression can be observed in the eye, a reference image is not shown in this panel. For imaging, mice were anesthetized with Nembutal (50–70 mg/kg body weight), and integration times of five minutes were typically used. Although integration times for monitoring bacterial infections have ranged from one second to 30 min in our laboratory, 5–10 min are typically used for gene expression studies where the dynamic range of light emission is less. All animals were handled under the strict institutional guidelines in the Department of Comparative Medicine at Stanford University.

cessory genes encoding the enzymes for substrate biosynthesis from *Photorhabdus luminescens*, were expressed constitutively in *Salmonella typhimurium*[3]. These light-emitting bacteria were then used to infect susceptible strains of mice and the bioluminescent light transmitted through the mouse tissues was imaged externally using an ICCD camera. Temporal analyses were performed following intraperitoneal and oral inoculations and the effect of antibiotic therapy on systemic disease was monitored. These studies revealed that low levels of bioluminescent light, emitted internally, could be detected externally. Thus, infection and the reduction of bacterial load following antibiotic therapy could be monitored in living mice.

A significant advantage to this approach is the ability to integrate *in vitro* and *in vivo* assays using luciferase as a reporter, which allows for a more cohesive experimental design. For example, in our initial infectious disease model, gastrointestinal infections by *S. typhimurium*, the *in vitro* assay for minimum inhibitory concentration (MIC) of antibiotic effective against these strains, and the epithelial entry assay in cell culture were performed with the same labeled strains as were administered to mice and detected *in vivo*. Other models for infectious disease are under development in our laboratories, including a pneumonia model (see Fig., panel *a*). In these studies neonatal mice are acutely susceptible to Gram-negative infections and succumb to *Salmonella* infections occurring at unique tissue sites compared to adults.

There are many *in vivo* models for determining the efficacy of antibiotics each quantifying bacterial growth at a different anatomical site in mice, rats or rabbits with *ex vivo* bacterial counting. Achieving statistical significance is possible only with the data from relatively large groups of animals. The predictive value of these models may be limited since an overview of the disease process in the entire animal is not always feasible. The sensitivity of photon counting through a living animal allows for initial or early quantitation of the signal from the pathogen; this signal can be followed over time in the same animal improving statistical analysis. In addition, specific bacterial genomic targets can be labeled with light, and response to target-directed drugs may be monitored throughout therapy and after the removal of the drug from the system.

Gene expression

Expression from a regulated viral promoter was monitored both in cell culture and as a transgene (Tg) in intact animals using the same reporter gene construct (panels *b–d*). Transactivation of the promoter from HIV by the viral protein Tat was demonstrated in living cells using luciferase as the reporter[1,7]. As *in vitro*, the HIV promoter (located in the long terminal repeat, LTR) can be induced specifically in selected regions *in vivo* with the chemical dimethyl sulfoxide (DMSO, panel *b*). The optimal concentration of substrate for transdermal delivery could be determined in the LTR-*luc* Tg mouse (panel *c*). Although the LTR-*luc* Tg mouse is not an ideal model for HIV replication or pathogenesis, due to a variety of reasons linked to the observation that HIV does not replicate in murine

SPECTRAL_0000542

© 1998 Nature Publishing Group http://www.nature.com/naturemedicine

cells, we have used this model to demonstrate the ability to monitor control of gene expression in living animals. In addition, developmental regulation of the HIV LTR was demonstrated in this Tg system when luciferase expression was monitored in neonatal Tg mice at various ages. This demonstrates that developmental gene expression can be monitored in living animals and that viral promoters can be used to probe transcription in development (panel *d*).

Discussion

Noninvasive monitoring of light emitted from within a living mammal, where the light is constitutively expressed or reporting gene expression, provides an opportunity for obtaining more specific information about physiological processes and whole biological systems in less time, using fewer animals. This is especially relevant to the costly processes of drug discovery where significant advances have been made in generating large numbers of potentially useful compounds (for example, combinatorial chemistries, genomics and high-throughput screening). In the absence of significant advances in *in vivo* analyses, the bottleneck in drug development at the animal model step has been accentuated. *In vivo* luciferase monitoring can address this limitation and has applications in infectious disease (viral, bacterial and fungal), oncology, gene therapy, development, and many other areas in which animal models are used as predictors for the human response to therapy.

Acknowledgments

We thank Hamamatsu for use of the photonic detection system in this study and John Morrey (Utah State) for the transgenic mouse line (LTR-luc) and many helpful discussions. This work was funded in part through grants from the California Universitywide AIDS Research Program, Stanford Office of Technology Licensing, ONR contract N-00014-94-1024, NIH RR00070 and unrestricted research funds from the Baxter Foundation and the Mary L. Johnson Fund.

1. Contag, C., *et al.* Visualizing gene expression in living mammals using a bioluminescent reporter. *Photochem. Photobiol.* **66**, 523–531 (1997).
2. Contag, C.H., Contag, P.R., Spilman, S.D., Stevenson, D.K. & Benaron, D.A. Photonic monitoring of infectious disease and gene regulation. in *OSA TOPS on Biomedical Optical Spectroscopy and Diagnostics.* (eds. Sevick-Muraca, E. & Benaron, D.) 220–224 (Optical Society of America, Washington, DC, 1996).
3. Contag, C.H., *et al.* Photonic detection of bacterial pathogens in a living host. *Molec. Micro.* **18**, 593–603 (1995).
4. Thompson, E.M., Adenot, P., Tsuji, F.I. & Renard, J.P. Real-time imaging of transcriptional activity in live mouse preimplantation embryos using a secreted luciferase. *Proc. Natl. Acad. Sci. USA* **92**, 1317–1321 (1995).
5. Hooper, C.E., Ansorge, R.E. & Rushbrooke, J.G. Low-light imaging technology in the life sciences. *J. Biolumin. Chemilumin.* **9**, 113–122 (1994).
6. Hooper, C.E., Ansorge, R.E., Browne, H.M. & Tomkins, P. CCD imaging of luciferase gene expression in single mammalian cells. *J. Biolumin. Chemilumin.* **5**, 123–130 (1990).
7. White, M.R.H., *et al.* Real-time analysis of the transcriptional regulation of HIV and hCMV promoters in single mammalian cells. *J. Cell Sci.* **108**, 441–455 (1995).
8. Petterson, J., *et al.* Modulation of virulence factor expression by pathogen target cell contact. *Science* **273**, 1231–1233 (1996).
9. Morrey, J.D., Bourn, S.M., Bunch, T.D., Sidwell, R.W. & Rosen, C.A. HIV-1 LTR activation model: Evaluation of various agents in skin of transgenic mice. *J. Acquir. Immune Defic. Syndr.* **5**, 1195–1203 (1992).
10. Morrey, J.D., *et al. In vivo* activation of human immunodeficiency virus type 1 long terminal repeat by UV type A (UV-A) light plus psoralen and UV-B light in the skin of transgenic mice. *J. Virol.* **65**, 5045–5051 (1991).
11. Zhang, L., Hellstrom, K.E. & Chen, L. Luciferase activity as a marker of tumor burden and as an indicator of tumor response to antineoplastic therapy *in vivo*. *Clin. Exp. Metastasis* **12**, 87–92 (1994).
12. Hickey, M.J., *et al.* Luciferase *in vivo* expression technology: Use of recombinant mycobacterial reporter strains to evaluate antimycobacterial activity in mice. *Antimicrob. Agents Chemother.* **40**, 400–407 (1996).
13. Morrey, J.D., Bourn, S.M., Morris, J.L., Bunch, T.D. & Sidwell, R.W. Activation of the human immunodeficiency virus long terminal repeat by abrasion of the skin in transgenic mice. *Intervirology* **37**, 315–320 (1994).

ON THE MARKET

GOING "GREEN"



Naiad Technologies offers two new ways to cut the cost of disposal of hazardous wastes.

Naiad Technologies has introduced two new product solutions that are designed to reduce the cost of disposal of hazardous wastes in labs: SolvCycle, a safe and inexpensive method for recycling alcohol solvents, such as those used in cytology and histology, and FluorAway, which works on a similar principle and is intended for removing toxic fluorescent dyes out of aqueous solutions. At the heart of these **alcohol solvent recycling and fluorescent dye removal systems** is the company's filtration technology, consisting of a benchtop system about the size of a drip coffee pot, along with replaceable filter cartridges containing proprietary slurries to which specific materials bind as liquid wastes or solvents pass through. Naiad Technologies' first product, RadAway, uses this technology to remove radioactive molecules from liquid wastes, condensing the waste volume some 20 to 30 times into an easily disposable solid.

Reader Service No. 84
Tel. (+1) 503-274-4407
Fax (+1) 503-241-0827

REAGENT ROUND-UP

In addition to the mainstays X-gal, X-gluc, MUG and PNP-glucuronide, Glycosynth produces a series of **enzyme substrates** for a host of applications. New compounds are added regularly to the list—many of them designed to address specific needs. Indeed, Glycosynth says that it welcomes inquiries for constructing custom-built enzyme substrates, of which Rose-gal (6-chloro-3-indolyl β-D-galactopyranoside) is an example. These materials are used not only for routine assays and diagnostic tests but also in trying to identify inherited diseases with a metabolic base and in the development of specific diagnostic tests.

Reader Service No. 85
Tel. (+44) (0) 1925-575075
Fax (+44) (0) 1925-575121

LTK-008 decontamination reagent is your license to kill.



LTK-008 is a new **decontamination reagent** from Racksys that removes contamination caused by DNA, RNA, DNase, RNase, bacteria and phages from work surfaces or laboratory equipment. Surfaces can be decontaminated in 5–10

SPECTRAL_0000543

Rainer Ochs and Enrico Kuhles October 1995

Camera types for Low Level Light Imaging

The image sensor : Tube and solid state cameras -

Different camera designs of individual advantages and disadvantages are available today for the purpose of Low Level Light Imaging. We distinguish camera types with and without an image amplifier. A camera including an image amplifier (intensified camera) provides as a first amplifier stage the tube image amplifier - typically a MCP (multi channel plate) or a cascade of MCP's within a vacuum tube. The output of the MCP is recorded by either a CCD = intensified CCD camera or an intensified tube camera on Vidicon or Saticon principle.

Some of this cameras operate within the Photon Counting Mode. Other cameras integrate the output of the intensifier and read it out analogously. The photocathode converts in average about 20 % of the specimen photons into the electrons required for the amplification.

Cameras without image amplifier record the image directly onto a semiconductor chip = CCD. This chip (sometimes an optimised custom design) provides the individual sensor elements for the desired localisation of the photon event.

The noise of these chips is reduced by cooling, the CCD is cooled by liquid nitrogen or by electrical cooling with a Peltier - element.

The heat transfer from the Peltier element by air convection, forced air stream or water cooling depends on the desired temperature level and its accuracy .

An additional method of noise reduction is provided by the " Slow Scan Camera". As the word explains - the electronic readout (scan) of the pixels inside the CCD is slow - so about 20 microseconds per pixel.

Properties and details of Imaging Amplifiers

A photocathode converts the photon in an electron - this electron is amplified within the MCP and projected onto a screen, re-converting these multiplied electrons into photons .

A variety of different cathode material = the photocathodes light sensitive layer enables an optimum wavelength matching of such systems. The typical quantum efficiency between 400 and 600 nanometer is for a typical photocathode is about 20 % in the maximum - with other words maximal 20 photons out of 100 photons can be recognized (= converted into an electron) by the cathode.

The MCP (or cascade of MCP's) is the intensifier . The intensifier consists of vacuum sealed body incorporating input and output window on either side of the MCP. Images are focused onto the input window = photocathode which releases electrons in proportion to the amount of light falling upon it. A voltage applied to these electrons forces them into the narrow acceleration / amplification channels (some million channels) of the MCP . The secondary

electrons collide with the channel wall surfaces and dislodge additional secondary electrons - this process provides the electron amplification = multiplication.

The electrons are once more accelerated as they leave the MCP and then strike a phosphor screen on the inner surface of the output window to generate a visible image. A camera is focused then to this intensified image on the output window by fiber optics or a relay lens.

For higher amplification, MCPs can be cascaded to several stages. Unfortunately (or normal in real physics) - the resolution of the image is inversely proportional to the amplification stages - more amplification means less spatial resolution.

The advantage of the high sensitivity is paid by the lower resolution. Mathematical photon counting algorithms allow a post recording resolution enhancement - at the cost of significant sensitivity loss besides of a huge computation work.

Photon Counting

Photon counting cameras use a double or triple stage intensifier to drive every photon event to saturation at the output screen. The Signal then is scanned with a TV camera and the image is binarized with a threshold. Then the binarized images are accumulated in memory, eventually forming a grey image out of the statistics.

Although the name implies that you can see single photons, to form up an image with some grey resolution, a great amount of events is needed to create a recognisable image. Photon counting is a method to reach very high sensitivity.

Cooled CCD Slow Scan Cameras

Cooled , integrating **CCD = Charge Coupled Devices** cameras can be used for long time integration / exposure periods to provide good images from low light specimens.

The technology is simple : the light falls directly onto an array of light sensitive elements which collect and accumulate the charges generated by the light. The readout = scan directs the charge of each pixel (pixel by pixel) to an amplifier.

The quantum efficiency of CCD's is remarkably high - so about 40% in the red range falling to 10 % in the blue range . The absence of a photocathode allows no customised wavelength shifting - but with a special fourecence coating, sensitivity is high even at the blue end.

Long integration time for the detection of less then one photon / second / pixel is required. Dark currents, fixed pattern noise and charge carrier fluctuations inside the CCD are drastically reduced and stabilised by active cooling at a fixed temperature to minimise noise during long exposures.

Chip temperature is one of the most important criterias for the sensitivity you get. Cooling down with liquid nitrogen produces best results, but this technique is inconvenient and expensive. The more comfortable way to cool is by multi-stage peltier elements. Sometimes, the produced heat must be removed by a water precooler, some cameras give the heat direct to the air. For good results, a minimum of -70°C must be reached, otherwise the background is too high for highest sensitivity.

The CCD is fixed into a hermetically sealed container, usually evacuated to minimise the temperature drain and to overcome condensation problems- one reason for the relatively high cost of such CCD.

Readout of the sensor chip creates noise which is dependent on the bandwidth of the readout process (typically 500kHz or less) therefore the readout speed is reduced for a better signal/noise ratio but live display is hardly possible . Only pseudo live transfer rates of up to 2 images of limited size per second can be sent to the computer.

BINNING sums groups of pixels to get higher sensitivity for decreasing the integration time at the cost of decreased spatial resolution. The binning is sometimes software selectable. Rule of the thumb: the reduction of resolution by factor 3 enhances the sensitivity by about factor 10.

Sub-array scanning defines a subsection of the image as a region of interest. This mode may enable a quasi-live display of i.e. one living cell.

Resolution, contrast and dynamic range of CCD's is superior to the Image Amplifiers whilst the total sensitivity at full resolution is (depending on the wavelength recorded) approximately equal to the image intensifier. Comparing the CCD at lower resolution - equal to the image intensifiers properties - then the CCD is more sensitive. The resolution of Photon Counting Systems (without center of gravity operation) equals the CCD at 10x10 pixel binning. In this resolution, the CCD is even more sensitive than photon counting systems !

A special effect of these chips are simulated light events created by cosmic radiation or by radioactive decays inside of the chip-sensor material in absence of light. High intensities qualify these events for elimination by appropriate, intelligent discriminating software.

Why we have chosen a cooled CCD for our new instrument:

The new Luminograph includes the state of the art technology of solid state detector instead of the one step image amplifier with an adapted high sensitivity Saticon Tube system of the former Model LB 980.

- The first advantage is the extraordinary image quality. In full resolution mode, the camera creates images in superb quality, much better than Intensifier Systems can do. Thereby both the spatial resolution and the grey resolution with 15 bit real grey values are excellent. Photon Counting Systems create their grey shades on a statistical basis as a superposition of binary images. This does not give a good grey resolution. The spatial resolution of Photon-Counting Systems is limited by the MCP-Stages, which is much less than what comes out of a CCD. In Photon Counting Mode, the resolution is comparable with that of the CCD with 10x10 pixels binning.
- The second advantage is the high sensitivity. Both the high quantum efficiency and the large pixel area give the CCD highest sensitivity. When binning together pixels, with a matrix of about 5x5 pixels, the sensitivity of photon counting system is met, but allows a much better image quality, because resolution is better and noise is lower. Because of the statistical characteristic of photon counting, there is high noise with a big grain, so you have to integrate considerably long to have a secure contrast from the background. With the CCD the background noise is low, so signals can easily determined. With higher binning rates, the sensitivity can be expanded even beyond the range of photon counting systems, or exposure times can be reduced to get faster operation.
- To combine that, you can exchange sensitivity for resolution and vice versa. So you have always the best images that are possible with that amount of light your sample gives. So you can have a extremely sharp illuminated image, that will be superexposed with a luminescence signal, that is taken with lower resolution at highest sensitivity. As

sensitivity is controlled by the exposure time, the camera can be used from dim room light to lowest light levels. So the flexibility of the CCD allows the use in various applications and always shows it's best side.

- The third advantage of this approach is the virtually indestructible quality of this system. There are no wearing out parts, as image intensifiers and cameras tube, so lifetime is extremely long. The camera is robust in operation, there are no memory effects or danger of destruction by too much light, as with intensifiers, that are very sensitive to over-illumination.
- For quantitation of results, the CCD shows maximum linearity and uniformity. Over the full 15-bit range, the response is strictly linear, the response is uniform over the whole image area.

The New Luminograph LB 981

Employing a CCD camera with a unique cooling system (four stage peltier element), that stabilises the CCD on 200K (-73°C) up to an ambient temperature of 35°C. The produced heat (only 10W!) is given off to the air, so no further cooling equipment is needed. At this temperature, the thermal dark current is negligible and the background is very low.

The Camera chip is hermetically sealed in a high vacuum container and is cooled down to the working temperature within 15 minutes at normal room temperature.

The integral sensitivity is improved, compared to the LB 980 and the resolution is increased to 578 x 384 pixels.

The camera head is small and light weight - the ideal candidate for microscopic applications - very easy mounting / fixing to a microscope.

The camera head is mounted inside of the LB 981 system onto a motor driven, computer controlled spindle , enabling a stepless focusing of specimens sizes from 30mm to 300 mm side length by one and the same objective only ! The objective is motor controlled as well and the software focuses automatically for brilliant results.

The software :

A powerful, easy to use software operating now under Windows™ will satisfy also the very critical and experienced customer type.

All camera parameters are controlled by this software, all special software was especially optimised for the Low Level Light Detection. Many subroutines as noise reduction , cosmics elimination and auto brightness scaling - run automatically in the background ; the user may decide about additional info as overlay between Luminescence signal and optical image or activate a Multi fluorescence color image.

The backbone of the software is a commercial Imaging software - but the entire user interface is written in the form of special application macro languages - thus keeping the door always open for additional, custom specific modification / implementation within a short time for reasonable cost.

An inexperienced operator without specific background in digital image processing (typically not such an easy task) can handle this system after minutes of basic introduction only.

Imaging on the Microscope

The Camera Head of the new LB981 is small and lightweight, so it easily can be mounted to the microscope with a C-Mount adapter.

The System is available as a microscope camera, or mounted in the dark box for macroscopic imaging. Taking the camera out and on the microscope is done in a few seconds, so with the dark box, both applications can be satisfied side by side.

Fluorescent imaging is not difficult, because here usually is plenty of light. The Camera is used in its highest resolution and produces brilliant high dynamic images in few seconds. Fluorescent Illumination and filtering is done by the microscope, only make sure, that you use the best filters for the applied dye to receive the maximum sensitivity possible.

If you are looking to living cells or have dyes that are sensitive to bleaching, the high sensitivity of the camera is useful, because you are able to dim the exitation light to a very faint illumination that does not bleach the samples.

Luminescence Imaging is much more challenging, because here we are at the physical limits. This is, because the amount of light available, decreases with the square of the magnification. If you are looking to a luminescenting cell culture with the macroscopic lens, one pixel will catch the light of hundreds and thousands of cells. If you are now looking through the microscope and are looking to one or several cells only, the light of one cell will be spreaded over many many pixels - resulting in very low light.

To form an image, even in an ideal camera, a lot of photons are needed. If you want to have only a contrast ratio of 10 (what is not very much, the system allows for contrast ratios up to 30000) a bright area of 100 x 100 pixels is composed of 100 thousand registrated photons. According to the quantum efficiency of the sensor, only 10 to 40% of the photons are registrated, so the 2.5 to 10fold of photons must reach the detector, depending on the wavelength.

But only a small portion of light that is emitted by the sample will reach the target. This is a result of optical principles: only a part of the room angle, that is radiated by the sample will be seen by the microscope lens. In the best condition, the camera sensor is placed directly behind the lens, without additional mirrors, prisms and lenses. If the beam path within the microscope is longer, considerable light is lost. This light loss can be magnitudes of 10.

But not to discourage you, it can be done. But not only the camera, the whole system of camera, microscope and chemistry must be optimised to get best results:

- Use the best microscope you can get. We made good experience with the Zeiss Axiovert 100TV. The camera is mounted trough a hole in the table and placed directly behind the lens.
- Use lenses with as much aperture as you can get. The highest aperture have immersion lenses. These use a drop of immersion oil or water between objective and sample carrier. From optical reasons, this allows for much better aperture - immersion lenses bring a Factor of 5 more light to the sensor. From Zeiss, for Example the Neofluar x40 1.3 is an excellent lens.
- Optimise your chemistry to get as much light as possible. Optimise the concentration of luminescence substrate, have the temperature right for good reactions, use cell clones with high efficiency. If you have the choice, with the CCD camera it is also helpful to use reactions that emit a longer wavelength. (Between 450 and 680 is a slope from 10% to 40% efficiency, more in the blue, 10% are constant, more in the red the efficiency slowly drops again).

Now you have all done to bring as much light to the sensor as possible. Depending on the amount of light, you have to wait until the needed number of photons will have arrived. The amount of light needed however, depends on the resolution. If for example, at full resolution, a 100 x 100 area will need about 1Million photons, at pixel binning of 5x5, only the 25th part of that 40,000 are needed, because now the number of pixels is reduced by that factor (the pixel are getting larger).

So with resolution and time, you can find a combination, where you can see your sample as good as possible. Binning factors up to 20 x 20 are usable, and the time can go up to an hour. For even longer expositions (if the sample remains stable) long time accumulation allows unlimited time.

CCD Image Acquisition Tutorial

Gatan, Inc.

5933 Coronado Lane,
Pleasanton,
CA 94588

Tel: (925) 463-0200
Fax: (925) 463-0204

May 2001

SPECTRAL_0000550

1. Introduction

This document will guide users of Gatan CCD camera through the process of viewing, acquiring and saving images.

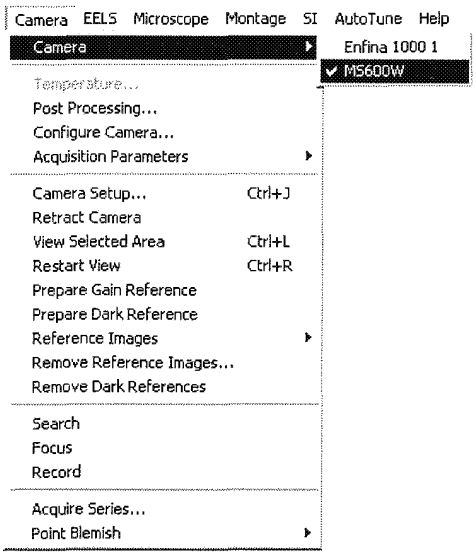
2. Hardware

The procedures in this document are applicable to all Gatan CCD camera (DualVision, MultiScan, UltraScan and GIF MSC).

3. Image Acquisition

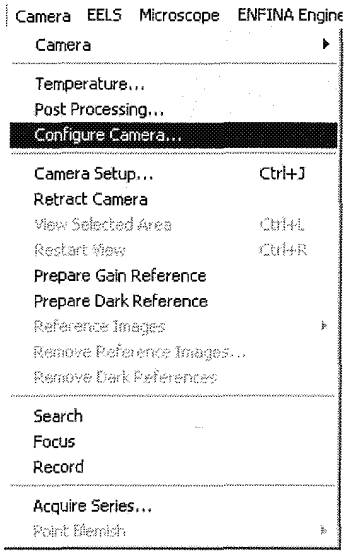
3.1. Camera configuration

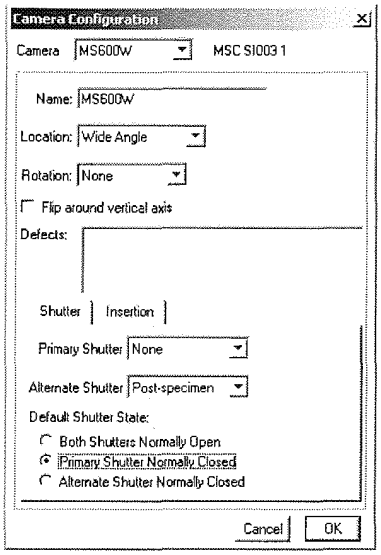
First, it is necessary to select the CCD camera that you will use to acquire images. Select Camera and a list of available cameras will be displayed, as shown below. Select the camera that you wish to configure from the list. The example below shows the Multiscan 600W camera selected.



SPECTRAL_0000551

The next step is to configure the CCD camera. This process is shown in the following figures.





In the Camera configuration dialog box, you can change the name of the camera by typing in the **Name** field. Image rotation can be specified in the Rotation pull-down menu. The coordinates for column defect correction are entered in the **Defects** field. It is very important to specify the **Primary** and **Alternate** (if there is one set up) shutter available to the camera. Finally you should specify the shutter status, i.e. the state of the shutter when the CCD camera is not acquiring any images. "Shutter Normally Closed" is the default setting.

3.2. Prepare dark reference image

This section only applies to DualVision 600 CCD camera which do not have a TEM shutter control. The DualVision 600 camera is shutterless. Since CCD dark current depends upon the temperature, CCD must reach its set target temperature before acquiring the dark reference image.

Before starting the preparation procedure, lower the TEM viewing screen (make sure no electron beam illuminates the CCD sensor during the procedure). Under the **Camera** menu, choose **Prepare Dark Reference** and follow the screen instructions.

3.3. Prepare gain reference image

It is important to prepare a new gain reference image after the CCD has reached the equilibrium temperature (normally this takes about 1-2 hours). The gain reference image should be checked daily.

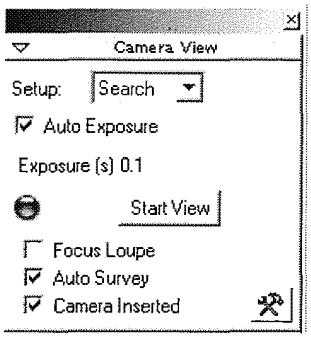
To prepare gain reference image, remove specimen from the field of view, evenly spread the illumination across the CCD sensor; for wide angle CCD cameras, this could mean that the illumination is evenly spread across the entire viewing screen in the TEM.

Under the **Camera** menu, choose **Prepare Gain Reference**. Set the target intensity to the value of about half the dynamic range. For example, for 14-bit cameras, set the value

to 8000 and 12-bit camera to 2500. Normally it is sufficient to set the frames to average to 4. Then simply follow the instructions on the screen.

3.4. View

The view mode allows user to observe **Live** (continuous) images on the monitor. Its control palette is shown below. The setup has two operation modes which are preset for easy use. The **Search** mode displays a continuous (low resolution) image with the entire CCD field of view. This is to allow the user to quickly conduct a sample search using the CCD camera. The **Focus** mode displays a continuous image at higher resolution than the **Search** image. Fine adjustment of focus setting can be done with this operation mode.

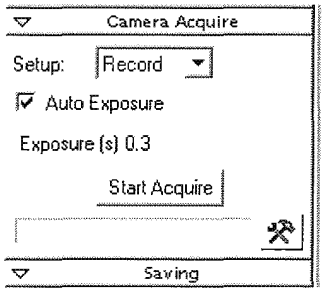


To increase the image update speed on the monitor, click on the **Focus Loupe**. This allows user to focus image by using a small image area with high speed. The **Auto Survey** updates the image display in real time.

Auto Exposure is enabled and disabled by clicking on the **Auto Exposure** selection box. Similarly the CCD camera is **Inserted or Retracted** with a simple mouse click.

3.5. Record

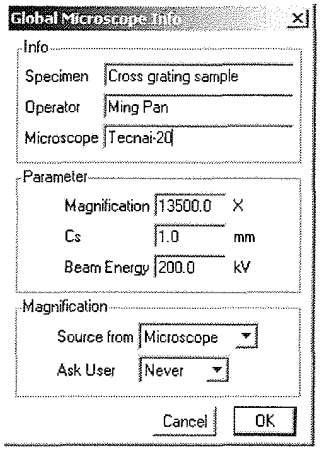
To record the final image, click on the **Start Acquire** button in the Acquire palette (shown below). This mode is preset to acquire a full resolution CCD image. **Auto Exposure** optimizes the CCD exposure to ensure the final image quality.



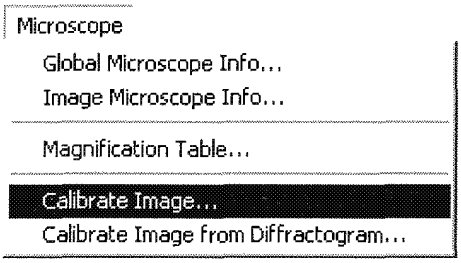
4. Magnification calibration

Since the CCD camera is at different plane in the electron beam path from the TEM photographic film, the magnification displayed on the TEM console does not represent the actual magnification on the CCD sensor. Hence calibration is necessary.

It is very important to make sure DigitalMicrograph software correctly reads the TEM magnification. If there is communication between the computer and the TEM, the magnification is read automatically. If there is no communication, please make sure DigitalMicrograph is set to prompt the user to enter a value for magnification every time an image is to be acquired. This can be set by choosing **Global Microscope Info...** under the **Microscope** menu.



For low magnifications, the user can utilize a standard calibration sample such as a "cross grating" sample which contains periodic lines with a spacing of 0.463 μm. Record a full frame CCD image by clicking the **Start Acquire** button. Under the **Microscope** menu, choose **Calibrate Image....** Follow the instructions on screen. Choose **Yes** when prompted by "Calibrate parent device based on this image?".

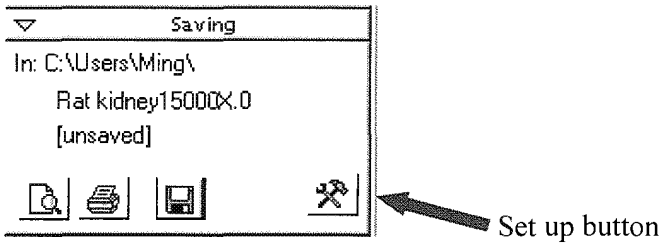


For high magnification, magnification calibration is best carried out by using high resolution lattice images such as graphitized carbon (d = 0.34nm) or gold crystals (d-(111) = 0.23nm).

Once an image with crystalline lattice fringes is acquired, choose **Calibrate Image from Diffractogram**. Then follow the instructions on screen.

5. Save

The recorded images are displayed on the monitor. The button with a floppy disk icon is used for saving images. Images can be easily saved in any user specified directory with a common root name. The **Saving** palette is shown below.

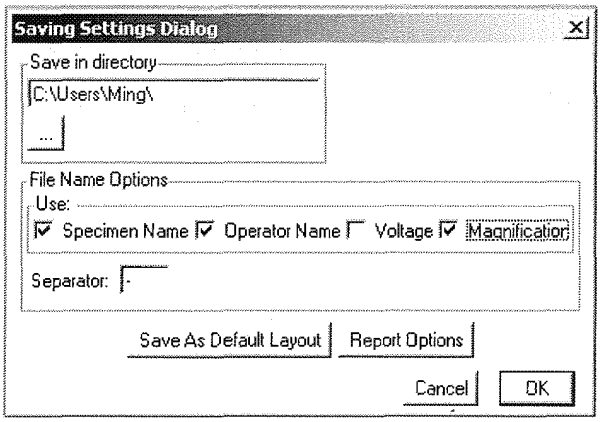


SPECTRAL_0000554

5.1 Choosing directory

Click on the **Set up** button (the one with tools). The **Set up** dialog box will be displayed.

In the **Save in directory,** click on the **Browse** button (the one with dots). Select or create a directory for saving images.

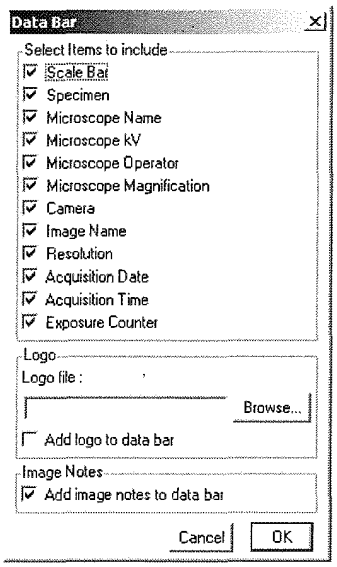


5.2 Construct image file name

In the **File Name Options,** specify the way you want the image file name to be constructed.

5.3 Report Options

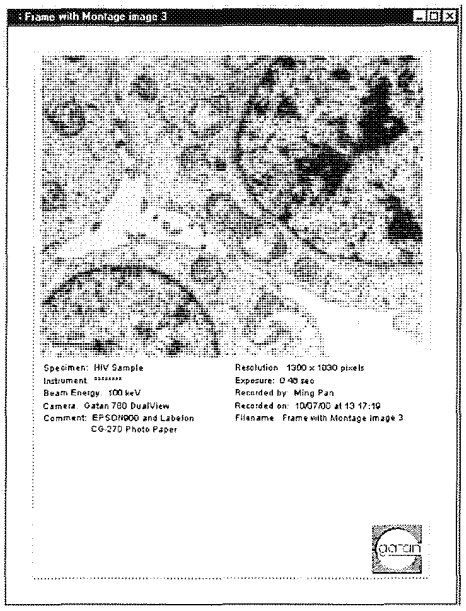
Click on the **Report Options** button to view the following dialog box. You can choose to have any parameters listed to be included in your report. You can also add a logo file and image notes to the report.



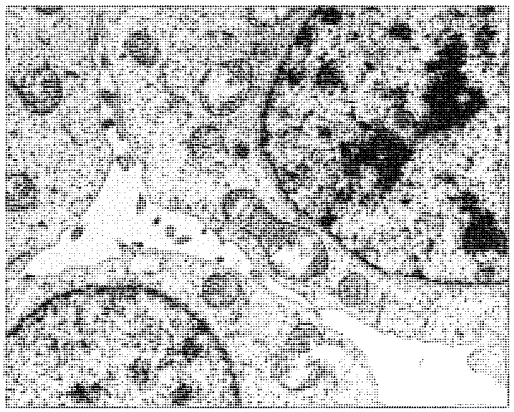
SPECTRAL_0000555

5.4 Report

The report button (the one with a page and a magnifier on the Save palette) will toggle between image view and report view. In the report view, an image is displayed of the print preview mode with parameters as specified in the **Report Options**. Click on the printer icon and the report will print out on your selected printer.



(Report view)

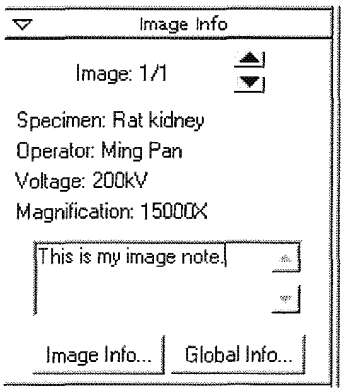


(Image view)

Users can customize the layout and selection of parameters on the page and save the setting as a report template. This is done by click the **Save As Default Layout** button in the **Save setup** dialog.

5.5 Image Notes

The user can type in notes in the **Image Note** window (shown below). Saving an image will automatically save the image notes with the image file. The **Up/down arrows** allow user to browse through the images saved in a session.



SPECTRAL_0000556

5.6 TEM Session Information (Global Info)

Before acquiring any images, it is recommended to enter the correct information about the sample, operator, TEM name, etc. Click on the **Global Info** button (shown above). The global information is saved automatically with every image that is acquired.

6 Quick Reference

The steps necessary for operating Gatan CCD camera are summarized here.

1. Check the TEM session information by clicking on the **Global Info** button on **Image Save** palette.
2. Prepare dark reference image. (For DualVision 600 CCD camera only)
3. Prepare gain reference image.
4. Click on "**Start View**" on the **View** palette to position sample area of interest. Enable **Auto Exposure.**
5. Click on **Focus Loupe** to check the final focus. Make sure **Auto Survey** is checked.
6. Click on **Start Acquire** button in the **Image Acquire** palette. Enable **Auto Exposure.**
7. Calibrate magnification (optional).
8. Click on **Report View** button to view image in print preview mode.
9. Click on **Save** button to save image in the designated folder.
10. Click on **Print**button to send image to printer.

Electronic Acknowledgement Receipt

EFS ID:	11391952
Application Number:	13222688
International Application Number:	
Confirmation Number:	5910
Title of Invention:	EXCITATION LIGHT SOURCE ASSEMBLY
First Named Inventor/Applicant Name:	Michael B. Nelson
Customer Number:	27104
Filer:	Bruce E. Dahl/Cynthia Sullivan
Filer Authorized By:	Bruce E. Dahl
Attorney Docket Number:	SPEC US-4 (027560-0014)
Receipt Date:	11-NOV-2011
Filing Date:	31-AUG-2011
Time Stamp:	17:57:00
Application Type:	Utility under 35 USC 111(a)

Payment information:

Submitted with Payment	no

File Listing:

Document Number	Document Description	File Name	File Size(Bytes)/ Message Digest	Multi Part /.zip	Pages (if appl.)
1	Information Disclosure Statement (IDS) Form (SB08)	SPEC_US-4_IDS-1.pdf	615454 b9a3e92cd8af0ca6284bea0146bc6e1939418482	no	12

Warnings:	
Information:	

2	Foreign Reference	EP0097060A2.pdf	1657702 da410b45662c5e18c138d99bc7a0c01e9e7 c8b2b	no	39
Warnings:					
Information:					
3	Foreign Reference	EP0228877A2.pdf	724201 160c4eaeb1770af127b91f0d59d162184a0 dd79f	no	20
Warnings:					
Information:					
4	Foreign Reference	EP0491131A1.pdf	453907 b116b38a09bd58482791874d5907be5d50 87ea64	no	42
Warnings:					
Information:					
5	Foreign Reference	EP0493707A2.pdf	372843 0bd1415602df7a7645dc1255df617dae597 7deb5	no	6
Warnings:					
Information:					
6	Foreign Reference	EP0718622A2.pdf	824545 b678b7b66bfe152d66563c614b94e9e3e47 04091	no	16
Warnings:					
Information:					
7	Foreign Reference	EP1478423B1.pdf	1327593 4c1b2c7f9c72084b0090de99d05c8178c3b 02d4e	no	24
Warnings:					
Information:					
8	Foreign Reference	EP1478916B1.pdf	2483868 1ab9bae0edcd4874a7c7dc87d4694758741 fdf61	no	50
Warnings:					
Information:					
9	Foreign Reference	WO0049938A1.pdf	907994 d89d27a3b2273777383c5c859b21e4051d 196cdb	no	24
Warnings:					
Information:					
10	Foreign Reference	WO0161324A1.pdf	948172 177eb5a6ae0975dc109202f65c6473fc21a8 1455	no	25
Warnings:					
Information:					

11	Foreign Reference	WO0163247A2.pdf	3004590 736c4dc70a6dd504ee5d7279c6c79875b887bf2e	no	70
Warnings:					
Information:					
12	Foreign Reference	WO9908233A1.pdf	2649791 38a73da0805b3204df084e79a1a9edbf6ba3301ca	no	65
Warnings:					
Information:					
13	Foreign Reference	WO94000742.pdf	563966 4ba48345c9d56c963839c8c704d6ea2be5827dda	no	17
Warnings:					
Information:					
14	Non Patent Literature	Absolute_Calibration_of_Luminometers_with_Low-Level_Light_Standards.pdf	866895 f7167cb7f8e10387fc812728095f564c4fad3c8d	no	10
Warnings:					
Information:					
15	Non Patent Literature	Absolute_Radiometric_Calibration_of_Digital_Imaging_Systems.pdf	324256 e4923b7f0fbdf2168c42a9357e594aa6ecdfa86a	no	9
Warnings:					
Information:					
16	Non Patent Literature	Auaomated_Calibration_of_Zoom_Lens_CCD_Image_System_for_Videogrammetry.pdf	190014 04b134a723e54b5833653c88b0474771b1bfdfa1	no	6
Warnings:					
Information:					
17	Non Patent Literature	Bioluminescence_and_Chemiluminescence.pdf	276348 57bd154578ec4d104de0f09175481af799907339	no	5
Warnings:					
Information:					
18	Non Patent Literature	Biioluminescent_indicators_in_living_mammals.pdf	264175 fa271adc39664f738befae829fe7f85c6a562d93	no	3
Warnings:					
Information:					
19	Non Patent Literature	Camera_types_for_Low_Level_Light_Imaging.pdf	242054 8543a1f6eb6ac9575de5351f48494b1993920439	no	6
Warnings:					
Information:					

20	Non Patent Literature	CCD_Image_Acquisition_Tutorial.pdf	194174 ec40c667df562b7b5ed4a2e6e44db3b2f8b04a2b	no	8
Warnings:					
Information:					
			Total Files Size (in bytes):	18892542	

This Acknowledgement Receipt evidences receipt on the noted date by the USPTO of the indicated documents, characterized by the applicant, and including page counts, where applicable. It serves as evidence of receipt similar to a Post Card, as described in MPEP 503.

New Applications Under 35 U.S.C. 111
If a new application is being filed and the application includes the necessary components for a filing date (see 37 CFR 1.53(b)-(d) and MPEP 506), a Filing Receipt (37 CFR 1.54) will be issued in due course and the date shown on this Acknowledgement Receipt will establish the filing date of the application.

National Stage of an International Application under 35 U.S.C. 371
If a timely submission to enter the national stage of an international application is compliant with the conditions of 35 U.S.C. 371 and other applicable requirements a Form PCT/DO/EO/903 indicating acceptance of the application as a national stage submission under 35 U.S.C. 371 will be issued in addition to the Filing Receipt, in due course.

New International Application Filed with the USPTO as a Receiving Office
If a new international application is being filed and the international application includes the necessary components for an international filing date (see PCT Article 11 and MPEP 1810), a Notification of the International Application Number and of the International Filing Date (Form PCT/RO/105) will be issued in due course, subject to prescriptions concerning national security, and the date shown on this Acknowledgement Receipt will establish the international filing date of the application.

PTO/SB/08a (01-10)
Approved for use through 07/31/2012. OMB 0651-0031
U.S. Patent and Trademark Office; U.S. DEPARTMENT OF COMMERCE
Under the Paperwork Reduction Act of 1995, no persons are required to respond to a collection of information unless it contains a valid OMB control number.

INFORMATION DISCLOSURE STATEMENT BY APPLICANT

(Not for submission under 37 CFR 1.99)

Application Number	13222688
Filing Date	2011-08-31
First Named Inventor	Michael B. Nelson
Art Unit	2828
Examiner Name	Not yet known
Attorney Docket Number	SPEC US-4 (027560.0014)

U.S.PATENTS Remove

Examiner Initial*	Cite No	Patent Number	Kind Code[1]	Issue Date	Name of Patentee or Applicant of cited Document	Pages,Columns,Lines where Relevant Passages or Relevant Figures Appear
	1					

If you wish to add additional U.S. Patent citation information please click the Add button. Add

U.S.PATENT APPLICATION PUBLICATIONS Remove

Examiner Initial*	Cite No	Publication Number	Kind Code[1]	Publication Date	Name of Patentee or Applicant of cited Document	Pages,Columns,Lines where Relevant Passages or Relevant Figures Appear
	1	20010028510	A1	2001-10-11	Ramm et al.	

If you wish to add additional U.S. Published Application citation information please click the Add button. Add

FOREIGN PATENT DOCUMENTS Remove

Examiner Initial*	Cite No	Foreign Document Number[3]	Country Code[2] ¡	Kind Code[4]	Publication Date	Name of Patentee or Applicant of cited Document	Pages,Columns,Lines where Relevant Passages or Relevant Figures Appear	T[5]
	1							☐

If you wish to add additional Foreign Patent Document citation information please click the Add button Add

NON-PATENT LITERATURE DOCUMENTS Remove

Examiner Initials*	Cite No	Include name of the author (in CAPITAL LETTERS), title of the article (when appropriate), title of the item (book, magazine, journal, serial, symposium, catalog, etc), date, pages(s), volume-issue number(s), publisher, city and/or country where published.	T[5]

INFORMATION DISCLOSURE STATEMENT BY APPLICANT (Not for submission under 37 CFR 1.99)		
	Application Number	13222688
	Filing Date	2011-08-31
	First Named Inventor	Michael B. Nelson
	Art Unit	2828
	Examiner Name	Not yet known
	Attorney Docket Number	SPEC US-4 (027560.0014)

	1	HAWORTH, "CCD Image Calibration Using AIP4WIN," http://www.stargazing.net/david, Copyright 2001 David Haworth v. 5.0, pages 1-12.	☐
	2	RODA et al., "Chemiluminescence Imaging Systems for the Analysis of Macrosamples: Microtiter Format, Blot Membrane, and Whole Organs," Methods in Enzymology," Vol. 305, Copyright 2000 by Academic Press, pages 120-132.	☐
	3	STANLEY, "Commercially Available Luminometers and Low-Level Light Imaging Devices," Methods in Enzymology, Vol. 305, Copyright 2000 by Academic Press, pages 96-103.	☐
	4	ROSS et al., "High-speed radiometric imaging with a gated, intensified, digitally-controlled camera[2869-29]," http://ucla.worldcat.org, Proceedings - SPIE the International Society for Optical Engineering, no. 2869, (1996): 386-394, British Library Serials, 2 pages.	☐
	5	RICE et al., "In vivo imaging of light-emitting probes," Journal of Biomedical Optics," Vol. 6, No. 4, October 2001, pages 432-440.	☐
	6	HENGERER et al., "In vivo Procedure for the Measurement Luciferase Reporter Gene Activity with a Low Light Imaging System," Reprint from BIOspektrum 4 (1998), pages 1-3.	☐
	7	BERTHOLD et al., "Luminometer Design and Low Light Detection," Methods in Enzymology, Vol. 305, Copyright 2000 by Academic Press, pages 62-87.	☐
	8	BRAUER et al., "Measuring luminescence with a low light level imaging system using electronic light standards," Siemens AG, Karlsruhe, Germany, Bioluminescence & Chemiluminescence status report," Chichester:Wiley 1993: 13-17, 1 page.	☐
	9	SZALAY et al., "Bioluminescence and chemiluminescence: status report: proceedings of the VIIth Bioluminescence and Chemiluminescence," Banff, March 1993, http://ucla.worldcat.org, 1 page.	☐
	10	FRANCIS et al.,"Monitoring Bioluminescent Staphylococcus aureus Infections in Living Mice Using a Novel luxABCDE Construct," http://iai.asm.org/cgi/content/full/68/6/3594, Xenogen Corporation, Alameda, CA and Division of Neonatal andDevelopmental Medicine, Department of Pediatrics, Stanford University Medical Center, Stanford, CA, Infection and Immunity, Vol. 68, No. 6, June, 2000, cover page and pages 3594-3600.	☐
	11	VOSS et al., "Radiometric and Geometric Calibration of a Visible Spectral Electro-Optic 'Fisheye' Camera Radiance Distribution System," Journal of Atmospheric and Oceanic Technology, Volume 6, (1989), pages 652-662.	☐

INFORMATION DISCLOSURE STATEMENT BY APPLICANT (Not for submission under 37 CFR 1.99)		
	Application Number	13222688
	Filing Date	2011-08-31
	First Named Inventor	Michael B. Nelson
	Art Unit	2828
	Examiner Name	Not yet known
	Attorney Docket Number	SPEC US-4 (027560.0014)

	12	NILES et al., "Radiometric calibration of a video fluorescence microscope for the quantitative imaging of resonance energy transfer," Rev. Sci, Instrum. 66 (6), June 1995, Copyright 1995 American Institute of Physics, pages 3527-3536.	☐
	13	EDIRISINGHE et al., "Radiometric Callibration of Multispectral Airborne Video Systems," International Journal of Remote Sensing, Vol. 20, No. 14, 1999, cover page and pages 2855-2870.	☐
	14	REHEMTULLA et al.,"Rapid and Quantitative Assessment of Cancer Treatment Response Using In Vivo Bioluminescence Imaging," Neoplasia, Vol. 2, No. 6, 2000, www.nature.com/neo, pages 491-495.	☐
	15	ZHANG et al., "Rapid in vivo funtional analysis of transgenes in mice using whole body imaging of luciferase expression," Transgenic Research 10: 2001 Kluwer Academic Publishers, The Netherlands, pages 423-434.	☐
	16	TSIN et al., "Statistical Calibration of CCD Imaging Process," Appeared in the Proceedings of the IEEE 2001 International Conference on Computer Vision, pages 1-8	☐
	17	CONTAG et al., "Use of Reporter Genes for Optical Measurements of Neoplastic Disease In Vivo," Neoplasia, Vol. 2, Nos. 1-2, January-April 2000, www.nature.com/neo, pages 41-52.	☐
	18	CONTAG et al., "Visualizing Gene Expression in Living Mammals Using a Bioluminescent Reporter," Photochemistry and Photobiology, 1997, 66(4): pages 523-531.	☐

If you wish to add additional non-patent literature document citation information please click the Add button Add

EXAMINER SIGNATURE

Examiner Signature		Date Considered	

*EXAMINER: Initial if reference considered, whether or not citation is in conformance with MPEP 609. Draw line through a citation if not in conformance and not considered. Include copy of this form with next communication to applicant.

[1] See Kind Codes of USPTO Patent Documents at www.USPTO.GOV or MPEP 901.04. [2] Enter office that issued the document, by the two-letter code (WIPO Standard ST.3). [3] For Japanese patent documents, the indication of the year of the reign of the Emperor must precede the serial number of the patent document. [4] Kind of document by the appropriate symbols as indicated on the document under WIPO Standard ST.16 if possible. [5] Applicant is to place a check mark here if English language translation is attached.

INFORMATION DISCLOSURE STATEMENT BY APPLICANT

(Not for submission under 37 CFR 1.99)

Application Number	13222688
Filing Date	2011-08-31
First Named Inventor	Michael B. Nelson
Art Unit	2828
Examiner Name	Not yet known
Attorney Docket Number	SPEC US-4 (027560.0014)

CERTIFICATION STATEMENT

Please see 37 CFR 1.97 and 1.98 to make the appropriate selection(s):

☐ That each item of information contained in the information disclosure statement was first cited in any communication from a foreign patent office in a counterpart foreign application not more than three months prior to the filing of the information disclosure statement. See 37 CFR 1.97(e)(1).

OR

☐ That no item of information contained in the information disclosure statement was cited in a communication from a foreign patent office in a counterpart foreign application, and, to the knowledge of the person signing the certification after making reasonable inquiry, no item of information contained in the information disclosure statement was known to any individual designated in 37 CFR 1.56(c) more than three months prior to the filing of the information disclosure statement. See 37 CFR 1.97(e)(2).

☐ See attached certification statement.

☐ The fee set forth in 37 CFR 1.17 (p) has been submitted herewith.

☒ A certification statement is not submitted herewith.

SIGNATURE

A signature of the applicant or representative is required in accordance with CFR 1.33, 10.18. Please see CFR 1.4(d) for the form of the signature.

Signature	/Bruce E. Dahl/	Date (YYYY-MM-DD)	2011-11-11
Name/Print	Bruce E. Dahl	Registration Number	33670

This collection of information is required by 37 CFR 1.97 and 1.98. The information is required to obtain or retain a benefit by the public which is to file (and by the USPTO to process) an application. Confidentiality is governed by 35 U.S.C. 122 and 37 CFR 1.14. This collection is estimated to take 1 hour to complete, including gathering, preparing and submitting the completed application form to the USPTO. Time will vary depending upon the individual case. Any comments on the amount of time you require to complete this form and/or suggestions for reducing this burden, should be sent to the Chief Information Officer, U.S. Patent and Trademark Office, U.S. Department of Commerce, P.O. Box 1450, Alexandria, VA 22313-1450. DO NOT SEND FEES OR COMPLETED FORMS TO THIS ADDRESS. **SEND TO: Commissioner for Patents, P.O. Box 1450, Alexandria, VA 22313-1450.**

Privacy Act Statement

The Privacy Act of 1974 (P.L. 93-579) requires that you be given certain information in connection with your submission of the attached form related to a patent application or patent. Accordingly, pursuant to the requirements of the Act, please be advised that: (1) the general authority for the collection of this information is 35 U.S.C. 2(b)(2); (2) furnishing of the information solicited is voluntary; and (3) the principal purpose for which the information is used by the U.S. Patent and Trademark Office is to process and/or examine your submission related to a patent application or patent. If you do not furnish the requested information, the U.S. Patent and Trademark Office may not be able to process and/or examine your submission, which may result in termination of proceedings or abandonment of the application or expiration of the patent.

The information provided by you in this form will be subject to the following routine uses:

1. The information on this form will be treated confidentially to the extent allowed under the Freedom of Information Act (5 U.S.C. 552) and the Privacy Act (5 U.S.C. 552a). Records from this system of records may be disclosed to the Department of Justice to determine whether the Freedom of Information Act requires disclosure of these record s.

2. A record from this system of records may be disclosed, as a routine use, in the course of presenting evidence to a court, magistrate, or administrative tribunal, including disclosures to opposing counsel in the course of settlement negotiations.

3. A record in this system of records may be disclosed, as a routine use, to a Member of Congress submitting a request involving an individual, to whom the record pertains, when the individual has requested assistance from the Member with respect to the subject matter of the record.

4. A record in this system of records may be disclosed, as a routine use, to a contractor of the Agency having need for the information in order to perform a contract. Recipients of information shall be required to comply with the requirements of the Privacy Act of 1974, as amended, pursuant to 5 U.S.C. 552a(m).

5. A record related to an International Application filed under the Patent Cooperation Treaty in this system of records may be disclosed, as a routine use, to the International Bureau of the World Intellectual Property Organization, pursuant to the Patent Cooperation Treaty.

6. A record in this system of records may be disclosed, as a routine use, to another federal agency for purposes of National Security review (35 U.S.C. 181) and for review pursuant to the Atomic Energy Act (42 U.S.C. 218(c)).

7. A record from this system of records may be disclosed, as a routine use, to the Administrator, General Services, or his/her designee, during an inspection of records conducted by GSA as part of that agency's responsibility to recommend improvements in records management practices and programs, under authority of 44 U.S.C. 2904 and 2906. Such disclosure shall be made in accordance with the GSA regulations governing inspection of records for this purpose, and any other relevant (i.e., GSA or Commerce) directive. Such disclosure shall not be used to make determinations about individuals.

8. A record from this system of records may be disclosed, as a routine use, to the public after either publication of the application pursuant to 35 U.S.C. 122(b) or issuance of a patent pursuant to 35 U.S.C. 151. Further, a record may be disclosed, subject to the limitations of 37 CFR 1.14, as a routine use, to the public if the record was filed in an application which became abandoned or in which the proceedings were terminated and which application is referenced by either a published application, an application open to public inspections or an issued patent.

9. A record from this system of records may be disclosed, as a routine use, to a Federal, State, or local law enforcement agency, if the USPTO becomes aware of a violation or potential violation of law or regulation.

CCD Image Calibration Using AIP4WIN

David Haworth

The purpose of image calibration is to remove unwanted errors caused by CCD camera operation. Image calibration is a very import first step in the processing of an astronomical image. Image calibration involves creating three master calibration frames: bias, dark and flat field frames. The goal is to combine multiple calibration images to create a low noise master bias, dark and flat field calibration frames. The challenge in creating these master calibration frames is to reduce noise and remove cosmic ray hits that affect the quality of these calibration frames. The high quality calibration frames applied to the astronomical image will remove or remove unwanted errors caused by CCD camera operation. Poor quality master calibration frames will introduce additional errors in the astronomical image. The goal is to create high quality calibration frames.

First a short overview of the image taking process is covered and then the following CCD image calibration tasks are covered

- Part 1: Find Gross Defect Images
- Part 2: Organize Files
- Part 3: Create Master Dark Calibration Frame
- Part 4: Create Master Bias Calibration Frame
- Part 5: Create Master Flat Calibration Frame
- Part 6: Image Calibration, Tracking and Stacking

Image Taking Process

The astronomical images came from an all night September 23, 2000 imaging session. The imaging equipment used was a SBIG ST-237 CCD camera, Celestron C8 Fastar on a Losmandy G-11 telescope mount. MaxIm DL CCD software was used to control the ST-237 camera. The imaging location was at home on the driveway.

The imaging session started on Saturday 9/23/00 evening at 21:14 PM PST and ended on Sunday morning 9/24/00 at 5:53 AM PST. This imaging session started about half hour after twilight, which was later than usual. Normally I setup the telescope at sunset and take dark frames until the end of twilight. I start imaging objects at twilight end.

On Saturday evening 9/23/00 the Sunset was 19:04 and twilight end was at 20:46. On Sunday morning 9/24/00 the Moonrise was 2:57, twilight started at 5:19 and Sunrise was 7:00. Most of the late Sunday morning objects were low in the east to southeast just above the trees and were in the moon's sky glow. Calibration frames were taken throughout the night and during Sunday morning twilight from 4:52 AM to 5:53 AM.

The images taking process was to manually take one 30 seconds image to check dynamic range of the astronomical object to check that the important image areas did not exceed the ST-237 camera maximum 4095 level. Maximum exposure was limited to 30 seconds because all images were unguided. This night's imaging plan was to obtain a large number of Messier and selected NGC objects before the northwest cloudy weather sets in for fall and winter. Therefore, most image sequences were eight images of 30 seconds for a total of 4 minutes. Some objects were too bright for 30 seconds images. For example, M13, M92 were 16 images x 15 seconds and M42 was 30 images x 2 seconds too prevent ST-237's 4095 saturation on key parts of the astronomical object of interest.

During the imaging session 502 frames (295 Mbytes) were taken. These frames included astronomical object images, bias frames, dark frames and flat frames. All frames were stored in a single directory call Master. This Master directory was a subdirectory of the 000923 directory. The 000923 directory name was made up of the first two digits for the year, the next two digits were for the month and last two digits were for the evening day. This naming directories scheme was a hang over from using a DOS PC to control the

Copyright 2001 David Haworth v5.0

Cookbook CB245. The advantage of this naming technique was the directory listing sorts the order of when the images were taken and was compatible with earlier image directory names.

Part 1: Find Gross Defect Images

The first task was to copy the 000923 directory of images to the computer in the house. This was easily done by connecting a temporary 50 foot LAN 10Base-T cable between the outside ST-237 control computer and the indoor image processing computer. On the indoor computer a work in progress (WIP) directory was created in the 000923 directory and all the images in the master directory were copied to the WIP directory. The images in the master directory were never edited or processed. Only the image copies in the WIP directory were moved, edited or processed. Also, the images are kept on the outside ST-237 control computer until a CD-R ROM backup is created.

The next task was to organize the 502 files and to identify gross image problems. At this point AIP4WIN Measure Statistics File was used to measure statistics on the image files. AIP4WIN version 1.2 includes a new feature to measure statistics on files, which was a very good time saver on checking for gross image problems. Using AIP4WIN Measure Statistics File 16 bad or problem images were found in the 502 images. Also, AIP4WIN Measure Statistics File was very help in organizing the image files by type and exposure time.

Using AIP4WIN Measure Statistics File I found all 502 files could not be measured at once because of a Microsoft limitation. AIP4WIN Measure Statistics File was used twice to create two statistics.txt files to cover the all 502 image files because of the 294 files limit. The two statistics.txt files were loaded into Microsoft Excel and combined into one spreadsheet. The spreadsheet was sorted by date/time and printed out as an over all image worksheet summary.

Most of the images were part of an eight image sequence group that was automatically taken by MaxIm DL CCD camera control sequence mode. MaxIm DL CCD takes an image sequence automatically saving each image with a three digit number at the end of image file name. In most imaging sessions I let the sequence number continue to increment throughout the imaging session. This provides an easy reference locator for any sequence image with the other sequence images. Images with less than a three digit number at the end of the file name were manually taken images used to check astronomical object centering or exposure time. In most cases these manually taken images are not used in the imaging processing, only the sequence images are calibrated, combined and processed.

Image file naming convections:

- m for Messier objects
- n for NGC objects
- dk for dark frames
- bias for bias frames
- flat for flat frames
- a, b, c, ...etc. letters after the above codes indicate a different sequence or some change in the image (object position, exposure time, etc.).

A few errors were easily seen using AIP4WIN Measure Statistics File summary table. These errors are found by checking the values for the Min PV, Max PV, Mean, Median, Mode and Std Dev for each sequence or each similar type of sequence like the 30 seconds dark frames. The following images errors were found because they had significantly different values than the other similar types of images.

Errors Frames Set 1

This sequence was to be 2 second dark frames for the M42 images, most of the values were too large. Inspecting the dark frames showed that they were star fields. The error was not correctly controlling the ST-237 CCD camera to take dark frames during the sequence.

File Name	Date	Time	Exp	Wid	Hght	Min	Max	Mean	Med	Mode	Std Dev
dk2s445.fit	9/24/00	11:52:51	2	640	480	0	4095	4	0	0	91.103
dk2s446.fit	9/24/00	11:53:04	2	640	480	0	4095	4	0	0	90.743
dk2s447.fit	9/24/00	11:53:16	2	640	480	0	4095	4	0	0	99.309
dk2s448.fit	9/24/00	11:53:29	2	640	480	0	4095	4	0	0	91.654
dk2s449.fit	9/24/00	11:53:42	2	640	480	0	4095	4	0	0	90.462
dk2s450.fit	9/24/00	11:53:55	2	640	480	0	4095	4	0	0	89.557
dk2s451.fit	9/24/00	11:54:07	2	640	480	0	1399	3	0	0	39.567
dk2s452.fit	9/24/00	11:54:20	2	640	480	0	2007	3	0	0	47.352

Errors Frames Set 2

This sequence was to be 30 seconds dark frames, most of the values were too large as compared to other 30 seconds dark frames. Inspecting the dark frames showed that they were star fields. The error was not correctly controlling the ST-237 CCD camera to take dark frames during the sequence.

File Name	Date	Time	Exp	Wid	Hght	Min	Max	Mean	Med	Mode	Std Dev
dkl453.fit	9/24/00	11:55:23	30	640	480	77	4095	209	206	218	265.215
dkl454.fit	9/24/00	11:56:03	30	640	480	80	4095	209	207	216	259.703
dkl455.fit	9/24/00	11:56:42	30	640	480	81	4095	210	207	216	264.854
dkl456.fit	9/24/00	11:57:24	30	640	480	84	4095	209	207	217	259.022
dkl457.fit	9/24/00	11:58:04	30	640	480	80	4095	208	206	216	264.672
dkl458.fit	9/24/00	11:58:43	30	640	480	84	4095	208	206	215	266.940

Error Frame 3

This error image was a flat frame named as a bias frame. This was easy seen with the statistics of the flat frames taken after this image and the bias frame taken before this image. The error was in file naming.

File Name	Date	Time	Exp	Wid	Hght	Min	Max	Mean	Med	Mode	Std Dev
biasd483.fit	9/24/00	12:47:22	30	640	480	297	4039	446	453	477	97.791

Error Frame 4

Flat frames were taken at morning twilight; this last flat frame was higher than the previous seven flats. This flat frame was not used in the calibration. The error was the twilight was changing too fast.

File Name	Date	Time	Exp	Wid	Hght	Min	Max	Mean	Med	Mode	Std Dev
lata491.fit	9/24/00	12:53:36	30	640	480	378	4095	536	543	565	99.463

Side Note

For the C8 Fastar telescope configuration all the images that were taken at 30 seconds have stars or astronomical objects bright enough to saturate the ST-237 at its maximum 4095 level. For example, the M31 core was max out at the 4095 in 0.1 seconds as shown in the following images statistics.

File Name	Date	Time	Exp	Wid	Hght	Min	Max	Mean	Med	Mode	Std Dev
m31d236.fit	9/24/00	8:59:32	0.1	640	480	0	4095	2	0	0	198.141
m31d237.fit	9/24/00	8:59:42	0.1	640	480	0	4095	2	0	0	192.776

Part 2: Organize Files

The next task was to organize files by creating directories for each object and each set of calibration frames. Also, using AIP4WIN statistics summary table it was easy to check the exposure time for each image sequence.

A calibration directory called DK Bias Flat was created for all the bias, flat and dark frames. Subdirectories in the DK Bias Flat directory were created for each sequence of calibration frames. Each directory starts with its sequence number range, 001-008. This makes it easer to list the directories in order in which they were taken. Next part of the directory name was the type of calibration frame, DK for dark frames, Bias for Bias frames and Flat for flat frames. Next part of the directory name was the exposure length and sometimes includes the temperature. Last part of the directory name was a note like error for the sequence images 445 to 458. The calibration frames were copied from the work in progress (WIP) directory to the appropriate named directory.

Directory of H:\000923\DK Bias Flat
001-008 DK 30s
057-072 DK 15s
105-115 DK 30s
172-179 DK 30s
246-261 DK 30s
262-277 Bias 0s
278-293 DK 30s
294-309 Bias 0s
310-325 DK 30s
445-452 Stars 2s error
453-458 Stars 30s error
459-466 DK 30s
467-474 DK 2s
475-482 Bias 0s
483-491 Flat 30s

The files left in the work in progress (WIP) directory were all astronomical image files. Directories were created for the following objects: B33, M01, M103, M110, M13, M27, M29, M31, M33, M34, M35, M36, M37, M38, M39, M42, M45, M50, M52, M56, M57, M71, M74, M76, M77, M78, M92, N2024, N7635, N891, and SATURN. The images were copied from the work in progress (WIP) directory to the appropriate named directory. Now the WIP directory was empty and was deleted.

Part 3: Create Master Dark Calibration Frame

This process step was to combine multiple dark frame images together to create a low noise master dark calibration frame. The challenge was to remove the gross errors and cosmic ray hits that add noise to the dark frame and affect the calibrated image quality.

AIP4WIN Multi-Image Average Combine and Median Combine were used for each set of dark calibration frames in a sequence subdirectory. For the seven dark sequence subdirectories there were seven average images and seven median images. These dark sequence averages and medians were copied into a temporary directory and AIP4WIN Measure Statistics File was performed on the 14 files. Notice in the below statistics file how the dark sequences 001-008 and 105-115 have a higher Std Dev than the other dark sequences.

File Name	Max PV	Std Dev
average001-008.fts	3752	43.052
average105-115.fts	3814	44.125
average172-179.fts	3649	41.975
average246-261.fts	3588	41.304
average278-293.fts	3602	41.565
average310-325.fts	3601	41.563
average459-466.fts	3553	40.962
median001-008.fts	3743	42.928
median105-115.fts	3819	44.063
median172-179.fts	3659	41.903
median246-261.fts	3586	41.256
median278-293.fts	3602	41.526
median310-325.fts	3599	41.520
median459-466.fts	3539	40.843

The span of 001-466 files contained 84 dark frames of 30 seconds.
The span of 172-466 files contained 64 dark frames of 30 seconds.

The next step was to copy all 30 seconds dark frames into one directory. AIP4WIN Multi-Image Average Combine and Median Combine were used to create the following four dark frames based on all 84 frames and on selected 64 frames that exclude the dark sequences of 001-008 and 105-115.

Statistics for average and median show that the median of 172-466 has the lowest Max PV and Std Dev.

File Name	Max PV	Std Dev	
average001-466.fts	3643	41.996	contains 84 frames
average172-466.fts	3598	41.469	contains 64 frames
median001-466.fts	3611	41.764	contains 84 frames
median172-466.fts	3595	41.463	contains 64 frames

The below calculations using AIP4WIN Multi-Image Image Math showed interesting results that the median is within 3-4 values being the lowest value. It would seem that cosmic rays or some other additive signal was becoming the primary noise component. At this point the median172-466.fts file is the best dark frame with the average172-466.fts file being the second best dark frame.

average001-466.fts minus average172-466.fts Max Pixel Value = 45
average172-466.fts minus average001-466.fts Max Pixel Value = 2
Analysis: average001-466.fts contains much higher values than average172-466.fts

median001-466.fts minus median172-466.fts Max Pixel Value = 16
median172-466.fts minus median001-466.fts Max Pixel Value = 4
Analysis: median001-466.fts contains much higher values than median172-466.fts

The median and average 172-466 files were lower values than 001-466 files.

Next compare the average versus median files of the same image frames.

average001-466.fts minus median001-466.fts Max Pixel Value = 32
median001-466.fts minus average001-466.fts Max Pixel Value = 3

average172-466.fts minus median172-466.fts Max Pixel Value = 12
median172-466.fts minus average172-466.fts Max Pixel Value = 3

Analysis: median files were lower than the average files for the same set of darks frames.

One may be tempted to use only median459-466.fts with its Std Dev 40.843 for 8 darks. Comparing median459-466.fts with the median172-466.fts shows a large difference. This would be expected with a median of a small set of 8 frames versus a median of 64 frames.

median172-466.fts minus median459-466.fts Max Pixel Value = 56
median459-466.fts minus median172-466.fts Max Pixel Value = 12

Summary: median172-466.fts was the best master dark frame.

Side Note: The Std Dev of a median or average image is not the best way to compare the quality of two calibration frame with each other. The Std Dev of an image is giving a measure of how spread out the pixels values are from the average pixel value of the image.

Part 4: Create Master Bias Calibration Frame

Creating a master bias calibration frame was a similar process to creating a master dark frame. AIP4WIN Multi-Image Average Combine and Median Combine were used to create an average and median bias calibration frames for each bias frame subdirectory. AIP4WIN Measure Statistics File was used to measure each average and median bias calibration frame for each bias frame subdirectory. Analysis: no obvious problems were identified.

Average and median bias calibration frames for the bias frame sequence subdirectories.

File Name	Max PV	Std Dev
median475-482.fts	239	1.812
median262-277.fts	250	1.862
median294-309.fts	249	1.881
average475-482.fts	242	1.923
average262-277.fts	248	1.930
average294-309.fts	250	1.945

An All Bias directory was created and all 40 bias frames were copy into it. AIP4WIN Measure Statistics File was used on all 40 bias files. The bias file statistics summary was loaded into Excel and sorted by Std Dev. Then the top three highest Std Dev bias files (biasa267.fit, biasa268.fit and biasd476.fit) were removed which left a total of 37 bias frames. AIP4WIN Multi-Image Average Combine and Median Combine were used to create a master average37 and median37 bias calibration frames for the remaining 37 bias frames.

File Name	Max PV	Std Dev
biasa267.fit	465	3.074
biasa268.fit	330	3.068
biasd476.fit	245	2.504
biasb299.fit	249	2.392

biasb302.fit	262	2.329
biasd477.fit	237	2.297
biasb300.fit	252	2.291
biasa271.fit	264	2.285
biasb295.fit	259	2.280
biasd479.fit	239	2.280
biasa262.fit	253	2.276
biasb296.fit	251	2.276
biasb304.fit	246	2.274
biasd480.fit	243	2.267
biasb301.fit	244	2.263
biasd478.fit	248	2.263
biasa273.fit	255	2.262
biasb306.fit	247	2.260
biasa270.fit	253	2.259
biasb297.fit	258	2.259
biasa266.fit	261	2.251
biasb298.fit	240	2.248
biasb309.fit	268	2.244
biasb307.fit	249	2.241
biasa263.fit	230	2.240
biasa276.fit	246	2.239
biasa277.fit	233	2.237
biasb305.fit	245	2.233
biasd482.fit	260	2.233
biasa274.fit	253	2.232
biasb303.fit	255	2.222
biasa265.fit	253	2.220
biasa269.fit	250	2.218
biasa275.fit	258	2.217
biasd481.fit	236	2.211
biasa272.fit	247	2.201
biasb294.fit	241	2.200
biasd475.fit	234	2.200
biasa264.fit	237	2.198
biasb308.fit	243	2.188

The resulting median and average statistics of the 37 bias frames.

File Name	Max PV	Std Dev
median37.fts	249	1.876
average37.fts	248	1.913

average37.fts minus median37.fts Max Pixel Value = 5
median37.fts minus average37.fts Max Pixel Value = 2
Analysis: median file was lower than the average file for the same set of bias frames.

Summary: median37.fts was the best master bias frame.

Part 5: Create Master Flat Calibration Frame

AIP4WIN Multi-Image Auto-Process Deep Sky was used to create a master flat calibration frame. First, AIP4WIN Measure Statistics File was used to measure each flat frame. Analysis: no obvious problems were identified with the flat frames.

Flat frames

File Name	Date	Time	Exp	Wid	Hght	Min	Max	Mean	Med	Mode	Std Dev
flata484.fit	9/24/00	12:48:51	30	640	480	307	4003	459	466	489	98.736
flata485.fit	9/24/00	12:49:31	30	640	480	286	4026	443	450	470	96.949
flata486.fit	9/24/00	12:50:12	30	640	480	254	3978	394	400	416	95.693
flata487.fit	9/24/00	12:50:53	30	640	480	239	3975	381	386	408	94.131
flata488.fit	9/24/00	12:51:34	30	640	480	275	4002	419	425	441	96.943
flata489.fit	9/24/00	12:52:15	30	640	480	287	4066	432	439	464	96.989
flata490.fit	9/24/00	12:52:55	30	640	480	286	4054	435	441	464	96.452

AIP4WIN Calibrate Setup Advanced menu settings were:

- use bias frame, median37.fts for bias frame,
- create master bias
- median172-466.ft for dark frame
- automatic dark matching
- create master dark
- applied flatfield correction
- select the above seven flatfield files
- normalize median combine since they were twilight flats
- subtract flat dark
- median172-466.ft for flat dark frame
- create master flat
- Save master flat as flatmaster7.fts

Close Advanced Calibration menu

AIP4WIN Calibrate Master Frames was used to verify the Master Dark Contents, Master Flat Contents and Master Bias Contents.

AIP4WIN Measure Statistics File was used on the flatmaster7.fts file. This data cannot be compared to the above seven flats because it was normalize and dark subtracted.

File Name	Date	Time	Exp	Wid	Hght	Min	Max	Mean	Med	Mode	Std Dev
flatmaster7.fts	9/24/00	7:47:36	30	640	480	298	539	422	430	459	81.023

Image calibration setup was now competed.

Part 6: Image Calibration, Tracking and Stacking

AIP4WIN Multi-Image Auto-Process Deep Sky was used to calibration, tracking and stack NGC 891 deep sky image. First the NGC 891 statistics on file summary table were check for abnormal readings between the eight 30 second images. None were found. Next AIP4WIN Multi-Image Auto-Process Deep Sky was used to calibrate, track and stack eight 30 second NGC 891 images.

AIP4WIN Multi-Image Auto-Process Deep Sky menu settings were

- Select files: n891a148.fit, n891a149.fit, n891a150.fit, n891a151.fit, n891a152.fit, n891a153.fit, n891a154.fit and n891a155.fit
- Stack
- Calibrate image
- 2X resample
- Prescale, prescale factor 16
- Nose Filter, deviation 1
- Select Master Frame n891a148.fit
- 2 star alignment, track radius 6
- Slave alignment, Star selection automatic
- No enhancement

Save n891 calibrated, tracked and stacked image as n891cal.fts.

Appendix A

Improving the Master Dark Frame

Cosmic ray hits add unwanted light to the dark frames. Cosmic ray hits can be seen by comparing/blinking the dark frames. AIP4WIN Measure Statistics File provides a quick visual multiple file blink feature. It opens an image, displays the image in the same window location, closes the image and gets the next image. This is very handy to see major cosmic ray hits and other defects that cause it to be different than the other dark frames. This section looks at ways to identify cosmic ray hits on dark frames based on analysis and not rely on visual interpretation.

Use AIP4WIN Multi-Image Image Math to take the absolute differences between median172-466.fts and each dark frame, save the absolute differences file. I used file name letter d plus the sequence number. This is a very, very slow and manual process for 84 dark frames.

Next use AIP4WIN statistics files on all of the absolute differences files d001.fts to d466.fts. Load the statistics file in to Excel and delete all columns except File Name, Max PV and Std Dev. Sort the data by Max PV. The dark frames with cosmic ray hits stand out with Max PV's greater than 1,000. Other candidates are any Max PV's greater than 500. Create a Cosmic Ray Hits directory and move the dark files that correspond to these absolute differences files to the Cosmic Ray Hits directory.

File Name	Max PV	Std Dev
d007.fts	3652	42.163
d311.fts	3604	41.586
d278.fts	3579	41.536
d105.fts	1983	9.332
d001x.fts	1428	6.805
d111.fts	877	4.707
d315.fts	688	3.891
d003.fts	679	3.429
d465.fts	589	4.382
d463.fts	509	2.959
d466.fts	341	3.417
d251.fts	303	2.332
d108c.fts	278	3.378
d255.fts	277	2.265
d110.fts	264	3.373
d323.fts	261	2.177
d108d.fts	243	3.462
d283.fts	242	2.718
d460.fts	240	2.310
d114.fts	239	3.049
d109.fts	236	3.305
d112.fts	234	3.208
d106.fts	224	3.188
d282.fts	200	2.149
d006.fts	199	2.254
d280.fts	199	2.133
d314.fts	195	2.122
d115.fts	192	3.115
d107.fts	184	3.097
d113.fts	184	3.088
d281.fts	173	2.085

d002.fts	164	2.393
d004.fts	163	2.182
d175.fts	157	1.755
d177.fts	156	1.915
d310.fts	156	2.252
d179.fts	155	1.787
d008.fts	148	2.168
d005.fts	120	2.171
d173.fts	104	1.712
d257.fts	101	2.034
d324.fts	97	1.980
d174.fts	92	1.662
d316.fts	91	1.997
d256.fts	84	1.985
d259.fts	84	1.972
d254.fts	83	2.017
d317.fts	80	1.998
d260.fts	69	2.006
d176.fts	66	1.585
d287.fts	66	1.982
d178.fts	57	1.668
d291.fts	57	1.958
d459.fts	57	2.106
d253.fts	56	1.986
d288.fts	56	1.979
d293.fts	56	1.972
d461.fts	56	2.076
d246.fts	52	2.015
d286.fts	52	1.924
d462.fts	50	2.097
d172.fts	49	1.653
d285.fts	48	1.930
d321.fts	48	1.956
d290.fts	47	1.965
d292.fts	47	1.972
d319.fts	47	1.970
d320.fts	47	1.991
d248.fts	46	2.059
d249.fts	46	2.004
d464.fts	46	2.180
d261.fts	45	1.924
d284.fts	44	1.931
d289.fts	44	1.992
d279.fts	42	1.984
d312.fts	42	1.977
d322.fts	42	1.913
d252.fts	41	1.980
d247.fts	40	2.031
d325.fts	40	1.951
d258.fts	38	1.999
d313.fts	38	1.986
d318.fts	37	1.904
d250.fts	33	1.935

All 84 absolute differences files
Median 94.500
Average 312.833

Stdeva 700.508

The bottom 74 absolute differences files
Median 81.500
Average 117.432
Stdeva 83.837
(3* Stdeva)+ Average = 368.944

Take the AIP4WIN Multi-Image Average Combine and Median Combine on the new set of 74 dark frames (84 – 10 cosmic ray hit frames).

Average74dks.fts minus median74dks.fts Max Pixel Value = 34
median74dks.fts minus Average74dks.fts Max Pixel Value = 3
Analysis: median has lower values that average.

median172-466.fts minus median74dks.fts Max Pixel Value = 4
median74dks.fts minus median172-466.fts Max Pixel Value = 11
Analysis: median172-466.fts has lower values than median74dks.fts.

median172-466.fts minus median64dks.fts Max Pixel Value = 4
median64dks.fts minus median172-466.fts Max Pixel Value = 16
Analysis: median172-466.fts has lower values than median74dks.fts.

median172-465crh.fts minus median172-466.fts Max Pixel Value = 5
median172-466.fts minus median172-465crh.fts Max Pixel Value = 4
Analysis: these two files may be similar.

average172-465crh.fts minus median172-465crh.fts Max Pixel Value = 13
median172-465crh.fts minus average172-465crh.fts Max Pixel Value = 3
Analysis: median172-465crh.fts has lower values than average172-465crh.fts.

File Name	Max PV	Std Dev
median172-466.fts	3595	41.463
average172-466.fts	3598	41.469
median172-465crh.fts	3598	41.491
average172-465crh.fts	3600	41.499
median64dks.fts	3611	41.703
median74dks.fts	3606	41.713
median001-466.fts	3611	41.764
average74dks.fts	3640	41.943
average001-466.fts	3643	41.996

According to Std Dev the median172-466.fts is the best calibration dark frame. See concerns on using Std Dev of an average or median frame to determine a merit of goodness in the below side note.

Side Note: The Std Dev of a median or average image is not the best way to compare the quality of two calibration frame with each other. The Std Dev of an image is giving a measure of how spread out the pixels values are from the average pixel value of the image. What is needed is a data set of Std Dev for each pixel against all the image frames that made up the calibration frame. For the ST-237 with 640 x 480 pixels there would be 640 x 480 Std Devs, one for each pixel location. One could average the data set of all the Std Devs and use this number to compare it to other calibration sets. The proposal is that the lower average of all pixels Std Dev is a lower noise and lower cosmic ray affected calibration frames set and will produce a higher quality calibrated image.

[8] Chemiluminescence Imaging Systems for the Analysis of Macrosamples: Microtiter Format, Blot Membrane, and Whole Organs

By ALDO RODA, PATRIZIA PASINI, MONICA MUSIANI, and MARIO BARALDINI

Introduction

Chemiluminescence (CL) is a versatile, ultrasensitive analytical tool with a wide range of applications in fields such as biotechnology, pharmacology, molecular biology, and clinical chemistry.[1,2]

By coupling enzymatic reactions to light-emitting systems, CL can be used to detect enzyme activity or substrates or to study the effect of enzyme inhibitors by the resultant modifications of the light emission kinetic profile.[3–5] The involvement of radical species in the mechanisms of CL reactions such as luminol/peroxidase/H_2O_2 or luminol/FeEDTA/xanthine/xanthine oxidase makes it possible to determine the antioxidant capacity of biologically active compounds in simple aqueous solution or in biological fluids such as serum.[6,7] Chemiluminescence also represents a sensitive detection system for filter membrane biospecific reactions such as Southern, Northern, or Western blot tests and dot blot hybridization reactions that avoids the use of radioisotopes and long exposure times.[8,9] Finally, ultraweak and enhanced CL have been widely employed to study oxygen-free radical (OFR) formation in different biological systems, including whole organs, tissue homogenates, isolated cells, and subcellular organelles, made possible

[1] L. J. Kricka, P. E. Stanley, G. H. G. Thorpe, and T. P. Whitehead, "Analytical Applications of Bioluminescence and Chemiluminescence." Academic Press, London/New York, 1984.
[2] A. K. Campbell, "Chemiluminescence: Principles and Applications in Biology and Medicine." Ellis Horwood, Chichester, 1988.
[3] M. DeLuca and W. McElroy, *Methods Enzymol.* **133,** 331 (1986).
[4] D. C. Vellom and L. J. Kricka, *Methods Enzymol.* **133,** 229 (1986).
[5] A. Roda, P. Rauch, E. Ferri, S. Girotti, S. Ghini, G. Carrea, and R. Bovara, *Anal. Chim. Acta* **294,** 35 (1994).
[6] T. P. Whitehead, G. H. G. Thorpe, and S. R. J. Maxwell, *Anal. Chim. Acta* **266,** 265 (1992).
[7] C. Pascual and C. Romay, *J. Biolumin. Chemilumin.* **7,** 123 (1992).
[8] S. Beck and H. Köster, *Anal. Chem.* **62,** 2258 (1990).
[9] M. Musiani, M. Zerbini, M. Gibellini, D. Gentilomi, S. Girotti, and E. Ferri, *Anal. Biochem.* **194,** 394 (1991).

Copyright © 2000 by Academic Press
All rights of reproduction in any form reserved.
METHODS IN ENZYMOLOGY, VOL. 305
0076-6879/00 $30.00

SPECTRAL_0000579

by a weak spontaneous photon emission associated with OFR-related oxidative processes.[10]

The light output generated by biospecific reactions is usually detected by photomultiplier- or photodiode-based luminometers or by instant photographic film. Luminographs, recently developed low-light imaging devices based on Vidicon or CCD video cameras, can be utilized to analyze macrosamples such as gel, membrane, microtiter plates, or petri dishes or, in conjunction with optical microscopy, microsamples such as tissue sections, single cells, or microchip devices.[11–14]

These imaging systems offer some advantages over conventional instrumentation. For example, when a microtiter format is used for enzymatic or antioxidant activity studies, a video camera-based imaging system allows the simultaneous measurement of 96 to 384 samples, whereas microtiter plate luminometers read microtiter wells one by one or strip by strip. This feature and the availability of CL reagents that reach steady-state light emission quickly (i.e., in a few minutes) make CL imaging particularly suitable for the development of high throughput screening (HTS) assays. As far as blot applications are concerned, the main advantage of CL imaging with respect to photographic film is the possibility of performing direct semiquantitative analysis. For the study of oxygen-free radical formation in whole organs, imaging devices allow not only quantification of the emitted photons, but also visualization of the spatial distribution of the CL signal corresponding to radical production in a specific area of the organ.

This article describes some systems for CL imaging of macrosamples developed in our laboratory, lists some applications, and critically evaluates their analytical performance in comparison with other systems.

Instrumentation

The basic instrumentation for CL imaging includes an ultrasensitive video camera, an optical system, and appropriate software for image analysis. The video camera has to be designed specifically to pick up the static CL signal and must be characterized by very low instrumental noise. The

[10] E. Cadenas, A. Boveris, and B. Chance, *in* "Free Radicals in Biology" (W. A. Pryor, ed.), p. 211. Academic Press, New York, 1984.
[11] Y. Hiraoka, J. W. Sedat, and D. A. Agard, *Science* **238,** 36 (1987).
[12] R. A. Wick, *BioTechniques* **7,** 262 (1989).
[13] A. Roda, P. Pasini, M. Musiani, S. Girotti, M. Baraldini, G. Carrea, and A. Suozzi, *Anal. Chem.* **68,** 1073 (1996).
[14] A. Roda, P. Pasini, M. Baraldini, M. Musiani, G. Gentilomi, and C. Robert, *Anal. Biochem.* **257,** 53 (1998).

SPECTRAL_0000580

instrumentation thus differs from that used to evaluate the fast transient excited state utilized in fluorescence analysis.

Detection and analysis of CL signals were performed using a high-performance, low-light level imaging apparatus (Luminograph LB 980, EG&G Berthold, Bad Wilbad, Germany), which permits the measurement of emitted light at the single-photon level. The video system consists of a 1-in. Saticon high dynamic range pick-up tube (a Vidicon-type tube with Se-As-Tl light target photoconductor) linked to an image intensifier, by high transmission lenses, and also to a video amplifier. This system is connected to a PC for quantitative image analysis, and a sample dark box is provided to prevent contact with external light. The system operates in the following consecutive steps: (i) the illuminated sample images are recorded; (ii) the luminescent signal is measured with optimized photon accumulation lasting 1–5 min, with 2-sec interval integration; and (iii) after computer elaboration of the luminescent signal with pseudocolors corresponding to the light intensity, an overlay of the sample photograph with the luminescent signal allows visualization of the spatial distribution of the target analytes. Light emission from the samples is quantified by delineating a given area and counting the number of photon fluxes from within it.

Alternatively, when higher detectability is required, a Luminograph LB 981 (EG&G Berthold, Bad Wilbad, Germany) based on a back-illuminated cooled CCD is used; thanks to its high sensitivity, it does not require the addition of an image intensifier. The instrument setup and CL imaging processing are quite similar to those of the LB 980 luminograph.

The analytical signal is usually expressed as relative light units for qualitative analysis or as photons/second/surface unit (pixel or mm^2) for quantitative data.

Materials and Methods

Reagents

Peroxidase (type VI-A, from horseradish, 1100 U/mg), acetylcholinesterase (AChE) (type V-S, from electric eel, 1000–2000 U/mg), choline oxidase (from *Alcaligenes* genus, approximately 10 U/mg), acetylcholine iodide, 5-amino-2,3-dihydro-1,4-phthalazinedone (luminol sodium salt), bis-*N*-methylacridinium nitrate (lucigenin), 9-amino-1,2,3,4-tetrahydroacridine (tacrine hydrochloride), and ascorbic acid are from Sigma (St. Louis, MO). Trolox, a water-soluble analog of α-tocopherol, and 4-iodophenol are from Aldrich (Milwaukee, WI). The ECL-enhanced chemiluminescent

SPECTRAL_0000581

reagent (luminol/enhancer/H_2O_2) for horseradish peroxidase (HRP) detection is from Amersham (Amersham, UK).

Principle of the Methods

Microtiter Format Chemiluminescent Assays

Evaluation of Antioxidant Activity. The luminol/enhancer/peroxidase/H_2O_2 reaction produces relatively steady-state light output for at least 5–40 min in the presence of an excess of peroxidase substrate. The addition of antioxidant compounds to the CL cocktail results in an activity- and concentration-dependent reduction in photon emission, followed by light resumption after a certain time period. The kinetic profile of the light output allows calculation of the relative antioxidant potency of a given molecule with respect to reference substances.

Evaluation of Acetylcholinesterase Inhibitors. The CL detection of AChE is based on coupled enzymatic reactions that involve choline oxidase and horseradish peroxidase as the indicator enzymes and uses luminol/enhancer to detect the H_2O_2 formed, thus leading to stable light emission. The addition of AChE inhibitors to the CL cocktail reduces the light emission as a function of inhibitor activity and concentration. AChE inhibitors include drugs commonly used in the treatment of Alzheimer's disease, such as tacrine, and pesticides like Aldicarb and Paraoxon.

Dot Blot Hybridization for the Detection of Human B19 Parvovirus DNA

Nucleic acid hybridization techniques are able to detect viral genomes directly in clinical samples, allowing rapid and sensitive diagnosis of viral infections, especially for viruses that do not grow in cell cultures or have a long replication cycle. In dot blot hybridization reactions the specimens are dotted on membrane and are hybridized with a specific gene probe labeled with a hapten and then the hybrid is detected using an enzyme-conjugated antihapten antibody and CL substrate such as peroxidase/luminol/H_2O_2 or alkaline phosphatase/dioxetane.

Chemiluminescent Imaging of Oxygen-Free Radical Formation in Isolated and Perfused Rat Liver

Oxygen-free radicals are known to be involved in the ischemia–reperfusion injury of organs.[15,16] OFR-related oxidative processes are char-

[15] J. M. McCord, *N. Engl. J. Med.* **312,** 159 (1985).
[16] H. Jaeschke, *Chem. Biol. Interact.* **79,** 115 (1991).

SPECTRAL_0000582

acterized by a weak spontaneous photon emission. Chemical light enhancers are employed to increase luminescent output by interaction with OFR. In particular, the acridinium salt lucigenin has been shown to react specifically with superoxide radical $\cdot O_2^-$ to form *N*-methylacridone in the excited state, which reverts to its ground state with the emission of light.[17]

Procedures

Microtiter Format Chemiluminescent Assays

Evaluation of Antioxidant Activity. Prepare aqueous serial dilutions (two to three decades) of the compounds to be examined for antioxidant activity and of ascorbic acid and Trolox as positive controls. In this system, ascorbic acid and Trolox are generally used at final concentrations ranging from 0.3 to 30 μM. Prepare a CL cocktail by adding 100 μl of a 100-ng/ml HRP solution in 0.1 *M* Tris buffer, pH 8.6, to 5 ml of ECL-enhanced chemiluminescent reagent containing luminol/H_2O_2/enhancer. Add 10 μl of antioxidant solution and 20 μl of CL cocktail to each well of a black 384-well microtiter plate (Corning Costar, Acton, MA). Acquire the CL signal for 1 min and monitor the reaction kinetics at 2-min intervals for 20–30 min.

Evaluation of Acetylcholinesterase Inhibitors. Prepare aqueous serial dilutions (two to three decades) of the compounds to be examined for AChE inhibition activity and of tacrine hydrochloride as a positive control. In this system, tacrine chlorohydrate is generally used at final concentrations ranging from 0.1 to 10 n*M*. Prepare a CL cocktail with the following: 0.1 m*M* acetylcholine iodide, 0.1 U/ml AChE, 0.3 U/ml choline oxidase, 6 μM luminol, 2 μM 4-iodophenol, and 0.22 U/ml HRP in 0.5 *M* potassium phosphate buffer, pH 8.0. Add 10 μl of inhibitor solution and 20 μl of CL cocktail to each well of a black 384-well microtiter plate (Corning Costar). Acquire the CL signal for 1 min and monitor the reaction kinetics at 2-min intervals for 20–30 min.

Dot Blot Hybridization for the Detection of Human B19 Parvovirus DNA

Specimen Preparation. Add 5-μl aliquots of serum (with B19 parvovirus present during active infection) to 195 μl of distilled water and filter the mixture by the Bio Dot apparatus on a nylon membrane (Amersham Hybond N, Amersham, UK) equilibrated in distilled water. Air dry and treat

[17] S. J. Rembish and M. A. Trush, *Free Radic. Biol. Med.* **17,** 117 (1994).

SPECTRAL_0000583

the membrane with UV for 5 min. Alkali denature the specimens on the membrane by 0.1 *M* NaOH–1 *M* NaCl and neutralize by 0.1 *M* Tris–HCl, pH 7.4. Soak membranes in 50 m*M* Tris–HCl, pH 7.6, 5 m*M* EDTA containing 1 mg/ml pronase and incubate with gentle shaking at 37° for 1 hr. After incubation, remove the pronase by three 5-min rinses in 2× SSC (1× SSC is 0.15 *M* NaCl, 0.015 *M* sodium citrate, pH 7).

As a control of sensitivity, prepare serial dilutions (100-0.001 pg) of B19 parvovirus DNA in 200 μl of distilled water, filter on nylon membrane, and then treat as described earlier.

Hybridization Reaction. Seal the nylon membrane with dotted specimens in a polypropylene bag with 200 μl/cm^2 of prehybridization mixture containing 4× SET (20× SET is 3 *M* NaCl, 0.4 *M* Tris–HCl, pH 7.8, 20 m*M* EDTA), 5× Denhardt solution (50× Denhardt is 1% Ficoll, 1% polyvinylpyrrolidone, 1% bovine serum albumin in distilled water), 100 μg/ml of denaturated calf thymus DNA, and 0.5% sodium dodecyl sulfate (SDS). Incubate the membranes at 65° for 1 hr. Remove the prehybridization mixture and replace it with 100 μl/cm^2 of hybridization mixture containing 4× SET, 5× Denhardt solution, 50% formamide, 0.5% SDS, 100 μg/ml denaturated calf thymus DNA, and 50 ng/ml of denaturated parvovirus B19 DNA probe labeled with digoxigenin. Incubate the membrane in a shaking water bath at 42° for 16–18 hr. After hybridization, wash the membrane in (i) 2× SSC, 0.5% SDS at room temperature for 5 min, (ii) 2× SSC, 0.5% SDS at room temperature for 15 min, (iii) 0.1× SSC, 0.1% SDS at 65° for 1 hr, and (iv) 0.1× SSC, 0.1% SDS at room temperature for 5 min.

Chemiluminescent Immunoenzymatic Detection. Wash briefly in 100 m*M* Tris–HCl buffer, pH 7.5, with 150 m*M* NaCl and then apply the blocking reagent (Boehringer, Mannheim, Germany) to the nylon membrane at room temperature for 30 min. Incubate the membrane at room temperature for 30 min with sheep antidigoxigenin Fab fragments conjugated to alkaline phosphatase (Boehringer, Mannheim, Germany) diluted 1:5000. Equilibrate it for 2 min with equilibration buffer (100 m*M* Tris–HCl, 100 m*M* NaCl, 50 m*M* $MgCl_2$, pH 9.5). Seal the dried nylon membrane in a polypropylene bag with 100 μl/cm^2 of a freshly prepared solution of Lumi-Phos Plus (Lumigen, Southfield, MI) chemiluminescent substrate. After a 45-min incubation, acquire the luminescent signal from the hybrid formation for 1 min.

Chemiluminescent Imaging of Oxygen-Free Radical Formation in Isolated and Perfused Rat Liver

Isolate livers from anesthetized Wistar male fed rats weighing 200–250 g. Cannulate the portal vein with an 18-gauge catheter, wash the organ with

SPECTRAL_0000584

Ringer's lactate solution, and expose to 1 hr ischemia at 37°. Place the liver in the luminograph chamber and perfuse for 1 hr at 37° through the portal catheter with oxygenated Krebs Henseleit buffer, containing 10 μM lucigenin. Drive the perfusion medium (maintained at 37°) by a Model 312 Minipuls 3 peristaltic pump (Gilson, Villiers le Bel, France) at a flow rate of 18 ml/min. Monitor the light emission from the organ surface for 50–60 min by acquiring the chemiluminescent signal for 1 min at 5-min intervals and record live images at the beginning and at the end of the experiment. Acquire chemiluminescent signals during ischemia and also during the reperfusion of nonischemic livers as negative controls.

Results and Discussion

Microtiter Format Chemiluminescent Assays

Evaluation of Antioxidant Activity. The light output from the luminol/enhancer/peroxidase/H_2O_2 reaction reached a maximum in a few minutes and maintained a steady state for at least 20–30 min. Figure 1a shows a 384-well microtiter plate used for determining activities of antioxidant compounds and AChE inhibitors at different concentrations. The addition of antioxidant compounds to the corresponding CL cocktail resulted in a concentration-dependent reduction in light output, as shown in Fig. 1b for ascorbic acid. After initial light suppression, photon emission resumed, starting at lower concentrations, then increasing to values similar to those of the control wells, followed by a subsequent decrease in light output in all wells. This pattern is consistent with CL reaction kinetics, indicating that the antioxidant activity should be evaluated during steady-state emission.

Evaluation of Acetylcholinesterase Inhibitors. The detection of AChE with a microtiter format was optimized to permit simultaneous analysis of the 384 wells of a microtiter plate with a luminograph device that uses a cooled ultrasensitive CCD camera. Light emission reached a steady state after 10–15 min and was stable for at least 10 min. Figure 1a shows a 384-well microtiter plate used for determining activities of AChE inhibitors and antioxidant compounds at different concentrations. The addition of AChE inhibitors to the corresponding CL cocktail resulted in a concentration-dependent reduction in light output, as shown in Fig. 1c for tacrine. Photon emission did not resume after this reduction and it never reached values similar to those of the control wells, even though tacrine is a reversible AChE inhibitor. The relatively rapid decrease in light output observed in all wells indicates that inhibition activity should be evaluated during steady-state emission.

SPECTRAL_0000585

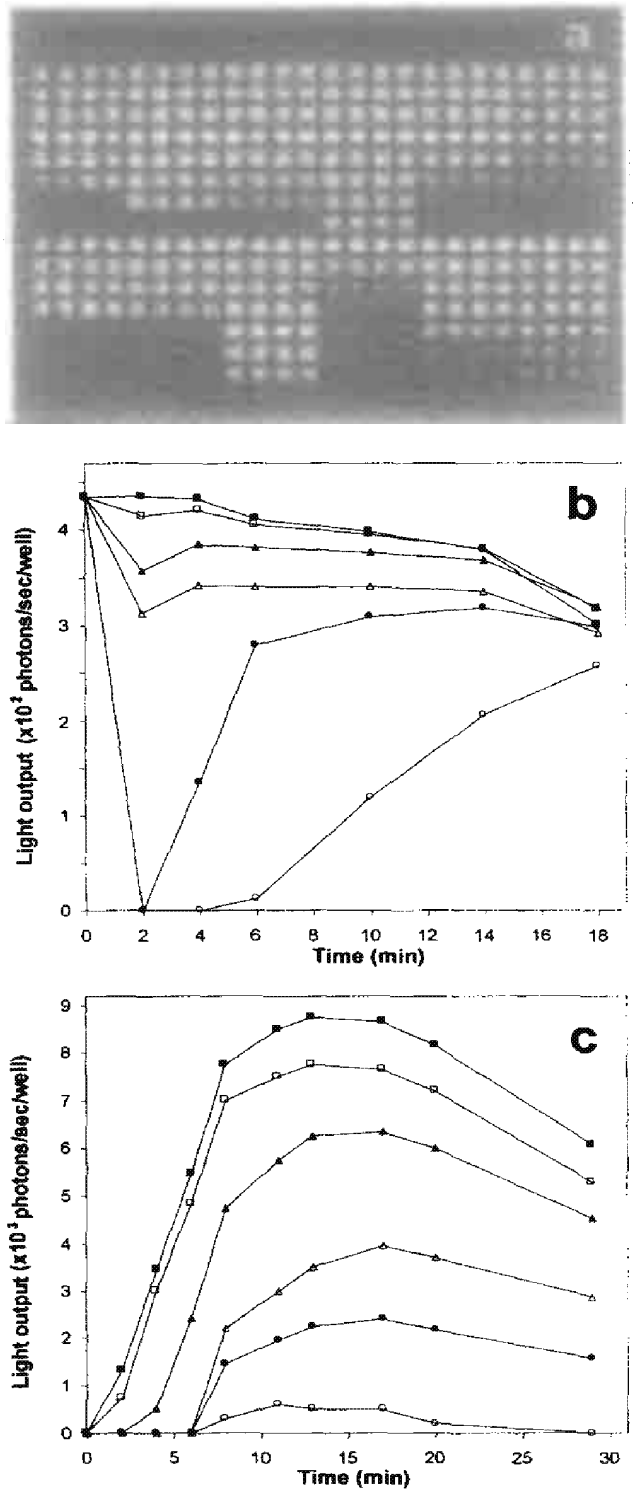


FIG. 1. Chemiluminescent signal detected at 15 min in a 384-well microtiter plate used for determining activities of antioxidant compounds and AChE inhibitors at different concentrations (a). Kinetic profile of the luminol/enhancer/peroxidase/H_2O_2 reaction and concentration-dependent reduction in light output due to the addition of ascorbic acid: ■, control; □, 0.3; ▲, 1.0; △, 3.0; ●, 10; and ○, 30 μM (b). Kinetic profile of the CL reaction for the detection of AChE and concentration-dependent reduction in light output due to the addition of tacrine: ■, control; □, 0.1; ▲, 0.25; △, 0.5; ●, 1.0; and ○, 10 nM (c).

SPECTRAL_0000586

For both of these microtiter format assays, with the luminograph software, it was possible to calculate the integral of the light emitted by each well or to directly visualize the dose-dependent inhibitory effect of the drugs. The methods fulfill the requirements of precision as the coefficients of variation calculated over different sets of experiments never exceeded 5%. When compounds poorly soluble in water have to be analyzed, a mixed solvent containing not more than 10–20% of dimethyl sulfoxide (DMSO) or dimethylformamide (DMF) should be used, and determination of the drug antioxidant activity or enzyme inhibitory effect must take into consideration the light-quenching effects of DMSO or DMF.

Chemiluminescence imaging has proved to be a suitable tool for the development of high throughput screening assays of drugs. Using a CCD camera, 384-well black polystyrene microtiter plates, and CL reagents that quickly (in a few minutes) reach a steady state of light output, an automated system can be set up easily to screen more than 5000 samples per hour. The high detectability of CL labels makes the technique very sensitive, thus allowing analysis of small sample amounts and very diluted specimens. For quantitative measurements, optical distortion and geometry must be considered; thus, image corrections, which can be included easily in the software for signal processing, are required.

Dot Blot Hybridization for the Detection of Human B19 Parvovirus DNA

It has been demonstrated that chemiluminescent enzyme substrates are the most sensitive tools available for detecting enzyme conjugates in a wide range of enzyme-based applications.[18] In order to assess the sensitivity of the developed assay using the imaging luminograph and Lumi-Phos Plus chemiluminescent substrate for alkaline phosphatase, different dilutions of B19 parvovirus DNA (ranging from 100 pg to 1 fg) were analyzed, and it was found that 20-10 fg of homologous DNA could be detected at end point dilution (Fig. 2a). This detection limit is similar to that achieved with photographic film, but lower than that obtained with colorimetric detection that has a detection limit of about 100 fg (Fig. 2b). The advantage of luminographic over photographic detection is that the amount of photons emitted by each dot can be quantified simultaneously, thus rendering the data analysis easy and rapid. Moreover, with luminographic detection, chemiluminescent reactions can be recorded permanently, as all sample images are stored in a computer; they can also be printed or sent to other laboratories for evaluation using floppy disks or computer network.

[18] L. J. Kricka, *in* "Nonisotopic Probing, Blotting, and Sequencing" (L. J. Kricka, ed.), p. 3. Academic Press, New York, 1995.

SPECTRAL_0000587

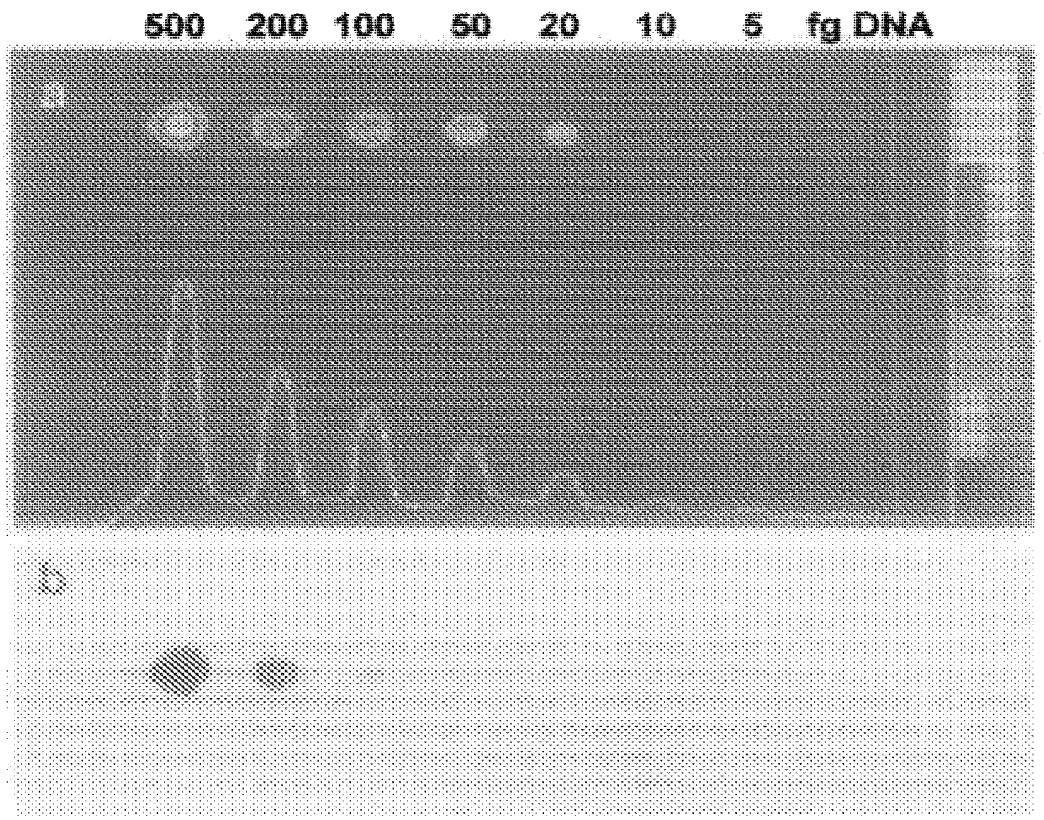


FIG. 2. Dot blot hybridization for the detection of serial dilutions (500-5 fg) of human B19 parvovirus DNA using chemiluminescent (a) or colorimetric (b) substrates. A bidimensional profile of light output showing a linear decrease in photon emission is reported in a.

The specificity of the chemiluminescent assay was ascertained on the basis of the following experiments: (a) chemiluminescent signal was detected when B19 parvovirus-positive reference sera were hybridized with the labeled DNA probe; (b) no chemiluminescent signal was detected when B19 parvovirus-negative reference sera were hybridized with the labeled DNA probe; (c) no chemiluminescent signal was observed when B19 parvovirus-positive reference sera were hybridized with the unlabeled DNA probe and treated with antidigoxigenin Fab fragments conjugated with alkaline phosphatase, followed by chemiluminescent detection; and (d) no chemiluminescent signal was shown after the hybridization of B19 parvovirus-positive reference sera with digoxigenin-labeled probe when incubation with antidigoxigenin Fab fragments was either omitted or replaced by incubation with sheep nonimmune serum.

The chemiluminescent dot blot hybridization system with luminographic detection can be a useful tool for the detection, quantitation, and study of specific viral genetic sequences inside clinical specimens and, thus, for sensitive, specific, and rapid diagnosis of viral infections.

SPECTRAL_0000588

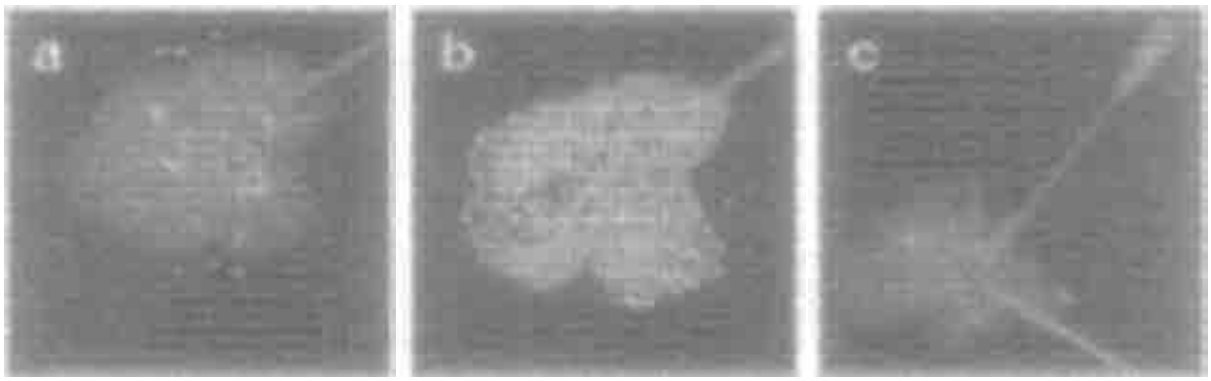


FIG. 3. Chemiluminescent imaging of oxygen-free radical formation in isolated and perfused rat liver. Spatial distribution of the luminescent signal in ischemic liver at 5 (a) and 40 (b) min after reperfusion. Luminescent emission is not detected in liver during ischemia (c).

Chemiluminescent Imaging of Oxygen-Free Radical Formation in Isolated and Perfused Rat Liver

The aim of our study was to develop a chemiluminescent method for *real time* quantitative detection and localization of oxygen-free radical formation in isolated and perfused rat livers exposed to ischemia–reperfusion.[19] A chemiluminescent signal was observed a few minutes after reperfusion. Superimposition of the chemiluminescent and live images acquired successively during reperfusion allowed localization of the luminescent emission, showing that it started around the hepatic vascular pedicle (Fig. 3a) and then spread progressively over the whole organ surface (Fig. 3b). Light output kinetics were evaluated by measuring the photon flux/second/organ surface at consecutive 5-min intervals: the signal increased, reaching the maximum value after 15–20 min, and then it decayed slowly, disappearing after 50–60 min. The supposition that the luminescent peak could correspond to a burst of superoxide radical production is supported by the following findings. The addition of 30 U/ml superoxide dismutase, a specific scavenger of $\cdot O_2^-$, to the perfusion medium caused a rapid decrease in light output, showing that the observed signal was truly dependent on superoxide radical formation. On the contrary, luminescent emission was not observed during ischemia, when the O_2 required for oxygen radical formation was, of course, lacking (Fig. 3c). Furthermore, light production was not detected during the reperfusion of nonischemic livers, probably because the postulated conversion of xanthine dehydrogenase to its oxygen radical-producing form, xanthine oxidase, during hypoxia did

[19] A. Gasbarrini, P. Pasini, B. Nardo, S. De Notariis, M. Simoncini, A. Cavallari, E. Roda, M. Bernardi, and A. Roda, *Free Radic. Biol. Med.* **24,** 211 (1998).

SPECTRAL_0000589

not occur.[20] Although the light emission may well correspond to superoxide radical formation on the liver surface, in previous studies it was postulated that it reflects metabolism of the whole organ and correlates with more global parameters such as lipid peroxidation.[10]

We have shown the possibility of assessing the rate and spatial distribution of oxygen-free radical formation on the surface of intact organs *in real time.* This system opens new prospects for the study of the physiopathogenesis of oxidative stress and provides a suitable model for screening substances with antioxidant activity. In addition, it could represent a useful tool for testing the effectiveness of storage conditions and media utilized in the preservation of organs for transplantation.

Concluding Remarks

The applications of CL imaging described earlier demonstrate the high versatility of this system. In the chapter "*In situ* Hybridization and Immunohistochemistry with Enzyme-Triggered Chemiluminescent Probes" by Roda *et al.* in this volume, we report the use of CL imaging coupled with optical microscopy, showing additional applications in immunohistochemistry and *in situ* hybridization.

These results have demonstrated that CL imaging is a valuable bioanalytical tool suitable for a wide range of applications. When used to measure CL reactions occurring in microtiter plates, the main advantage is that it permits simultaneous monitoring of up to 4 × 384 microtiter wells, thus facilitating kinetic studies and the measurement of time-dependent CL signals. However, the main limitation of CCD-based imaging is the narrow dynamic range with respect to photomultiplier detection (two to three decades lower). In addition, its sensitivity is 5–10 times lower than those of conventional CL microtiter readers. When imaging is used to measure CL reactions detecting blot format biospecific probes, its analytical performance is superior to those of systems such as photographic film or other systems using different principles to detect immunological or genetic reactions such as radioisotopes or color-producing substrates.[21,22] The main advantages are higher detectability as well as the possibility of performing quantitative analysis. CL imaging of whole organs to detect oxygen-free radicals or, in principle, any kind of CL reaction is a promising tool. Because

[20] Y. Amaya, K. I. Yamazaki, M. Sato, K. Noda, and T. Nishino, *J. Biol. Chem.* **265,** 14170 (1990).

[21] I. Bronstein, J. C. Voyta, K. G. Lazzari, O. Murphy, B. Edwards, and L. J. Kricka, *BioTechniques* **8,** 310 (1990).

[22] S. Girotti, M. Musiani, P. Pasini, E. Ferri, G. Gallinella, M. L. Zerbini, A. Roda, G. Gentilomi, and S. Venturoli, *Clin. Chem.* **41,** 1693 (1995).

SPECTRAL_0000590

the analytical information is derived from an intact organ or even an intact live laboratory animal, it offers an enormous advantage over *in vitro* systems using cultured isolated cells. The system must be standardized carefully in terms of sample geometry, and the permeability, diffusion, and partition of the CL substrate in a given organ, cellular, and subcellular compartment have to be considered.

In conclusion, CL imaging is an important tool in the modern bioanalytical laboratory, at times complementary to other systems but, in many cases, unique.

SPECTRAL_0000591

larities between emission spectra of potential chemiluminescence calibrators and the oxyluciferin. Another area where much needs to be accomplished is in the area of low-level light imaging where calibration is still primitive.[14–16]

[14] D. J. O'Kane and J. E. Wampler, *Proc. Soc. Photo-Opt. Instr. Eng.* **1161,** 205 (1989).
[15] F. Berthold, K. Hafner, and D. DiPrato, *in* "Bioluminescence and Chemiluminescence: Fundamental and Applied Aspects" (A. K. Campbell, L. J. Kricka, and P. E. Stanley, eds.), p. 617. Wiley, Chichester, 1994.
[16] D. H. Leaback, *in* "Bioluminescence and Chemiluminescence: Molecular Reporting with Photons" (J. W. Hastings, L. J. Kricka, and P. E. Stanley, eds.), p. 545. Wiley, Chichester, 1997.

[6] Commercially Available Luminometers and Low-Level Light Imaging Devices

By PHILIP E. STANLEY

The study of bioluminescence (BL) and chemiluminescence (CL) and assays and techniques based on them usually requires the measurement of light output. Today, the life scientist uses a commercially available instrument because there are many from which to choose in the marketplace. This article discusses briefly some aspects of the various types of instruments and provides a list of many of the suppliers.

In Volume 133 of "Methods in Enzymology" the specifications of various types of luminometers are described in some detail.[1] In this volume, Berthold *et al.*[2] review this topic in light of today's technology, whereas Voss[3] describes the mode of action of detectors used in this instrumentation. Technical specifications of many other luminometers are given elsewhere.[4–12]

[1] P. E. Stanley, *Methods Enzymol.* **133,** 587.
[2] F. Berthold, K. Herick, and R. M. Siewe, *Methods Enzymol.* **305** [4] 2000 (this volume).
[3] K. J. Voss, *Methods Enzymol.* **305** [3] 2000 (this volume).
[4] P. E. Stanley, *in* "Clinical and Biochemical Luminescence" (L. J. Kricka and T. J. N. Carter, eds.), p. 219. Dekker, New York, 1982.
[5] P. E. Stanley, *J. Biolumin. Chemilumin.* **7,** 77 (1992).
[6] P. E. Stanley, *J. Biolumin. Chemilumin.* **7,** 157 (1992).
[7] P. E. Stanley, *J. Biolumin. Chemilumin.* **8,** 237 (1993).
[8] P. E. Stanley, *J. Biolumin. Chemilumin.* **9,** 51 (1994).
[9] P. E. Stanley, *J. Biolumin. Chemilumin.* **9,** 123 (1994).
[10] P. E. Stanley, *J. Biolumin. Chemilumin.* **11,** 175 (1996).
[11] P. E. Stanley, *J. Biolumin. Chemilumin.* **12,** 61 (1997).
[12] P. E. Stanley, *Luminescence* **14,** 215 (1999).

Copyright © 2000 by Academic Press
All rights of reproduction in any form reserved.
METHODS IN ENZYMOLOGY, VOL. 305
0076-6879/00 $30.00

SPECTRAL_0000592

Luminometers typically comprise a photomultiplier that is operated either as a current measuring device or, more commonly now, as a photon counting device, a sample chamber to hold a cuvette or other container, perhaps a device(s) for injecting reagents automatically into the cuvette either before placing it in the sample chamber or while in the darkened sample chamber itself. Automatic sampling handling may also be featured.

In the last decade or so there has been a move toward multisample processing and the use of a personal computer to control the instrument and also software to deal with the data produced. There has also been an increase in sensitivity of the instruments by virtue of improved optics as well as photomultiplier performance.

Some luminometers are now available that are designed for a specific task or range of tasks; for example, hygiene testing in the food processing industry in which microbial adenosine triphosphate is measured with firefly luciferase built into a disposable unit within the luminometer. Another example would be luminometers designed for toxicity assays using luminous bacteria or for testing water for the tracing of pollutants.

A major change that has occurred in the last decade is the ever increasing number of microtiter plate luminometers coming to the marketplace. Some are designed to measure BL or CL which exhibit glow luminescence whereas others will measure BL and CL with either glow or flash luminescence. Some manual or semiautomatic cuvette luminometers will measure glow or both glow and flash luminescence.

So-called glow luminescence occurs when the light output from the reaction remains more or less constant over many tens of seconds (often minutes or even hours). In this situation, light measurement can be made comfortably at any reasonable time during the glow period. In contrast, flash luminescence occurs when the light output rises to a maximum and then falls rather quickly; the whole process may take only a very few seconds. In this situation, the time when the light measurement is made is of critical importance. In measurements involving flash luminescence there must be consistency in timing and reagent mixing, and injector design plays an important role. Luminometers only able to measure glow reactions may not be equipped with automatic injectors. At present, luminometers are available for 96- to 384-well plates and beyond. A feature that should be addressed in choosing a microtiter plate luminometer is its ability to discriminate the signal produced by adjacent wells, so-called cross-talk. It may be that one well is producing many photons while the adjacent one is producing none at all. A unit with good cross-talk characteristics will discriminate the light generated by the two wells and show minimum spill of light from the bright well into the dark well. Another important feature is the ability of the injectors to ensure good mixing of reagents in the well

SPECTRAL_0000593

while avoiding splashing. Some workers require the microtiter plate to be temperature controlled and this feature is not always available as an option. A number of manufacturers of microtiter plate luminometers provide models that may be used in conjunction with robotic systems to enable large numbers of samples to be processed, which are finding considerable usage by those workers engaged in high throughput screening in the pharmaceutical discovery arena.

Automatic injection of reagents is often considered a very desirable feature. Care should be taken in choosing a system with the following points in mind: ease of cleaning; sterilizability, if needed; ease of disassembly; and ease of replacement of disposable parts. Some injectors have software that will permit control of the injected volume as well as variation of the injection rate. Others have a simple single injection volume that is not variable by the user.

There is a very wide range of software available, either built-in or available as an option. Sometimes the software is available on a PC or a Mac computer that is connected to, and may also operate, the luminometer.

A number of low-level light imaging systems are now available. These are used for the two-dimensional imaging of, for example, chemiluminescent gels, and some have software to assay the bands. Some systems can be connected to a microscope so that bio- or chemiluminescence produced by cells can be assessed. In the list that follows are a number of companies that produce high-sensitivity charge-coupled device (CCD) cameras that may be built into custom designed instruments.

New models of luminometers are now being introduced into the marketplace at a steady rate and some older models are inevitably withdrawn from time to time. Consequently, a contribution such as this becomes outdated rather quickly. The following list of manufacturers was compiled in August 1998 and adjusted in January 2000 to take account of some changes to company names and contact details. See Reference 12 for more detailed information about some current instruments. Contact details are given together with a brief mention of the types of luminometers they currently provide.

When choosing a luminometer or CCD imaging system the purchaser would be advised to test the competing instruments in his laboratory with his own reagents and ancillary equipment.

Manufacturers of Luminometers

Although the list is extensive, the author does not guarantee that it is comprehensive, complete, or free from errors. Instruments not included in this list are (1) large automatic dedicated luminometers used in clinical

SPECTRAL_0000594

laboratories for immunoassays and (2) imaging systems based on phosphor screen detectors.

Anthos Labtec Instruments GmbH, Lagerhausstrasse 507, A-5071 Wals/Salzburg, Austria
Tel: +43 662 857-220; Fax: +43 662 857-223

Microtiter plate luminometers

ATTO Corporation, 2-3, Hongo 7-chome, Bunkyo-Ku, Tokyo 113, Japan
Tel: +81 3 3814 4861; Fax: +81 3 3814 4868

Microtiter plate luminometer

Azur Environmental, 2232 Rutherford Road, Carlsbad, CA 92008
Tel: +1 619 438-8282; Fax: +1 619 438-2980

Specialized luminometers for toxicity testing

BBI-Source Scientific, Inc., 7390 Lincoln Way, Garden Grove, CA 92841
Tel: +1 714 898-9001; Fax: +1 714 891-1229

Luminometers

Berthold Detection Systems GmbH, Bleichstrasse 3A, D-75173 Pforzheim, Germany
Tel: +49 7231 92060; Fax: +49 7231 920650

High sensitivity luminometer, microtiter plate luminometer

Bio-Orbit Oy, P.O. Box 36, FIN-20521 Turku, Finland
Tel: +358 2 410-1100; Fax: +358 2 410-1123

Luminometers, manual and automatic, microtiter plate

Bio-Rad, Inc., 1000 Alfred Nobel Drive, Hercules, CA 94547
Tel: +1 510 724-7000; Fax: +1 510 741-5817

CCD imaging system and microtiter plate system

Bioscan, Inc., 4590 MacArthur Bvld. NW, Washington, DC 20007
Tel: +1 202 338-0974; Fax: +1 202 338-8514

Luminometer

BioThema AB, Strandvägen 36, S-130 54 Dalarö, Sweden
Tel: +46 8501 51641; Fax: +46 8501 50952

Portable luminometer

Biotrace Ltd., The Science Park, Bridgend, CF31 3NA, UK
Tel: +44 1656 768844; Fax: +44 1656 768835

Specialized luminometers for hygiene and similar assays in food and allied industries

BMG-LabTechnologies GmbH, Hanns-Martin-Schleyer-Strasse 10, D-77656 Offenburg, Germany
Tel: +49 781 969-680; Fax: +49 781 969-6867

Microtiter plate luminometer

SPECTRAL_0000595

Boehringer-Mannheim GmbH, Sandhoffer Strasse 116, D-68305 Mannheim, Germany
Tel: +49 621 7598545; Fax: +49 621 7598830

Imaging device for analysis of blots and microtiter plates

Camspec Ltd., 11 High Street, Sawston, Cambridge CB2 4BG, UK
Tel: +44 1223-8326971; Fax: +44 1223-836414

Chemiluminescence detector for HPLC

Capitol Controls Ltd., 8 Hawksworth, Southmead Industrial Park, Didcot, Oxfordshire OX11 7HR, UK
Tel: +44 1235-512000; Fax: +44 1235-512020

Specialized luminometer for water pollution assays

Cardinal Associates Inc., P.O. Box 5220, Santa Fe, NM 87502
Tel: +1 505 473-0033; Fax: +1 505 473-5637

Microtiter plate luminometer

Celsis · Lumac, Cambridge Science Park, Milton Road, Cambridge CB4 4FX, UK
Tel: +44 1223 426008; Fax: +44 1223 426003

A range of specialized luminometers for hygiene assays in food and allied industries

Charm Sciences Inc., 36 Franklin Street, Malden, MA 02148
Tel: +1 617 322-1523; Fax: +1 617 322-3141

A range of specialized luminometers for hygiene assays in food and allied industries

CLIMBI Ltd., P.O. Box 20, Moscow 125422, Russia
Tel: +7 095-976-4055; Fax: +7 095-976-7586

Portable and manual luminometer

ConCell BV, Wevelinghoven 26, D-41334 Nettetal, Germany
Tel: +49 2153 911-833; Fax: +49 2153 911-835

Specialized luminometer for hygiene and similar assays in food and allied industries

Cypress Systems, Inc., 2500 West 31st Street, Suite D, Lawrence, KS 66047
Tel: +1 913 842-2511; Fax: +1 913 832-0406

Luminometer for hygiene and environmental monitoring

Dr Bruno Lange GmbH Berlin, Willstättersreasse 11, D-40549 Düsseldorf, Germany
Tel: +49 211-52-880; Fax: +49 211-52-88175

Specialized luminometers for toxicity testing

Dynex Technologies Inc., 14340 Sullyfield Circle, Chantilly, VA 20151
Tel: +1 703 631-7800; Fax: +1 703 631-7816

A range of microtiter plate luminometers

SPECTRAL_0000596

Electron Tubes Ltd., Bury Street, Ruislip, Middlesex HA4 7TA, UK
Tel: +44 1895-630771; Fax: +44 1895-635953

Manufacturer of photomultipliers and associated equipment

F.A.T. Research Institute for Antioxidant Therapy Ltd., Chausseestrasse 8, D-10115 Berlin, Germany
Tel: +49-30-39789376; Fax: +49-30-39789386

Specialized luminometers for assay of antioxidants.

GEM Biomedical, MGM Instruments, 925 Sherman Avenue, Hamden, CT 06514
Tel: +1 203 248-4008; Fax: +1 203 288-2621

A range of luminometers (manual, automatic, and microtiter plate) and hygiene and reporter genes

Hamamatsu Photonics K.K., 314-5 Shimokanzo, Toyooka-village, Iwata-gun, 436-01 Japan
Tel: +81 539-62-5248; Fax: +81 539-62-2205

Manufacturers of photomultipliers and associated equipment and of CCD imaging systems

Hughes Whitlock Ltd., Wonostow Road, Singleton Court, Monmouth, Gwent NP5 3AH, UK
Tel: +44 1600-715632; Fax: +44 1600-715674

Specialized luminometer for hygiene and similar assays in food and allied industries

IDEXX Laboratories, Inc., One IDEXX Drive, Westbrook, ME 04092
Tel: +1 207 856-0300; Fax: +1 207 856-0630

Specialized luminometer for hygiene and similar assays in food and allied industries

Imaging Associates, 8 Thame Park Business Centre, Wenman Road, Thame, Oxfordshire OX9 3XA, UK
Tel: +44 1844-213790; Fax: +44 01844-213644

CCD cameras and imaging systems

Kikkoman Corporation, 399 Noda, Noda City, Chiba Pref, 278 Japan
Tel: +81 471 23 5517; Fax: +81 471 23 5959

Luminometer for hygiene testing

Labsystems Oy, P.O. Box 8, FIN-00881 Helsinki, Finland
Tel: +358 9 329 100; Fax: +358 9 3291 0312

Microtiter plate luminometers and tube luminometer

Labtech International Ltd., 1 Acorn House, The Broyle, Ringmer, East Sussex BN8 5NW, UK
Tel: +44 1273 814-888; Fax: +44 1273 814-999

Manual luminometer, microtiter plate luminometer; hygiene monitoring

Mediators Diagnosticka GmbH, Simmeringer Haupstrasse 24, A-1100 Vienna, Austria
Tel: +43 1 740-40-350; Fax: +43 1 740-40-359

Microtiter plate luminometer

SPECTRAL_0000597

Merck KgaA, Frankfurterstrasse 250, 64271 Darmstadt, Germany
Tel: +49 6151 725410; Fax: +49 6151 723380

Specialized luminometer for hygiene testing of foods and similar products

Millipore Corporation, 80 Ashby Road, Bedford, MA 01730
Tel: +1 617 275-9200; Fax: +1 617 533-2889

Specialized luminometers for microbiological testing of foods and similar products; also CCD camera for sterility testing using filters

Molecular Devices Corporation, 1311 Orleans Drive, Sunnyvale, CA 94089
Tel: +1 408 747-1700; Fax: +1 408 747-3602

Specialized CCD imaging microtiter plate reader

New Horizons Diagnostics Corporation, 9110 Red Branch Road, Columbia, MD 21045
Tel: +1 410 992-9357; Fax: +1 410 992-0328

Specialized luminometers mainly for food safety and sanitation

Packard Instrument Co., 800 Research Parkway, Meriden, CT 06450
Tel: +1 203 238-2351; Fax: +1 203 639-2172

Microtiter plate luminometers

PerkinElmer Berthold, P.O. Box 100163, D-75312 Bad Wildbad, Germany
Tel: +49 7081 1770; Fax: +49 7081 177166

A wide range of manual and automatic luminometers, microtiter plate luminometers, CCD imaging unit for blots, microtiter plates, etc.

PerkinElmer Wallac, P.O. Box 10, FIN-20101 Turku, Finland
Tel: +358 2-2678-111; Fax: +358 2-267-8357

A range of microtiter plate luminometers and CCD imaging units for blots, microtiter plates, etc.

Photek Ltd., 26 Castleham Road, St. Leonards-on-Sea, East Sussex TN38 9NS, UK
Tel: +44 1424-850555; Fax: +44 1424-850051

Manufacturer of photomultipliers, image intensifiers, and custom-built CCD cameras

Photonic Science Ltd., Millham, Mountfield, Robertsbridge, East Sussex TN32 5LA, UK
Tel: +44 1580 881199; Fax: +44 1580 880910

Manufacturer of specialized CCD cameras and imaging systems

Randox Laboratories Ltd., Diamond Road, Crumlin, Co. Antrim, UK
Tel: +44 1849-422413; Fax: +44 1849-422413

Specialized luminometer for water quality assays

SPECTRAL_0000598

Roper Scientific, Tucson Office: 3440 East Britannia Drive, Tucson, AZ 85706
Tel: +1 602 889-9933; Fax: +1 602 573-1944
Trenton Office: 3660 Quakerbridge Road, Trenton, NJ 08619
Tel: +1 609 587-9797; Fax: +1 609 587-1970

Manufacturer of specialized CCD cameras and imaging systems

St. John Associates, Inc., 4806 Price George's Avenue, Beltsville, MD 20705
Tel: +1 301 595-5605; Fax: +1 301 595-2738

Manual luminometer for cuvettes and flow

STRATEC Electronic GmbH, Gewerbestrasse 11, D-75217 Birkenfeld 2, Germany
Tel: +49 7082-79160; Fax: +49 7082-20559

Manual luminometer and microtiter plate luminometer

TECAN Austria GmbH, Untersbergstrasse 1A, 5082 Grödig/Salzburg, Austria
Tel: +43 6246 8933; Fax: +43 6246 72770

Microtiter plate instruments

Tropix, Inc., 47 Wiggins Avenue, Bedford, MA 01730
Tel: +1 617 271-0045; Fax: +1 617 275-8581

Microtiter plate luminometer

Turner Designs, 845 W. Maude Avenue, Sunnyvale, CA 94086
Tel: +1 408 749-0994; Fax: +1 408 749-0998

Manual luminometer

Valbiotech, 57 bvd de la Villette, F-75010 Paris, France
Tel: +33 1 40 03 89 14; Fax: +33 1 44 52 92 69

Microtiter plate luminometer

Wright Instruments Ltd., Unit 10, 26 Queensway, Enfield, Middlesex EN3 4SA, UK
Tel: +44 181-4433339; Fax: +44 181-4433638

CCD cameras

Zylux Corporation, 1742 Henry G. Lane Street, Maryville, TN 37801
Tel: +1 423 379-6016; Fax: +1 423 379-6018

Manual luminometer and microtiter plate luminometer

SPECTRAL_0000599

UCLA Library | Search | WorldCat

WorldCat (Sign in)

Off-Campus Access
UCLA Library Catalog
A-Z List of Databases
E-journals
Ask a Librarian
Return to Search Results

Search

Libraries to search: Libraries Worldwide | Advanced Search

Cite/Export | Print | E-mail | Add to list | Share | Permalink | Ask a Librarian

High-speed radiometric imaging with a gated, intensified, digitally-controlled camera[2869-29]

Chat with a librarian
More like this

Author: C C Ross; R A Sturz

Edition/Format: Article : English

Publication: PROCEEDINGS- SPIE THE INTERNATIONAL SOCIETY FOR OPTICAL ENGINEERING, no. 2869, (1996): 386-394

Database: British Library Serials

Search this publication for other articles with the following words:
Search

Find a copy online

Get this article

UC eLinks

Find a copy in the library

University of California Libraries

Get it from this library group

3 group libraries own this item

UC Berkeley Libraries — check availability for this item

UC Davis Libraries — check availability for this item

UC Santa Cruz Library — check availability for this item

WorldCat

Find it in libraries globally

Worldwide libraries own this item

Buy it

Details

Document Type:	Article
All Authors / Contributors:	C C Ross; R A Sturz
ISSN:	0361-0748
BL Shelfmark:	6823.100000
OCLC Number:	198456222
Language Note:	English

Reviews

User-contributed reviews

Tags

Add tags for "High-speed radiometric imaging with a gated, intensified, digitally-controlled camera[2869-29]". Be the first.

Similar items

User lists with this item ()

Languages: Deutsch | English | Español | Français | Nederlands | 中文
You: Sign in | Register | My WorldCat | My Lists | My Watchlist | My Reviews | My Tags | My Saved Searches
WorldCat: Home | About | Help | Get E-mail Updates | Feedback | Search | WorldCat Blog
Legal: Copyright © 2001-2010 OCLC. All rights reserved. | Privacy Policy | Terms and Conditions

WorldCat is the world's largest library catalog, helping you find library materials online.

Journal of Biomedical Optics 6(4), 432–440 (October 2001)

In vivo imaging of light-emitting probes

B. W. Rice
M. D. Cable
M. B. Nelson
Xenogen Corporation
860 Atlantic Avenue
Alameda, California 94501

Abstract. *In vivo* imaging of cells tagged with light-emitting probes, such as firefly luciferase or fluorescent proteins, is a powerful technology that enables a wide range of biological studies in small research animals. Reporters with emission in the red to infrared (>600 nm) are preferred due to the low absorption in tissue at these wavelengths. Modeling of photon diffusion through tissue indicates that bioluminescent cell counts as low as a few hundred can be detected subcutaneously, while $\sim 10^6$ cells are required to detect signals at ~2 cm depth in tissue. Signal-to-noise estimates show that cooled back-thinned integrating charge coupled devices (CCDs) are preferred to image-intensified CCDs for this application, mainly due to their high quantum efficiency (~85%) at wavelengths >600 nm where tissue absorption is low. Instrumentation for *in vivo* imaging developed at Xenogen is described and several examples of images of mice with bioluminescent cells are presented. © *2001 Society of Photo-Optical Instrumentation Engineers.* [DOI: 10.1117/1.1413210]

Keywords: imaging; bioluminescence; luminescence; fluorescence; luciferase; *in vivo*.

Paper 080379 received Jan. 26, 2001; revised manuscript received July 16, 2001; accepted for publication July 17, 2001.

1 Introduction

The use of light-emitting probes, such as luciferase or fluorescent proteins, as a reporter of gene expression in living cells is a well-established technique for the study of biological activity.[1] Such probes have been widely used *in vitro* where light detection is easily accomplished using standard photomultiplier tubes or inexpensive charge coupled device (CCD) arrays for imaging applications. Detection of light-emitting probes *in vivo* within small living animals is also possible due to the semitransparent nature of mammalian tissue,[2–5] but improved instrumentation is required, consisting of high-sensitivity low-noise detectors, a more advanced imaging system, and sophisticated software tools for interpreting images.

The ability to track light-emitting cells in small laboratory animals such as mice or rats opens up a wide range of applications in pharmaceutical and toxicological research. These include *in vivo* monitoring of infectious diseases, tumor growth and metastases, transgene expression, compound toxicity, and viral infection or delivery systems for gene therapy. The ability to detect signals in real time in living animals means that the progression of a disease or biological process can be studied throughout an experiment with the same set of animals without the traditional need to sacrifice for each data point. This results in higher quality data using fewer animals and ultimately will speed the process of screening compounds leading to more rapid drug discovery.

Compared with more traditional structural imaging modalities such as magnetic resonance imaging (MRI) or computed tomography (CT), *in vivo* bioluminescent imaging offers several advantages. From a practical standpoint, bioluminescent/fluorescent imaging systems are lower cost, have shorter imaging times of <5 min, are easier to use by the nonspecialist, and can image multiple animals at once. In terms of quantitation, MRI/CT systems provide structural size information only, whereas bioluminescent signals provide information about both the location and number of metabolically active cells. Detection of infections in soft tissue such as bacterial pneumonia is also easily accomplished with bioluminescence and is not possible with MRI/CT. Finally, bioluminescent or fluorescent reporters linked to tissue-specific gene promoters provide functional and spatial information on gene expression, opening up an exciting area of research using light-producing transgenic animals.

In this paper, we examine the photonic issues associated with *in vivo* imaging and describe the design of instrumentation that has been optimized for this application. More specifically, we discuss briefly the tagging of cells with light-emitting markers and look at the trade-offs between bioluminescent and fluorescent probes. The basic physics issues associated with the diffusion of light through tissue are reviewed, along with the spectral properties of tissue. Design of *in vivo* imaging instrumentation and selection of a CCD is presented, using the general purpose *in vivo* imaging system (IVIS™) developed at Xenogen as an example. Finally, calibration and signal-to-noise issues are addressed, illustrated using several examples of *in vivo* images of mice. Most of the photon diffusion and instrumentation design issues discussed in this paper are common to both bioluminescence and fluorescence applications; however, the majority of calculations and image examples in the later part of this paper are for bioluminescent tags (luciferase) because that has been the focus of most of our work to date at Xenogen.

2 Light-Emitting Reporters

For most *in vivo* imaging applications, it is desirable to use genetic light-emitting reporters that propagate with the la-

Address all correspondence to Brad Rice. Tel: 510-291-6182; Fax: 510-291-6136; E-mail: brice@xenogen.com

1083-3668/2001/$15.00 © 2001 SPIE

SPECTRAL_0000602

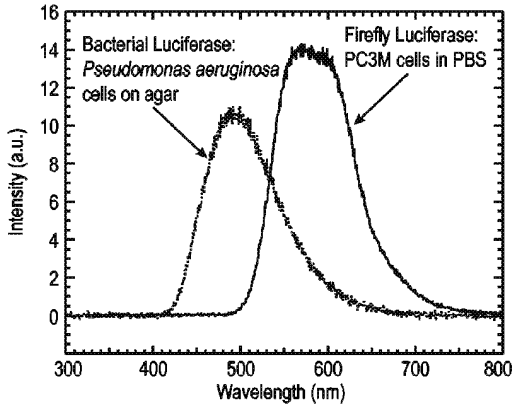


Fig. 1 Spectral emission measurements for bacterial luciferase in *Psuedomonas aeruginosa* and firefly luciferase in PC-3M-*luc* protstate tumor cells. The bacteria is measured on agar while the PC3M cells are measured in a phosphate buffered solution.

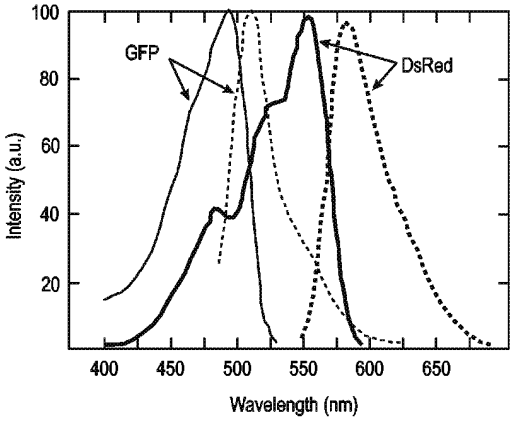


Fig. 2 Excitation (solid) and emission (dashed) spectra for fluorescent proteins GFP and DsRed (Clonetech Living Colors™ fluorescent proteins).

beled cells as they multiply in an animal. This avoids problems with signal dilution that would be associated with cell division when using exogenous dyes, for example. Luciferases and fluorescent proteins are two common genetic markers. The luciferase enzyme, when combined with the substrate luciferin, oxygen, and ATP, generates light through a chemical reaction resulting in bioluminescence.[1,6] In the case of fluorescent proteins, the tagged cells must be illuminated with an excitation source in order to fluoresce.

Bioluminescence in mammalian (eukaryotic) cells is accomplished by incorporating the *luc* gene into the cell's DNA in order to express the luciferase enzyme. A required substrate, luciferin, is added exogenously and distributes quickly (within minutes) throughout the entire animal. The *luc* gene originates from the North American firefly, *Photinus pyralis*, and produces light at an emission peak at ~560 nm. In prokaryotic cells, the luciferase *lux* gene from soil bacterium (*Photorhabdus luminescens*) along with substrate-encoding genes are incorporated into the targeted cell so that both luciferase and luciferin are produced endogenously. The spectra for both types of luciferase are shown in Figure 1. The firefly luciferase is especially attractive for *in vivo* imaging because the spectrum is very broad and contains a large component above 600 nm where transmission through tissue is higher (see Sec. 3).

Two common fluorescent proteins are green fluorescent protein and red fluorescent protein or DsRed. The excitation and emission spectra for each are shown in Figure 2. Again, the DsRed is more attractive for *in vivo* applications because there is significant emission above 600 nm. Note, however, that the excitation remains in the 500–575 nm range where tissue absorption is very high.

Bioluminescence has an advantage over fluorescence as an *in vivo* reporter in that no external light source is required for excitation. This means that background levels are very low compared to those of fluorescent proteins where significant autofluorescence of the tissue surface results from the use of high power external excitation light sources, especially in cases where the luminescent cells are deep in the tissue. Another advantage of bioluminescence is that signals are more easily quantitated because, for tagged cells at a fixed location, the signal level observed on the surface of the animal is directly proportional to the number of cells. In the case of fluorescence, the signal level is related to both the number of cells and the intensity of excitation light, which is difficult to quantify because the excitation light is strongly absorbed as it passes into tissue. In most cases, fluorescent proteins require excitation in the green part of the spectrum where tissue absorption is particularly high. Despite these complications, researchers have made progress in developing diffuse optical tomography codes that treat the propagation of both the excitation and emission through tissue.[7]

For *in vitro* applications, where cells are not embedded in tissue, fluorescent proteins have an advantage since they are usually brighter than bioluminescent reporters provided that the excitation source is bright enough. It is generally easier to observe individual cells *in vitro* using fluorescence compared with bioluminescence.

3 Photon Diffusion in Tissue

Mammalian tissue is a turbid medium that both scatters and absorbs photons.[8] Photons are scattered due to changes in refractive index at cell membranes and internal organelles. Absorption varies greatly with the type of cell or tissue, but is generally affected by the presence of hemoglobin, which absorbs strongly in the blue-green region of the visible spectrum, but is fairly transparent in the red at wavelengths >600 nm. Typically, for $\lambda > 600$ nm, the $1/e$ absorption length is ~2 cm, while the effective length for scattering is much shorter at ~0.05 cm (see Refs. 8 and 9 for a review of the optical properties of tissue). In this regime, where scattering is dominant, a significant amount of bioluminescent emission can escape the tissue, but the emission is highly diffuse as illustrated schematically in Figure 3.

In order to predict *in vivo* imaging signal levels and spatial resolution as a function of depth, and to help define the requirements for imaging instrumentation, it is important to have a quantitative model for the diffusion of photons in tissue. For the case of homogeneous tissue where the scattering length is short compared with the absorption length (generally true in tissue for $\lambda > 600$ nm), photon propagation is well de-

SPECTRAL_0000603

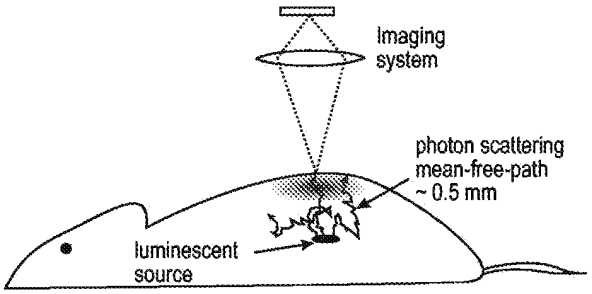


Fig. 3 *In vivo* imaging systems view diffuse (scattered) light emitted from an embedded source. The imaging system focuses on the surface of the animal.

scribed by a diffusion model.[10] In this model, for continuous waves, the photon fluence ϕ (W/cm^2) decays exponentially away from a point source according to

$$\phi(\mathbf{r}) = \frac{P}{4\pi D r}\exp(-\mu_{\text{eff}} r), \tag{1}$$

where r is the distance away from the source, P is the source power, D is the diffusion coefficient given by $D = 1/[3(\mu_s' + \mu_a)]$, and $\mu_{\text{eff}} = \sqrt{3\mu_a(\mu_s' + \mu_a)}$ where μ_s' is the reduced scattering coefficient (cm^{-1}) and μ_a is the absorption coefficient (cm^{-1}) for the tissue. The reduced scattering coefficient μ_s' is related to the scattering coefficient through $\mu_s' = (1-g)\mu_s$, where g is the average cosine of the scattering angle. The scattering angle in tissue is usually small giving $g \sim 0.9$. The radiance L (W/cm^2/sr) in tissue along a unit vector $\hat{s}$ is given by[11]

$$L(\mathbf{r},\hat{s}) = \frac{1}{4\pi}[\phi(\mathbf{r}) + 3\mathbf{j}(\mathbf{r})\cdot\hat{s}], \tag{2}$$

where $\mathbf{j}(\mathbf{r})$ is the flux, which is related to the fluence through $\mathbf{j}(\mathbf{r}) = -D\nabla\phi(\mathbf{r})$.

Consider the case of an imaging system viewing down on a homogeneous slab of turbid media with an embedded source as shown in Figure 4. The radiance observed at the tissue

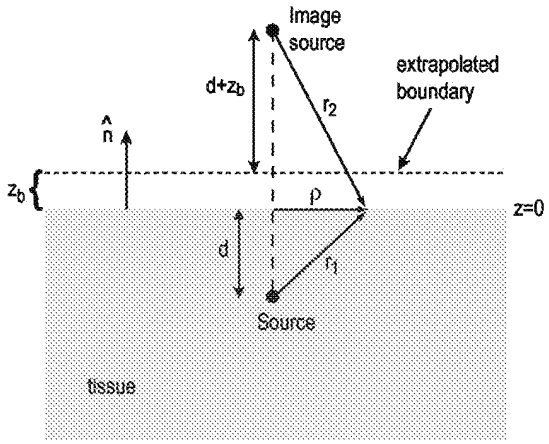


Fig. 4 Geometry for the extrapolated boundary photon diffusion model. The extrapolated boundary is a distance z_b above the actual tissue surface.

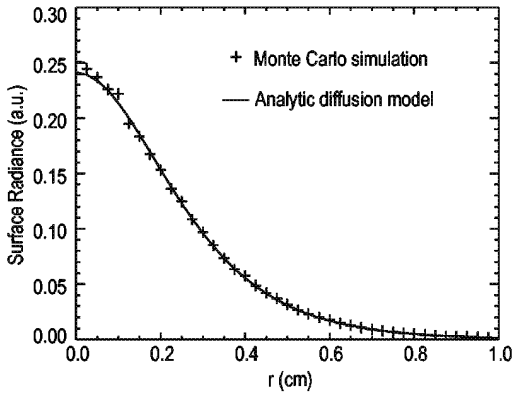


Fig. 5 Surface radiance profile calculated from extrapolated boundary diffusion model (line) and from Monte Carlo simulations (plus symbol). Parameters for this simulation are $d = 4$ mm, $\mu_a = 0.5$ cm^{-1}, $\mu_s' = 15$ cm^{-1}.

surface can be calculated from Eqs. (1) and (2) above with appropriate boundary conditions. Here we use the extrapolated boundary condition,[11] which is fairly simple and has been shown to agree well with Monte Carlo simulations and measurements. In this case, an image source is reflected about a plane located a distance z_b above the surface as shown in Figure 4, where

$$z_b = \frac{1+R_{\text{eff}}}{1-R_{\text{eff}}}\frac{2}{3(\mu_a+\mu_s')} \tag{3}$$

and R_{eff} is the effective reflection coefficient averaged over all angles of incidence at the boundary.[11] The photon fluence at the boundary is the sum of the contribution from the source and its image

$$\phi(z=0) = \frac{P}{4\pi D}\left[\frac{\exp(-\mu_{\text{eff}} r_1)}{r_1} - \frac{\exp(-\mu_{\text{eff}} r_2)}{r_2}\right] \tag{4}$$

and the normal derivative of the fluence is given by

$$\frac{\partial\phi}{\partial z}(z=0) = \frac{-P}{4\pi D}\left[\frac{d}{r_1^2}\left(\mu_{\text{eff}} + \frac{1}{r_1}\right)\exp(-\mu_{\text{eff}} r_1) + \frac{d+2z_b}{r_2^2}\left(\mu_{\text{eff}} + \frac{1}{r_2}\right)\exp(-\mu_{\text{eff}} r_2)\right], \tag{5}$$

where $r_1 = [\rho^2 + d^2]^{1/2}$ and $r_2 = [\rho^2 + (d+2z_b)^2]^{1/2}$ and d is the source depth. Inserting Eqs. (4) and (5) into Eq. (2) gives the surface radiance

$$L_{z=0} = \frac{1}{4\pi}\left(\frac{P}{4\pi D}\right)\left\{\frac{\exp(-\mu_{\text{eff}} r_1)}{r_1} - \frac{\exp(-\mu_{\text{eff}} r_2)}{r_2} + 3D\left[\frac{d}{r_1^2}\left(\mu_{\text{eff}} + \frac{1}{r_1}\right)e^{-\mu_{\text{eff}} r_1} + \frac{d+2z_b}{r_2^2} \times \left(\mu_{\text{eff}} + \frac{1}{r_2}\right)e^{-\mu_{\text{eff}} r_2}\right]\right\}. \tag{6}$$

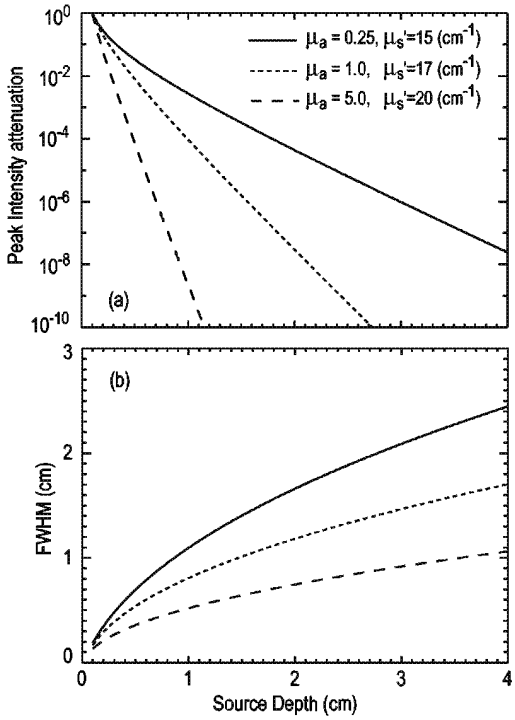


Fig. 6 Calculation of peak intensity (a) and full width at half maximum (FWHM) (b) as a function of source depth for three sets of tissue parameters corresponding roughly to 650 nm (solid), 590 nm (short dash), and 550 nm (long dash). The intensity curves are normalized to one at 1 mm depth.

Equation (6) is plotted as a function of ρ in Figure 5 for typical tissue scattering and absorption parameters. For comparison, a Monte Carlo calculation of the surface profile is also shown, performed using a modified version of the MCML code.[12] For these parameters the agreement between the Monte Carlo and the analytical diffusion model is quite good.

A real animal is neither homogeneous nor a slab shape, but, nevertheless, for source depths that are small compared to the radius of the animal, the above diffusion model can be used to get reasonably good qualitative estimates of signal level and spot size as a function of source depth. In Figure 6(a) the peak radiance ($\rho = 0$) obtained from Eq. (6) is plotted as a function of source depth for three sets of tissue parameters, corresponding roughly to green (550 nm), orange (590 nm), and red (650 nm) wavelengths. At a 1 cm depth the peak signal is attenuated by $\sim 10^{-2}$ for wavelengths at ~650 nm while the attenuation is very large $\sim 10^{-10}$ for shorter wavelengths (~550 nm). Clearly, to observe signals from deep inside the tissue, it is essential to have high sensitivity in the red and near-infrared part of the spectrum. The spot size, or full width at half maximum, of the surface radiance profile is plotted in Figure 6(b). Although wavelengths >600 nm provide much higher signal levels, the trade-off is that the spot size is larger and hence spatial resolution is worse. We note that spatial resolution can actually be much better than the surface spot size indicated in Figure 6(b) if we use the diffusion model with an appropriate fitting algorithm to reconstruct the location and size of the original internal light source.

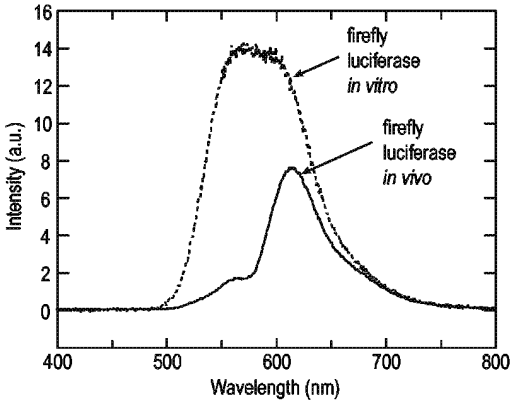


Fig. 7 *In vitro* (dashed) and *in vivo* (solid) spectral measurements for firefly luciferase in PC-3M-*luc* protstate tumor cells. *In vivo* measurements are for a subcutaneous thigh tumor in a nude mouse.

The fact that the absorption coefficient μ_a varies with wavelength results in a redshifting of the peak of the luciferase emission spectrum *in vivo* compared with *in vitro*. In Figure 7 we compare the yellow-green firefly (*Photinus pyralis*) luciferase spectrum measured *in vitro* in PBS with a subcutaneous tumor *in vivo* in a nude mouse. The host cell is the PC-3M-*luc* prostate tumor cell line. The strong attenuation of the signal at wavelengths<600 nm is apparent and is characteristic of the hemoglobin absorption spectrum. In Figure 7, the tumor is only ~0.5–1 mm deep so some of the emission below 600 nm is still present; however, for sources deeper in tissue, located in internal organs such as the liver, kidney, and lungs, the emission below 600 nm would be completely extinguished.

4 CCD Selection

Selection of the proper CCD camera is critical for *in vivo* imaging applications. As seen in Figures 6 and 7, the CCD camera must have high sensitivity or quantum efficiency at wavelengths >600 nm and must have the lowest noise possible in order to detect sources up to a few centimeters deep. An image intensified photon counting CCD camera is one popular choice for many bioluminescent applications. The high-gain image intensifier allows individual photons to be counted with very little noise. However, these cameras, frequently equipped with bialkali photocathodes, suffer from relatively low quantum efficiency (QE) of just 10%–15% at 450 nm, dropping to less than 1% at 650 nm as shown in Figure 8 (Hamamatsu C2400-30 Series). Multialkali (S20) and GaAs photocathodes are available that have higher QE above 600 nm, but these tend to have higher thermal noise and cooling issues and are not readily available with large detector areas. Photon counting electronics associated with image intensified systems typically have an electronic threshold that eliminates subthreshold signals and reduces noise. It has been our observation that this threshold can effectively reduce the QE further. Another practical difficulty with photon counting systems is that the count rate is limited by pulse width and counting electronics considerations resulting in

SPECTRAL_0000605

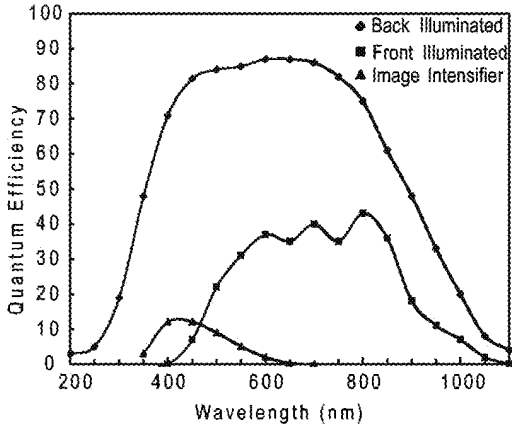


Fig. 8 Quantum efficiency for a bialkali photocathode (triangle), back illuminated (diamond), and front illuminated (square) integrating CCDs.

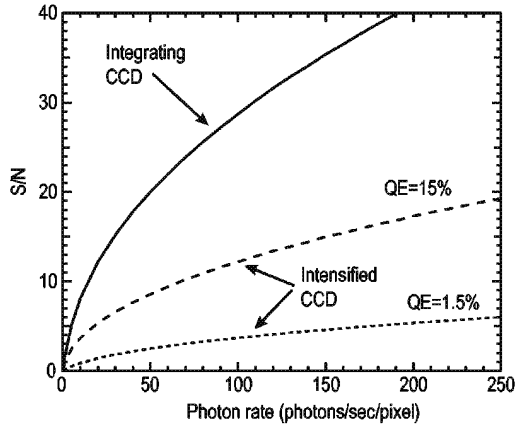


Fig. 9 Comparison of S/N for an integrating CCD (solid) and an intensified CCD (dashed). Two quantum efficiencies are plotted for the intensified CCD corresponding to $\lambda = 450$ nm (QE = 15%) and $\lambda = 600$ nm (QE = 1.5%).

limited dynamic range for bright signals. In this case, image brightness must be controlled through some external means such as apertures or neutral density filters.

A better CCD choice for *in vivo* applications is a cooled back-thinned (and back-illuminated) integrating CCD (e.g., Spectral Instruments 620 Series or Roper Scientific EEV 36-40b). These devices have very high quantum efficiency approaching 85% as shown in Figure 8, and the QE remains high in the red and near-IR spectral regions. Dark current can be a source of noise with integrating CCDs, but cooling the CCD to $-105\,^{\circ}$C reduces the dark current to near negligible levels, typically $<4\times10^{-4}$ e/s/pixel for 24 μm pixels. Until recently, cooling detectors to $-105\,^{\circ}$C required liquid nitrogen, but convenient cryogenic refrigerators have become available making operation at these temperatures relatively easy. There is also electronic noise associated with the CCD readout (read noise) of ~5 e rms that represents the minimum noise floor that the signal must exceed. Higher spatial resolution is another advantage of integrating CCDs. The Xenogen IVIS™ system typically uses a 25 mm CCD size with a 1024×1024 format and 24 μm pixels (formats 1300×1340 with 20 μm pixels and 2048×2048 with 13.5 μm pixels are also available).

Quantitative comparisons of image intensified versus integrating CCDs can be made by calculating the signal required to achieve a given signal-to-noise ratio for each device. The total noise for a given signal is the rms sum of the read noise, R_N, the noise associated with dark charge, D_c, and the statistical noise associated with the signal itself.[13] The signal and dark charge follow a Poisson distribution so the noise is simply the square root of the signal. The signal to noise can then be written as (all quantities are in units of electrons)

$$S_N \equiv \frac{S_e}{N} = \frac{S_e}{\sqrt{S_e + R_N^2 + D_c}}, \tag{7}$$

where S_e is the signal per pixel in electrons. Solving this equation for S_e gives

$$S_e = \frac{S_N\left(S_N + \sqrt{S_N^2 + 4(R_N^2 + D_c)}\right)}{2}. \tag{8}$$

The photon rate incident on a pixel is then given by $S_p = S_e/(Q_E\tau)$ where Q_E is the quantum efficiency and τ is the integration time. Note that amplifier and digitizer noise can also be considered in calculating signal/noise (S/N) at the CCD digitizer output. However, these noise sources are usually negligible relative to the quantities in Eq. (7) and therefore are not included in this analysis.

The signal in Eq. (7) can be increased relative to the read noise by binning pixels together prior to readout. A binning value of 5, for example, means that a 5×5 group of pixels is summed together to form one larger superpixel. In this case, the superpixel has an area of 25 times the original pixel and hence 25 times the signal (and dark current). The read noise remains roughly constant as binning is increased, so binning effectively increases the ratio of signal to read noise. This trade-off of spatial resolution for sensitivity is usually beneficial for *in vivo* imaging where signal levels are low and the diffuse images do not demand high spatial resolution.

A comparison of S/N from Eq. (7) for integrating and intensified CCDs is shown in Figure 9. For this figure we assume the high resolution CCD described above is binned to $\sim200\times200$ pixels, i.e., bin = 5. For integrating CCDs we have $R_N \sim 5$ electrons, $D_c \sim 0.01\tau$ electrons/pixel, and $Q_E \sim 0.85$. Photon counting CCDs do not have a dark current specification, but for a typical 26 mm bialkali photocathode there is a thermal emission of ~10 electrons/s/image which gives an effective dark current of $2.5\times10^{-4}\tau$ electrons/pixel. The read noise is assumed to be zero for the photon counting CCD and quantum efficiencies of 15% (~450 nm) and 1.5% (~600 nm) are plotted in Figure 9 for this device. For very low signals (S/N ~ 1), both the integrating and intensified (QE = 15%) CCDs give similar performance. However, at S/N ~ 10, the intensified CCD requires about five times as much signal as the integrating CCD. Physically, what is happening here is that for S/N ~ 1 the higher QE of the integrating system combined with higher read noise ends up giving essentially the same S/N for the same signal as the intensified

SPECTRAL_0000606

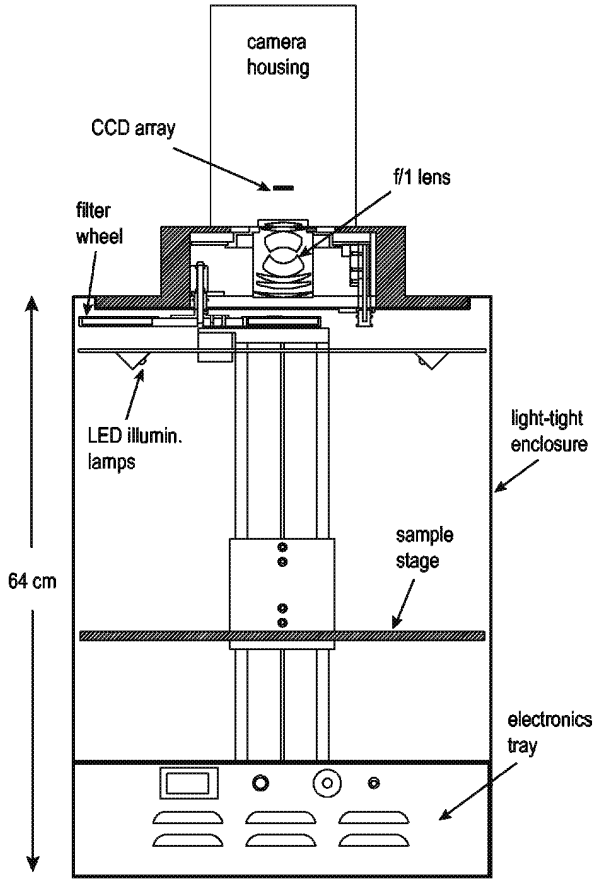


Fig. 10 Illustration of the IVIS™ imaging system.

CCD. But as the S/N increases to 10, the read noise and dark charge noise become negligible compared with the signal noise itself, and so the higher QE of the integrating system ends up giving better performance. As seen in Figure 9, at the red wavelengths of interest for *in vivo* imaging, the low QE gives very poor performance.

5 Imaging System Design

In consideration of the above arguments, a general purpose *in vivo* imaging system (IVIS™) has been developed at Xenogen based on a cooled back-illuminated integrating CCD. A schematic of the instrument is shown in Figure 10. The CCD camera is located on top of a light-tight imaging chamber. The door to the chamber is made extremely light tight through the use of a double baffle seal while the remainder of the enclosure is constructed in such a way as to minimize any penetrations into the box. Light is collected from the specimen and imaged onto the CCD using a fast 50 mm f/1 lens. The sample stage moves up and down to vary the field of view (FOV) from 10–25 cm. A seven-position filter wheel is also provided to enable spectral imaging capability. The sample stage, lens focus, f/stop, and filter wheel are all stepper motor controlled through Xenogen's Living Image® control software. Light-emitting diodes (LEDs) are located on the top plate to illuminate the specimen for photographic images. Other convenient features include a gas anesthesia system and a heated sample shelf to help maintain an animal's body temperature during anesthesia.

A typical *in vivo* image is shown in Figure 11 where 10^6 cells tagged with bacterial luciferase (*Strep. pneumonia*) were administered through the trachea with a ball-tipped needle. The sequence of steps required to produce this image can be summarized as follows. For the initial image (start of an experiment) bioluminescent cells are injected into the animal. If using firefly luciferase, then the luciferin substrate must also be injected prior to each image, while for bacterial luciferase the substrate is produced endogenously. The animal is then anesthetized with isoflurane and placed in the imaging chamber. A gas manifold with a nose cone is provided in the chamber to maintain anesthesia during imaging (see top of Figure 11). In a typical image sequence, the LEDs are turned on and a photographic image is acquired and displayed with a gray-scale color table, equivalent to black and white photograph. Then the LEDs are turned off and a longer exposure image of the bioluminescent (or fluorescent) light is taken. The bioluminescent image is overlaid on top of the photographic image using a pseudo-color intensity scale as seen in Figure 11, where red indicates the highest intensity and violet the lowest intensity. The exposure time and f stop were 0.2 s, f/8 for the photographic image and 30 s, f/1 for the bioluminescent image. Note that the individual lobes of the lungs can be distinguished in this image.

The units on the color bar in Figure 11 and all other images shown in this paper are analog-to-digital converter units, or ADU. The signal in ADU is related to the number of photoelectrons in a pixel by $S_{\mathrm{ADU}} = S_e G$ where G is the CCD amplifier gain. Typically, for the CCD cameras used in this study, $G \sim 1$ so it is appropriate to equate $S_{\mathrm{ADU}} \sim S_e$.

6 Calibration and Signal-to-Noise Estimates

Absolute intensity calibration of the CCD camera and overall imaging system is necessary to calculate brightness (in physical units) of luminescent cells and to estimate the number of cells inside an animal from the intensity of the surface image. To accomplish this, we utilize an absolutely calibrated 8 in. integrating sphere from Optronic Laboratories, Inc. (OL Series 425 Variable Low-Light-Level Calibration Standard). The integrating sphere is illuminated with a tungsten lamp, and the light level entering the sphere can be controlled using a set of reducing apertures and by moving the lamp away from the aperture. This combination allows very low radiance levels of $\sim 10^{-10}$ W/cm^2/sr (sr=steradian) across the 2 in. output aperture of the sphere. By imaging this aperture, counts detected by the CCD camera digitizer (ADU) can be converted to physical units of radiance in W/cm^2/sr or photons/s/cm^2/sr. The camera calibration depends on f-stop and shelf position. A typical calibration for a wide open lens (f/1) and a 15 cm FOV is 4×10^5 photons/s/sr/cm^2 at the object plane per ADU/s/pixel at the CCD (for 24 μm pixel size and $\lambda = 600$ nm.) To give an example of sensitivity, if we assume a 5 min image with binning of 8 (64 pixels grouped together to form a larger pixel) and a total noise of 7 ADU per binned pixel, then the minimum detectable radiance is

SPECTRAL_0000607

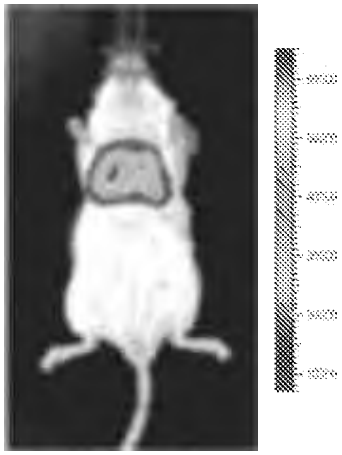


Fig. 11 Pneumonia model in a Balb/c mouse with 10^6 cells of *Strep. pneumoniae-xen*10 administered through the trachea. Image taken at 42 h with a 30 s integration time and binning=10. The pseudocolor bioluminescent image is overlaid on top of a grayscale photographic image of the mouse. Color bar units are in digitizer units, or ADU.

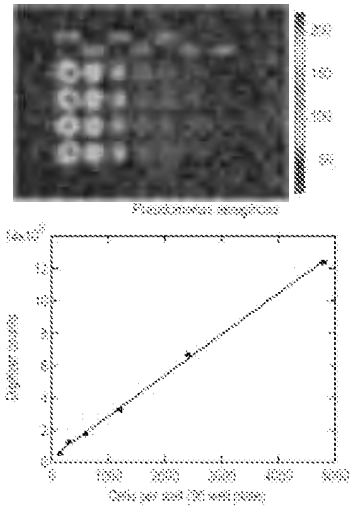


Fig. 12 Image of well plate containing *Pseudomonas aeruginosa* cells tagged with bacterial luciferase (top). Cell counts range from 5000 on the left to 150 on the right. The lower plot shows the total counts per well versus the number of cells, indicating good linearity.

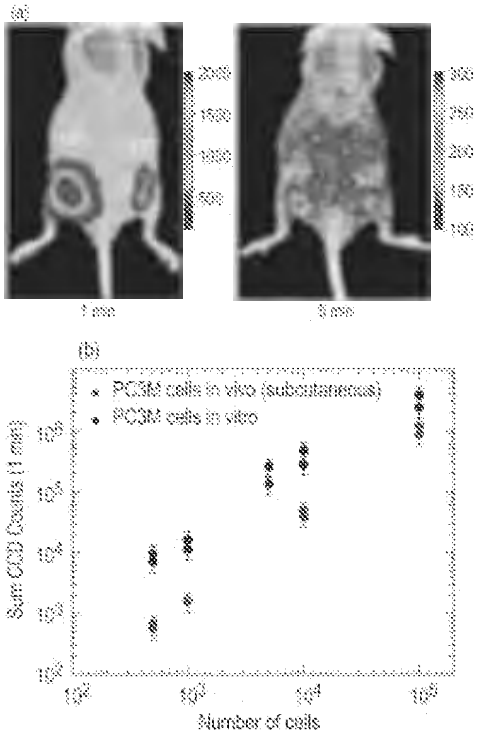


Fig. 14 (a) Subcutaneous injection of PC3M-*luc* prostate tumors cells. Cell counts from left to right are 10^5, 10^4, 1000, and 500. (b) Sum of counts from ROIs around each site in (a), normalized to a 1 minute image time (red). Counts for cells in a 96-well plate are also shown (blue). There are two images and hence two data points for each cell count number.

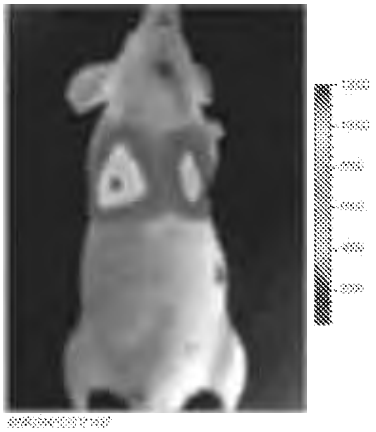


Fig. 15 Image showing bioluminescence from the lungs after an intravenous tail injection of 4×10^6 PC3M-*luc* cells. Imaging time is 1 min and binning=8.

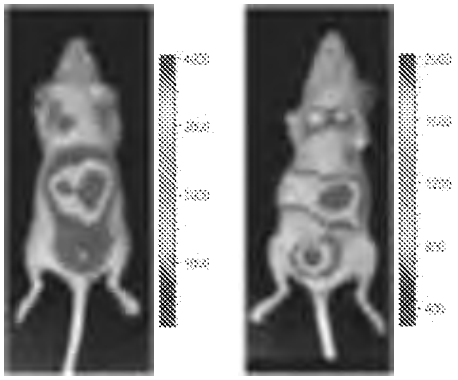


Fig. 16 Dorsal (left) and ventral (right) views of metastatic signals from breast cancer cell line MDA-MB-231-*luc*, week 14 after intravenous injection of tumor cells. Imaging time is 2 min and binning=4.

SPECTRAL_0000608

$$4\times10^5\frac{\text{photons}}{\text{s sr cm}^2}\frac{1}{\text{ADU/s/pixel}}\times\frac{7\text{ ADU}}{300\,s\,64\text{ pixels}}$$

$$\approx 145\frac{\text{photons}}{\text{s sr cm}^2}.$$

The area of a binned pixel in the object plane (object-to-image demagnification = 5.8) for this configuration is 0.013 cm^2, so the minimum detectable photon emission into 4π steradians (e.g., from an isotropically radiating cell) is 24 photons/s/pixel. The bioluminescent emission per cell varies depending on the cell line, but in the cell lines we have measured to date emission is in the range of 5–100 photons/s/cell into 4π steradians. Thus the IVIS™ imaging system can detect on the order of 0.25–5 cells per pixel *in vitro* with a S/N ~ 1.

An *in vitro* image of a 96-well plate containing a dilution series of bioluminescent bacteria (*Pseudomonas aeruginosa*) is shown in Figure 12. The cell count per well ranges from 5000 down to 150. The 150-count well is barely visible above the CCD noise and represents the minimum detectable number of cells for this particular cell line in a 96-well plate. There are about 60 binned (bin = 10) pixels in a well giving ~2.5 cells per pixel sensitivity in this case, consistent with the discussion above.

Of particular interest to the application of *in vivo* imaging is the minimum observable cell as a function of depth in an animal. The number of CCD signal electrons, S_e, required to give a certain signal-to-noise ratio, S_N, is given by Eq. (8). We can combine this with Eq. (6) to find the minimum number of cells that can be detected at a depth d. Defining a normalized radiance as $L_n \equiv L_{z=0}/P$ and replacing the emission power P with the integrated photon count, which is given by $C_n\rho_c\tau$ where C_n is the number of bioluminescent cells, ρ_c is the photon emission rate per cell, and τ is the integration time, we can write

$$S_e = dA\,d\Omega\,C_n\rho_c\tau L_n Q_E, \tag{9}$$

where dA is the pixel area element at the object plane, $d\Omega$ is the collection solid angle which is assumed small. Substituting Eq. (8) for S_e and solving for C_n gives

$$C_n = \frac{S_N\left(S_N + \sqrt{S_N^2 + 4(R_N^2 + D_c)}\right)}{dA\,d\Omega\rho_c\tau L_n Q_E}. \tag{10}$$

This equation gives the number of cells required to give a signal-to-noise ratio S_N at a depth d in tissue. In Figure 13 we plot the cell count versus depth for S_N values of 1, 10, and 100 for two different absorption coefficients of 0.25 and 1.0 cm^{-1} (corresponding roughly to wavelengths of 650 and 590 nm, respectively). We set $\tau = 300$ s, $\rho_c = 30$ photons/cell/s, and used 24 μm pixels with bin = 8 for this plot. According to this calculation, for cells ~0.5 mm deep (subcutaneous), we can detect on the order of a few hundred cells with $S_N \sim 10$. To make measurements at the deepest organs in a mouse (~1 cm deep) at red wavelengths requires 10^4–10^5 cells. For shorter wavelengths (see $\mu_a = 1$ cm^{-1} curves) significantly more cells are required to see deep tissue signals. These results provide general guidance on the minimum number of detectable cells; the exact number will depend on the brightness of the cell line and the type of tissue the photons must pass through.

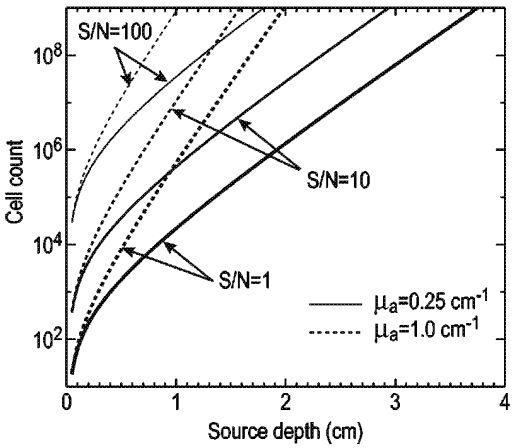


Fig. 13 Cell count vs source depth calculated using the diffusion model for three different S/N ratios. Solid lines are $\mu_a = 0.25$ cm^{-1} ($\lambda > 600$ nm) and dashed lines are $\mu_a = 1.0$ cm^{-1} ($\lambda < 600$ nm). A scattering coefficient of $\mu_s' = 15$ cm^{-1} and a bioluminescent emission of 30 photons/cell/s was used for all curves.

The results from Figure 13 are in good agreement with measurements in real animals. In Figure 14(a) we show images of PC3M-*luc* prostate tumor cells injected subcutaneously into a nude mouse. Cell counts of 500, 1000, 10^4, and 10^5 were injected into the thigh of each animal. In this case, 500 cells is close to the minimum cell count that can be observed. The sum of the counts in an Region of Interest (ROI) surrounding each spot is plotted in Figure 14(b). For comparison, *in vitro* measurements of the same cell counts are also shown in Figure 14(b). A deep-source lung signal is shown in Figure 15. For this animal, 4×10^6 PC3M-*luc* cells were injected into a tail vein, where cells are promptly transported to the lungs. The peak signal levels and signal-to-noise values from both Figures 14 and 15 are given in Table 1. The signal units in this table are ADU, but since the CCD amplifier gain is ~1 we can assume $S_{ADU} \sim S_e$ for comparison with Figure 13. Although the data in Table 1 are limited, the S/N versus depth trend is in qualitative agreement with that predicted in Figure 13.

The signal-to-noise calculations above only consider the CCD and intrinsic signal noise. In addition, there can be other

Table 1 Summary of signal measurements from Figures 14 and 15.

No. cells	Depth (estimate)	Peak signal (ADU)	S/N
500 (subcu)	~0.5 mm	180	12
10^3 (subcu)	~0.5 mm	350	18
10^4 (subcu)	~0.5 mm	5000	70
10^5 (subcu)	~0.5 mm	1.5×10^5	390
4×10^6 (lung)	~5 mm	6.5×10^4	250

SPECTRAL_0000609

sources of background light that create what is effectively a higher noise floor. As seen in Figure 14(a), background light can be observed on the animal with the 500-cell injection. This background level is small and is usually only a factor when looking for the very lowest bioluminescent signals. The background emission can result from phosphorescence of the skin, fur, or impurities on the animal. There also appears to be a low-level light emission due to metabolic activity in live animals, although this is not very well understood at the present time. Regardless of the source, every effort must be made to reduce the background light in order to approach the intrinsic noise floor of the CCD camera.

As a final example of the power of *in vivo* imaging, we show an example of tumor metastases in Figure 16. Here 5×10^6 breast cancer cells (MDA-MB-231-*luc*) were injected into a tail vein and this image was taken at week 14 after injection. The image shows clear metastatic signals from the lungs and lower body organs. These tumors are small and certainly would not have been palpable externally. The animal was dissected shortly after this image was taken, and *ex vivo* signals were found in the lungs, spine, adrenal glands, and lymph nodes.

7 Conclusion

In vivo imaging of cells or viruses tagged with light-emitting probes promises to be an important technology for the study of biological activity, the screening of potential drugs, and the assessment of toxicological effects of compounds. Both bioluminescent luciferase and fluorescent proteins are potential tags that can be used, although bioluminescence has a significant advantage due to extremely low backgrounds. Long-wavelength (>600 nm) probes will give the best signal levels in mammalian tissue due to lower absorption in tissue. The use of state-of-the-art cooled integrating CCD cameras along with imaging chambers optimized for *in vivo* applications allow the detection of bioluminescent signals throughout the body of small laboratory animals such as mice or rats. Experiments with luciferase tagged cells have demonstrated that minimum cell counts in the range of ~500 cells can be detected subcutaneously, while higher cell counts are required for larger depths in tissue. The sensitivity of detection is adequate to observe metastases of cancer cells, demonstrating the potential of *in vivo* imaging technology.

Acknowledgments

The authors would like to thank Darlene Jenkins, Kevin Francis, and Carole Bellinger-Kawahara and their respective research groups for data and assistance in performing the experiments discussed in this paper.

References

1. *Fluorescent and Luminescent Probes for Biological Activity*, W. T. Mason, Ed., Academic, London (1999).
2. C. H. Contag, P. R. Contag, J. I. Mullins, S. D. Spilman, D. K. Stevenson, and D. A. Benaron, "Photonic detection of bacterial pathogens in living hosts," *Mol. Microbiol.* **8**, 593–603 (1995).
3. C. H. Contag, D. Jenkins, P. R. Contag, and R. S. Negrin, "Use of reporter genes for optical measurements of neoplastic disease *in vivo*," *Neoplasia* **2**, 41–52 (2000).
4. A. Rehemtulla, L. D. Stegman, S. J. Cardozo, S. Gupta, D. E. Hall, C. H. Contag, and B. D. Ross, "Rapid and quantitative assessment of cancer treatment response using *in vivo* bioluminescence imaging," *Neoplasia* **2**, 491–495 (2000).
5. M. Yang, E. Baranov, P. Jiang, F. Sun, X. Li, L. Li, S. Hasegawa, M. Bouvet, M. Al-Tuwaijri, T. Chishima, H. Shimada, A. Moossa, S. Penman, and R. Hoffman, "Whole body optical imaging of green fluorescent protein-expressing tumors and metastases," *Proc. Natl. Acad. Sci. U.S.A.* **97**, 1206–1211 (2000).
6. J. W. Hastings, "Chemistry and colors of bioluminescent reactions: A review," *Gene* **173**, 5–11 (1996).
7. D. J. Hawrysz and E. M. Sevick-Muraca, "Developments toward diagnostic breast cancer imaging using near-infrared optical measurements and fluorescent contrast agents," *Neoplasia* **2**, 388–417 (2000).
8. V. Tuchin, *Tissue Opt.*, SPIE, Bellingham, WA (2000).
9. W. F. Cheong, S. A. Prahl, and A. J. Welch, "A review of the optical properties of biological tissues," *IEEE J. Quantum Electron.* **26**, 2166–2185 (1990).
10. A. Ishimaru, *Wave Propagation and Scattering in Random Media*, Academic, New York (1978).
11. R. C. Haskell, L. O. Svaasand, T. Tsay, T. Feng, M. S. McAdams, and B. J. Tromberg, "Boundary conditions for the diffusion equation in radiative transfer," *J. Opt. Soc. Am. A* **11**, 2727–2741 (1994).
12. L.-H. Wang, S. L. Jacques, and L.-Q. Zheng, "MCML-Monte Carlo modeling of photon transport in multilayered tissues," *Comput. Methods Programs Biomed.* **47**, 131–146 (1995).
13. G. C. Holst, *CCD Arrays, Cameras, and Displays*, SPIE, Bellingham, WA (1998).

SPECTRAL_0000610

BIOspektrum

In vivo Procedure for the Measurement Luciferase Reporter Gene Activity with a Low Light Imaging System

Bastian Hengerer, Novartis AG, Basel
Klaus Herick, EG&G BERTHOLD, Bad Wilbad



Reprint from BIOspektrum 4 (1998)

SPECTRAL_0000611

In vivo Procedure for the Measurement Luciferase Reporter Gene Activity with a Low Light Imaging System

Bastian Hengerer, Novartis AG, Basel
Klaus Herick, EG&G BERTHOLD, Bad Wilbad

The differential control of gene expression is a central theme of modern molecular biology. Interactions between transcription factors and DNA are commonly studied by a number of different techniques:

- Electrophoretic gel mobility shift assays;
- Binding tests, as with Avidin-Biotin-Complexed DNA (ABCD);
- Pull Down tests, and
- Reporter Gene assays.

These methods, however, are associated with certain disadvantages inherent to *in vitro* assay systems, for example non-physiological concentrations and the constraint of working with cellular extracts. This article presents an alternative for the detection of regulatory DNA-binding proteins in living cells.

The initial goal was to search for new, unknown transcription factors belonging to the Nuclear Hormone Receptor (NHR) superfamily [1]. Nuclear hormone receptors are bound by structurally diverse molecules such as retinoids, steroids, thyroids and vitamin D_3. These hormones regulate cellular development and differentiation as well as organ physiology through a common mechanism: hormone binding to specific receptors effects an allosteric change in receptor conformation which enables the receptor-hormone complex to interact with the transcription complex, thereby ultimately regulating the transcription of single genes [2]. Members of the NHR family are therefore at once hormone receptors and transcription factors, most binding as homo- or heterodimers to their specific recognition sequences in the promotor region of the gene being regulated. Since the dimerization partner influences ligand affinity, the activity of the nuclear hormone receptors can themselves be specifically regulated [3, 4].

In the present work, a nuclear hormone receptor was stably expressed in a cell line containing a luciferase reporter gene. Coexpression of a dimerization partner in the same cell line allowed induction of transcriptional regulatory activity in the resulting complex. The NHR-heterodimer then activates the expression of the *luc* reporter gene, whose product, the firefly-derived luciferase, is detected in the living cells with a low light imaging system.

This *in vivo* cotransfection assay was used to identify new heterodimer partners for specific NHR variants of unknown function and ligand specificity. For this purpose, a known nuclear hormone receptor was expressed in a neuron cell line. A cDNA bank was cotransfected for the expression of the heterodimerization partner. Since the cells expressing an active heterodimerzation partner are still alive during measurement of luciferase activity, it is possible to identify them using PCR techniques. As a control, 9-*cis*-retinoic acid receptor (RXR) was coexpressed instead of the cDNA bank. This example is here presented (Fig. 1).

As a positive control to prove the viability of the assay itself, an immortal cell line containing no endogenous RXR activity was transfected with a total of 3 plasmids:

- The reporter gene plasmid carries the luciferase reporter gene *luc*, the expression of which is regulated by the nuclear hormone receptor. This cis-vector was stably transfected into the cell line. The luciferase gene is located behind a thymidine kinase (TK) promoter with very low baseline activity. In front of the TK promoter, the hormone receptor-specific promoter sequence (RE) has been cloned in fourfold tandem repeat (Fig. 2).
- The pTRACER-NHR expression plasmid (Invitrogen, Leek, NL) is also stably integrated into the genome of the transfected cells. NHR expression is strongly and constitutively controlled by the CMV promoter.
- Finally, the cells were transiently transfected with a third plasmid, the pTRACER-RXR expression plasmid. This plasmid carries the gene for the 9-*cis*-retinoic acid receptor. In the presence of 10 nM 9-*cis*-retinoic acid, the NHR heterodimer complex is activated in the transfected cells, leading to luciferase expression. If instead of the RXR a cDNA bank is cloned into

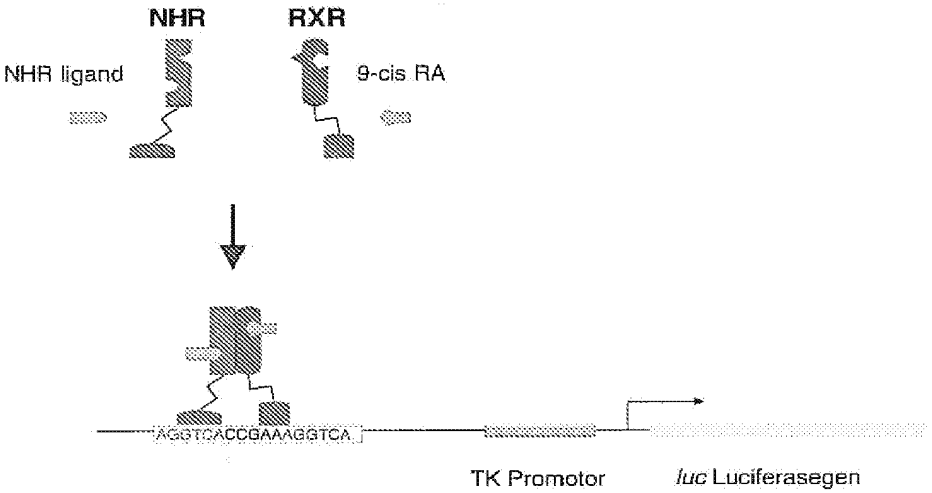


Fig. 1: The binding of a nuclear hormone receptor heterodimer to a specific promoter sequence. The receptors are comprised of a hormone (red, green) and a DNA-binding domain (blue). The stably expressed NHR is depicted in red, and the heterodimerization partner (in this case the positive control 9-cis-retinoic acid receptor RXR) in green. Expression of the reporter gene luciferase can only be effected by prior binding of the heterodimer. Although a monomer is capable of interacting with one of the binding sequences, it alone can not exert transcriptional control [5]. The DNA binding sequence is characterized by two repeating motifs of six base pairs each, separated by a five base-pair spacer. (9-cis-RA: 9-cis-retinoic acid; NHR: nuclear hormone receptor; TK: thymidine-kinase promoter)

SPECTRAL_0000612

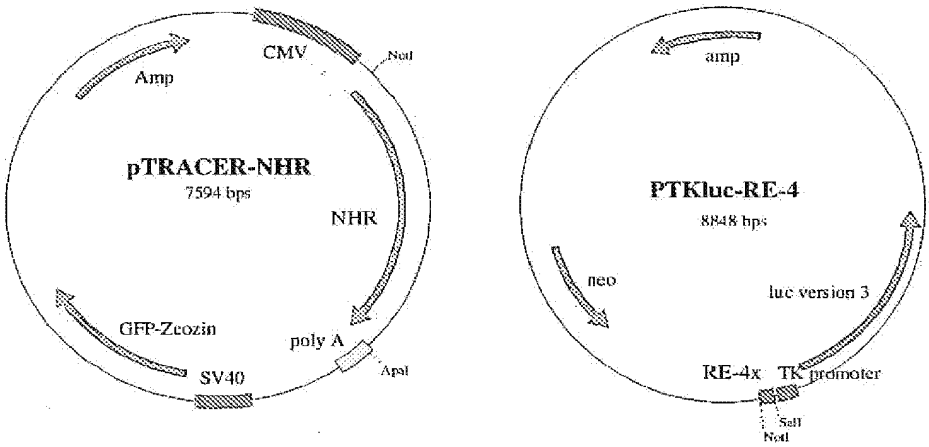


Fig. 2: Plasmid Constructs. In the pTRACER-NHR expression plasmid, the cDNA (here RXR) is under the control of the strong CMV promoter. In addition, the resistance genes for Ampicillin and GFP-Zeozin have been cloned into this vector. The reporter gene plasmid pTKluc-RE-4 expresses luciferase as dictated by the NHR-RE (Responsive Element), which has been cloned into this vector in fourfold tandem repeat. The thymidine-kinase promoter (TK) demonstrates a very low baseline activity which is beyond the limit of the method's detection.

the expression vector, it becomes able to express and identify hitherto unknown heterodimers.

The assay system has been constructed such that the presence of 10 nM 9-*cis*-retinoic acid is required for luciferase gene expression when an NHR/RXR heterodimer complex binds to its own specific sequence. In the experiment shown, the cells were stably transfected with the NHR expression and reporter plasmid. As the baseline luciferase expression of the plasmid containing the reporter gene was below the experimental detection limit, light emission due to luciferase activity was observed only for cells in which the missing component – the retinoic acid receptor (RXR) – had been expressed as well. To measure the luciferase activity, the living cells were washed once with PBS, spread with 500 ml luciferase substrate (Promega, Mannheim) per 10 cm culture dish, and detected immediately. To ensure the survival of the cells, there was no lysis buffer treatment prior to the addition of the luciferase substrate. The presence of the corresponding RXR expression plasmid was corroborated by single-cell PCR (data not shown). Luciferase activity was detected with the NightOWL Imaging System (EG&G Berthold, Bad Wildbad). This system's CCD-camera allows rapid detection of luciferase in femtomolar concentrations.

This simple *in vivo* technique allowed the identification of individual transfected cells in which a functional nuclear hormone receptor complex had induced reporter gene activity. The cells had been previously modified to express only parts of the expression and reporter system. A complete, active system was only present after the cells had been supplemented with the missing RXR component. Following the *in vivo* studies, the cells remained available for further experimentation.

By implementing a cDNA bank it is also possible to identify and characterize hitherto unknown binding partners. Furthermore, since the method is not dependent on specific promoters or expression plasmids, it is also extendable in application to other experimental systems.

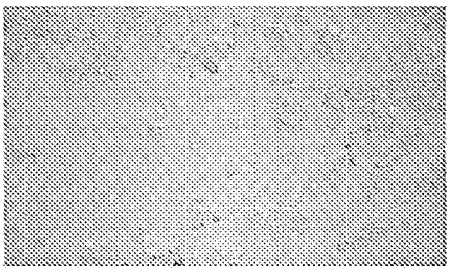


Fig. 3: Luciferase detection with the imaging system. The cells were systematically probed for luciferase activity in petri dishes. The positive control is shown above: cells were transiently transfected with the RXR expression plasmid. The picture is the result of a superimposition of a light-transmission photograph and the corresponding luminescence recording. The luminescence signals were depicted in an intensity-dependent manner, with red and blue representing, respectively, high and low intensity. The light-transmission photograph was taken at the maximum possible resolution (578 x 385 pixels) with a 20 ms exposure time, and the luminescence signal was recorded in the dark at the highest possible resolution with a 5 s exposure time. The „slow-scan" CCD-Camera (cooled to –70 °C) in the NightOWL Imaging System (EG&G Berthold, Bad Wildbad) was connected through a video input to an Axioplan microscope at 40x magnification (Zeiss, Oberkochen).

References

[1] ***Mangelsdorf, D.J., Thummel, C., Beato, M., Herrlich, P., Schütz, G., Umesono, K., Blumberg, B., Kastner, P., Mark, M., Chambon, P., Evans, R.M. (1995):*** The nuclear receptor superfamily: The second decade. *Cell 83, 835-839.*

[2] ***Vivat, V., Zechel, C., Wurtz, J.M., Bourguet, W., Kagechika, H., Unemiya, H., Shudo, K., Moras, D., Gronemeyer, H., Chambon, P. (1997):*** A mutation mimicking ligand-induced conformational change yields a constitutive RXR that senses allosteric effects in heterodimers. *EMBO J. 16, 5697-5709.*

[3] ***Evans, R.M. (1988):*** The steroid and thyroid hormone receptor superfamily. *Science 240, 889-894.*

[4] ***Kastner, P., Mark, M., Chambon, P. (1995):*** Nonsteroid nuclear receptors: What are genetic studies telling us about their role in real life? *Cell 83, 859-869.*

[5] ***Forman, B.M., Umesono, K., Chen, J., Evans, R.M. (1995):*** Unique response pathways are esthabished by allosteric interactions among nuclear hormone receptors. *Cell 81, 541-550.*

Address for correspondence

Dr. Klaus Herick
EG&G Berthold
Calmbacher Straße 22
75323 Bad Wildbad
Germany
Tel.: +49 - 7081 - 177272
Fax: +49 - 7081 - 177439
EMail: Klaus_Herick@egginc.com

SPECTRAL_0000613

[4] Luminometer Design and Low Light Detection

By FRITZ BERTHOLD, KLAUS HERICK, and RUTH M. SIEWE

Introduction

This article describes the methods of low level light detection that are used in bioluminescence and chemiluminescence and the application of these principles in instrumentation, both luminometers and imaging systems.

The availability, quality, and decreasing cost of commercial luminometers have reached a level that makes the use of "home-built" instruments a rare exception. Accordingly, we will focus on those physical and engineering principles that are, or could be, employed in commercial instrumentation and describe and discuss specific features in a critical fashion.

For low level light imaging, progress has been driven by dramatic advances in solid-state technology, particularly charge-coupled devices (CCDs). Tube and microplate luminometers, however, have been improved in more of an incremental fashion.

It is amazing how well the photomultiplier has held up as the detector of choice in luminometry. In view of the enormous progress in solid-state optoelectronics, it had seemed to be only a question of time until the photomultiplier, a vacuum tube, would be replaced. However, photomultipliers have improved considerably in recent years, and especially when operated as photon counters, they are the most sensitive light detectors presently available at a reasonable cost.

Following the wide popularity of microplates, many plate luminometers are now available. Luminometers for 384-well plates have also become available, and as the trend goes to an even higher sample density, the development of instrumentation can be expected to follow.

Portable, battery-driven luminometers have been developed in recent years, mostly in the use of rapid ATP measurement in industrial hygiene monitoring and other microbiological applications.

First, basic principles of luminometry and instrument design will be explained, in particular the function of the photomultiplier, the measuring chamber, and reagent injectors. Furthermore, we will discuss quality control, calibration, the definition and determination of sensitivity, dynamic range, and units used in luminometry. This should enable the reader to judge the performance of his luminometer critically and to optimize his experimental procedures to obtain correct results.

Copyright © 2000 by Academic Press
All rights of reproduction in any form reserved.
METHODS IN ENZYMOLOGY, VOL. 305
0076-6879/00 $30.00

SPECTRAL_0000614

The features needed in a luminometer depend both on the applications and on the type of luminescent chemistry used. For example, an injector is needed for flash-type kinetics, but is not necessary for glow kinetics. In some applications, such as reporter gene assays using a luciferase gene, high sensitivity may be the first consideration; in other cases, a high dynamic range is more important. The requirement for sample throughput will determine the level of automation. We will then describe luminometers by categories rather than individual instruments. Commercial suppliers are listed in the overview by Phil Stanley in this volume.

Basics of Luminometry

Instrumentation

The basic design, including measuring chamber, detector, and reagent injectors, will be discussed using a semiautomatic instrument as an example (Fig. 1).

Detector. The standard detector used in almost all luminometers is still the photomultiplier tube. So far, it has held up well against semiconductor technology, as it is hard to match the signal-to-noise ratios of photomultipliers at comparable cost. However, in the future, avalanche diodes may be developed into an alternative to multipliers, especially for portable luminometers with space constraints. Different types of low-noise silicon

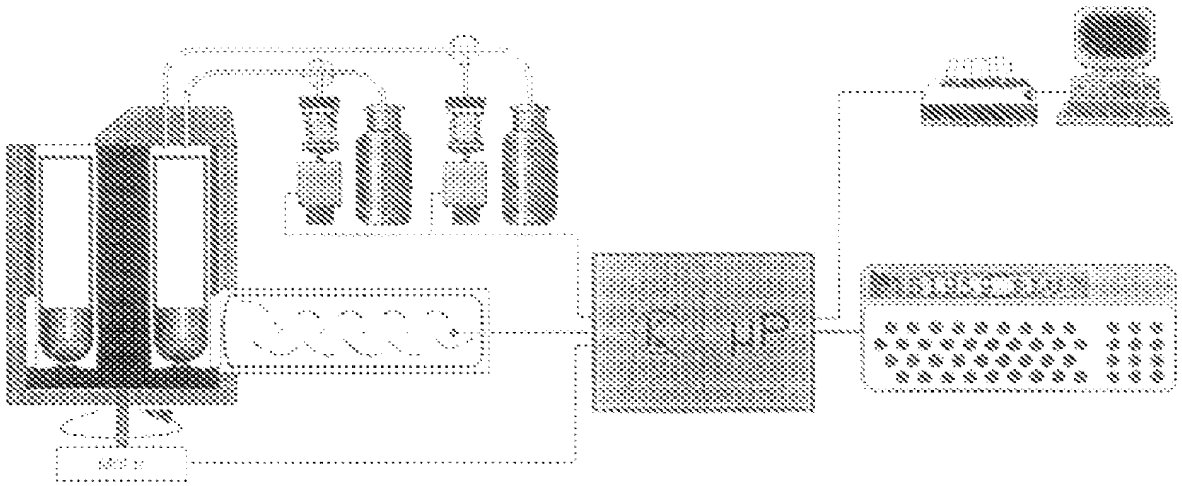


FIG. 1. Schematics of a semiautomatic tube luminometer. Hardware components include a motor-driven turret with a light-tight measuring chamber, two automatic injectors, a photomultiplier unit, an electronic board with microprocessor, and an alphanumeric keyboard and display. Note that connection of an external PC is optional.

SPECTRAL_0000615

detectors have been used in luminometry, but their sensitivity is several orders of magnitude lower than for photomultipliers.

At the cathode of a photomultiplier, photons release electrons by the photoelectric effect. These electrons are accelerated electrostatically and focused onto the first dynode, where they release secondary electrons, typically four to six. These electrons subsequently pass through a chain of further dyodes, with the multiplication process recurring every time. In total, up to 14 dynodes are used in commercial photomultipliers. Finally, the electron bunch is collected on an anode.

The amplitude–time function of anode current signals at low light levels is shown in Fig. 2. Individual events have full width at half maximum of about 2–6 nsec in relatively fast multipliers. The pulse amplitudes vary considerably and can be classified into three categories.

Only pulses with amplitudes between A and B correspond to electrons released at the cathode, representing the photons to be measured, plus noise electrons released spontaneously from the cathode.

Pulses smaller than A are due to noise events from dynodes or other low amplitude noise sources, whereas pulses greater than B originate from radioactivity in the glass and cosmic radiation.

Two methods to process these signals are available.

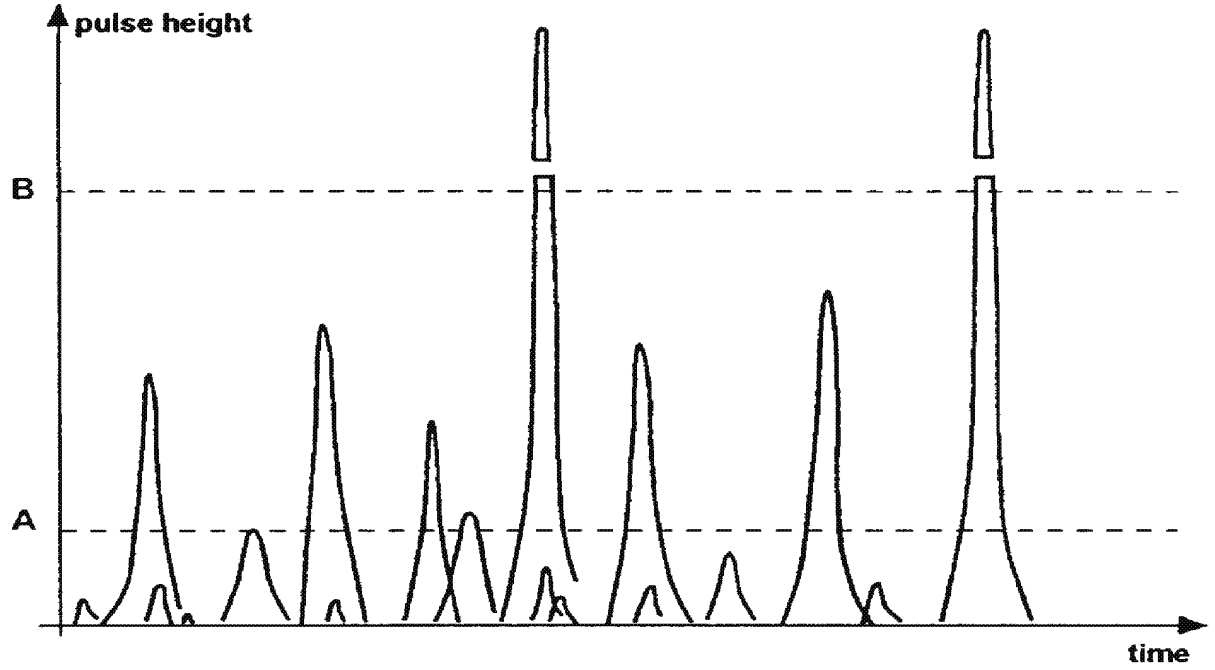


FIG. 2. Output pulses from a photomultiplier falling into three pulse height ranges: below A, dynode noise, etc.; between A and B, signal plus cathode noise; and above B, high energy events.

SPECTRAL_0000616

i. Current measurement by integrating the charge signals with a direct current (DC) amplifier.
ii. Amplifying the signals with a fast pulse amplifier and digitally counting only those pulses with an amplitude greater than A using a threshold discriminator circuit that is set accordingly. This is called photon counting. To exclude the contribution from radioactivity, one could use an upper level discriminator set at level B that would exclude all pulses greater than B. However, this is rarely done because the contribution from this noise source is small.

Photon counting leads to higher sensitivity than current measurement, mainly because the noise contribution from small pulses is excluded. Another advantage is much better stability, making frequent readjustments unnecessary.[1] The only disadvantage of photon counting is that saturation at high light levels occurs at pulse rates of around 2.5×10^7 counts per second, whereas current measurement extends to light levels higher by about one or two orders of magnitude.

To avoid the effect of saturation, it is normally possible to reduce light levels, e.g., by placing a neutral-density light filter between the sample and the photo cathode. It should also be noted that after exposure to very high light levels, most photomultipliers have elevated background levels for a certain time. Some luminometers are equipped with overload warning and protection.

The spectral sensitivity of a photomultiplier is determined by the type of cathode used. For bioluminescence and chemiluminescence measurements, bialkali or rubidium-bialkali photocathodes are normally used, covering a spectral range from about 350 to 700 nm. For special applications, like the measurement of singlet oxygen, a sensitivity extension into the red range is desirable. This would require the use of S20 or extended S20 cathodes covering the spectrum up to about 900 nm or S1 cathodes that extend even to 1100 nm. As a general rule, more red sensitivity also means more dark current so that cooling becomes almost mandatory. Bialkali tubes, however, can be operated at ambient temperature with tolerable dark count rates: about 10–50 counts per second. This value can be reduced by a factor of four by cooling to 6°.

Measuring Chamber. The measuring chamber and sample-loading mechanism have the following functions.

[1] F. Berthold, *in* "Advances in Scintillation Counting" (S. A. McQuarrie, C. Ediss, and L. I. Wiebe, eds.), p. 230. Faculty of Pharmacy and Pharmaceutical Sciences, University of Alberta, Edmonton, Canada, 1983.

SPECTRAL_0000617

i. The sample must be transported from outside the instrument into the measuring position in a reliable way, and the sample-loading mechanism must also be well designed ergonomically.
ii. The measuring chamber has to be absolutely light tight in its closed position. When it is open, the detector should be protected against excessive light levels that could cause memory effects in the detector (see section on detectors).
iii. Because light emission occurs practically isotropically, only a fraction of the light will reach the detector directly. Therefore, reflecting surfaces must be used, and a well-designed geometry employed. The efficiency ε of a measuring chamber is defined as the ratio of the number of photons reaching the photocathode divided by the number of photons emitted from the sample. A value for ε of 40% can be obtained (F. Berthold, unpublished results), but it is normally considerably lower. This number is dependent on sample format and wavelength.
iv. According to its design, the measuring chamber may allow quite different sample formats.

Reagent Injectors. The injection of starter reagent into the sample while the sample is in the measuring chamber in front of the detector allows tracing of the light emission instantaneously from the beginning. This is imperative for luminescence systems with so-called flash kinetics such as acridinium esters or aequorin, where light emission reaches its peak after 1 sec or less, and 90% of the light is emitted within 2 to 3 sec. However, in the case of glow kinetics, the reagent(s) starting the reaction may be added outside the luminometer. The definition of "glow" versus "flash" is somewhat arbitrary. For measurement with a microplate, the light output should not vary by more than about 1% per minute to allow operation without an on-board reagent injector. However, for a manual luminometer, it may be possible to start measurement within 1 to 2 sec after manual reagent addition. Therefore, the requirements regarding constant light output may be relaxed greatly, and a signal decay of 10–20% per minute might not cause a problem.

Injection of liquid volumes, such as 100–300 μl, may take several hundred milliseconds. Note that this is about the time for a flash kinetics signal to reach maximum, which has two implications: (i) the intrinsic rise time of the luminescence flash is slowed down and (ii) until injection is completed, the reagent mixture is in a transient state of rapidly changing concentrations. Good precision can only be obtained when not only the volume, but also the time and pressure profile of injection (velocity over time) are highly reproducible. In many applications this profile must also ensure rapid

SPECTRAL_0000618

mixing of reagents. Rotation or shaking devices normally do not allow mixing fast enough for a flash kinetics system, but are useful in maintaining the long-term homogeneity of samples.

The liquid injector may have the additional function to resuspend magnetic or other microparticles, which can be achieved with a "jet"-type injection. In practice, a 1–2% precision of relative light unit (RLU) values can be achieved and maintained, which is generally considered to be sufficient.

Automatic reagent injection may also be used to initiate sequential luminescent reactions, as in dual luciferase assays. Furthermore, injection and measurement of an internal standard following measurement of the analyte can be advantageous because it can make the establishment of a standard curve unnecessary. Such protocols can be used for ATP determination alone or for the simultaneous measurement of ATP, ADP, and AMP when only very low amounts of ATP are present.[2]

Two types of injector design are used, based on either pistons or bellows. Total dead volume, from reagent container to injector nozzle, should be minimized. A useful feature is the possibility of pumping unused reagents back into their original container.

The pressure profile has to be adapted to the actual measuring problem. In the case of sequential reactions such as dual reporter gene assays or internal calibrations, the injection process must avoid squirting droplets to the upper part of the tube as these cannot be reached by subsequent injections. Furthermore, the integrity of cells might be impaired by too high injection speed.

In conclusion, an ideal injector allows setting the volume over a wide range with high precision and has an adjustable pressure profile.

Special Considerations for Microplate Luminometers. For fast flash kinetics, the reagent triggering the light emission has to be injected into the sample while it is in the measurement position. For opaque microplates, which are used in most luminometers, both the nozzle of the reagent injector and the light detector have to be positioned above the microplate, therefore competing for space. An effective and elegant solution is the use of an optical fiber transporting the light from the microplate to the photomultipliers, while an optically transparent reagent duct practically replaces one of the fibers in the bundle.[3]

Commercial microplate luminometers are equipped with up to four reagent injectors. Two is the number used mostly, with the one injecting into the measuring position the most critical and important one.

[2] F. Berthold, S. Kolehmainen, and V. Tarkkanen, U.S. Patent 4,390,274 (1983).
[3] F. Berthold and W. Lohr, FRG Patent 41 23 818 (1994).

SPECTRAL_0000619

Units and Performance

Units

Raw data from luminometers are generally presented as relative light units. RLU is not a scientifically defined unit, but only a relative measure for the light output from the sample. A priori one cannot expect identical RLU readings from different luminometers when measuring the same sample. Each luminometer has to be calibrated individually using known analyte concentrations or special calibrators (see section on calibration and quality control). The situation differs somewhat between photon counting and current measuring systems.

In a current measuring device using a photomultiplier, the output signal not only depends on light intensity, but also on parameters such as applied high voltage, amplifier gain, and the digitizing factor converting current (or voltage) into RLUs.

Let us now look at a photon counter. As explained in the section on detectors, practically each photoelectron produces a logic pulse (except very few that do not reach the first dynode or do not produce secondary electrons). The number of photoelectrons released is equal to the number of photons hitting the photocathode multiplied by the quantum efficiency. Therefore, the counting rate registered by a photon counter, expressed as counts per second (cps), is a meaningful unit. It is generally used by the manufacturers of photomultiplier tubes to specify their product for their intended use as photon counters.

The situation becomes somewhat blurred because most luminometers convert the count rate into RLUs internally, using different conversion factors that are frequently not known or accessible to the user.

Some instruments allow the user to enter so-called RLU factors on top of the internally set conversion factors. These can be set so that different instruments of the same type show identical RLU readings for samples with the same photon emission, compensating for inevitable variations in quantum efficiency between individual photomultiplier tubes.

We think that an option to present results as counts per second, in addition to RLUs, is desirable. Basic performance criteria of photon counters, such as dead time and background that determine dynamic range, are reported as counts per second.

Furthermore, it is recommended to always report measuring results normalized to time as RLU per second. In the case of glow kinetics producing a practically constant signal during measurement, results reported as RLU per second are preferable over RLU because the results are independent of measuring time.

SPECTRAL_0000620

Dynamic Range and Sensitivity

Both dynamic range and sensitivity are important specifications for a luminescence system and will be discussed along a calibration curve for ATP measurements (Fig. 3). This example was chosen because this chemistry exhibits both a high dynamic range and a low reagent background.

Three regions can be distinguished clearly. The horizontal part in region 1 is background, normally the addition of instrument and reagent background. It should be noted that the term "relative light unit" might be a misleading unit for instrument background because this is (normally) due to noise electrons emitted from a photocathode, without any contribution from photons. Region 2 is the linear range that is best suited for quantitative work. Region 3 is characterized by increasing saturation effects of the photon counter, leading to a flat part of the curve without any further increase of output vs concentration. With very high light levels the output will decrease eventually.

In the case of a photon counter, the saturation effect is due to its dead time, determining the maximum intensity that can be registered (I_{max}).

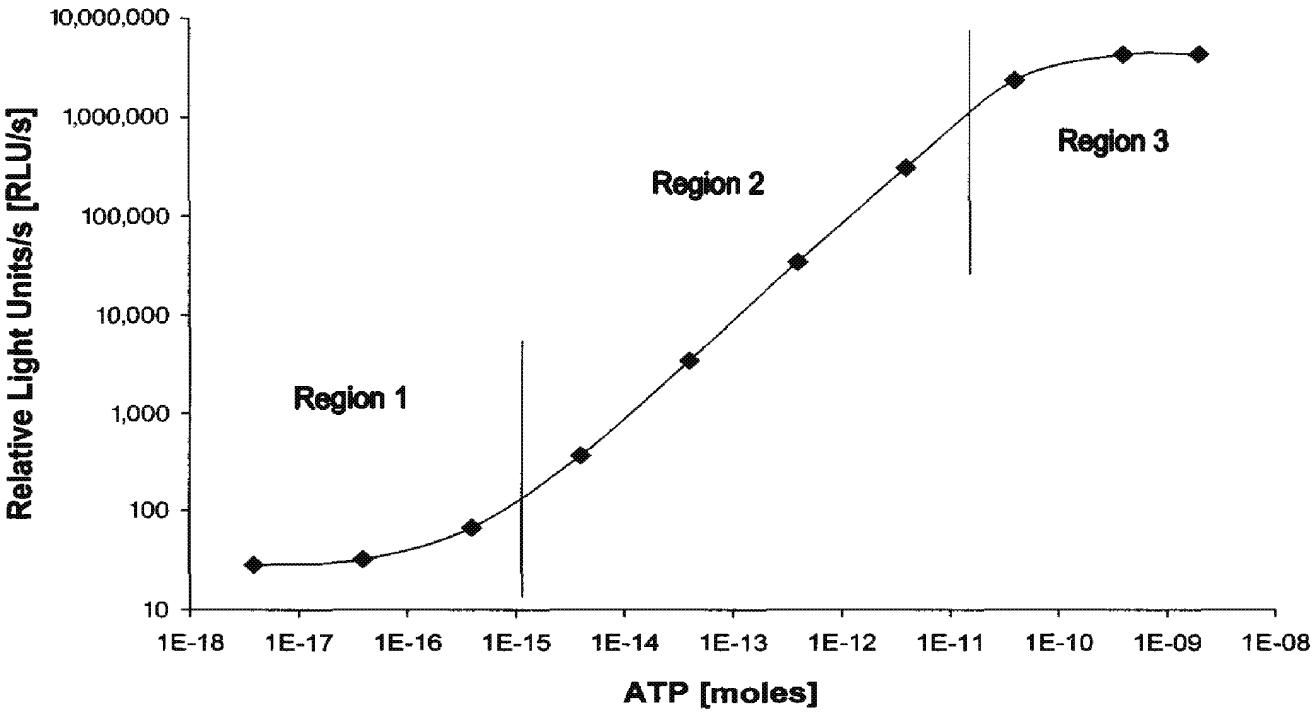


FIG. 3. ATP standard calibration curve measured on a EG&G Berthold (Bad Wildbad, FRG) Lumat LB 9507. ATP was diluted in distilled water to given quantities. Measurement was performed using the ATP detection kit from Analytical Luminescence Laboratory (Ann Arbor, MI) according to manufacturer's instructions. Different regions indicated are described in the text.

SPECTRAL_0000621

Over a limited range, a dead time correction is possible using, in good approximation, the following formula:

$$I_{\text{true}} = \frac{I_{\text{m}}}{1 - \frac{I_{\text{m}}}{I_{\text{max}}}}$$

where I_{true} is the corrected true intensity, I_{m} is the measured intensity, and I_{max} is the maximum intensity that can be detected. It may be useful to remember that if I_{m} is 10% of I_{max}, the result is already 10% too low due to counting losses. This formula is a good approximation up to $I_{\text{m}}/I_{\text{max}} = 0.5$; above this value errors become too great to be corrected properly.

For photomultipliers in the current measuring mode, the linear range is extended by typically two orders of magnitude before saturation occurs. A good way to increase the linear range at the high end is to use an optical filter, say OD 2 absorbing 99% of the light.

Calibration and Quality Control

The standard calibration procedure is to establish a calibration curve as shown in Fig. 3. We will now discuss additional methods for calibration and quality control and their usefulness.

Absolute Calibration. This means calibrating a luminometer in terms of the absolute number of photons emitted from a sample (see by O'Kane and Lee, this volume). Ideally, the calibrator source should have the same optical spectrum as the samples containing unknown analyte quantities and should also have the same sample format. Such calibrations are necessary in basic luminescence research, but would rarely be required by those using luminescence as a tool, as in biochemistry and molecular biology.

System Performance Check. This test allows checking not only of the function of the light detector, but also of the entire system, including reagent quality and injector function. It is performed by measuring the signal obtained for a standardized amount of a suitable luminophor. The result is then compared to a reference value and deviations are indicated. Such performance tests are particularly useful in clinical applications to indicate system failure, thereby avoiding false results for patient samples.

Light Calibrators. Their purpose is to calibrate or to just check the function of the light detector in a luminometer. These light sources are normally not themselves calibrated in terms of the number of photons emitted, but must have excellent long-term stability. Radioactive light sources using scintillation as the light generation process are very stable, and any decrease due to radioactive decay is exactly calculable. A common approach is the combination of tritium or another low energy β emitter,

SPECTRAL_0000622

with a suitable scintillator.[4,5] Because luminescence is a random emission of single photons, scintillation test sources should be sufficiently quenched to exhibit single-photon characteristics.[6]

The use of radioactivity is considered undesirable, as one of the driving forces of luminescence technology is to avoid the use of radioactivity. An interesting approach is the use of naturally occurring ^{238}U, minimizing regulatory concerns.[7] Autoradioluminescence in luminescent solid uranyl salts is generated from the α particles emitted.

Light-emitting diodes (LEDs) are convenient light sources and can be stabilized to obtain low drift. Green LEDs emit around 560 nm, matching the spectrum of firefly bioluminescence quite well. Some luminometers are equipped with built-in LEDs. For instruments using DC measurement, it is advantageous to use such light sources for automatic gain control. Good photon counters, however, are so stable that recalibrations are normally not required, and they are more stable than most nonisotopic light calibrators. Nevertheless, light calibration can be very useful in indicating any major problem in the luminometer before actual samples are measured.

Internal Calibration. The purpose is to correct inhibition of the light-generating chemistry (chemical quench) or absorption of light within the sample (optical quench). It is applied to glow-type reagent systems. The procedure is to add a calibrated quantity of analyte to the sample, comparing the signal before and after calibrator addition, and correcting the result using straightforward calculations. Internal calibration may be performed with manual calibrator addition, but automatic injection is more convenient.[2] The ratio of calibrator to sample volume must be sufficiently small so that the conditions to be tested are not influenced by the calibrator addition. This might necessitate sample rotation or shaking to affect mixing.

Sensitivity

Determining sensitivity as the minimum detectable number of photons would be an interesting specification. However, this is only possible when the luminometer is first calibrated in terms of photons emitted from the sample. As discussed in the preceding section, this is somewhat complicated

[4] T. ET. Oikari, I. A. Hemmil, and E. J. Soini, *in* "Analytical Applications of Bioluminescence and Chemiluminescence" (L. J. Kricka, P. E. Stanley, G. H. G. Thorpe, and T. P. Whitehead, eds.), p. 475. Academic Press, New York, 1984.

[5] D. J. O'Kane and J. Lee, *Photochem. Photobiol.* **52,** 723 (1990).

[6] E. Schram, H. Van Esbroeck, and H. Roosens, *in* "Proc. 1978 Int. Symp. on Anal. Appl. of Biolumin. Chemilumin" (E. Schram and P. E. Stanley, eds.). State Printing and Publishing, Westake Village, CA, 1979.

[7] D. J. O'Kane and D. F. Smith *in* "Bioluminescence and Chemiluminescence: Current Status" (P. E. Stanley and L. Kricka, eds.), p. 38. Wiley, Chicester, 1993.

SPECTRAL_0000623

to perform and may also be of limited interest to the user employing luminescence as a tool wishing to know the minimum measurable quantity of a particular analyte.

Most data sheets for commercial instrumentation therefore state sensitivity in terms of the minimum amount of analyte detectable, such as ATP or firefly luciferase. However, it must be understood that this number is not a characteristic of the luminometer alone, but also of reagent quality. As shown in the section on microplate luminometers, one can get almost one order of magnitude difference in signal levels between black and white microplates for the same luminometer and analyte concentration. An exact definition of sensitivity is therefore only possible for one particular system configuration, comprising luminescence reagent, sample cuvette or microplate, and sample volume. Furthermore, it would be useful to adhere to certain definitions and procedures when defining sensitivity. The work of Jago *et al.*[8] determining the sensitivity of 10 different luminometers is still exemplary because of its methodological approach.

We recommend the following simple method for determining the sensitivity of a luminometer for a specific reagent system.

i. Take a statistically significant number ($\geq$10) of background measurements (with all reagents, but zero analyte concentration).
ii. Measure a known amount of analyte in the midrange, e.g., 100 to 1000 times above background.
iii. Calculate sensitivity using the formula

$$S = (A * 3\sigma_{BG})/(S_A - BG)$$

where S is the sensitivity (same unit as A), A is the amount of analyte used for calibration (in mol, g, etc.), S_A is the result for measurement of A (in counts, cps, relative light units, or any other unit), BG is the mean value for background measurement (same unit as S_A), and σ_{BG} is the standard deviation of background measurement.

Example: In Fig. 3, the amount of 3.94×10^{-13} mol ATP (A) results in 34,140 RLU/sec (S_A). The mean value with a standard deviation of background measurement is 25 $\pm$ 4 RLU/sec (BG and σ_{BG}). Therefore, a sensitivity of the ATP detection kit used, measured on the indicated instrument, can be calculated to be 1.39×10^{-16}.

[8] P. H. Jago, W. J. Simpson, S. P. Denyer, A. W. Evans, M. W. Griffiths, J. R. M. Hammond, T. P. Ingram, R. F. Lacey, N. W. Macey, B. J. McCarthy, T. T. Salusbury, P. S. Senior, S. Sidorowicz, R. Smither, G. Stanfield, and P. E. Stanley, *J. Biolumin. Chemilumin.* **3,** 131 (1989).

SPECTRAL_0000624

Practical Hints

Because luminometers are about the most sensitive instruments to measure light, they should be placed where they are not exposed to very bright light, particularly sunlight.

Many reagent tubes exhibit strong phosphorescence after being exposed to light so it is good practice to always store tubes in the dark (in a drawer, not on a table).

Most instruments have no cooling for their detector (and normally do not need it). However, it should be remembered that background increases considerably with temperature; an increase of a factor of two for a temperature increase of 7° might be typical.

Factors Determining the Choice of Instrumentation

In almost all analytical fields of chemistry, biochemistry and medicine, bioluminescence and chemiluminescence techniques are used for the measurement of analytes in the attomole and femtomole range. Luminescent reactions are also widely used in food technology (for review, see Stanley *et al.*[9] and Navas and Jimenez[10]). The exploding market is reflected in the increasing number of luminescence-based reagents and the variety of luminometers currently available (for a review, see Stanley[11]).

The application determines the choice of a suitable luminometer because special features, e.g., injectors or temperature control, are required for some applications. All assays can be performed either in a microplate or in a tube luminometer. Additionally, for spatial resolution, imaging systems are used (see later).

Luminophors and Light-Generating Systems

A variety of bioluminescent and chemiluminescent luminophors or light-generating systems are described. Table I shows some common luminophors and their characteristics. The given values summarize characteristics under particular *in vitro* conditions. Kits and reagents available on the market often show different behavior of the same luminophor.

In principle, light emission kinetics are distinguished functionally into two groups: the flash type, when light is emitted within a few seconds, and

[9] P. E. Stanley, R. Smither, and W. J. Simpson (eds.), *in* "A Practical Guide to Industrial Uses of ATP-Luminescence in Rapid Microbiology." Cara Technology Limited, Lingfield, UK, 1997.

[10] M. J. Navas and A. M. Jimenez, *Food Chem.* **55,** 7 (1996).

[11] P. E. Stanley, *J. Biolumin. Chemilumin.* **12,** 61 (1997).

SPECTRAL_0000625

TABLE I
CHARACTERISTICS OF COMMON LIGHT-GENERATING SYSTEMS

Light-generating system	λ_{max}(nm)[a]	Emission kinetics
Acridiniume esters (e.g., Lucigenin)	530	Flash
Dioxetane derivatives	450–477	Glow
Aequorin	469	Flash
Luciferin/luciferases (Vibrio)	490	Flash
Luciferin/luciferase (firefly),	562 (615)	Flash
e.g., addition of coenzyme A		Glow
Luminol/isoluminol,	425	Flash
e.g., with enhancers		Glow

[a] Values are dependent on reaction conditions.

the glow type, when light emission is extended for a longer time period, e.g., up to several hours. The time scale of this classification is arbitrary. It should be used to distinguish between reactions where, on the one hand, the manual pipetting of reagents is possible (glow) and, on the other hand, when automatic injection to allow immediate measurement of the samples is essential (flash). Even very similar proteins, e.g., luciferases of the glowworm *Lampyris noctiluca* and the firefly *Photinus pyralis,* can show different emission kinetics.[12] The firefly emits light within seconds (flash type) whereas light emission of the glowworm is much more continuous (glow type).

It is important to note that for some applications, the luminophor itself, e.g., luminol, is used as the label, whereas in other applications the label is an enzyme catalyzing a luminescent reaction. The quantum efficiency reflects the number of photons produced per reacting molecule of luminophor. When an enzyme such as alkaline phosphatase is used as a label, one should consider that light output can be high despite a low quantum efficiency, as it can be overcompensated by a high number of substrate molecules turned over per molecule enzyme.

As shown in Table I, the label affects not only the emission kinetics, but also the spectrum of light emission. The wavelength of emitted light depends on the conditions used. The light output of firefly luciferase reaches a maximum at 562 nm. In the presence of certain divalent metal ions, such as Cd^{2+} or Zn^{2+}, or at low pH, light output is shifted into the red region of the spectrum (λ_{max} 610–615 nm). This affects light measurement because the quantum efficiency of photomultipliers depends on the wavelength.

[12] G. B. Sala-Newby, C. M. Thomson, and A. K. Campbell, *Biochem. J.* **313,** 761 (1996).

SPECTRAL_0000626

Some kits available on the market include enhancers. These compounds also often lead to a shift in wavelength.

Applications and Demands for Instrumentation

This section discusses common bioluminescent and chemiluminescent applications in the context of the required luminometer features. Depending on the other reagents, the same luminophor may show flash or glow characteristics. The handling of glow-type luminescence not requiring an automatic injection of reagents is more convenient, but luminol (without enhancer)-, acridinium ester-, and aequorin-based assays with flash kinetics maintain their ground because of certain advantages.

Reporter Gene Assays

In most of the reporter gene assays currently on the market (for review, see Bronstein *et al.*[13]), light emission is quite stable (glow type), which allows, in general, measurement without using injectors. Common reporter genes are luciferases, β-galactosidase, β-glucuronidase, secreted alkaline phosphatase, and the photoprotein aequorin. For the use of aequorin, injectors are required due to the flash kinetics of light emission. In general, temperature control is not necessary for reporter gene assays.

For the use of dual-label assays,[14,15] injectors might be recommended. Some of the available luminometers even provide software that allows the automatic injection of reagents, measurement, and evaluation (ratio calculation) of measured data.

For spatial resolution of gene expression, imaging systems can be used (see section on imaging).

ATP Measurements

In principle, the firefly luciferase leads to a flash-type luminescence, requiring reagent injectors, but a glow-type light emission can be obtained, e.g., when coenzyme A is present.[16] In this case, injectors are not needed. However, it should be mentioned that injectors can also be used for the addition of different reagents, e.g., for lysis buffer and luciferin/luciferase, leading to high sample throughput.

[13] I. Bronstein, J. Fortin, P. E. Stanley, G. S. A. B. Stewart, and L. J. Kricka, Anal. *Biochem.* **219,** 169 (1994).
[14] B. A. Sherf, S. L. Navarro, R. R. Hannah, and K. V. Wood, *J. NIH Res.* **9,** 56 (1997).
[15] C. S. Martin, P. A. Wight, A. Dobretsova, and I. Bronstein, *Biotechniques* **21,** 520 (1996).
[16] K. V. Wood, *in* "Bioluminescence and Chemiluminescence: Current Status" (P. E. Stanley and L. J. Kricka, eds.), p. 543. Wiley, New York, 1991.

SPECTRAL_0000627

Glow-type luminescence is applied in industrial hygiene applications, where small portable luminometers without injectors are used.

Measurement of Enzymes and Metabolites

Many enzymes and metabolites can be coupled to the production or utilization of ATP, NAD(P)H, or H_2O_2, and luminescent detection of these compounds is possible. Luminescent detection methods have been described for more than 100 enzymes and metabolites (for review, see Campbell[17]). General statements on instrumentation requirements are difficult, as, for example, enzymes are temperature dependent and reaction kinetics of light emission depend on the particular assay.

Room temperature to 25° is usual. Because the temperature should be maintained constant, especially for continuous measurements, temperature control might be useful. Luminescent systems for the measurement of ATP, NAD(P)H, or H_2O_2 in principle show flash kinetics, but, as described earlier, glow luminescence can be obtained by the addition of other compounds, such as enhancers.

Cellular Chemiluminescence (Phagocytosis)

Because the determination of cellular chemiluminescence uses living cells, adjustable temperature control (e.g., from 25 to 41°) is necessary. The kinetic of light emission is measured over long time periods of up to several hours. Frequently a group of samples derived from a primary sample must be measured simultaneously. This necessitates parallel measurement, which can be affected in an automatic sample changer (tube or microplate), taking cyclic measurements from a multitude of samples, or a multidetector instrument.

Immunoassays

From a commercial point of view, immunoassays are certainly the most important application of bioluminescence and chemiluminescence. In clinical diagnostics, fully automated systems, which include pipetting, incubation, separation, and measurement, are available, but on a smaller scale, tube and microplate luminometers are widely used.

In clinical diagnostics, acridinium esters and dioxetane derivatives are the most common luminophors; however, other sensitive luminescent systems, based for example on acetate kinase or aequorin, can be attractive.[18]

[17] A. K. Campbell, "Chemiluminescence: Principles and Applications in Biology and Medicine," Chapter 5. Ellis Horwood, Chichester, UK, 1988.
[18] L. J. Kricka, *Pure Appl. Chem.* **68,** 1825 (1996).

SPECTRAL_0000628

Temperature control is not necessary for this application. Referring to Table I, the number of required injectors depends on the light emission kinetics of the luminescence system and also on the degree of automatic sample preparation.

DNA Probe Techniques

Nonisotopic DNA probe techniques are becoming more and more important in the field of nucleic acids research (for review, see Kricka[19]). For many luminescent applications, the use of photographic films is still sufficient for light detection. If quantification of light emission is required, luminometers or imaging systems are recommended. Using filter membrane adapters, dot blots in a 96-well format can be measured in microplate luminometers.[20] For a detailed analysis of gels and blots of different formats, low light imaging systems are best suited.

From Single Sample to Fully Automated Luminometers

Single Sample Tube Luminometers

We will start with the simplest (and least expensive) type of luminometer, which is best suited for low or medium throughput. Each sample has to be loaded into the instrument manually, is usually measured promptly, then unloaded, and the sequence can be repeated.

Single sample instruments can be equipped with automatic or manual reagent injectors so that every assay using flash or glow kinetics can be performed. Their only limitation is lack of automatic sample changing.

In certain respects, single sample luminometers can even be superior to automatic instruments. Some models can accommodate a wide range of sample formats, including different tubes with diameters of 8–16 mm and a height of 40–100 mm, a design with cap, liquid scintillation vials, and also flat sample formats such as culture tubes and filters with up to a 35 mm diameter.

Because a single sample instrument may have less space constraint for the design of an optimized measuring chamber (see measuring chamber section), one finds instruments with the highest sensitivity in this category.

Portable Luminometers. Portable, battery-driven luminometers have been developed for industrial microbiology applications.[9] A typical protocol for rapid hygiene monitoring may be the following: wettened swab samples

[19] L. J. Kricka (ed.), *in* "Nonisotopic DNA Probe Techniques." Academic Press, San Diego, 1992.
[20] N. Walter and C. Steiner, *Biotechniques* **15,** 926 (1993).

SPECTRAL_0000629

are taken from the surface to be tested. The ATP content is then determined using the firefly reaction. Some systems use extraction reagents, extracting ATP from somatic cells or bacteria, whereas others measure free ATP only. Light-generating reagents (luciferin/luciferase) are frequently either freeze-dried or immobilized for convenience and stability.

Reagents and instrumentation are both designed for error-free operation under adverse conditions and must observe sterility requirements in food-processing plants.

In advanced commercial products, all consumables come in single-dose packages, avoiding any pipetting steps. This type of packaging frequently results in special sample formats so that most portable luminometers are part of a proprietary reagent/instrument system. For instance, it may be necessary to measure a swab of 10 cm length directly, which is only possible in specially designed luminometers. Weight is an important consideration; it is typically less than 1500 g.

Portable luminometers may allow storage of the results of 1000 or more samples that have been measured in the field, together with sample identification entered via keyboard or downloaded from a computer. These results can be downloaded to a PC for further analysis.

Portable luminometers for hygiene applications are usually less sensitive than those for scientific use. However, portable instrumentation has become available that is sensitive enough for scientific or industrial use beyond rapid hygiene monitoring. Such applications include the distinction of bacterial from somatic ATP, identification of coliform bacteria by specific enzymatic reactions, resulting in a luminescence signal, and immunoassay and DNA probe assays also using luminescent labels.

Automatic Tube Luminometers

Automatic tube luminometers are available in two configurations, either with a chain or with racks for sample holding and transport. A popular rack-type luminometer can load and measure up to 400 samples in 40 racks with 10 samples each.

Some automatic tube luminometers are equipped with temperature stabilization and other features, making them particularly useful for cellular chemiluminescence studies.

Microplate Luminometer

Because of the popularity of microplates, automatic plate luminometers have found a considerable market. Some not only accommodate 96-well plates, but also plates with 384 wells.

In a microplate luminometer the measuring chamber consists of both the

SPECTRAL_0000630

instrument and the microplate. Therefore, microplates have to be chosen carefully in terms of detection performance parameters such as cross-talk (see later).

Measuring luminescence from microplates presents some unique design challenges, which are reflected in considerable performance differences among such instruments, particularly cross-talk and reagent injection.

Cross-talk. Because of the close proximity of neighboring sample wells, it is difficult to avoid spillover of light between wells, called cross-talk. A practical method for cross-talk determination is the following: A quasi-constant signal (S_m) is generated in well m, and the apparent signals in neighboring empty wells S_d (diagonal position) and S_a (adjacent position) are measured. For neighboring wells in the diagonal position, the cross-talk is defined as $CT_d = S_d/S_m$; for neighboring wells in adjacent positions, the cross-talk is defined as $CT_a = S_a/S_m$ (Fig 4). Ideally, cross-talk would be zero. In reality, values of 10^{-4} are normally acceptable. Because adjacent wells are closer than diagonal ones, CT_a is higher. Of course, cross-talk is only an issue for glow luminescence because light emission for flash-type luminescence will occur only from the well in the measurement position. Cross-talk and sensitivity are characteristics of the combined system (luminometer and microplate), a fact that is frequently not reflected in the manufacturers' documentation.

Table II shows diagonal and adjacent cross-talk values for different commercially available 96-well microplates, i.e., white, black, clear, clear bottom, and strips. In addition, the relative efficiency of S_m is given, which is related to a white plate with maximum reflection.

Clear microplates are used if, in addition to luminescence, absorbance is also of interest, e.g., in cell growth determination. Using clear plates, or

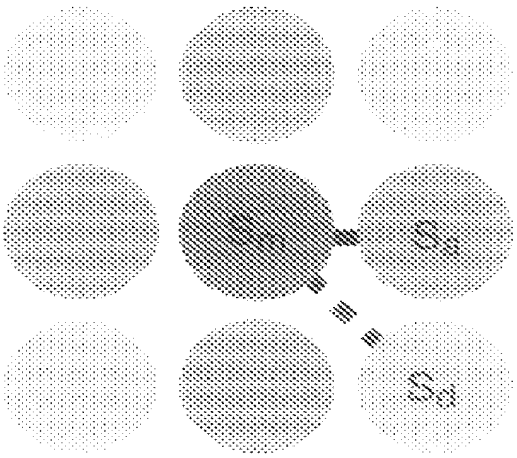


FIG. 4 Determining cross-talk.

SPECTRAL_0000631

TABLE II
CROSS-TALK VALUES AND RELATIVE SIGNAL EFFICIENCIES FOR DIFFERENT 96-WELL MICROPLATES

Type	Relative signal efficiency (%)	Cross-talk CT_d	CT_a
White, opaque	81–100	$3.55–5.94 \times 10^{-5}$	$1.55 \times 10^{-5}–1.15 \times 10^{-4}$
White strips	50–80	$1.70 \times 10^{-6}–3.37 \times 10^{-5}$	$4.56 \times 10^{-6}–6.26 \times 10^{-5}$
White, clear bottom	34–37	$1.83–3.37 \times 10^{-5}$	$3.02–6.27 \times 10^{-5}$
Clear	12–14	$3.45–3.73 \times 10^{-2}$	$8.43–8.93 \times 10^{-2}$
Clear strips	12–15	$2.01–3.37 \times 10^{-2}$	$6.30–7.08 \times 10^{-2}$
Black	6–7	$<10^{-6}–1.09 \times 10^{-5}$	$6.31 \times 10^{-6}–3.42 \times 10^{-5}$

[a] Diagonal and adjacent cross-talk values (CT_d and CT_a, respectively) were determined using 18 different commercially available 96-well microplates, the ATP bioluminescence assay kit CLS II from Boehringer Mannheim (FRG) according to the instructions, and the luminometer MicroLumat-Plus LB 96V from EG&G Berthold (FRG). The same quantity of ATP was pipetted into each plate; the relative signal efficiency of 100% corresponds to 7×10^6 RLUs per 10 sec. The cross-talk, e.g., from well B2 into A1, A3, C1, and C3, was averaged as CT_d and from well B2 (S_m) to B1, B3, A2, and C2 as CT_a ($n = 3$). The averaged background of wells containing buffer was subtracted before calculation. Standard deviations were in a range of 5–30%.

strips inserted into plate holders, the highest cross-talk values were obtained in a range of 2 to 9% of S_m. Adjacent cross-talk could be measured even in wells two (CT_{a2}) and three positions (CT_{a3}) away from the well generating the signal S_m: $CT_{a2} = 0.63–2.33 \times 10^{-2}$ and $CT_{a3} = 1.05–4.02 \times 10^{-3}$. The relative efficiency of S_m shows only small values of about 12 to 15% because the isotropic light is not reflected inside the well. Because light shines through the clear plate material, resulting in enormous cross-talk, clear microplates are not suitable for measuring luminescence.

To reduce this high cross-talk, white microplates with clear bottoms, which are optically not connected to neighboring wells, are used. These plates show CT values up to three orders of magnitude less than completely clear plates. Also, the efficiency is increased to 34–37%, due to more reflection from the white walls of the wells.

Maximum signal efficiency was obtained using white opaque microplates as well as white opaque strips inserted into holders, as here the optical reflection reaches the highest values. Furthermore, these plates show very small cross-talk values that are in the same range as clear bottom plates. White microplates have become standard in luminescent measurement because they combine very low cross-talk and high signal efficiency.

Black microplates show the best cross-talk values—about 10 times lower than for white ones—but because of their low efficiency, they are recommended only when enough light is available.

SPECTRAL_0000632

Furthermore, there are differences in cross-talk and efficiency between plates of the same type from different manufacturers; e.g., S_m of white strip plates differs from 50 to 80%.

Reagent Injection. The limited space for both detector and injector(s) above a well is an engineering challenge that can be solved quite elegantly by using light conductors to the detector, which are partly substituted by optically transparent injection nozzles.

Additional design criteria for plate luminometers are their interfaces to robot and stacker systems. For high throughput screening, either the integration into a fully automated robot system or the use of a stacker system, where a series of microplates is measured automatically, is a prerequisite.

The trend to higher sample numbers and smaller volumes has led to the design of microplates with 384 wells and beyond. Correspondingly, several luminometers accommodating 384-well plates have been introduced. The measuring time for a plate with 384 wells is roughly four times that for 96 wells and can therefore reach 10 min or more.

Throughput can be increased with multidetector systems. A system with eight detectors operated in parallel reduces the measuring time by a factor of 8, compared to only one detector.

The problem of cross-talk is even more critical for 384-well plates than for 96-well plates because of the greater proximity of neighboring wells. Cross-talk values between 10^{-3} and 10^{-4} may be considered acceptable. The authors are not aware of a 384-well instrument allowing reagent injection into the measuring position, which would be difficult but not impossible to realize. Consequently, 384-well luminometers are presently used for glow kinetics.

For even higher sample density, the conventional luminometer design with the sequential or parallel measurement of single wells may no longer be suitable; the use of imaging systems might be the better choice, albeit associated with a different set of limitations.

Multi-functional Instruments

Some instruments have been designed to measure not only luminescence, but also fluorescence, light absorption, or radioactivity. A combination of different instruments in one has the advantage of lower costs and less use of space. However, there are also some disadvantages. Just one type of measurement at one time can be done. Therefore, the use of the instrument by many people is difficult. The major problem is that a combined instrument cannot be optimized for the measurement of each label. For example, luminescent and fluorescent labels differ in emission spectrum.

SPECTRAL_0000633

Whereas luminescent labels emit their light mainly in the range of 400 to 600 nm (Table I), the emission of light of some common fluorescent labels is at a much higher wavelength, e.g., Cy5.5™ 694 nm, Cy7™ 767 nm. Because detectors with sensitivity in the red area show a higher background noise, these detectors are less suitable for low light luminescence applications.

In a microplate scintillation counter, cross-talk values for luminescence measurements are higher than for scintillation applications. This is due to the fact that coincidence and other discrimination methods used in scintillation counting not only suppress noise, but cross-talk as well, and corresponding methods are not available in luminescence measurement.

Luminescence Imaging

For particular applications, besides the amount of luminescence, information about spatial resolution is required. Imaging is the point of interest in this recently established field of luminescence measurements. The sample size ranges from a single cell, using microscopes, to complete animals, such as a mouse, using light-tight housings.[21] Examples involving spatial resolution include luminescent blot detection and analysis of reporter gene expression.[22,23]

The spatial measurement of bio- and chemiluminescent signals demands a high-density array of highly sensitive detectors. The photon multiplier technique as described earlier is not suitable for this purpose, So imaging detectors are used. The most important detector technologies for luminescence imaging are (i) slow-scan cooled CCD cameras, (ii) intensified CCD cameras, and (iii) video cameras with an intensifier.

Detector Techniques

The CCD is a semiconductor detector containing an array of picture elements called pixels. These arrays show various formats and consist of up to about 9×10^6 pixels. Because the pixel size is in the range of a few micrometers, i.e., less than 10 μm to about 25 μm, a high-density array performance leads to high optical resolutions. Inside the pixels, electron-hole pairs are generated by the impinging photons, and the electrons are accumulated. The number of generated electrons is proportional to the number of incoming photons. At the end of the exposure, the charges are

[21] G. Taubes, *Science* **276,** 1993 (1997).
[22] J. C. Nicolas, *J. Biolumin. Chemilumin.* **9,** 139 (1994).
[23] B. Kost, M. Schnorf, I. Potrykus, and G. Neuhaus, *Plant J.* **8,** 155 (1995).

SPECTRAL_0000634

read out pixel by pixel and are stored. The resulting pattern represents the image.

In principle, CCDs are divided into standard (front)- and back-illuminated chips according to their installed orientation. The spectral sensitivity of a front-illuminated CCD differs from that of a bialkali photocathode and ranges from 400 to 1100 nm; it can be extended down to 200 nm by a UV-to-VIS converter. At 650 nm a maximum quantum efficiency of about 40% is reached. Spectral sensitivity and quantum efficiency are limited by absorption of the incoming light through the silicon dioxide layer before generating charges inside the pixel. By exposing the chip from the other side (back-illuminated CCD), quantum efficiency can be increased to a maximum of about 85% at 650 nm, as there is no light absorption by the silicon dioxide layer.

Low light imaging is restricted by two sources of background noise: thermal noise (dark current) and readout noise. Thermal noise is generated due to statistical fluctuations of thermal electrons within the pixel and can be reduced by cooling either cryogenically or by Peltier elements. Because the use of liquid nitrogen or water cooling may not be convenient in many laboratories, only multiple-stage Peltier cooling will be considered here. At 200 K (four-stage Peltier/air cooling of the CCD chip) the thermal noise of a state-of-the-art detector is less than four electrons/pixel/hour. This means the CCD chip is almost free of thermal noise even for exposure times up to hours.

The readout noise is generated during the readout process. It increases with scan speed. Because the readout noise becomes significant at low signal levels, such as luminescence imaging, CCD detectors usually operate in a slow-scan mode of less than 100 kHz, e.g., a chip of 512 × 512 pixels can be read out at a rate of 50 kHz within about 5 sec. The readout noise, given in statistical terms, is called root mean square (RMS) and can be reduced to less than six electrons RMS.[24]

In the case of intensified CCD systems, where an image intensifier is placed in front of a CCD, the intensified signal-to-background noise ratio is influenced only marginally by the noise level. Therefore, intensified CCD's usually operate at higher readout rates of up to 5 MHz. Further cooling is not strictly required.[25,26] Yet another approach is the combination of a very

[24] C. D. Mackay, *Photonics Spectra* **2,** 113 (1992).

[25] P. L. Jones, I. M. Greenfield, C. E. Hooper, R. Ansorge, and M. A. Stanley, *in* "Bioluminescence and Chemiluminescence: Current Status" (P. E. Stanley and L. J. Kricka, eds.), p. 175. Wiley, New York, 1991.

[26] C. E. Hooper and R. E. Ansorge, *in* "Bioluminescence and Chemiluminescence: Current Status" (P. E. Stanley and L. J. Kricka, eds.), p. 337. Wiley, New York, 1991.

SPECTRAL_0000635

low noise saticon tube, which is a special type of high dynamic, low noise vidicon tube, with an age intensifier.[27]

The relative advantages of different detector types have been discussed repeatedly.[28,29] In our view, it has not been proved that any particular type of detector is superior to others, but there are considerable performance differences within each class of detectors. The benefits of cooled slow-scan CCDs are image quality, sensitivity, and a broad dynamic range (1>10,000), whereas the advantage of an intensified detector is fast image acquisition, e.g., in the case of calcium ion imaging. All detector principles are used in high-quality commercial instruments.

Technical Construction

Sample formats vary from microscopic, such as single cells or tissue sections, to macroscopic, such as culture dishes, blots, thin-layer chromatograms, or gels. Therefore, the detector can be adapted to a microscope for microscopic imaging or, for imaging of a macroscopic-sized sample, the detector can be mounted inside a light-tight dark housing containing a suitable sample support.

Figure 5 presents a schematic of a macroscopic imaging system. The detector is mounted mechanically onto a vertical drive inside the dark cabinet to allow adjustment of the magnification. The lens is mounted independently on a second vertical precision drive for focus adjustment. By combining both positioning capabilities under computer control, it is possible to bring images from about a 3- to 30-cm edge length into full view of the detector, with the system autofocused continually. The sensitivity of microscopic imaging systems is mainly influenced by the quality of the microscope.

Imaging Software

The software of an imaging system controls three main functions: (i) image acquisition, (ii) image correction, and (iii) image processing.

[27] R. Bräuer, B. Lübbe, R. Ochs, H. Helma, and J. Hoffmann, *in* "Bioluminescence and Chemiluminescence: Current Status" (P. E. Stanley and L. J. Kricka, eds.), p. 13. Wiley, New York, 1991.

[28] R. E. Ansorge, C. E. Hooper, W. W. Neale, and J. G. Rushbrooke, *in* "Bioluminescence and Chemiluminescence: Current Status" (P. E. Stanley and L. J. Kricka, eds.), p. 349. Wiley, New York, 1991.

[29] R. A. Wick, G. Iglesias, and M. Oshiro, *in* "Bioluminescence and Chemiluminescence: Current Status" (P. E. Stanley and L. J. Kricka, eds.), p. 47. Wiley, New York, 1991.

SPECTRAL_0000636

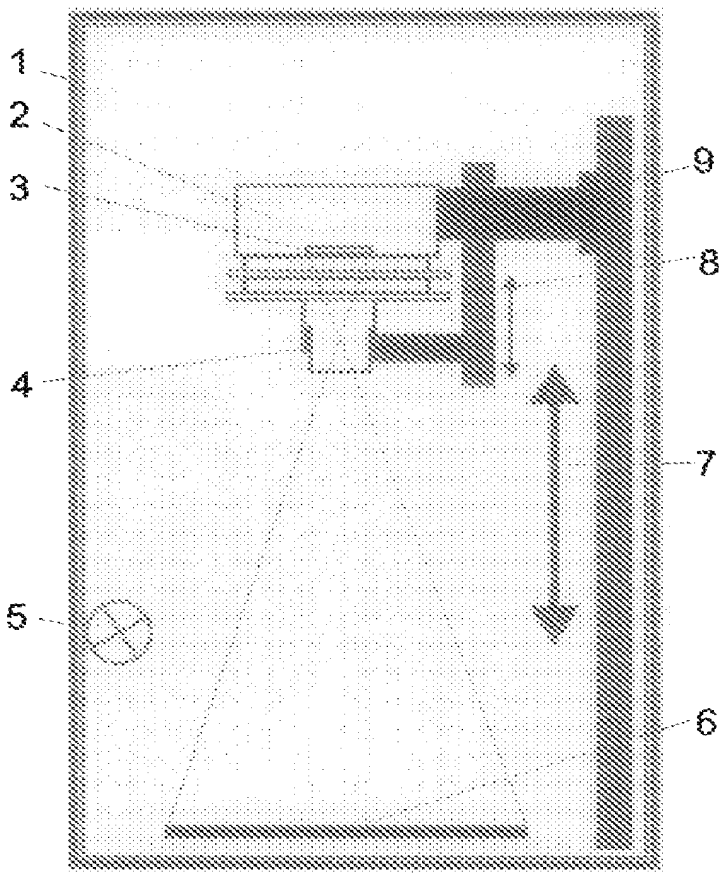


FIG. 5. Schematics of a low level imager. The light-tight housing (1) of a macroscopic imaging system is presented containing the detector (2) with a motor-driven vertical adjustment of magnification (7, 9), the sensor element (3), the lens (4) with a second vertical precision drive for focus adjustment (8), a weak and fluorescence light source with interchangeable filters (5), and the sample table (6).

i. The acquisition software has to control camera parameters such as the exposure time, optical parameters such as the focus adjustment/magnification, and the display/storage of raw data.
ii. The image correction software includes functions to control background subtraction, sensitivity correction to compensate for variations in pixel sensitivity, and geometrical correction, which is necessary because of "cushion" or "fish-eye" distortion associated with large solid angle imaging. Additionally, the image brightness and contrast have to be controlled because the 14- to 16-bit gray levels of the CCD camera have to be converted into 8-bit gray levels that can be recognized by the human eye.
iii. Finally, the image processing software performs the addition and subtraction of images and the conversion of black and white images

SPECTRAL_0000637

of the CCD into pseudocolor images. Furthermore, this software controls pattern recognition to allow counting and classifying objects such as cells or colonies, as well as quantitative reading of the microplate. Blot and gel documentation function is also included in imaging processing software. For these purposes, many analysis programs are available from other types of imaging, including fluorescence or radioactivity methods.

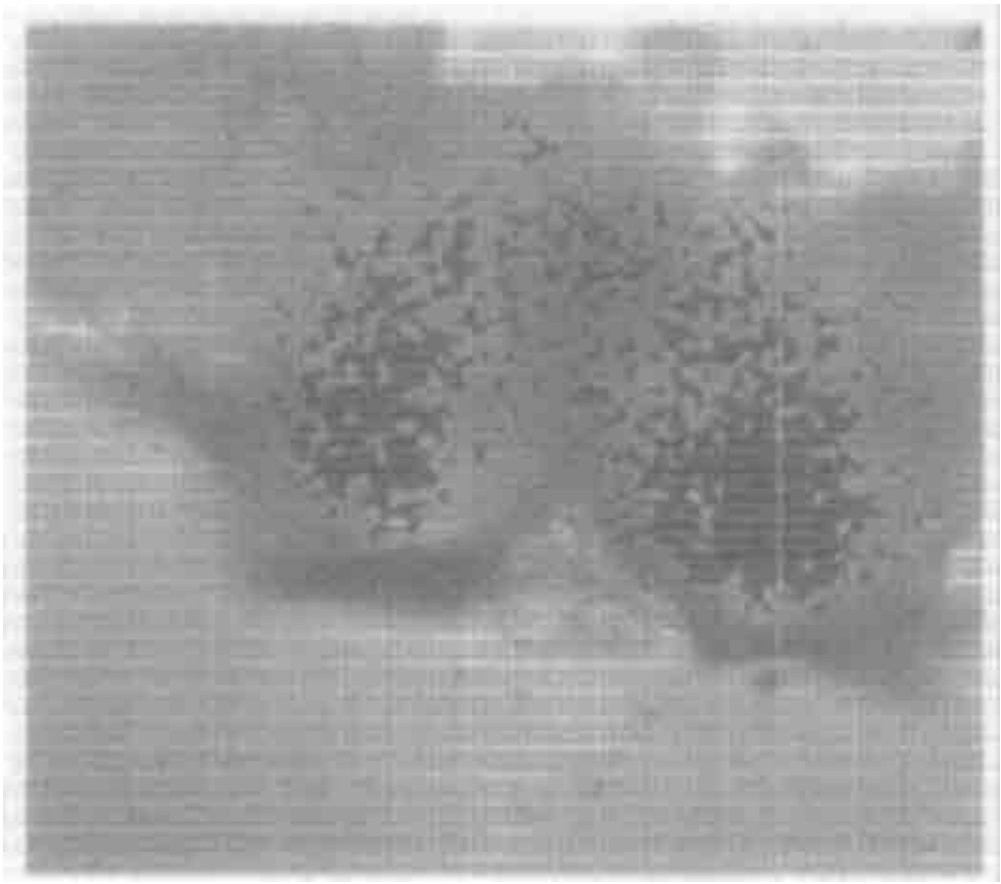


FIG. 6. Detection of luminescence emitted from the jelly fish photoprotein aequorin expressed in a brain section of the fruit fly *Drosophila melanogaster* (line 103Y) using a back-illuminated slow-scan CCD camera coupled to an inverse microscope (courtesy of D. J. Amstrong, Glasgow). Luminescence, shown as rough black areas and spots, appeared from the Calyx region (approximately 30–40 μm across) of the mushroom bodies of the brain of an adult fruit fly. The imaging system NightOWL from EG&G Berthold (Bad Wildbad, FRG) was connected to the inverse microscope Axiovert TV 100 from Zeiss (Jena, FRG) equipped with a Neofluar 20× lens (0.50 NA). A 20-fold magnification was used. An overlay of a transilluminated and a luminescent image is presented. Two copies of aequorin (cDNA clone pAQ2) have been targeted into the mushroom bodies using the P[GAL4] expression system as described in Rosay *et al.*,[31] Tettamanti *et al.*,[32] and Yang *et al.*[33]; coelenterazine was purchased from Molecular Probes (Eugene, OR).

SPECTRAL_0000638

Example of Application

Luminescence imaging is only possible for glow-type luminescence because it would be almost impossible to dispense reagents into (intact) samples and take an image at the same time. Even so, the weak and chemical flash-type luminescence of the jellyfish photoprotein aequorin can be detected. Figure 6 shows aequorin expression in the brain of a transgenic fruit fly *Drosophila melanogaster* as an actual example for reporter gene analysis.

The macroscopic and microscopic imaging system NightOWL from EG&G Berthold[30] was used for this spatial detection of the luminescent label aequorin. Figure 6 presents an overlay of two images. First, a transilluminated image was acquired using a 20-msec exposure time. For this image, less sensitivity was required due to the illumination, but high resolution was required for maintaining good spatial resolution. Therefore, each pixel was read out separately. Second, a luminescent image was acquired. Here, camera parameters were set mainly for high sensitivity but less for spatial resolution: An exposure time of 3 min was chosen and groups of 5×5 pixels were connected together (pixel binning) to increase sensitivity. For comparison, the emitted aequorin luminescence was quantified to about 200 to 500 RLU per 15 sec using a LB 9507 luminometer from EG&G Berthold (Bad Wildbad, FRG) (J. D. Amstrong, personal communication).

[30] B. Möckel, J. Grand, and R. Ochs, *in* "Bioluminescence and Chemiluminescence" (J. W. Hastings, L. J. Kricka, and P. E. Stanley, eds.), p. 539. Wiley, Chicester, 1996.
[31] P. Rosay, S. A. Davies, Y. Yu, M. A. Sozen, K. Kaiser, and J. A. T. Dow, *J. Cell Sci.* **110,** 1683 (1997).
[32] M. Tettamanti, J. D. Amstrong, K. Endo, M. Y. Yang, K. Furukubo Tokunaga, K. Kaiser, and H. Reichert, *Dev. Genes Evol.* **207,** 242 (1997).
[33] M. Y. Yang, J. D. Amstrong, I. Vilinsky, N. J. Strausfeld, and K. Kaiser, *Neuron* **15,** 45 (1995).

[5] Absolute Calibration of Luminometers with Low-Level Light Standards

By DENNIS J. O'KANE and JOHN LEE

Relative light units are commonly reported in the measurement of bioluminescent and chemiluminescent reactions. The reason is that the calibration of the absolute photon sensitivity of the detector system entails overcoming severe technical problems. Absolute photon calibration is essential if one is to determine the absolute quantum yields of these reactions, important information required for elucidating the mechanisms of

Copyright © 2000 by Academic Press
All rights of reproduction in any form reserved.
METHODS IN ENZYMOLOGY, VOL. 305
0076-6879/00 $30.00

SPECTRAL_0000639

Bioluminescence & Chemiluminescence status report
Ed.: A.A.Szalay L.J.Kricka P.Stanley, Chichester: Wiley 1993: 13-17

Measuring luminescence with a low light level imaging system using electronic light standards

Bräuer R., B. Lübbe, R. Ochs, H. Helma and J. Hoffmann
Siemens AG, Karlsruhe, Germany

Summary
The 2D detection of the luminescence by images has the advantage of being a very good evidence, it is quantitative, fast and non-polluting. Based on the described methods the design principals of the Luminograph LB 980 (BERTHOLD) are given. The instrument can be calibrated, is very sensitive and has a high resolution. The user can define circular or rectangular image areas where the intensity is calculated either in relative light units, watts or photons. This makes the system very powerful and flexible, suited for many applications in bio- and chemiluminescence. A UV lamp in the inside of the sample chamber makes the system applicable also for fluorescent images. This makes the system a very useful instrument in the molecular biology laboratory.

Keywords: bioluminescent imaging, reporter gene assay, Western Blot,

SPECTRAL_0000640

UCLA Library Search WorldCat WorldCat (Sign in)

melvyl@UCLA

Pilot

Search

Libraries to search Libraries Worldwide | Advanced Search

<< Return to Search Results Cite/Export Print E-mail Add to list Share Permalink Ask a Librarian

Bioluminescence and chemiluminescence : status report : proceedings of the VIIth International Symposium on Bioluminescence and Chemiluminescence, Banff, March 1993

Author: Aladar A Szalay; Larry J Kricka; P E Stanley

Published: Chichester, England ; New York : Wiley, ©1993.

Edition/Format: Book : Conference publication : English

Chat with a librarian

More like this

Subjects

Bioluminescence assay -- Congresses.

Chemiluminescence assay -- Congresses.

Bioluminescence -- Congresses.

View all subjects

Similar items

Find a copy in the library

University of California Libraries

Get it from this library group Request

3 group libraries own this item

UC Berkeley Libraries check availability for this item

UC Davis Libraries check availability for this item

UCR Libraries check availability for this item

WorldCat

Find it in libraries globally Request

Worldwide libraries own this item

Buy it

Details

Material Type: Conference publication

Document Type: Book

All Authors / Contributors: Aladar A Szalay; Larry J Kricka; P E Stanley

Find more information about: Aladar A Szalay Go

ISBN: 0471941646 : 9780471941644

OCLC Number: 28631466

Description: xiii, 548 p. : ill. ; 24 cm.

Responsibility: edited by A. Szalay, L. Kricka, and P. Stanley.

Reviews

User-contributed reviews

Tags

Add tags for "Bioluminescence and chemiluminescence : status report : proceedings of the VIIth International Symposium on Bioluminescence and Chemiluminescence, Banff, March 1993".

Similar Items

Related Subjects: (5)

Bioluminescence assay -- Congresses.

Chemiluminescence assay -- Congresses.

Bioluminescence -- Congresses.

Chemiluminescence -- Congresses.

Luminescence -- Measurement -- Instruments -- Congresses.

User lists with this item ()

Languages: Deutsch | English | Español | Français | Nederlands | 中文
You: Sign in | Register | My WorldCat | My Lists | My Watchlist | My Reviews | My Tags | My Saved Searches
WorldCat: Home | About | Help | Get E-mail Updates | Feedback | Search | WorldCat Blog
Legal: Copyright © 2001-2010 OCLC. All rights reserved. | Privacy Policy | Terms and Conditions

WorldCat is the world's largest library catalog, helping you find library materials online.

DOWNLOADED FROM iai.ASM.ORG - at UCLA BIOMEDICAL LIB/SERIALS July 14, 2010

Infection and Immunity

Monitoring Bioluminescent Staphylococcus aureus Infections in Living Mice Using a Novel luxABCDE Construct

Kevin P. Francis, Danny Joh, Carolyn Bellinger-Kawahara, et al.

2000. Monitoring Bioluminescent Staphylococcus aureus Infections in Living Mice Using a Novel luxABCDE Construct. Infect. Immun. 68(6):3594-3600. doi:10.1128/IAI.68.6.3594-3600.2000.

Updated information and services can be found at:
http://iai.asm.org/cgi/content/full/68/6/3594

These include:

CONTENT ALERTS

Receive: RSS Feeds, eTOCs, free email alerts (when new articles cite this article), more>>

Information about commercial reprint orders: http://journals.asm.org/misc/reprints.dtl
To subscribe to an ASM journal go to: http://journals.asm.org/subscriptions/

Journals.ASM.org

SPECTRAL_0000643

INFECTION AND IMMUNITY, June 2000, p. 3594–3600 Vol. 68, No. 6
0019-9567/00/$04.00+0
Copyright © 2000, American Society for Microbiology. All Rights Reserved.

DOWNLOADED FROM iai.ASM.ORG - at UCLA BIOMEDICAL LIB/SERIALS July 14, 2010

Monitoring Bioluminescent *Staphylococcus aureus* Infections in Living Mice Using a Novel *luxABCDE* Construct

KEVIN P. FRANCIS,[1] DANNY JOH,[1] CAROLYN BELLINGER-KAWAHARA,[1] MATTHEW J. HAWKINSON,[1] TONY F. PURCHIO,[1] AND PAMELA R. CONTAG[1,2]*

Xenogen Corporation, Alameda, California 94501,[1] and Division of Neonatal and Developmental Medicine, Department of Pediatrics, Stanford University Medical Center, Stanford University, Stanford, California 94305[2]

Received 27 January 2000/Returned for modification 1 March 2000/Accepted 23 March 2000

Strains of *Staphylococcus aureus* were transformed with plasmid DNA containing a *Photorhabdus luminescens lux* operon (*luxABCDE*) that was genetically modified to be functional in both gram-positive and gram-negative bacteria. *S. aureus* cells containing this novel *lux* construct, downstream of an appropriate promoter sequence, are highly bioluminescent, allowing the detection of fewer than 100 CFU in vitro (direct detection of exponentially dividing cells in liquid culture). Furthermore, these bacteria produce light stably at 37°C and do not require exogenous aldehyde substrate, thus allowing *S. aureus* infections in living animals to be monitored by bioluminescence. Two strains of *S. aureus* 8325-4 that produce high levels of constitutive bioluminescence were injected into the thigh muscles of mice, and the animals were then either treated with the antibiotic amoxicillin or left untreated. Bioluminescence from bacteria present in the thighs of the mice was monitored in vivo over a period of 24 h. The effectiveness of the antibiotic in the treated animals could be measured by a decrease in the light signal. At 8 h, the infection in both groups of treated animals had begun to clear, as judged by a decrease in bioluminescence, and by 24 h no light signal could be detected. In contrast, both groups of untreated mice had strong bioluminescent signals at 24 h. Quantification of CFU from bacteria extracted from the thigh muscles of the mice correlated well with the bioluminescence data. This paper shows for the first time that bioluminescence offers a method for monitoring *S. aureus* infections in vivo that is sensitive and noninvasive and requires fewer animals than conventional methodologies.

Many strains of *Staphylococcus aureus*, which cause a wide variety of diseases ranging from pyoderma to toxic shock syndrome, are methicillin and gentamicin resistant, with some strains also showing limited resistance to vancomycin. Such bacteria are a major problem in nosocomial, or hospital-acquired, infections (3, 9, 18). Without the development of new antibiotics it is possible that, given time, such bacteria will be untreatable by conventional means. In order to combat such bacterial infections, novel and effective drugs will be needed. In addition, new approaches for screening candidate antibiotics both in vitro and in vivo are essential to accelerate the development of new antiinfectives. To this end, bioluminescence offers a method that is sensitive and innocuous and allows only live, or viable, cells to be detected. Furthermore, in vivo detection of bioluminescent bacteria is noninvasive, allowing rapid monitoring of the infective state of eukaryotic cells both in culture and in animals (4, 7). Such a method of monitoring in vivo bioluminescent organisms in living animals has been described for gram-negative bacteria and it was demonstrated to correspond to bacterial CFU data with a correlation coefficient of 0.98 (H. L. Rocchetta, J. W. Foley, C. J. Boylan, P. W. Iverson, P. R. Contag, D. E. Jenkins, and T. R. Parr, Abstr. 39th Intersci. Conf. Antimicrob. Agents Chemother., abstr. 797, 1999). However, until now, in vivo monitoring has not been achieved for gram-positive bacterial infections.

Synthesis of light in naturally occurring bioluminescent bacteria is encoded by five essential genes that are organized in an operon such as *luxCDABE*. Blue-green light is emitted from these bacteria with a peak at 490 nm as a result of a heterodimeric luciferase (encoded by *luxAB*) catalyzing the oxidation of reduced flavin mononucleotide ($FMNH_2$) and a long-chain fatty aldehyde (synthesized by a fatty acid reductase complex encoded by *luxCDE*). Although a number of additional *lux* genes in bioluminescent bacteria have been identified, only *luxA-E* are essential for the biosynthesis of light (10). The *lux* operon can be readily moved into a variety of gram-negative bacteria to confer a bioluminescent phenotype. However, because all identified species of naturally occurring marine and terrestrial bioluminescent bacteria are gram negative, the transformation of gram-positive bacteria to a light phenotype has been somewhat limited due to the differing genetics of these two bacterial groups.

Bioluminescent strains of *S. aureus* have been constructed (5, 13). However, these bacteria contain the firefly luciferase gene (*luc*) or variations of isolated bacterial *luxAB* luciferase genes, each of which require the addition of an exogenous substrate to allow bioluminescence. Moreover, most bioluminescent gram-positive bacteria have been generated using bacterial luciferase genes that encode enzymes that are unstable at temperatures above 30°C (8). Although such bacteria are useful for environmental studies (e.g., the assessment of food products for contamination by such bacteria), *luxAB* constructs that only permit bioluminescence to occur below 30°C are of limited use for experimentation on pathogenicity carried out at 35°C and above in vivo.

In this report, we describe the construction of a novel *Photorhabdus luminescens lux* operon, where each gene (*luxA*, *-B*, *-C*, *-D*, and *-E*) has been modified by the introduction of a gram-positive ribosome binding site (RBS). This novel operon, preceded by an appropriate promoter sequence, allowed several highly bioluminescent *S. aureus* strains to be generated.

* Corresponding author. Mailing address: Xenogen Corporation, 860 Atlantic Ave., Alameda, CA 94501. Phone: (510) 291-6100. Fax: (510) 291-6196. E-mail: prcontag@xenogen.com.

SPECTRAL_0000644

DOWNLOADED FROM iai.ASM.ORG - at UCLA BIOMEDICAL LIB/SERIALS July 14, 2010

TABLE 1. Oligonucleotide sequences used to amplify the *P. luminescens* genes from pSB417[a]

Gene	Primer	Sequence	Restriction endonucleases
luxA	XAF3	CCCC**GGATCCTGCAG**ATGAAGCAAGAGGAGGACTCTCTATG	*Bam*HI, *Pst*I
	XAR	GGC**GGATCCGTCGAC**TTAATATAATAGCGAACGTTG	*Bam*HI, *Sal*I
luxB	XBF	GG**GAATTCTCGAG**GAGGAGAGAAAGAAATGAAATTTGGA	*Eco*RI, *Xho*I
	XBR	GGC**GGATCCGTCGAC**TTAGGTATATTCCATGTGGTAC	*Bam*HI, *Sal*I
luxC	XCF	GG**GAATTCTCGAG**GAGGATGGCAAATATGACTAA	*Eco*RI, *Xho*I
	XCR	GGC**GGATCCGTCGAC**TTATGGGACAAATACAAGGAAC	*Bam*HI, *Sal*I
luxD	XDF	GG**GAATTCTCGAG**GAGGAGTAAAAGTATGGAAAATGA	*Eco*RI, *Xho*I
	XDR	GGC**GGATCCGTCGAC**TTAAGACAGAGAAATTGCTTGA	*Bam*HI, *Sal*I
luxE	XEF	GG**GAATTCTCGAG**GAGGAAAACAGGTATGACTTCATATG	*Eco*RI, *Xho*I
	XER	GGC**GGATCCGTCGAC**TTAACTATCAAACGCTTCGGTTA	*Bam*HI, *Sal*I

[a] Oligonucleotide sequences used to amplify the *P. luminescens luxA*, *B*, *C*, *D*, and *E* genes from pSB417 by PCR (see main text for PCR conditions). Nucleotides highlighted in bold show the positions and sequences of the different restriction sites (identified in far-right column) incorporated to facilitate cloning. Gram-positive RBSs sites are underscored by solid lines. Start and stop codons are underscored by broken lines.

These labeled bacteria could be detected in vivo noninvasively, allowing antibiotic efficacy to be efficiently assessed in real time.

MATERIALS AND METHODS

Incorporation of gram-positive RBSs upstream of *luxA*, *-B*, *-C*, *-D*, and *-E* by PCR. The five genes of the *P. luminescens lux* operon, *luxA*, *-B*, *-C*, *-D*, and *E*, were amplified using PCR. The primers were designed to replace the gram-negative RBS AGG with the gram-positive RBS AGGAGG, ensuring that this site was at least 7 nucleotides upstream of the start codon (ATG) of each gene. PCR was performed with a Geneamp PCR system 9700 automated thermocycler (Perkin-Elmer Applied Biosystems, Norwalk, Conn.) in 200-μl thin-walled PCR tubes (Molecular BioProducts, San Diego, Calif.). Reactions were carried out in 50-μl volumes containing 5 μl of 10× PCR buffer (supplied with *Taq* DNA polymerase; Boehringer Mannheim, Indianapolis, Ind.), 2.0 mM $MgCl_2$, 50 pmol of each oligonucleotide primer (Table 1), a 0.2 mM concentration of each deoxynucleotide triphosphate (dATP, dCTP, dGTP, and dTTP; Amersham Pharmacia Biotech, Piscataway, N.J.), 1 U of *Taq* DNA polymerase (Boehringer Mannheim) and 10 ng of plasmid DNA containing the *P. luminescens luxCDABE* cassette (pSB417) (17). Amplification of each gene was achieved with 30 cycles at 95°C for 15 s, 50°C for 30 s, and 72°C for 60 s, followed by a final extension step at 72°C for 2 min. PCR-amplified DNA was purified prior to cloning procedures by passing complete reaction volumes through spin columns (PCR purification kit; Qiagen, Valencia, Calif.).

Assembly of a modified *luxABCDE* cassette on pBluescript. The luciferase (*luxAB*) and fatty acid reductase genes (*luxCDE*) were assembled on separate pBluescript SK(−) vectors (Stratagene, La Jolla, Calif.) using restriction enzymes sites introduced by PCR. *luxA* PCR-amplified DNA was inserted into pBluescript SK(−) at the *Bam*HI and *Sal*I sites (directionally orientated downstream of the *lacZ* promoter), and the plasmid was electroporated into *Escherichia coli* strain DH5α. Positive *luxA* clones, grown overnight at 37°C on Luria-Bertani (LB) medium containing 100 μg of ampicillin per ml (as were all subsequent clonings in *E. coli*) were selected by PCR (conditions as described above) using M13 forward (5′ - GTA AAA CGA CGG CCA GT - 3′) and reverse (5′-GGA AAC AGC TAT GAC CAT G - 3′) primers, whose sequences flank the pBluescript SK(−) polylinker. Templates in these reactions were added as whole cells, and lysis occurred at the first 95°C incubation. Plasmid DNA from selected clones and all clones subsequently deemed positive was prepared using standard alkaline lysis procedures (Plasmid Spin Miniprep kit; Qiagen). *luxB* PCR-amplified DNA was then cut with *Sal*I/*Xho*I and inserted at the *Sal*I site downstream of the cloned *luxA* gene. This ligation was again electroporated into *E. coli* DH5α, and *luxAB* clones and selected by screening for bioluminescence in the presence of exogenously added *n*-decyl aldehyde (Sigma, St. Louis, Mo.). Bioluminescence was detected using a photon-counting intensified charge-coupled device (ICCD) camera (model 2400-32; Hamamatsu Photonics, Bridgewater, N.J.).

Assembly of a separate *luxCDE* cassette in pBluescript SK(−) was achieved by the sequential cloning of *luxC*, *-D*, and *-E* using the compatible enzymes *Sal*I and *Xho*I. Each step of the cloning procedure was confirmed by screening potential *E. coli* transformants by PCR using M13 forward and reverse primers (as described above). The fidelity of the final *luxCDE* cassette was confirmed by inserting this sequence, cut with *Sal*I/*Xho*I, at the *Sal*I site downstream of the luciferase genes in the above pBluescript SK(−) *luxAB* vector and screening for bioluminescent colonies using the ICCD camera. The modified *lux* operon containing the rearranged *lux* genes preceded by gram-positive RBS was designated *luxABCDE*, to distinguish it from the unmodified native operon *luxCDABE*.

Transformation of *Staphylococcus aureus* to a bioluminescent phenotype. The above *luxABCDE* construct was inserted into the gram-positive or -negative shuttle vector pMK4 (14) and tested for bioluminescence in different *S. aureus* strains using random host DNA fragments as promoters. The *luxABCDE* cassette was cut from pBluescript SK(−) using the restriction enzymes *Bam*HI and *Sal*I and ligated with similarly cut pMK4 plasmid DNA (oriented so that no promoter lay upstream of this cassette) (Fig. 1). This ligation was electroporated into *E. coli* DH5α and *luxABCDE* clones, grown overnight at 37°C on LB medium containing 100 μg of ampicillin (the gram-negative selectable marker found on pMK4) per ml, selected by screening for colonies emitting low levels of bioluminescence (light barely detectable using the Hamamatsu ICCD camera). Genomic DNA from a clinical isolate of methicillin-resistant *S. aureus* (MRSA) was cut with *Sau*3A in a partial digest (1) and ligated into pMK4 *luxABCDE* plasmid DNA cut with *Bam*HI (*Bam*HI enzyme left active to reduce background from religation of the empty vector DNA). This ligation mix was then electroporated into *E. coli* DH5α, and the resulting transformants were plated on LB medium containing 100 μg of ampicillin per ml. The colonies were scraped from the plates and pooled, and their plasmid DNA was extracted (Plasmid Spin Miniprep kit; Qiagen). This plasmid DNA was electroporated into competent *S. aureus* RN4220 cells, and the resulting transformants were selected on LB medium containing 5 μg of chloramphenicol (the gram-positive selectable marker found on pMK4) per ml. Highly bioluminescent colonies were then selected using the ICCD camera.

Comparing bioluminescence from *S. aureus* RN4220 strains containing the modified *luxABCDE* versus the native *luxCDABE*. Plasmid DNA was prepared from several highly bioluminescent strains of *S. aureus* RN4220 containing pMK4 *luxABCDE* with different promoter fragments upstream of *luxA* (see above). The DNA was isolated using alkaline lysis (Plasmid Spin Miniprep kit; Qiagen) subsequent to treatment of the *S. aureus* cells with lysostaphin (Sigma) for 30 min at 37°C. A *luxA* backprimer (5′ - CCA CAC TCC TCA GAG ATG CG - 3′) was then used to sequence the *S. aureus* promoter fragments lying upstream of the *lux* operon in each plasmid. These promoter sequences were termed P1 through P73, and the plasmids were designated pMK4 *luxABCDE* Pn (where n is a number in the range of 1 to 73) Sequencing of the strain *S. aureus* RN4220 pMK4 *luxABCDE* P1 (data not shown) showed that this plasmid still contained an active *Bam*HI site between the promoter sequence and *luxA*. This enabled the directional replacement of the modified *luxABCDE* with the native *luxCDABE* cassette cut from pSB417 (17) by using the restriction enzymes *Bam*HI and *Sal*I. The latter plasmid, pMK4 *luxCDABE* P1, was constructed in *E. coli* DH5α and then moved into *S. aureus* RN4220 using cloning and transformation procedures similar to those described above.

Bioluminescence from *E. coli* DH5α and *S. aureus* RN4220 containing either pMK4 *luxABCDE* P1 or pMK4 *luxCDABE* P1 was compared. Cultures of each of the latter bacterial strains, grown to exponential phase at 37°C in LB medium containing 100 μg of ampicillin per ml or 15 μg of chloramphenicol per ml, were diluted in 100-μl volumes across black 96-well microtiter plates in doubling dilutions (−0.3 log) and monitored for light over a period of 30 min at 37°C using the ICCD camera. The content of each well was then plated on LB agar to allow the number of CFU, ranging from approximately 10^1 to 10^7 CFU/ml, to be compared to levels of bioluminescence (in relative light units [RLU]).

Determining the temperature stability of bioluminescence in *S. aureus*. Exponential cultures of the bacterial strains were grown to a concentration of approximately 10^7 CFU/ml at 30°C in LB medium containing 100 μg of ampicillin per

SPECTRAL_0000645

ml or 15 μg of chloramphenicol per ml, and 1-ml volumes of each were placed in heating blocks set at 31, 33, 35, 37, 39, 41, 43, 45, and 47°C. After allowing the bacteria to acclimate and grow at each temperature for a period of 1 h, the nine heating blocks were sequentially placed inside a dark chamber, and light from each of the three cultures was recorded for a period of 1 min using the ICCD camera. To eliminate errors in the number of RLU arising from variations in bacterial numbers, each culture was plated on LB agar to allow the number of CFU to be recorded and the bioluminescence data to be normalized to the viable-cell number.

Estimating the minimum number of bioluminescent *S. aureus* CFU detectable in liquid culture. Exponential cultures of bioluminescent *S. aureus* RN4220 pMK4 *luxABCDE* P1 were monitored using a highly sensitive liquid nitrogen-cooled integrating charge-coupled device (CCD) camera (model LN/CCD 1340-1300-EB/1; Princeton Instruments, Tucson, Ariz.) to determine the minimum number of CFU of this strain of bacteria detectable at 37°C. Volumes (100 μl) of exponentially growing cells were diluted across black 96-well microtiter plates from approximately 10^5 to 10^1 CFU/ml in doubling dilutions (−0.3 log) and monitored for light over a period of 10 min. The content of each well was then plated on LB agar to allow the number of CFU to be compared to levels of bioluminescence (in RLU).

Monitoring bioluminescent *S. aureus* 8325-4 infections in mice. Plasmid DNA was isolated from *S. aureus* RN4220 pMK4 *luxABCDE* P1 and *S. aureus* RN4220 pMK4 *luxABCDE* P2 (as described above) and used to transform the pathogenic strain *S. aureus* 8325-4 (M. Smeltzer, University of Arkansas, Little Rock). Bioluminescent transformants of *S. aureus* 8325-4 were then tested in vivo in mice. Exponential cultures of *S. aureus* 8325-4 pMK4 *luxABCDE* P1 and *S. aureus* 8325-4 pMK4 *luxABCDE* P2, grown at 37°C in LB medium containing 15 μg of chloramphenicol per ml, were pelleted and then resuspended in phosphate-buffered saline (PBS). Bacterial concentrations were estimated spectrophotometrically by determining the absorbance at 600 nm, and concentrations were adjusted to approximately 5×10^7 CFU/ml by dilution with PBS. These cells were then held on ice for a short period until the mice were ready to be inoculated. Cell numbers were verified by plating dilutions of inoculum onto LB agar.

Mice were anesthetized with ketamine (100 mg/ml) and xylazine (20 mg/ml), mixed at a 4:1 ratio (vol/vol) just before use. A ketamine-xylazine mixture (100 mg/kg of body weight [dose based on ketamine concentration]) was injected intramuscularly into the right hamstring muscle. After anesthesia was established, the mice were injected in the left anterior tibialis with approximately 5×10^6 CFU in a total volume of 100 μl of PBS (twelve mice were injected with *S. aureus* 8325-4 pMK4 *luxABCDE* P1 and twelve mice were injected with *S. aureus* 8325-4 pMK4 *luxABCDE* P2). Six mice from each group were treated with a single oral dose of amoxicillin (10 mg/kg) immediately prior to anesthesia, with the remaining six mice from each group serving as untreated controls. Mice were imaged at 0, 4, 8, and 24 h postinfection using the Hamamatsu ICCD camera. At each time point, both dorsal and ventral images were taken. All images were collected for 5 min.

Quantification of bioluminescence data from mice. Total photon emission from selected and defined areas within the images of each mouse was quantified with the LivingImage software package (Xenogen Corporation, Alameda, Calif.). The photon signal from the anterior tibialis muscle was quantified from the dorsal and ventral images of each mouse, and a dorsal-ventral average was calculated. This averaging corrects for light scattering differences due to mouse-to-mouse variation in the tissue depth of the bacteria.

Extraction and quantification of bacteria from the thigh muscle of mice. After the 24-h imaging time point, the mice were sacrificed and the infected thigh muscles (both the anterior tibialis and the quadriceps muscle) were surgically removed. The muscle tissue was homogenized in 500 μl of PBS with a loose Dounce homogenizer. The tissue and bacterial suspension was then diluted in PBS by 10^5, 10^6, and 10^7 to a final volume of 1 ml for each dilution. A 100-μl volume of each dilution was plated out in duplicate onto LB agar plates and incubated overnight at 37°C. The following morning colonies were counted and the numbers of CFU for each tissue sample were estimated.

RESULTS

Gram-positive RBSs allow the *P. luminescens lux* operon to function in *S. aureus*. Vallanoweth and Rabinowitz (17) have reported that gram-positive ribosomes are unable to translate mRNAs containing weak gram-negative RBSs. In addition, they stated that the spacing between the RBS and the start codon (most commonly ATG) on gram-positive mRNAs should ideally be 7 to 10 nucleotides. In the present study we used PCR to alter the RBS of each gene in the *P. luminescens lux* operon from AGG to AGGAGG, ensuring that this site was a minimum of 7 bases upstream of the start codons of each gene (Table 1). Interestingly, in *E. coli*, bioluminescence from clones containing the modified *luxABCDE* operon (that containing a gram-positive RBS) was found to be significantly greater than that from those containing the unmodified *luxCDABE* operon (that containing a gram-negative RBS), but only when both constructs lay downstream of a weak uninduced pBluescript *lacZ* promoter. Increasing transcription of both *lux* operons on pBluescript in *E. coli* by the addition of isopropyl-β-D-thiogalactopyranoside (IPTG) to the medium (solid or liquid culture) resulted in significantly more light from the unmodified *luxCDABE* operon but in a decrease in light from the modified *luxABCDE* operon. Low levels of bioluminescence could also be seen from *E. coli* clones containing a promoterless *luxABCDE* operon, greatly aiding the cloning of this cassette into the shuttle vector pMK4 lacking a recognized promoter (Fig. 1).

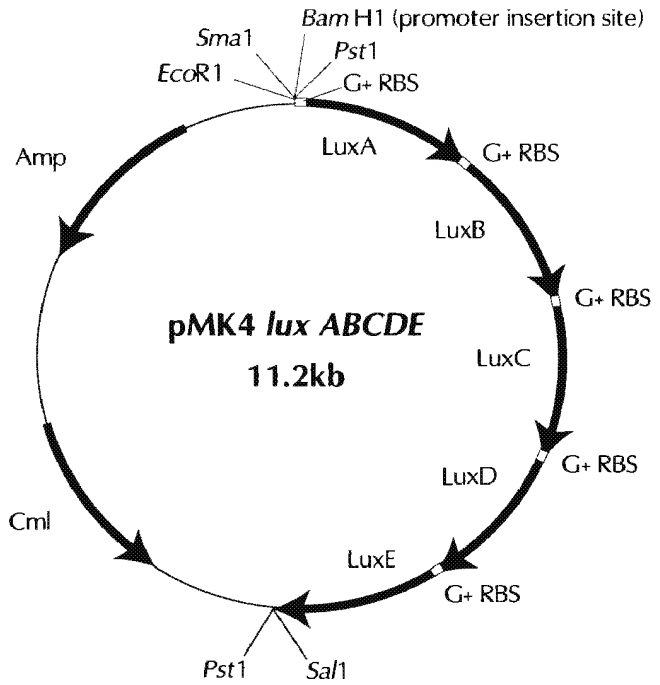


FIG. 1. Schematic diagram of the plasmid pMK4 *luxABCDE*. Nucleotide sequences of the *lux* genes, ordered as shown, are as given in GenBank (accession number M90093) flanked by the relevant sequences shown in Table 1. This plasmid can be used to generate constitutive bioluminescent strains by ligating genomic DNA (partially digested by 4-base cutter) at the unique *Bam*HI or *Sma*I site and selecting for light in the gram-positive bacterium from which the DNA was derived.

Random fragments of genomic DNA from *S. aureus* were ligated into pMK4 *luxABCDE*, such that efficiently expressed constitutive promoters could be identified using the modified *lux* operon as a reporter. Electrotransformation of *S. aureus* RN4220 with the mixture of plasmid DNAs in this ligation reaction mixture resulted in approximately 20,000 transformants, with between 5 and 10% of these colonies showing some degree of bioluminescence. From the 2,000 or so bioluminescent colonies, 73 moderately to highly bioluminescent transformants were isolated and further characterized for constitutive bioluminescence. The level of bioluminescence from the majority of these strains was comparable to that seen from gram-negative bacteria, such as *E. coli*, carrying an expressed *luxCDABE* operon (data not shown). Bioluminescence from pure cultures of many of these *S. aureus* strains was at a level that could be observed by the naked eye in a darkroom after less than a minute of acclimatization.

Plasmid DNA from the six brightest strains, designated *S. aureus* RN4220 pMK4 *luxABCDE* P1 through P6, was purified, and the flanking 500 bp upstream of *luxA* were se-

DOWNLOADED FROM iai.ASM.ORG - at UCLA BIOMEDICAL LIB/SERIALS July 14, 2010

SPECTRAL_0000646

DOWNLOADED FROM iai.ASM.ORG - at UCLA BIOMEDICAL LIB/SERIALS July 14, 2010

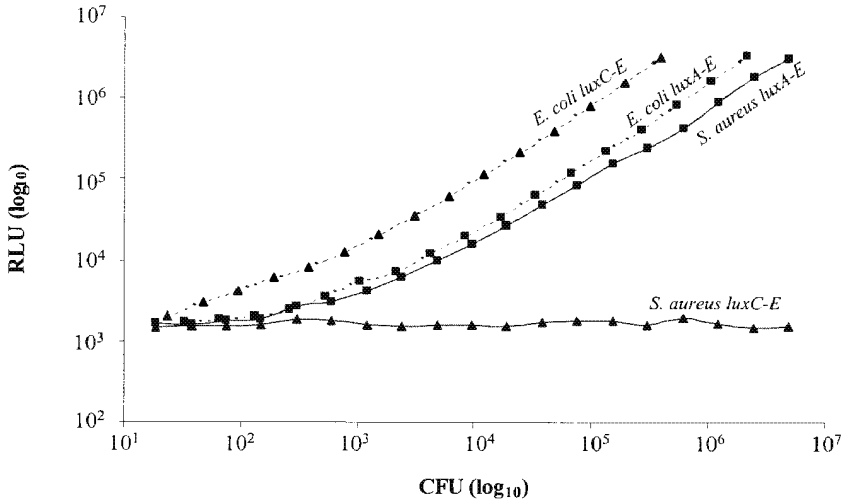


FIG. 2. Comparison of bioluminescence from *S. aureus* and *E. coli* containing the native *luxCDABE* operon versus that in strains containing the modified *luxABCDE* operon. Exponential cultures of *S. aureus* RN4220 pMK4 *luxABCDE* P1 (-■-), *S. aureus* RN4220 pMK4 *luxCDABE* P1 (-▲-), *E. coli* DH5α pMK4 *luxABCDE* P1 (··■··) and *E. coli* DH5α pMK4 *luxCDABE* P1 (··▲··) were diluted across black 96-well microtiter plates in doubling dilutions (−0.3 log) and monitored for light over a period of 30 min using the ICCD camera. The content of each well was then plated to allow the number of CFU to be compared to the level of bioluminescence (RLU).

quenced. All six sequences were different (suggesting that different promoters had been selected), and each showed a high level of homology to gram-positive sequences (especially to *S. aureus* and *Bacillus subtilis* sequences) in GenBank (data not shown). Fortuitously, pMK4 *luxABCDE* P1 was found to still contain an active *Bam*HI site between the promoter sequence and *luxA*. This enabled the directional replacement of *luxABCDE* with a *luxCDABE* cassette cut from pSB417 (18). By interchanging the *lux* cassettes so exactly, discrepancies in light due to promoter activity could essentially be eliminated, allowing a true comparison of the activity of the two operons to be made. Figure 2 shows that both *luxCDABE* and *luxABCDE* function similarly in *E. coli* (approximately fourfold difference), but only *luxABCDE* gives significant bioluminescence in *S. aureus*. The minimum number of *S. aureus* RN4220 pMK4 *luxABCDE* P1 CFU detectable at 37°C using a photon-counting ICCD camera was approximately 400 CFU. However, using a more sensitive liquid nitrogen-cooled integrating CCD camera we were able to detect as few as 80 CFU at 37°C.

Bioluminescence from *S. aureus* RN4220 pMK4 *luxABCDE* P1 is optimal at 37°C. To monitor bioluminescence emitted from pathogenic bacteria within animals (4), it is essential that both the *lux* genes and Lux proteins function adequately at body temperature (i.e., around 37°C). Thus, in order to determine whether modification of the *lux* genes had altered the temperature range over which optimal bioluminescence occurs in bacterial cells, light arising from the modified *luxABCDE* cassette was compared to that from the native *luxCDABE* operon in both gram-negative and gram-positive bacteria between 31 and 47°C. Since *S. aureus* RN4220 pMK4 *luxCDABE* P1 was previously shown to be nonbioluminescent (Fig. 2), only *S. aureus* RN4220 pMK4 *luxABCDE* P1, *E. coli* DH5α pMK4 *luxABCDE* P1, and *E. coli* DH5α pMK4 *luxCDABE* P1 were tested over the above-mentioned temperature range. Figure 3 shows that the maximum light to be recorded from a culture of *S. aureus* RN4220 pMK4 *luxABCDE* P1 was at 37°C. Furthermore, between 31 and 41°C the light emission from this strain remained above 60% maximum, and it continued to do so for more than 4 h (data not shown), indicating that the Lux enzymes are stable over this temperature range. In contrast, both *E. coli* DH5α pMK4 *luxABCDE* P1 and *E. coli* DH5α pMK4 *luxCDABE* P1 gave maximum light at 41°C. Comparison of the light profiles from these two *E. coli* strains indicates that the *luxABCDE* construct functions less efficiently at lower temperatures than *luxCDABE*. Whether this is an accurate reflection of the functioning of this modified *lux* construct or of the P1 promoter is not known. However, since this construct was designed to work optimally in gram-positive bacteria, optimization of bioluminescence in gram-negative bacteria can still be performed using the native *luxCDABE* cassette.

Bioluminescent *S. aureus* allows effective antibiotic treatment to be monitored in living animals. A number of pathogenic strains of *S. aureus* were transformed with the plasmids pMK4 *luxABCDE* P1 and pMK4 *luxABCDE* P2, including RN6390, 8325-4, and a clinical isolate of MRSA. Interestingly, RN6390 and 8325-4 were both found to produce similar levels

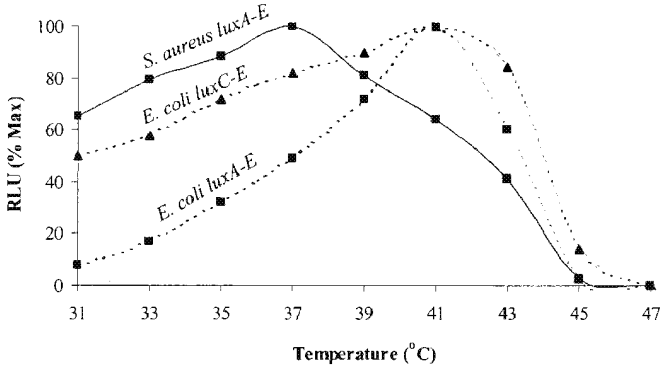


FIG. 3. Temperature stability of the modified *luxABCDE* operon. Exponential cultures of *S. aureus* RN4220 pMK4 *luxABCDE* P1 (-■-), *E. coli* DH5α pMK4 *luxABCDE* P1 (··■··), and *E. coli* DH5α pMK4 *luxCDABE* P1 (··▲··) were grown to approximately 1×10^7 CFU/ml at 30°C and 1-ml volumes of each were placed in heating blocks set at 31, 33, 35, 37, 39, 41, 43, 45, and 47°C. After 1 h at each of these elevated temperatures, the nine heating blocks were sequentially placed inside a dark chamber and light from each of the three cultures was recorded for a period of 1 min using the ICCD camera. Shown are the number of RLU at each of the temperatures, with this data expressed as a percentage of the maximum (Max) bioluminescence attained and adjusted for variation in the number of CFU.

SPECTRAL_0000647

DOWNLOADED FROM iai.ASM.ORG - at UCLA BIOMEDICAL LIB/SERIALS July 14, 2010

of bioluminescence to RN4220 when transformed with each of the above-mentioned plasmids, whereas the transformed strain of MRSA was significantly brighter (two- to fourfold). Whether this increase in light was due to increased transcription or translation (the promoter sequences being derived from this MRSA strain) or was simply a factor of higher metabolic activity in this strain was not determined. However, the fact that fewer MRSA cells could be detected with these strains, both in culture and in vivo, than could be detected with other transformed *S. aureus* strains (data not shown), indicated that increased screening for more highly bioluminescent constructs may increase the sensitivity of detection still further.

Figure 4 shows how bioluminescent *S. aureus* can be effectively monitored in living animals in real time and can be used to determine the efficacy of antibiotic therapy. Both *S. aureus* 8325-4 pMK4 *luxABCDE* P1 and *S. aureus* 8325-4 pMK4 *luxABCDE* P2 produced significant bioluminescent signals in mice, allowing treatment with amoxicillin to be effectively assessed (only P1 ventral images shown). Cumulative bioluminescence data collected from both the dorsal and ventral sides of each animal is shown in Fig. 5. At 8 h, the infection in both groups of treated animals had begun to clear, as judged by a decrease in bioluminescence, and by 24 h no signal could be detected. In comparison, both groups of untreated mice had strong bioluminescent signals at 24 h, corresponding to an apparent poor state of health as indicated by ruffled fur and dragging of the hindquarters during movement.

Extraction of bacteria from the thigh muscles of each of the mice confirmed the bioluminescence data to be extremely accurate at predicting the number of viable bacteria in the tissue. For both strains of bacteria, *S. aureus* 8325-4 pMK4 *luxABCDE* P1 and *S. aureus* 8325-4 pMK4 *luxABCDE* P2, the number of CFU recovered from the thigh muscles of the untreated mice at 24 h postinfection was found to have increased approximately 25-fold (2×10^9 CFU/ml) over the inoculating dose (8×10^7 CFU/ml). In comparison, the number of CFU (P1 and P2) in the thigh muscles of the antibiotic-treated mice varied between 1.1×10^3 and 6.8×10^4 CFU/ml at 24 h postinfection, representing a decrease of at least 1,000-fold from the number of CFU used to inoculate the mice. Moreover, by plating all of the recovered bacteria on media containing no antibiotics, the plasmid stability of both bioluminescent *S. aureus* strains could be assessed. *S. aureus* 8325-4 pMK4 *luxABCDE* P2 was slightly more stable than *S. aureus* 8325-4 pMK4 *luxABCDE* P1, with 95% of P2 CFU retaining a high level of bioluminescence, as opposed to 85% of P1 CFU when plated in the absence of selection. However, since each CFU recovered from a mouse thigh muscle consists of approximately 10^5 to 10^6 cells derived from a single cell in the absence of selective pressure to maintain the *lux* plasmid, the percentage of bacteria still carrying plasmid DNA upon extraction from the animal was probably significantly higher.

DISCUSSION

Among the *lux* operons from bioluminescent bacteria, that from *P. luminescens* (2, 12) appears to be ideally suited for use in mammalian animal models, given that mammalian body temperatures lie within the temperature optimum for the bioluminescent enzymes from this bacterium (Fig. 2) (6, 15, 19). This is in contrast to the low optimum temperature for beetle luciferases (Luc) and other characterized bacterial luciferases, such as those from species of *Vibrio* (8, 10). In vivo monitoring of luciferase was initially pioneered with a gastrointestinal infectious disease model using bioluminescent gram-negative *Salmonella enterica* serovar Typhimurium (4). This study indicated not only that in vivo bioluminescent imaging is feasible but also that it can be quantitative and its use, as predicted, results in more information in less time than conventional assays. Although a large variety of gram-negative bacterial species can be labeled with the *P. luminescens lux* operon, the introduction of these or other bacterial *lux* operons into gram-positive bacteria results in little or no light, regardless of the strength of the promoter preceding this operon (our unpublished data). Data presented in this paper show that for the first time it is possible to generate bioluminescent gram-positive bacteria capable of producing high levels of light at 37°C without the addition of exogenous substrate (Fig. 2). The consequence of this finding is far reaching, especially in the development of real-time in vivo assays for antibiotic efficacy studies designed to monitor gram-positive infections in animal models, as is demonstrated in this study with bioluminescent *S. aureus* (Fig. 4).

In recent years there has been a dramatic increase in the number of antibiotic-resistant strains of gram-positive bacteria causing serious, life-threatening diseases in humans. This is especially true for strains of *S. aureus*, *Streptococcus pneumoniae*, *Mycobacterium tuberculosis*, and enterococci (3, 11), with a large number of these bacteria being resistant to a wide range of or, in some cases, all conventional antibiotics (e.g., MRSA and vancomycin-resistant enterococci). The occurrence of such multidrug-resistant bacteria is of increasing concern, since they represent a disease threat of epidemic proportions. Conventional methodologies for monitoring these gram-positive pathogens in vivo are not only cumbersome, but they also usually include biological assessment regimens that represent late or end stages of the disease process and often use death as an endpoint. The late-stage animal protocols are also considered more stressful to the animal in these models and less likely to give important information about the events early in disease. Alternatively, ex vivo assays can be employed to reveal disease processes. These assays require removal of tissue and, usually, sacrifice of the animal. As a consequence there is the loss of the contextual influences of the living animal. Ex vivo assays can be extraordinarily sensitive (e.g., PCR, with single-molecule sensitivity). However, such assays are typically plagued with various artifacts such as sampling limitations, where only a small amount of tissue or limited numbers of cells can be analyzed. The use of bioluminescent noninvasive imaging strategies to reveal the real-time effects of potential therapeutic agents on gram-positive bacterial infections in animal models would greatly accelerate the analyses of compounds under development. The spatial and temporal differences in the bioluminescent signals between treated and untreated animals (Fig. 4) can be used to assess the effects of compounds on specific biological processes in vivo.

Although this study only describes bioluminescent *S. aureus*, we have used the modified *luxABCDE* operon to successfully transform a wide range of gram-positive bacteria, including strains of *S. pneumoniae* and *Listeria monocytogenes* (data not shown). In each case, the gram-positive bacteria carrying this modified *lux* operon are highly bioluminescent and can be monitored in vivo in animals. Plasmid loss in the absence of antibiotic selection has been shown to be minimal from each of the latter bacteria over a period of 24 to 48 h in vivo (>80% plasmid retention), with no observable genetic structural instability. However, since plasmids are of limited use for monitoring regulation due to artifacts involving, among other things, copy number and supercoiling, we have recently constructed a number of *luxABCDE* transposons. These have been successfully used to stably transform and monitor gene regulation in a number of gram-positive bacteria (our unpublished results).

SPECTRAL_0000648

DOWNLOADED FROM iai.ASM.ORG - at UCLA BIOMEDICAL LIB/SERIALS July 14, 2010

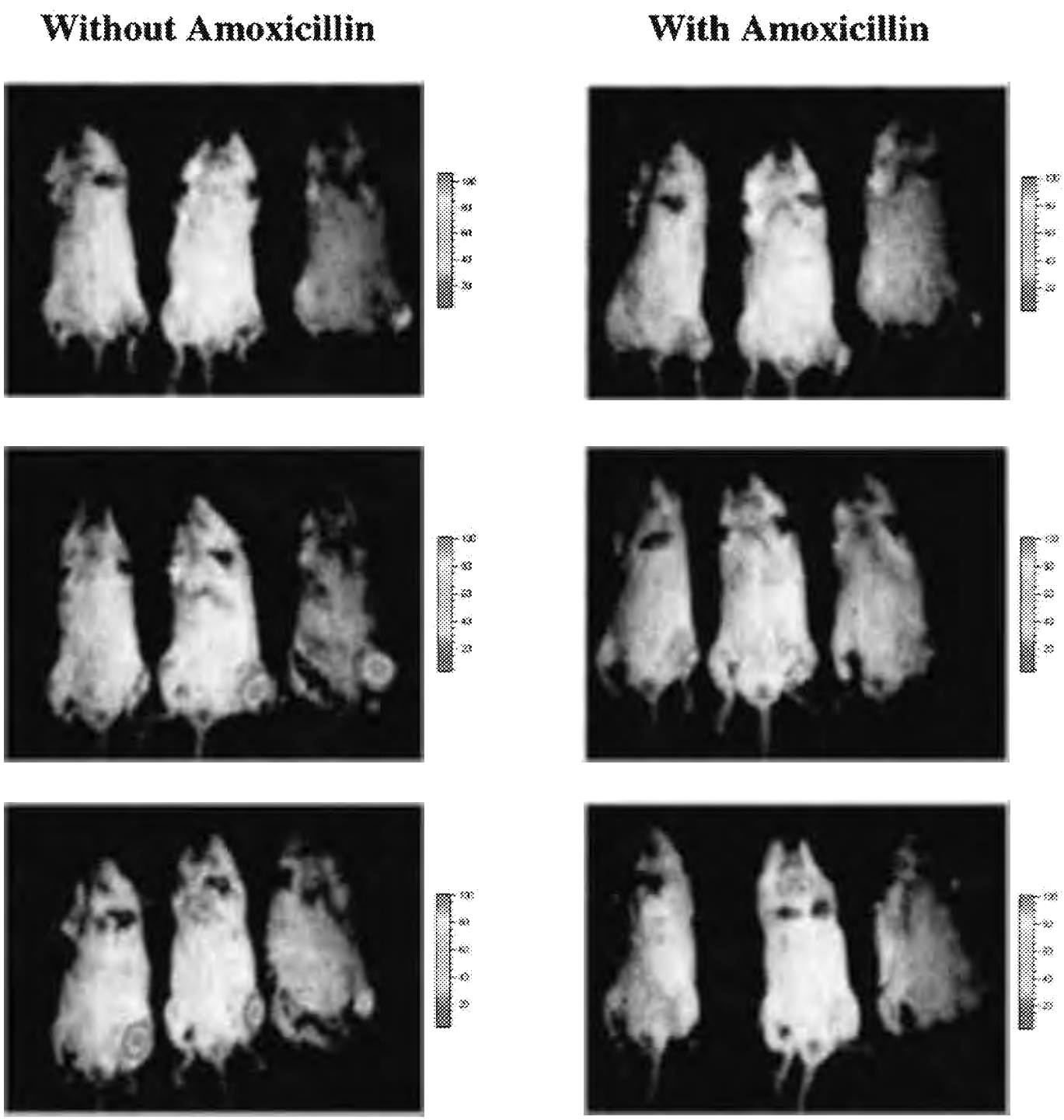


FIG. 4. Monitoring the effects of amoxicillin on bioluminescent *S. aureus* in mice. Exponential cultures of the bioluminescent bacteria were injected intramuscularly into the left anterior tibialis (8×10^6 CFU) of 24 anesthetized mice, 12 mice with *S. aureus* 8325-4 pMK4 *luxABCDE* P1 and 12 mice with *S. aureus* 8325-4 pMK4 *luxABCDE* P2. Six mice from each group were treated with a single oral dose of amoxicillin (10 mg/kg) immediately prior to anesthesia, with the remaining six mice from each group serving as untreated controls. Shown are three treated and three untreated *S. aureus* 8325-4 pMK4 *luxABCDE* P1-infected mice, imaged ventrally for 5 min at 0, 8, and 24 h postinfection using the ICCD camera.

The ability to monitor gene regulation in gram-positive bacteria using bioluminescence should also prove extremely valuable for in vitro uses, such as environmental monitoring and for applications in the food industry.

The noninvasive approach described here allows for experimental protocols that are significantly faster. Furthermore, because biostatistics are improved through collection of multiple data points in the same animal, the overall number of

SPECTRAL_0000649

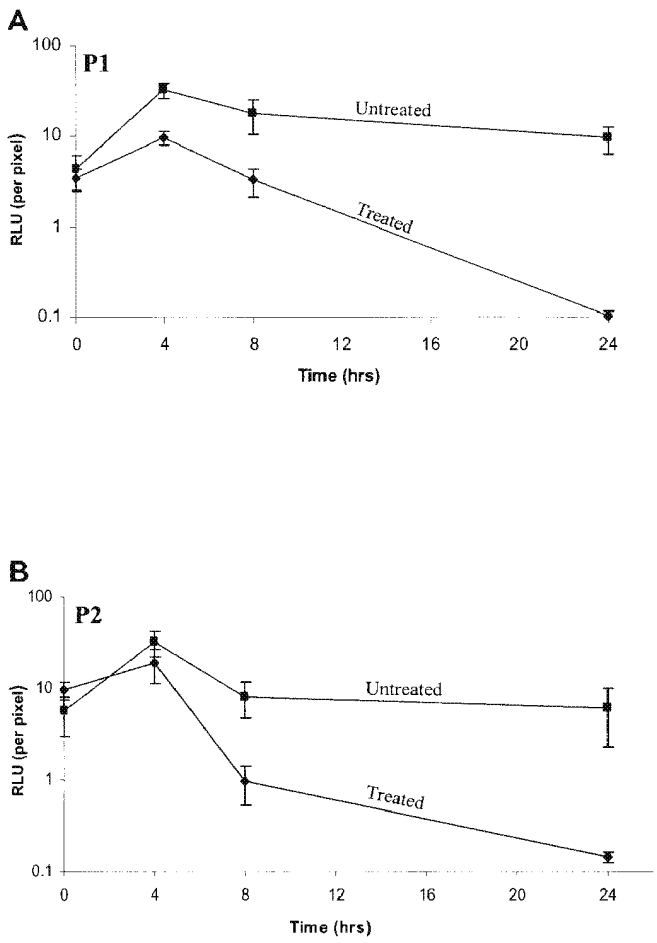


FIG. 5. Bioluminescence data recorded from *S. aureus* 8325-4 pMK4 *luxABCDE* P1 (A)- and *S. aureus* 8325-4 pMK4 *luxABCDE* P2 (B)-infected mice. Each data set represents the mean number of RLU from six mice either untreated (■) or treated (◆) with amoxicillin (10 mg/kg), imaged both dorsally and ventrally for 5 minutes at 0, 4, 8, and 24 h postinfection using the ICCD camera. Error bars, standard errors of the means.

animals required is reduced. These two benefits should improve the capacity to relieve the bottleneck of animal studies that occurs in drug development as high-throughput technologies increase the number of potential lead compounds that require animal evaluation. We believe that this technology also increases the quality of animal model data to provide more information for selecting the drug candidates that will be clinically successful.

ACKNOWLEDGMENTS

We thank B. Nelson and M. Cable (Bioimaging Section, Xenogen Corporation) for their assistance with experimental design and data collection using the two CCD cameras, C. Safieddine (Animal Husbandry Section, Xenogen Corporation) and R. Gungon (Infectious Disease Section, Xenogen Corporation) for assisting with the animal work, and D. Jenkins (Oncology Section, Xenogen Corporation) and C. Contag (University of Stanford, Stanford, California) for help with preparing the manuscript. We also thank M. Winson (University of Wales, Aberystwyth, United Kingdom) for kindly supplying us with the *P. luminescens lux* plasmid, pSB417, and M. Smeltzer (University of Arkansas) for the *S. aureus* strain 8325-4.

REFERENCES

1. **Ausubel, F. M., R. Brent, R. E. Kingston, D. D. Moore, J. G. Seidman, J. A. Smith, and K. Struhl.** 1995. Current protocols in molecular biology, vol. 1. John Wiley & Sons, Inc., New York, N.Y.
2. **Boemare, N. E., R. J. Akhhurst, and R. G. Mourant.** 1993. DNA relatedness between *Xenorhabdus* spp. (*Enterobacteriaceae*), symbiotic bacteria of entomopathogenic nematodes, and a proposal to transfer *Xenorhabdus luminescens* to a new genus, *Photorhabdus* gen. nov. Int. J. Syst. Bacteriol. **43:**249–255.
3. **Carbon, C.** 1999. Costs of treating infections caused by methicillin-resistant staphylococci and vancomycin-resistant enterococci. J. Antimicrob. Chemother. **44:**31–36.
4. **Contag, C. H., P. R. Contag, J. I. Mullins, S. D. Spilman, D. K. Stevenson, and D. A. Benaron.** 1995. Photonic detection of bacterial pathogens in living hosts. Mol. Microbiol. **18:**593–603.
5. **Corbisier, P., G. Ji, G. Nuyts, M. Mergeay, and S. Silver.** 1993. *luxAB* gene fusions with the arsenic and cadmium resistance operons of *Staphylococcus aureus* plasmid pI258. FEMS Microbiol. Lett. **110:**231–238.
6. **Frackman, S., M. Anhalt, and K. H. Nealson.** 1990. Cloning, organization, and expression of the bioluminescence genes of *Xenorhabdus luminescens*. J. Bacteriol. **172:**5767–5773.
7. **Francis, K. P., and M. P. Gallagher.** 1993. Light emission from a Mu*lux* transcriptional fusion in *Salmonella typhimurium* is stimulated by hydrogen peroxide and by interaction with the mouse macrophage cell line J774.2. Infect. Immun. **61:**640–649.
8. **Hill, P. J., C. E. Rees, M. K. Winson, and G. S. Stewart.** 1993. The application of *lux* genes. Biotechnol. Appl. Biochem. **17:**3–14.
9. **Howe, R. A., M. Wootton, T. R. Walsh, P. M. Bennett, and A. P. MacGowan.** 1999. Expression and detection of hetero-vancomycin resistance in *Staphylococcus aureus*. J. Antimicrob. Chemother. **44:**675–678.
10. **Meighen, E. A.** 1993. Bacterial bioluminescence: organization, regulation, and application of the lux genes. FASEB J. **7:**1016–1022.
11. **Petrini, B., and S. Hoffner.** 1999. Drug-resistant and multidrug-resistant tubercle bacilli. Int. J. Antimicrob. Agents **13:**93–97.
12. **Rainey, F., R.-U. Ehlers, and E. Stackebrandt.** 1995. Inability of the polyphasic approach to systematics to determine the relatedness of the genera *Xenorhabdus* and *Photorhabdus*. Int. J. Syst. Bacteriol. **45:**379–381.
13. **Steidler, L., W. Yu, W. Fiers, and E. Remaut.** 1996. The expression of the *Photinus pyralis* luciferase gene in *Staphylococcus aureus* Cowan 1 allows the development of a live amplifiable tool for immunodetection. Appl. Environ. Microbiol. **62:**2356–2359.
14. **Sullivan, M. A., R. E. Yasbin, and F. E. Young.** 1984. New shuttle vectors for *Bacillus subtilis* and *Escherichia coli* which allow rapid detection of inserted fragments. Gene **29:**21–26.
15. **Szittner, R., and E. Meighen.** 1990. Nucleotide sequence, expression and properties of luciferase coded by lux genes from terrestrial bacterium. J. Biol. Chem. **265:**16581–16587.
16. **Vellanoweth, R. L., and J. C. Rabinowitz.** 1992. The influence of ribosome-binding-site elements on translational efficiency in *Bacillus subtilis* and *Escherichia coli* in vivo. Mol. Microbiol. **6:**1105–1114.
17. **Winson, M. K., S. Swift, P. J. Hill, C. M. Sims, G. Griesmayr, B. W. Bycroft, P. Williams, and G. S. Stewart.** 1998. Engineering the *luxCDABE* genes from *Photorhabdus luminescens* to provide a bioluminescent reporter for constitutive and promoter probe plasmids and mini-Tn*5* constructs. FEMS Microbiol. Lett. **163:**193–202.
18. **Wong, S. S., P. L. Ho, P. C. Woo, and K. Y. Yuen.** 1999. Bacteremia caused by staphylococci with inducible vancomycin heteroresistance. Clin. Infect. Dis. **29:**760–767.
19. **Xi, L., K. W. Cho, and S. C. Tu.** 1991. Cloning and nucleotide sequences of *lux* genes and characterization of luciferase of *Xenorhabdus luminescens* from a human wound. J. Bacteriol. **173:**1399–1405.

Editor: E. I. Tuomanen

DOWNLOADED FROM iai.ASM.ORG - at UCLA BIOMEDICAL LIB/SERIALS July 14, 2010

SPECTRAL_0000650

Radiometric and Geometric Calibration of a Visible Spectral Electro-Optic "Fisheye" Camera Radiance Distribution System

KENNETH J. VOSS

Institute of Marine Resources, Scripps Institution of Oceanography, University of California, San Diego, La Jolla, California

GIUSEPPE ZIBORDI

Institute for the Study of Geophysical and Environmental Methodologies, National Council of Research, Modena, Italy

(Manuscript received 22 July 1988, in final form 27 December 1988)

ABSTRACT

Camera systems which measure a complete hemispherical field ("fisheye" lens systems), can be applied to the measurement of the radiance, but accurate radiometric and geometric calibrations are required to obtain absolute radiance data. The calibration procedure applied to an instrument built for spectral and geometrical radiance distribution measurements in the visible wavelength region (450–650 nm), based on an electro-optic fisheye camera system, is described and validated through comparison with a more standard radiometer.

1. Introduction

Methods for making measurements of the total sky radiance distribution, and total underwater radiance distribution can be used for many purposes: ground truth of satellite data, validation of radiative transfer models, determination of physical and optical properties such as absorption and scattering phase function. In many studies, such as auroral emissions (Babey et al. 1986), bidirectional reflectance properties (Deering and Eck 1987), sky and underwater visibility (Boileau and Gordon 1966; Tyler 1960), and radiative transfer (Smith 1974), measurements of either the total sky or underwater radiance distributions (or both) are required. These measurements have not been performed widely in the past, however, because of the difficulty in making accurate measurements with sufficient angular resolution in a time short enough to avoid changes in the distribution during data collection. Recent advances in solid state camera systems have opened up methods of collecting this type of data quickly and accurately. "Fisheye" optics cover a hemispherical field of view and, coupled with an electro-optic camera system, allow a hemisphere of the radiance distribution to be gathered in a single image. Thus measurement takes place rapidly in a single frame period which, with implementation of a filter changer mechanism, allows measurement at several spectral bands to be performed in a short time.

A system for spectral measurement of the underwater and sky radiance distribution (composed of two cameras to obtain the upwelling and downwelling underwater radiance, and a third camera to obtain the sky radiance at the surface) has been developed and successfully applied in field measurements (Voss 1989). Particular care has been devoted to the radiometric and geometric calibration of the system in order to obtain absolute radiance values.

In this paper, with reference to the electro-optic fisheye Radiance Distribution Camera System used in atmospheric measurements, the calibration procedure is described and validated through comparison of contemporaneous measurements taken with the instrument and with a more standard sky radiometer.

2. Description of the instrument

The electro-optic fisheye Radiance Distribution Camera System (RADS) consists of a fisheye lens, a filter changer assembly, and a solid state camera (GE 2509 CID). Figure 1 shows a schematic of this system.

A fisheye converter lens (Bicar) is used as input stage to the filter changer optics. This lens typically extends the field of view of a more conventional lens to allow a 2π solid angle in the object space to be projected onto the image plane. The filter changer optics are used to provide an appropriate optical path for light filtration and to enable image formation on the sensing device of the camera. The resultant optical system makes possible measurement of the radiance distribution from 0 to 87.5 degrees zenith and 360 degrees azimuth: almost an entire hemisphere.

The filter changer allows four spectral filters (to select desired spectral bands in the visible and near infrared regions) and four absorption neutral density filters (to

Corresponding author address: Dr. Kenneth Voss, Institute of Marine Resources/Scripps Institution of Oceanography, University of California, San Diego, Mail Code A-018, La Jolla, CA 92093.

© 1989 American Meteorological Society

SPECTRAL_0000651

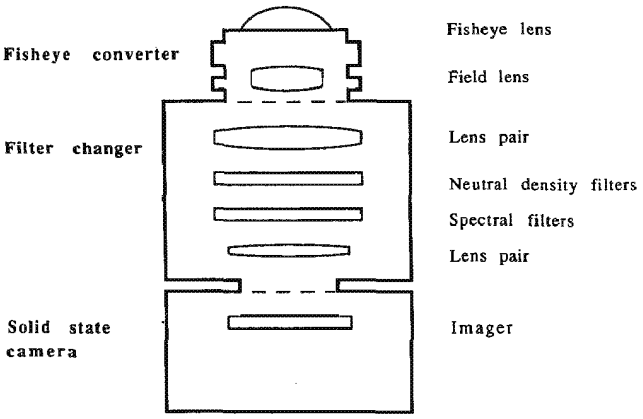


FIG. 1. A schematic of the electro-optics fisheye camera system.

adjust the overall scene dynamic range to the optimum camera level) to be inserted into the optical path of the instrument. The optical rays are not focused at the position occupied by the neutral density and spectral filters, so small spatial variations in the optical properties of the filters can be neglected. The maximum deviation of any ray from the optical axis of the camera system is 16 degrees, causing a maximum shift of 1.5% in the transmittance peak of the interference filters. The filter changer is remotely controlled allowing multiple spectral measurements in rapid succession to be performed.

The GE-2509 CID is a solid state camera with a Charge Injection Device (CID) imaging sensor, a resolution of 253 (vertical) × 260 (horizontal) elements, with the characteristics of low blooming [compared with Charge Coupled Devices (CCD) cameras (Sims and Denton 1987)], dynamic range of over two orders of magnitude, spectral responsivity between 400 and 1100 nm and frame period of approximately $\frac{1}{30}$ s. The camera can perform, through remote control, on-chip integration of the incident irradiance, making possible an extension of the lower limit of the camera sensitivity.

A frame grabber (Poynting 509) is used to convert the analog signal from the camera into eight bit digital form (256 grey levels). A microcomputer (Hewlett Packard 310C) is used for overall system control, data handling, processing and storage. A color CRT allows data to be displayed on screen as false color images, and a $\frac{1}{4}''$ cartridge tape drive (Hewlett Packard 9144A) with a storage capacity of 182 megabytes data per cartridge is used for permanent archiving of data.

3. Calibration

The irradiance in the image plane of ideal optics is proportional to the radiance field in the object space (Slater 1980). Therefore, radiometric and geometric calibration factors can be applied to digitized data of the radiance field, obtained with the optical system, to compute absolute radiometric values and determine their absolute spatial location. The necessary factors for the calibration of data taken with RADS have been derived from measurements carried out in the laboratory. In the following subsections, a description and quantitative results are given for each step of the applied calibration procedure.

a. Linearity calibration

Response of the measuring system to input flux is determined by both the camera and frame grabber (uniformity of the imager in linearity and sensitivity, frame grabber linearity), so the system linearity must be calibrated as a unit, and substitution of one or the other part requires recalibration. To test the uniformity in response of the imager, it is required that the imager be uniformly illuminated during measurements. To this end, the lens and filter changer were removed from the camera and the imager was illuminated by diffuse, unfocused light from a plastic diffusing plate which was itself illuminated on the back side with a lamp. The lamp supply current was constantly monitored during measurements to avoid changes in irradiance due to variation in the output of the power source. The lamp was moved away from the diffusing plate in steps which were calibrated to cause a 0.1 logarithmic (1 dB) reduction in irradiance. Images were saved at each step and were used to determine the linearity from a relative intensity of 1.0 to 0.01 irradiance units.

The result of this calibration is shown in Fig. 2, where the logarithm of the digitized values are plotted versus the logarithm of the relative irradiance incident on the imager; this illustrates the very linear response of the system. The count values given in Fig. 2 were determined by a 100 × 100 element average taken from the center of the imager. Before sampling, a "dark frame" was subtracted off, pixel by pixel. This frame consisted of an average of 5 frames of the dark field (obtained with the camera completely obscured), and it was used to remove the dark noise due to thermal generation of charges (noise dependent on temperature and integration time), manufacturing defects in the elements of the imager (spatially dependent noise), and the read out process (random noise).

To test the uniformity in response of the imager, the images obtained for the linearity calibration were divided into 4 × 4 element segments, and linearity tests and response curves were determined for each subsample. The imager was found to be very uniform, with a total variation of 3% in linearity and sensitivity.

Because of the uniformity exhibited by the imager, and for simplicity of processing, the elements of the imager were considered to have a linearity response equal to that given by the central 100 × 100 elements. The error associated with this assumption is less than 3%. Thus the relative linearized radiance, L_l, is given by

$$L_l = b(\mathrm{DN} - \mathrm{D0})^m, \qquad (1)$$

SPECTRAL_0000652

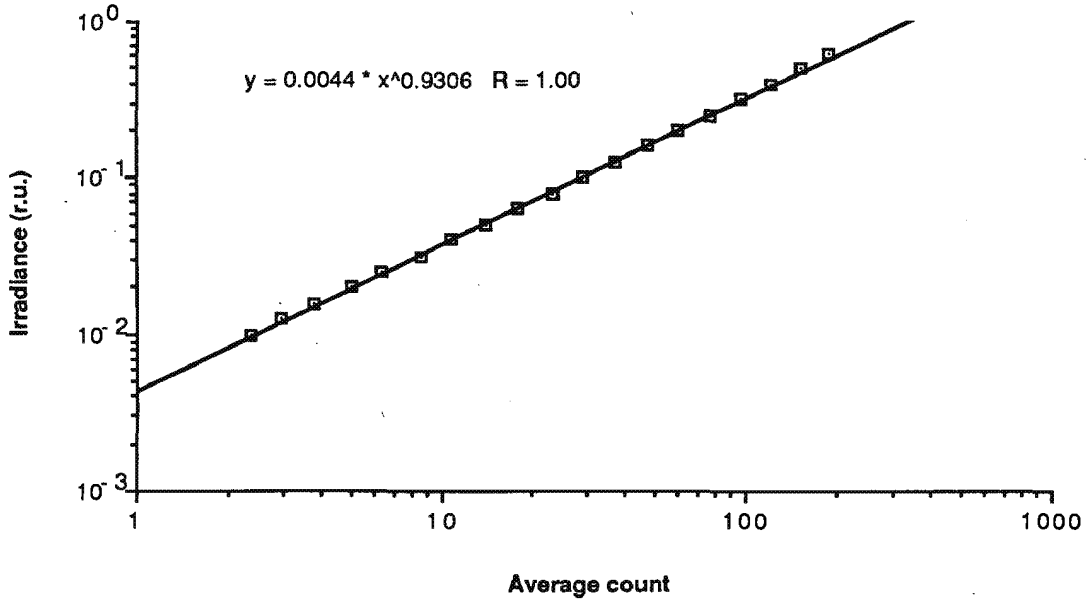


FIG. 2. Linearity of the system to input irradiance.

where DN is the digital number obtained from the irradiance measured by the analyzed element of the imager, D0 is the correspondent dark noise, and b (offset) and m (slope) are the coefficients derived from a logarithmic least-squares fit to digitized data of the relative irradiance measured by the imager (see Fig. 2).

b. Spectral calibration

Spectral calibration of the camera system was performed for each spectral filter in conjunction with the camera and lens response. The spectral response of the system is predominantly determined by the bandpass interference filters and to a lesser extent by the spectral sensitivity of the imager. The calibration was performed by illuminating the camera system with light from a monochromator. Images were obtained at 1 nm increments through the band pass of the system. From the average of a 3 × 3 subsample of the illuminated area the spectral characteristic of each channel were derived. Figure 3 shows the spectral response of the system and Table 1 lists the center wavelength and band pass for each channel.

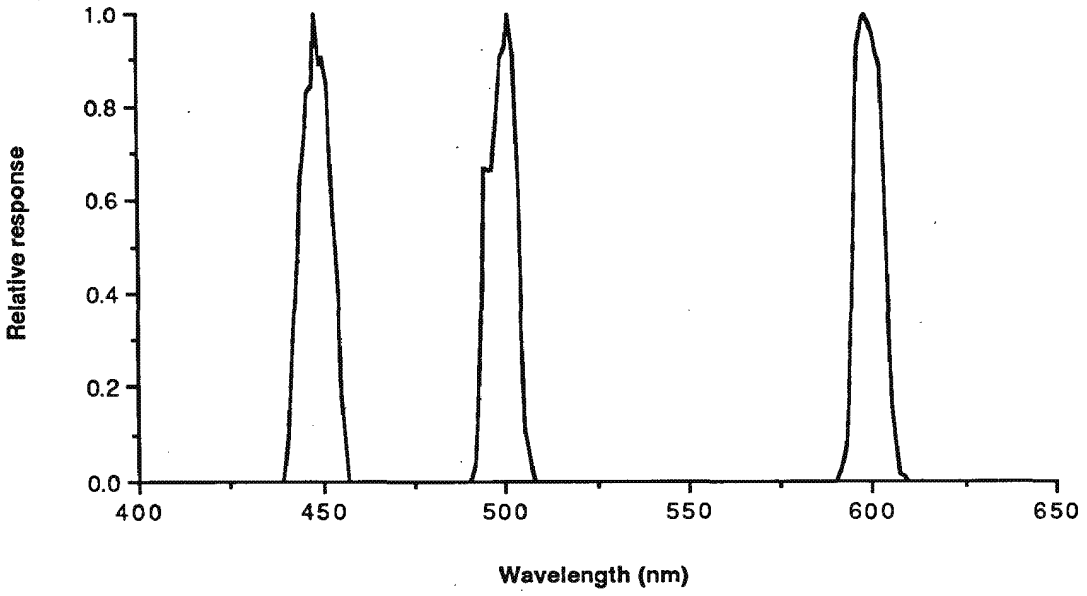


FIG. 3. Spectral response of the instrument; each filter response individually normalized.

SPECTRAL_0000653

TABLE 1. Spectral characteristics of the instrument.

Channel	Central wavelength (nm)	Bandwidth (nm)
1	449	10.5
2	499	10.0
3	600	9.5
4*	—	—

* Channel 4 was not implemented.

c. Geometric projection

The fisheye lens characteristically projects via an equidistant projection. For this type of lens

$$r = f\theta, \tag{2}$$

where r is the radial distance from the center on the image plane, f is the focal length of the lens system and θ is the view angle of the point source at infinity projected onto the image plane.

Geometric mapping of the radiance field onto the imager surface must be determined through calibration, thus checking the projection accuracy and experimentally evaluating f. To do this, the camera system was placed on a precision rotation mount at a distance over 3 meters from a small bright source (the source took up about 2 × 2 pixels in the image). The camera was rotated and images of the source were obtained at every 10 degrees. Figure 4 shows the result of this calibration step. These data prove that the optics exhibit a very linear projection, thus it follows an almost ideal equidistant projection. The derived f (given by slope of the curve in Fig. 4) allows view angles, θ, to be computed for each element of the imager through Eq. (2).

d. Rolloff

Rolloff of a lens (attenuation of radiance on increase in view angle) is an important aspect in the calibration of any imaging optical system. The optics of RADS is composed of the fisheye lens and a set of achromatic lenses in the filter changer. Theoretically, a fisheye lens following an equidistant projection (Miyamoto 1964) has a rolloff $R(\theta)$ given by

$$R(\theta) = \frac{\alpha \cos\theta(\sin\theta/\theta)}{f^2}, \tag{3}$$

where α is the area of the entrance aperture seen by the sensing element in the image plane and θ the view angle. Fisheye lenses have been built with the factor $\alpha \cos\theta$ nearly constant, in which case the rolloff is determined almost wholly by the $\sin\theta/\theta$ factor. But in general each fisheye lens design has its own inherent optical rolloff which must be determined through careful calibration. Conventional lenses exhibit a rolloff attenuation factor following a power of the cosine of the view angle (Slater 1980), so the general form for rolloff of the RADS optics may be given by

$$R(\theta) = \frac{\alpha \cos^n\theta(\sin\theta/\theta)}{f^2}. \tag{4}$$

To measure this factor, a barium sulfate plaque (of 20 cm diameter and exhibiting nearly lambertian characteristics) was placed approximately 100 cm from a standard calibration lamp, thus providing a stable, uniform radiance source. The plaque was viewed at approximately 45 degrees by the camera system which was placed on a rotating mount. Since the plaque-lamp geometry was not changed during measurements, the camera viewed a source of constant radiance. Images

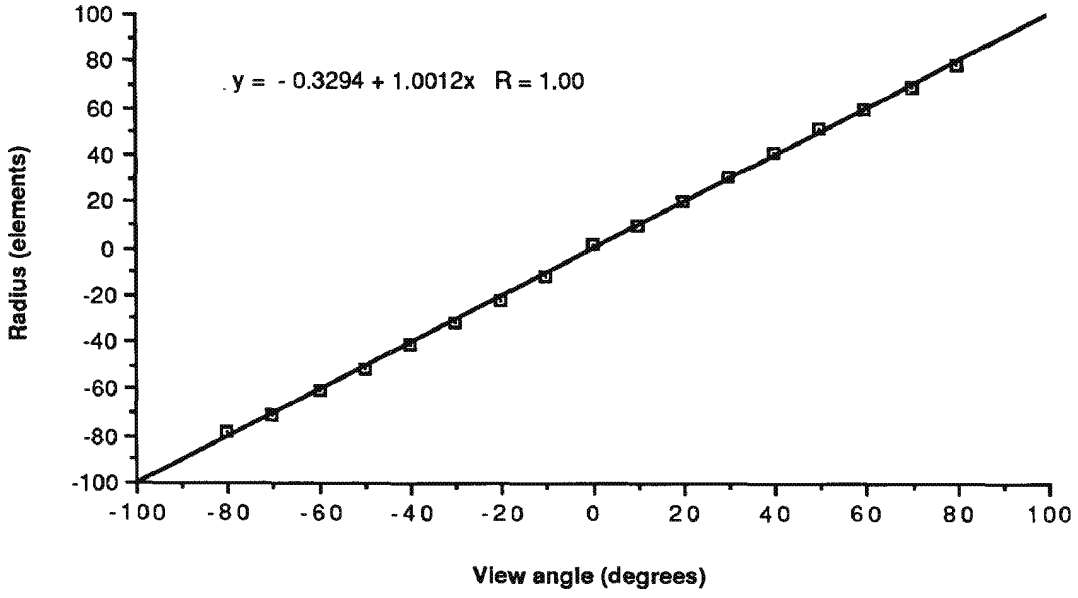


FIG. 4. Projection of the optics.

SPECTRAL_0000654

of the plaque were obtained at various view angles and investigated to determine the apparent rolloff of the optics system.

For calibration purposes a factor is desired which, when multiplied by the linearized radiance, will result in a rolloff corrected value. It was found that the rolloff, in our case, was best fit by a fifth order polynomial, in which all parameters appearing in Eq. (4) are accounted for. Figure 5 shows data obtained from measurements and the resulting curve fit used for rolloff correction.

The equation, derived from the fit, was found to reproduce the true optics rolloff within 2% (standard error of estimate resulting from fit was 1.8%). Tests were performed to determine the sensitivity of the rolloff correction to various factors, such as spectral bandpath, neutral density filters value and the mutual position of plaque and camera. No appreciable sensitivity to these factors has been discerned.

e. Polarization sensitivity

Sky light is polarized, and its polarization varies with direction, atmospheric conditions, and sun zenith angle (Plass and Kattawar 1970). The water radiance field is also polarized and its degree of polarization varies with depth and water optical properties (Waterman 1955). With a lens system the possibility of polarization sensitivity exists due to the fresnel coefficients at each surface of the lens. Polarization is therefore an important aspect in the performance analysis of a system designed to measure the radiance distribution of sky light, or the underwater radiance distributions.

To test the polarization sensitivity of RADS, the barium sulfate plaque was illuminated at approximately 60 degrees with an incandescent light source to provide an unpolarized radiance source. RADS was placed in a position to view the plaque, and a polarizer was inserted between the camera and the radiance plaque. Images were then obtained with different positions of the polarizer. RADS was also tilted with respect to the plaque, to enable measurement at various view angles (0, 15, 25, 45, 50, 70 degrees). The results of this test indicated that the camera does not have any significant polarization sensitivity. This implies that measurements of the radiance distribution with this system have negligible error due to polarization sensitivity.

f. Absolute calibration

To determine the absolute radiometric calibration factor, the barium sulfate plaque was illuminated at normal incidence with a 1000 W standard of spectral irradiance (calibration of which is traceable to National Bureau of Standards). The plaque was centered in the field of view of RADS at a distance of 50 cm from the lamp and viewed at 45 degrees.

The equation relating the irradiance $E(\lambda)$ incident on the plaque with the radiance $L(\lambda)$ reflected by the plaque (assuming a lambertian reflector) is

$$L(\lambda) = \rho \frac{E(\lambda)}{\pi}, \tag{5}$$

where ρ is the reflectance of the plaque (in this case, $\rho = 0.95$ with normal light incidence and 45 degrees viewing angle and it is almost constant in the spectral regions of interest).

Images of the plaque were obtained for each of the spectral filters, and the signal level counts were deter-

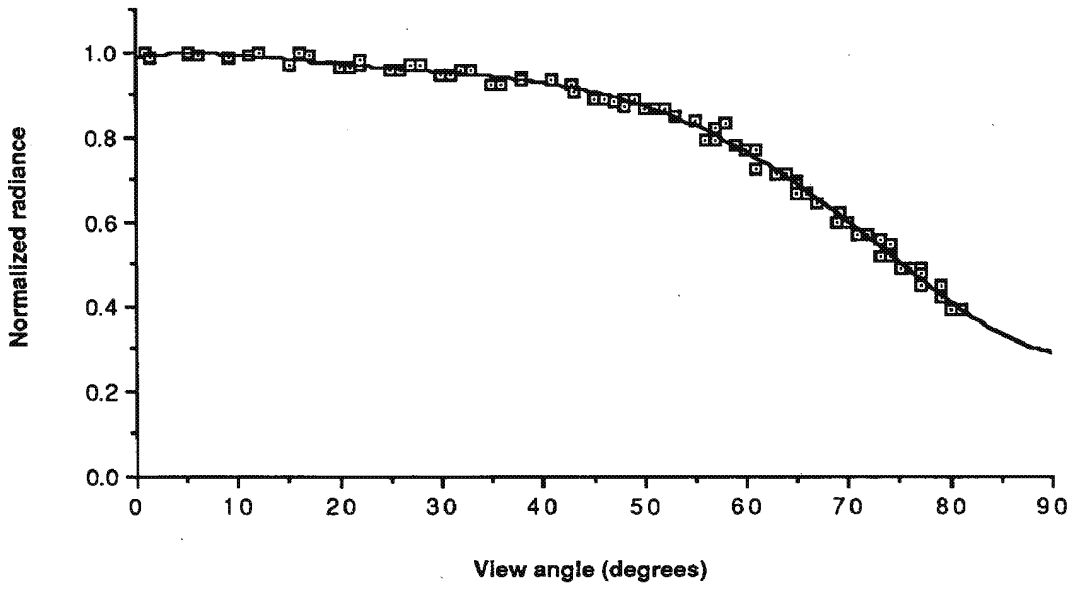


FIG. 5. Rolloff of the optics.

SPECTRAL_0000655

TABLE 2. Calibration constants.

Channel	$A(\lambda)$ (mW cm^{-2} μm^{-1} sr^{-1})	ND_1	ND_2	ND_3	ND_4
1	26.42	1.0	0.510	0.257	0.112
2	15.57	1.0	0.515	0.264	0.115
3	8.53	1.0	0.536	0.286	0.121
4*	—	—	—	—	—

* Channel 4 was not implemented.

mined from a 3 × 3 pixel area in the center of the plaque image. The absolute calibration factor $A(\lambda)$ was computed for each channel, dividing the plaque radiance by the average linearized value obtained from images:

$$A(\lambda) = \frac{L(\lambda)}{L_l}. \quad (6)$$

The possible errors in this factor are mainly caused by instabilities in the standard lamp irradiance, least count errors in the values obtained from the images (reduced by averaging pixels), and random noise in the imager. The error in the value of $A(\lambda)$ was found to be less than 5%, determined through multiple calibrations with two different standard lamps. In Table 2, the computed absolute calibration factors are given.

g. *Flare and blooming analysis*

To determine the flare and blooming characteristics of the camera lenses and imager, a simple test was performed. A helium neon laser was directed at the barium sulfate plaque that was imaged by the camera. The image of the laser beam subtended no more than one element on the sensor. No spill over to neighboring elements was detected with the imaged element saturated. In this manner the flare and blooming of the images were determined to be negligible (when reasonable care is taken to maintain the flux levels close to or below saturation).

h. *Neutral Density filters attenuation*

The attenuation values of the Neutral Density (ND) filters were determined by imaging the barium sulfate plaque through each neutral density filter (and with each spectral filter) and adjusting the signal level through use of the integration capability of the camera. The signal levels obtained from neighboring filters (ND1 and ND2, ND2 and ND3, and ND3 and ND4) were expressed as ratios and the attenuation value of each filter was determined by multiplying these ratios together. Measurements were taken with each spectral filter to account for wavelength dependence of the ND filters. The error in the final values are estimated to be less than 2%, with this error due to pixel to pixel variations in the mean used to determine the ratios. The computed data of the relative attenuation for each ND and spectral filter combination, are shown in Table 2.

i. *Injection Inhibit timing*

Photogenerated charge in solid state devices (such as CID or CCD), is linearly dependent on the integration time. RADS can perform, under remote control, on-chip integration of the incident irradiance through the use of the Injection Inhibit function of the camera. This function inhibits clearing of the imager between frame periods (the process of clearing is called "injection") so that the photogenerated charge is accumulated over several frame periods. Use of the Injection Inhibit function of the camera allows lower irradiance levels to be measured, but requires the determination of the inhibit time used in the function. This was determined by imaging a stable source repeatably with many different integration times (whose absolute value is determined by the Injection Inhibit time step: 1, 2, 3, . . .), determining the average of the response's intercept versus the Injection Inhibit time step, and comparing this value with the response for the basic integration period. In this system (camera and frame grabber) it was found an additional delay of 2.5 frame periods existed between the step of 1 and 2; for each additional increment above 2, each step corresponds to an additional frame period. Result of this analysis is shown in Fig. 6a.

The derived integration time I_t (frame periods) as a function of the Injection Inhibit time step I_s is given by

$$I_t = 1, \qquad (I_s = 1) \quad (7)$$

$$I_t = 2.5 + I_s, \quad (I_s > 1). \quad (8)$$

The applicability of the Injection Inhibit function is limited by the thermally generated dark noise and loses its usefulness when accumulation of charge due to thermally generated dark noise outstrips accumulation of light generated charge. Figure 6b illustrates the generation of dark noise as a function of the integration time at 25°C. Data have been obtained averaging 200 × 200 pixels in the center of the detected dark images, error bars give the standard deviation (less than 3.0 counts) of dark noise in the analyzed area.

j. *Final calibration factor*

The above factors taken together give the final calibration procedure of

$$L(\theta, \lambda) = (L_l - l_0)[A(\lambda)R(\theta)^{-1}\mathrm{ND}(\lambda)^{-1}I_t^{-1}], \quad (9)$$

where L_l is the linearized radiance in channel with central wavelength λ and computed through Eq. (1) for the output digital value of the considered element in the imager and l_0 accounts for variations in dark noise between calibration and field measurements.

SPECTRAL_0000656

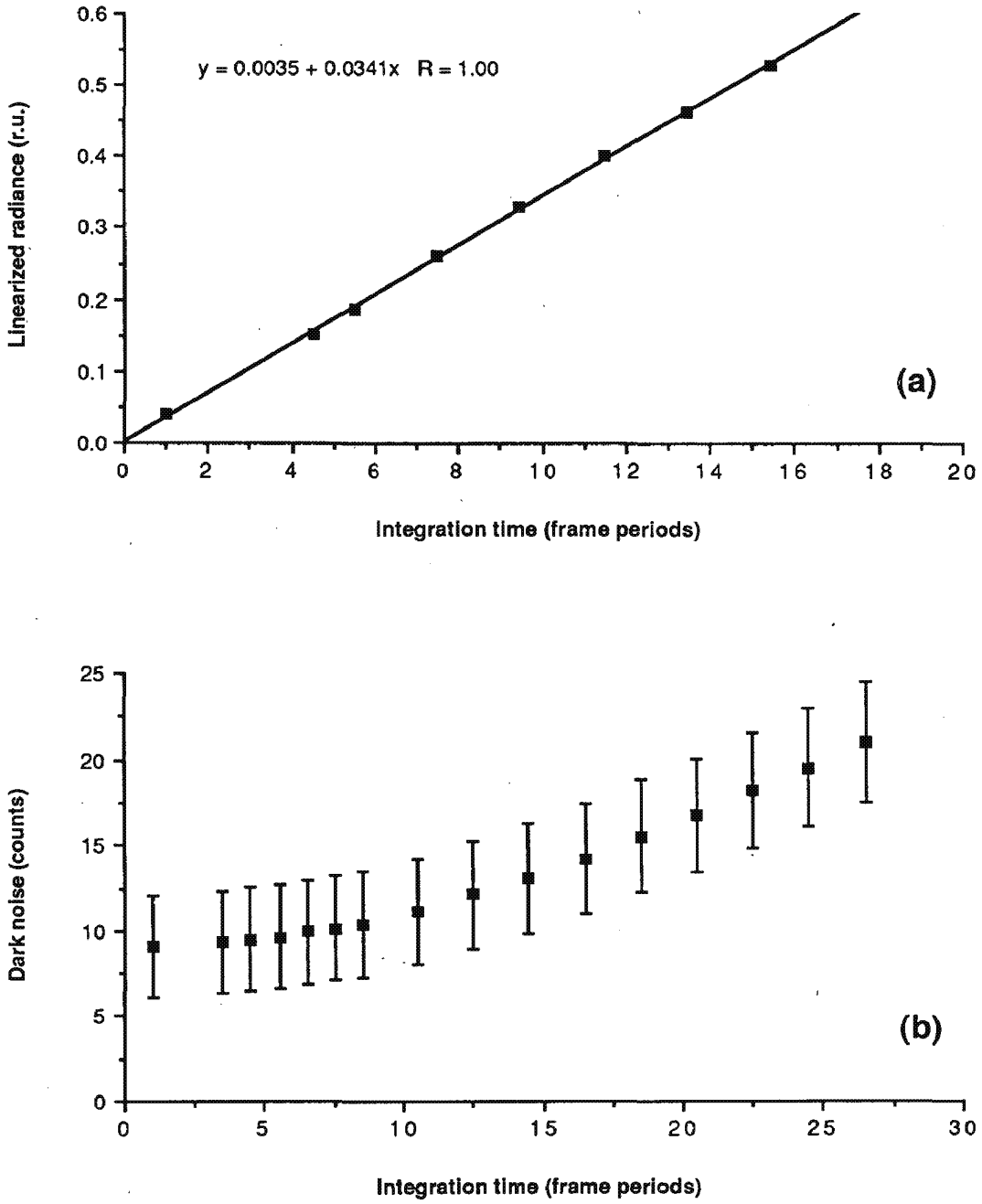


FIG. 6. Radiance (a) and dark noise (b) as a function of the integration time.

The dark noise D0, subtracted off the raw frame image in the linearization step, is obtained during calibration. In field measurements, variations in the dark noise of the imager can be caused by ambient temperature changes or use of different integration times or both. The term l_0 is obtained from an average linearized value of a sample of elements taken outside the projected image and accounts for the operational variations of the dark noise. So, while the dark field subtracted off pixel by pixel in the image during linearization removes the spatially dependent portion of the dark noise, l_0 accounts for temperature differences in the imager between the calibration and field use, and excess charge generated with increasing the integration time. This procedure has been validated by measurements showing no appreciable dependence on temperature or integration time in the spatially dependent contribution to dark noise.

The overall error in the RADS absolute calibration is less than 12% where the maximum relative error

SPECTRAL_0000657

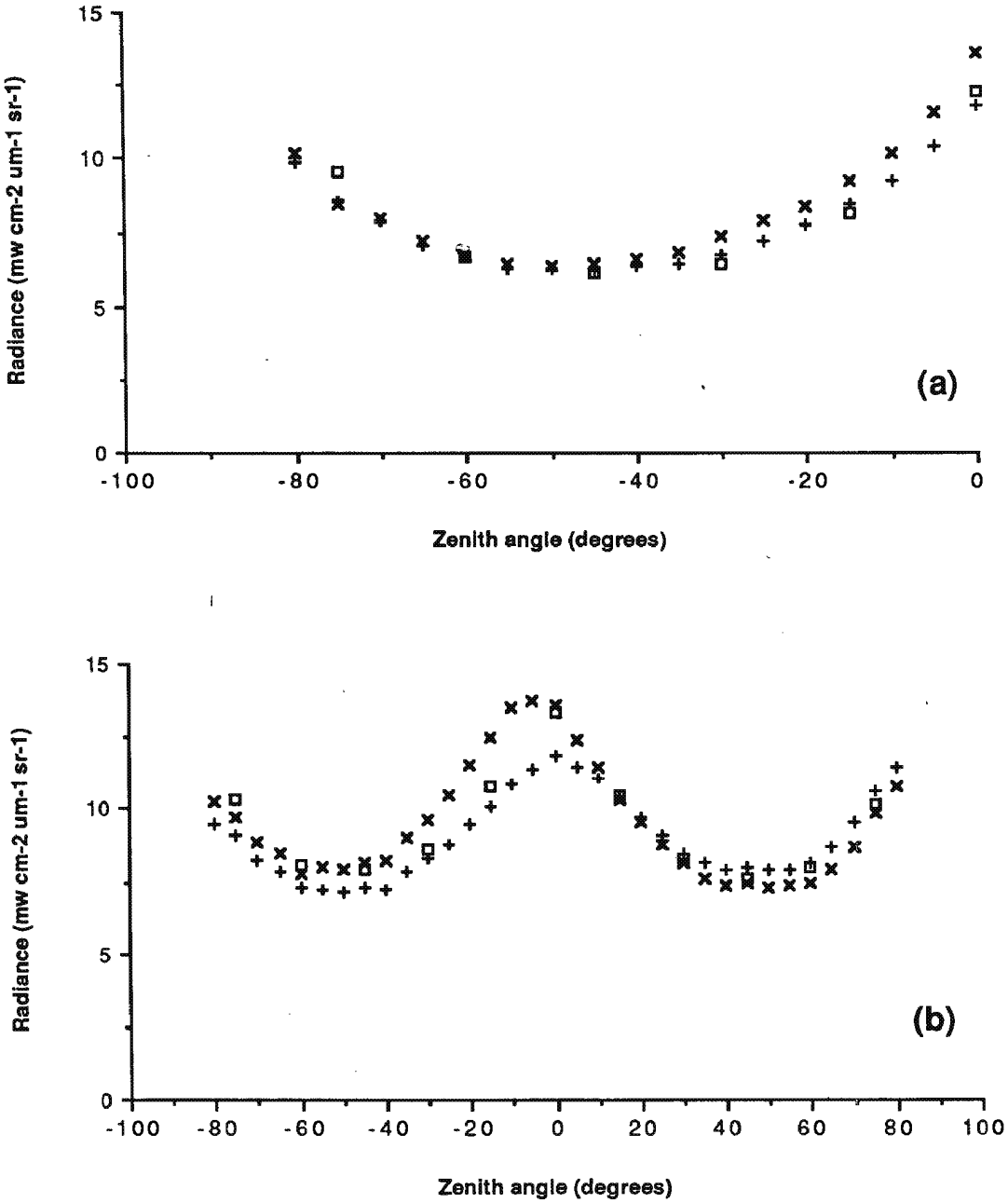


FIG. 7. Comparison between RADS data (×, +) and HHCRM data (□) taken at 449 nm and 441 nm central wavelengths respectively, in the sun plane (a) and in the sun-normal plane (b).

among data obtained from the same image is about 5% (due to methodologies applied in the linearization and rolloff correction).

4. Comparison with HHCRM data

a. Description of the experiment

On 13 May 1988 clear sky field measurements were obtained with RADS, and the Hand Held Contrast Reduction Meter (HHCRM). The HHCRM (Wilson 1979) is a gershun tube type radiometer with a 1 degree field of view and 10 spectral filters (10 nm wide) centered in the visible spectrum. This instrument was installed on an alta-azimuth mount to perform measurement of the sky radiance for selected angles in relation to the sun zenith plane. Measurements with the HHCRM (with error in absolute value within 4%) were performed at channels with central wavelength 441, 490 and 611 nm (close to the central wavelengths of RADS), at every 15 degrees in sky planes passing through the zenith. Before and after these measure-

SPECTRAL_0000658

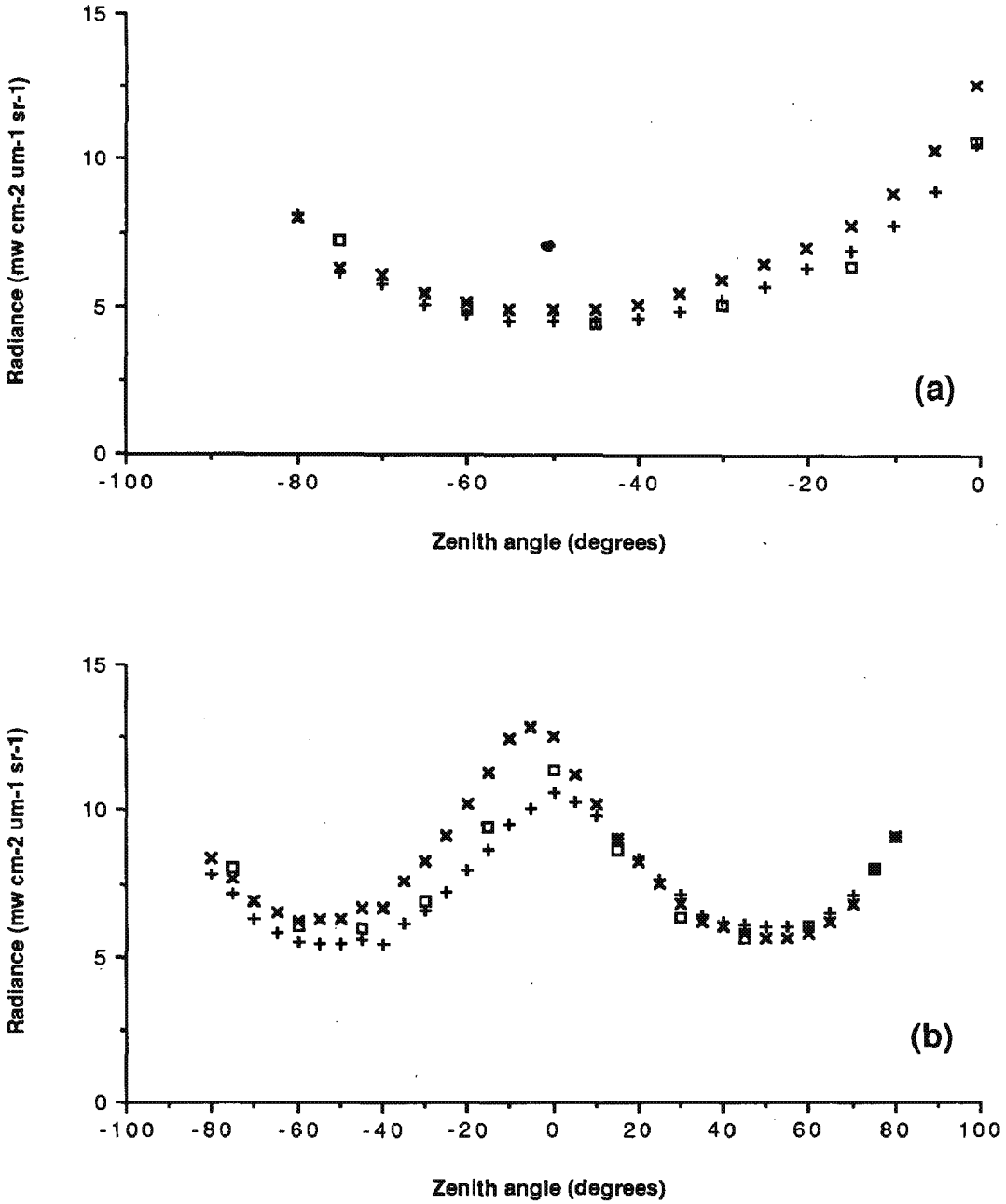


FIG. 8. Comparison between RADS data (×, +) and HHCRM data (□) taken at 499 nm and 490 nm central wavelengths respectively, in the sun plane (a) and in the sun-normal plane (b).

ments, an image was acquired and stored for each channel of RADS.

b. Data and discussion

Qualitative comparisons (because of the different central wavelengths) have been performed, between the radiance data derived from the HHCRM and RADS, to show the capability of the latter instrument in reproducing the radiance field. All data are given for the same sky planes at, or near (due to change in sun position during measurements), the sun and sun-normal zenith planes. In Figs. 7–9 HHCRM data (taken with sun zenith of 18 degrees and azimuth of 142 degrees) are shown for the sun (a) and sun-normal (b) zenith planes and compared with RADS data taken just before and after the HHCRM measurements. Comparisons are affected by the error in collocating the azimuth planes of the two instruments (less than 3 degrees) and the change in sun zenith and azimuth angles (about 2 and 9 degrees respectively) between beginning and conclusion of a measurement set. In the

SPECTRAL_0000659

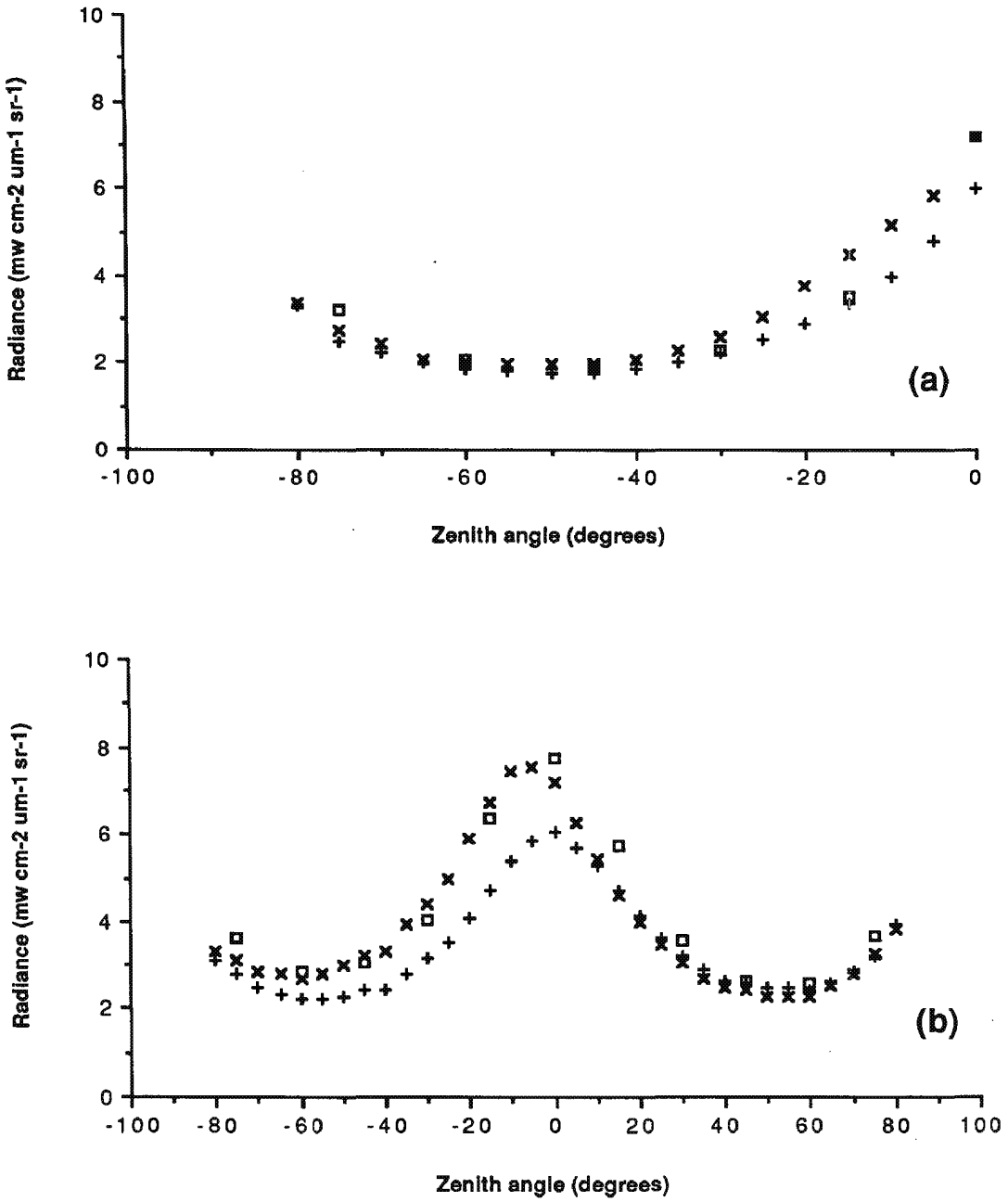


FIG. 9. Comparison between RADS data (×, +) and HHCRM data (□) taken at 600 nm and 611 nm central wavelengths respectively, in the sun plane (a) and in the sun-normal plane (b).

sun zenith plane, the radiance distribution is not sensitive to small variations in azimuth and RADS and HHCRM data agree quite well in all the cases. In the RADS measurements an occulter shadows the direct solar irradiance, as this is several decades higher than the maximum input value of the camera, and moreover causes undesired scattering in the optics. The occulter used in our measurements blocks the sky radiance at all zenith angles in the direction of the solar azimuth, and because of this the graphs in Figs. 7–9 (a) do not extend in this direction. In the sun-normal plane, the radiance distribution is very sensitive to azimuth angle, and data show more variation (the error in collocating the azimuth planes of the two instruments is estimated to be on the order of 3 degrees). In general, though, good agreement is found between measurements taken with the two instruments, thus experimentally validating the calibration procedure used for RADS.

The fisheye camera system, compared with traditional instruments (such as the HHCRM), excels as a method of obtaining radiance information for the complete distribution over an hemisphere. Figure 10

SPECTRAL_0000660

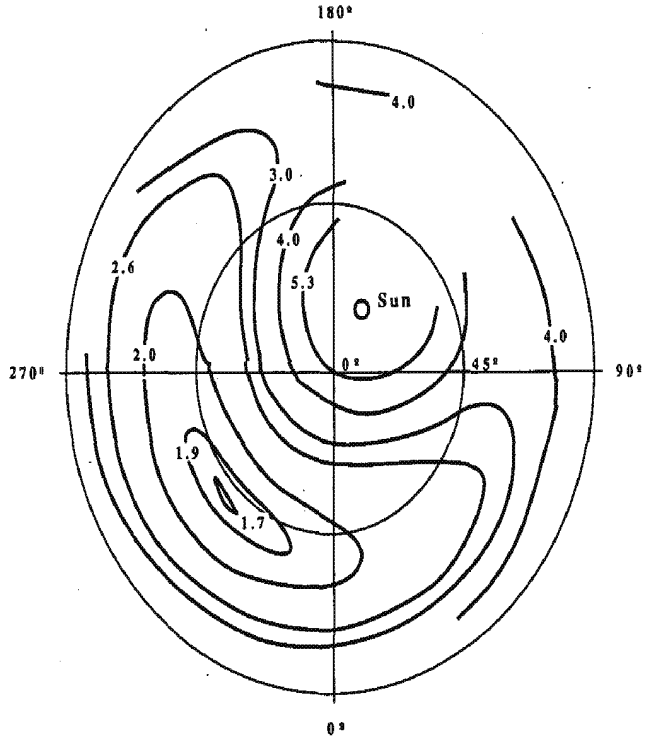


FIG. 10. Contour plot of radiances (units of mw cm^{-2} um^{-1} sr^{-1}) obtained from data taken with RADS at 600 nm (after Zibordi and Voss 1988).

shows a contour plot derived from a calibrated image obtained with channel 3 of RADS. The undefined area corresponds to the circumsolar zone shadowed by the occulter.

5. Conclusion

The calibration techniques applied to a fisheye electro-optic camera system have been described and validated through comparisons with measurements taken by a standard sky radiometer. Results demonstrate the capability of the camera to give data with good accuracy and illustrate its usefulness in performing spectral radiance distribution measurements with a high geometrical resolution, in the short time required for a changing light field.

Acknowledgments. RADS was developed at the Visibility Laboratory of the Scripps Institution of Oceanography and supported by the Office of Naval Research under contract N00014-85-C-0730. This work has been supported by the U.S. Office of Naval Research under this same contract and N00014-85-K-0005, and with the additional support of the Italian National Council of Research. Preliminary design work on the filter changer was supported by the U.S. Air Force Geophysics Laboratory contract F19628-84-K-0047. We would also like to thank Ms. Janet Shields and Mr. Roswell Austin for their critical review of the manuscript.

REFERENCES

Babey, S. K., J. S. Murphree, E. P. King, L. L. Cogger and C. D. Anger, 1986: Intensified charge-coupled-device imager for auroral studies. *Opt. Eng.*, **25**, 1149–1154.

Boileau, A. R., and J. I. Gordon, 1966: Atmospheric properties and reflectances of ocean water and other surfaces for a low sun. *Appl. Opt.*, **5**, 803–813.

Deering, D. W., and T. F. Eck, 1987: Atmospheric optical depth effects on angular anisotropy of plant canopy reflectance. *Int. J. Remote Sens.*, **8**, 893–916.

Miyamoto, K., 1964: Fisheye lens. *J. Opt. Soc. Amer.*, **54**, 1060–1061.

Plass, G. N., and G. W. Kattawar, 1970: Polarization of the radiation reflected and transmitted by the earth's atmosphere. *Appl. Opt.*, **9**, 1122–1130.

Sims, G. R., and M. B. Denton, 1987: Characterization of a charge-injection-device camera system as a multichannel spectroscopic detector. *Opt. Eng.*, **26**, 1008–1019.

Slater, P. N., 1980: Remote sensing. *Optics and Optical Aspects*, Addison-Wesley, 116–119.

Smith, R. C., 1974: Structure of solar radiation in the upper layers of the sea. *Optical Aspects of Oceanography*, N. G. Jerlov and E. S. Nielsen, Eds., Academic Press, 95–119.

Tyler, J. E., 1960: Observed and computed path radiance in the underwater light field. *Marine Res.*, **18**, 157–167.

Voss, K. J., 1989: An underwater electro-optic radiance distribution camera system. *Opt. Eng.*, **28**, 241–247.

Waterman, H., 1955: Polarization of scattered sunlight in deep water. *Marine and Biology in Oceanography.* Pergamon Press, 426–434.

Wilson, W., 1979: Measurements of atmospheric transmittance in a maritime environment. *Atmospheric Effects on Radiative Transfer*, SPIE Vol. 195, 153–159.

Zibordi, G., and K. J. Voss, 1988: Geometrical and spectral distribution of sky radiance: comparison between simulations and field measurements. *Remote Sens. Environ.* (in press)

SPECTRAL_0000661

Radiometric calibration of a video fluorescence microscope for the quantitative imaging of resonance energy transfer

Walter D. Niles and Fredric S. Cohen
Department of Molecular Biophysics and Physiology, Rush Medical College, 1753 West Congress Parkway, Chicago, Illinois 60612

(Received 18 October 1994; accepted for publication 14 March 1995)

A video microscope for radiometric imaging of resonance energy transfer (RET) between donor and acceptor fluorophores is described and calibrated. The donor is excited by epi-illumination with monochromatic light. Light emitted by donor and acceptor fluorophores in the specimen is filtered into separate emission images, which are viewed with a pair of multichannel plate image intensifiers in tandem with charge-coupled device (CCD) cameras. The RET rate constant is calculated at each location in the specimen from the ratio of the donor and acceptor emission intensities. These intensities are computed from the video brightnesses after transformation to irradiances using an experimentally obtained calibration, which accounts for the spectral transmission of the optical pathways and the spectral response of the detectors to determine the energies emitted by the probes in the specimen. We describe procedures for measuring the input irradiance–output brightness relations of the intensifier-CCD cameras. With these calibrations, the RET ratio image enables measurement of molecular-scale (nanometer) distances between probes within membranes of biological and biophysical interest. © *1995 American Institute of Physics.*

I. INTRODUCTION

Quantitative video microscopy has become a powerful tool in the study of biological structure.[1] New video cameras, particularly charge-coupled devices (CCDs), offer high spatial resolution, high sensitivity, wide dynamic range, and geometric accuracy.[2,3] When coupled with fluorescence labeling of macromolecules, video microscopy has revealed new insights into cellular structure and dynamics in two- and three-dimensional images.[4–6] With the new cameras coupled to amplification devices such as image intensifiers,[7,8] a small number of photons emitted by a few probes localized in a small area can be detected.[9] This has opened the possibility for measuring distances between molecules, that are below the diffraction limit, by resonance energy transfer (RET).[10–12] RET occurs between two dyes when the absorption spectrum of the acceptor dye overlaps the emission spectrum of the donor, and the relative orientation of the absorption dipole of the acceptor is not perpendicular to the emission dipole of the donor.[13] The excited donor's electromagnetic field overlaps with the acceptor's excitation wave function only when the probes are separated by less than 10 nm.[14] RET imaging enables separations on the molecular scale of distances to be spatially localized within a specimen.[10]

Distances in the RET image are determined from the rate constant, k_t. For any donor–acceptor pair,

$$k_t = k_D(R_0/R)^6, \tag{1}$$

where k_D is the rate constant for fluorescence of an excited donor in the absence of acceptor, R is the radial separation between the probes, and R_0 is the characteristic distance at which an excited donor transfers its energy to the acceptor with a probability of 1/2.[14] k_t is proportional to the sensitization ratio $\Delta I_A/I_D$, where ΔI_A is the ratio of the acceptor's emission intensity above its background level of excitation, and I_D is the door emission intensity.[10,12,15] Thus RET imaging requires two video cameras, one to view the donor emission and one for the acceptor. Because k_t indicates the transfer between probes of energy over a continuous wavelength band rather than by the transfer of discrete photons, the luminance voltages (brightnesses) of the video images must be converted to the amount of energy falling on the camera faceplate (irradiances). To relate these irradiances to the emission radiances of the probes in the specimen, the energy transmission properties of the electro-optical system are also needed.[12]

Previous calibrations of RET imaging systems have relied on correlating the brightness ratio measured in the video microscope to a standard ratio without measuring the irradiance–brightness relation of the video cameras. Studies of RET between fluorescent DNA-intercalating dyes in leukocytes related the video brightness ratios obtained with labeled cells to external intensity ratios of the same cells measured with a calibrated photomultiplier tube.[12] In measures of protein kinase activation by cyclic nucleotides within Aplysia sensory neurons,[16] conditions were varied to determine the range of internal ratios. More generally, video imaging has relied on the linearity of brightness with increasing exposure of the camera's sensing element to a constant photon flux.[3,4] This photometric linearity within a single range of wavelengths has been used to calibrate image sharpness in video microscopes.[17–19] Video cameras deliver an image frame every 1/30 s, however, rather than integrating a constant intensity with increasing time. Moreover, energy transfer microscopy requires measuring two separate wavelength ranges simultaneously, and the video brightnesses of the probes must be related to energy fluxes. We describe a RET imaging video microscope that is calibrated radiometrically using a photodetector. Our microscope was designed to detect RET and measure distances between coumarin and rhodamine dyes attached to phospholipids. The microscope

SPECTRAL_0000662

can be adapted to any pair of RET probes and improved cameras. The RET microscope is applied to the determination of R_0 for coumarin- and rhodamine-labeled phospholipids contained in planar depositions.

A. A model for quantitative fluorescence imaging

Radiometric video imaging requires a transformation of the brightness $c(\lambda)$ of each pixel in an image to the radiant intensity of the light energy at a particular wavelength $I(\lambda)$ emitted from the corresponding location in the object plane.[20] Radiant intensities have units of radiance (W/cm^2) when the exit pupil of the objective lens subtends a small solid angle with respect to the specimen. The lens captures a fraction f of the total power emitted by the specimen and transmits a fraction $T(\lambda)$. We assume that the lens is aplanatic and forms a focused image of an object pixel with an irradiance equal to $fT(\lambda)I(\lambda)$. After transfer through the microscope, the irradiance on the image intensifier faceplate is $i'(\lambda)=fS(\lambda)I(\lambda)$, where $T(\lambda)$ is incorporated into $S(\lambda)$, the spectral transfer efficiency of the optical pathway for wavelength λ. For an intensifier responsivity to wavelength λ of $R(\lambda)$, $i'(\lambda)$ is equivalent to a spectrally matched irradiance $i(\lambda)=i'(\lambda)R(\lambda)$ that produces a brightness independent of λ for identical irradiances.[6,15] The video brightness produced is $c(\lambda)=F[i(\lambda)]$, where $F[\ ]$ is a function that relates the light energy impinging on the detector to the output brightness at the corresponding image pixel. Calibration requires determining $S(\lambda)$, $R(\lambda)$, $F[\ ]$, and the inverse function $G[\ ]$, where $G[c(\lambda)]=i(\lambda)$. The light emanating from the object pixel has spectral character. Its total radiance, $I=\int I(\lambda)d\lambda$, is reduced to $i=\int i(\lambda)d\lambda$ at the intensifier and produces brightness $c=\int c(\lambda)d\lambda$ in the video image, so that $G[c]=i=\int fS(\lambda)R(\lambda)I(\lambda)d\lambda$.[12] In RET, the light emitted by each probe in the specimen is isolated by filters into a narrow range of wavelengths in each emission pathway. As the spectral transmission and responsivities are relatively constant over the range in each pathway, they can be replaced by $S=\int S(\lambda)d\lambda$ and $R=\int R(\lambda)d\lambda$. Thus, $G[c]=fSRI$, and the measured average brightness c corresponds to the average radiance I of the specimen by $I=G[c][fSR]^{-1}$, although more detailed studies of RET require the decalibration of I to obtain its spectral character.[12]

B. Light amplification by image intensifiers

In an image intensifier, photons strike a photocathode, such as a multialkali S-25 deposition, and generate primary photoelectrons, which are electrostatically focused on the multichannel plate (mcp).[8,9] At each stage in the mcp, the number of secondary electrons produced by the incident electrons is a power function of the voltage drop across the stage plus the work function. The emitted electrons strike a phosphor output screen, in our case P20 (or a mixture of P20 and P39). The emitted light, now greatly amplified with respect to the original image formed on the photocathode, is focused on a video camera. With many mcp stages, the low intensities of the input image are amplified several decades to produce an output image with intensities above the input sensitivity of the video camera. In essence, the intensifier relation can be described as $d(\log W_o)=Ad(\log W_i)$, where W_i is the light energy falling on the input photocathode, and W_o is the light energy emitted by the output screen.[9] The output image radiance is then related to the input image by

$$W_o=(W_i)^A. \tag{2}$$

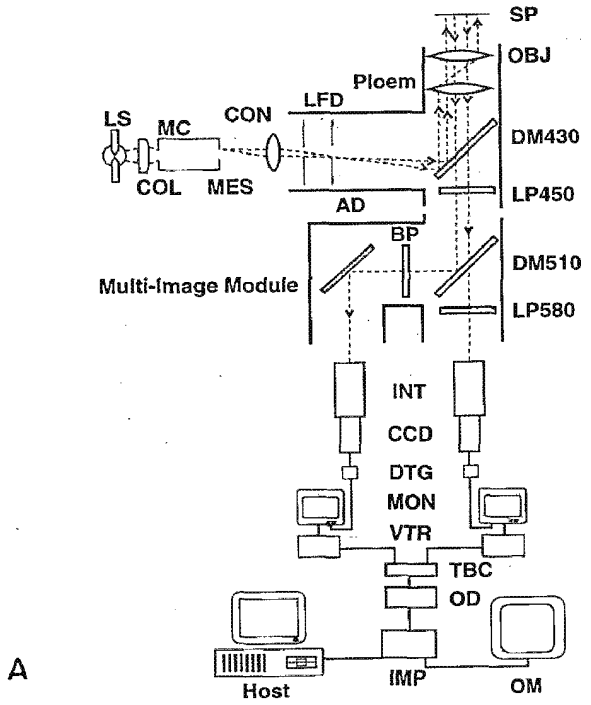
II. A VIDEO FLUORESCENCE MICROSCOPE FOR RET IMAGING

General. A schematic diagram of the optical and video components of the microscope is shown in Fig. 1(A). The components include a monochromatic light source, a microscope with two sets of filter mounts, and two video cameras. The microscope (Laborlux 11, E. Leitz, Inc., Rockleigh, NJ) was laid on its backbrace and bolted to a vibration-free air table. The stage was replaced with a custom-machined specimen holder for mounting a special planar membrane chamber with No. 1 glass cover slips for front and backsides. The planar membrane chamber, in which RET between planar lipid membranes and vesicles is studied,[21] was modified to hold quartz substrates containing lipid depositions. The specimen holder was mounted to a set of micrometer-resolution manipulators (460XYZ, Narishige Scientific Instruments, Tokyo, Japan) to situate the specimen within the object plane of the microscope. During calibrations, the specimen holder was replaced with a beam steerer (Newport–Klinger Corp., Fountain Valley, CA), a resolution target (M70-S, Sine Patterns, Penfield, NY), or a ruled grating. The grating and resolution target were used to determine geometric distortion and shading in the image by measuring line separations and modulation transfer in different parts of the image.[1] Specimens were viewed with Leitz infinity-corrected MPlan series (flat-field, achromatic) objective lenses, either 25×/0.4 NA 11/mm w.d. or 50×/0.6 NA 6 mm w.d.

Monochromatic light source. A 100 W Hg arc lamp (HBO 100) operated with a current-voltage stabilized power supply (E. Leitz, Inc.) served as the light source. Its housing was detached from the microscope to allow interposition of a grating monochromator with sweep motor (Jobin–Yvon H-10, ISA Associates, Metuchen, NJ) between the lamp and the epi-illumination tube (Infinity Ploemopak, E. Leitz, Inc.) of the microscope. An entrance slit 1×0.2 cm and an exit slit, 1 cm high and either 0.5, 1, or 2 mm wide produced excitation light with a full width at half-maximum bandwidth of 8 nm/mm. A 10× $f/4$ condenser lens enabled Köhler illumination of the object plane by focusing the image of the exit slit at the aperture diaphragm and at the exit pupil of the objective.

Excitation and emission pathways. Excitation light from the monochromator was directed through the objective and toward the specimen by a cube-mounted dichroic mirror with a transmission cut-on of 430 nm (Omega Optical, Brattleboro, VT) for RET experiments. A 450 nm long-pass filter fixed behind the dichroic mirror separated probe emissions from scattered excitation light. Probe emissions were separated into donor and acceptor components and directed to separate camera ports with a second cube in a Multi-image module (Nikon, Inc., Garden City, NY). Emissions were first split with a 510 nm transmission cut-on dichroic mirror; the

SPECTRAL_0000663



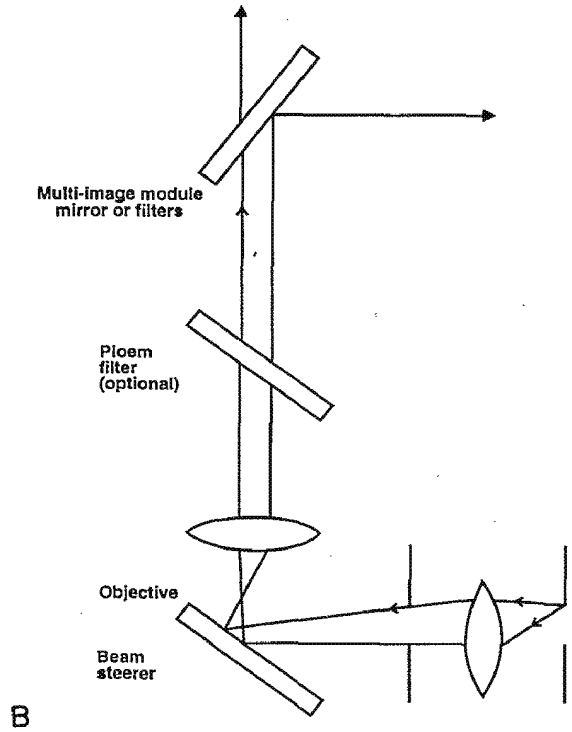


FIG. 1. (A) Schematic layout of the RET microscope and video and image processing equipment. LS, light source; COL, collector; MC, monochromator; MES, monochromator exit slit; CON, condenser; LFD, luminous field diaphragm; AD, aperture diaphragm; SP, specimen plane; OBJ, objective; DM430, 430 nm cut-on dichroic mirror; LP450, 450 nm cut-on long-pass filter; DM510, 510 nm cut-on dichroic mirror; LP580 nm cut-on long-pass filter; BP, 450–490 nm bandpass filter; INT, intensifier; CCD, charge-coupled device camera; DTG, date–time generator; MON, video monitor; VTR, video tape recorder; TBC, time-base corrector; OD, optical disk recorder; IMP, image processor; OM, output monitor. The apertures of the intensifier-CCD coupling optics were set at $f/1.2$ at the intensifier and $f/2.0$ at the camera. (B) Layout for the direct illumination of the specimen plane with the beam steerer used to reflect light into the objective. This configuration eliminated scattering by the dichroic mirror at wavelengths greater than the cut-on wavelength and misdirection of the light away from the emission pathway.

donor coumarin emission was passed through a 450–490 nm bandpass filter while the acceptor rhodamine emission was passed through a 580 nm long-pass filter. In some calibrations, a 50/50 mirror (Nikon, Inc.) was used in the Multi-image module to direct equal amounts of light toward both camera ports.

Video recording. Video images of donor and acceptor emissions were obtained with two image intensifiers (KS1380 and KS1381, Videoscope International, Washington, D.C.), each coupled to a CCD camera (CCD-72, Dage-MTI, Inc., Michigan City, IN). Intensifier gains were set by the mcp voltages. These were adjusted either manually with calibrated potentiometers or by computer control. Computer control was used to gate the mcps to 0 V with 1 ms duration pulses during the vertical blanking interval of each frame to decrease intensifier noise due to persistence charges. The CCD cameras, in frame integration mode (readout in RS-170A video format), were operated at maximum gain and resolution and at a gamma of 1. The preset black reference level was set at 10–50 mV above the 0 V reference voltage (back porch) with a potentiometer in each CCD control box.[22] This eliminated autoblacking of the video signal.[22] Video images from the intensifier-CCDs were continuously displayed on a pair of video monitors (EVM-1719, Electrohome Ltd., Kitchener, Ontario, Canada; WV-5410, Panasonic Co., Secaucus, NJ). The fields of view displayed on the monitors at reduced scan were 375 and 187 μm wide (4:3 aspect ratio) for the 25× and 50× objectives, corresponding to solid angles of $2.8\times10^{-4}\pi$ and $2.3\times10^{-4}\pi$ sr.

Video signals were recorded on 3/4 in. U-matic video tape using two high-resolution monochrome video tape recorders (VO-5800H, Sony Communications Corp., Park Ridge, NJ; NV-9240XD, Panasonic Co., Parsippany, NJ). The two video records were synchronized by sending each signal to separate data–time generators (Video Timer VTG-33, For-A Corp., Ltd., West Newton, MA) that superimposed a 0.01 s resolution time stamp in a lower corner of each video frame. The data–time generators were simultaneously activated with a ganged relay switch (delay<1 μs) and were accurate to within 0.01 s for a continuous run of 3 h. For digitization, the tape signals were transferred to a high-resolution monochrome optical disk to stabilize the video frames (TQ-3038F, Panasonic Co.). A time base corrector (Sync 2F, Nova Systems, Inc., Canton, CT) with <15 ns jitter per line was interposed between the tape and disk recorders to resynchronize each transferred frame.

Image processing. An image processor (Series 151, Imaging Technology, Inc., Bedford, MA) controlled by a 386 AT-class host microcomputer was used to transform video brightnesses to irradiances and to calculate ratio images. The image processor contained an analog-to-digital converter (ADI), 8 frame buffers, and an arithmetic logic unit connected by a 24 address-bit partial VME specification video bus, which allowed full-frame computations to be performed at the frame rate of 30 Hz. Programmable control registers in the ADI were used to adjust the analog video signal level prior to digitization. Video frames were digitized at 8 bits brightness resolution per pixel and the 512×480 pixel images were displayed on a color monitor (ECM 1301, Elec-

SPECTRAL_0000664

trohome Ltd.). Custom-written programs were used to average video frames, calculate average brightnesses in small areas of each image, convert brightnesses to radiances, and calculate intensity ratios.

Video level matching. Prior to calibration, the video reference levels and gains of the devices with 75-Ω terminated outputs were manually set to coincide. A wave-form vectorscope (1750, Tektronix Corp, Beaverton, OR) was used to display video signals and to match the 0 V levels. A 9 bar brightness scale switched into each CCD camera output was used to match the 0.714 V white level for the cameras, the optical disk recorder, the time base corrector, and the ADI. The input and output gains and levels of the tape recorders, which were unterminated, were also adjusted to reproduce the 0 V and brightness-scale levels of the cameras. The offset of the luminance component produced by the synchronization stripper of the ADI was compensated for by programming the ADI control registers. This produced a unit change in the digitized brightness for each 2.789 mV change in the input luminance signal.

Radiometric measurements. A silicon photodetector with a 1-cm-diam faceplate (883-SL, Newport–Klinger Corp.) was connected in photovoltaic mode (for output stability) to an optical power meter (835, Newport–Klinger Corp.) that corrected the spectral response of the photodetector. The photodetector produced a radiometric output at each set wavelength (the bandpass at each wavelength was 10 nm). The meter was operated with a 500 Hz output cycle; the noise level was 0.15 pW *p-p*. Irradiances were measured in a darkened room. The photodetector was attached to a camera port at the location of the intensifier faceplate and zeroed against ambient light. To direct light into the microscope objective, a beam steerer with >95% reflectance over the wavelength range of 390–620 nm (Newport–Klinger Corp.) was placed in the specimen plane.

To normalize the power readings to radiances, the areas of the light beam incident on the photodetector at each camera port were measured. Areas were determined by recording images of the light spots on high-contrast film (Technical Pan 135, Eastman Kodak Co., Rochester, NY) with a 55 mm macrolens (Nikkor, Nikon, Inc.) and by using a series of exposure times and apertures to avoid overestimation by diffusive saturation in the film. Areas were also obtained by viewing the light spots on a translucent screen placed over each port and measuring the diameter with a caliper. At both camera ports, the spots had circular areas of 0.386 ± 0.021 cm^2. Power readings obtained at the camera ports were divided by this area to obtain irradiances on the intensifiers. At the object (specimen) plane, illumination areas were measured with a transparent grating with 20 lines/mm attached to the specimen holder. These areas varied in size with the aperture diaphragm setting and the method of illumination; but the usual area used in RET experiments was 1.257×10^{-3} cm^2.

Neutral density filters of 1%, 5%, and 32% transmittances (Edmund Scientific Co., Barrington, NJ) were calibrated for spectral transmittance and attenuation and used to decrease the light intensity below the saturation level of the intensifiers. The cameras saturated at irradiances in excess of 0.01 nW/cm^2. The 1% and 5% filters transmitted 1.05% (±0.15%, standard deviation for 6 measurements) and 5.1% (±0.10%) of the incident power. The filters were placed in front of the intensifier photocathodes to extend the minimum attained irradiance to 3.9×10^{-6} nW/cm^2. The calibration irradiance was obtained as the product of the filter's transmission coefficient and the reading of the photodetector.

The cameras were calibrated with monochromatic intensities. Irradiances measured at different wavelengths were spectrally matched by using published spectral responsivity curves of the image intensifiers,[23] with coefficients given as percentages of the peak response. To obtain the intensifier responsivity $R(\lambda)$, the coefficients were multiplied by the individual responsivities of S-25 and P20.[24] The KS1380 intensifier phosphor was a mixture of P20 and P39; these phosphors have nearly identical spectral responsivities,[24] so we used the curve for P20 for both intensifiers. The peak response for S-25 is 56% at 620 nm and for P20 is 96% at 530 nm. For example, at $\lambda=500$ nm the intensifiers have a relative spectral efficiency of 100%, while the efficiencies of S-25 and P20 are 41% and 67%. Thus $R(\lambda=500\text{ nm})=1.00\times0.41\times0.67=0.275$. At each wavelength used, irradiances measured with the photodetector at the position of the intensifier faceplate were multiplied by the spectral responsivity coefficient to obtain the spectrally matched irradiance. To determine radiances originating at the object plane in RET experiments, the spectral response was incorporated into the spectral transfer coefficients as $S'(\lambda)=S(\lambda)R(\lambda)$.

III. RESULTS

A. Spectral transmission by the microscope

Irradiances at the object plane. The donor coumarin is excited directly in RET with a maximum at 390 nm. We obtained the power available to the donors by measuring the intensity of the epi-illumination light incident on the photodetector placed in specimen plane. A 390 nm light beam was reflected from the 430 nm dichroic mirror and the aperture diaphragm was adjusted to provide a spot diameter of 400 μm at the object plane with the 25× objective. The incident power (with Köhler illumination) was 2.08 ± 0.17 μW (standard deviation for $n=5$) with the 2.0 mm slit and 521 ± 47 nW with the 0.5 mm slit, corresponding to irradiances of 1.655 ± 0.134 and 0.414 ± 0.037 mW/cm^2.

Spectral transfer functions of the emission pathways. The spectral transfer function of the microscope $S(\lambda)$ indicates the relative efficiency of the optical pathway in transmitting incident light and is used to convert the power at the camera into the power originating from the specimen. To measure $S(\lambda)$ of each emission pathway without partial reflection by the dichroic mirror, the light beam was directed into the objective lens with the beam steerer placed at 45° in the specimen plane, as depicted in Fig. 1(B). The area of the primary objective lens, 3.14 cm^2, was used to normalize the incident powers. The illumination arrangement of Fig. 1(B) did not produce Köhler illumination and magnification of the exit slit image by the condenser greatly attenuated the power incident at the photodetector.

The incident radiances $I(\lambda)$ measured with the photodetector at the position of the objective for the wavelength

SPECTRAL_0000665

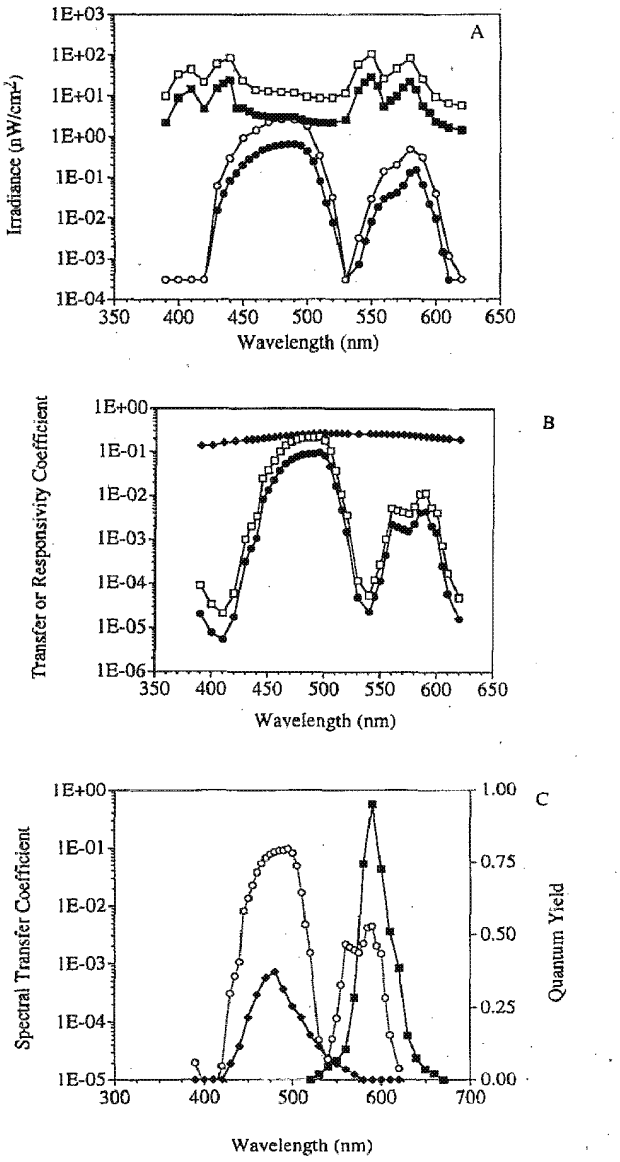


FIG. 2. Spectral transfer function of the RET microscope. (A) Irradiances measured with the photodetector at the specimen plane $I(\lambda)$ using the 2.0 (open squares) and 0.5 mm (closed squares) monochromator exit slits and the irradiances measured at both camera ports $i'(\lambda)$, (open circles), 2.0 mm, and (closed circles) 0.5 mm exit slits. At wavelengths greater than 525 nm, powers at the coumarin port were within the noise of the radiometer. At the rhodamine port, wavelengths below 535 nm were not detected. (B) Spectral transfer function of the microscope $S(\lambda)$ between the objective and the camera ports, calculated as $i'(\lambda)/I(\lambda)$ (open squares), spectral responsivity coeffficients of the intensifiers $R(\lambda)$ calculated from quantum efficiencies of the photocathode and output phosphor (closed diamonds), and spectral transfer and responsivity coefficients $S'(\lambda)$ calculated as $R(\lambda)S(\lambda)$ (closed circles). (C) Quantum distribution functions of coumarin-PE (closed diamonds) and rhodamine-PE (closed squares) emission, plotted with $S'(\lambda)$ (open circles). The rhodamine emission is passed only by the acceptor pathway with no spillover into the donor pathway. The coumarin emission is transmitted with greater efficiency by the donor pathway than the rhodamine emission is passed by the acceptor pathway.

range of 390–620 nm are shown in Fig. 2(A) for the 2.0 (open squares) and 0.5 mm (closed squares) slits. Transmitted irradiances $i'(\lambda)$ were measured with the photodetector at each camera port for the same range of wavelengths. The optical pathways contained the 430 nm dichroic and 450 nm long-pass emission filters in the Ploem and the RET filters in the Multi-image module. The transmitted radiances for the

TABLE I. Spectral transfer characteristics of emission pathways.

	Coumarin (donor)	Rhodamine (acceptor)
Spectral limits (nm)	430–535	550–610
Peak transfer (nm)	495	595
Peak coefficient	0.2238	0.0117
Total power transfer (%)	5.521	0.335

25× objective are shown in Fig. 2(A) for both 2 (open circles) and 0.5 mm exit slits (closed circles). $S(\lambda)$, calculated for both emission pathways as $i'(\lambda)/I(\lambda)$, is displayed in Fig. 2(B) (open squares), together with $R(\lambda)$ (closed diamonds) and the product $S'(\lambda)=S(\lambda)R(\lambda)$ (closed circles), which was used to spectrally match $i'(\lambda)$. The donor and acceptor emissions were effectively separated by the microscope.

The total relative power transferred by the 25× objective and the peak transmittances for each pathway are shown in Table I. Transfer coefficients measured with the 50× objective lens were decreased relative to the 25× lens by 43% at all wavelengths. This was greater than the 25% reduction expected on the basis of the ratio of numerical aperture to magnification, indicating additional optical density in the 50× objective. The quantum distribution functions of the donor coumarin (filled squares) and the acceptor rhodamine (filled squares) dye emissions, as measured by spectrofluorimetry of liposomes containing probe-labeled phospholipids,[25] are shown in Fig. 2(C) together with $S'(\lambda)$ (filled diamonds). The spectral transfer function of each pathway overlaps with the peak emission range of the corresponding dye. With the 25× objective, the donor pathway transfers about 5.5% of the total incident power, while the acceptor pathway passes only about 0.34%. The greater transmissivity of the donor pathway is compensated by the smaller emission intensity of coumarin relative to the acceptor rhodamine.[26]

B. Video camera calibrations

Varying the irradiance. Irradiances were varied by combining illumination arrangements, bandpass and neutral density filters, and objectives of different magnification and numerical aperture to cover the brightness range of the cameras. The different illumination arrangements included reflecting the light beam into the objective with the beam steerer at 45° in the specimen plane [Fig. 1(B)], and epi-illuminating the beam steerer (using the 430 nm dichroic or the beam splitter) placed in the specimen plane at 90° to the optical axis [Fig. 1(A)]. The spectral transfer characteristics of the emission pathways enabled a large number of irradiances to be obtained by varying the wavelength.

The cameras were calibrated by fixing the intensifier gain and monochromator wavelength and alternately measuring the power at the camera port with the photodetector and then the brightness with the camera (and neutral density filter). Prior to all calibrations, the intensifier was allowed to stabilize for 45 min after the mcp power supply was turned on. At each gain, irradiances and brightnesses were measured for each monochromator exit slit and the full range of inci-

SPECTRAL_0000666

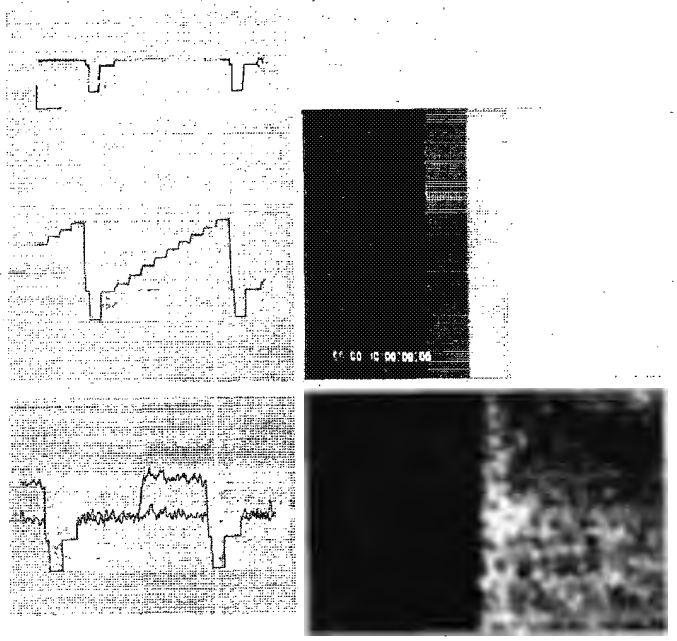


FIG. 3. Video brightnesses and luminance voltages of the KS1381 intensifier-CCD camera. The left-hand panels show tracings of single horizontal line sweeps of the video signal. The oscilloscope was triggered at the line frequency of the video camera, 15.75 kHz. In the top trace, the flat portion extending for 59 μs after the sync pulse is the preset black level of +42 mV. The middle trace shows the brightness scale of 9 steps each with an amplitude of 79.3 mV above the previous step. The initial step is divided between the preset black level for the brightness scale circuit and 79.3 mV. The right-hand panel shows the video image produced by the voltage steps. The bottom panel on the left-hand side shows a line tracing of the camera signal recorded with a neutral density step between 1.2 and 0.7 in the specimen plane that was transilluminated with a constant light intensity. Superimposed on the tracing is the voltage recorded with the specimen consisting of a uniform ND 1.2 filter transilluminated by the same light intensity. The right-hand panel shows the video image produced by the step. All video images in the figure were obtained with a 55 mm Nikkor lens placed 110 cm away from the video monitor in a darkened room, with the film exposed for 1/30 s at f/8.0. The prints were obtained on high-contrast paper at identical exposure conditions. The coincidence of the voltage levels obtained with a uniform dark field and with a contrast step in the field having the same ND as the uniform field indicates that the black level of the camera was fixed by the preset level and the calibrations were not affected by autoblacking. The shading apparent in the brightness scale image was due to refraction by the highly curved faceplate of the video monitor and was not present in the digitized frames stored in the frame buffers. Scale bars: vertical 220 mV, horizontal 10 μs.

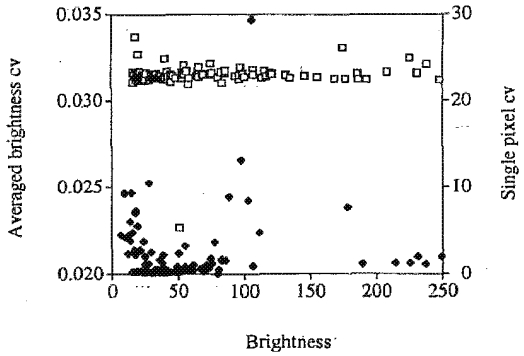


FIG. 4. Coefficients of brightness variation (standard error/mean) for single pixels (open symbols) and area averages (closed symbols) measured in 32 consecutive video frames obtained at maximum intensifier gain for different irradiances. The cv are plotted as a function of the average pixel brightness. The right-hand ordinate denotes the cv for individual pixels tracked from frame to frame, in which the average was measured as the arithmetic mean brightness for the 32 samples. This cv is larger at low mean brightness due to the speckled nature of images obtained at low irradiances. The left-hand ordinate denotes the cv obtained by averaging the mean brightnesses of 1024 pixels in a compact area in the 32 frame average. These cv are less than 3.5% and are invariant with the mean brightness.

dent wavelengths. After the gain was adjusted, the mcp was allowed to stabilize for up to 15 min. Measurements were repeated over an 11 month period to determine reproducibility. Although the irradiance resulting from a particular arrangement was variable, due to lamp aging and positional variation of the arc, the brightness produced by each irradiance was constant.

The brightness scale of the video camera. We ensured that the video luminance voltages always corresponded to absolute irradiances by checking that the preset black level was used as the reference voltage.[26] In addition, we set the analog control registers of the ADI to produce linearity of the digitized brightness with the camera voltage. Oscilloscope tracings of single video line sweeps from the KS1381-CCD camera are shown in Fig. 3. The top trace is the preset black level. The middle and bottom traces are paired with single, digitized video frames. The middle trace shows that the digitized brightness was linear with the video voltage. Each step in amplitude of 79.3 mV (left-hand panel) produced a constant increase of 28.4 brightness units (right-hand panel). Reproducibility of dark levels is seen in the superimposed traces at the bottom. The dark voltage level obtained with a uniform field of ND 1.2 in the specimen plane coincided with the dark level obtained with a step of neutral density (from ND 0.7 to 1.2) in the field. The modulation transfer function (mtf) ultimately limits imaging intensity steps at fine resolution and the estimation of brightness as a function of irradiance. The mtf falls to 80% at 128 line pairs/mm in the specimen plane. Calibrations were made with uniformly illuminated fields to avoid amplitude compression by the optics at high spatial frequencies.

Determining brightnesses. At gains >10% of maximum, the intensifiers produce speckled images at irradiances less than 10^{-4} nW/cm^2. At each pixel in the image, the brightness varied greatly from frame to frame. The measured coefficients of variation (standard error/arithmetic mean) for single pixels in averages of 32 frames, as shown in Fig. 4 (right-hand ordinate), were typically large, particularly for low mean pixel brightnesses. The variation originates from non-Gaussian noise processes in the intensifiers including thermionic emission at the photocathode, shot noise in the mcp, and fluorescence noise in the output phosphor.[24] To obtain a brightness estimate that reliably corresponded to an irradiance, images were spatiotemporally averaged. First, 32 video frames obtained at fixed irradiance and intensifier gain were averaged. Then, the resulting arithmetic mean pixel brightnesses were averaged for 1024 pixels in a user-selected compact area. As seen in Fig. 4 (left-hand ordinate), this averaging produced coefficients of variation (cv) that were <3.5% for each area and were invariant with the average brightness. Shading was determined by measuring the average brightness at different positions in the frame. Geometric distortion was assessed with a ruled grating by measuring a line spac-

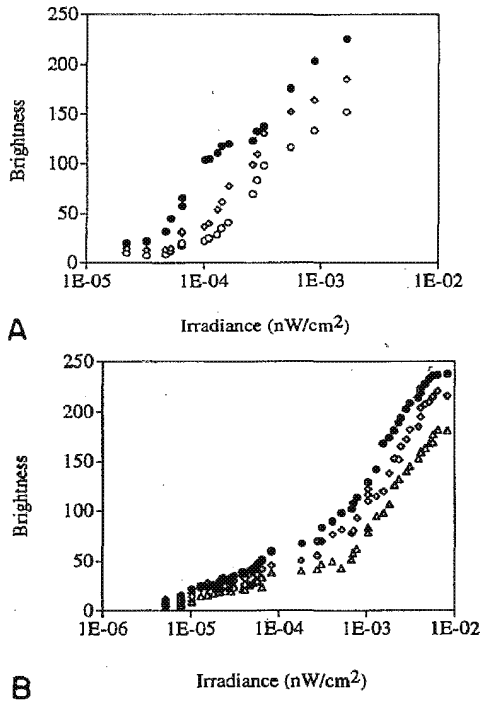


FIG. 5. Irradiance–brightness relations for the KS1380 intensifier-CD camera. (A) High mcp gains. The 32-video frame average brightnesses recorded at mcp gains 19% (open circles), 43% (open diamonds), and 100% (closed circles) of maximum are shown plotted as a function of irradiance. The brightnesses were obtained by averaging the individual pixel brightnesses of a square area consisting of 1024 pixels. Irradiances were obtained at wavelengths ranging from 430 to 600 nm. Irradiances greater than 10^{-4} nW/cm^2 were obtained using the beam splitter and the 50/50 mirror. Irradiances below this value were obtained with the full set of RET filters in the microscope and with the camera at the donor port, which restricted the wavelengths to between 430 and 530 nm. The irradiances shown were spectrally matched by multiplying by the spectral responsivity coefficient for the wavelength of the irradiance. This intensifier has a minimum detectable irradiance of 10^{-5} nW/cm^2. The brightness increases less steeply for irradiances greater than 3×10^{-4} nW/cm^2, particularly at the lower gains, suggesting an excessive mcp voltage. (B) Low gains used in RET experiments. Relations obtained at mcp gains 0.7% (open triangles), 1.5% (open diamonds), and 3.5% (closed circles) of maximum are shown together. At these gains, the minimum detectable irradiance is 10^{-4} nW/cm^2. The maximum slope is maintained up to 10^{-2} nW/cm^2, where the brightness saturates at <250.

ing at the center of the frame and then moving the line pair to a corner of the frame. Both shading and geometric distortion were <5%, due to the flat-field correction inherent in the objective. In addition, the image fell on only the central region of the mcp and on the central 512 pixels of each line in the CCD (which has a width of <750 pixels). Thus, flat-field correction was unnecessary.

Irradiance–brightness relations. Each intensifier-CCD camera was unique in its response. Nonetheless, key features were common to both cameras. When the averaged brightnesses were plotted on a linear ordinate as a function of the spectrally matched irradiances on a logarithmic abscissa, the relation at each fixed mcp gain resembled a sigmoid or a power function with abrupt saturation. Irradiance–brightness relations are shown in Fig. 5 for the KS1380 intensifier and in Fig. 6 for the KS1381. Each relation was typified by a region of low slope at small irradiances, then a region where small increments in irradiance produced a large increase in

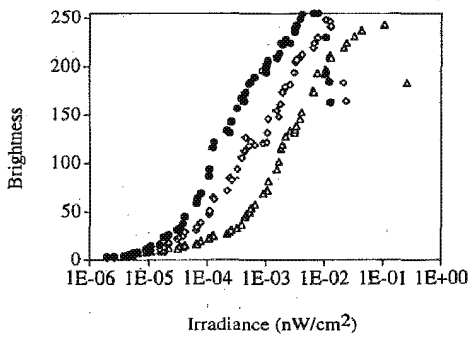


FIG. 6. Irradiance–brightness relations for the KS1381 intensifier-CCD cameras at mcp gains used in RET experiments. Relations for the KS1381 intensifier are shown for gains of 100% (closed circles), 43% (diamonds), and 19% (triangles) of maximum. This intensifier has greater sensitivity at lower irradiances by about one-half decade compared to the KS1380/1381. In addition, the slopes of the relations at irradiances just exceeding the minimum detected levels are also greater. Thus, this intensifier is most useful for detecting the emission of the sensitized acceptor in RET experiments.

brightness, and finally a region where the brightness either remained relatively constant with further increases in irradiances or fell to submaximal values. We found that the brightness at a fixed irradiance was not strictly proportional to the intensifier gain, even in the region of maximum slope. The slope in this region depended on the mcp gain setting and was larger at greater gains (Figs. 5 and 6).

The errors of measurement in these relations originated from the error in determining the irradiance, because the average brightness error was small (Fig. 4). The irradiance error, calculated by assuming that the measured power, area, and filter transmission means were uncorrelated, linear random variables, was 9.6×10^{-6} nW/cm^2.

Minimum detectable irradiances. The background brightness produced at maximum gain with the faceplate shielded from any light was less than 1.0 ± 0.4 units (standard error). Low levels of light ($<0.5\times10^{-5}$ nW/cm^2) produced brightnesses <20 units, but these brightnesses were typically constant for further increases in the irradiance, making them impossible to calibrate, until a minimum detectable irradiance was reached. The minimum detectable irradiance was determined as the lowest irradiance producing a brightness that scaled with the gain and varied with small changes in the irradiance. For the KS1380, the minimum detectable irradiance was greater than 10^{-5} nW/cm^2 at all gains [Figs. 5(A) and 5(B)]. At large gains, this intensifier was less sensitive than the KS1381, which produced calibratable brightnesses for irradiances $<10^{-5}$ nW/cm^2 at gains >19% (Fig. 6). Thus, the KS1381 was used to detect the fainter emission of the acceptor, which is sensitized to fluorescence by RET from the directly excited donor.

Saturation of the intensifier brightness. Saturation of the brightness occurred with both intensifiers at all gains at large irradiances ($>10^{-3}$ nW/cm^2). At large gains with the KS1381, the brightness reached the maximum value of 255 units at 10^{-2} nW/cm^2. At greater irradiances, the overload protection of the mcp caused the brightness to decline to about 160 units. With the KS1380 intensifier, however, the brightness saturated at <255 units without the steep decline in brightness found with the KS1381. To avoid possible dam-

SPECTRAL_0000668

TABLE II. Parameters for gain relations of KS1380/81 and KS1381 intensifier-CCD cameras.

Intensifier gain (as % maximum)	Fit parameters[a]		
	Amplitude	Exponent	R^2
KS1381			
100	8577.134	0.550	0.924
43	5830.434	0.556	0.945
19	1657.166	0.464	0.983
3.5	1035.908	0.483	0.912
KS1380/1381			
100	14 202.848	0.577	0.845
43	37 259.938	0.745	0.906
19	46 878.114	0.818	0.931
3.5	2462.708	0.428	0.953
1.5	1734.427	0.398	0.968
0.67	1656.637	0.432	0.951

[a]The parameters obtained by fitting the function brightness$=a$(irradiance)^b to the irradiance–brightness data are shown. The amplitude is denoted by a and the exponent b.

age to the intensifiers, we did not explore the differences between these saturation behaviors. In general, we found the KS1381 to be more sensitive to the lowest light levels and useful over a greater range of intensities than the KS1380.

Determining irradiance from brightnesses. The utility of the cameras is hinged not only on sensitivity and gain, but ultimately around the conversion of brightnesses to irradiances. This poses the question of the best conversion method. One way is to use the measured relations as a look-up table in which each brightness is compared with an ordered list of brightness–irradiance pairs. Interpolation would produce an irradiance value, but with considerable computation. A faster way is to fit a functional form to the irradiance–brightness relation with estimated parameters. During experiments, the video image is transformed using the set of parameters appropriate to the mcp gain. We chose the latter method for reasons of implementation.

The relations at each gain were quantitatively characterized by fitting power functions of the form brightness $=a$(irradiance)^b to the data. The coefficient a and the exponent b were obtained by linear regression on the logarithm of the brightness function. This form was chosen because it is expected by the theoretical relation given in Eq. (2), and we found that linear and polynomial functions up to order 3 produced worse fits ($R^2<0.5$). We excluded the data at the upper irradiance regions where the brightness saturated or decreased due to overload protection. Data at the lowest irradiances were included in the fits, however. All relations were adequately described by single functions. The fitted parameters for each intensifier at each gain are shown in Table II.

The two fitted parameters varied as a function of the gain. The amplitude a denotes the magnitude of the brightness at a particular irradiance, while the exponent b is the increment in brightness for an increase in irradiance. With the KS1381, both the amplitude and exponent were increased at higher gain, as expected for the increased slope of the irradiance–brightness relation at large gains. The amplitude varied more consistently than the exponent with the gain. While the exponent did not vary as greatly with the gain, it also was greater at larger gains. With the KS1380, neither the amplitude nor the exponent varied consistently with gains >10% of maximum. At gains below 5%, the amplitude varied with the gain, but the exponent was relatively constant. To ensure that the fitted parameters provided the most accurate conversion, the KS1380 was operated at low gains to measure the emission of the directly excited donor, while the KS1381 was used at high gains to detect the acceptor.

C. RET measurements with the calibrated intensifier-CCDs

To verify the calibration, we measured RET between coumarin-phosphatidyl ethanolamine (PE) and rhodamine-PE dispersed in unlabeled phosphatidylcholine spread in planar depositions on quartz substrates.[27] The planar lipid depositions were formed from liposomes prepared by detergent dialysis of lipid containing fixed mole fraction ratios of labeled to unlabeled lipids. The ratio of coumarin-PE to rhodamine-PE was fixed at 1:1 for easy calculation of the median distance of separation between probes in each mixture. The liposomes were spread on Ar plasma-cleaned quartz substrates,[27,28] which were washed and then mounted in the specimen holder. The liposomes break open on the quartz surface to produce plane smectic mesophases. The amount of deposited material was checked by measuring the emission of rhodamine directly excited at 540 nm. Substrates were used only when the directly excited rhodamine intensity was proportional to the amount of rhodamine-PE in the liposomes.

To measure RET, the coumarin was excited at 390 nm, and the emitted light was separated by the RET filters into coumarin and rhodamine components, which were viewed as separate images simultaneously with the two intensifier-CCD cameras. Brightnesses (c) in each full-frame image were transformed on a pixel-by-pixel basis to irradiances (i) at the intensifier faceplates using the inverse calibration function $i=G[c]$, where $G[c]=(c/a)^{(1/b)}$, with a and b chosen for the mcp gain. These irradiances were then divided by $S'=\int R(\lambda)S(\lambda)d\lambda$, (the total fractional power transferred by the passband of the emission path) to obtain the radiances originating from the specimen that were captured by the objective. For RET between a single donor–acceptor pair, the median separation R between probes for a particular probe mixture is related to the ratio of the sensitized rhodamine radiance ΔI_A to the coumarin radiance I_D by $(R_0/R)^6=(\Delta I_A/I_D)A_t$, where A_t is the area density of rhodamine-PE.[12] ΔI_A was determined by removing from the total rhodamine intensity the contribution from direct excitation of the dye at 390 nm. This was obtained from lipid depositions containing only rhodamine-PE at the same density as in the RET experiments and excited at 390 nm. The radiance ratios for each pixel were calculated and averaged for the image, and the average ratio as a function of the median separation distance for each probe mixture was plotted (Fig. 7). The median distance of separation, $1/2\sqrt{2}(R_p)$, was calculated from the radial distribution function for donor–acceptor separation ($\int 2rdr/R_p^2$), where R_p is the radius of the statis-

SPECTRAL_0000669

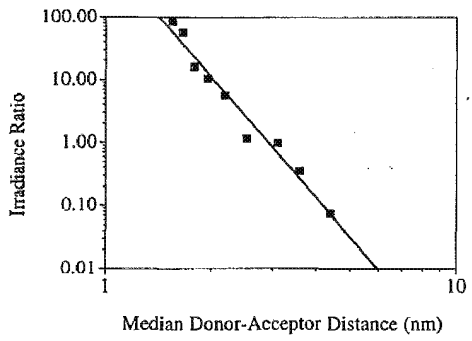


FIG. 7. RET between coumarin and rhodamine within lipid depositions containing fixed densities of fluorescently labeled phospholipids. The lipid depositions were made on quartz substrates as described in the text. In all preparations, the ratio of coumarin-PE to rhodamine-PE was fixed at 1:1. Donor–acceptor distances were varied by changing the mole fraction ratio of labeled to unlabeled lipids. The coumarin-PE was excited at 390 nm, and the emissions of both probes were recorded simultaneously using two cameras. Brightnesses in the two images were converted to irradiances using the inverse of the fitting function and the acceptor:donor ratio was determined by dividing the rhodamine irradiance by the coumarin irradiance. The ratios were averaged for 3 quartz substrates of each lipid composition. The ratios are plotted as a function of the median donor–acceptor distance for the lipid composition as described in the text. The line $A/D=879.34\ (R)^{-6.02}$ was obtained by regression $R^2=0.971$. The inverse-sixth power dependence of the sensitization ratio is in accord with the distance dependence expected for RET. The characteristic distance for 50% RET was determined to be 3.04 ±0.37 nm for the deposited lipid bilayers.

tical disk for which $2R_p$ is the median separation between two donors (or two acceptors).[25,29,30] R_p was calculated from the mole fraction m of donor as $\sqrt{(n/\pi m)}$, where n is the area per phospholipid which was taken to be 0.6 nm^2. At the point where the ratio equals 1, indicating 50% RET efficiency, the characteristic distance for energy transfer R_0 was 3.04±0.37 nm, in agreement with other measurements for this pair of probes.[26] This confirms the necessity of calibrating the video cameras to determine radiance ratios, as the untransformed brightness ratios do not provide accurate estimates of k_t. In addition, the RET ratio varied with the inverse-sixth power of the median donor–acceptor separation, as expected, thus validating the accuracy of the calibrations. Therefore, the calibrated cameras enable the quantitative determination of RET.

IV. DISCUSSION

Intensified-CCD cameras in the quantitation of low light levels. The intensifier-CCD cameras calibrated in this study are sensitive to low light levels. The brightness amplitude of the video image was related quantitatively to the energy flux of light emitted by the specimen that reaches the detector. We calibrated our cameras radiometrically (as energy fluxes), rather than photometrically (as photon fluxes), in order to directly quantitate RET. RET is characterized as the transfer of excitation energy from a bluer probe to a redder one by electromagnetic interaction rather than by quantum transfer.[14] Thus, transforming the video brightnesses to radiometric intensities enables RET to be determined from the energies emanating from the probes in the specimen. This conversion consists of 4 steps: transforming the video brightnesses into irradiances using the camera relations, correcting the irradiances for the spectral response efficiencies of the intensifier, transforming these irradiances into radiances from the probes entering the microscope using the spectral transfer function for the emission pathway, and correcting these radiances by the solid angle of the field of view to obtain the total flux of energy from the probes in the specimen. Computations of RET rely on specific models of probe–pair interaction and depend on the geometrical arrangement of the probes in the specimen as each donor interacts with several acceptors. Lipid membranes provide an ordered arrangement of molecules and are well-suited specimens for the microscope.

Validity of the calibration. The microscope is suitable for measurements of RET because the brightnesses of both the donor and acceptor probes can be simultaneously monitored and converted into the irradiance values needed to calculate k_t. The errors in the calculated irradiances depend on the type of conversion used. We have found that R_0 for the coumarin–rhodamine pair is accurately estimated when the conversion is made using inverses of the irradiance–brightness relations obtained by fitting power functions to the data. The error in this conversion can be appreciable with large brightnesses (>200), because the fit parameters leave large residuals. But the errors introduced into the intensities by the inverses of the fitted functions do not impede the estimation of RET parameters in a uniformly illuminated field. Because both the mcps and CCD cameras are comprised of discrete sensing units, the calibration is valid in practical situations where RET is localized to small areas in the image. We used video equipment rather than a direct digital readout approach because we ultimately want to use the RET microscope to follow the time course of dynamic RET images that occur during membrane fusion. When cooled CCD cameras are developed with better sensitivities at video rates than intensifier-CCD cameras, and bandwidth limitations on direct memory access are overcome, then the interposition of video encoding can be eliminated in favor of direct collection and transfer of digital data.

Spillover of the emission of one probe into the emission pathway is always a potential source of error with RET.[12] With this microscope, the useful range of spectral transmission coefficients is 10^{-1}–10^{-5} [Fig. 2(B)]; the cameras respond to a range of irradiances less than four orders of magnitude at any gain. Thus, the 390 nm excitation light is excluded from the donor pathway and the wavelength bands passed by emission paths are separated by 15 nm, according to this criterion. The overlap between coumarin and rhodamine emission quantum distribution functions is entirely within the rhodamine bandpass region of the microscope. During RET, the coumarin emission is absorbed by the acceptor which has a large extinction over this range of wavelengths. In the absence of RET, the coumarin emission that spills over into the rhodamine pathway appears as background, which is subtracted from the total sensitized rhodamine image. Rhodamine has low excitation at 390 nm, and its directly excited emission remains undetected by the less sensitive KS1380 that is used to detect the donor coumarin.

RET measurement with the calibrated video microscope.

SPECTRAL_0000670

The magnitudes of the radiances measured are expected to be encountered in RET experiments, as is shown by the following calculations. The amount of excitation light energy delivered to the fluorescent probes in the specimen is more than enough to produce large emission intensities detectable by the cameras. With an incident excitation irradiance of 1.6 mW/cm^2 at 390 nm (5.1×10^{-10} nJ/$h\nu$), each donor coumarin molecule, with a molecular cross section of 6.06×10^{-17} cm^2, absorbs energy at a rate of 9.69×10^{-11} nW. For probes distributed evenly in a planar bilayer at 1 mol % (3.33×10^{12} cm^{-2}), the energy absorption density is 320 nW/cm^2. With a quantum yield for coumarin of 0.5, the emission density of the donor in the specimen is 160 nW/cm^2. The objective lens subtends only a small solid angle, and captures a fraction of about 7.85×10^{-4} of the total radiated flux. Thus the power entering the microscope relative to the field of view is 0.126 nW/cm^2 in the focused image, and, with a spectral transfer coefficient integral of the donor emission pathway over the emission range 430–535 nm of ~5%, the irradiance reaching the image intensifier from the unquenched coumarin is 6.3×10^{-3} nW/cm^2. This is a large value for the intensifier-CCD cameras and produces brightnesses in excess of 150 units at gains >2% of maximum. If the acceptor rhodamine is present at the same density as the donor, then the median distance of separation is 3.1 nm. With the R_0 of 3.0 nm for the coumarin–rhodamine pair, $(R_0/R)^6=0.82$, and the fraction of the coumarin excitation energy transferred to rhodamine is 0.45. With a quantum yield for rhodamine of 0.9, the acceptor radiance at the specimen is 65 nW/cm^2. With $\int S(\lambda)d\lambda=0.004$ for the acceptor emission pathway over the emission range of rhodamine (540–610 nm) and the same solid angle for capture by the objective, the irradiance at the rhodamine camera is 2.0×10^{-4} nW/cm^2. The coumarin emission reaching the coumarin camera is 3.7×10^{-3} nW/cm^2. At intensifier gains of about 1% of maximum for the coumarin camera and 100% for the rhodamine camera, the coumarin brightness is decreased to 100 units and the rhodamine brightness is increased to ~100 units. If the donor and acceptor are each present at 0.5 mol %, then the median separation is 4.37 nm, the fraction of the coumarin excitation energy transferred to rhodamine is 0.09, and the irradiances reaching the coumarin and rhodamine cameras are 2.7×10^{-3} and 4.5×10^{-5} nW/cm^2, respectively, which produce brightnesses of about 100 and 50. The intensifier-CCD cameras detect the low light levels predicted by these calculations and are able to distinguish the brightnesses produced by the radiances of probes at different distances in the specimen both theoretically and experimentally. The microscope measures distances on the nanometer scale. We are applying it to the phenomenon of membrane fusion.

ACKNOWLEDGMENT

This work was supported by NIH No. GM27367.

[1] S. Inoué, *Video Microscopy* (Plenum, New York, 1986).
[2] R. S. Aikens, D. A. Agard, and J. W. Sedat, Methods Cell Biol. **29**, 291 (1989).
[3] I. S. McLean, *Electronic and Computer-aided Astronomy: From Eyes to Electronic Sensors* (Horwood, Chichester, 1989).
[4] Y. Hiraoka, J. W. Sedat, and D. A. Agard, Science **238**, 36 (1987).
[5] D. L. Taylor and E. D. Salmon, Methods Cell Biol. **29**, 207 (1989).
[6] D. L. Taylor and E. D. Salmon, Methods Cell Biol. **29**, 239 (1989).
[7] G. R. Bright and D. L. Taylor, in *Applications of Fluorescence in the Biomedical Sciences* (Liss, 1986), pp. 257–288.
[8] M. Chodorow and R. Symons, in *Reference Data for Engineers: Radio, Electronics, Computer, and Communications*, edited by M. E. Van Valkenburg (Prentice Hall, Carmel, IN, 1993), Chap. 16, pp. 32–34.
[9] K. R. Spring and R. J. Lowy, Methods Cell Biol. **29**, 270 (1989).
[10] B. Herman, Methods Cell Biol. **30**, 219 (1989).
[11] U. Kubitscheck, M. Kircheis, R. Schweitzer-Stenner, W. Dreybrodt, T. M. Jovin, and I. Pecht, Biophys. J. **60**, 307 (1991).
[12] M. Ludwig, N. F. Hensel, and R. J. Hartzman, Biophys. J. **61**, 845 (1992).
[13] R. E. Dale and J. Eisinger, in *Biochemical Fluorescence: Concepts*, edited by R. F. Chen and H. Edelhoch (Dekker, New York, 1974), Chap. 1, pp. 115–284.
[14] Th. Förster, Ann. Phys. **2**, 55 (1948). Translated from German by R. S. Knox, Department of Physics and Astronomy, University of Rochester, as Biological Physics Group Tech. Report No. 46.
[15] L. Brand and B. Witholt, Methods Enzymol. **11**, 776 (1967).
[16] B. J. Bacskai, B. Hochner, M. Mahaut-Smith, S. R. Adams, B.-K. Kaang, E. R. Kandel, and R. Y. Tsien, Science **260**, 222 (1993).
[17] R. A. Baldock and I. Poole, J. Microsc. **172**, 49 (1993).
[18] J. M. Beach and B. R. Duling, J. Microsc. **172**, 41 (1993).
[19] R. Oldenbourg, H. Terada, R. Tiberio, and S. Inoué, J. Microsc. **172**, 31 (1993).
[20] W. J. Smith, *Modern Optical Engineering* (McGraw-Hill, New York, 1966), pp. 188–193.
[21] W. D. Niles and F. S. Cohen, J. Gen. Physiol. **90**, 703 (1987).
[22] *Reference Manual for CCD-72 Series Camera* (Dage, MTI, Michigan City, IN, 1989).
[23] *Reference Manual for KS1380/1381 and KS1381 Image Intensifiers* (Video Scope International, Washington, D.C., 1989), pp. A1–10.
[24] G. E. Stillman, in *Reference Data for Engineers: Radio, Electronics, Computer, and Communications*, edited by M. E. Van Valkenburg (Prentice Hall, Carmel, IN, 1993), Chap. 21, pp. 1–31.
[25] W. D. Niles and F. S. Cohen (unpublished).
[26] G. P. McGinty, *Video Cameras: Theory and Servicing* (Sams, Indianapolis, IN, 1984), pp. 140–142, 219.
[27] C. L. Poglitsch and N. L. Thompson, Biochemistry **29**, 248 (1990).
[28] N. L. Thompson, A. A. Brian, and H. M. McConnell, Biochim. Biophys. Acta **772**, 10 (1984).
[29] T. N. Estep and T. E. Thompson, Biophys. J. **26**, 195 (1979).
[30] B. Snyder and E. Friere, Biophys. J. **40**, 137 (1982).

SPECTRAL_0000671

This article was downloaded by: *[University of California, Los Angeles]*
On: *29 July 2010*
Access details: *Access Details: [subscription number 918974530]*
Publisher *Taylor & Francis*
Informa Ltd Registered in England and Wales Registered Number: 1072954 Registered office: Mortimer House, 37-41 Mortimer Street, London W1T 3JH, UK



International Journal of Remote Sensing
Publication details, including instructions for authors and subscription information:
http://www.informaworld.com/smpp/title~content=t713722504

Radiometric Calibration of Multispectral Airborne Video Systems

A. Edirisinghe; J. P. Louis; G. E. Chapman

To cite this Article Edirisinghe, A. , Louis, J. P. and Chapman, G. E.(1999) 'Radiometric Calibration of Multispectral Airborne Video Systems', International Journal of Remote Sensing, 20: 14, 2855 — 2870
To link to this Article: DOI: 10.1080/014311699211831
URL: http://dx.doi.org/10.1080/014311699211831

PLEASE SCROLL DOWN FOR ARTICLE

Full terms and conditions of use: http://www.informaworld.com/terms-and-conditions-of-access.pdf

This article may be used for research, teaching and private study purposes. Any substantial or systematic reproduction, re-distribution, re-selling, loan or sub-licensing, systematic supply or distribution in any form to anyone is expressly forbidden.

The publisher does not give any warranty express or implied or make any representation that the contents will be complete or accurate or up to date. The accuracy of any instructions, formulae and drug doses should be independently verified with primary sources. The publisher shall not be liable for any loss, actions, claims, proceedings, demand or costs or damages whatsoever or howsoever caused arising directly or indirectly in connection with or arising out of the use of this material.

INT. J. REMOTE SENSING, 1999, VOL. 20, NO. 14, 2855–2870

Radiometric Calibration of Multispectral Airborne Video Systems

A. EDIRISINGHE, J. P. LOUIS and G. E. CHAPMAN

Spatial Analysis Research Group, Charles Sturt University, Wagga Wagga, NSW 2678, Australia; e-mail: edirisi@camar.csiro.au

(*Received 20 May 1997; in final form 26 October 1998*)

Abstract. This paper describes the operational characteristics and radiometric calibration of the Multispectral Airborne Video System (MAVS) at Charles Sturt University. The system consists of an array of four high-resolution Charge-Coupled Device (CCD) cameras, each with a narrow band filter. The four channels of image data are digitised in real time using a data acquisition system, which also provides for continuous interactive viewing while the system is in operation. The characteristics of system performance, the results of aperture calibration and the results of system radiometric calibration are presented. The video imaging system is found to have a highly linear response. The differences of the radiance based and reflectance based system calibration curves are investigated through a newly developed radiometric calibration model. As a result of this, a method for calculation of atmospheric optical thickens is presented. Calibrated imagery from this system is now being used routinely for remote monitoring of land and water.

Downloaded By: [University of California, Los Angeles] At: 04:17 29 July 2010

1. Introduction

The need to derive quantitative data from images obtained from satellite or aircraft borne sensors requires the proper calibration of these systems. Calibrated systems can then be used in cost-effective monitoring activities. Images from most of the satellite sensors are not suitable for operational, small-scale, non-homogeneous applications such as agricultural monitoring. The main reasons for this are lack of high spatial resolution and fixed revisit schedules, coupled with long data turn-around times. Therefore, multispectral airborne videography is becoming a widely used operational remote sensing tool, with it's high spatial and flexible spectral wavebands. There have been a number of air-video systems developed (Nixon *et al.* 1987; King 1988; Everitt *et al.* 1991 and Neale, Black and Crowther 1994) and operated in the past. King (1995) has comprehensively reviewed most of the existing air-video sensor systems in regard to design and application aspects. A historical account of the evolution of airborne videography can be found in Mausel *et al.* (1992).

Airborne videography has been used for monitoring of agriculture (Jackson 1982; Jackson *et al.* 1987), natural resources such as forestry (King and Vlcek 1990) and rangeland (Pickup *et al.* 1995), vegetation (Nixon, Escobar and Menges 1985) and habitat (Homer *et al.* 1993).

For these systems to achieve their full potential, particularly for multi-temporal

International Journal of Remote Sensing
ISSN 0143-1161 print/ISSN 1366-5901 online ©1999 Taylor & Francis Ltd
http://www.tandf.co.uk/JNLS/res.htm
http://www.taylorandfrancis.com/JNLS/res.htm

SPECTRAL_0000673

studies, it is important that radiometric calibration procedures be developed to quantify multispectral air-video imagery.

2. Multispectral airborne video system

The Multispectral Airborne Video Imaging System (MAVS) presently in use at Charles Sturt University is based on the Digital Multispectral Video (DMSV) camera array (McKenzie *et al.* 1992). The MAVS consists of four high-resolution monochrome CCD video cameras with narrow band interference filters, mounted in a 96 mm square array, using a precision mounting frame (Mckenzie *et al.* 1992). The precision frame allows the camera axes to be precisely aligned parallel to one another. The camera array is fixed to the side of an equipment rack, which is secured to the seat rails in a Cessna 210 aircraft, in place of the co-pilot's seat. The camera frame extends out far enough to allow the cameras to look down through a bubble in a modified aircraft door.

The equipment rack contains the data acquisition and processing unit, which is an industrial IBM 486 compatible PC containing a 4 MB, 8 bit, AT-VISTA frame grabber to simultaneously digitise the analogue video signals from the four cameras. Image acquisition during flight is manually controlled via the keyboard, using image capture and processing software. The frame grabber transforms the video frames into 740 × 576 pixel digital image files in four channels, corresponding to the four camera bands. The digitised images are stored in Band Interleaved by Pixel (BIP) format to a hard disk. A 14″ VGA colour monitor is used for data acquisition control and may also be switched for use as a real time image display. A 600 watt power supply and a 240 volt AC inverter mounted in the equipment rack allow an operating time of 2–3 hours.

The cameras are a CCIR model high-performance CCD video camera. Each video camera acquires an image in a preset spectral band determined by an interchangeable narrow band (25 nm) interference filter centred at: band 1 (blue) 460 nm, band 2 (green) 550 nm, band 3 (red) 650 nm, and band 4 (near infrared) 770 nm. A 12 mm focal length lens is used on each camera, which gives a ground resolution of approximately 1.1 m when flying at 1500 m above ground level (AGL) and a ground area coverage of almost 0.25 km^2. The camera field of view (FOV) in the horizontal and vertical video directions is 28 and 22°, respectively.

An image processing software package (ABVIP) developed in the Spatial Data Analysis Unit at CSU also facilitates operational tasks such as camera aperture control and continuous interactive viewing (McKenzie *et al.* 1992 and Louis *et al.* 1995).

2.1. *Preliminary adjustments to the system*

Initial camera adjustments are required to balance the outputs from each camera and to maximise the camera signal-to-noise ratio. This is done by setting the camera gain close to minimum, setting the integration time to 1 ms and adjusting the initial aperture to approximately 70% open (*f*/1.8–*f*/2.1). These settings provide a useful starting point for many agricultural and vegetation monitoring applications. An experimental procedure has been devised to allow initial camera adjustments to be made in a systematic manner. Briefly, the procedure consists of imaging a set of natural or artificial targets with grey levels ranging from white to black, under normal solar illumination conditions, and adjusting each camera until the output dynamic range is optimally utilised. The automatic gain control on the CCD camera

Downloaded By: [University of California, Los Angeles] At: 04:17 29 July 2010

SPECTRAL_0000674

was disabled in order to facilitate the radiometric calibration process. The lens aperture settings are controlled by a stepper motor using keyboard commands in flight and may be changed as required, for different illumination conditions. There are 24 different aperture settings.

Accurate spatial registration of MAVS imagery is achieved through the pre-flight parallel alignment (Louis *et. al.* 1995) of each of the cameras. This significantly reduces the time required for post-processing of imagery.

The speed of the aircraft must be taken into account to make sure that a clearly focused image is obtained. The camera's 'electronic shutter' (CCD integration time) must be fast enough to 'freeze' the relative motion of the ground. The normal setting of 1 ms is a trade-off between light availability and motion blur. In addition, the video signal produced has a standard interlaced TV line scan configuration. Each image frame is made up of two interlaced image fields, with a field scan rate of 50 Hz. The aircraft flies in the same direction as the image horizontal scan direction. It takes 1/50 s to scan each field and therefore 1/25 s to complete each image frame. There is 1/50 s between adjacent odd and even field scan lines. The optimal aircraft speed is that which corresponds to a multiple of the ground resolution distance being covered in 1/50 s. At a flying height of 1500 m, this is about 1.1 m in 1/50 s, corresponding to an aircraft speed of 55 m s^{-1} (107 knots). At this flying speed, the odd field is 'sheared' from the even field by exactly one pixel. This interlace shear between the odd and even image fields is removed from the imagery as part of the post flight image processing procedures.

3. Aperture calibration

A calibrated aperture is helpful in setting the optimum contrast levels in each airborne image when planning flights. The MAVS camera lens aperture is controlled by a stepper motor through a RS232 computer connection. There are 24 control steps in total to change the aperture through 25 stops from 0 (fully closed) to 24 (fully open). For a circular aperture, the calibration allows a unique *f*/number to be assigned to each aperture stop. In this case the *number* belonging to *f*/number is defined as follows:

$$number = \left(\frac{l}{d}\right) \tag{1}$$

where l (= 12 mm) is the focal length of the camera and d is the diameter of the aperture opening. According to the MAVS specification, $d = 8.6$ mm for the largest aperture opening at 25th stop. As a part of the MAVS aperture calibration procedure, the assumption of a circular aperture was experimentally investigated.

3.1. *Method*

The aperture calibration was conducted under both laboratory and field conditions. In the laboratory a 500 W lamp projected on to an off-white screen was used as the light source. The stability of the light source was estimated to be $\pm$ 9%. An image of the illuminated screen was acquired for each aperture stop. In the field, a single grey-scale target, laid out on a flat open grass surface, was imaged for each aperture. Solar illumination variations throughout the field experiment were minimised by acquiring all the images in a relatively short time span (5 min). The average image digital numbers were calculated for each band for both experiments.

For a circular pupil of diameter d and area A, of an optical system, the light

Downloaded By: [University of California, Los Angeles] At: 04:17 29 July 2010

SPECTRAL_0000675

transmission W is given as

$$W = K_p A = K_p \pi d^2/4 \tag{2}$$

where K_p is a constant of proportionality.

Equation (2) shows that the light-gathering power of the lens is proportional to the entrance pupil area (A). However, the amount of light gathered is directly proportional to DN, corrected for the offset created by camera dark current (DC) for each band (see table 1). Therefore, $(DN - DC)$ is proportional to A. As a consequence of this, $(DN - DC)$ is proportional to d^2. Since the aperture size is uniquely defined by d, d^2 is directly proportional to (aperture stop number)^2. Therefore, DN in each spectral band is proportional to (aperture stop number)$^2 + DC$.

3.2. *Results*

The curves in figures 1 and 2 show the experimentally obtained relationships between the MAVS-recorded 8-bit digital number (DN) and the aperture stop number. The DN is averaged over the centre portion of the image to minimise the influence of any spatial non-uniformity characteristics of the imagery. Figure 1 shows the results of field measurements for the blue and the red bands. The result of the laboratory measurements for the blue band is shown in figure 2. The difference in the MAVS response levels in figures 1 and 2 is due to the two entirely different light levels that prevailed in the field and the laboratory environments.

Statistical analysis of data relating to these curves confirmed the quadratic nature

Table 1. Summary of the MAVS fundamental radiometric characteristics.

Band	Dark current (DN)	System Noise (DN)	Dynamic range (DN)	Signal-to-noise ratio (dB)	Radiometric precision (DN)
Blue	12	0.90	243	56.60	135.00
Green	12	0.76	243	48.60	157.80
Red	13	0.80	242	49.60	151.30
NIR	13	0.92	242	48.40	131.50

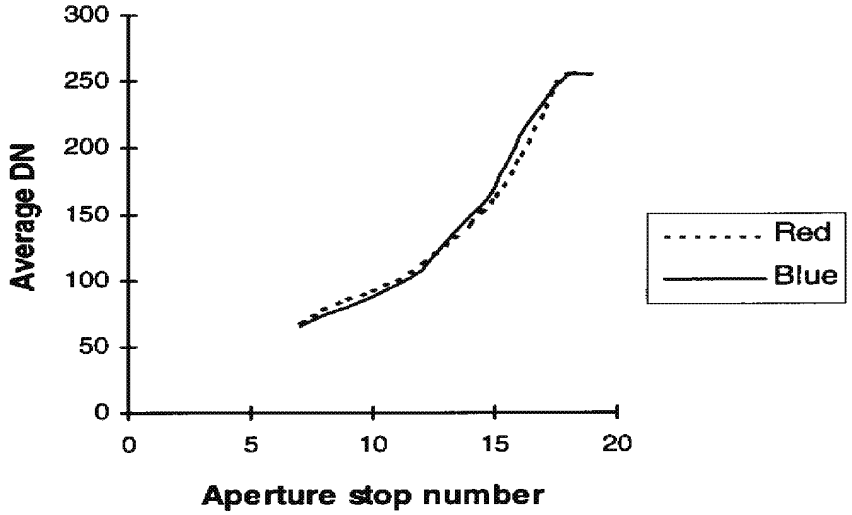


Figure 1. System DN versus aperture size for red and blue bands in the field.

SPECTRAL_0000676

Downloaded By: [University of California, Los Angeles] At: 04:17 29 July 2010

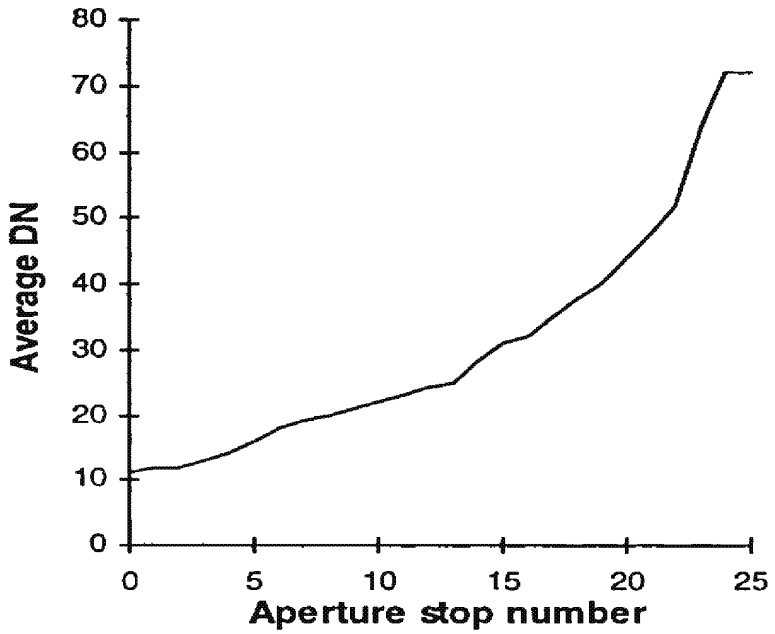


Figure 2. System response in DN for blue band versus aperture stop number in the laboratory.

of the relationships, $r^2 = 0.98$ for each curve, indicating that the MAVS aperture opening is circular (Edirisinghe 1997).

A constant shift (increment or decrement) in d between any two consecutive aperture openings is calculated by dividing the difference between the fully open aperture diameter $d = 8.6$ mm by the number of available openings (24). This gives the shift value between any two apertures as $8.6/24 = 0.358$ mm. This shift is used to calculate the corresponding d for each of the 24 aperture openings, simply by multiplying with the corresponding aperture opening number. Using equation (1) with calculated d and $l = 12$ mm, an f/number is assigned to each aperture opening starting from the largest $f/1.4$ to the smallest $f/33.3$.

For a given constant illumination level, the following relationship holds between two images acquired with different MAVS apertures:

$$\frac{(DN_i - DC)}{(DN_j - DC)} = \left(\frac{n_j}{n_i}\right)^2 \tag{3}$$

where DN is the system response, i and j represent the aperture stop number from 1 to 24 and n is the corresponding f/number for each i and j. This yields

$$(DN_j - DC) = (DN_i - DC) \times \left(\frac{n_i}{n_j}\right)^2 \tag{4}$$

4. Fundamental characteristics of the MAVS

The fundamental characteristics of imaging systems include dynamic range, noise, dark current, radiometric precision, system response linearity and spatial resolution. These characteristics represent the response of the system as whole rather than the manufacturer's specifications for each component of that system or for each camera alone.

Knowledge of these characteristics is required for the MAVS radiometric calibration. The evaluation of the MAVS characteristics are conducted (Edirisinghe 1997) according to established methods of performance assessment for CCD devices

SPECTRAL_0000677

Downloaded By: [University of California, Los Angeles] At: 04:17 29 July 2010

(Janesick 1987; Mackay 1992) and for an air-video system (King 1992). Except for the linearity parameters, table 1 summarises the result of this evaluation.

The CCD sensor response is generally linear to incident radiation (Janesick *et al.* 1987, Mackay 1992). When CCD sensors are connected to the video system components, such as the display, and frame grabber board, their linear response is subject to degradation. The effect of this for the MAVS is investigated in §5.1.

5. Radiometric calibration of the MAVS

In general, the radiometric calibration of an imaging sensor involves the establishment of the relationship between the detector output and the input radiation intensity, so that data values may meaningfuly be compared from one image to another or from image to ground target characteristics. The radiometric calibration of the MAVS is conducted using the empirical line method (Farrand *et al.* 1994). This involves the production of system response curves either of the form DN versus reflectance or DN versus radiance. Reflectance values refer to the Bi-directional Reflectance Factor (BRF) of a target as measured by referencing to pressed halon powder as a near ideal reflector. The calibration allows the DN recorded in a band (i) of the MAVS with a given aperture to be related to the spectral radiance (R_i) for that band at the sensor, by the linear relationship:

$$DN_i = K_i R_i + F_i \tag{5}$$

where $i = 1$ to 4 is the band number, K_i is the slope and F_i is the offset of the linear relationship. R_i represents the target radiance given in watts per square meter per micro-meter per steradian ($\mathrm{W\,m^{-2}\,\mu m^{-1}\,sr^{-1}}$) as measured by a calibrated hand-held radiometer, an Analytical Spectral Devices' Personal Spectrometer (PSII).

The offset and the slope of the calibration equation are commonly known as calibration coefficients. The calibration coefficients for each spectral band with a particular camera/aperture combination remain unique and constant depending on the consistency of the system response. For the sake of simplicity, the general form of the calibration equation, given above for all four bands, can be rewritten without subscripts to represent a single spectral band as follows:

$$DN = K \times R + F \tag{6}$$

The result of the MAVS system radiometric calibration is a file containing the coefficients F and K belonging to all the operational apertures for each camera band.

5.1. *Linearity of the system response in the laboratory*

The MAVS response curves of the form of equation (6) give important information on the degree of linearity of the system. Response curves derived under controlled environmental conditions in the Laboratory are useful for studying the system behaviour.

5.1.1. *Method of the experiment*

The experimental arrangement in the laboratory dark-room made use of a variable intensity light source consisting of two 3 kW halogen lamps with a stability of $\pm$ 9% overall. The lamps were projected onto a vertical white screen, to produce 17 different illumination levels. A diffusing glass screen was placed immediately in front of the camera array to produce uniform irradiance levels at the cameras. The camera array was positioned horizontally, 4 m from the screen. The average DN values of the images were calculated from the middle portion of each image to

SPECTRAL_0000678

Downloaded By: [University of California, Los Angeles] At: 04:17 29 July 2010

minimise effect caused by spatial non-uniformity, such as vignetting (King 1992, Russ 1992). All experiments were conducted with 12 mm lenses fitted to the cameras.

The system response relationship in the form of DN versus radiance was obtained in the laboratory environment. The calibrated PSII, with a 7% radiometric precision was used to measure the radiance and reflectance of all targets used in the experiment. The PSII has a 10° FOV fore-optic and a wavelength range of 350–1100 nm over 512 channels. The PSII measurements were taken under the same illumination conditions as the video imagery, at right angles to the target and at the same distance. The reflectance values, relative to a white halon reference, were directly acquired from the PSII, and were later converted to absolute radiance values in $W\,m^{-2}\,\mu m^{-1}\,sr^{-1}$ as described in the manufacture's manual. Images were collected for different aperture settings with each camera/filter combination under different light intensity levels. The results of these laboratory experiments enabled the system response to be determined.

5.1.2. *Results*

Figure 3 shows the linearity of the MAVS laboratory-based response curves for the four spectral bands, plotted as DN against the relative light intensity. The results of the linear least square regression between these two data sets produced a regression coefficient (r^2) of 0.99 and a residual standard error in the video response of 3–5 DN. This demonstrates that the additional step of digitisation and the attachment of other electronic components to the CCD sensors did not affect the linear form of the response curve. The results indicate that the system as a whole responds in highly linear manner to the incident light flux in the laboratory environment.

Table 2 shows the results of application of linear least squares regression analysis to the laboratory data sets of DN and radiance, for the four MAVS spectral bands. These laboratory-based MAVS calibration coefficients, in conjunction with equation (5), characterise the linear response of the system. The high r^2 values (=0.99) in this table indicates the high degree of linearity of the MAVS response in each of the four bands.

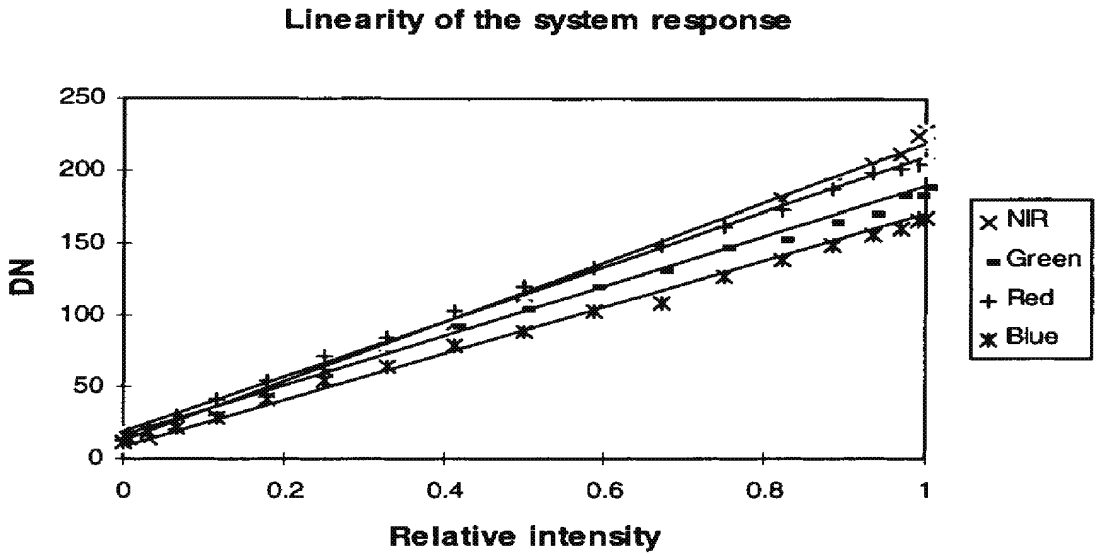


Figure 3. System response versus relative intensity for the four MAVS bands with aperture $f/1.4$ (laboratory results).

Downloaded By: [University of California, Los Angeles] At: 04:17 29 July 2010

SPECTRAL_0000679

Table 2. Laboratory-based results of the MAVS calibration statistics with aperture $f/1.4$ for $DN \sim R$ ($W m^{-2} sr^{-1} \mu m^{-1}$).

Band	Offset (DN)	Std error offset (DN)	Slope ($DN\ sr\ m^2\ \mu m\ W^{-1}$)	Std error slope ($DN\ sr\ m^2\ \mu m\ W^{-1}$)	Residual std. error (DN)	Coefficient of the regression r^2
Blue	12.74	1.41	6.086	0.091	3.62	0.99
Green	14.80	2.10	2.123	0.044	3.60	0.99
Red	16.90	3.10	2.152	0.058	5.30	0.99
NIR	10.11	1.55	1.204	0.016	3.98	0.99

5.2. *Field calibration*

There has been little success at calibrating airborne video data using response curves derived in the laboratory, due to the fact that the illumination conditions and the apertures differ markedly in the two situations (King 1992). However Vane *et al.* (1993) have calibrated the AVIRIS in the laboratory to within 90% of their in-flight calibration results. In terms of the illumination and operational apertures, for the MAVS, the field calibration conditions are much closer to the airborne situations than those in the laboratory environment. Based on these facts it had been decided to investigate the use of the field-based calibration curves for airborne video interpretation. As a result, the field-based MAVS response curves were obtained and analysed to determine their linearity characteristics.

5.2.1. *Method of the experiment*

A field calibration experiment was conducted using the normal blue-sky conditions. As the sensor and the target in the field were exposed to the same atmospheric conditions and illumination levels, a direct comparison between the video data and the hand-held radiometer reflectance data is possible, without the need for an atmospheric model to correct for the effects of the atmosphere. The PSII was used to measure the reflectance and radiance of all targets used in the calibration process. Linear calibration curves of the form of equation (6) were determined for each camera/aperture combination and for each spectral band.

A standardized grey scale was used for the field calibration experiment. Five polyester sheets, with different shades ranging from very dark green (almost black) to white, were selected as field calibration targets. These grey scale sheets produced 7–90% BRF values relative to pressed halon powder and were sufficiently rough and non-specular reflective, to be considered as having near Lambertian reflectance characteristics. All of the sheets were uniform in reflectance with less than 1% variation within the spectral resolution of the MAVS. The size of the target samples relative to pixel size, and their radiometric brightness range, are important factors. The targets were large enough to fully cover the MAVS camera FOV. The measured BRF, assuming nadir observations with the PSII, of the grey scale polyester sheets for each camera band is given in table 3.

The CSU cherry picker, anchored in an open grass area with minimum obstacles around, was used for the field calibration experiment. The MAVS was placed in the bucket of the cherry picker and the camera array fixed to a specially constructed steel frame, which in turn was bolted onto the bottom of the bucket.

The target polyester sheets were placed under the cherry picker at a distance of 4–5 m. Special care was taken to ensure that the vertical axis of the camera array

Downloaded By: [University of California, Los Angeles] At: 04:17 29 July 2010

SPECTRAL_0000680

Table 3. Measured BRF of the polyester sheet grey scale calibration targets with normal incidence.

Band	Target-1	Target-2	Target-3	Target-4	Target-5
Blue	0.91	0.61	0.51	0.35	0.09
Green	0.91	0.64	0.53	0.34	0.08
Red	0.90	0.58	0.50	0.34	0.07
NIR	0.90	0.57	0.50	0.33	0.11

was at right angles to the target sheet. A number of images were acquired for each target, with different apertures and for two heights. As in the laboratory experiment, all field experiments were conducted with 12 mm lenses fitted to the cameras. The calibrated PSII, with a 10° FOV, was again used to measure the radiance and reflectance of all targets used in this calibration experiment.

5.2.2. *Results*

Table 4 shows the calibration coefficients resulting from the linear regression analysis between DN and corresponding radiance values. The MAVS response is again demonstrated to be a highly linear ($r^2 = 0.99$).

5.3. *Radiance-based MAVS calibration curves*

Lambert's law of irradiation (illumination) states that the solar irradiation in the field varies with the solar zenith angle, and hence varies with the time of day. Lambert's law of radiation also applies to the reflected radiance from the target surface (Jenkins and White 1957). In the case of the MAVS, the sensor observation angle is fixed at 0° to the nadir at all times. Hence only the law of irradiation is effective in this situation. Therefore, the derived field-based calibration curves given below in equation (16), in the form of DN versus reflectance (BRF), are valid only for images obtained with the Sun at the particular zenith angle at which the calibration experiment was conducted. This conclusion is based on the assumption that our calibration target surfaces are sufficiently flat and Lambertian and are unaffected by azimuthal variations of the incoming solar irradiance. The shape of the radiance-based calibration curve indicates the intrinsic system response, with given camera/aperture combination, to incoming radiation. Both DN and radiance (R) depend only on the total number of photons received, respectively, by the MAVS sensor and the PSII. Hence, under identical illumination conditions, both instruments should respond in a related and absolute way to the incoming radiation. As both the measuring instruments are under the same radiation influence, the two data sets

Table 4. Field-based results of the MAVS calibration statistics with aperture $f/1.9$ ($DN \sim R$ in $\mathrm{W\,m^{-2}\,sr^{-1}\,\mu m^{-1}}$).

Band	Offset (DN)	Std error offset (DN)	Slope ($DN\,\mathrm{sr\,m^2\,\mu m\,W^{-1}}$)	Std. error slope ($DN\,\mathrm{sr\,m^2\,\mu m\,W^{-1}}$)	Residual std. error (DN)	Coefficient of the regression r^2
Blue	9.90	3.12	1.126	0.030	3.79	0.99
Green	13.54	2.46	0.598	0.020	2.90	0.99
Red	14.10	1.57	0.673	0.020	1.92	0.99
NIR	12.37	1.00	0.654	0.013	1.14	0.99

Downloaded By: [University of California, Los Angeles] At: 04:17 29 July 2010

SPECTRAL_0000681

should be consistent with each other. Hence the characteristics of the response curve in terms of F and K are unique, reproducible and constant for each MAVS spectral band.

In the field calibration trial, DN and R data were recorded at the same height under identical atmospheric, environment and illumination conditions for each aperture. In addition to the standard target values, the dark current DN value of each band has also been included as an additional control point representing a zero radiance target. The inclusion of this band specific dark current control point guarantees the consistency of the offset for every calibration curve, which belongs to different apertures, including the situation where the aperture is completely closed. The slope and offset and associated statistics of the resultant field calibration curves are given in table 4.

5.4. *Reflectance-based MAVS calibration curves*

The radiance-based calibration curve, equation (6), can be rewritten in terms of target BRF (I) and global irradiance (S) to give a reflectance-based calibration curve as in equation (9). The offset and the slope of a reflectance-based calibration curve can be determined theoretically, given knowledge of the corresponding radiance calibration curve. Experience has shown that the measurement of I is more effective and efficient than the measurement of R, in either the field or the laboratory. This is due to the fact that I is measured as a relative ratio of two PSII responses whereas R is an absolute quantity and can only be calculated with the aid of pre-existing PSII calibration files. With time, deterioration of the PSII instrument may cause the calibration files, supplied by the manufacturer, to be incompatible with the instrument's current operational characteristics. Calibration in terms of I removes this reliance on the accuracy of the PSII calibration files. Another advantage of calibrating the MAVS to I rather than R is that most agronomic variables of interest are generally correlated with I to remove the effects of illumination variations.

Consider a situation in the field where a calibration target from table 2 is placed horizontally on the ground under clear sky and in direct sun illumination. The reflected R in the vertically upward direction from the target surface is measured in $\mathrm{W\,m^{-2}\,\mu m^{-1}\,sr^{-1}}$ using the PSII. This instrument is placed directly above the target with observation angle at 0° to vertical direction, at a height of 2 m. I is the BRF of the target, measured relative to pressed halon powder acting as a near ideal Lambertian reflector. I is obtained directly from the PSII using a special BRF mode and recorded accordingly. Most remotely sensed target surfaces are known to have quasi-Lambertian reflectance characteristics at most observer angles and assessed to be close to ideal Lambertian reflectors at small solar zenith angles (Slater 1980, Kaufman 1989, Rees 1990) with nadir observations.

For a perfect Lambertian reflector approximated by pressed halon powder, the diffuse albedo is equal to one. The diffuse albedo is the ratio of total scattered radiant energy from a target to the total incident solar energy. In general, the incident solar energy is also called incident flux and the irradiance is the incident flux density. It can be shown that the Bi-directional Reflectance Distribution Function or BRDF (L) of a target in a given direction is the product of the BRF (I) of the target and the BRDF of the pressed halon powder ($L(hl)$) for the same direction and illumination conditions. Therefore,

$$L = IL(hl) \tag{7}$$

Further, $L(hl)$ can shown to be constant and always less than one.

SPECTRAL_0000682

Downloaded By: [University of California, Los Angeles] At: 04:17 29 July 2010

Using Lambert's cosine law, R can be expressed as a function of either BRF or BRDF. Choosing BRDF gives

$$R = LS\cos\phi \tag{8}$$

where S is the global irradiance on the target and it is defined in equation (11) and ϕ is the observation angle. For the PSII measurements in the field, $\phi = 0$ and $\cos\phi = 1$. Substituting equation (6) into equation (8), and replacing L by I, gives

$$DN = KIL(hl)S + F \tag{9}$$

where $I = \dfrac{L}{L(hl)}$ and, again, $L(hl)$ is a constant representing the BRDF of the pressed halon powder. Since $L(hl) < 1$, then we can see that $I > L$.

It can also be shown for an ideal Lambertian surface (Rees 1990) that

$$L(hl) = \frac{1}{\pi} \tag{10}$$

S is a function of the extra terrestrial solar irradiance, the solar zenith angle (θ), the optical thickness (τ) of the atmosphere, down-welling diffused irradiance and environmental irradiance (Slater 1980, Iqbal 1983, Jackson and Slater 1986, Moran *et al.* 1992) and can be expressed as

$$S(\lambda) = [E(\lambda)e^{-\tau^{\sec\theta}}\cos\theta + S_{de}(\lambda)] \tag{11}$$

where $E(\lambda)$ is the extra terrestrial solar irradiance at top of the atmosphere, θ is the solar zenith angle at the time of the radiance measurement in the field and λ is the wavelength. $E(\lambda)$ is assumed to be a constant for a given day. However, it varies with seasonal changes of the sun–earth distance (Hill and Sturm 1991). Seasonally adjusted tabulated values of $E(\lambda)$ can be found in Iqbal (1983) and Neckel and Labs (1984). τ is the atmospheric optical thickness and is less than 1. S and $S(\lambda)$ represent the same quantity except the later explicitly indicates the wavelength dependence of S. $S_{de}(\lambda)$ is the sum of down-welling diffused irradiance $S_d(\lambda)$ and environmental irradiance $S_e(\lambda)$ at the target.

According to Lambert's law of illumination, the amount of direct solar irradiance on a horizontal target surface is given by $E(\lambda)e^{-\tau^{\sec\theta}}\cos\theta$, which is the first part in the right-hand side of equation (11). Provided θ is not too large (less than 30°), S is not very sensitive to changes in θ. For a typically clear atmosphere, $\tau = 0.3$ in the 550 nm (green) wavelength band (Rees 1990) and for variations in $\theta < 30°$, the variation in direct solar irradiance on the target surface calculated to be less than 4%. This, according to equation (11), amounts to even less variation of S, provided $S_{de}(\lambda) > 0$. However, for θ up to 60°, S may vary by as much as 26%.

Substituting equation (11) into equation (9) gives

$$DN = \frac{1}{\pi}KI[E(\lambda)e^{-\tau^{\sec\theta}}\cos\theta + S_{de}(\lambda)] + F \tag{12}$$

By combining all the constants together into one constant (G), equation (12) may be rewritten as follows:

$$DN = G\left[e^{-\tau^{\sec\theta}}\cos\theta + \frac{S_{de}(\lambda)}{E(\lambda)}\right]I + F \tag{13}$$

Downloaded By: [University of California, Los Angeles] At: 04:17 29 July 2010

SPECTRAL_0000683

where

$$G = \frac{1}{\pi} K E(\lambda) \tag{14}$$

The $G\left[e^{-\tau^{\sec\theta}}\cos\theta + \frac{S_{de}(\lambda)}{E(\lambda)}\right]$ term represents the new slope of the DN versus I equation. The $\cos\theta$ term models the variation of the solar illumination with changing incident angle. For $\theta < \pm 30°$, and clear atmospheric conditions with $\tau < 1$, $\tau\cos\theta \ll 1$, the exponential term $e^{-\tau^{\sec\theta}}$ can be expanded in terms of a Taylor polynomial as

$$e^{-\tau^{\sec\theta}} = 1 - \tau\sec\theta + \frac{(\tau\sec\theta)^2}{2} + \ldots \tag{15}$$

For small θ values, the 3rd term of this polynomial expansion can be neglected. In this case, the reflectance calibration equation (13) can be written as

$$DN = G\left[\cos\theta + \frac{S_{de}(\lambda)}{E(\lambda)} - \tau\right] I + F \tag{16}$$

Equation (16) presents the general form of the reflectance-based MAVS calibration equation. The dependence of the slope term on θ suggests that the reflectance-based calibration cannot be uniquely defined as in the case with the radiance-based calibration equation. It is interesting to note here that the offset remains unchanged regardless of whether the relationship takes the form DN versus I or the earlier form DN versus R. Therefore, θ and τ limit the use of the reflectance-based calibration curves to the time and date of air calibration trial.

During the field calibration experiment, reflectance values I and the corresponding DN values were recorded for known ground targets. As in the case with the radiance based calibration curves, an additional control point consisting of the dark current DN value and respective zero reflectance point are included in DN and reflectance data vectors. The slope and intercept for each camera/aperture combination is obtained from a linear regression of DN on I. Table 5 summarizes regression results for all four MAVS bands with aperture $f/1.9$ and for $\theta = 23.2°$.

The slope $G\left[\cos\theta + \frac{S_{de}(\lambda)}{E(\lambda)} - \tau\right]$ of the reflectance-based calibration equation given in table 5 is obtained statistically from the field-based data vectors of DN and I. The estimated field calibration curves represent the response of the MAVS in the field and should be identical to the response curves obtained in the air with identical

Table 5. Field based results of the MAVS calibration statistics with aperture $f/1.9$ ($DN \sim$ BRF or reflectance with $\theta = 23.2°$).

Band	Offset (DN)	Std. error offset (DN)	Slope (DN/BRF)	Std error slope (DN/BRF)	Residual std error (DN)	Coefficient of the regression r^2
Blue	9.90	3.08	633.44	14.96	3.74	0.99
Green	13.54	2.47	301.97	12.19	2.47	0.99
Red	14.12	1.58	286.64	7.85	1.93	0.99
NIR	12.37	1.00	247.94	4.89	1.14	0.99

SPECTRAL_0000684

Downloaded By: [University of California, Los Angeles] At: 04:17 29 July 2010

acquisition conditions. The MAVS in-flight calibration curves derived from a subsequent experiment confirmed this fact (Edirisinghe 1997). Once the slope is estimated using the regression on the field or air-based data, G can be calculated as

$$G = \frac{slope}{\cos\theta + e - \tau} \tag{17}$$

where

$$e = \frac{S_{de}(\lambda)}{E(\lambda)} \tag{18}$$

According to Iqbal (1983), Moran *et al.* (1992) and Vermote *et al.* (1994), $0 < e < 0.25$.

It is important to note here that G and F are unique for any calibration curve and can be directly used for routine airborne missions with the relevant θ and assuming there is no significant change of τ and e. The limitation of fixed τ and e is not critical, since most operational flights are conducted under very clear skies. Once G and F are properly estimated for a particular band and camera/aperture combination, they are stored in a computer file to be used in future airborne missions.

5.5. *Calculation of atmospheric optical thickness using field-based reflectance calibration model*

Equation (17) can be used to calculate τ using known values of $E(\lambda)$, $S_{de}(\lambda)$, θ, slope, G and K. In the MAVS green band, the resulting τ shows an agreement to better than 95% with the value of atmospheric optical thickness (0.3) given by Rees (1990) and Vermote *et al.* (1994) for typically clear atmospheric conditions. A better than 96% agreement is obtained between the reflectance model calculated τ and the 6S (Vermote *et al.* 1994) simulated value of atmospheric optical thickness with *in situ* parameters (Edirisinghe 1997). These results indicate the accuracy of the model presented in §5.2 and the field-based MAVS calibration procedure.

5.6. *Retrieval of apparent target BRF at the airborne sensor by using the field-based radiance calibration coefficients*

The radiance-based offset (F) and slope (K) values given in table 4 can be used to estimate the apparent target reflectance in the form of BRF ($I(h)$) at the altitude of the MAVS sensor as follows. For any θ where $0° < \theta < 30°$,

$$DN = F + GI(h)(\cos\theta + e - \tau) \tag{19}$$

where $G = \frac{1}{\pi} K E(\lambda)$ from equation (14). Therefore,

$$I(h) = \frac{DN - F}{G(\cos\theta + e - \tau)} \tag{20}$$

where DN is the video image data value recorded in-flight with aperture $f/1.9$ and where τ and θ are known parameters for the air trial. When θ and τ are both small, the calculation of $I(h)$ can be simplified further by replacing $(\cos\theta + e - \tau)$ by $\cos\theta$. These conditions can be met if the airborne mission is conducted around midday under typical clear sky conditions. In this case it can be written

$$I(h) = \frac{DN - F}{G\cos\theta} \tag{21}$$

Downloaded By: [University of California, Los Angeles] At: 04:17 29 July 2010

SPECTRAL_0000685

Equation (21) is useful for calculating the apparent reflectance at altitude $I(h)$ of the MAVS targets using known values of G and F, for each spectral band, in routine operations. For each target, the value of DN is obtained from airborne imagery.

6. Conclusion

The CSU MAVS has been operational since 1992 and is currently being used for agricultural and environment monitoring. An accurate calibration procedure has been developed to enable the MAVS to be used for quantitative reflectance measurements.

The fundamental system characteristics of the MAVS indicate a highly linear system with very low system noise levels and a high signal-to-noise ratio level (Edirisinghe 1997). These MAVS response characteristics both in the field and in the laboratory were shown to be remarkably consistent for the two very different illumination environments. This also confirmed the linearity of the system throughout the dynamic range in both environments.

The camera apertures have been calibrated in terms of *f*/number from *f*/33.3 to *f*/1.4. This enables the radiometric corrections for the MAVS images under different apertures to be carried out in a systematic way. It also allows for the selection of the optimum aperture for a given target field, taking account of the required contrast levels.

The system is radiometrically calibrated in the laboratory and in the field. The larger aperture stops used in the laboratory are unsuitable for field experiments, as these larger apertures generally cause the field video signal to be saturated. The relatively small aperture stops are also suitable for the in-flight environment.

A theoretical model has been developed to investigate the relative merits and limitations of radiance-based and reflectance-based radiometric calibration procedures. The model predictions revealed close agreement between the experimentally obtained offsets of radiance-based and reflectance-based calibration curves. However, in both cases the slope is dependent on the chosen aperture setting. The model highlights the importance of using the correct solar angle and therefore the correct time of day when conducting reflectance-based radiometric calibrations either in the field or in the air.

Using this model, a method has been devised to determine the apparent target reflectance or radiance at the altitude of the sensor, using field-based calibration coefficients. This method is based on the assumption that system response in the air remains unchanged. This premise is supported by the consistency of the system response between the field and laboratory environment. The method has proved useful in routine airborne monitoring applications and for comparisons of apparent reflectance or radiance derived using other similar systems and atmospheric radiative transfer models.

The radiometric calibration reflectance model, outlined in this paper, is used to calculate the atmospheric optical thickness (τ) over the field site. In the four MAVS spectral bands, the model-based τ values show an agreement to better than 96% with the corresponding values of τ simulated using the 6S radiative transfer code. This agreement provides an indirect conformation of the accuracy of the MAVS radiometric calibration procedures developed in this paper. The knowledge gained in this study has been used to support a more comprehensive in-flight radiometric calibration study that includes an analysis of atmospheric transmission effects on airborne video imagery (Edirisinghe 1997).

Downloaded By: [University of California, Los Angeles] At: 04:17 29 July 2010

SPECTRAL_0000686

Acknowledgments

The authors are grateful to the staff of the Spatial Analysis Unit for their continued support of this research.

References

EDIRISINGHE, A., 1997, Development of radiometric and geometric correction procedures for low cost airborne video image processing systems. PhD thesis, Faculty of Science and Agriculture, Charles Sturt University, Australia.

EVERITT, J. H., ESCOBAR, D. E., VILLARREAL, R., NORIEGA, J., and DAVIS, M. R., 1991, Airborne video systems for agricultural assessment. *Remote Sensing of Environment*, **35**, 231–242.

FARRAND, H. W., SINGER, B. R., and MERENYI, E., 1994, Retrieval of apparent surface reflectance from AVIRS data: a comparison of empirical line, radiative transfer, and spectral mixture methods. *Remote Sensing of Environment*, **47**, 311–321.

HILL, J., and STURM, B., 1991, Radiometric correction of multitemporal Thematic Mapper data for use in agricultural and land-cover classification and vegetation monitoring. *International Journal of Remote Sensing*, **12**, 1471–1491.

HOMER, C. G., EDWARDS, T. C., RAMSEY, R. D., and PRICE, K. P., 1993, Use of remote sensing method in modelling sagegrouse winter habitat. *Journal of Wildlife Management*, **57**(1), 78–84.

IQBAL, M., 1983, *An Introduction to Solar Radiation* (New York: Academic Press).

JACKSON, R. D., 1982, Canopy temperature and crop water stress. In *Advances in Irrigation*, edited by D. Hill (New York: Academic Press).

JACKSON, R. D., MORAN, M. S., SLATER, P. N., and BIGGAR, S. F., 1987, Field calibration of reflectance panels. *Remote Sensing of Environment*, **22**, 145–158.

JACKSON, R. D., and SLATER, P. N., 1986, Absolute calibration of field reflectance radiometers. *Photogrammetric Engineering and Remote Sensing*, **52**, 189–196.

JANESICK, J. R., ELLIOT, T., COLLINS, S., BLOUKE, M. M., and FREEMAN, J., 1987, Scientific charge-coupled devices. *Optical Engineering*, **26**, 692–714.

JENKINS, F. A., and WHITE, H. E., 1957, *Fundamentals Of Optics*, 3rd edn (New York: McGraw-Hill).

KAUFMAN, Y. J., 1989, The atmospheric effect on remote sensing and its corrections. In *Theory and Applications of Optical Remote Sensing*, edited by G. Asrar (New York: John Wiley), pp. 336–428.

KING, D., 1988, Development of a multispectral arial video system and its application in forest and land cover type analysis. PhD dissertation, Faculty of Forestry, University of Toronto, Canada.

KING, D., 1992, Evaluation of radiometric quality, statistical characteristics, and spatial resolution of multispectral videography. *The Society for Imaging Science and Technology*, **36**, 394–404.

King, D., 1995, Airborne multispectral digital camera and video sensors: a critical review of system design and application. *Canadian Journal of Remote Sensing* (Special Issue on Airborne Remote Sensing), **21**, 245–273.

KING, D., and VLCEK, J., 1990, Development of a multispectral arial video system and its application in forestry. *Canadian Journal of Remote Sensing*, **16**, 15–22.

LOUIS, J., LAMB, D., MCKENZIE, G., CHAPMAN, G., EDIRISINGHE, A., MCCLOUD, I., and PRATLEY, J., 1995, Operational Use and Calibration of Airborne Video Imagery for Agricultural and Environmental Land Management Applications. *Proceedings of the 15th Biennial Workshop on Colour Photography and Air Videography, Terre Haute, Indiana, USA*, pp. 326–333.

MACKAY, C. D., 1992, The role of charge coupled devices in low light level imaging. Technical guide, Astromed, Cambridge Science Park, Milton Road, Cambridge, CB4 4GS, England, UK.

MAUSEL, P., EVERITT, J. H., and KING, D. J., 1992, Airborne videography: current status and future perspectives. *Photogrammetric Engineering and Remote Sensing*, **58**, 1189–1195.

MCKENZIE, G., DARE-EDWARDS, A., LOUIS, J., VAN DER RIJT, V., and PRATLEY J., 1992,

Downloaded By: [University of California, Los Angeles] At: 04:17 29 July 2010

SPECTRAL_0000687

Application of low-cost airborne video technology to Australian agriculture. *6th Australasian Remote Sensing Conference, Wellington, New Zealand*, pp. 293–297.

MORAN, M. S., JACKSON, R. D., SLATER, P. N., and TEILLET, P. M., 1992, Evaluation of simplified procedures for retrieval of land surface reflectance factors from satellite sensor output. *Remote Sensing of Environment*, **41**, 169–184.

NEALE, C. M. U., and CROWTHER, B. G., 1994, An airborne multispectral video/radiometer remote sensing system: development and calibration. *Remote Sensing of Environment*, **49**, 187–194.

NECKEL, H., and LABS, D., 1984, The solar radiation between 3300 and 12 500 A. *Solar Physics*, **90**, 205–258.

NIXON, P. R., ESCOBAR, D. E., and BOWEN, R. L., 1987, A multispectral false color video imaging system for remote sensing applications. *Proceedings of the 11th Biennial Workshop on Color Aerial Photography and Videography in the Plant Sciences*, American Society of Photogrammetry and Remote Sensing, Falls Church, Virginia, pp. 295–305.

NIXON, P. R., ESCOBAR, D. E., and MENGES, R. M., 1985, Use of a multiband video system for quick assessment of vegetal condition and discrimination of plant species. *Remote Sensing of Environment*, **17**, 203–208.

PICKUP, G., BASTIN, G. N., CHEWINGS, V. H., and PEARCE, G., 1995, Correction and classification procedures for assessing rangeland vegetation cover with airborne video data. *Proceedings of the 15th Biennial Workshop on Colour Photography and Air Videography, Terre Haute, Indiana, USA*, pp. 305–314.

REES, W. G., 1990, *Topics in Remote Sensing—1: Physical Principles of Remote Sensing* (Cambridge: Cambridge University Press).

RUSS, J. C., 1992, *The Image Processing Handbook* (Boca Raton, Florida: CRC Press).

SLATER, P. N., 1980, *Remote Sensing: Optics and Optical Systems* (Addison-Wesley).

VANE, G., GREEN, R. O., CHRIEN, T. G., ENMARK, H. T., HANSEN, E. G., and POTER, W. M., 1993, The Airborne Visible/Infrared Imaging Spectrometer (AVIRIS). *Remote Sensing of Environment*, **44**, 127–143.

VERMOTE, E., TANRE, D., DEUZE, J. L., HERMAN, M., and MORCRETTE, J. J., 1994, Second simulation of the satellite signal in the solar spectrum (6S). User Guide, Version 0, Laboratoire d'Optique Atmospherique, Universite des Sciences et Techniques de Lille, 59655 Villeneuve d'Ascq Cedex, France.

Downloaded By: [University of California, Los Angeles] At: 04:17 29 July 2010

SPECTRAL_0000688

Neoplasia • Vol. 2, No. 6, 2000, pp. 491–495

www.nature.com/neo

Rapid and Quantitative Assessment of Cancer Treatment Response Using *In Vivo* Bioluminescence Imaging[1]

Alnawaz Rehemtulla, Lauren D. Stegman†‡, Shaun J. Cardozo†, Sheila Gupta†, Daniel E. Hall†, Christopher H. Contag§ and Brian D. Ross†‡*

The Center for Molecular Imaging and the Department of *Radiation Oncology, †Radiology, ‡Biological Chemistry, University of Michigan Medical School, 1150 West Medical Center Drive, Medical Sciences Research Building III, Room 9303, Ann Arbor, MI 48109-0648; §Department of Pediatrics, Stanford University School of Medicine, Stanford, CA 94305-5208

Abstract

Current assessment of orthotopic tumor models in animals utilizes survival as the primary therapeutic end point. *In vivo* bioluminescence imaging (BLI) is a sensitive imaging modality that is rapid and accessible, and may comprise an ideal tool for evaluating antineoplastic therapies [1]. Using human tumor cell lines constitutively expressing luciferase, the kinetics of tumor growth and response to therapy have been assessed in intraperitoneal [2], subcutaneous, and intravascular [3] cancer models. However, use of this approach for evaluating orthotopic tumor models has not been demonstrated. In this report, the ability of BLI to noninvasively quantitate the growth and therapeutic-induced cell kill of orthotopic rat brain tumors derived from 9L gliosarcoma cells genetically engineered to stably express firefly luciferase (9L^{Luc}) was investigated. Intracerebral tumor burden was monitored over time by quantitation of photon emission and tumor volume using a cryogenically cooled CCD camera and magnetic resonance imaging (MRI), respectively. There was excellent correlation (r=0.91) between detected photons and tumor volume. A quantitative comparison of tumor cell kill determined from serial MRI volume measurements and BLI photon counts following 1,3-bis(2-chloroethyl)-1-nitrosourea (BCNU) treatment revealed that both imaging modalities yielded statistically similar cell kill values (P=.951). These results provide direct validation of BLI imaging as a powerful and quantitative tool for the assessment of antineoplastic therapies in living animals. *Neoplasia* (2000) **2,** 491–495.

Keywords: luciferase, bioluminescence, *in vivo* imaging, cell kill, therapeutic response.

Introduction

Rodent tumor models have become indispensable in the discovery and assessment of new anticancer therapies [4]. Many preclinical *in vivo* studies of experimental therapeutics utilize rapidly growing transplantable mouse or human tumor cell lines injected subcutaneously in syngeneic or immunodeficient rodents, to facilitate quantitation of tumor growth and treatment response using caliper measurements of tumor volume. However, these studies may not be representative of tumor biology as the phenotypes of neoplastic cells can be modulated by interaction with surrounding normal tissue, and both treatment responses and therapy-induced toxicities can vary at different organ sites [5–8]. Orthotopic tumor models are arguably more appropriate models of human cancer because they may reproduce some of the organ-specific properties of human tumor growth. However, quantitative measurements of therapeutic-induced changes in tumor growth in orthotopic models are more difficult to obtain, usually requiring that large numbers of animals be killed at multiple time points to overcome variability between animals. These facts underscore the need for high-throughput surrogate markers for evaluating therapeutic response in preclinical studies of new therapeutic strategies.

Materials and Methods

Production of 9L^{luc} Cell Line

The luciferase expression plasmid pGL3 (Promega, Madison, WI) was cotransfected into 9L cells in the presence of an expression vector for neomycin resistance (*neo*^{R}) at a ratio of 10:1. The resulting G418^R colonies were isolated and cultured independently and the best expressing lines were identified based on the level of bioluminescent activity in the presence of luciferin in living cells. A highly bioluminescent clone (9L^{Luc}) that demonstrated *in vivo* growth characteristics similar to the parental 9L cell line was selected for further studies.

Animal Model

Rat 9L^{Luc} cells were grown as monolayers in minimal essential medium (MEM) supplemented with 10% fetal calf

Address all correspondence to: Dr. Brian D. Ross PhD, University of Michigan, Center for Molecular Imaging, 1150 West Medical Center Drive, 9303 Medical Science Research Building III, Ann Arbor, MI 48109-0648. E-mail: bdross@umich.edu

[1]Support for this work was provided by the National Cancer Institute (R24-CA83099, P20-CA86442, NOI-C0-07013).

Received 3 November 2000; Accepted 17 November 2000.

Copyright © 2000 Nature America, Inc. All rights reserved 1522-8002/00/$15.00

SPECTRAL_0000689

serum, 100 IU/ml penicillin and 100 mg/ml streptomycin, and 2 mM L-glutamine at 37°C in a 95/5% air/CO_2 atmosphere. Intracerebral $9L^{Luc}$ tumors were induced in male Fischer 344 rats weighing between 125 and 135 g by implantation of 10^5 cells in 5 μl serum-free MEM in the right forebrain at a depth of 3 mm through a 1-mm burr hole. The surgical field was cleaned with 70% ethanol and the burr hole was filled with bone wax to prevent extracerebral extension of the tumor. For chemotherapeutic studies, 1,3-bis(2-chloroethyl)-1-nitrosourea (BCNU) was dissolved in absolute ethanol and diluted in saline (10% final ethanol) at the time of treatment and administered by a single i.p. injection at a dose of $1.0\times LD_{10}$ (n=5) corresponding to 13.3 mg BCNU/kg body weight. Control $9L^{Luc}$ animals (n=5) received an i.p. injection of vehicle (10% ethanol in saline) only.

Magnetic Resonance Imaging

Magnetic resonance imaging (MRI) was performed every other day beginning 10 days after tumor cell implantation on a Varian Unity Inova system equipped with a 7.0-T, 18.3-cm horizontal bore magnet (Oxford Instruments Inc., Oxfordshire, UK) and a quadrature rat head coil. Rats were anesthetized with a 2% isofluorane/air mixture and maintained at 37°C inside the magnet using a heated, thermostated circulating water bath. A single-slice sagittal gradient–echo sequence was used to confirm proper animal positioning and to prescribe subsequent acquisitions. T_2-weighted transverse brain images were obtained using a spin–echo sequence with the following parameters: 3.0-second repetition time, 60-msec echo time, field of view=30×30 mm using a 128×128 matrix, slice thickness=1 mm, number of slices=15 with no gap, and one

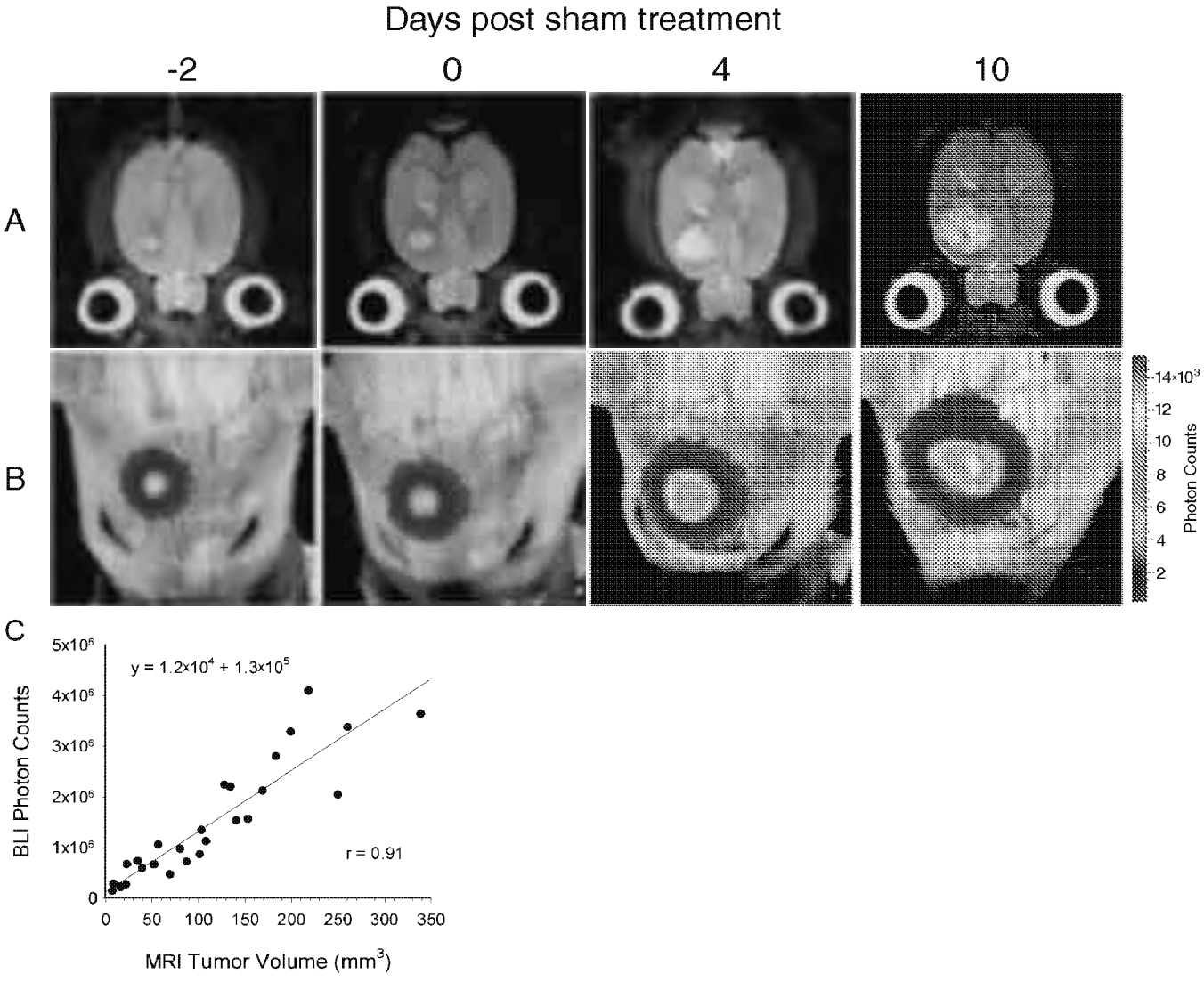


Figure 1. *Kinetics of intracranial glioma growth in a representative animal. $9L^{Luc}$ cells were implanted intracerebrally at 16 days before sham treatment with ethanol vehicle and tumor progression was monitored with MRI (A) and BLI (B). The days, post–sham treatment, on which the images were obtained are indicated at the top. The MR images are T_2-weighted and are of a representative slice from the multislice dataset. The scale to the right of the BL images describes the color map for the luminescent signal. Correlation of tumor volume with in vivo photon emission is shown where tumor volume was measured from T_2-weighted MR images and plotted against total measured photon counts (C). The relationship between the two measurements was defined by regression analysis (r=0.91).*

SPECTRAL_0000690

excitation. Tumor volumes were derived from multislice MR data sets as previously described [9]. In brief, the tumor boundary visualized in each slice was defined as a region-of-interest (ROI) using image-processing software (Advanced Visual Systems, Waltham, MA). The sum of the number of tumor-containing pixels in each slice was then multiplied by the MR voxel volume to obtain the total tumor volume. Voxel volume was calculated as:

$$\text{Voxel volume} = (\text{slice thickness}) \times \left[\frac{(\text{field of view})^2}{(\text{matrix})^2}\right].$$

In Vivo Bioluminescence Imaging

In vivo bioluminescence imaging (BLI) was conducted on a cryogenically cooled IVIS™ system (Xenogen Corp., Alameda, CA) coupled to a data-acquisition PC running LivingImage™ software (Xenogen Corp.) as an overlay on IGOR (Wavemetrics, Seattle, WA) under Windows 98. This system has been recently developed by Xenogen Corporation to provide outstanding signal-to-noise images of luciferase signals emerging from within living animals. Before imaging, animals were anesthetized in a plastic chamber filled with 2% isofluorane/air mixture and 150 mg/ml of luciferin (potassium salt, Xenogen Corp.) in normal saline was injected (i.p.) at a dose of 150 mg/kg body weight. This dose and route of administration has been previously shown to be optimal for studies in rodents when images were acquired between 10 and 20 minutes post-luciferin administration [10]. During image acquisition, isofluorane anesthesia was maintained using a nose cone delivery system and animal body temperature was regulated using a digitally thermostated bed integrated within the IVIS system. A gray scale body surface image was collected in the chamber under dim illumination, followed by acquisition and overlay of the pseudocolor image representing the spatial distribution of detected photon counts emerging from active luciferase within the animal. An integration time of 1 minute was used for luminescent image acquisition. Signal intensity was quanti-

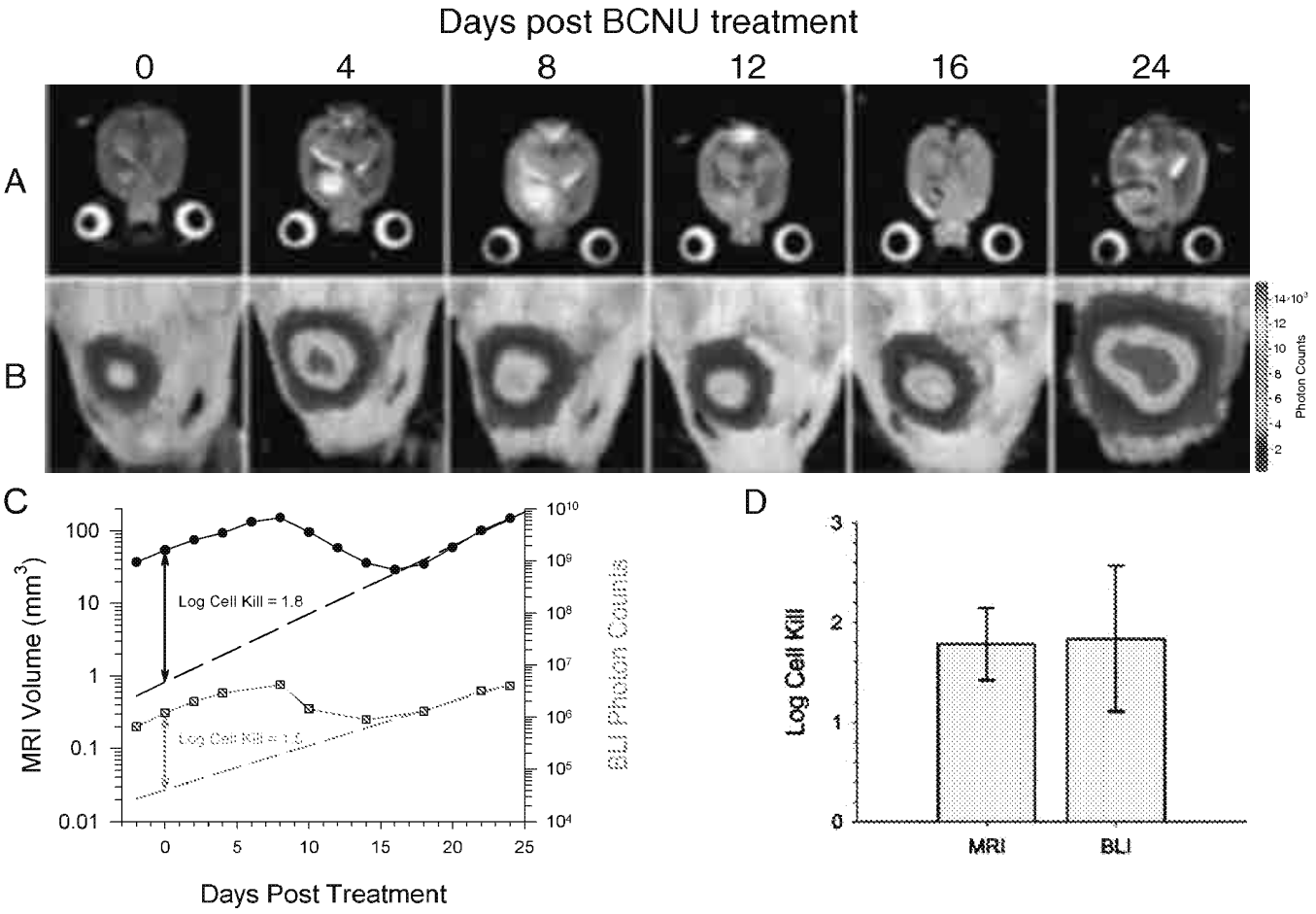


Figure 2. *Temporal analysis of the response of a 9L^{Luc} tumor to BCNU chemotherapy. Tumor cells were implanted 16 days before treatment. Tumor volume was monitored with T_2-weighted MRI (A) and intratumoral luciferase activity was monitored with BLI (B). The days post-BCNU therapy on which the images were obtained are indicated at the top. The scale to the right of the BL images describes the color map for the photon count. Quantitative analysis of tumor progression and response to BCNU chemotherapy (C). Tumor volumes (●) and total tumor photon emission (■) obtained by T_2-weighted MRI and BLI, respectively, are plotted versus days post-BCNU treatment. The dashed lines are the regression fits of the exponential tumor repopulation following therapy. The solid vertical lines denote the apparent tumor-volume and photon-production losses elicited by BCNU on the day of treatment from which log cell kill values were calculated as previously described [9]. Comparison of log cell kill values determined from MRI and BLI measurements (D). Log cell kill elicited by BCNU chemotherapy was calculated using MRI (1.78±0.36) and BLI (1.84±0.73). Data are represented as mean±SEM for each animal (n=5). There was no statistically significant difference between the log kills calculated using the MRI and BLI data (P=.951).*

fied as the sum of all detected photon counts within a region of interest prescribed over the rat head using the LivingImage™ software package.

Tumor Cell Kill Calculations and Statistical Analysis

Quantitation of tumor cell kill from imaging data for each animal was accomplished as previously described [9]. In brief, $\log(\text{cell kill}) = \log_{10}[V_{pre}/V_{post}]$ where V represents the tumor volume or summed photon counts from MRI and BLI measurements, respectively. Statistical comparisons between log cell kill values obtained by MRI and BLI were made using unpaired Student's t test. Differences in animal survival rates were determined by Kaplan-Meier Analysis. A probability value of $P<.05$ was considered significant.

Results

The ability of BLI to quantitate *in vivo* tumor burden in an orthotopic animal model was investigated through *in vivo* measurements of both the tumor volume and photon emission from the same group of animals over time. A time series of transverse T_2-weighted MR images of a representative tumor-bearing rat brain demonstrates the growth of a $9L^{Luc}$ tumor, which appears as a hyperintense lesion in the right forebrain (Figure 1*A*). Corresponding BL images of the same animal, displayed as a pseudocolor image overlaid on a gray scale reference image of the rat head, reveal an intense signal arising from the tumor (Figure 1*B*). Scatter of tumor-emitted photons as they pass through the brain, bone, and skin likely account for the BL pseudocolor image exceeding the tumor dimensions as measured by MRI. Over time, the bioluminescence signal from the tumor increased in both apparent diameter and intensity as the tumor volume, as measured by MRI, increased. The detected luminescent signal at each time point was quantified and plotted against the corresponding MRI-determined tumor volume for each of the five sham-treated animals. Linear regression analysis revealed an excellent correlation ($r=0.91$) between the measurement of intracerebral tumor burden using these two imaging modalities (Figure 1*C*).

Quantitation of therapeutic efficacy was accomplished on a separate group of rats with intracerebral $9L^{Luc}$ tumors, which were treated with the chemotherapeutic agent BCNU. MR and BL images of a representative animal from this experiment are shown in Figure 2*A* and *B*, respectively. The first images were acquired within 2 hours of BCNU administration followed by repeat scans acquired at selected posttreatment intervals. The MR images revealed that the tumor continued to expand up to 8 days after treatment followed by regression and subsequent regrowth. The corresponding BL images revealed parallel changes in detected photon emission over this same time period. Similar results were observed for the other four animals in the BCNU-treatment group. A plot of tumor volume and detected photon counts versus time for this animal is shown in Figure 2*C* along with an exponential fit of the tumor regrowth data. Extrapolation of the tumor regrowth back to the time of treatment, allowed for quantitation of cell kill in each animal studied, as previously described [9]. Mean log cell kill values determined by MRI and BLI were 1.78±0.36 ($n=5$ animals) and 1.84±0.73 ($n=5$ animals), respectively (Figure 2*D*), indicating that these two independent imaging methods were statistically identical ($P=.951$). The BCNU-induced tumor cell kill resulted in a statistically significant increase ($P=.007$) in the survival of the treated animals (41.0±0.7 days) compared with the controls (25.2±7.2 days) as shown in Figure 3.

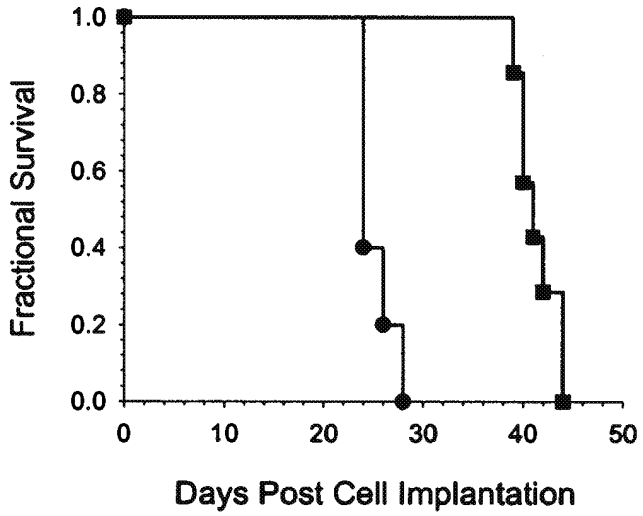


Figure 3. *Kaplan-Meier survival analysis of 1× LD_{10} BCNU-treated (■) and sham-treated control (●) animals. The mean survival times were 41.0±0.7 and 25.2±7.5 days, respectively, for the treated and control groups (mean±SEM, n=5). There was a statistically significant increased life span in the treated animals (P=.007 Mantel-Cox logrank test).*

Discussion

We have previously reported that serial measurements of tumor volume obtained from standard T_2-weighted MR images of intracerebral 9L tumors can be used to accurately quantitate tumor cell kill in individual animals [9]. In this study, MRI-based measurements were used to validate BLI-based measurements of orthotopic tumor growth and therapy-induced tumor cell kill in individual animals. There appears to be a linear relationship between MRI-determined tumor volume and tumor light output as measured through BLI. Both living and dead tumor cells, as well as dead tumor cell debris, infiltrating host cells, and peritumoral edema may all contribute to the MRI-determined tumor volume. In contrast, tumor light output is presumably derived solely from metabolically active transformed tumor cells. This may result in less robust correlation between MRI-determined tumor volume and photon counts in treated tumors or large untreated tumors in which regions of the tumor may be necrotic. In support of this hypothesis, we have observed less significant correlations between tumor volume and photon counts following treatment (data not shown). This may represent an advantage of BLI over direct measurements of tumor volume using MRI or calipers as it provides a

SPECTRAL_0000692

quantitative surrogate measure of the number metabolically active tumor cells.

Other advantages of the BLI approach for preclinical evaluation of therapeutic interventions include reasonable equipment costs, short scanning times of only 1 to 5 minutes, simultaneous scanning of multiple animals in a single image acquisition, and minimal postprocessing requirements. However, BLI is currently a two-dimensional imaging modality with only 1- to 2-mm spatial resolution due to photon scattering, which impairs detailed assessment of tumor anatomy and invasion. The quantitative nature and higher throughput of BLI should significantly reduce the cost of preclinical drug discovery and development by accelerating *in vivo* analyses of orthotopic animal models of neoplastic disease.

Acknowledgement

We thank Phillip Kish for technical assistance.

References

[1] Contag CH, Jenkins D, Contag PR, and Negrin RS (2000). Use of reporter genes for optical measurements of neoplastic disease *in vivo*. *Neoplasia* **2**, 41–52.

[2] Sweeney TJ, Mailander V, Tucker AA, Olomu AB, Zhang W, Cao Y, Negrin RS, and Contag CH (1999). Visualizing the kinetics of tumor-cell clearance in living animals. *Proc Natl Acad Sci USA* **96**, 12044–12049.

[3] Edinger M, Sweeney TJ, Tucker AA, Olomu AB, Negrin RS, and Contag CH (1999). Noninvasive assessment of tumor cell proliferation in animal models. *Neoplasia* **1**, 303–310.

[4] Curt GA (1994). The use of animal models in cancer drug discovery and development. *Stem Cells* **12**, 23–29.

[5] Dong Z, Radinsky R, Fan D, Tsan R, Bucana CD, Wilmanns C, and Fidler IJ (1994). Organ-specific modulation of steady-state mdr gene expression and drug resistance in murine colon cancer cells. *J Natl Cancer Inst* **86**, 913–920.

[6] Fidler IJ, Wilmanns C, Staroselsky A, Radinsky R, Dong Z, and Fan D (1994). Modulation of tumor cell response to chemotherapy by the organ environment. *Cancer Metastasis Rev* **13**, 209–222.

[7] Killion JJ, Radinsky R, and Fidler IJ (1998). Orthotopic models are necessary to predict therapy of transplantable tumors in mice. *Cancer Metastasis Rev* **17**, 279–284.

[8] Ross BD, Mitchell SL, Merkle H, and Garwood M (1989). *In vivo* ^{31}P and ^{2}H NMR studies of rat brain tumor pH and blood flow during acute hyperglycemia: differential effects between subcutaneous and intracerebral locations. *Magn Reson Med* **12**, 219–234.

[9] Ross BD, Zhao YJ, Neal ER, Stegman LD, Ercolani M, Ben-Yoseph O, and Chenevert TL (1998). Contributions of cell kill and posttreatment tumor growth rates to the repopulation of intracerebral 9L tumors after chemotherapy: an MRI study. *Proc Natl Acad Sci USA* **95**, 7012–7017.

[10] Contag CH, Spilman SD, Contag PR, Oshiro M, Eames B, Dennery P, Stevenson DK, and Benaron DA (1997). Visualizing gene expression in living mammals using a bioluminescent reporter. *Photochem Photobiol* **66**, 523–531.

Transgenic Research **10:** 423–434, 2001.
© 2001 *Kluwer Academic Publishers. Printed in the Netherlands.*

Rapid *in vivo* functional analysis of transgenes in mice using whole body imaging of luciferase expression

Weisheng Zhang[1], Jian Q. Feng[2], Stephen E. Harris[3], Pamela R. Contag[4], David K. Stevenson[1] & Christopher H. Contag[1,*]

[1]*Division of Neonatal and Developmental Medicine, Departments of Pediatrics, and Microbiology and Immunology, Stanford University Medical Center, Stanford University, Stanford, CA 94305-5208*
[2]*Department of Oral Biology, University of Missouri-Kansas City, Kansas City, MO 64108*
[3]*Department of Medicine, University of Texas Health Science Center at San Antonio, San Antonio, TX 78284*
[4]*Xenogen Corporation, 860 Atlantic Avenue, Alameda, CA 94501*

Received 5 September 2000; revised 12 December 2000; accepted 15 December 2000

Key words: heme oxygenase, bone morphogenic protein, transgene, functional, *in vivo* molecular imaging, luciferase, photoprotein, reporter gene

Abstract

The use of transgenic animals in biomedical research is increasing rapidly and may be the best means of determining gene function. Generating transgenic animals typically requires time-consuming screening processes, and gene function is assessed by an array of difficult phenotypic and biochemical assays performed *ex vivo*. To address the unmet need in transgenic research for functional assays performed with ease in living animals, we demonstrate here that *in vivo* detection of luciferase enzyme as a transcriptional reporter facilitates rapid screening for both the presence and function of transgenes in intact living mice. Using this approach we identified three bioluminescent transgenic founders where the transgene consisted of the heme oxygenase promoter fused to the modified coding sequence of the luciferase gene. These founders were identified from 183 pups and confirmed by PCR analysis. Identification of HO-1-*luc* homozygotes from back- crossed F_2 littermates was then accelerated by *in vivo* imaging. In another transgenic mouse line, where the transgene was comprised of the bone morphogenic-4 (BMP4) promoter fused to the modified luciferase gene, we were able to identify transgenic animals and in each line we were able to visualize patterns of expression in living animals over time. The light production from these transgenic mice indicated that the desired DNA fragment was functional and different expression profiles apparent at different ages and after gene induction.

Introduction

General strategies for generating transgenic (Tg) animals have been well described (Pinkert 1994; Monastersky & Robl 1995), however, the time-consuming processes of screening for the presence and function of the transgene remain as rate limiting steps. Typically, screening involves the polymerase chain reaction (PCR), Southern blot hybridization or slot-blot hybridization (Tinkle et al., 1994), to demonstrate the presence of integrated DNA. To determine if the gene products are expressed, steady-state levels of mRNA transcripts can be assessed by northern blot or slot-blot hybridization, coupled reverse transcription and polymerase chain reaction (RT-PCR), or *in situ* hybridization, and protein expression assayed using western blots, or immunofluorescent staining. Finally, a wide range of assays is needed to determine function as an indication of the appropriate phenotype. Tissues from the Tg animal are required to perform these molecular and functional analyses (Bieberich et al., 1994), and removal of tissues may not be possible until a line is well established. Thus, a rapid noninvasive screen-

* Author for correspondence:
E-mail: ccontag@cmgm.stanford.edu

SPECTRAL_0000694

ing method is needed as a functional assay for the generation and study of Tg animals.

A number of lines of Tg mice that employ reporter gene constructs have been developed and tested. For example, Tg mice containing viral long terminal repeat (LTR) promoter fusions have been used to study the range of tissues and cell types that are capable of supporting HTLV-1 expression and the development of neurofibromatosis-like tumors associated with HTLV-1 retrovirus (Bieberich, 1993). The LTR from HIV-1 has been fused to luciferase to evaluate transcriptional regulation by UV light and various sensitizing agents (Morrey et al., 1991, 1992). Cardiovascular biology and associated disease states have been investigated in Tg mouse models using tissue-specific promoters (Johnson et al., 1989; Tsika et al., 1990; Seidman et al., 1991; Rindt et al., 1993), and regulation of insulin-responsive glucose transporter GLUT4 and Apo A-I genes have also studied in models of diabetes, obesity (Liu, M. L. et al., 1992) and coronary artery disease (Walsh et al., 1989, 1993). These are only a few examples of where reporter genes that encode proteins with optical signatures have been used to study regulation in transgenic animal studies.

Photoproteins as biological labels have been used for more than a decade for the study of gene expression in cell culture or using excised tissues (Campbell 1988; Morrey et al., 1991, 1992; Hashings 1996). Low-light imaging of internal bioluminescent signals has been used to study temporal and spatial gene regulation in relatively thin or nearly transparent organisms (Millar et al., 1992; Brandes et al., 1996; Stanewsky et al., 1997). The advance of external detection of light generated internally using the transmitted signal as an indicator of reporter gene expression, has opened the door to visualizing mammalian biology in real time. We now can quantify *in vivo* gene expression profiles, progression of infectious disease, and tumor growth and regression in animal models (Contag et al., 1995, 1997, 1998, 1999). This *in vivo* functional imaging approach has been used in the present study to dramatically simplify the selection and evaluation of photoprotein-based transgenes in mice. We used *in vivo* photoprotein detection to rapidly identify 3 HO-1-*luc* Tg mouse founder mice. To identify HO-1-*luc* homozygous mice and back-crossed Tg mice with the bone morphogenic-4 promoter driving expression of the luciferase coding sequence (BMP4-*luc*), we monitored luciferase expression in young animals, and demonstrated a functional response to a known stimulus. The results from the *in vivo* assays were further confirmed by more conventional *ex vivo* molecular analyses for DNA and protein levels. The results suggested that *in vivo* imaging of luciferase expression provided a rapid functional screen for the presence of photoprotein encoding transgenes and for *in vivo* gene expression profiling of the labeled genes.

Materials and methods

Generation of HO-1-luc transgene

The plasmid, pHO-1-*luc*15, comprised of a 15 kb genomic fragment containing the mouse HO-1 promoter upstream of the coding sequence of the modified firefly luciferase present in the pGL-3 series of vectors (Alam J. et al., 1994; Promega Corp. Madison, WI) was linearized using restriction enzyme *Not*I and purified using GeneClean Kit (Bio101, Vista, CA). The purified linear plasmid at 10 ng/μl was injected into FVB mouse pronuclei, and the embryos were then transferred into pseudopregnant FVB mice. Injections and embryo transfers were performed in Tg Mouse Facility at Stanford University under the direction of Dr. Hugh McDivitt. At 2–3 weeks of age mice were screened by both *in vivo* bioluminescent imaging and PCR.

DNA extraction and PCR

Mouse tail DNA was extracted using QIAamp Tissue Kit (Qiagen Inc. Valencia, CA). The PCR reactions for detection of the HO-1-*luc* fusion utilized primers that span the junction of the HO-1 sequence and the luciferase coding sequence. The primers were 5′-CAGACTTGCCA-GAGTCATATGATT-3′ at the 5′ end corresponding to positions −149 to −125 bp upstream of the murine HO-1 transcriptional start, and 5′-GGTCGACGGATCCTTATTCGATTTAG-3′ located downstream from the polyadenylation signal (poly A) in the pGL3-basic vector (Promega Corp.). The PCR reactions were carried out in a total volume of 100 μl containing 10 pmoles of each primer, 1.75 mM of $MgCl_2$, 0.5 μg of either mouse genomic DNA or 10 ng of plasmid DNA (pHO-1-*luc*15). These reactions utilized a commercial PCR buffer system (Gibco-BRL, Grand Island, NY) and recombinant Taq DNA polymerase (Gibco-BRL, Grand Island, NY) and amplification was performed with 30 cycles of 94°C for 1 min, 55°C for 1 min, and 72°C for 1.5 min

SPECTRAL_0000695

using Genius Thermocycler (Techne Inc., Princeton, NJ). The luc primers for detecting the BMP4-*luc* fusion were contained within the luciferase coding region and were 5′-AGAGATACGCCCTGGTTCC-3′ (corresponding to luciferase position 179–197) and 5′-CATCGACTGAAATCCCTGG-3′ (corresponding to positions 561–579). These primers amplified a 400 bp sequence.

Southern hybridization

A 1.7 kb *Hin*dIII and *Xba*I fragment containing the entire luciferase coding sequence from pGL3-Basic vector was isolated from an agarose gel using the QIAquick Gel Extraction Kit (Qiagene Inc. Valencia, CA). This luciferase probe was randomly labeled by nick translation using α-^{32}P dATP (Amersham, Pharmacia Biotech, Inc. Piscataway, NJ) and a commercial labeling kit (Primer-It II Kit, Strategene, La Jolla, CA). The genomic DNA from mouse tail tissue was digested with *Kpn*I and *Sal*I. DNA digests were then analyzed using the standard Southern hybridization method (Sambrook, J. et al., 1989).

Ex vivo *luciferase assay*

Mouse tissues were homogenized and sonicated using a tissue disrupter (Sonic Dismembrator 60, Fisher Scientific, Pittsburgh, PA) in 500 µl of PBS buffer. Luciferase activity was determined for 30 s integration using Luciferase Assay System according to the recommendations of the vendor (Promega Corp, Madison, WI) and normalized to relative light intensity per milligram of tail protein measured by Bradford Protein Assay System (Sigma, St. Louis, MO).

Imaging

For imaging, one of two low light imaging systems was used that either employed an intensified CCD camera (Hamamatsu, Japan) or a cooled camera (Xenogen, Corp., Alameda CA). The intensified CCD camera (ICCD; model C2400-32, Hamamatsu, Japan) was fitted with a 50 mm f 1.2 Nikkor lens (Nikon, Japan) and an image processor (Argus 20, Hamamatsu) as hardware package that is integrated with LivingImage software (Xenogen, Corp.). The other system employed a cryogenically cooled camera (Roper Scientific, Trenton, NJ) fitted with a 50 mm f 0.95 Navitar (Buhl Optical, Pittsburgh, PA) available as an integrated imaging system (Xenogen, Corp.). Twenty minutes prior to imaging, the substrate luciferin was injected into the peritoneal cavity using a dose of 150 mg/kg body weight (15 mg/ml stock). Mice were then anesthetized using Nembutal (25–50 mg/kg body weight) and imaged with integration times of 1 to 10 min as indicated in figures (Contag et al., 1995, 1997). Grayscale reference images of the animals were obtained under low light illumination from light emitting diodes (LED) built into the imaging dark boxes. The transmitted light originating from the luciferase expressing cells in the bodies of the transgenic mice was detected in total darkness, and the intensity of this light was represented as a pseudocolor image where blue is the least intense and red the most intense bioluminescent signals. The two images were superimposed using the LivingImage software overlay (Xenogen, Corp.) and Igor image analysis software (Wavemetrics, Seattle, WA). Following the imaging animals were kept warm and allowed to recover. If animals were imaged more than once, luciferin was injected prior to each image to ensure that each measurement was performed in luciferin excess.

The relative light intensity, photon counts, from a region of the whole animal image approximating 1.1 cm of the tail tips from the 2-week-old BMP4-*luc* Tg mice was determined using the program NIH Image (NIH, Bethesda, MD). Light intensity for the HO-1-*luc* transgenic animals was quantified using the quantitative functions in the software LivingImage and Igor. These *in vivo* counts were collected and compared to the relative light intensity as determined by *ex vivo* biochemical assays for luciferase activity (Promega Corp.).

Inducible expression in the homozygous HO-1-luc Tg line

$CdCl_2$ (2 mM), a known inducer of HO-1 transcription, was injected into left thigh of each of 15 mice (20 µl per tissue), and 20 µl of H_2O was injected into the contralateral thigh as a negative control. Mice were imaged using two low light imaging systems (ICCD and cooled CCD cameras) over a 24 h time course with 3 h intervals for the first 9 h and then at 24 h post injection of $CdCl_2$. Integration times of 1 and 10 min were used for the cooled and intensified CCD cameras, respectively. At 0, 3, 6, 9, 12 and 24 h mice were sacrificed and proteins from each thigh muscle were extracted. The proteins were analyzed by western blot using antibody to the native HO-1 protein.

SPECTRAL_0000696

Western blot analyses

Quantification of HO-1 protein levels was performed by western blot. Protein concentration in tissue sonicates was determined via the Bradford protein assay as recommended by the manufacturer (Sigma, St. Louis, MO). Proteins from either 50 μg of tissue sonicates was subjected to size selection on 10% SDS/PAGE gels and transferred to Nitrocellulose membranes (Bio-Rad, CA) using a Bio-Rad electroblot device as recommended by the manufacturer. HO-1 protein was detected using the primary rabbit polyclonal human HO-1 antibody (Stressgen, Toronto, Canada), and secondary goat anti-rabbit IgG (Bio-Rad). Bound antibody was detected by chemiluminescence according to manufacturer protocol (Amersham, Piscatawag, NJ).

Results

Rapid screening of HO-1-luc Tg mouse founders

HO-1-*luc* fusion DNA was introduced into FVB mouse eggs by microinjection and the fertilized eggs were then transferred into pseudopregnant mice. Two to three-week-old pups were sedated, treated with luciferin, and light emission was measured with the ICCD camera. Three positive founders (F_0), which emitted bioluminescent signals were identified from 183 pups. In Figure 1 (panel A and B) images of two of the HO-1-*luc* Tg founders and their littermates are shown. To confirm integration of the entire luciferase gene into the mouse genome, tail DNA samples from 105 pups, including the three that were positive for *in vivo* light emission, were analyzed by PCR, using primers which amplify a 2.1 kb transcriptional unit including the basal promoter and proximal enhancer of the HO-1 gene, the entire luciferase coding region, and the 3′ poly A termination sequence. All three bioluminescent founders identified by the ICCD camera were also PCR positive while all of their littermates were negative. Figure 1 (panel C and D) shows the PCR results for two of the three HO-1-*luc* founders and selected littermates.

Identification of homozygous HO-1-luc transgenic mice

To generate a homozygous HO-1-*luc* Tg line, a female founder was bred with a wildtype FVB male. Four pairs of luciferase positive F_1 offspring that had been identified by imaging were then bred to produce the F_2 generation. We identified homozygous F_2 HO-1-*luc* Tg mice using the classic Mendel's Equal Segregation Law after backcrossing each of the F_2 Tg mice onto a nontransgenic background (FVB). Ten glowing F_2 females were backcrossed with wild type FVB males and two-week-old pups from individual matings were imaged. In this analysis, two homozygous F_2 females were identified. Examples of the resulting pups from the backcrosses are shown in Figure 2. In one litter all eight pups were bioluminescent and from another, only four of nine pups had a detectable signals. From this analysis the first female was determined to be homozygous and the second, heterozygous. Using the same strategy, three homozygous F_2 males were identified from 10 F_2 males. One pair of homozygous F_2 mice were used to generate the homozygous HO-1-*luc* Tg colony.

Expression patterns in young HO-1-luc Tg mice

HO-1 is widely expressed in tissues of young mice (Rodgers & Stevenson, 1990) and in these studies basal levels of reporter gene expression was detectable over the entire body of each HO-1-*luc* Tg mouse (Figure 2). The signal intensity, however, was greater over the cranium in each of the HO-1-*luc* positive pups than over other regions. This expression pattern was observed in each of the pups and the pattern was reproducible, but the intensity appeared to vary slightly from mouse to mouse. Expression of HO-1 in the brain of neonates is consistent with observations made by immunocytochemistry (Bergeron et al., 1998).

Screening and gene expression patterns in BMP4-luc Tg mice

This imaging technology has also been used to examine two-week-old pups from an expressing BMP4-*luc* Tg heterozygous female backcrossed with a wild-type male (C57BL/Balb/C). Out of 11 offspring, four pups expressed luciferase at a similar level as measured by whole body luciferase imaging, and with a very reproducible pattern of increasing intensity from the dorsal to ventral side of the animal and expression in the ears (Figure 3). In these two-week-old mice the observed dorsal to ventral gradient of expression is in agreement with the proposed role of BMP4 in participating in the dorsal ventral organization during mammalian development (Liem et al., 1995; Hammerschmidt et al., 1996, Watanabe and Le Douarin 1996).

SPECTRAL_0000697

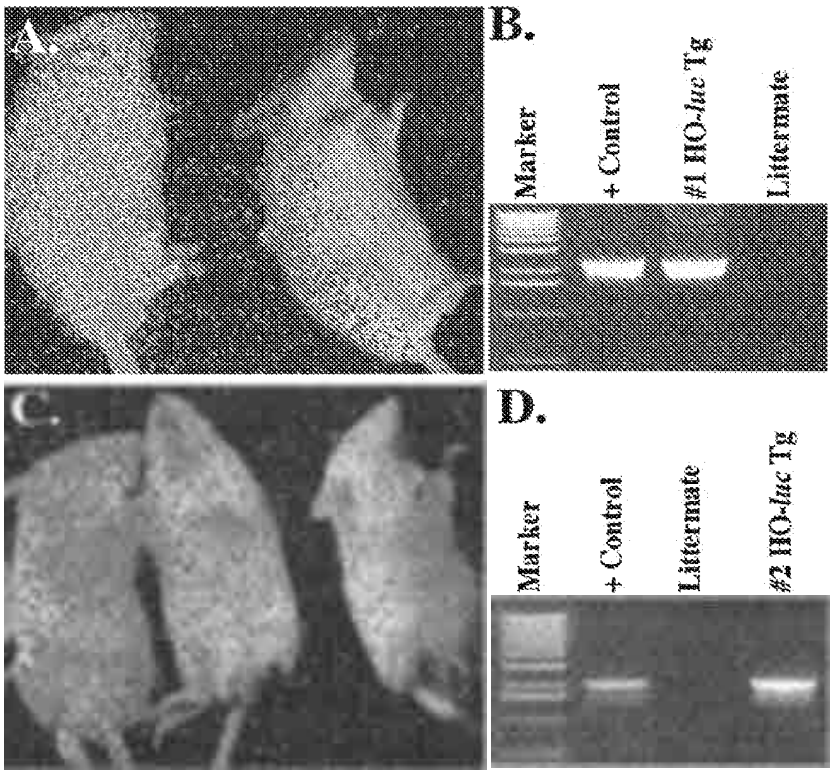


Figure 1. Screening of HO-1-*luc* transgenic mice. HO-1-*luc* Tg founders (F_0; 1 and 2) were identified via monitoring luciferase expression *in vivo* in comparison to levels in their littermates (A, C). Presence of the HO-1-*luc* transgene in selected mice was determined by PCR (B, D). The PCR reaction targeted a 2.1 kb DNA fragment that included the HO-1 basal promoter and proximal enhancer region, as well as the luciferase gene and the 3′ SV40 poly-A signal. Positive control DNA was the plasmid pHO-1-*luc*15, which was used to generate transgenic mice and the samples were mouse tail DNA.

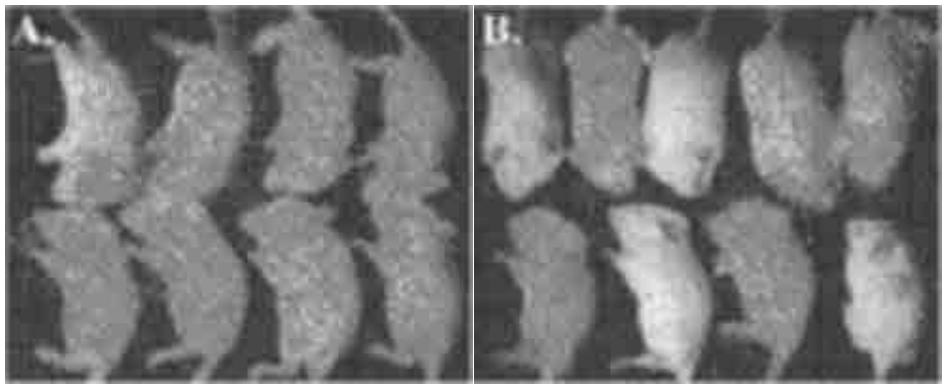


Figure 2. Identification of homozygous HO-1-*luc* F_2 mice. Luciferase positive F_2 mice were bred with wildtype mice (strain FVB). The offspring were examined with ICCD camera for luciferase expression. Pups from one of homozygous females (A) and from one of heterozygous females (B) are shown.

SPECTRAL_0000698

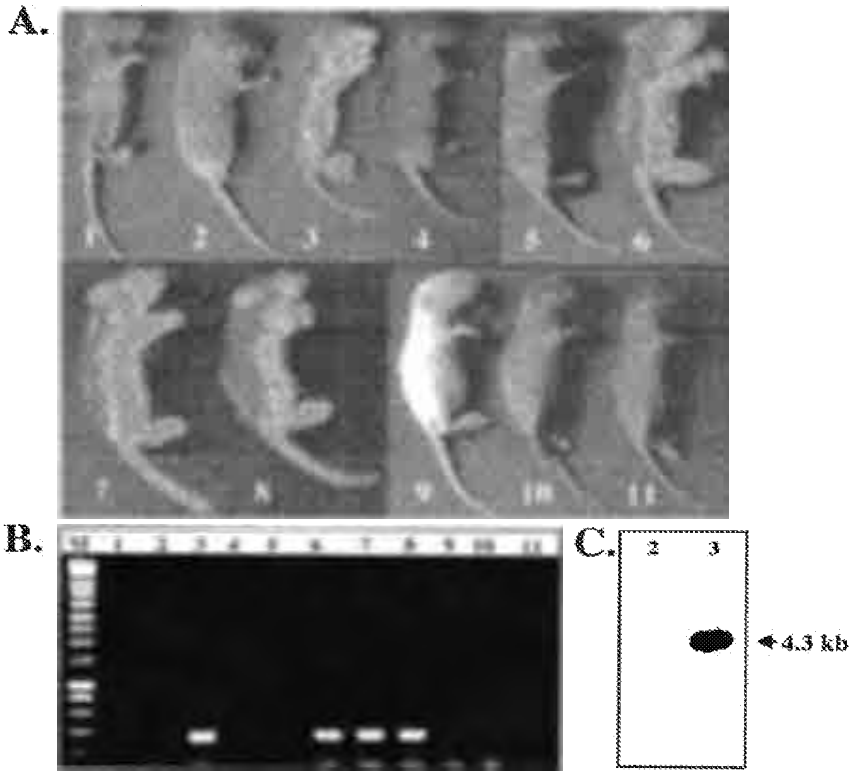


Figure 3. Identification of BMP4-*luc* Tg mice. A heterozygous BMP4-*luc* Tg female was backcrossed with a wildtype male (C57BL/Balb/C) and presence of the BMP4-*luc* gene fusion was assessed using *in vivo* imaging of the 11 pups at two weeks of age (A). Presence of the transgene was verified by PCR using primers that amplify a 400 bp region of the luciferase coding region (B), and by Southern analysis for a *luc* negative (animal 2) and a *luc* positive (animal 3), the probe was ^{32}P-labeled DNA corresponding to the entire luciferase coding sequence (C). In each assay the Tg positive animals were identified, and the whole body imaging further revealed the overall expression pattern with increasing signal from the dorsal to ventral side in each of the Tg positive animals.

Tail DNA from selected positive and negative pups was analyzed by PCR and DNA from selected animals was digested with the restriction endonucleases *Kpn*I and *Sal*I and analyzed by Southern blot hybridization (Figure 3). Results from whole animal imaging and PCR were in agreement with all luminescent animals identified as Tg positive in each assay. Using the entire luciferase coding sequence as probe Southern blot hybridization was performed using a 4.6 kb DNA fragment containing the BMP4 promoter (2.6 kb), luciferase (1.7 kb) and the SV40 late poly A signal (0.3 kb) was used as a probe; two selected animals were analyzed by Southern blot hybridization. The animal with a detectable luminescent signal *in vivo* that was positive in the PCR analyses (animal 3) was also positive by Southern blot hybridization. The animal without detectable *in vivo* signal that was negative by PCR analysis was also negative in the Southern blot analysis (animal 2). Mouse tail tissue was also examined using the *ex vivo* enzyme assay for luciferase activity for all 11 mice. The *ex vivo* result showed that only the animals with detectable *in vivo* signals had detectable luciferase activity in the *ex vivo* assay (Table 1). Thus, the data from the biochemical assays, the Southern blot hybridizations, the PCR analyses and the whole body *in vivo* imaging were all in agreement.

Basal levels of expression in adult male homozygous HO-1-luc Tg mice

In the screening process, high basal levels of expression were detected in the testes of adult male homozygous HO-1-*luc* Tg mice. This pattern of basal expression was apparent in images from both the ICCD and cooled CCD camera systems with 10 and 1 min

SPECTRAL_0000699

Table 1. Summary of identification of BMP4-luc transgenic mice

Animal number	*Ex vivo* luciferase activity[a]	PCR[b]	*In vivo* imaging[c]
1	0.133	–	– (ND)
2	0.053	–	– (ND)
3	124	+	+ (ND)
4	0.071	–	– (ND)
5	0[d]	–	– (170)
6	338	+	+ (5.81×10^4)
7	1176	+	+ (1.27×10^5)
8	63	+	+ (4.49×10^4)
9	0.085	–	– (10)
10	0.092	–	– (30)
11	0.054	–	– (0[c])

[a]Relative Light Intensity/mg Protein.
[b]PCR scored as +/– data shown in Figure 3.
[c]Scored +/– by whole body image; relative light intensity/1.1 cm tail tip for several animals is given in parentheses.
[d]Numbers equal or below background.
ND: Not determined, the numerical data was not available for these images.

integration times, respectively (Figure 4). However, the overall low levels of expression in tissues other than the testes were only apparent with the cooled CCD camera (Figure 4B). Low basal levels of HO-1 have been reported in many tissues including the liver (Rodgers & Stevenson, 1990) and our *in vivo* data are consistent with these observations. To determine if the detectable levels of reporter gene expression in the testes were representative of HO-1 expression from the native HO-1 gene, or an artifact of the HO-1-*luc* integration site, we used a western blot analysis to compare the native levels of HO-1 protein in the testes to that of the control tissue, liver (Figure 4C). Consistent with the *in vivo* luciferase imaging data, higher levels of HO-1 protein were apparent in the testes in comparison to the liver. The liver had very low levels of *ex vivo* luciferase activity that were near background levels (Figure 4D); this appeared to be true for the *in vivo* assay as well.

Inducible expression of the HO-1 promoter in the homozygous HO-1-luc Tg mice

After intramuscular injection of $CdCl_2$ the animals were imaged at several time points with both low light imaging systems, and HO-1 protein, expressed from the native HO-1 locus, was assayed by western blot analyses (Figure 5). In each animal, expression of the reporter gene was detected, via *in vivo* luciferase imaging, in the treated thigh muscle, but not in the thigh that did not receive the heavy metal inducer $CdCl_2$. Reporter gene expression appeared to peak at 9 h post induction and decreases were observed at the 24 h time point. Expression of the HO-1 protein from the native HO-1 gene was also elevated in the muscle that received the inducer (western blot), but not in the thigh muscle treated with water alone. The signal intensity observed with the cooled CCD camera was, on average two fold greater with a 1 min integration time, than the ICCD camera with a 10 min integration time.

Correlation of signal intensity for in vivo *and* ex vivo *measurements*

Relative luminescence from the *ex vivo* measurements in BMP4 mouse tail-tip homogenates were measured and normalized to relative luciferase units (RLU) per milligram of tail protein, and *in vivo* RLU from approximately 1.1 cm of the tail tips of images were quantified for five animals. *In vivo* measurements of RLU quantified over the liver and testes of HO-1-*luc* Tg mice using the cooled CCD and *ex vivo* RLU obtained from the liver testes homogenates camera were determined for three mice. *In vivo* RLU for these animals and tissues was plotted against *ex vivo* RLU and a strong correlation ($r = 0.985$ for BMP4-*luc* and $r = 0.964$ for HO-1-*luc* mice) was observed (Figure 6).

Discussion

The imaging strategy described here makes use of the observation that light penetrates tissues, at a low yet detectable level, and the fact that reporter genes that encode light-producing enzymes can be engineered into biological systems as functional *in vivo* reporter genes (Contag et al., 1997, 1998). The efficiency of light transmission through the relatively opaque tissue of mammals is wavelength dependent; blue light penetrates poorly and red light penetrates more efficiently; this is due primarily to absorption of shorter wavelengths of light by hemoglobin (Chance et al., 1997). Light is also lost, as it passes through tissues, due to scatter. The net reduction of bioluminescent signal is estimated from *in vitro* studies to be approximately 10-fold for every centimeter of tissue depth, however this estimation will vary with tissue type (Contag et al., 1995). Despite the loss of bioluminescent signal due to absorbance and scattering,

SPECTRAL_0000700

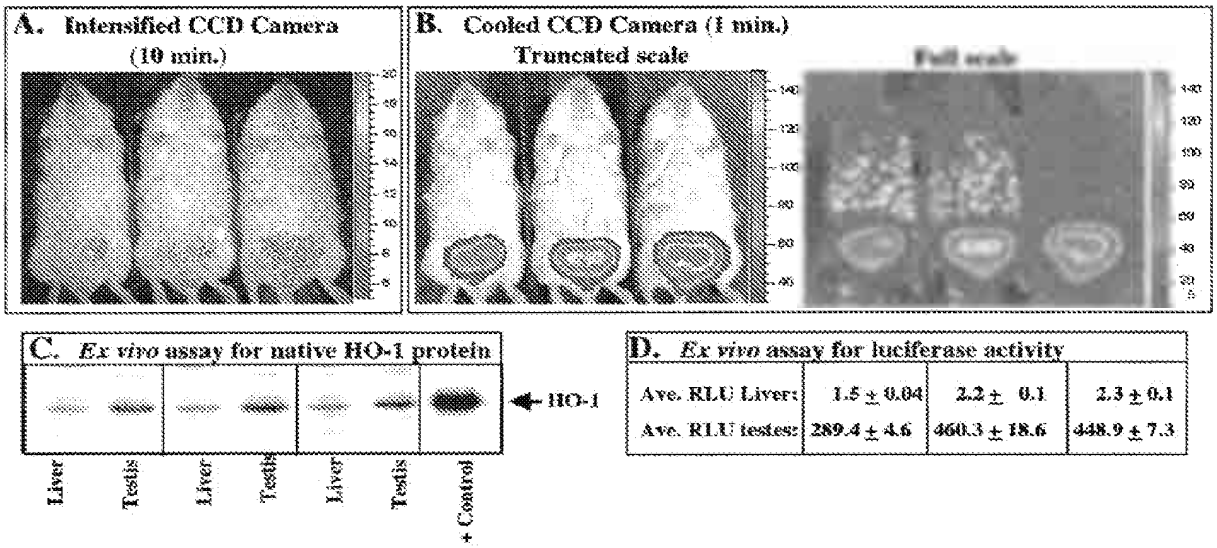


Figure 4. Basal levels of expression in the testes and comparison of two camera systems. Basal levels of HO-1-*luc* expression were detected in animals using either an intensified CCD camera with integration times of 10 min (A) or a cooled CCD camera with a 1 min integration time (B). The cooled camera is more sensitive and therefore the data is shown without the weaker signal (truncated scale) or with the weak signals (full scale). The levels of HO-1 protein were determined by western blot analyses as an indication of expression of the native gene relative to the reporter construct in liver and testes (C). Liver and testes tissue were removed, the cell lysed and the luciferase levels measured in an *ex vivo* assay (D). Basal levels of expression were highest in the testes by all measurements, and luciferase signal in the liver was not above background *in vivo* or *ex vivo*.

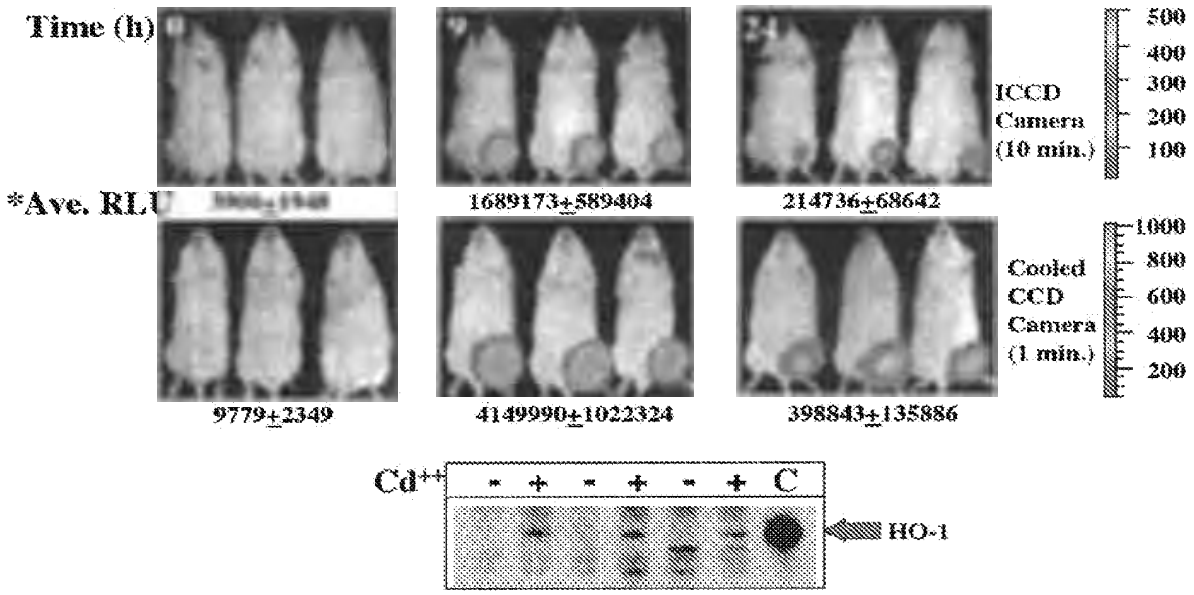


Figure 5. Increased HO-1 transcription in muscle following treatment with $CdCl_2$. 20 µl of 2 mM $CdCl_2$ was injected into left thighs of 8-week-old HO-1-*luc* Tg females and H_20 was injected to right thighs as control. Mice were imaged at 0, 3, 6, 9, 12, 24 h (images from 0, 9 and 24 h time points are shown). Thigh muscle was excised and homogenized in 4 volumes of PBS. 50µg of total protein from each sample from the 24 h time point was analyzed by western blot. Ave. RLU – Average relative luminescnece units from left leg of three mice.

SPECTRAL_0000701

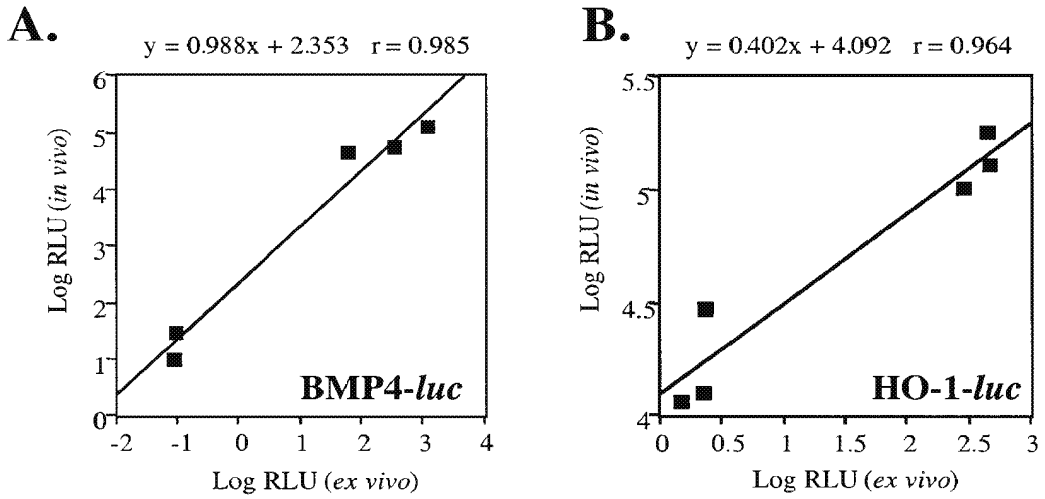


Figure 6. Correlation of relative luciferase activities between *in vivo* and *ex vivo* data. *Ex vivo* relative luciferase activities of BMP4 mouse tail-tip homogenates were measured and normalized to relative luciferase units (RLU) per milligram of tail protein. *In vivo* RLU from approximating 1.1 cm of the tail tips of images of BMP4-luc mice were quantified. *In vivo* RLU was plotted against *ex vivo* RLU in Log scales (data from #6, 7, 8, 9 and 10 mice were used; (A). *In vivo* RLU quantified over the liver and testes of HO-1-*luc* Tg mice using a cooled CCD camera; this data was plotted against *ex vivo* RLU obtained from the liver and testes homogenates (B).

the weak signals that are transmitted through the relatively opaque tissues can be detected, even from deep internal sources such as the liver, lung and intestine (Contag et al., 1997; Weng et al., 2000). The sensitivity of the *in vivo* measurements rivals that obtained by *ex vivo* luciferase activity measurements (Lipshutz et al., 2001). In the study by Lipshutz et al., the detection limit in the liver was 35 picograms of luciferase enzyme per gram of liver tissue and 1 in a million transduced liver cells (Lipshutz et al., 2001).

The conventional assays of PCR and Southern hybridization only detects presence of integrated target DNA in transgenic lines, and information regarding promoter activity requires further analysis by assays such as RT-PCR northern blot hybridization, *ex vivo* luciferase assay in cell lysates, or western blot. These conventional assays are hampered by a sampling limitation in that only a small portion of a few target tissues can be analyzed to determine the relevance of the Tg model to the biological question. This is further exacerbated at the subsequent steps required for understanding function and levels of expression need to be assessed at multiple time points in response to various stimuli.

Using this *in vivo* monitoring method, the luciferase expression from whole HO-1-*luc* Tg animals was directly visualized in relatively short periods of time (1–10 min). Light emission indicated that the functional transcription unit comprised of the HO-1 promoter-luciferase fusion, was incorporated into the genome of the recipient embryo. Noninvasive functional imaging of the photoprotein reporter resulted in an overall picture of the expression pattern superimposed over the whole body of the animal, thus both quantitative and spatial data can be obtained. Strong correlations between the *in vivo* signal intensity and cell number have been described with a linear relationship between signal intensity and cell number over six orders of magnitude (1×10^3 to 1×10^8 cells in the peritoneal cavity of mice) (Edinger et al., 1999; Contag et al., 2000). The *in vivo* signal, however, must be considered to be relative to signals of nontransgenic mice, and as with any measurement of expression, a comparison must be determined between mice that carry the transgene and those that do not.

The imaging step also serves as a high quality prescreen for a more directed analysis of specific tissues using conventional *ex vivo* analyses. This approach allows analyses of transgenes even if the target tissue for analysis is a vital organ. The correlation between *in vivo* measurements of luciferase activity and other *in vivo* imaging measurements of cell number (magnetic resonance imaging, MRI) is extremely good with a correlation of $r = 0.91$ (Rehemtulla et al., 2000). Conventional assays require removal of the tissue and as such can not be utilized until the founders have

SPECTRAL_0000702

been bred and time has been invested in generating a transgenic line. *In vivo* assays permit functional analyses of vital organs even of the founder animals. By imaging the intact mouse, expression in all tissues can be determined non-invasively allowing the assay to be performed early in the life of the founder animals thus, accelerating the selection of relevant lines for further study.

The response of the promoter to various stimuli can also be assessed early in the process of generating a Tg line by monitoring changes in light emission after stimulating the animals with known effectors, such as heavy metals in the HO-1-*luc* Tg line. Induction of expression may be necessary in screening the Tg founders if basal levels of expression are extremely low during development. Knowledge of the expression pattern following induction also serves to reveal the integrity of the promoter in the transgenic line. Many fewer animals can be used in the analysis of photoprotein reporters since the functional assay can be performed *in vivo* prior to the more labor-intensive assays. In the case of the HO-1-*luc* Tg mice, increased expression in response to the heavy metal Cd^{++}, suggested that HO-1 promoter was intact and functional since responsive elements for this stimulus are located over the length of the 10 kb HO-1 promoter (Alam, 1994).

Selection of homozygous Tg mice is often necessary, but due to the random integration of the transgene, such analyses can be difficult using conventional molecular approaches. Homozygosity of F_2 mice is determined by back-crossing with wild type and determining the phenotype of the offspring (Figure 2). This process was dramatically accelerated using *in vivo* imaging since tissue sampling and analysis by *ex vivo* luciferase assay, determining mRNA or protein levels was obviated. For identification of the BMP4-*luc* Tg mice, the *in vivo* imaging results were confirmed by Southern analysis, PCR and *ex vivo* luciferase assays (Figure 3A and 3B, Table 1). In this analysis, the patterns of the signal intensity *in vivo* were consistent with those observed by Southern bolt hybridization, PCR and in *ex vivo* luciferase assays. Inconsistencies in *ex vivo* assays may occur due to incomplete homogenization of tissue and sampling limitations since only a fraction of the tissue can be analyzed in biochemical assays. Substrate availability in the *in vivo* assay is not a source of inconsistency, since in earlier studies adequate levels of luciferin were detected in all tissues by 20 min after injection, and additional doses of luciferin did not result in increased signal intensity (Contag et al., 1997).

Homologous recombination is the traditional method for the generation of specific gene knockouts. The neomycin resistant gene (*neo*) is generally used as a selectable marker allowing the selection of the transfected stem cells. However, identification of the knock-out animals containing the *neo* cassette still relies on PCR or Southern analysis. If a luciferase reporter gene is used in the replacement vector as the reporter gene, identification of the knock-out founders would be accelerated by the imaging method. One use of this technology would be the analysis of coordinate regulation or interactive regulatory pathways. For example, the *noggin* gene product regulates transcription of the BMP4 gene (Kim et al., 1998), and crossing the BMP4-*luc* Tg line with a *noggin* knockout mouse may allow *in vivo* analyses of the responsive regions of the promoter. Similarly the luciferase reporter gene could be used to noninvasively verify conditional knockouts in cre-lox systems such that the response could be normalized to luciferase expression.

In vivo detection of light from photoprotein reporters can be used to quantify spatial and temporal fluctuations in gene expression from living Tg animals. In both examples in this study, the expression of the native gene was paralleled by the reporter transgene expression as detected by several methods. The use of such dynamic assays to measure and image transgene expression will result in increased information under both physiological and pathophysiological conditions. The imaging of reporter gene expression *in vivo* provides real time data pertaining to perturbations in gene expression in living animals. In both the HO-1-*luc* and the BMP4-*luc* Tg lines of mice significant signal above background was detected at birth and basal levels of luciferase activity were detectable throughout life. However, this may not be the case for all Tg lines and investigators should be aware that a tightly regulated promoter may not express basal levels that can be detected without activation.

Rapid screening and analysis of the transgenic lines will facilitate the process of generating Tg animals and selecting the most informative lines. The *in vivo* imaging approach described here provides a rapid functional screen for photoprotein-based Tg mice. The information from living animals more accurately represents responses to therapies than that from conventional biochemical assays performed *in vitro* and *ex vivo*.

SPECTRAL_0000703

Animal models with molecular indicator lights, such as luciferase, that can be used to predict changes in gene expression patterns represent a powerful tool for multiparameter analyses of gene expression. With the development of target directed therapies that are intended to alter disease- related gene expression, it is necessary to refine Tg models to accelerate the preclinical stage of drug development. The effects of potentially useful therapeutic compounds on expression of specific genes can be evaluated in over the entire body and over time. Therapeutic intervention at the level of the gene, the mRNA or the protein has to take into account the multifunctionality of the gene product and the multiple levels of regulation during physiology and metabolism. Thus, we are required to understand the full scope of gene function in complex metabolism and the result of intervention as it relates to the hierarchy of pathway interaction. This is only possible in the context of a living intact animal. Access to real time data in living transgenic animals can greatly enhance the study of biological processes in the areas of metabolism, infectious disease, tumor progression and metastasis, gene therapy, mammalian development, among many other areas.

Acknowledgements

This work was funded in part through grants from NIH, 1R01 HL58013 and RR00070; the ONR, contract N-00014-94-1-1024 and unrestricted gifts from the Mary L. Johnson and Hess Research Funds.

References

Alam J (1994) Multiple elements within the 5′ distal enhancer of the mouse heme oxygenase-1 gene mediate induction by heavy metals. *J Biol Chem* **269**(40): 25049–25056.

Bergeron M, Ferriero DM and Sharp FR (1998) Developmental expression of heme oxygenase-1 (HSP32) in rat brain: an immunocytochemical study. *Brain Res Dev Brain Res* **105**: 181–194.

Bieberich CJ, King CM, Tinkle BT and G Jay (1993) A transgenic model of transactivation by the tax protein of HTLV-I. *Virol* **196**: 309–318.

Bieberich CJ, Ngo L and Jay G (1994) Molecular approaches involved in mammalian gene transfer: Evaluation of transgene expression. *In*: Pinkert CA (ed.), Transgenic Animal Technology: A Laboratory Handbook. pp. 235–262. Academic Press, San Diedo, California.

Brandes C, Plautz JD, Stanewsky R, Jamison CF, Straume M, Wood KV et al. (1996) Novel features of *Drosophila* period transcription revealed by real-time luciferase reporting. *Neuron* **16**: 687–692.

Campbell AK (1988) Chemiluminescence. Principles and applications in biology and medicine. Ellis Horwood Ltd. and VCH Verlagsgesellschaft mbH, Chichester, England.

Chance B, Luo Q, Nioka S, Alsop DC, Detre JA (1977) Optical investigations of physiology: a study of intrinsic and extrinsic biomedical contrast. *Philos Trans R Soc Lond B Biol Sci* **352**: 707–716.

Contag PR, Olomu I, Stevenson DK and Contag CH (1998) Bioluminescent reporters in living mammals. *Nature Med* **4**: 245–247.

Contag CH, Spilman SD, Contag PR, Oshiro M, Eames B, Dennery P et al. (1997) Visualizing gene expression in living mammals using a bioluminescent reporter. *Photochem Photobiol* **66**: 523–531.

Contag CH, Contag PR, Mullins JI, Spilman SD, Stevenson DK and Benaron DA (1995) Photonic detection of bacterial pathogens in living hosts. *Mol Microbiol* **18**: 593–603.

Contag CH, Jenkins D, Contag PR and Negrin RS (2000) Use of reporter genes for optical measurements of neoplastic disease *in vivo*. *Neoplasia* **2**: 41–52.

Edinger M, Sweeney TJ, Tucker AA, Olomu AB, Negrin RS and Contag CH (1999) Noninvasive assessment of tumor cell proliferation in animal models. *Neoplasia* **1**: 303–310.

Feng JQ, Harris MA, Ghosh-Choudhury N, Feng M, Mundy GR, Harris SE (1994) Structure and sequence of mouse bone morphogenetic protein-2 gene (BMP-2): comparison of the structures and promoter regions of BMP-2 and BMP-4 genes. *Biochimica et Biophysica Acta* **1218**: 221–224.

Hammerschmidt M, Serbedzija GN, McMahon AP (1996) Genetic analysis of dorsoventral pattern formation in the zebrafish: requirement of a BMP-like ventralizing activity and its dorsal repressor. *Genes Dev* **10**: 2452–2461.

Hastings JW (1996) Chemistries and colors of bioluminescent reactions: a review. *Gene* **173**: 5–11.

Johnson J, Wold B and Hauschka S (1989) Muscle creatine kinase sequence elements regulating skeletal and cardiac muscle expression in transgenic mice. *Mol Cell Biol* **9**: 3393–3399.

Liem KF Jr, Tremml G, Roelink H and Jessell TM (1995) Dorsal differentiation of neural plate cells induced by BMP-mediated signals from epidermal ectoderm. *Cell* **82**(6): 969–979.

Lipshutz G, Gruber C, Cao Y-A, Hardy J, Contag C and Gaensler K (2001) Utero delivery of adeno-associated viral vectors: Intraperitoneal gene transfer produces long-term expression. *Mol Ther* (in press).

Liu ML, Olson AL, Moye-Rowley WS, Buse JB, Bell GI and Pessin JE (1992) Expression and regulation of the human GLUT4/muscle-fat facilitative glucose transporter gene in transgenic mice. *J Biol Chem* **267**: 11673–11676.

Kim J, Ault KT, Chen HD, Xu RH, Roh DH, Lin MC et al. (1998). Transcriptional regulation of BMP-4 in the Xenopus embryo: analysis of genomic BMP-4 and its promoter. *Biochem Biophys Res Commun* **250**(2): 516–530.

Millar AJ, Short SR, Chua NH and Kay SA (1992) A novel circadian phenotype based on firefly luciferase expression in transgenic plants. *Plant Cell* **4**: 1075–1087.

Monastersky GM and Robl JM (ed.) (1995) Strategies in Transgenic Animal Science. ASM Press, Washington D.C.

Morrey JD, Bourn SM, Bunch TD, Thomas D, Siddwell RW and Rosen CA (1992) HIV-1 LTR activation model: Evaluation of various agents in skin of transgenic mice. *J Acquir Immune Defic Syndr* **5**: 1195–1203.

Morrey JD, Bourn SM, Bunch TD, Jackson MK, Siddwell RW, Barrows LR et al. (1991) *In vivo* activation of human immunodeficiency virus type 1 long terminal repeat by UV type A (UV-A)

SPECTRAL_0000704

light plus psoralen and UV-B light in the skin of transgenic mice. *J Viol* **65**: 5045–5051.

Rindt H, Gulick J, Knotts S, Neumann J and Robbins J (1993) *In vivo* analysis of the murine beta-myosin heavy chain gene promoter. *J Biol Chem* **268**: 5332–5338.

Pinkert CA (ed.) (1994) Transgenic Animal Technology: A Laboratory Handbook. Academic Press, San Diedo, California.

Rehemtulla A, Stegman L, Cardozo S, Gupta S, Hall D, Contag C et al. (2000). Rapid and quantitative assessment of cancer treatment response using *in vivo* bioluminescence imaging. *Neoplasia* **2**: 491–495.

Rodgers PA and Stevenson DK (1990) Developmental biology of heme oxygenase. *Clin Perinatol* **17**(2): 275–291.

Sambrook J, Fritsch EF and Maniatis T (1989) Molecular Cloning: A Laboratory Manual (2nd edn). Cold Spring Harbor Laboratory Press, USA.

Seidman CE, Schmidt EV and Seidman JG (1991) *Cis*-dominance of rat atrial natriuretic factor gene regulatory sequences in transgenic mice. *Can J Physiol Pharmacol* **69**: 1486–1492.

Stanewsky R, Jamison CF, Plautz JD, Kay SA and Hall JC (1997) Multiple circadian-regulated elements contribute to cycling period gene expression in *Drosophila*. *EMBO J* **16**: 5006–5018.

Tinkle BT, Bieberich CJ and Jay G (1994) Molecular approaches involved in mammalian gene transfer: Analysis of transgene integration. *In*: Pinkert CA (ed.), Transgenic Animal Technology: A Laboratory Handbook. (pp. 221–234). Academic Press, San Diedo, California.

Tsika RW, Bahl JJ, Leinwand LA and Morkin E (1990) Thyroid hormone regulates expression of a transfected human alpha-myosin heavy chain fusion gene in fetal rat heart cells. *Proc Natl Acad Sci USA* **87**: 379–383.

Walsh A, Azrolan N, Wang K, Marcigliano A, O'Connell A and Breslow JL (1993) Intestinal expression of the human apo A-I gene in transgenic mice is controlled by a DNA region 3′ to the gene in the promoter of adjacent convergently transcribed apo C-II gene. *J Lipid Res* **34**: 617–623.

Walsh A, Ito Y and Breslow JL (1989) High levels of human apolipoprotein A-I in transgenic mice result in increased plasma levels of small high density lipoprotein (HDL) particles comparable to human HDL3. *J Biol Chem* **264**: 6488–6494.

Watanabe Y and Le Douarin NM (1996) A role for BMP-4 in the development of subcutaneous cartilage. *Mech Dev* **57**(1): 69–78.

Weng Y-H, Tatarov A, Bartos BP, Contag CH and Dennery PA (2000) Bioluminescent and doxycycline-regulatable HO-1 expression in type II pneumocytes via transpulmonary delivery. *Am J Physiol Lung Cell Mol Physiol* **278**: L1273–1279.

Wozney J, Mosen V, Celeste AJ, Mitsock LM, Whitters MJ, Kriz MJ et al. (1988) Novel regulators of bone formation: molecular clones and activities. *Science* **242**: 1528–1534.

SPECTRAL_0000705

Statistical Calibration of CCD Imaging Process

Yanghai Tsin *
Robotics Institute
Carnegie Mellon University
Pittsburgh, PA 15213

Visvanathan Ramesh
Imaging Department
Siemens Corporate Research
Princeton, NJ 08540

Takeo Kanade
Robotics Institute
Carnegie Mellon University
Pittsburgh, PA 15213

Abstract

Charge-Coupled Device (CCD) cameras are widely used imaging sensors in computer vision systems. Many photometric algorithms, such as shape from shading, color constancy, and photometric stereo, implicitly assume that the image intensity is proportional to scene radiance. The actual image measurements deviate significantly from this assumption since the transformation from scene radiance to image intensity is non-linear and is a function of various factors including: noise sources in the CCD sensor, as well as various transformations occurring in the camera including: white balancing, gamma correction and automatic gain control. This paper illustrates how careful modelling of the error sources and the various processing steps enable us to accurately estimate the "response function", the inverse mapping from image measurements to scene radiance for a given camera exposure setting. It is shown that the estimation algorithm outperforms the calibration procedures known to us in terms of reduced bias and variance. Further, we demonstrate how the error modelling helps us to obtain uncertainty estimates of the camera irradiance value. The power of this uncertainty modeling is illustrated by a vision task involving High Dynamic Range image generation followed by change detection. Change can be detected reliably even in situation where the two images (the reference scene image and the current image) are taken several hours apart.

1 Introduction

Charge-Coupled Device (CCD) cameras are used widely in computer vision systems. Many photometric algorithms, such as shape from shading [8], color constancy [11],and photometric stereo [15], implicitly assume that the image intensity is proportional to scene radiance. However, the CCD imaging process usually deviates from this ideal linear model. This is due to the fact that there are several independent sources of error in the sensor and that the operation pipeline in the camera includes additional operators such as color correction/white balancing and gamma correction. The camera non-linearities make the above mentioned vision algorithms to be systematically biased since they expect the real scene irradiance as input. Thus it is desirable to calibrate the process of imaging, including typical operations such as γ-correction and white balancing. Given a static scene with constant camera irradiance, the calibration procedure aims to estimate the camera response function, i.e. the mapping from the cross product space of image intensity and exposure time to camera irradiance, by acquiring images with multiple exposure settings. Since the irradiance is assumed to be constant within the acquisition period, the calibration step essentially estimates the response function by minimizing prediction disagreements across the images.

The calibration can be greatly improved if the noise characteristics and the various processing steps in the conventional CCD sensor are modeled carefully. In this paper we present a calibration technique that is motivated from statistical model of the transformation steps and errors in the CCD camera. It is shown that the model helps in obtaining accurate estimates of the camera response function, the scene radiance, and its uncertainty. We illustrate how the calibration results can be used in a vision operation sequence involving High Dynamic Range (HDR) image generation followed by illumination invariant change detection. The knowledge of uncertainty in the radiance is used to automatically setup the change detection measure threshold so that a given false alarm rate can be achieved. The paper is organized as follows. Section 2 describes the CCD imaging process and the error sources at various steps. Section 3 describes the probabilistic generative model for the image observations. Section 3.1 describes the statistical model and the iterative calibration algorithm. Section 4 describes the experiments performed on synthetic and real data to validate our calibration algorithm. Section 5 discusses the application of the calibration method to perform illumination invariant change detection. We conclude in section 6 with a discussion and outlook.

In this paper we denote true values of scalars as Roman

*The first author acknowledges the research fellowship from Siemens Corporate Research.

SPECTRAL_0000706

letters, such as g. Observations or estimates of a random variable are denoted with a hat, $\hat{g}$. Matrices and vectors are denoted by using bold face letters.

2 Imaging Process

Before we address the problem of estimating the camera response function, we first provide an overview of the nature of various transformations and error sources in a typical color CCD camera.

A typical CCD camera imaging process is shown in figure 1. The camera irradiance, i.e. the energy incident on the CCD is usually considered to be proportional to the attenuated scene radiance under normal weather conditions [8] . The lens system transmits this camera irradiance unevenly because of factors including: the $cos^4\theta$ *law* and *vignetting* [8]. Modern cameras usually correct the "$cos^4\theta$" distortion while the *vignetting* effect could be accounted for by calibration (see for instance [2]). The light energy transmitted through the lens system is then converted to electrons in the CCD array. In color CCD cameras, a red, green, blue filter array (called the *Bayer pattern*) is used in the sensor. Two rows in a *Bayer pattern* consists of a sequence of alternating red/green filter elements in one row followed by alternating green/blue filter elements in the subsequent row. The photoelectronic transformation is corrupted by various sources of errors (noise). For an excellent review the readers are referred to [7]. Due to manufacturing defects, the CCD well sizes fluctuate with a small variance. Thus, different CCD units output different voltage for the same light input. This phenomenon is called the *fixed pattern noise* and is usually modeled by a constant multiplier associated with each site. In addition, there is the *dark current* due to the thermal energy. The dark current usually adds a constant offset to the observed intensity, plus a small fluctuation which can be modeled as Gaussian noise. In this paper we will model the ideal CCD output, after scaled by the fixed pattern noise and offset by the dark current , as E. The CCD unit response is integrated over an exposure time t. Usually E is corrupted by the *shot noise* N_s and the thermal noise N_{c1}. The variance of the shot noise is proportional to Et. The output of the CCD unit can then be modeled as following.

$$\hat{E_1} = tE + N_s + N_{c1} \tag{1}$$

To obtain the color image values from the Bayer Image, some form of interpolation (e.g. bilinear interpolation) is carried out to obtain the full resolution color image [1]. This operation is followed by *white balancing* [17], a processing step that attempts to generate output images that are consistent with human perception of color under different illumination conditions. In this paper we will model white balancing as separate transformations on each channel involving the scaling of values and an offset. Now equation (1) can be rewritten as the following.

$$\hat{E_2} = aE + N_s + N_{c1} + b \tag{2}$$

Here a is the combined scaling factor that incorporates the scale due to white balancing and the exposure time.

To account for the non-linear transfer function relating the input voltage in the display monitor to the display brightness, γ *correction* is usually applied to the sensed image value. Considering other noise effects such as: quantization error, amplifier noise, D/A and A/D noise, as an additional noise term N_{c2} with a constant variance, we have the expression for the observed image measurements:

$$\hat{z} = f\left(aE + N_s + N_{c1} + b\right) + N_{c2} \tag{3}$$

3 Calibration algorithm

We are interested in the estimation of the inverse function $g = f^{-1}$. We call this function the $responsefunction$ of the imaging process. Using equation (3) and using a Taylor series approximation:

$$g(\hat{z}) \approx aE + N_s + N_{c1} + b + g'(\hat{z})N_{c2} \tag{4}$$

Without noise, the true values have the following relation.

$$g(z) = aE + b \tag{5}$$

We write the zero mean noise term as

$$N(a, \hat{z}) = N_s + N_{c1} + g'(\hat{z})N_{c2} \tag{6}$$

The variance of the noise term is given by

$$\sigma^2(a, \hat{z}) = aE\sigma_s^2 + \sigma_{c1}^2 + g'(\hat{z})^2\sigma_{c2}^2 \tag{7}$$

While the response function can be modeled by a continuous/smooth parametric function, we simplify the problem by following [5] to compute values of g at discrete values only. In this paper we will assume 256 gray levels are used.

Besides the error sources mentioned above, other factors contribute to deviations in the image measurements. These factors include, but are not limited to, the following: blooming, color aberration, and spectral sensitivity. The readers are referred to [16] for further discussion. In this paper we deal with blooming by removing the infected pixels, i.e. the pixels surrounding a saturated pixel within a certain radius. The radius is usually 3 pixels for our cameras and is chosen empirically. To perform the calibration of the imaging process, we essentially use the same idea as the approaches in [12], [5], and [14]. We assume a constant, but spatially varying, camera irradiance, E, (within the given acquisition time) at a given pixel. Under this assumption, it is clear that spatially varying errors such as fixed pattern noise, dark current noise and vignetting are not relevant since these spatial

SPECTRAL_0000707

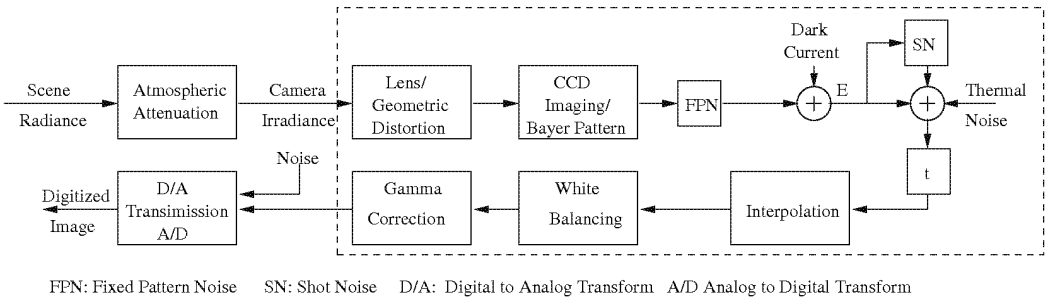


Figure 1: *CCD camera imaging pipeline*

variations are decoupled from the temporal random noise. The prediction of E can be done by using our statistical model from a collection of image measurements at a given pixel (with various exposure settings). When calibration of g, a and b is finished, other error sources can be calibrated using [7] and [2] . In this paper our focus is only on the estimation of the response function g, white balancing coefficients a and b.

We build upon the approaches of [5][14], with some major improvements. First, instead of considering a small group of representative pixels for calibration purposes, we will study all the valid pixels. Statistics on pools of pixels helps us to properly form and weight calibration functions. Second, we model white balancing explicitly to account for color correction that is carried out during the process of taking images. Third, the noise is modeled and the variance is computed. Consequently, when we construct our HDR image, the blending step involves a meaningful weight function and the output HDR map has an predictable variance map. Fourth, we realize the problem of *u-ambiguity* is worse than the authors of [14] have expected. Moderate noise level and small error tolerance bring their solution to a trivial one. We put constraints on the variations of exposure times to avoid the trivial solutions. The next subsection details the statistical estimation process.

3.1 Parameter estimation

The estimation problem will be formally defined in this section. Let $\mathcal{I}(x) = \hat{z}(x)$ denote the image measurement at a given spatial location x. A set of images $\mathcal{I}_1, \mathcal{I}_2, \ldots, \mathcal{I}_N$ of a static scene is taken under different exposure settings $t_1, t_2, \ldots, t_N$. Denote the observed intensity value in the kth image at pixel location x as $\hat{z}_k(x)$. At each pixel x, we observe a pixel trace over the N images $\hat{z}_1(x), \hat{z}_2(x), \ldots, \hat{z}_N(x)$. They all correspond to the same unknown $E(x)$. Denote by $\mathcal{P}(k, \hat{z}, \epsilon) = \{x : \|\mathcal{I}_k(x) - \hat{z}\| < \epsilon\}$, the *pool* of pixels in the kth image that centered at $\hat{z}$ with a radius ϵ. Then from equations (4) and (6):

$$g(\hat{z}_k(x)) = E(x)a_k + b_k + N(a_k, \hat{z}_k). \tag{8}$$

The objective is to obtain the maximum-likelihood estimate of the response function $g(.)$, a_k, b_k and $E(x)$. This is done in an iterative fashion. Let $\hat{g}^{(j)}(.)$, $\hat{a}_k^{(j)}$, $\hat{b}_k^{(j)}$ denote the estimates at the start of the j'th iteration. Given these values it is possible to predict $\hat{E}^{(j)}(x,k), k = 1, \ldots, N$ and the weighted average of these predictions across the pixel trace provides the iteration estimate (of the true unknown scene radiance $E(x)$), $\hat{E}^{(j)}(x)$ as seen in equation (9). The weights are set to a constant value in our calibration process.

$$\begin{aligned} \hat{E}^{(j)}(x,k) &= \frac{\hat{g}^{(j)}(\hat{z}_k(x)) - \hat{b}_k^{(j)}}{\hat{a}_k^{(j)}}, k = 1, 2, \ldots, N \\ \hat{E}^{(j)}(x) &= \sum_{i=1}^{N} \hat{w}_i^{(j)} \frac{\hat{g}^{(j)}(\hat{z}_i(x)) - \hat{b}_i^{(j)}}{\hat{a}_i^{(j)}} \end{aligned} \tag{9}$$

Given the new estimates for the scene radiance, we can recover the residuals $\hat{e}_k^{(j)}(x, \hat{z}_k)$, and the mean error across pools $\hat{e}_k^{(j)}(\hat{z}_k)$. In addition, we can recover the standard deviation of the errors in scene radiance estimate $\hat{\sigma}_k^{(j)}(\hat{z}_k)$ by using the residuals in each pixel pool. To deal with outliers we use robust versions of the above estimates. For example, we use the 66 percent trimmed mean in our estimation step involving $\hat{e}_k^{(j)}(\hat{z}_k)$ (see equation (11)). Note that $\phi(.)$ in this equation corresponds to the trimmed mean estimator. In addition, in equation (12) $\hat{\sigma}_k^{(j)}(\hat{z}_k)$ uses the median of the residuals to estimate the standard deviation.

$$\hat{e}_k^{(j)}(x, \hat{z}_k) = \hat{a}_k^{(j)} \hat{E}^{(j)}(x) + \hat{b}_k^{(j)} - \hat{g}^{(j)}(\hat{z}_k) \tag{10}$$

$$\hat{e}_k^{(j)}(\hat{z}_k) = \phi(\hat{e}_k^{(j)}(x, \hat{z}_k), x \in \mathcal{P}(k, \hat{z}, \epsilon)) \tag{11}$$

$$\begin{aligned} \frac{1}{\hat{w}_k^{(j)}} &= \hat{\sigma}_k^{(j)}(\hat{z}_k) \\ &= c \cdot \underset{x \in \mathcal{P}(k, \hat{z}, \epsilon)}{median} \|\hat{e}_k(x, \hat{z}_k) - \hat{e}_k^{(j)}(\hat{z}_k)\| \end{aligned} \tag{12}$$

SPECTRAL_0000708

Denote by $e_k(\hat{z}_k)$ the theoretical errors at each iteration as a function of $\Delta g(.)$, Δa, and Δb, then it can be shown that:

$$\begin{aligned} & e_k(\hat{z}_k) = \mu\left(e_k(x, \hat{z}_k)\right) \\ \approx & \sum_{i \neq k} w_i \frac{a_k}{a_i} \left[\Delta g(\hat{z}_i(x)) - \Delta b_i - E\Delta a\right] \\ & + (w_k - 1)\left[\Delta g(\hat{z}_k) - \Delta b_k - E\Delta a_k\right] \\ \stackrel{\text{def}}{=} & \mathcal{F}(\Delta\mathbf{g}, \Delta\mathbf{a}, \Delta\mathbf{b}, \hat{z}_k, k) \end{aligned} \tag{13}$$

The constant c in (12) is affected by two issues. First, a correction factor has to be applied since a robust estimate of σ is obtained by taking the median of the absolute deviations. This factor is 1.483 for the Gaussian distribution. A second factor has to be multiplied to correct for the correlations induced by the Bayer pattern in the color image. For color images, neighboring pixels are usually correlated due to interpolation of the Bayer pattern. While independence can be achieved by pre-selection of pixels, we model the impact of the correlations on our variance prediction and correct for it. This correction factor can be shown to be 1.265 for green bands and 1.333 for red and blue bands.

Define the updates $\Delta\mathbf{g}$, $\Delta\mathbf{a}$ and $\Delta\mathbf{b}$:

$$\begin{aligned} & \Delta\mathbf{g} = \{\Delta g(z)\}, z = 1, 2, \ldots, 256, \\ & \Delta\mathbf{a} = a_i, i = 1, 2, \ldots, N, \; and, \\ & \Delta\mathbf{b} = b_i, i = 1, 2, \ldots, N \end{aligned} \tag{14}$$

The update step at each iteration involves the computation of the updates by determining:

$$\underset{\Delta\mathbf{g}, \Delta\mathbf{a}, \Delta\mathbf{b}}{\mathbf{argmin}} \sum_{k, \hat{z}_k} \frac{\left(\hat{e}_k^2(\hat{z}_k) - \mathcal{F}(\Delta\mathbf{g}, \Delta\mathbf{a}, \Delta\mathbf{b}, \hat{z}_k, k)\right)^2}{\hat{\sigma}_k^2(\hat{z}_k)} \tag{15}$$

and updating the current estimates:

$$\begin{aligned} \hat{\mathbf{g}}^{(j+1)} &= \hat{\mathbf{g}}^{(j)} - \eta\Delta\mathbf{g} \\ \hat{\mathbf{a}}^{(j+1)} &= \hat{\mathbf{a}}^{(j)} - \eta\Delta\mathbf{a} \\ \hat{\mathbf{b}}^{(j+1)} &= \hat{\mathbf{b}}^{(j)} - \eta\Delta\mathbf{b} \end{aligned} \tag{16}$$

At the end of the iterations, we use the relationship given by (7) to obtain a system of linear equations relating the parameters σ_{c1}, σ_{c2}, and σ_s to $\sigma^2(a, z)$. The estimates $\hat{\sigma}_k(\hat{z}_k)$, $\hat{g}(.)$, $\hat{E}(.)$, and $\hat{a_k}$ are used as measurements and a least squares fitting step is used to estimate the unknown CCD sensor parameters. The system of equations relating the ideal parameters is given below:

$$\sigma_k^2(\hat{z}_k) = \sum_{i \neq k} w_i^2 \sigma^2(a_i, z_i) + (w_k - 1)^2 \sigma^2(a_k, \hat{z}_k) \tag{17}$$

After the calibration has finished, and the variances of the noise estimated, the HDR image can be blended using (9). The weighting function is given by

$$w_k = \frac{a_k / \sigma(a_k, \hat{z}_k)}{\sum_i a_i / \sigma(a_i, \hat{z}_i)} \tag{18}$$

The standard deviation of scene radiance estimation (9) is given by

$$\sigma_E(x) = \frac{\sqrt{N}}{\sum_i a_i / \sigma(a_i, \hat{z}_i)} \tag{19}$$

3.2 Iterative Calibration Algorithm

While the above estimation algorithm is in theory reasonable, we have to adapt it to address practical considerations. First, there are several types of known outliers in a typical digitized image,including boundary pixels and blooming contaminated pixels. They can be easily identified and the corresponding pixels can be taken care of by preprocessing the input image. Equations of form (13) must be properly constrained to avoid trivial solutions. Notice that what we are going to recover is the affine transformed version of the original scene radiance. The true scene radiance remains unknown without first calibrating for the spatial variations and the dark current. Therefore, a shifted and scaled version of $g(z)$ gives the same consistency over different images. To fix the ambiguity, it is necessary to fix the values of two points of the response function. Let the two points be x_1 and x_2. $\Delta g(x_1)$ and $\Delta g(x_2)$ are set to zero once $g(x_1)$ and $g(x_2)$ have been initialized. A further ambiguity arises when different b_k's are allowed for different images. For instance, when we add a value $c \cdot a_k$ to b_k, different images agree the same . To remove this ambiguity, we fix one of the b_k's and let $\Delta b_k = 0$. These constraints can be used directly by setting appropriate values to zeroes in the equations of form (13).

In [14] the authors mentioned the so called $u - ambiguity$ arose when both $\mathbf{g}$ and $\mathbf{a}$ are allowed to change. Consider the case when $b_k = 0$ for all k. The ideal imaging process becomes $g(z) = Ea$. It is easy to see that the imaging process can also be interpreted as scene E^u scaled by a^u, with corresponding response curve $g^u(z)$. In one extreme case, $u = 0$, the response curve is flat, and all the a_k's are the same. This will make arbitrary images "agree" on each other. Mitsunaga and Nayar ([14]) claimed that their polynomial formulation alleviates this ambiguity if the true response curve is indeed a polynomial. However, the true response curve can seldom be represented exactly by a low degree polynomial. The model approximation error translates to a larger variance in the estimated response function. This problem is fundamental and cannot be solved without ground truth of the scene radiance. In our algorithm, we bound the changes in the scaling factors by placing *a priori* knowledge on them. For example, we punish large deviations of a_i from the nominal exposure times. For electronically controlled shutters and small white balancing, this is usually a reasonable assumption.

Finally, we put smoothness and monotone constraints on the response function. To enforce smoothness we add an ex-

SPECTRAL_0000709

tra term $\lambda \sum_{k=2}^{254} (\Delta g(k-1) - 2\Delta g(k) + \Delta g(k-1))$ to the cost function (15). Usually the response curve is monotonically increasing. Algorithms to solve order constrained optimization problem are within the field of isotonic regression [3] . To simplify the problem we post process the estimated response function by *pool-adjacent-violators (PAV)* algorithm. More rigorous algorithms, such as quadratic-programming should be used if the order constraint is to be imposed along with the optimization.

The algorithm can now be summarized as follows:

1. Preprocess the image. This involves:
   - Taking out all the outlier pixels;
   - Building a look up table to all the pooled pixel sets $\mathcal{P}(k, \hat{z}, \epsilon)$;
   - Building pixel traces, and estimating the most likely intensity values that correspond to a pool under a given exposure. This is done by taking the median of the intensity values of the pooled pixels for a given exposure.
2. Initialize the response curve to be a straight line passing through the fixed point x_1 and x_2. Set the initial scale factors a_i to be the nominal exposure times, and the initial offsets to be all zeros. For color images, each channel has its own g,a and b. Each channel is calibrated separately.
3. Build HDR using (9). In the place of g, a and b use current estimate.
4. Calculate the prediction error for each pixel using (10).
5. Estimate $\hat{e}_k(\hat{z}_k)$ and $\hat{\sigma}_k^2(\hat{z}_k)$ from equations (11) and (12). Form equations of (13) and (17) for each pool of pixels.
6. Enforce smoothness constraints. The constraints $\Delta g(x_i) = 0, i = 1, 2$ can be approximated by linear equations $K\Delta g(x_i) = 0$, where K is a large number.
7. Solve for Δg, Δa and Δb,σ_s, σ_{c1}, and σ_{c2} by using equations (15) and (17).
8. Update $\hat{g}$, $\hat{a}$ and $\hat{b}$ using (16);
9. Impose monotonic constraints by pool-adjacent-violator (PAV) algorithm.
10. Iterate 3 until the 1-norm of $\mathbf{\Delta g}$ is smaller than error tolerance.

4 Experiments

4.1 Simulated Images

In each sequence eight images were generated. Consecutive images had exposure ratio of $\sqrt{2}$. The response function was $g(z) = (z/255)^{1.2}, z = 0, 1, 2, \ldots, 255$. The radiance E was designed to have uniform distribution in $[0, 1]$. Pixel pools on average had about 200 elements. Pools with at least 100 pixels were considered. The noise levels were set to be $\sigma_s = 0.015$, $\sigma_{c1} = 0.01$ and $\sigma_{c2} = 1$. These noise terms were chosen to simulate real camera noises.

To compare our algorithm with that of [5] and [14], 50 sequences were produced without white balancing. We applied all three algorithms on the same data set.

For each algorithm, response functions estimated from the 50 sequences were compared with the true one. Average and standard deviation of the response function error were computed. Though the algorithms of [5] and [14] had already achieved high accuracy, less than 0.5% at high intensity end, our algorithm showed further improvement in terms of reduced bias 2(a) and variance 2(b).

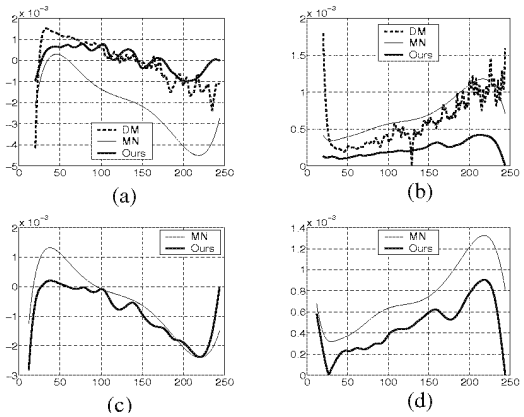


Figure 2:
Comparison on the response function estimation error: First row, estimation errors without white balancing; second row, with white balancing. (a)(c) average estimation errors for the 50 sequences; (b)(d) standard deviation of the estimation errors.

In addition to the response function, our algorithm output estimation of the variance term. The average estimated σ_s, σ_{c1} and σ_{c2} were 0.0150, 0.0101, and 0.8617, with standard deviation 0.0004, 0.0003 and 0.3839. We didn't use any constrained optimization on the variance terms. 4 out of 50 sequences output negative value on σ_{c2} and were forced to be 0 after optimization. If the 4 sequences were taken out, average of the variance term σ_{c2} for the remaining 46 sequences were 0.9366 with standard deviation 0.2978.

Readers should realize the limitations of the noise model

SPECTRAL_0000710

(7). When calibrated, $aE \approx g(z)$ for a given pixel. If $g(z)$ has similar function form as $g'(z)^2$, it is not easy to discriminate the individual contributions of σ_s^2 and σ_{c2}^2. For example, when $g(z) = z^2 = g'(z)^2$, it is impossible to quantify shot noise individually. In such case, however, the total noise variance can still be estimated by combining σ_s^2 and σ_{c2}^2.

Next, 50 sequences with white balancing introduced were studied. Our algorithm was able to recover both the scale factor and offset reliably. The nominal scale factor a was multiplied by a Gaussian random variable with mean 1 and standard deviation 0.05 and was provided to the program. Our algorithm was able to recover the scale factor to the accuracy of 0.5% in the above mentioned noise settings. Our algorithm also recovered the offset factor reliably. The extent to which the offset can be recovered especially depends on the noise term N_{c1}. In all the cases, the larger the pixel pool size, the better the accuracy on estimation. Performance of [14] were comparable (see figure 2(c)(d)). Our algorithm has smaller deviations.

4.2 Real Images

We took 21 sequences of outdoor images using a Sony EVI 330 camera. One representative image is shown in figure 3(a). We changed shutter speed ranging from $1/60$ to $1/10000$ in 14 stops to capture the high dynamic scene. Figure 3(b) is the pixel pool size histogram of the image in (a).

Figure 3(c) shows the histogram of the prediction error $e_k(x, \hat{z}_k)$ in the pool centered at 199 before calibration. Initially the bias is large, about 30% relative error. After a couple of iterations our algorithm is able to bring the whole pool to very small bias 3(d).

Estimated response curves for the sequence in figure 3(a) are shown in 3(e). Curves of the three channels are superimposed and it is interesting to observe that the three curves are very close to each other despite that they were estimated independently. Figure 3(f) shows the results of camera variance estimation step using the model equations (17). Over the 21 sequences, the average estimated σ_s, σ_{c1}, σ_{c2} are 0.0138, 0.0037,0.9965 for the green channel, with standard deviation 0.0025,0.0007, and 0.5473 respectively.

We further tested our algorithm on the Cathedral sequence down-loaded from the web site of Debevec [5]. As a comparison, we ran the code of both [5] and [14] on the set of images. The estimated response curves and the blended HDR images were then used to test the prediction agreement (10)(11) of different images. Representative prediction errors are shown in figure (4). Our algorithm gives much better accuracy than those of [5] and [14].

We don't have ground truth white balancing information for our data set. However, we frequently observed much improved agreement across images when scale and offset

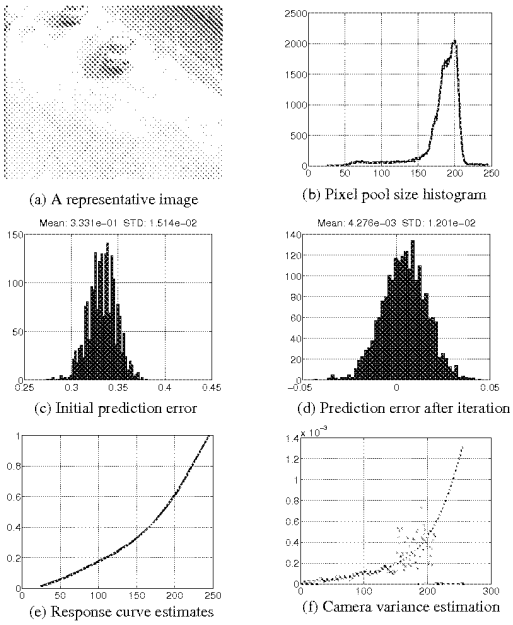


Figure 3:
Calibration of a Sony camera. See text for explanations..

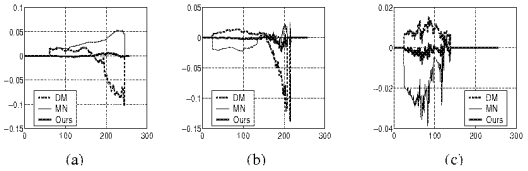


Figure 4:
Real image results: (a)-(c) prediction errors for images 1,6 and 12 in the Cathedral sequence.

factors are allowed to be calibrated. Intuitively scale factors change the slope of curves shown in figure 4, and offset factors shifts the curves in vertical direction. Our better performance in the Cathedral sequence is largely due to these extra degrees of freedom.

5 Application: Illumination Invariant Change Detection

Since our calibration provides an uncertainty estimate of $E(x)$, we believe it is possible to make use of this information to demonstrate significant improvements of various vision algorithms such as change detection, color constancy, etc. In this paper, we address the problem of change detection under varying illumination.

For simplicity we only consider the case of static Lambertian scene, static camera, and planar background. In our

SPECTRAL_0000711

example we took a sequence of images of a empty parking lot. Hours later we took a second set of images. In both cases images were calibrated, and HDR images with uncertainty model were obtained. Two such images are shown in figure (5a,c). Our goal is to detect the parked cars under significantly changed lighting while having the ability to discriminate shadow from the changes due to reflectance.

Past works have shown that the illumination change can be modeled as linear transformations in the RGB space (see for instance [20]). The argument is supported by early research that the surface reflectance can be represented by low dimensional linear systems [10]. Representing the measured color vector at a pixel x as a row vector $E(x) \in \mathcal{R}^{1\times 3}$, and the radiance of the same pixel under a different illumination as $E'(x)$, the authors of [20] claimed $E'(x) = E(x)\mathbf{M}, \mathbf{M} \in \mathcal{R}^{3\times 3}$. If a population of K pixels are coplanar in the 3D world, and they are illuminated by the same light source in each case, they all obey the same transformation $\mathbf{M}$. The transformation can be estimated using the observed radiance at these pixels. Thus we can stack all the color vectors into two $K \times 3$ matrices $\hat{\mathbf{E}}$ and $\hat{\mathbf{E}}'$, and we have the system of equations:

$$\hat{\mathbf{E}}\mathbf{M} = \hat{\mathbf{E}}' \tag{20}$$

The estimate $\hat{\mathbf{M}}$ that minimizes the error in a least squares sense can be computed.

Let $\hat{\mathbf{E}} = \mathbf{E} + \mathbf{N_E}$ and $\hat{\mathbf{E}}' = \mathbf{E}' + \mathbf{N}'_{\mathbf{E}}$. Here $\mathbf{E}$ is composed of the true radiance and $\mathbf{N_E}$ is composed of zero mean independent random variables whose variances are estimated by (19). Using standard perturbation analysis techniques [18] (i.e. first order error propagation) the covariance matrix of the prediction error at a given pixel x, $e(x) = \hat{E}(x)\mathbf{M} - \hat{E}'(x)$, can be calculated as a function of Σ_E and $\Sigma_{E'}$ and the E and E'.Here $\hat{E}(x)$ and $\hat{E}'(x)$ corresponds to 1 by 3 data vectors.

Given the prediction error $e(x)$ and the covariance $\Sigma(e(x))$, the test statistic: $d^2 = e(x)'\Sigma^{-1}(e(x))$ has a χ^2 distribution with 3 degrees of freedom. However, in our situation, we have to use $\hat{\Sigma}$, the estimate of the true unknown covariance matrix evaluated at $\hat{E}(x)$ and $\hat{E}'(x)$. Thus, the test statistic calculated, $\hat{d}^2$, is only approximately χ^2. A more closer look points out that $\hat{d}^2$ is distributed as the sum of two random variables one having a χ^2 distribution with 3 degrees of freedom and another having the distribution of the quadratic form $e(x)'\Delta\Sigma e(x)$. Here $\Delta\Sigma$ corresponds to the error in the covariance matrix estimate. This is verified in our real experiments (Please see figure 6). Thus, it is necessary to have an additional empirical estimation step to estimate the mapping between probability of false alarm and the threshold.

In the above discussion, we mainly considered all pixels in a given surface patch with same illumination effect. In reality, we don't know clustering of the pixels according to change of reflectance or illumination distribution before hand. This is exactly the problem to be solved. Estimating the transformation matrix in (20) requires such clustering information. To deal with this dilemma we adopted robust estimation algorithms. The basic idea is to iteratively partition the data into clusters through the use of robust techniques that can detect and handle outliers. We use the least trimmed sum of squares(LTS) [13] [19] to give an initial guess of the largest region with same illumination effect. The M-estimator [9] is then used to refine the estimation. When the estimation of M converges, all the pixels obeying this transformation are considered to be within the same cluster. For example, in figure 5(d), all pixels in region A is identified as belonging to the same cluster because they were previously lit by morning skylight (figure 5)(a) and now by sunlight (figure 5(b)). Color changes of the remaining pixels are due to another lighting, the skylight, or parked car. To detect shadows we re-apply the estimation technique to identify the next cluster of pixels among the non-labelled pixels. Shadows of different shade are detected in the second and third run. At each step the test statistic $\hat{d}^2$ is measured for the cluster pixels and the iterations stop when this test statistic is greater than the chi-square threshold discussed above. In the example, the pixels that are labelled black are considered "change".

The detected changes and shadows are shown in figure (5d). Despite dramatic change in light spectrum and intensity, shadows and parked cars are successfully detected. We applied the algorithm on 21 other HDR images that were taken as much as 10 hours apart from the time the reference images was taken. We get good results for all the cases.

From theory, the mean of the $\hat{d}^2$ test statistic in the "unchanged" regions should be approximately 3 (assuming zero mean error for $\Delta\Sigma$). We computed this value for the dominant background cluster for the 21 images. The population mean is 3.3792 with the standard deviation of this estimate being 0.5064. For each of the 21 sequences we plotted the distribution of the χ^2 value against the theoretical value in figure 6. The estimated probability density function matches well with the theoretical predictions [1].

6 Conclusion

In this paper we proposed a statistical method to calibrate the imaging process. We use a statistical model of the measurement errors in a CCD camera that accounts for various transformations in the sensor. We proposed an iterative non-linear estimation algorithm to estimate the camera response function, the white balancing coefficients, and the scene irradiance predictions. We verified the correctness of the al-

[1] Theory predicts that there will be some discrepancy between the chi-squared distribution and the observed distribution

SPECTRAL_0000712

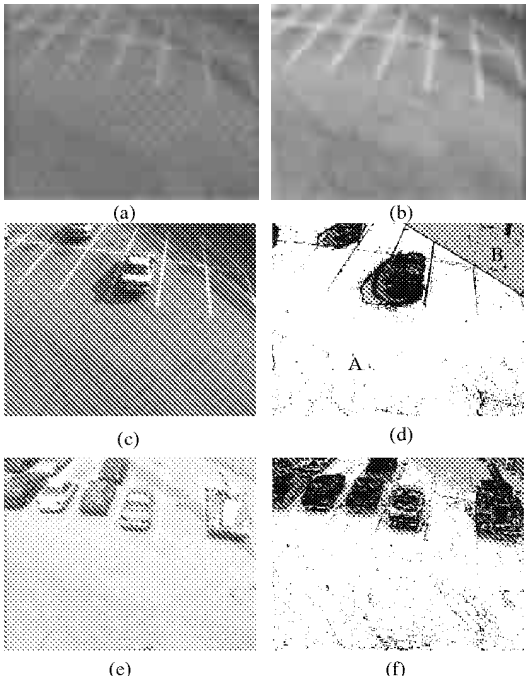


Figure 5: *Change detection under varying illumination. (a) Reference image, taken at 7:00. (b) The predicted image: what the background would look like if it is lit by sun at 9:20 of that day. (c) Target image, taken at 9:20 of the same day. (d) Detected changes: light and dark gray: different shades of shadows. Black: change. (e) Another target image, taken at 14:30 of the same day. (f) detected change at 14:30.*

gorithm through extensive simulations and by experiments on real data. A major aspect of the proposed method is that estimates of the uncertainties of irradiance estimates are also obtained. These uncertainties can be used to improve the robustness of computer vision methods. We used illumination invariant long-term change detection in outdoor environments as an example to illustrate this aspect of the work. The change detection algorithm here considered only the most simple case: flat background, fixed camera and static scene. However, the method can be extended to treat more general cases. For example, we can combine our algorithm with SSD method [6] to register two images of the same scene under different illumination. Under varying lighting, the registration algorithm can be used for object recognition, memory based robot localization, color constancy.

7 Acknowledgement

We thank Dr. Sathyakama Sandilya for valuable comments that helped improve the paper.

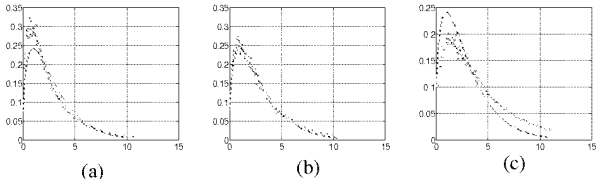


Figure 6: χ^2 *distribution: estimation versus theory. (a)-(c) clearly showed that* $\hat{d}^2$ *is only approximately distributed as a chi-square distribution with 3 degrees of freedom.*

References

[1] J. E. Adams, "Design of Practical Color Filter Array Interpolation Algorithms for Digital Cameras", *Proceeding of SPIE*vol. 3028, pp 117-125

[2] N. Asada, A. Amano and M. Baba, "Photometric Calibration of Zoom Lens Systems", *Proc. of IEEE International Conference on Pattern Recognition:, 1996.*

[3] R.E. Barlow, D. J. Bartholomew, J.M.Bremner and H. D. Brunk, *Statistical Inference under Order Restrictions* . John Wiley & Sons, 1972.

[4] V. Brajovic, R. Miyagawa, and T. Kanade, " Temporal Photoreception for Adaptive Dynamic Range Image Sensing and Encoding," *Neural Networks, Vol. 11, No. 7-8, October, 1998, pp. 1149-1158.*

[5] P. E. Debevec, J. Malik, "Recovering High Dynamic Range Radiance Maps from Photographs", *In SIGRAPH '97.*

[6] G.D. Hager and P.N. Belhumeur,"Efficient Region Tracking With Parametric Models," *IEEE Trans. on Patt. Analysis and Machine Intelligence, 20(10):1025–1039, 1998.*

[7] G. E. Healey, R. Kondepudy, "Radiometric CCD Camera Calibration and Noise Estimation", *IEEE Transaction on Pattern Recognition and Machine Intelligence, Vol. 16, No. 3, March 1994.* ;

[8] B.K.P.Horn, *Robot Vision* . MIT Press, Cambridge. 1986.

[9] P. J. Huber, *Robust Statistics* . New York, Wiley, 1980.

[10] L. T. Maloney, "Evaluation of linear models of surface spectral reflectance with small numbers of parameters", *J. Opt. Soc. Am.* A/Vol. 3, No. 10, October 1986.

[11] L. T. Maloney and B. A. Wandell, " Color Constancy: a method for recovering surface spectral reflectance," *Journal of the Optical Society of America",* A, 3(1):29-33, 1986.

[12] S. Mann and R. W. Picard, "Being 'Undigital' with digital cameras: Extending Dynamic Range by Combining Differently Exposed Pictures", *IS&T 48th Annual Conference.*

[13] P. Meer, "Robust Techniques for Computer Vision,", Tutorial at the *1997 Computer Vision & Pattern Recognition Conference, San Juan, Puerto Rico.*

[14] T. Mitsunaga, S. Nayar, "Radiometric Self Calibration", *CVPR '99.*

[15] S. Nayar, K. Ikeuchi, and T. Kanade, "Shape from Interreflections," *Int'l Journal of Computer Vision, vol. 6, no. 3, 1991, pp. 73-195.*

[16] C. L. Novak, S. A.Shafer, and R. G. Wilson, "Obtaining accurate color images for machine vision research," in *Proc. SPIE Conf. Perceiving, Measuring and Using Color,* Santa Clara, CA, Feb. 1990.

[17] D. Qian, J. Toker and S. Bencuya, "An Automatic Light Spectrum Compensation Method for CCD White Balance Measurement," *IEEE Trans. Consumer Electronics, Vol. 43, No. 2 May 1997, pp. 216-220.*

[18] G. S. Rogers, *Matrix Derivatives,*, Marcel Dekker, inc, New York, 1980.

[19] P. J. Rousseeuw, *Robust regression and outlier detection* , Annick M. Leroy, 1987.

[20] D. Slater and G. Healey, "The Illumination Invariant Matching of Deterministic Local Structure in Color Images," *IEEE Transaction on Pattern Analysis and Machine Intelligence,*Vol. 19, No. 10, October 97.

SPECTRAL_0000713

Neoplasia • Vol. 2, Nos. 1–2, January-April 2000, pp. 41–52 41
www.nature.com/neo

Use of Reporter Genes for Optical Measurements of Neoplastic Disease *In Vivo*[1]

Christopher H. Contag, Darlene Jenkins†, Pamela R. Contag†* and Robert S. Negrin‡*

Departments of *Pediatrics and ‡Medicine, Stanford University Medical Center, Stanford University, Stanford, CA; †Xenogen Corporation, 860 Atlantic Avenue, Alameda, CA

Abstract

Revealing the cellular and molecular changes associated with cancer, as they occur in intact living animal models of human neoplastic disease, holds tremendous potential for understanding disease mechanisms and elucidating effective therapies. Since light is transmitted through mammalian tissues, at a low level, optical signatures conferred on tumor cells by expression of reporter genes encoding bioluminescent and fluorescent proteins can be detected externally using sensitive photon detection systems. Expression of reporter genes, such as the bioluminescent enzyme firefly luciferase (Luc) or variants of green fluorescent protein (GFP) in transformed cells, can effectively be used to reveal molecular and cellular features of neoplasia *in vivo*. Tumor cell growth and regression in response to various therapies have been evaluated non-invasively in living experimental animals using these reporter genes. Detection of Luc-labeled cells *in vivo* was extremely sensitive with signals over background from as few as 1000 human tumor cells distributed throughout the peritoneal cavity of a mouse with linear relationships between cell number and signal intensity over five logs. GFP offers the strength of high-resolution *ex vivo* analyses following *in vivo* localization of the tumor. The dynamic range of Luc detection allows the full disease course to be monitored since disease progression from small numbers of cells to extensive disease can be assessed. As such, therapies that target minimal disease as well as those designed for late stage disease can be readily evaluated in animal models. Real time spatiotemporal analyses of tumor cell growth can reveal the dynamics of neoplastic disease, and facilitate rapid optimization of effective treatment regimens. Thus, these methods improve the predictability of animal models of human disease as study groups can be followed over time, and can accelerate the development of therapeutic strategies. *Neoplasia* (2000) **2,** 41–52.

Keywords: luciferase, photon counting, non-invasive, imaging, *in vivo*, CCD.

Introduction

Development of neoplastic disease is a stepwise process involving loss of genetic regulation, changes in cellular physiology, and failure of effective immune surveillance [1–9]. The progression of neoplastic states to disseminated disease requires interactions between the transformed cells and normal tissues as occurs in invasion, extravasation, migration and neovascularization [10–12]. Although individual steps in these processes may be modeled in correlative cell culture assays, evaluation of the dynamic and interactive processes of the complete disease requires the context of living animals. However, animal models have typically served as "black boxes" where well-defined signals can be applied, but the ultimate evaluation is performed outside of the animal via *ex vivo* assays. Sophistication of these *ex vivo* assays has increased dramatically with the development of confocal and two-photon microscopy for the interrogation of thick tissues, reporter proteins with diverse optical signatures, multiparameter flow cytometry and DNA microarrays [13–20].

Tremendous sensitivity can be achieved using amplification methods such as polymerase chain reaction (PCR) to detect tumor cell DNA or mRNA levels, but these assays are time-consuming and severely limited by the size of the sample that can be reasonably evaluated. Thus, the fraction of a given tissue that can be analyzed is limited [21,22]. Studies employing these assays may, therefore, be subject to sampling biases such that results may not represent overall expression levels in the target tissue or organ. In the absence of a signal that can be detected in the intact animal, or even the intact organ, targeting specific tissues for analyses is also difficult, and all tissues cannot be evaluated. Thus, only a small fraction of a few selected tissues is studied when *ex vivo* assays are employed. To achieve statistical significance with temporal studies, large numbers of animals are used with groups being sacrificed at each time point. Thus, analyses using *ex vivo* assays are both limited and require large numbers of animals.

Address all correspondence to: Dr. Christopher H. Contag, Department of Pediatrics, Stanford University, Stanford, CA. E-mail: ccontag@cmgm.stanford.edu

[1]This work was funded, in part, through grants from a Translational Award from The Leukemia Society (609099), the National Cancer Institute (R01 CA80006), and unrestricted gifts from the Mary L. Johnson and Hess Research Funds.
Received 29 November 1999; Accepted 14 December 1999.

Copyright © 2000 Nature America, Inc. All rights reserved 1522-8002/00/$15.00

SPECTRAL_0000714

The limitations of the *ex vivo* assays indicate that accessible, versatile and sensitive assays that can rapidly reveal cellular and molecular changes as they occur in intact animal models of human neoplasia are necessary to advance our understanding of disease processes and accelerate the development of effective intervention strategies. In particular, refinement of animal models to include markers for imaging the multiple stages of cancer development *in vivo* would complement current *ex vivo* assays and would dramatically accelerate and enrich the analyses of animal models of human neoplastic disease by revealing cellular and molecular changes *in vivo* and directing the *ex vivo* assays to critical target tissues.

A variety of imaging strategies designed to reveal the physiologic changes associated with neoplasia and response to therapy have been described. The modalities utilized in these approaches include fluorescence imaging, magnetic resonance imaging (MRI), single photon emission computed tomography (SPECT), and positron emission tomography (PET) [23–34]. Contrast agents that enhance MRI are being developed and molecular reporter genes for MRI have enabled cellular and molecular analyses [35,36]. Similarly, fluorescent dyes that are concentrated at the tumor site or that can be activated by the target cell have been described and utilized to localize tumor cells in animal models [33,37,38]. PET is, by design, a method of revealing metabolic changes and can be used to localize cells and molecules labeled with radioactive tracers. However, many of these imaging strategies are not well-suited for small animals and can be encumbered by long scan times and expensive instrumentation for detection and support. In addition, some of these methods can be difficult to quantify and lack sensitivity.

Sensitive *in vitro* molecular assays have been developed using light-emitting enzymes, luciferases, as reporters [39–42]. Luciferases comprise a family of photoproteins that can be isolated from a wide variety of species including bacteria and a large number of eukaryotic organisms [43]. Luciferase from the firefly, *Photinus pyralis*, is the most commonly used photoprotein in molecular biology studies and has been used to evaluate gene expression in transformed cell lines in culture [44,45], and to monitor tumor growth and response of tumors to antineoplastic therapy in animal models of human disease [21,46]. This reporter gene is not only the most widely used member of the photoprotein family of enzymes; it is also the most-studied and has been modified such that it is well suited for studies of neoplastic disease. These modifications include mutations for optimal mamma-

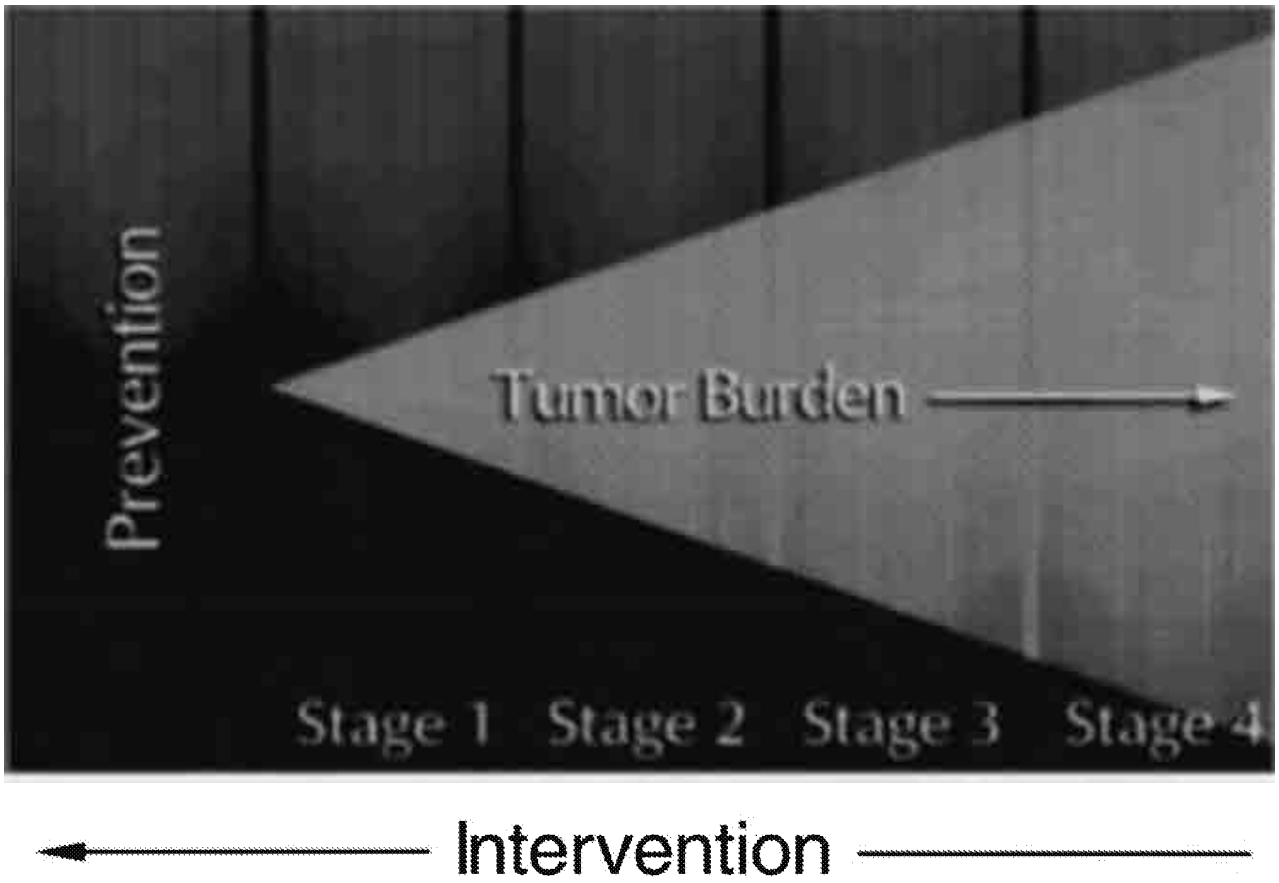


Figure 1. *New developments in cancer therapy. With the advancement of diagnostics and therapy, there is a need to develop new therapies that target small numbers of tumor cells to prevent both initiation of disease and relapse after treatment. Therefore, development of animal models that represent minimal disease is necessary to evaluate new therapeutic strategies that target these conditions.*

SPECTRAL_0000715

lian codon usage and increased expression due to removal of a peroxisome targeting site [41,42]. These features of the firefly enzyme make it an ideal choice for *in vivo* monitoring of tumor cell growth. Another luciferase that has been used as a reporter in mammalian cells includes that from the sea pansy (*Renilla reniformis*). The wavelength of emission from this enzyme (blue, with a peak at 460 nm) and its use of a substrate other than luciferin have led to its use in dual-reporter assays [47,48]. Many luciferases from bioluminescent marine organisms, including that of *R. reniformis*, use the high-energy compound, coelenterazine, as a substrate. Analyses of these photoproteins as indicators of gene expression have, in the past, required removal of the tissues and assessment of enzymatic activity in cell lysates. This type of assay has many of the same limitations as other *ex vivo* assays; however, the fact that light can pass through

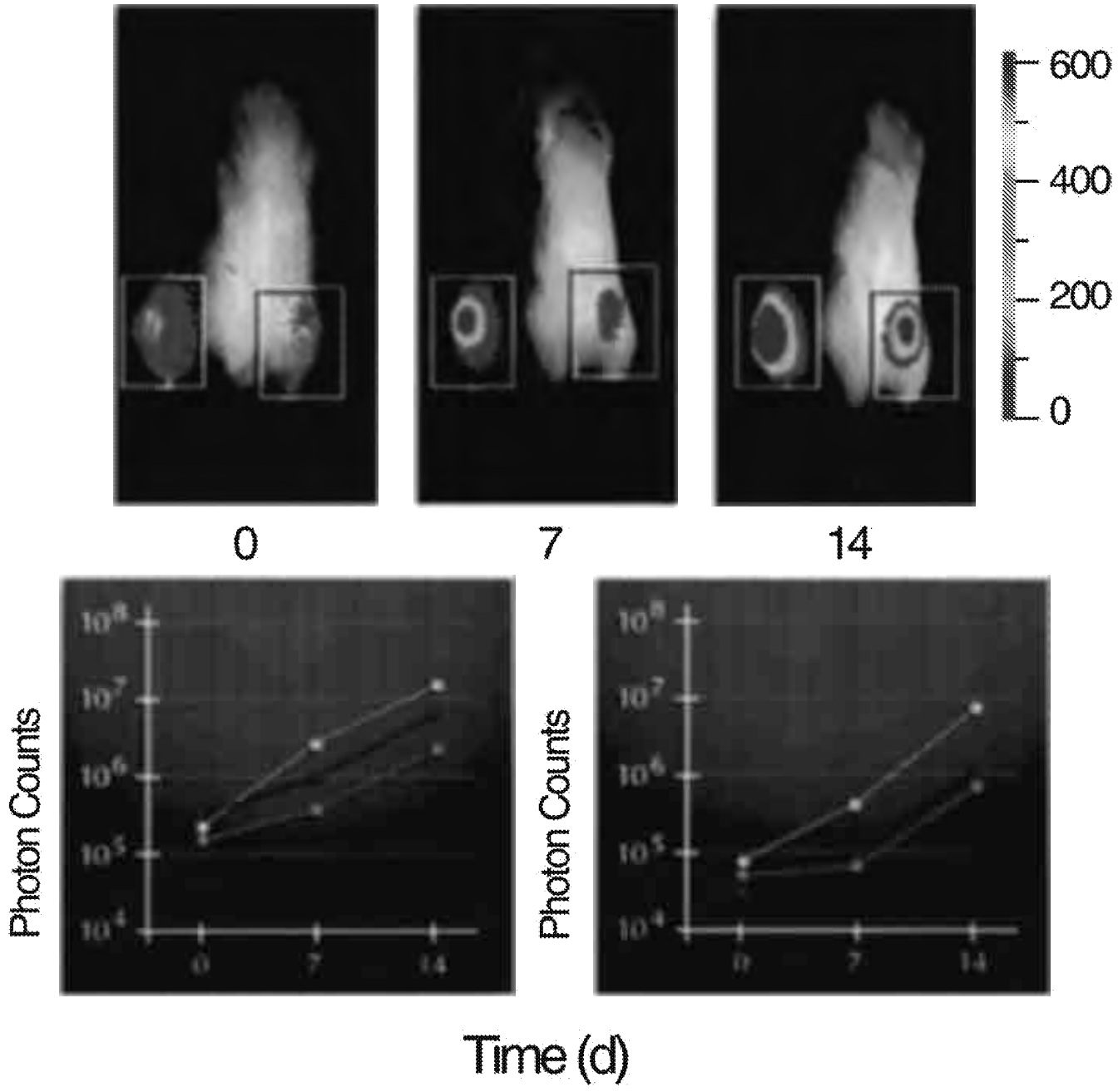


Figure 2. *Monitoring tumor growth at subcutaneous sites. PC-3M cells labeled with constitutive expression of a modified luciferase gene (PC-3M-luc) were injected at subcutaneous sites on each hind flank of three animals and growth of the cells was monitored by photon emission over a 14-day time course. A pseudocolor image representing light intensity is superimposed over a grayscale reference image of representative mice from each group of three (upper). Time (day) is indicated below each image. The color bar indicates average signal intensity per pixel represented by a color scheme used in the pseudocolor image. Total signal intensity over the tumor sites (boxes) was determined and plotted with respect to time for each group of three (lower). Inoculum was 1×10^6 cells in the left flank, n=3 (left); and 1×10^5 cells in the right flank, n=3 (right).*

mammalian tissues and the absence of bioluminescence from mammalian cells, suggested that it may be possible to use these reporter genes for the *in vivo* analysis of neoplasia.

It has previously been demonstrated that internal bioluminescent signals from bacteria and cells of transgenic mice can be externally detected *in vivo*, even when located at deep tissue sites [49,50]. Using this technology, it has been possible to non-invasively monitor infection, gene expression, and passive transfer of mammalian cells [51]. This approach has recently been applied to the study of tumor progression and response to therapy in living animal models [52,53]. The reporter genes used in these studies included the modified firefly luciferase for eukaryotic gene expression and a bacterial luciferase from the soil bacterium, *Photorhabdus luminescens*, for prokaryotic expression. Tagging biological processes with reporter genes that are propagated along with the labeled cells permit monitoring cell growth, and transcriptional events without the problem of dilution or loss of signal with cell division. The ability to monitor labeled processes from an external vantage point provides a tremendously powerful tool.

The use of external detection of an internal bioluminescent signal differs from other optical imaging strategies and offers some distinct advantages. Optical imaging typically involves the use of external light sources to either interrogate the inherent optical properties of tumor tissue, or to assess the concentration of exogenous dyes that accumulate or are activated at tumor sites [33,37,38,54]. In contrast, photons originating from photoproteins in labeled cells can serve as internal biological sources of light that transmit through mammalian tissues to reveal spatial and temporal information in the near absence of background bioluminescence [51]. The weak bioluminescent signal emitted from the labeled cells and transmitted through the animal tissue can be detected and quantified using low light imaging systems such as intensified and ultra-cooled charge-coupled device (CCD) cameras [50]. Bioluminescent reporters may offer greater versatility than fluorescent or other types of markers in mammalian tissues due to the nearly complete absence of spontaneous emission of light from mammalian cells. The use of outside light sources for fluorescence markers can result in tissue autofluorescence, creating background that is greater than the signal. As reporter genes are integrated into the chromosomes of the tumor cells, they are replicated with cell division, which is a distinct advantage over other labeling techniques using dyes that can be diluted out as the cells divide. Published research has demonstrated that real time, non-invasive analyses of pathogenic events, pharmacological monitoring and assessment of promoter activity can be performed *in vivo* [49–51]. These studies indicate that reporter genes can provide a window through which biological processes can be viewed in living animals, and thus may be useful in illumination of the temporal and spatial distribution of tumor growth and metastasis *in vivo.*

Detection of bioluminescence from beetle luciferases expressed in mammalian cells either in culture or *in vivo* requires exogenous delivery of the substrate for the enzymatic reaction. It has been determined that the substrate for the firefly luciferase, luciferin (D-(-)-2-(6′-hydroxy-2′-benzothiazolyl)thiazone-4-carboxylic acid), can be added to cell culture medium such that expression in living cells can be monitored [50]. This contrasts what has been observed for coelenterazine, the substrate used by luciferases from marine eukaryotes (e.g., *R. luciferase* from *R. reniformis*), which appears to have significant autoluminescence in the presence of serum proteins (Zhang and Contag, unpublished results). The ability of luciferin to enter into cells is likely due to its small size (280.33 g/mol) and its zwitter ionic nature. Typical studies utilizing luciferase genes as transcriptional reporters require cell lysis with enzymatic activity being analyzed in a luminometer with the attendant loss of temporal information. For detection in living animals, the substrate, luciferin, can be supplied via intraperitoneal injection and luciferase activity can be evaluated at many different tissue sites simultaneously [50], including the central nervous system and fetal tissues in utero (C.H.C., unpublished results). The small size of luciferin also makes it a poor antigen and immune responses to luciferin are unlikely; this will be useful as the models move from xenografts in immunodeficient mice to syngeneic and autologous cell transfers.

Many of the assays for tumor cell growth and regression in animal models of neoplastic disease rely on changes in the volume of large superficial tumors where changes in three orthogonal diameters can be determined using calipers. These tumor models resemble late stages in human disease, and thus, therapies developed using these models are most applicable to late stage disease. In contrast, therapies that target minimal residual disease either after removal of the tumor, via surgery or therapy, or early in the disease course, cannot readily be developed using these conventional assays. Real time accurate assays that employ reporter genes for rapid detection of minimal disease in animal models will change the paradigm of drug development, and therapies that effectively treat small numbers of transformed cells will be developed (Figure 1).

Luciferase as a Reporter for Tumor Cell Growth *In Vivo*

The bioluminescent signal from human tumor cells expressing luciferase can be used to follow their growth in mouse xenograft models of human disease. This has been demonstrated using several human tumor lines. For example, growth of a highly metastatic human prostate cancer cell line (PC-3M) [55] has been followed over time in severe combined immunodeficient (SCID) mice (Figure 2). The PC-3M cells were transfected with the SV40-driven modified luciferase gene and stable clonal transfectants were selected by light emission and antibiotic resistance to generate the line designated PC-3M-*luc*. The luciferase in this construct was optimized for expression in mammalian cells removed [41,42]. Populations of cells arising from single cell clones were generated. Selected clones were used to initiate tumors at subcutaneous sites in the hind flanks of SCID mice, and growth of these cells *in vivo* was

SPECTRAL_0000717

followed over time using an intensified CCD camera to generate whole body images (Figure 2). Light emission was detectable within minutes of injecting the tumor cells, and signals continued to increase logarithmically over a 2-week time period. These data indicate that the bioluminescent light from the transformed cells was detectable externally and that tumor growth can be followed non-invasively. Studies are underway to correlate tumor size with photon counts in this prostate cancer model and to assess the minimal detectable cell number *in vivo*.

A human cervical carcinoma cell line (HeLa) has also been used in similar studies, which have indicated that tumor growth and inhibition in response to several different therapeutic agents could be monitored in living mice (Figure 3) [52,53]. Similar to the PC-3M-*luc* cells, a stable reporter cell line of HeLa cells (HeLa-*luc*) was generated through selection of an integrated reporter construct consisting of a portion of the viral promoter from SV-40 driving expression of the modified luciferase gene. HeLa-*luc* cells were introduced into animals via subcutaneous, intraperitoneal and intravenous inoculation, and the kinetics of cellular proliferation of labeled cells in irradiated SCID mice was non-invasively assessed [53]. The signals from luciferase-labeled cells in these 5-minute images were used to rapidly localize tumors in anesthetized animals and to quantify tumor cell proliferation. In this manner, as few as 1000 cells could be quantitatively detected following injection into immunodeficient mice [52,53]. The dynamic range of this assay permitted the study of disease progression from early (non-palpable tumors) to late stages, indicating that this reporter gene system could be used to evaluate therapies directed at various stages in the disease course including minimal disease states.

Detection of Minimal Disease and Evaluation of Therapy in Animal Models

Advancements in imaging that increase the sensitivity of tumor cell detection will have a dramatic effect on the study of minimal disease models where few cells exist early in diagnosis, or remain after therapeutic intervention. Effective intervention strategies that target the small numbers of neoplastic cells that persist after therapy remain major treatment challenges [56,57]. The observation, that while a majority of cancer patients enter a complete remission following chemotherapy or autologous transplantation, a significant proportion go on to relapse, underscores the importance of controlling minimal residual disease (MRD). The limited ability to detect neoplastic cells at these stages and to predict response to therapy in the absence of reliable assays has hampered progress.

Advancements in the treatment of MRD have been limited by a lack of adequate animal models where small numbers of tumor cells can be reliably and quantitatively detected. In some situations, the ability of the tumor cells to grow in SCID mice has been a powerful predictor of the clinical course of the patient [58]. However, detection of neoplastic cells in current animal models of human disease requires a large number of target cells and such models typically use the therapeutic endpoints of gross tumor growth or death of the animal. Molecular techniques, such as DNA amplification using PCR, have been used, but are hampered by sampling limitations, and the need to sacrifice the animal subjects [21,22]. Several other surrogate markers of tumor growth that can be detected in serum and do not require sacrifice of the animal have been used (e.g., human lactate dehydrogenase (LDH) isoenzymes or human nuclear matrix protein 41/7 (NMP 41/7) in sera of SCID mice) [59]. Even though human-derived serologic markers in xenograft models may

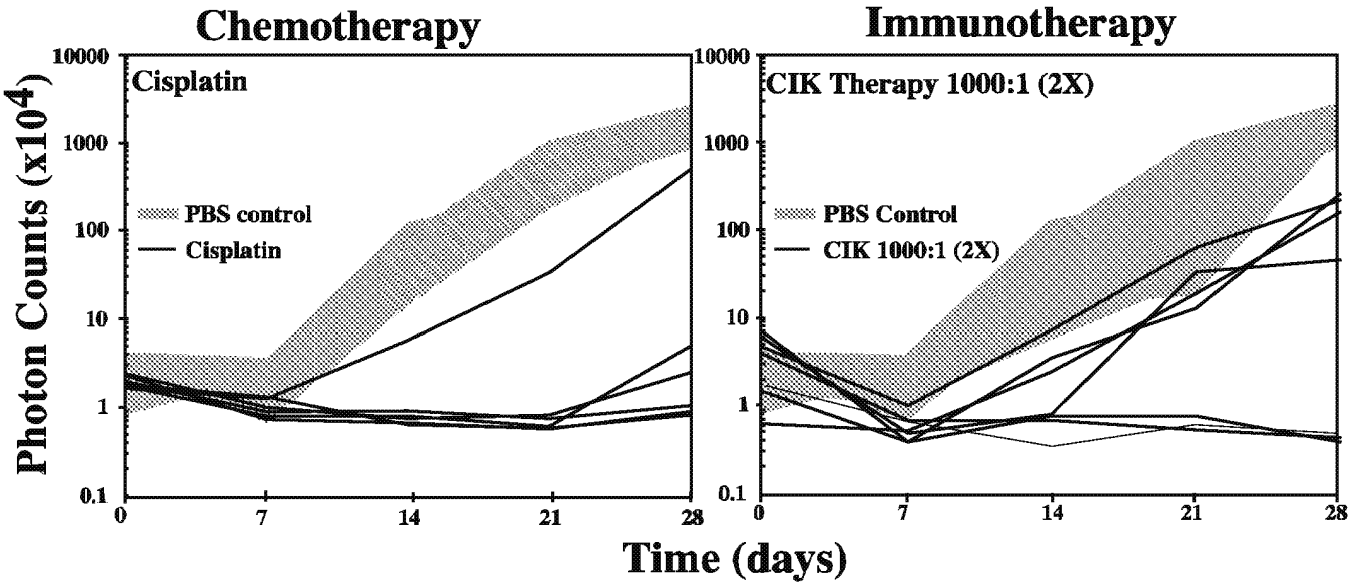


Figure 3. *Effects of chemotherapy and immunotherapy on HeLa-luc cell growth in vivo. HeLa-luc cells were injected into the peritoneal cavity (time 0) at 1×10^4 cells per animal. Groups of animals were either not treated (n=7), or treated with cis-platinum (n=6) or CIK cells at an effector to target ratio of 1000:1 (n=7). Tumor cell growth, as indicated by transmission of bioluminescent light, was assessed at weekly intervals and plotted for each animal with respect to time. The range of tumor cell growth in the untreated control animals is represented by the gray area.*

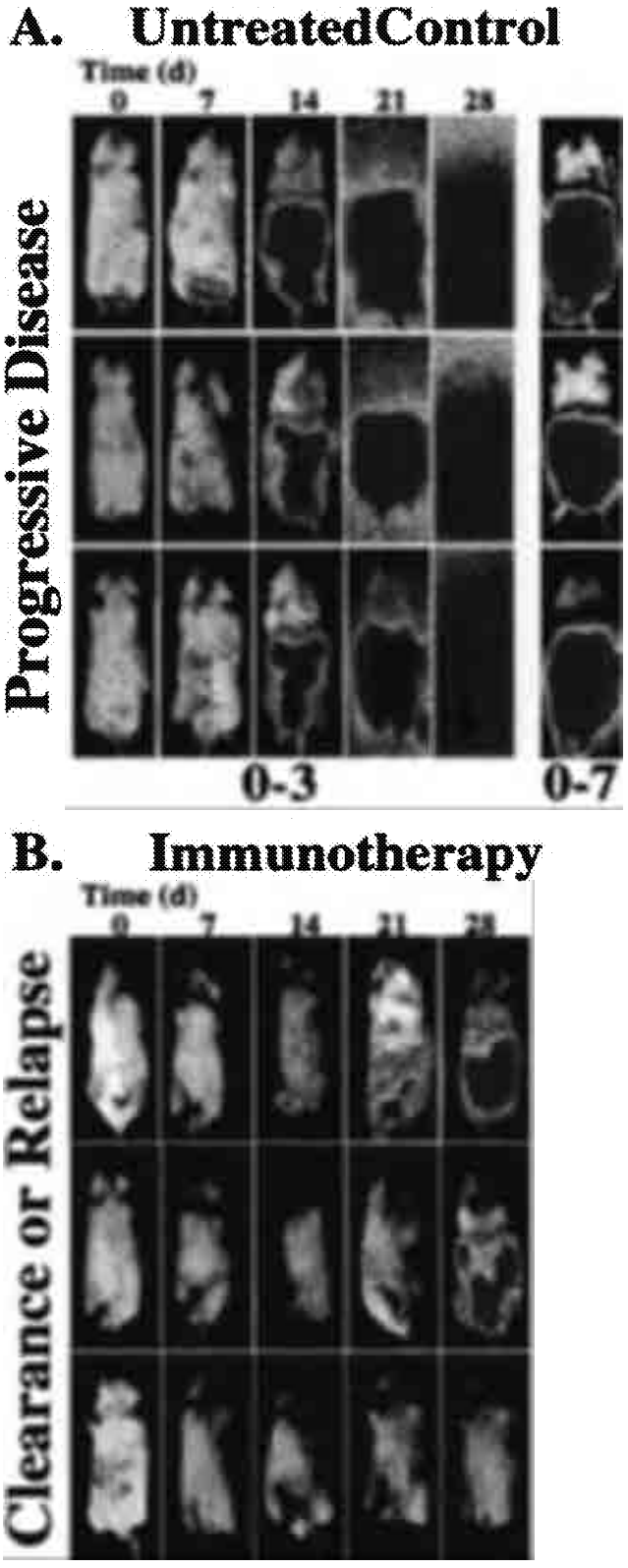


Figure 4. *Effects of immunotherapy on HeLa-luc cell growth in vivo. SCID mice bearing human xenografts, HeLa-luc cells, were either untreated (A) or treated with CIK cells at an effector to target ratio of 1000:1 (B). The growth of the tumor was followed over a 28-day time course. The pseudocolor images represent light intensity collected with a 5-minute integration time, and are all presented at the same display range (0–3 bits) with the exception of the 28-day time point for the untreated controls which is also shown at the 0–7 bit range to reveal spatial information.*

provide predictable indicators of tumor cell growth, these are indirect assays of tumor cell growth, are only detectable at a week to several weeks after introduction of the tumor cells, and require blood sampling and processing. Thus, further advancements in non-invasive detection and quantification of tumor burden in xenograft models are desirable.

Employing a luciferase-based methodology, conventional chemotherapies and a novel immune cell therapy, utilizing cytokine induced killer (CIK) T cells, have been evaluated in minimal disease xenograft models (Figure 4). The chemotherapeutic agents included cyclophosphamide, 5-fluorouracil, and *cis*-platinum. These three agents had different effects on the growth of HeLa-*luc* cells *in vivo*, with cyclophosphamide being the least effective and *cis*-platinum the most effective at reducing the signals in tumor-bearing animals [52]. Following treatment responses to therapy could be evaluated in as few as 24 to 72 hours. Long-term evaluation of the animals was also readily accomplished [52].

The immune cytotherapy arms of this study utilized CIK cells. These cells were generated by culturing peripheral blood mononuclear cells in the presence of IFN-γ, followed 1 day later by IL-2 and an anti-CD3 monoclonal antibody [60–62]. This incubation resulted in the dramatic expansion of effector cells which have cytolytic activity against a broad array of tumor cell targets including multidrug resistant cell lines and autologous fresh tumor isolates [63–65]. The cell type with the most robust anti-tumor activity expresses the surface marker CD3, a general T cell marker, and the natural killer (NK) cell marker, CD56. Initially, an effector to target ratio of 100:1 was used; by 2 weeks, only a modest effect was noted — thus, second and third treatment arms were tested using ratios of 1000:1. In these treatment arms, the signals were reduced to background in many of the animals indicating effective treatment. These studies demonstrated that the non-invasive assays could be used for the rapid development of effective doses and schedules of therapy [52]. The evaluation of novel additional approaches that may enhance the effects of CIK therapy, such as with the use of bi-specific antibodies which crosslink the effector cells with tumor markers, will be accelerated through the use of the luciferase imaging approach.

In these studies, the number of animals required to reach statistically meaningful endpoints was five to seven per treatment group. Differences among the different arms of the study were apparent at 7 days post-treatment with statistically significant results being obtained at 14 days. In conventional tumor models, based upon animal survival, experiments are conducted over several months. Therefore, using this quantitative *in vivo* assay where a single group of animals can be followed over time and differences between treatment groups can be evident in the first week, a greater number of different treatment strategies can be evaluated.

Luciferase Reporters in Metastatic Models

Detection of metastatic tumor growth in animals has been largely dependent on *ex vivo* analysis of excised tissues.

SPECTRAL_0000719

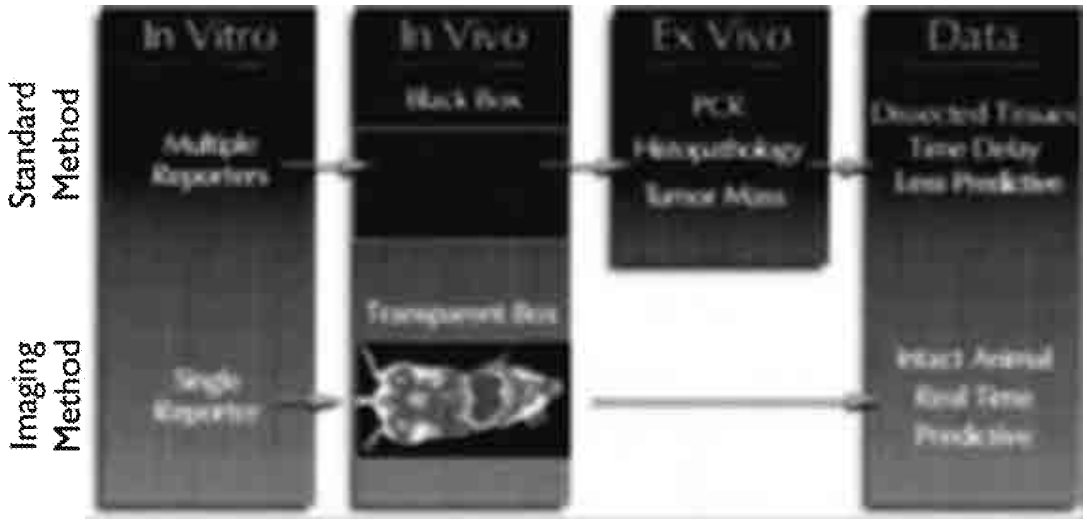


Figure 5. *Refinement of animal models using photoprotein reporters. Standard methods of monitoring tumor cell growth utilize multiple reporters and indicators to reveal the effects of experimental therapies on tumor cell growth in correlative cell culture assays. These assays often cannot be applied to in vivo analyses and assessing tumor growth in vivo is limited to measuring tumor size at superficial sites. Thus, ex vivo assays such as PCR, histological examination and weighing tumors have been necessary to assess tumor growth. These ex vivo assays often require sacrifice of the animals at multiple time points. Imaging tumor cell growth in culture and in vivo can be performed using a single reporter gene and signals for this reporter gene can be used to direct the ex vivo assays such that times and tissues can be targeted for analyses. This approach results in animal models and preclinical data that can be more predictive of human disease states.*

Histological analyses have been traditionally used to localize and document neoplastic and metastatic growth. These assays, however, suffer from the limitation of sampling selection and extensive labor involvement. GFP expression in tumor cell lines has facilitated directed analyses of tissue samples in these models and represents first steps toward linking the *in vivo* study of metastasis to tissue culture correlates [66,67]. In these studies, fluorescing metastatic colonies of cells could be detected on murine lung tissue via the GFP tag, and selected tissue samples could then be excised and cultured using a matrix-supported histoculture method to model *in vivo* tumor colonization. Throughout the studies, GFP expression permitted constant measurement and a means of detection that facilitated manipulation of both the *in vivo* model and the culture system. This approach demonstrated the strength of using an optical signature to track cells and monitor their growth both *in vivo* and in culture. Extending this approach to monitoring disease progression in three dimensions in living animal models is the goal of many imaging strategies.

As a step in the direction of real time, three-dimensional tumor cell imaging, luciferase-based methods offer the opportunity of whole body imaging and scanning for tumor growth with fairly short integration times (5 minutes per image). Furthermore, the ability to detect small numbers of luciferase-positive tumor cells enhances the potential to analyze experimental or spontaneous metastatic growth *in vivo*. Following intravenous injection of HeLa-*luc* cells, Edinger et al. [53] were able to detect microcolonies at a variety of tissue sites non-invasively. These microcolonies were detectable at 7 days after introduction of the tumor cells and appeared to be located in bone, lung and other tissues. The sensitivity of this assay and the ability to detect microcolonies using a whole body analysis indicated that this approach would be particularly useful in the detection of metastases at sites that are difficult to assay, such as bone or brain. The short time required for the imaging would allow quick screening of large numbers of animals and may permit imaging from multiple angles.

Since reporter gene expression can be monitored in living cells in culture, in animals and in cell lysates derived from tumor tissue, each step in the experimental design can be monitored with a single reporter gene. Examples of this are the studies by Chishima et al. [66] and Edinger et al. [53] and where either GFP or luciferase, respectively, was used both in culture and in animal models. Use of a single reporter gene at multiple steps in an experiment results in a more streamlined approach, and the added advantages of being quantitative and rapid make the use of these methods more efficient and informative than conventional studies. This is especially relevant to the study of metastasis where localizing microcolonies in the whole animal is tantamount to looking for a needle in a haystack. Since the *in vivo* data can be used to direct *ex vivo* analyses (i.e., localization of metastatic lesions for subsequent analyses), the labor-intensive assays such as PCR, expression profiling via DNA microarrays and histopathological assays can be performed on targeted tissues as directed by the *in vivo* analysis. This refinement to the animal models for neoplastic disease will result in more predictive models and improved clinical studies (Figure 5).

Green Fluorescent Protein (GFP) as an Indicator of Tumorigenesis

A wide variety of tumor cells have been labeled with GFP including human xenografts and syngeneic transfers. The gene encoding GFP from the jellyfish, *Aequeora victoria*, has been mutated for optimal mammalian expression and

alteration of its excitation and emission wavelengths. A family of genes encoding GFP variants that excite and emit at wavelengths other than the green wildtype excitation and emission of 397 and 509 nm offer versatility for gene expression studies [68–74]. Some of these variants have been used to tag tumor cells and monitor growth and metastasis in animal models [66,67]. The methods used to visualize the fluorescent proteins in living tissues include transillumination of the living animal [75] or intravital microscopy [76,77]. Transillumination of intact living animals produced detectable signals from tumors labeled with GFP, and metastases were visualized in the lung, liver, bones, and brain [75,78,79]. The detection limits were improved by utilizing nude mice or removing fur to reduce the light scatter. Maximum sensitivity was obtained following sacrifice of the animal and removal of the skin and other tissues. Following laparotomy, it was possible to obtain single-cell level resolution [79]. These steps enhanced the ability to detect tumors in mice; however, this approach eliminates temporal analyses and is not easily applied to larger-scale studies.

Orthotopic transplantation of cancer cells that express GFP has been used to visualize metastasis and angiogenesis [66,67,79–81]. Using intravital microscopy, it is also possible to detect single cells labeled with GFP and monitor their migration through blood vessels [77]. While this method allows for temporal analyses, it requires removal of the tissue over the tumor in order to make direct observations of the labeled cells. The excised tissue is replaced with a transparent window to permit repeated analyses. Studies using this technique have revealed migration patterns for immune cells and cancer cells at the tumor site. Studies utilizing intravital microscopy have also revealed expression patterns using the promoter for vascular endothelial growth factor (VEGF) [77].

The utility of fluorescent reporter genes in these types of analyses will be greatly enhanced by the introduction of red fluorescent proteins since the longer wavelength of red light transmits tissues more efficiently than green light. Weissleder et al. [33] have demonstrated the utility of red fluorescence for tumor imaging using an autoquenched red fluorescent dye (Cy5.5) that accumulates at the tumor site and is activated by lysosomal proteases of tumor cells. Quenched fluorochromes were bound to a copolymer consisting of poly-L-lysine and methoxypolyethylene glycol succinate. Following intravenous injection, the conjugates accumulated in solid xenograft tumors presumably after passing through the neovasculature of the tumor. The quenched fluorochrome was released in the tumor by lysosomal proteases in the tumor cells such that the signal was increased 12-fold at the tumor site and submillimeter-sized tumors were detectable subcutaneously. Fluorescent proteins that excite and emit at longer wavelengths may permit detection of labeled cells several millimeters or centimeters within mammalian tissue. Such reporter proteins have recently been described [16]. However, these orange-red fluorescent proteins have not yet been used in studies of *in vivo* tumor cell growth.

As transcriptional reporters, GFP and luciferase can be indicative of gene expression when a tumor-specific promoter is linked to the coding sequence, and when constitutively expressed, these reporters can be used to indicate the sites of tumor growth. *In vivo* assays that utilize reporter genes can also be set up as indicators of other steps in neoplastic disease progression, such as microvessel density (MVD) as an indicator of neovascularization of tumors. Moore et al. [83] have used a 9L cell line constitutively expressing GFP for assessing MVD. In this study using fluorescence microscopy, non-fluorescent regions at the borders of the tumor tissue were interpreted as vascularized regions lacking tumor cells. This was confirmed by utilizing conventional histological methods, anti-CD31 immunohistology, and Hoechst 33258 dye exclusion. MVD allowed quantification of tumor angiogenesis in tissue specimens, thus providing additional information about tumor growth and regression in animal models. Such analysis holds promise in evaluating the efficacy of anti-angiogenic therapies.

Multifunctional Reporters

The various optical reporter genes, including luciferase and GFP, have unique properties that make each useful for particular experimental applications. Luciferase is a real time indicator of transcription; due to its relatively short half-life, it indicates diminution of expression unlike the longer-lived GFP protein. In contrast, GFP can be used for higher resolution imaging in cells. Combining these reporter genes into a single gene could provide additional tools for the analysis of cancer cells *in vivo* and *ex vivo*. A recombinant protein consisting of the coding regions for GFP and luciferase would provide the sensitivity of fluorescence and the ease and real-time imaging of bioluminescence. Such a dual-function reporter gene was created and the single encoded protein was shown to be fluorescent and bioluminescent [48]. The GFP portion of the protein allowed for analyses of single living cells expressing the chimeric protein within a population by fluorescence microscopy, and the luciferase activity could be detected from the same living cells.

Luciferases comprise a family of enzymes that use different substrates and biochemical mechanisms to emit light of different wavelengths and that use different biochemical mechanisms [41–43,84–86]. In addition, directed and random mutageneses of firefly genes have resulted in shifts in the wavelength of emission [84,88], offering the possibility of multiparameter *in vivo* assays. Sets of bioluminescent enzymes with different biochemical requirements and different emission spectra have been used in *in vitro* and culture-based assays to assess expression of two different genes, usually one as control and the other as the inducible test gene [47,89]. Combining the various fluorescent proteins to the wide range bioluminescent enzymes increases the potential for assays and models to evaluate high throughput multiparameter analyses of oncogenesis.

SPECTRAL_0000721

Summary and Conclusions

Advancing our understanding of neoplastic disease requires the ability to effect biological processes *in vivo* and evaluate the changes non-invasively at the molecular and cellular levels. A basic premise of biology is that the investigator specifically perturbs a biological process and then studies the effects of this perturbation on the entire system to learn about interactive processes, mechanisms and pathways. A large number of biological events only occur in the context of intact organ systems that cannot be modeled in culture. For this reason, animal models are routinely utilized in biomedical research. However, the ability to interrogate cellular and molecular processes in living animal models has been limited, and thus evaluating the effects of various stimuli on complex biological processes *in vivo* was not previously possible. In the study of neoplastic disease, many of the molecular and cellular changes that are linked to the initiation and progression of disease only occur *in vivo* and may be largely undiscovered due to our inability to access these changes in the living animal. With advancements in molecular and cellular imaging, *in vivo* perturbation and evaluation of steps in interwoven pathways may be possible.

Similarly, improvements and modifications to animal model systems are needed to further understand various mechanisms of immune containment of neoplasia and to develop new therapies to prevent and treat small numbers of neoplastic cells present in minimal disease states. Since as few as 1000 luciferase-labeled tumor cells distributed throughout the peritoneal cavity were reliably detected and quantified in living animals, and the signals were proportional to tumor cell inocula over a broad dynamic range spanning at least five orders of magnitude, the kinetics of tumor growth from early stages of minimal disease to late stage disease could be evaluated over time [52,53]. The ability to monitor kinetics of tumor cell growth and localize micrometastases non-invasively will reveal novel features of these processes as well as elucidate cellular and tissue responses to tumor growth.

The demonstrated ability to non-invasively detect small numbers of tumor cells in living animals will permit the assessment of therapies designed to treat minimal disease states. Minimal residual disease that persists after elimination of the initial tumor mass often results in relapse of disease and remains a major therapeutic challenge [57]. In addition, as neoplastic diagnostic tests improve, therapies that are directed at minimal disease states early in the disease course would need to be developed. The approaches reviewed here can accelerate development of therapeutic strategies by providing a rapid *in vivo* assay for efficacy that is inexpensive and accessible. *In vivo* imaging approaches, in general, will improve the predictability of animal models of human neoplastic disease by providing spatiotemporal information, and the ease and versatility of photoprotein imaging can additionally be applied in high throughput animal models for drug discovery. In addition, information about the kinetics of tumor cell growth and effects of endogenous immunological mechanisms can be directly assessed; thus, more information is provided despite the rapid nature of the assay.

In vivo imaging of optical reporter genes is a broadly applicable tool for the study of neoplasia. This approach can provide real time data that indicate the spatial distribution of tumor cells at multiple time points during the disease course. Use of optical reporter genes provides information with relatively short scan times; thus, rapid assessment of a potential intervention in a fully quantitative manner is possible. Since groups of animals can be followed over time, far fewer animal subjects are required to obtain statistically meaningful results. The stress on the animals in these studies is dramatically reduced since whole body imaging replaces the use of death as an endpoint and the models can be evaluated in minimal disease states where the tumor burden is small. Rapid whole body imaging and the use of repeated measurements on groups of animals improve the data set, accelerate the study and reduce stress to the animals; taken together, these serve to generally refine animal studies of neoplastic disease.

This method may also extend to assessing the tissue distribution of host immune cells that recognize and eliminate tumor cells. With these molecular tools for *in vivo* studies, investigators can begin to analyze the mechanisms of immune surveillance of neoplastic disease in living animal models of human disease. Theoretically, other cell populations or biological functions that can be suitably labeled are also amenable for study in living animal models. Further modifications to the photoprotein reporters used in the imaging strategy may permit the development of multiparameter or dual color assays for monitoring tumor progression and interaction of the host response in the same animal. Studies thus far using optical reporter gene imaging have demonstrated that it is possible to track the fate of tumor cells *in vivo*.

Advances

Developments in optical reporter gene technologies have been dramatic since the discovery of GFP as an optical tag to indicate promoter activity, intracellular trafficking (by creating fusion proteins with GFP), or cell migration in small nearly transparent animals [90,91]. The lessons learned from the modifications of GFP can be applied to other optical reporter genes such as luciferase. For example, shifting of the emission wavelength of luciferase reporters from primarily blue and green emission to those that are more readily transmitted through tissues will greatly enhance their utility for *in vivo* analyses [69,70,92]. The barriers to transmission of light through tissues include scattering and absorption. Absorption is largely due to hemoglobin at shorter wavelengths up to 600 nm; above 800 nm, absorption is due to water. Reporter genes that emit within this window would be ideal for *in vivo* detection.

Advancements in imaging technologies will revolutionize the study, treatment and prevention of neoplastic disease by providing a wealth of critical information that has not been

previously available. Continued commitment to imaging research will lead to additional tools to reveal *in vivo* biological events leading to essentially transparent animal models, and the ability to assess cellular and molecular events non-invasively. Further advancement of non-invasive *in vivo* methods to study neoplasia will facilitate rapid development of novel therapeutics against new molecular targets, and enable assessment of therapeutic outcomes. Development of multimodality imaging approaches will greatly improve our ability to obtain structural and functional data in animal models, and these advancements will likely have direct bearing on clinical imaging and treatment of human cancers.

Acknowledgements

PC3M cells were kindly provided to Xenogen and Novartis Pharmaceuticals by J.I. Fidler from the M.D. Anderson Medical Center in Houston, TX and the prostate model was evaluated in collaboration with Novartis Pharmaceuticals.

References

[1] Clemens MJ, and Bommer UA (1999). Translational control: the cancer connection. *Int J Biochem Cell Biol* **31**, 1–23.

[2] Dang CV, and Semenza GL (1999). Oncogenic alterations of metabolism. *Trend Biochem Sci* **24**, 68–72.

[3] Devereux TR, Risinger JI, and Barrett JC (1999). Mutations and altered expression of the human cancer genes: what they tell us about causes. *IARC Sci Publ*, 19–42.

[4] Holt SE, and Shay JW (1999). Role of telomerase in cellular proliferation and cancer. *J Cell Physiol* **180**, 10–18.

[5] Jacobson S, and Pillus L (1999). Modifying chromatin and concepts of cancer. *Curr Opin Gen Dev* **9**, 175–184.

[6] Markiewicz MA, and Gajewski TF (1999). The immune system as anti-tumor sentinel: molecular requirements for an anti-tumor immune response. *Crit Rev Oncogen* **10**, 247–260.

[7] McBurney MW (1999). Gene silencing in the development of cancer. *Exp Cell Res* **248**, 25–29.

[8] Kavanaugh DY, and Carbone DP (1996). Immunologic dysfunction in cancer. *Hem/Oncol Clin N Am* **10**, 927–951.

[9] Whiteside TL, and Herberman RB (1995). The role of natural killer cells in immune surveillance of cancer. *Curr Opin Immunol* 7, 704–710.

[10] Christofori G, and Hanahan D (1994). Molecular dissection of multi-stage tumorigenesis in transgenic mice. *Sem Cancer Biol* **5**, 3–12.

[11] Hanahan D, and Folkman J (1996). Patterns and emerging mechanisms of the angiogenic switch during tumorigenesis. *Cell* **86**, 353–364.

[12] Coussens LM, Hanahan D, and Arbeit JM (1996). Genetic predisposition and parameters of malignant progression in K14-HPV16 transgenic mice. *Am J Pathol* **149**, 1899–1917.

[13] Bigos M, Baumgarth N, Jager GC, Herman OC, Nozaki T, Stovel RT, Parks DR, and Herzenberg LA (1999). Nine color eleven parameter immunophenotyping using three laser flow cytometry. *Cytometry* **36**, 36–45.

[14] Brown PO, and Botstein D (1999). Exploring the new world of the genome with DNA microarrays. *Nat Gen* **21**, 33–37.

[15] Eisen MB, and Brown PO (1999). DNA arrays for analysis of gene expression. *Methods Enzymol* **303**, 179–205.

[16] Matz MV, Fradkov AF, Labas YA, Savitsky AP, Zaraisky AG, Markelov ML, and Lukyanov SA (1999). Fluorescent proteins from non-bioluminescent *Anthozoa* species. *Nat Biotechnol* **17**, 969–973.

[17] Perou CM, Jeffrey SS, van de Rijn M, Rees CA, Eisen MB, Ross DT, Pergamenschikov A, Williams CF, Zhu SX, Lee JC, Lashkari D, Shalon D, Brown PO, and Botstein D (1999). Distinctive gene expression patterns in human mammary epithelial cells and breast cancers. *Proc Natl Acad Sci USA* **96**, 9212–9217.

[18] Piston DW (1999). Imaging living cells and tissues by two-photon excitation microscopy. *Trends Cell Biol* **9**, 66–69.

[19] Pollack JR, Perou CM, Alizadeh AA, Eisen MB, Pergamenschikov A, Williams CF, Jeffrey SS, Botstein D, and Brown PO (1999). Genome-wide analysis of DNA copy-number changes using cDNA microarrays. *Nat Gen* **23**, 41–46.

[20] Potter SM (1996). Vital imaging: two photons are better than one. *Curr Biol* **6**, 1595–1598.

[21] Zhang L, Hellstrom KE, and Chen L (1994). Luciferase activity as a marker of tumor burden and as an indicator of tumor response to antineoplastic therapy *in vivo*. *Clin Exp Metastasis* **12**, 87–92.

[22] Negrin RS, and Blume KG (1991). The use of the polymerase chain reaction for the detection of minimal residual malignant disease. *Blood* **78**, 255–258.

[23] Bogdanov A, Jr, and Weissleder R (1998). The development of *in vivo* imaging systems to study gene expression. *Trends Biotechnol* **16**, 5–10.

[24] Chenevert TL, McKeever PE, and Ross BD (1997). Monitoring early response of experimental brain tumors to therapy using diffusion magnetic resonance imaging. *Clin Cancer Res* **3**, 1457–1466.

[25] Ross B, Zhao Y-J, Neal E, Stegman L, Ercolani M, Ben-Yoseph O, and Chenevert T (1998). Contributions of cell kill and posttreatment tumor growth rates to the repopulation of intracerebral 9L tumors after chemotherapy: an MRI study. *Proc Natl Acad Sci USA* **95**, 7012–7017.

[26] Galons J-P, Altbach M, Paine-Murrieta G, Taylor C, and Gillies R (1999). Early increases in breast tumor xenograft water mobility in response to paclitaxel therapy detected by non-invasive diffusion magnetic resonance imaging. *Neoplasia* **1**, 113–117.

[27] Gambhir SS, Barrio JR, Herschman HR, and Phelps ME (1999). Imaging gene expression: principles and assays. *J Nucl Cardiol* **6**, 219–233.

[28] Gambhir SS, Barrio JR, Phelps ME, Iyer M, Namavari M, Satyamurthy N, Wu L, Green LA, Bauer E, MacLaren DC, Nguyen K, Berk AJ, Cherry SR, and Herschman HR (1999). Imaging adenoviral-directed reporter gene expression in living animals with positron emission tomography. *Proc Natl Acad Sci USA* **96**, 2333–2338.

[29] Jacobs A, Dubrovin M, Hewett J, Sena-Esteves M, Tan C-W, Slack M, Sadelain M, Breakefield X, and Tjuvajev J (1999). Functional coexpression of HSV-1 thymidine kinase and green fluorescent protein: implications for non-invasive imaging of transgene expression. *Neoplasia* **1**, 154–161.

[30] Tjuvajev JG, Finn R, Watanabe K, Joshi R, Oku T, Kennedy J, Beattie B, Koutcher J, Larson S, and Blasberg RG (1996). Non-invasive imaging of herpes virus thymidine kinase gene transfer and expression: a potential method for monitoring clinical gene therapy. *Cancer Res* **56**, 4087–4095.

[31] Tjuvajev JG, Avril N, Oku T, Sasajima T, Miyagawa T, Joshi R, Safer M, Beattie B, DiResta G, Daghighian F, Augensen F, Koutcher J, Zweit J, Humm J, Larson SM, Finn R, and Blasberg R (1998). Imaging herpes virus thymidine kinase gene transfer and expression by positron emission tomography. *Cancer Res* **58**, 4333–4341.

[32] Uehara H, Miyagawa T, Tjuvajev J, Joshi R, Beattie B, Oku T, Finn R, and Blasberg R (1997). Imaging experimental brain tumors with 1-aminocyclopentane carboxylic acid and alpha-aminoisobutyric acid: comparison to fluorodeoxyglucose and diethylenetriaminepentaacetic acid in morphologically defined tumor regions. *J Cereb Blood Flow Metab* **17**, 1239–1253.

[33] Weissleder R, Tung CH, Mahmood U, and Bogdanov A, Jr (1999). *In vivo* imaging of tumors with protease-activated near-infrared fluorescent probes. *Nat Biotechnol* **17**, 375–378.

[34] Tjuvajev JG, Joshi A, Callegari J, Lindsley L, Joshi R, Balatoni J, Finn R, Larson SM, Sadelain M, and Blasberg RG (1999). A general approach to the non-invasive imaging of transgenes using *cis*-linked herpes simplex virus thymidine kinase. *Neoplasia* **1**, 315–320.

[35] Harisinghani MG, Saini S, Weissleder R, Hahn PF, Yantiss RK, Tempany C, Wood BJ, and Mueller PR (1999). MR lymphangiography using ultrasmall superparamagnetic iron oxide in patients with primary abdominal and pelvic malignancies: radiographic–pathologic correlation. *AJR Am J Roentgenol* **172**, 1347–1351.

[36] Josephson L, Tung CH, Moore A, and Weissleder R (1999). High-efficiency intracellular magnetic labeling with novel superparamagnetic-Tat peptide conjugates. *Bioconjugate Chem* **10**, 186–191.

[37] Reynolds JS, Troy TL, Mayer RH, Thompson AB, Waters DJ, Cornell KK, Snyder PW, and Sevick-Muraca EM (1999). Imaging of spontaneous canine mammary tumors using fluorescent contrast agents. *Photochem Photobiol* **70**, 87–94.

[38] Nioka S, Yung Y, Shnall M, Zhao S, Orel S, Xie C, Chance B, and Solin L (1997). Optical imaging of breast tumor by means of continuous waves. *Adv Exp Med Biol* **411**, 227–232.

SPECTRAL_0000723

[39] de Wet JR, Wood KV, Helinski DR, and DeLuca M (1985). Cloning of firefly luciferase cDNA and the expression of active luciferase in *Escherichia coli*. *Proc Natl Acad Sci USA* **82**, 7870–7873.

[40] de Wet J, Wood K, DeLuca M, Helinski D, and Subramani S (1987). Firefly luciferase gene: structure and expression in mammalian cells. *Mol Cell Biol* 7, 725–737.

[41] Sherf B, and Wood K (1994). Firefly luciferase engineered for improved genetic reporting. *Promega Notes Mag* **49**, 14–21.

[42] Wood KV (1995). Marker proteins for gene expression. *Curr Opin Biotechnol* **6**, 50–58.

[43] Hastings JW (1996). Chemistries and colors of bioluminescent reactions: a review. *Gene* **173**, 5–11.

[44] Willard ST, Faught WJ, and Frawley LS (1997). Real-time monitoring of estrogen-regulated gene expression in single, living breast cancer cells: a new paradigm for the study of molecular dynamics. *Cancer Res* **57**, 4447–4450.

[45] Chen H, Biel MA, Borges MW, Thiagalingam A, Nelkin BD, Baylin SB, and Ball DW (1997). Tissue-specific expression of human achaete-scute homologue-1 in neuroendocrine tumors: transcriptional regulation by dual inhibitory regions. *Cell Growth Differ* **8**, 677–686.

[46] Takakuwa K, Fujita K, Kikuchi A, Sugaya S, Yahata T, Aida H, Kurabayashi T, Hasegawa I, and Tanaka K (1997). Direct intratumoral gene transfer of the herpes simplex virus thymidine kinase gene with DNA–liposome complexes: growth inhibition of tumors and lack of localization in normal tissues. *Jpn J Cancer Res* **88**, 166–175.

[47] Grentzmann G, Ingram JA, Kelly PJ, Gesteland RF, and Atkins JF (1998). A dual-luciferase reporter system for studying recoding signals. *RNA* **4**, 479–486.

[48] Day RN, Kawecki M, and Berry D (1998). Dual-function reporter protein for analysis of gene expression in living cells. *Biotechnology* **25**, 848–850.

[49] Contag CH, Contag PR, Mullins JI, Spilman SD, Stevenson DK, and Benaron DA (1995). Photonic detection of bacterial pathogens in living hosts. *Mol Microbiol* **18**, 593–603.

[50] Contag C, Spilman S, Contag P, Oshiro M, Eames B, Dennery P, Stevenson D, and Benaron D (1997). Visualizing gene expression in living mammals using a bioluminescent reporter. *Photochem Photobiol* **66**, 523–531.

[51] Contag PR, Olomu IN, Stevenson DK, and Contag CH (1998). Bioluminescent indicators in living mammals. *Nat Med* **4**, 245–247.

[52] Sweeney T, Mailander V, Tucker A, Olomu AB, Zhang W, Negrin RS, and Contag CH (1999). Visualizing tumor cell clearance in living animals. *Proc Natl Acad Sci USA* **96**, 12044–12049.

[53] Edinger M, Sweeney TJ, Tucker AA, Adesuwa B Olomu AB, Negrin RS, and Contag CH (1999). Non-invasive assessment of tumor cell proliferation in animal models. *Neoplasia* **1**, 303–310.

[54] Chance B, Luo Q, Nioka S, Alsop DC, and Detre JA (1997). Optical investigations of physiology: a study of intrinsic and extrinsic biomedical contrast. *Philos Trans R Soc London B Biol Sci* **352**, 707–716.

[55] Koslowski JM, Fidler IJ, Campbel D, Xu Z, Kaigh ME, and Hart IR (1984). Metastatic behavior of human tumor cell lines grown in the nude mouse. *Cancer Res* **44**, 3522–3529.

[56] Cave H, van der Werff ten Bosch J, Suciu S, Guidal C, Waterkeyn C, Otten J, Bakkus M, Thielemans K, Grandchamp B, and Vilmer E (1998). Clinical significance of minimal residual disease in childhood acute lymphoblastic leukemia. European Organization for Research and Treatment of Cancer — Childhood Leukemia Cooperative Group. *New Engl J Med* **339**, 591–598.

[57] Hirsch-Ginsberg C (1998). Detection of minimal residual disease: relevance for diagnosis and treatment of human malignancies. *Annu Rev Med* **49**, 111–122.

[58] Uckun FM, Sather H, Reaman G, Shuster J, Land V, Trigg M, Gunther R, Chelstrom L, Bleyer A, and Gaynon P (1995). Leukemic cell growth in SCID mice as a predictor of relapse in high-risk B-lineage acute lymphoblastic leukemia. *Blood* **85**, 873–878.

[59] Arguello F, Sterry JA, Zhao YZ, Alexander MR, Shoemaker RH, and Cohen HJ (1996). Two serologic markers to monitor the engraftment, growth, and treatment response of human leukemias in severe combined immunodeficient mice. *Blood* **87**, 4325–4332.

[60] Schmidt-Wolf IGH, Negrin RS, Kiem HP, Blume KG, and Weissman IL (1991). Use of a SCID mouse/human lymphoma model to evaluate cytokine-induced killer cells with potent antitumor cell activity. *J Exp Med* **174**, 139–149.

[61] Lu PH, and Negrin RS (1994). A novel population of expanded human CD3+CD56+ cells derived from T cells with potent *in vivo* antitumor activity in mice with severe combined immunodeficiency. *J Immunol* **153**, 1687–1696.

[62] Ochoa AC, Gromo G, Alter BJ, Sondel PM, and Bach FH (1987). Long-term growth of lymphokine-activated killer LAK cells: role of anti-CD3, beta-IL 1, interferon-gamma and -beta. *J Immunol* **138**, 2728–2733.

[63] Schmidt-Wolf IG, Lefterova P, Johnston V, Scheffold C, Csipai M, Mehta BA, Tsuruo T, Huhn D, and Negrin RS (1996). Sensitivity of multidrug-resistant tumor cell lines to immunologic effector cells. *Cell Immunol* **169**, 85–90.

[64] Schmidt-Wolf IG, Lefterova P, Mehta BA, Fernandez LP, Huhn D, Blume KG, Weissman IL, and Negrin RS (1993). Phenotypic characterization and identification of effector cells involved in tumor cell recognition of cytokine-induced killer cells. *Exp Hematol* **21**, 1673–1679.

[65] Hoyle CH, Bangs CD, Cahng P, Kamel O, Mehta BA, and Negrin RS (1998). Expansion of Philadelphia-chromosome-negative CD3+ CD56+ cytotoxic cells from CML patients: *in vitro* and *in vivo* efficacy in SCID mice. *Submitted*.

[66] Chishima T, Yang M, Miyagi Y, Li L, Tan Y, Baranov E, Shimada H, Moossa AR, Penman S, and Hoffman RM (1997). Governing step of metastasis visualized *in vitro*. *Proc Natl Acad Sci USA* **94**, 11573–11576.

[67] Chishima T, Miyagi Y, Wang X, Tan Y, Shimada H, Moossa A, and Hoffman RM (1997). Visualization of the metastatic process by green fluorescent protein expression. *Anticancer Res* **17**, 2377–2384.

[68] Brejc K, Sixma TK, Kitts PA, Kain SR, Tsien RY, Ormo M, and Remington SJ (1997). Structural basis for dual excitation and photoisomerization of the *Aequorea victoria* green fluorescent protein. *Proc Natl Acad Sci USA* **94**, 2306–2311.

[69] Cubitt AB, Heim R, Adams SR, Boyd AE, Gross LA, and Tsien RY (1995). Understanding, improving and using green fluorescent proteins. *Trends Biochem Sci* **20**, 448–455.

[70] Heim R, Prasher DC, and Tsien RY (1994). Wavelength mutations and posttranslational autoxidation of green fluorescent protein. *Proc Natl Acad Sci USA* **91**, 12501–12504.

[71] Heim R, Cubitt AB, and Tsien RY (1995). Improved green fluorescence. *Nature* **373**, 663–664.

[72] Tsien RY (1998). The green fluorescent protein. *Annu Rev Biochem* **67**, 509–544.

[73] Ormo M, Cubitt AB, Kallio K, Gross LA, Tsien RY, and Remington SJ (1996). Crystal structure of the *Aequorea victoria* green fluorescent protein. *Science* **273**, 1392–1395.

[74] Ito Y, Suzuki M, and Husimi Y (1999). A novel mutant of green fluorescent protein with enhanced sensitivity for microanalysis at 488 nm excitation. *Biochem Biophys Res Commun* **264**, 556–560.

[75] Yang M, Jiang P, Sun F, Hasegawa S, Baranov E, Chishima T, Shimada H, Moossa A, and Hoffman R (1999). A fluorescent orthotopic bone metastasis model of human prostate cancer. *Cancer Res* **59**, 781–786.

[76] Naumov G, Wilson S, MacDonald I, Schmidt E, Morris V, Groom A, Hoffman R, and Chambers A (1999). Cellular expression of green fluorescent protein, coupled with high-resolution *in vivo* videomicroscopy, to monitor steps in tumor metastasis. *J Cell Sci* **112**, 1835–1842.

[77] Fukumura D, Xavier R, Sugiura T, Chen Y, Park EC, Lu N, Selig M, Nielsen G, Taksir T, Jain RK, and Seed B (1998). Tumor induction of VEGF promoter activity in stromal cells. *Cell* **94**, 715–725.

[78] Yang M, Hasegawa S, Jiang P, Wang X, Tan Y, Chishima T, Shimada H, Moossa A, and Hoffman R (1998). Widespread skeletal metastatic potential of human lung cancer revealed by green fluorescent protein expression. *Cancer Res* **58**, 4217–4221.

[79] Hoffman R (1999). Orthotopic transplant mouse models with green fluorescent protein-expressing cancer cells to visualize metastasis and angiogenesis. *Cancer Met Rev* **17**, 271–277.

[80] Hofmann B, Bogdanov A, Jr, Marecos E, Ebert W, Semmler W, and Weissleder R (1999). Mechanism of gadophrin-2 accumulation in tumor necrosis. *J Magn Reson Imaging* **9**, 336–341.

[81] Fillmore HL, Shurm J, Furqueron P, Prabhu SS, Gillies GT, and Broaddus WC (1999). An *in vivo* rat model for visualizing glioma tumor cell invasion using stable persistent expression of the green fluorescent protein. *Cancer Lett* **141**, 9–19.

[82] MacDonald TJ, Tabrizi P, Shimada H, Zlokovic BV, and Laug WE (1998). Detection of brain tumor invasion and micrometastasis *in vivo* by expression of enhanced green fluorescent protein. *Neurosurgery* **43**, 1437–1442.

SPECTRAL_0000724

[83] Moore A, Marecos E, Simonova M, Weissleder R, and Bogdanov A, Jr (1998). Novel gliosarcoma cell line expressing green fluorescent protein: a model for quantitative assessment of angiogenesis. *Microvasc Res* **56**, 145–153.

[84] Kajiyama N, and Nakano E (1991). Isolation and characterization of mutants of firefly luciferase which produce different colors of light. *Protein Eng* **4**, 691–693.

[85] Wood KV, Lam YA, Seliger HH, and McElroy WD (1989). Complementary DNA coding click beetle luciferases can elicit bioluminescence of different colors. *Science* **244**, 700–702.

[86] Wood KV, Lam YA, and McElroy WD (1989). Introduction to beetle luciferases and their applications. *J Biolumin Chemilumin* **4**, 289–301.

[87] Wood KV (1990). *Luc* genes: introduction of colour into bioluminescence assays. *J Biolumin Chemilumin* **5**, 107–114.

[88] Eames BF, Benaron DA, Stevenson DK, and Contag CH (1999). Construction and *in vivo* testing of a red-emitting firefly luciferase. Proceedings of SPIE Annual Meeting. SPIE, pp. 36–39.

[89] Stables J, Scott S, Brown S, Roelant C, Burns D, Lee MG, and Rees S (1999). Development of a dual glow-signal firefly and *Renilla* luciferase assay reagent for the analysis of G-protein-coupled receptor signalling. *J Recept Signal Transduction Res* **19**, 395–410.

[90] Chalfie M, Tu Y, Euskirchen G, Ward WW, and Prasher DC (1994). Green fluorescent protein as a marker for gene expression. *Science* **263**, 802–805.

[91] Chalfie M (1995). Green fluorescent protein. *Photochem Photobiol* **62**, 651–656.

[92] Heim R, and Tsien RY (1996). Engineering green fluorescent protein for improved brightness, longer wavelengths and fluorescence resonance energy transfer. *Curr Biol* **6**, 178–182.

SPECTRAL_0000725

Photochemistry and Photobiology, 1997, 66(4): 523–531

Visualizing Gene Expression in Living Mammals Using a Bioluminescent Reporter

Christopher H. Contag*[1], Stanley D. Spilman[1], Pamela R. Contag[2], Masafumi Oshiro[3], Brian Eames[1], Phyllis Dennery[1], David K. Stevenson[1] and David A. Benaron[1,4]

[1]Department of Pediatrics, Stanford University School of Medicine, Stanford University, Stanford, CA, USA;
[2]Xenogen Corporation, Stanford, CA, USA;
[3]Hamamatsu Corporation, Bridgewater, NJ, USA and
[4]Hansen Experimental Physics Laboratory, Stanford University, Stanford, CA, USA

Received 25 April 1997; accepted 28 July 1997

ABSTRACT

Control of gene expression often involves an interwoven set of regulatory processes. As information regarding regulatory pathways may be lost in *ex vivo* analyses, we used bioluminescence to monitor gene expression in living mammals. Viral promoters fused to firefly luciferase as transgenes in mice allowed external monitoring of gene expression both superficially and in deep tissues. *In vivo* bioluminescence was detectable using either intensified or cooled charge-coupled device cameras, and could be detected following both topical and systemic delivery of substrate. *In vivo* control of the promoter from the human immunodeficiency virus was demonstrated. As a model for DNA-based therapies and vaccines, *in vivo* transfection of a luciferase expression vector (SV-40 promoter and enhancer controlling expression) was detected. We conclude that gene regulation, DNA delivery and expression can now be noninvasively monitored in living mammals using a luciferase reporter. Thus, real-time, noninvasive study of gene expression in living animal models for human development and disease is possible.

INTRODUCTION

We set out to establish a method to access real-time information pertaining to gene expression in living adult mammals. Gene regulation is fundamental to both normal development and pathologic conditions. Consequently, a considerable amount of research effort is devoted to assessing levels of expression from genetic regulatory elements under various conditions. Fusion of regulatory elements to reporter genes can be used to monitor levels of expression, typically via *ex vivo* methods. These methods involve excision of tissue and assessing levels of the reporter molecule in histological sections or in cell lysates using optically distinct substrates for the reporter enzymes (1,2). Such analyses are performed on biopsy or postmortem samples, which eliminates the possibility of understanding regulation in living animals in real-time, and limits these assays to single points in time. Temporal analyses require large numbers of animals, as several animals are used for each time point. Considerably more data could be obtained if the assays were performed *in vivo*, and the cost and effort of animal studies would be reduced.

Monitoring physiological processes using external sources of light has been accepted as a clinical tool (*e.g.* pulse oximetry) and is gaining acceptance as an imaging modality that can reveal both structure and function (3,4). These technologies are based on the ability of photons to pass through mammalian tissue despite its light absorbing and scattering properties (5). Advances in this area of research prompted us to investigate external detection of internal sources of light to determine the location of pathogens (6), and the temporal and spatial expression of mammalian genes. This method could be broadly applied to monitoring expression from transgenes, DNA- or cell-based therapies and host response to infection, as well as the tracking of pathogens and tumor cells in living animal models.

Real-time, *in vivo* monitoring of bioluminescent reporters has been described. However, such assays to date have been limited to organisms that are thin or essentially transparent (7–12) or to stages in development when the organism is translucent (9,13). We previously demonstrated noninvasive monitoring of bacterial pathogens in living adult mice using an internal bioluminescent light source (6), raising the possibility of real-time monitoring of gene expression in adult animals using bioluminescent reporters. Several animal model systems were available for developing this methodology, of which two were selected: a transgenic mouse where the transgene consists of the promoter from the human immunodeficiency virus (HIV)† fused to the firefly luciferase gene (*luc*) and an *in vivo* transfection of a luciferase expression vector in rats.

*To whom correspondence should be addressed at: Neonatal and Developmental Medicine, Grant Building, S-257, MC 5119, Department of Pediatrics, Stanford University School of Medicine, Stanford, CA 94305-5119, USA. Fax: 650-725-7724; e-mail: ccontag@cmgm.stanford.edu

© 1997 American Society for Photobiology 0031-8655/97 $5.00+0.00

†*Abbreviations:* CCD, charge-coupled device; DMSO, dimethylsulfoxide; HIV, human immunodeficiency virus; ICCD, intensified charge-coupled device; i.p., intraperitoneal; LTR, long terminal repeat; MCP, microchannel plate; p.i., postinfection; TCID, tissue culture infective dose; Tg, transgenic.

SPECTRAL_0000726

In the first luciferase animal model that we describe, the HIV promoter has been placed upstream of the luciferase coding sequence. In the viral genome, the HIV promoter resides in the long terminal repeats (LTR). A transgenic (Tg) mouse line with luciferase expressed from the HIV promoter (LTR–*luc* Tg) has been described (14). Although regulated differently in rodent and human cells, expression from the HIV promoter in rodent cells has some similarities to that in human cells and is inducible with various treatments including illumination with UV light (14,15), skin abrasion (2) and chemical induction (16–18). In the dermis of transgenic mice, the HIV promoter can be induced by topical treatment with dimethyl sulfoxide (DMSO), with maximum induction after 24 h (16).

The development of DNA-based therapies and vaccines would benefit from the ability to externally monitor gene delivery and expression. In our second model, we evaluated *in vivo* transfections using a luciferase expression vector and cationic liposome-mediated delivery as has been suggested for DNA-based therapies and vaccines (19–23). DNA has also been successfully delivered to cells in tissues and expressed in living animals by direct DNA injection, electroporation and particle bombardment. Based on a review of the literature, liposome-mediated gene transfer appeared to be the most efficient and cost effective means of assessing the usefulness of noninvasive luciferase monitoring in the evaluation of *in vivo* transfection. Unlike the transgenic animal model, not all cells in a given tissue are likely to contain the reporter construct, and weak signals may be expected in this type of assay. Therefore, we used a luciferase expression vector in which the luciferase gene was modified for optimal mammalian codon usage and removal of the peroxisome targeting site, which was driven by a strong viral promoter and enhancer (SV-40).

In this report, we noninvasively monitored the expression of both stably integrated and transiently transfected bioluminescent reporter gene fusions in both cell culture and living rodents. In our previous pathogenesis model, the bacterial pathogen could be modified to express enzymes for intracellular biosynthesis of the luciferase substrate (6,24). Intracellular biosynthesis of substrate, D-luciferin, is not yet possible in mammalian cells expressing firefly luciferase, thus it must be added exogenously. We demonstrate that D-luciferin can be delivered to living cells in culture and to tissue sites of luciferase expression *in vivo*. Furthermore, we report noninvasive monitoring of gene expression in living mammals from both superficial and deep tissue sites of expression and demonstrate visualization of gene delivery in transient transfections as used in gene therapies and gene vaccines. Finally, we demonstrate efficient control of the HIV promoter in adult transgenic mice and developmental regulation in neonates. These studies indicate that substrate availability and photon passage through tissues are not limiting in the use of bioluminescent reporters in living animals and suggest that promoters, with reasonably high expression, can be noninvasively evaluated in some tissues of living laboratory animal models.

MATERIALS AND METHODS

Cell culture. A human T cell line (Jurkat-derivative; 1G5) stably transfected with an HIV LTR–*luc* construct, originally prepared by E. Aguilar-Cordova and J. Belmont (25) was obtained from the AIDS Research and Reference Reagent Program of the NIH. This line was propagated in RPMI medium supplemented with penicillin, streptomycin, glutamine (2 m*M*) and fetal calf serum (10%). Cells were plated in 24 well dishes at 5×10^5 cells per well and infected with 1×10^4 tissue culture infectious doses (TCID) of HIV-1 strain A111 (laboratory isolate of a subtype B North American HIV-1, kindly provided by Drs. R. Shafer and T. Merigan of the Center for AIDS Research at Stanford) in a total volume of 200 μL. The cells and viral inoculum were maintained in this volume for 4 h after which an additional 800 μL of medium was added. At 22 h post-infection (p.i.) the substrate luciferin (50 m*M*; Molecular Probes, Seattle, WA) was added to each well at a final concentration of 0.5 m*M*. Wells were imaged at 24 h p.i. and at subsequent times as indicated. Cells were maintained for 7 days in luciferin-containing medium.

Animal subjects. Transgenic mice, containing the HIV LTR–luciferase fusion (mouse line 333 generated by Dr. John Morrey and coworkers (14), Utah State University), were initially obtained from Jackson Laboratories (Bar Harbor, ME). Subsequently, a breeding nucleus was obtained directly from Dr. Morrey and then bred and maintained in the Research Animal Facility at Stanford University under strict adherence to institutional guidelines.

To activate LTR–*luc* expression, DMSO (17) (100%, J. T. Baker) was applied twice topically to regions of skin at 24 and 16 h prior to imaging. If necessary, skin was shaved to remove hair just prior to application of DMSO. This method of promoter induction was found to be optimal for expression of luciferase in adult transgenic mice of this line (data not shown). In neonatal LTR–*luc* Tg mice the LTR was not induced chemically or by any other known means. Thus, only basal levels of expression were studied (*i.e.* gene expression in these animals was not modulated by any of the above-described treatments or any other known activators).

For imaging, mice and rats were anesthetized and imaged as previously described (6) using pentobarbital (70 mg/kg body weight). An aqueous solution of the substrate, luciferin (50 m*M*, 126 mg/kg), was injected into the peritoneal cavity 20 min prior to imaging for systemic delivery or applied topically (50 m*M* unless otherwise indicted) in 100% DMSO for transdermal delivery. Luciferin was also electroporated into skin of the ear using a caliper electrode (Gentronics/BTX, San Diego, CA) connected to an electroporator (Electro Cell Manipulator, model 600, Gentronics/BTX) under the following conditions: 120 V, 100 μF, 72 Ω, resulting in a time constant of 6–7 ms.

Imaging. At the time of imaging, animals were placed in a light-tight chamber, and a gray-scale body surface image was collected as a reference in the low room light provided by leaving the chamber door slightly open. Subsequently, the door to the chamber was closed to exclude the room light that obscured the relatively dimmer luciferase bioluminescence. Photons emitted from luciferase within the animal, and then transmitted through the tissue, were collected and integrated for a period of time between 5 and 30 min. A pseudocolor image representing light intensity (blue least intense and red most intense) was generated on an Argus 20 image processor (Hamamatsu, Japan); images were transferred using a plug-in module (Hamamatsu, Japan) to a computer (Macintosh 8100/100, Apple Computer, Cupertino, CA) running an image processing application (Photoshop, Adobe, Mountain View, CA). Gray-scale reference images and pseudocolor images were superimposed using the image processing software, and annotations were added using another graphics software package (Canvas, Deneba, Miami, FL).

An intensified charge-coupled device (CCD) camera (C2400-32, Hamamatsu), fitted with a 50 mm Nikkor lens (Nikon, Japan) and an image processor (Argus 20, Hamamatsu), was used in this study. In the comparison of this system to a cooled CCD (C4880-06, Hamamatsu) equipped with the same lens (subjects at the same distance from the lens), images were collected on a PC and then transferred to a Macintosh computer and processed as above.

Biochemical assays. Luciferase activity in tissue homogenates was determined with a commercially available assay kit (Promega, Madison, WI) that included acetyl Co-A to prolong light emission. A standard luminometer (LKB/Wallac, Stockholm, Sweden) was used to measure total light emission in conditions recommended by the manufacturers. Conversely, for substrate assays, luciferase (1

SPECTRAL_0000727

ng/mL) was substituted for luciferin in the same assay system and relative levels of substrate were determined in tissues of BALB/c mice (Stanford University) not expressing luciferase. An aqueous solution of luciferin (50 m*M*, 126 mg/kg) was injected intraperitoneally (i.p.) into BALB/c mice, and substrate levels in brain, skin and liver were assayed after 20 min.

In vivo *DNA delivery.* Seven day old Wistar rats were obtained from Simonsen (Gilroy, CA). A cationic liposome solution, Lipofectin (100 μL, Gibco-BRL, Gaithersberg, MD) was mixed with 100 μg of plasmid DNA (pGL3control vector, Promega, Madison, WI). The luciferase expression in this commercially available vector is under control of the SV-40 promoter and SV-40 enhancer, and the luciferase gene has been modified for higher levels of expression in some mammalian cells by removal of the peroxisome targeting site and optimization of codon usage for mammalian cells. Following incubation at 22°C for 15 min, DNA and liposome complexes were injected directly into the lungs of 7 day old rats in groups of three animals. Treated animals were then injected with an aqueous solution of luciferin (i.p.), and imaged at 24, 48 and 72 h. Images were obtained with an integration time of 30 min.

RESULTS

Bioluminescence in culture

Luciferase as a transcriptional reporter was used as a means to monitor viral replication in living cultured cells, using LTR activation as a molecular indicator of viral replication. We chose this approach because the LTR of HIV-1 contains elements that respond to both viral encoded factors (Tat protein) and host transcription factors. Thus, these genetic elements can function together as a molecular indicator reporting either viral replication or changes in cellular transcription factor profiles. In the case of infection, viral-encoded Tat can transactivate the LTR in promoter fusions, therefore transactivation can be used as an indicator of infection. Currently, analysis of transactivation of the HIV LTR *via* Tat is performed using lengthy biochemical assays (26). When LTR activity is coupled to luciferase expression, the LTR becomes a molecular switch controlling a biochemical light bulb, permitting noninvasive monitoring. This approach had previously been demonstrated to indicate levels of viral replication as measured in cell lysates (27) and more recently to assess transcription, microscopically, in single living cells (28). However, rapid analysis and detection of transactivation at a macroscopic level had not been previously demonstrated.

Expression of luciferase as a rapid, real-time macroscopic indicator of viral replication in cell culture is shown (Fig. 1). In these studies of infected cell populations, a stably integrated LTR–*luc* construct was used as the reporter (1G5 cell line). Luciferin was added directly to the living cells, and infected cultures were followed over time. Signal above background was apparent at 96 h p.i. and increased to a peak at 7 days. The numbers of syncytia (cytopathic effect due to replication of HIV) corresponded to levels of bioluminescence at each time point (data not shown), suggesting that bioluminescence was a reliable indicator of viral replication. This approach may accelerate viral assays, and reduce handling because detection, photon counting, can be done remotely with minimal human handling.

Substrate availability in cell culture was adequate to detect luciferase activity in this human T cell line. In addition, luciferase enzyme assays could also be performed in living rodent cells (NIH 3T3) and another human cell line (HeLa) transiently expressing luciferase from the pGL3 vector (data not shown). With a single addition of substrate, transiently transfected 3T3 and HeLa cells were uniformly bioluminescent from 48 to 72 h, and the decline after this time likely corresponds to loss of the reporter through cell division. Therefore, the availability of luciferin to intracellular luciferase appeared to be sufficient in these cell lines.

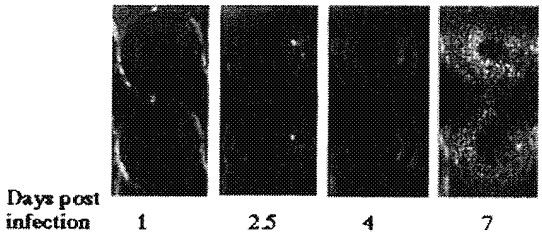


Figure 1. Bioluminescent reporter for promoter activity in cultured cells. Jurkat cells stably transfected with a plasmid containing the HIV LTR (1G5 (25); AIDS Research and Reference Reagent Program) upstream of the coding sequence of firefly luciferase were infected, in duplicate, with a laboratory isolate of HIV-1 (strain A111) using standard laboratory conditions and followed for a period of 7 days for emission of bioluminescent light. Four time points are shown: 1, 2.5, 4 and 7 days. At each time point a gray-scale image of the plate was generated in low room light followed by collection of photons emitted from the cultured cells in complete darkness for a period of 10 min. A color pseudoimage representing the intensity of bioluminescent light was superimposed over the gray-scale image of the plate. At 7 days p.i. a clear signal is present in the duplicate cultures indicating high levels of replication. The images at different time points represent the same two wells over the 7 day period.

Bioluminescence in whole animals

Application of the method described above for cells in culture to living mammals required demonstration that luciferin could be delivered to cells in target organs. As the intracellular biosynthesis of the substrate, D-luciferin, is not yet possible in mammalian cells, it must be delivered exogenously. We evaluated the delivery of luciferin to different cells in the body after i.p. injections. In this experiment, D-luciferin was injected i.p. into BALB/c mice, tissues were removed after 20 min, and luciferin assays, in which luciferase replaced luciferin in the buffer system, were performed on tissue homogenates from brain, skin and liver. Detectable levels of the substrate were found in all tissues analyzed (data not shown) indicating that substrate availability may not limit the ability to assess gene expression in various tissues of living animals.

Use of luciferase as a rapid, real-time *in vivo* indicator of genetic transfection in mammals is shown (Fig. 2). In these experiments, a luciferase expression vector was used to transfect cells of tissues in living rodents. Young Wistar rats were given a single unilateral injection of DNA–liposome complexes intrapleurally. The pGL3–control vector encoding a modified firefly luciferase was used in these assays. After 48 h, bioluminescence was detected unilaterally (a representative animal is shown in Fig. 2). Signals above background were not detected at other times. The contralateral lungs in these rats were used as internal negative controls as only the liposome preparation without DNA was injected at this site. These data suggest that peak levels of expression

SPECTRAL_0000728



Figure 2. Monitoring transient gene expression in chimeric animals. The luciferase expression vector, pGL3control, was delivered to *cells in the lung of* neonatal rats *via* cationic liposome delivery, and substrate was injected i.p. at 24 and 48 h post-DNA delivery. A representative image at the 48 h time point is shown. This image indicates that luciferase expression (color) from transient *in vivo* transfections of the lung can be monitored externally.



Figure 3. Unilateral induction of expression. The left half of the shaved dorsal surface of animals and the left ear were treated twice daily for 2 days with DMSO to activate expression of the HIV-1 LTR. Luciferin was applied topically over the entire surface of the back and both ears, and animals were imaged immediately after addition of substrate. Unilateral emission of bioluminescence (color) corresponding to the induced region was observed in groups of mice and a representative image is shown.

in the transfected tissues occurred after 2 days and indicate that luciferase expression, as measured by photon emission, can be used to noninvasively monitor *in vivo* transfections of cells in deep tissues of laboratory rodents. Moreover, the i.p. injection of luciferin appeared to adequately supply the intrapleural luciferase reaction with substrate. Such monitoring of reporter gene expression in deep tissues may be limited by absorbing and scattering tissues such as liver, and weak signals may not be apparent with external monitoring. Subsequent empirical determinations of the limits of detection will enhance our understanding of these anticipated limitations.

To further investigate use of *in vivo* luciferase monitoring for studying gene regulation in living animals, we used a transgenic mouse line where the promoter fusion (LTR–*luc*) is present in all cells. In this transgenic mouse, the promoter can be regulated and luciferase expressed in a variety of tissues. This transgene was initially selected for evaluation due to known activity of the HIV LTR in the skin; given the uncertainty of tissue penetration by photons from a weakly bioluminescent internal signal, a superficial site of expression was preferred for preliminary studies monitoring luciferase expression *in vivo*.

Use of luciferase as a rapid, real-time *in vivo* indicator of gene activation in a mammal is shown (Figs. 3 and 4). In the skin of LTR–*luc* Tg mice, expression of the HIV LTR has been reported to possibly occur in Langerhans cells (14,15); in skin cells the promoter can be activated with DMSO. Topical application of substrate appeared to be the most direct means of delivery. Of the various methods for transdermal delivery of small molecules, use of DMSO appeared to be suitable given the size and charge of the luciferin molecule. The extent of our ability to control and monitor gene expression in the skin of transgenic mice was tested by activating the gene in cells of approximately half of the shaved back and one ear of each LTR–*luc* Tg mouse. Twenty-four hours after initial activation with DMSO, the entire surface and both ears of each mouse were treated with 50 m*M* luciferin in 100% DMSO and a representative image is shown (Fig. 3). The effects of DMSO, which was used to deliver substrate to the expressing cells, on LTR expression was negligible in the time from substrate addition to imaging (less than 1 h).

A uniform bioluminescent signal from the region of the

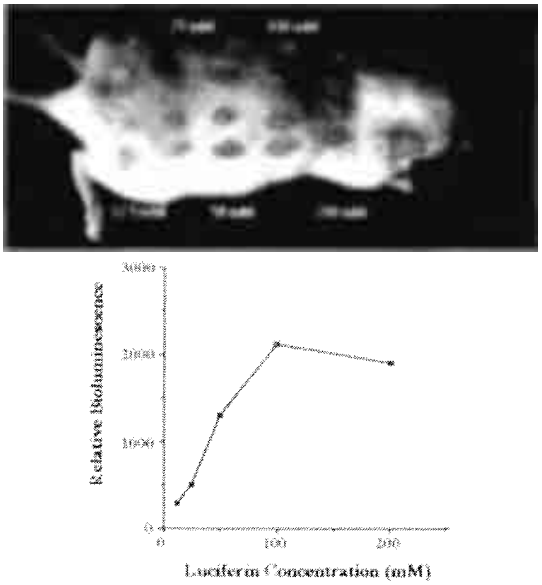


Figure 4. Transdermal delivery of substrate using DMSO. The HIV-1 LTR was induced in the skin of mice with twice daily treatments of DMSO over the entire surface of the back and the right ear for 2 consecutive days. Substrate was applied to the skin in solutions prepared in DMSO at a concentration of 200, 100, 50, 25 and 12.5 m*M*. A volume of 5 μL of each concentration was spotted in quadruplicate on skin using a multichannel pipette, with the highest concentrations near the head. Five microliters of the 50 m*M* luciferin solution was applied to each ear. (A) Two minutes after application, the animal was imaged as described in Fig. 1, and the bioluminescent response is shown (color). (B) The bioluminescent response appeared to increase linearly over the concentrations from 12.5 to 100 m*M*. Bioluminescence from 200 m*M* luciferin was roughly equivalent to, or slightly less than, that from 100 m*M*. DMSO solutions of luciferin containing water (25% H_2O in DMSO to 100% H_2O) resulted in no detectable bioluminescence (data not shown).

SPECTRAL_0000729



Figure 5. Transdermal delivery of substrate electrically and chemically. The LTR was activated in each ear of three mice, and then 24 h later substrate was delivered to the cells in DMSO or *via* electroporation and the animals were imaged. Bioluminescent signals were detected whether the substrate is delivered (A) electrically or (B) *via* electroporation.

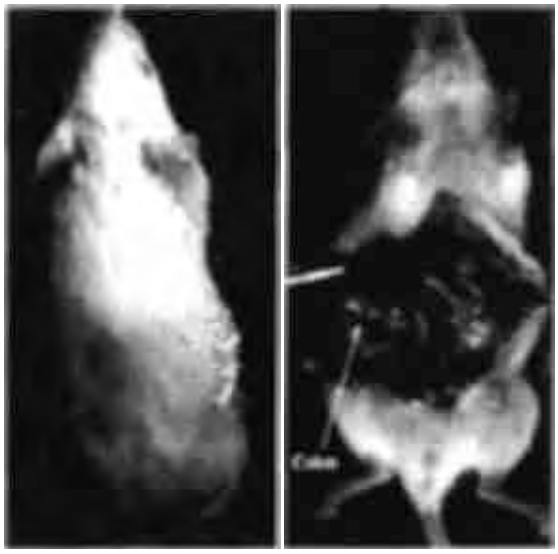


Figure 6. Detectable bioluminescence from internal tissues. (A) Bioluminescent signals were detectable from the abdomens of animals treated with DMSO on one ear only. This signal is assumed to be due to ingestion of DMSO during grooming. (B) Animals demonstrating signal from the abdomen were laparotomized and imaged. Bioluminescent signal localized to the colon in each of four animals studied, and in the animals shown in this figure, bioluminescence was tightly localized to a region of the colon (arrow), about 1 cm in length. In some other animals, the entire colon appeared to emit light.

backs in which the gene was activated was observed (Fig. 3), whereas signal from the nonactivated skin remained at background levels despite the presence of substrate in DMSO at the time of imaging. The ears served as internal negative and positive controls. Within the limits of this system, Fig. 3 demonstrates fairly good control of the HIV promoter in living animals and the ability to assay luciferase in large numbers of cells over large surface areas.

In experiments using various ratios of H_2O and DMSO for transdermal delivery of luciferin, the fraction of DMSO in these mixes ranged from 12.5 to 100%, bioluminescence could not be detected with luciferin made in solutions containing even 12.5% water (data not shown). A preparation of D-luciferin in pure DMSO, however, mediated transdermal delivery, as bioluminescence was easily detected from treated areas (Fig. 3) (24). To determine optimal substrate concentration for transdermal delivery, solutions of 12.5–200 m*M* luciferin in DMSO were spotted in quadruplicate directly on the skin 24 h after LTR activation (Fig. 4). In these experiments, the backs of mice were shaved, and the HIV-1 LTR was activated with twice daily treatments of DMSO 24 h and 16 h prior to analysis. Signals were quantified on images and data were plotted (Fig. 4). Bioluminescence increased linearly from 12.5 to 100 m*M* but remained relatively constant from 100 to 200 m*M* luciferin. These data suggest that 100 m*M* luciferin in 100% DMSO is the optimal concentration for transdermal delivery of this small molecule.

Gene activation due to the DMSO used to carry substrate into the expressing cells would not be apparent in the time from substrate addition to imaging. However, the use of DMSO for transdermal substrate delivery may be limiting in some studies of the HIV LTR as the promoter is simultaneously activated by DMSO. Therefore, electrodelivery of substrate to the skin was investigated as an alternative method. A representative comparison of chemical transdermal delivery (DMSO) and electrodelivery is demonstrated in Fig. 5. In three of three animals, electrodelivery of luciferin was comparable to chemical delivery. Cells in the ear may be more accessible than other tissues and with similar conditions electrodelivery of substrate was not achieved on the shaved backs of mice (data not shown). Electrodelivery is unidirectional relative to electron flow. Therefore, optimal bioluminescence would likely be obtained from the ears if the substrate was delivered to both sides by pulsing the tissue, reversing the polarity and giving an additional pulse.

During the initial evaluation of this imaging method, the active, inducible nature of the HIV LTR in cells of the skin was useful. However, following successful visualization of transient *in vivo* transfection with the mammalian expression vector (pGL3) and the initial studies demonstrating detection of LTR expression in superficial tissues, it appeared that photonic detection of luciferase expression from a variety of tissue sites was possible. After a single dose of luciferin (126 mg/kg) was injected into the peritoneal cavity, photon emission from the skin of the ears peaked at 20 min (29). With systemic rather than topical application of substrate, additional sites of expression from the LTR, other than the skin, could be identified (Fig. 6A). Photons originating from cells in the colon (Fig. 6B) were apparent externally, indicating that LTR–*luc* expression from deep tissues was also possible. This was also observed with expression from pGL3control vector in the lungs (Fig. 2). In earlier studies, externally viewed bioluminescent signals from the colon were not as intense as those obtained after removal of the skin and peritoneal wall exposing the viscera (6). This reduction in signal may affect studies using either weak bio-

SPECTRAL_0000730

luminescent signals, larger animal models or signals originating from more absorbing and scattering tissues such as liver.

Comparison of CCD detectors

Two different types of imaging systems were compared, as the optimal system for use in low-light imaging of biological processes in living animals was not previously determined. We focused on systems based upon the CCD, as it is a readily available, low-cost detector with many features supporting use for luciferase imaging. A CCD operates by converting photons that strike a CCD pixel into electrons and accumulating a charge that represents the number of photons striking each pixel. Maximum conversion of photons to electrons occurs at wavelengths between 400 and 1000 nm, and thus a CCD can detect visible through near infrared light. However, there are several important limitations in using a standard video rate CCD for *in vivo* luciferase imaging. First, in order to quantitate the electrons in each pixel, the stored charge must be read out. The signal produced when the photons first strike the CCD is too small to be sensed by the readout circuitry. Thus, to be recognized as a signal over noise, there is a minimum number of photons that must strike each pixel before the stored charge is converted to signal. This read noise is about 150 electrons for a typical video rate CCD design. Second, not all photons striking the detector are converted to electrons. The response of a CCD is wavelength dependent, and the standard efficiency of video rate CCD is about 35% (*e.g.* the probability that a given photon will strike the CCD and produce a change in stored charge is about 1 in 3). Last, there are background count sources, such as thermal energy or gamma rays, that can trigger false charges not originating from the luciferase construct. A good detector is shielded from background radiation and uses materials and components that are low in emitter-containing substances.

These CCD limitations can be overcome in several ways. First, intensified CCD (ICCD) amplify the signal relative to the noise by using an image intensifier that has both a photocathode and a microchannel plate (MCP) attached to a high-voltage element, such that many electrons are released when struck by a single photon. The camera noise is then discriminated by photon counting imaging. One advantage of these devices is that a single photon now results in a detectable signal, and single photon detection becomes possible. With an intensifier, some loss of image resolution occurs as the electron spray produced by the intensifier results in a blurring of the image, particularly if more than one intensifier stage is used in series. An advantage of the ICCD approach is that the intensifier can be designed to serve as a high-pass filter that amplifies only those photons with an energy at or above a desired level. In the ICCD system used in this study, amplification occurred only for photons with a wavelength of 600 nm or shorter, thus the background noise is minimal. A second alternative to the ICCD is a system where the CCD detector is cooled to reduce the background thermal noise, the signal is read slowly to reduce the read noise (less than 10 electrons), and the CCD chip used has higher photon to electron conversion rate (higher than 60%). In this cooled CCD the improvement scales linearly with integration time. Thus, short exposures benefit minimally from this approach. A combination of technologies can also be employed in which the intensifier of an ICCD is cooled. Cooled ICCD or alternatives to CCD-based systems were not explored in this study.

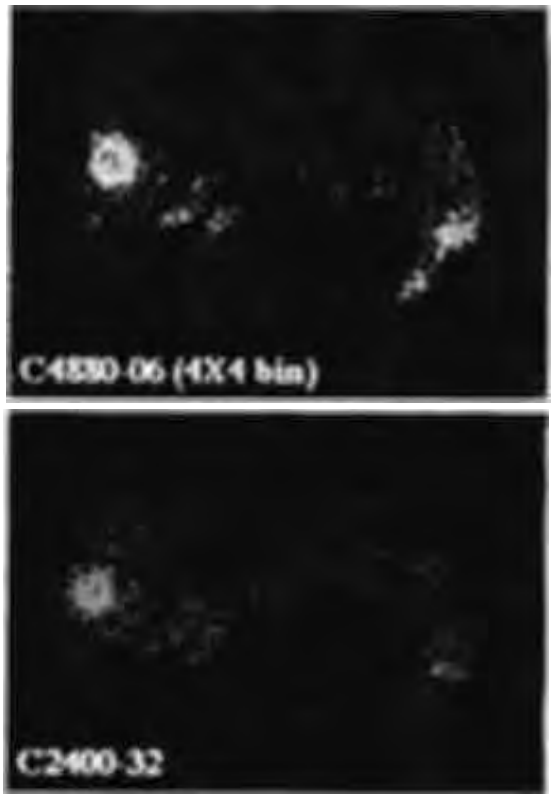


Figure 7. The LTR expression in neonatal mice and comparison of intensified and cooled CCD cameras. Four day old LTR–*luc* transgenic mice were imaged after luciferin injection with (A) a cooled CCD detector (C4880-06) and (B) an intensified CCD detector (C2400-32). Pixels were binned (4 × 4) with the cooled device, and 10 min integration times were used with each system. The images of bioluminescent light emission are nearly equivalent with each device. Gray-scale reference images are not shown.

A comparison of images from cooled and intensified CCD cameras using the neonatal LTR–*luc* Tg mouse model is shown (Fig. 7). Two images that were taken within minutes of each other of the same neonatal mouse (4 days of age) are presented (Fig. 7). These images were obtained with an ICCD (C2400-32) and a cooled CCD (C4880-06 cooled to −30°C, 16 pixels were binned; 4 × 4). The two images appear approximately equivalent. Thus, in the current model, no significant difference was seen between the two types of systems. Practically, however, an ICCD with the photon counting imaging method offers the advantage of showing real-time images as the signal accumulates, allowing for continuous monitoring of the process.

Developmental expression of the LTR

In Fig. 7 expression from the LTR in the 4 day old mouse was not induced by chemical treatment or by any other

SPECTRAL_0000731

known exogenous method. That is, the observed expression was under endogenous control of the regulatory element (HIV LTR). In these neonatal LTR–*luc* Tg mice, luciferase expression appeared to be elevated in the eye and limbs, and an overall basal level of activity was apparent over the entire animal. These patterns of expression were consistent with newborn LTR–*luc* Tg mice up to 4 days of age, at which time the elevated levels of expression in the eye decreased to background. Elevated levels of expression in the limbs appeared to be more variable. This suggests that the HIV LTR may serve as a probe for developmental gene regulation that marks steps in development of this animal model.

DISCUSSION

This study demonstrates our ability to visualize genetic responses of living cells in culture and in intact mammals by using bioluminescent light to report gene activity under varied conditions, such as viral replication and gene activation. Further, we demonstrate that the substrate for the luciferase reaction can be provided to mammalian cells in the intact animal. Delivery was optimized for systemic and transdermal delivery. Transdermal delivery was achieved by chemical or electrical means. All of the events described here can be monitored using commercially available ICCD detectors.

Mammalian development, host response to infection and house-keeping operations of organisms are ultimately controlled by a complex genetic program allowing the organism to respond to and interact with numerous environmental factors. This genetic program includes regulatory elements that act as switches for spatiotemporal control of gene expression in response to specific signals. Organisms have the ability to modulate gene expression over a wide range of dose–response relationships, where no expression and full-blown expression represent the ends of a continuous spectrum. An ability to study these genetic events noninvasively will increase our understanding of these processes in living mammals.

Since luciferin is taken up by mammalian cells in culture without overt signs of cytotoxicity and provides reasonable bioavailability of the substrate in living mammals, it appears that luciferase can function as a reporter for DNA delivery directly to living tissues. Monitoring expression of a modified luciferase gene fused to the SV-40 promoter transfected by cationic liposome delivery was used as a rapid assay for testing delivery of substrate to tissue sites. The ability to observe a bioluminescent signal from cells expressing luciferase in this model for DNA-based therapies and vaccines suggests that the substrate reaches useful concentrations in cells of the lung and perhaps other tissues following i.p. injections. Codelivery of the reporter gene or co-expression from a single promoter may allow rapid evaluation of different methods of delivery and duration of expression in the development of emerging DNA- and cell-based therapies. The luciferase expression detected optically in various tissues, and our data on substrate levels in different tissues indicate that substrate availability is not limiting and that a variety of promoters expressed in different tissues can be studied using this method.

Reproducible, qualitative signals can be obtained from both superficial and deep tissue photon emissions, indicating a qualitative correlation between detected light levels and two-dimensional detection of the desired event. It is likely that, at least within the same tissue, levels of light can be qualitatively compared, because graded responses were obtained from skin, ears and eyes. At present, quantitation of a genetic event coupled to luciferase by measurement of the bioluminescent light traversing live, intact tissue has not been achieved. This is due in part to the unknown kinetics of the reaction (*e.g.* uncertain local physiologic conditions, substrate and enzyme concentrations) as well as uncertainties regarding the tissue optics (*e.g.* variable transmission of the generated light based upon depth, and the dependence of transmission upon variable and unknown tissue-specific absorbance and scattering characteristics of the tissues interspersed between light generation and light detection).

The *in vivo* study of LTR–*luc* Tg mice demonstrated that in this mammalian model: (1) a number of variables can be tested simultaneously in a single animal noninvasively, (2) luciferase can be used as a reporter for expression in deep tissues, (3) developmental control of expression from the HIV promoter can be assessed in living animals and (4) transdermal delivery of small molecules (luciferin) can be evaluated in living mice. Therefore, *in vivo* monitoring of luciferase expression can be used to titrate, in real-time, the effective doses of individual compounds or their combinations for transfection of living tissue, which is useful for optimizing the DNA delivery and expression of DNA-based therapies. In addition, a number of inhibitory molecules as potential therapeutic agents could be tested rapidly and in real-time, accelerating their development for use in human therapies. A significant amount of data from each rapid assay can be collected, allowing evaluation of several different conditions simultaneously, at different time points and without *ex vivo* sample processing (*e.g.* removing the tissues, lysis of the cells or other sample preparations). Performing the assays directly on tissues in the living animal can be an alternative to *in vitro* biochemical assays or a complementary *in vivo* approach to test predictions made from *in vitro* data.

The ability to use such probes in living animals is a powerful tool for revealing steps in the complex regulatory pathways involved in development and response to infection. Toward this end we have evaluated the HIV promoter in culture and in living transgenic mice. Viral promoters utilize host and viral transcription factors to achieve levels of expression that are commensurate with requirements of viral replication. Some viral proteins are expressed to relatively high levels during infection, and promoters for genes encoding these proteins have been exploited to achieve elevated expression of experimental and therapeutic genes (*e.g.* SV-40 promoter in pGL3control vector). In neonatal LTR–*luc* Tg mice, a basal level of bioluminescence was detected in the absence of chemical or physical induction, and elevated signals have been observed in the developing eye and limbs with a rapid postnatal decline in all tissues over the first few weeks of life (Contag *et al.*, unpublished results). The reliance of viral promoters on host factors may thus make them useful as molecular probes for understanding host cell gene regulation.

The HIV LTR is regulated differently in mouse cells compared to cells of human origin; however, the ability to con-

SPECTRAL_0000732

trol LTR expression in rodent cells with DMSO and UV light has significance in understanding the role of host transcription factors in viral replication. The regulatory region (−167 to +80) in the HIV LTR contains numerous canonical binding sites for cellular transcription factors (30,31). Ultraviolet light-mediated activation of HIV-1 replication has been proposed in infections of humans, and the Tg mice serve as a model for this environmental factor (32). Moreover, Langerhans cells in the skin of infected humans appear to support HIV-1 replication (33), and increased tropism for Langerhans cells has been linked to heterosexual transmission (34). Because LTR–*luc* appears also to be expressed in these cells in Tg mice, analysis of these animals may reveal host factors that mediate expression from the LTR in human Langerhans cells thus providing clues to the role of different cell tropisms in increased transmission and the involvement of UV light in human disease.

Even though the relationship of LTR regulation in transgenic mice to the pathogenesis of HIV in humans remains speculative, the use of the LTR–*luc* fusion in mouse cells serves as an excellent model for demonstrating the potential of *in vivo* monitoring and may help to identify and characterize human cellular factors that interact with viral-encoded Tat (35). The Tat transactivation of the HIV LTR differs in cells derived from humans and rodents (36); thus, studies comparing host factors from these two species may lead to an understanding of the transactivation mechanism and ultimately to the generation of rodent models for studying HIV pathogenesis. Small animal models for HIV pathogenesis would be invaluable in the discovery of vaccines and new antiviral therapies for HIV. Despite the obvious caveats related to using HIV LTR–*luc* Tg mice as a model for HIV pathogenesis at this time, initial data suggest that the differential expression of this promoter during murine development may also hold tremendous potential for understanding gene regulation involved in mammalian ontogeny. Moreover, development of therapies for a wide variety of human diseases could be accelerated with access to real-time gene expression data from living mammalian animal models.

Acknowledgements—We thank Hamamatsu Corporation for use of the photonic detection systems for comparisons in this study, Dr. John Morrey (Utah State) for the transgenic mouse line (LTR–*luc*) and his many helpful discussions and Dr. Michael Bachmann for critical review of this manuscript. This work was funded in part through grants from the California Universitywide AIDS Research Program (D.A.B. and C.H.C.), Stanford Office of Technology Licensing (C.H.C.), ONR contract N-00014-94-1024 and unrestricted research funds from Baxter Foundation (D.A.B. and C.H.C.), Mary L. Johnson (D.K.S.), and a grant from the Packard Fund at the Lucille Salter Packard Children's Hospital (D.A.B.).

REFERENCES

1. Lee, K. J., *et al.* (1992) Myosin light chain-2 luciferase transgenic mice reveal distinct regulatory programs for cardiac and skeletal muscle-specific expression of a single contractile protein gene. *J. Biol. Chem.* **267**, 15875–15885.
2. Morrey, J. D., S. M. Bourn, J. L. Morris, T. D. Bunch and R. W. Sidwell (1994) Activation of the human immunodeficiency virus long terminal repeat by abrasion of the skin in transgenic mice. *Intervirology* **37**, 315–320.
3. Benaron, D. A., J. P. Van Houten, W. F. Cheong, E. L. Kermit and R. A. King (1995) Early clinical results of time-of-flight optical tomography in a neonatal intensive care unit. *SPIE* **2389**, 582–596.
4. Muller, G., B. Chance, and R. Alfano (eds.) (1993) *Medical Optical Tomography: Functional Imaging and Monitoring.* SPIE Press, Bellingham, WA.
5. Benaron, D., W.-F. Cheong and D. Stevenson (1997) Tissue optics. *Science* **276**, 2002–2003.
6. Contag, C. H., P. R. Contag, J. I. Mullins, S. D. Spilman, D. K. Stevenson and D. A. Benaron (1995) Photonic detection of bacterial pathogens in a living host. *Mol. Microbiol.* **18**, 593–603.
7. Brandes, C., J. D. Plautz, R. Stanewsky, C. F. Jamison, M. Straume, K. V. Wood, S. A. Kay and J. C. Hall (1996) Novel features of *Drosophila* period transcription revealed by real-time luciferase reporting. *Neuron* **16**, 687–692.
8. Schneider, M., D. W. Ow and S. H. Howell (1990) The in vivo pattern of firefly luciferase expression in transgenic plants. *Plant Mol. Biol.* **14**, 935–947.
9. Matsumoto, K., M. Anzai, N. Nakagata, A. Takahashi, Y. Takahashi and K. Miyata (1994) Onset of paternal gene activation in early mouse embryos fertilized with transgenic mouse sperm. *Mol. Reprod. Dev.* **39**, 136–140.
10. Tamiya, E., T. Sugiyama, K. Masaki, A. Hirose, T. Okoshi and I. Karube (1990) Spatial imaging of luciferase gene expression in transgenic fish. *Nucleic Acids Res.* **18**, 1072.
11. Anderson, S. L., G. R. Teakle, S. J. Martino-Catt and S. A. Kay (1994) Circadian clock- and phytochrome-regulated transcription is conferred by a 78 bp cis-acting domain of the *Arabidopsis* CAB2 promoter. *Plant J.* **6**, 457–470.
12. Langridge, W., A. Escher, G. Wang, B. Ayre, I. Fodor and A. Szalay (1994) Low-light image analysis of transgenic organisms using bacterial luciferase as a marker. *J. Biolumin. Chemilumin.* **9**, 185–200.
13. Thompson, E. M., P. Adenot, F. I. Tsuji and J. P. Renard (1995) Real time imaging of transcriptional activity in live mouse preimplantation embryos using a secreted luciferase. *Proc. Natl. Acad. Sci. USA* **92**, 1317–1321.
14. Morrey, J. D., S. M. Bourn, T. D. Bunch, M. K. Jackson, R. W. Sidwell, L. R. Barrows, R. A. Daynes and C. A. Rosen (1991) In vivo activation of human immunodeficiency virus type 1 long terminal repeat by UV type A (UV-A) light plus psoralen and UV-B light in the skin of transgenic mice. *J. Virol.* **65**, 5045–5051.
15. Cavard, C., A. Zider, M. Vernet, M. Bennoun, S. Saragosti, G. Grimber and P. Briand (1990) In vivo activation by ultraviolet rays of the human immunodeficiency virus type 1 long terminal repeat. *J. Clin. Invest.* **86**, 1369–1374.
16. Morrey, J. D., S. M. Bourn, T. D. Bunch, R. W. Sidwell and C. A. Rosen (1992) HIV-1 LTR activation model: evaluation of various agents in skin of transgenic mice. *J. Acquired Immune Defic. Syndr.* **5**, 1195–1203.
17. Morrey, J. D., M. K. Jackson, T. D. Bunch and R. W. Sidwell (1993) Activation of the human immunodeficiency virus type 1 long terminal repeat by skin-sensitizing chemicals in transgenic mice. *Intervirology* **36**, 65–71.
18. Simon, G., C. Moog and G. Obert (1994) Valproic acid reduces the intracellular level of glutathione and stimulates human immunodeficiency virus. *Chem. Biol. Interact.* **91**, 111–121.
19. Zhu, N., D. Liggitt, Y. Liu and R. Debs (1993) Systemic gene expression after intravenous DNA delivery into adult mice. *Science* **261**, 209–211.
20. Stribling, R., E. Brunette, D. Liggitt, K. Gaensler and R. Debs (1992) Aerosol gene delivery in vivo. *Proc. Natl. Acad. Sci. USA* **89**, 11277–11281.
21. Alexander, M. Y. and R. J. Akhurst (1995) Liposome-mediated gene transfer and expression via the skin. *Hum. Mol. Genet.* **4**, 2279–2285.
22. Philip, R., D. Liggitt, M. Philip, P. Dazin and R. Debs (1993) In vivo gene delivery. Efficient transfection of T lymphocytes in adult mice. *J. Biol. Chem.* **268**, 16087–16090.
23. Liu, Y., D. Liggitt, W. Zhong, G. Tu, K. Gaensler and R. Debs (1995) Cationic liposome-mediated intravenous gene delivery. *J. Biol. Chem.* **270**, 24864–24870.
24. Contag, C. H., P. R. Contag, S. D. Spilman, D. K. Stevenson and D. A. Benaron (1996) Photonic monitoring of infectious disease and gene regulation. In *OSA TOPS on Biomedical Optical Spectroscopy and Diagnostics*, Vol. 3 (Edited by E. Sev-

SPECTRAL_0000733

ick-Muraca and D. Benaron), pp. 220–224. Optical Society of America, Washington, D.C.
25. Aguilar-Cordova, E., J. Chinen, L. Donehower, D. E. Lewis and J. W. Belmont (1994) A sensitive reporter cell line for HIV-1 tat activity, HIV-1 inhibitors, and T cell activation effects. *AIDS Res. Hum. Retroviruses* **10**, 295–301.
26. Rosen, C. A., J. G. Sodroski and W. A. Haseltine (1985) Location of cis-acting regulatory sequences in the human T-cell leukemia virus type I long terminal repeat. *Proc. Natl. Acad. Sci. USA* **82**, 6502–6506.
27. Sodroski, J. G., C. A. Rosen and W. A. Haseltine (1984) Trans-acting transcriptional repeat of human T lymphotropic viruses in infected cells. *Science* **225**, 381–385.
28. White, M. R. H., M. Masuko, L. Amet, G. Elliott, M. Braddock, A. Kingsman and S. Kingsman (1995) Real-time analysis of the transcriptional regulation of HIV and hCMV promoters in single mammalian cells. *J. Cell Sci.* **108**, 441–455.
29. Contag, C. H. and P. R. Contag (1996) Viewing disease progression through a bioluminescent window. *Optics & Photon. News*, pp. 22–23.
30. Reddy, E. P. and P. Dasgupta (1992) Regulation of HIV-1 gene expression by cellular transcription factors. *Pathobiology* **60**, 219–224.
31. Jones, K. and B. Peterlin (1994) Control of RNA initiation and elongation at the HIV-1 promoter. *Annu. Rev. Biochem.* **63**, 717–743.
32. Vicenzi, E. and G. Poli (1994) Ultraviolet irradiation and cytokines as regulators of HIV latency and expression. *Chem.-Biol. Interact.* **91**, 101–109.
33. Stingl, G., K. Rappersberger, E. Tschachler, S. Gartner, V. Groh, D. L. Mann, K. Wolff and M. Popovic (1990) Langerhans cells in HIV-1 infection. *J. Am. Acad. Dermatol.* **22**, 1210–1217.
34. Soto-Ramirez, L., B. Renjifo, M. McLane, R. Marlink, C. O'Hara, R. Sutthent, C. Wasi, P. Vithayasai, V. Vithayasai, C. Apichartpiyakul, P. Auerwarakul, V. Peña Cruz, D.-S. Chui, R. Osathanondh, K. Mayer, T. H. Lee and M. Essex (1996) HIV-1 Langerhans' cell tropism associated with heterosexual transmission of HIV. *Science* **271**, 1291–1293.
35. Zhou, Q. and P. Sharp (1996) Tat-SF1: cofactor for stimulation of transcriptional elongation by HIV-1 Tat. *Science* **274**, 605–610.
36. Winslow, B. J. and D. Trono (1993) The blocks to human immunodeficiency virus type 1 Tat and Rev functions in mouse cell lines are independent. *J. Virol.* **67**, 2349–2354.

SPECTRAL_0000734

Electronic Acknowledgement Receipt

EFS ID:	11392030
Application Number:	13222688
International Application Number:	
Confirmation Number:	5910
Title of Invention:	EXCITATION LIGHT SOURCE ASSEMBLY
First Named Inventor/Applicant Name:	Michael B. Nelson
Customer Number:	27104
Filer:	Bruce E. Dahl/Cynthia Sullivan
Filer Authorized By:	Bruce E. Dahl
Attorney Docket Number:	SPEC US-4 (027560-0014)
Receipt Date:	11-NOV-2011
Filing Date:	31-AUG-2011
Time Stamp:	18:05:20
Application Type:	Utility under 35 USC 111(a)

Payment information:

Submitted with Payment	no

File Listing:

Document Number	Document Description	File Name	File Size(Bytes)/ Message Digest	Multi Part /.zip	Pages (if appl.)
1	Information Disclosure Statement (IDS) Form (SB08)	SPEC_US-4_IDS-2.pdf	614560 0c709847d8dadcfa46aeb4b6e079babc0031d93a	no	5

Warnings:	
Information:	

2	Non Patent Literature	CCD_Image_Calibration_Using_AIP4WIN.pdf	220393 322704857cb6252cdcfd62310df20533a06c8362	no	12
Warnings:					
Information:					
3	Non Patent Literature	Chemiluminescence_Imaging_Systems_for_the_Analysis_of_Macrosamples.pdf	2011551 be4cb10005a9cf979e7318375fdbdaff867ebb1e	no	13
Warnings:					
Information:					
4	Non Patent Literature	Commercially_Available_Luminometers_and_Low-Level_Light_Imaging_Devices.pdf	360393 3eec61f23b37e1984242ddcd0c69decbf163aa71	no	8
Warnings:					
Information:					
5	Non Patent Literature	High_speed_radiometric_imaging_with_a_gated_intensified_digitally_controlled_camera.pdf	113565 83a43ac58411de0533db45a50baa5b08b02863ad	no	2
Warnings:					
Information:					
6	Non Patent Literature	In_vivo_imaging_of_light-emitting_probes.pdf	353999 aad9d20c2fceccf727b732e90770db95e137b6d3	no	9
Warnings:					
Information:					
7	Non Patent Literature	In_Vivo_Procedure_for_Measurement_Luciferase_Reporter_Gene_Activity.pdf	1321407 471332cda92ba38569d6ee7ed423a93c90ad2559	no	3
Warnings:					
Information:					
8	Non Patent Literature	Luminometet_Design_and_Low_Light_Detection.pdf	2916610 65344840dad902a587acb516daa442e6bf3b0ddf	no	26
Warnings:					
Information:					
9	Non Patent Literature	Measuring_luminescence_with_a_low_light_level_imaging_system_using_electronic_light_standards.pdf	20965 78a18fbe37f3b16f5a19657c9bd000986f3c19a2	no	1
Warnings:					
Information:					
10	Non Patent Literature	Bioluminescence_and_chemiluminescence_status_report_proceedings.pdf	104185 b5ed7876478f0970c54dcb8f1c7206f0755d0204	no	2
Warnings:					
Information:					

11	Non Patent Literature	Monitoring_Bioluminescent_Staphylococcus_aureus_Infections_in_Living_Mice_Using_a_Novel.pdf	366245 9069b30f02ab18a56429476fb6e6f0e443dfb90a	no	8
Warnings:					
Information:					
12	Non Patent Literature	Radiometric_and_Geometric_Calibration_of_a_Visible_Spectral.pdf	624280 ca351e46bb99af759ec54018a9bd3d418a2ca296	no	11
Warnings:					
Information:					
13	Non Patent Literature	Radiometric_calibration_of_a_video_fluorescence_microscope_for_the_quantitative_imaging_of.pdf	1311524 ec40fa219a1ef2ef0e216fc8692b1f6a0b136754	no	10
Warnings:					
Information:					
14	Non Patent Literature	Radiometric_Calibration_of_Multispectral_Airborne_Video_Systems.pdf	299965 5c8a9043babdcab1c47986dda7b9e5f76846e90e	no	17
Warnings:					
Information:					
15	Non Patent Literature	Rapid_and_Quantitative_Assessment_of_Cancer_Treatment_Response_Using_In_Vivo_Bioluminescience.pdf	325682 15c52f7a03a0448075017ce0fb0b9ded7511d9b8	no	5
Warnings:					
Information:					
16	Non Patent Literature	Rapid_in_vivo_functional_analysis_of_transgenes_in_mice_using_whole_body_imaging_of.pdf	471882 7616db1339b1d55ad442d9f47835fabec3636190	no	12
Warnings:					
Information:					
17	Non Patent Literature	Statistical_Calibration_of_CCD_Imaging_Process.pdf	306387 afdfe9f0c5384d09d34dba28e875208821955037f	no	8
Warnings:					
Information:					
18	Non Patent Literature	Use_of_Reporter_Genes_for_Optical_Measurements_of_Neoplastic_Disease_In_Vivo.pdf	654630 ffa2083cc553ab9b5b8b785e7d272791df22589a	no	12
Warnings:					
Information:					
19	Non Patent Literature	Visualizing_Gene_Expression_in_Living_Mammals_Using_a_Bioluminescent_Reporter.pdf	659638 c86c0344a6e702063b26d3d8f5620f73ea8f5920	no	9
Warnings:					
Information:					

Total Files Size (in bytes):	13057861

This Acknowledgement Receipt evidences receipt on the noted date by the USPTO of the indicated documents, characterized by the applicant, and including page counts, where applicable. It serves as evidence of receipt similar to a Post Card, as described in MPEP 503.

New Applications Under 35 U.S.C. 111
If a new application is being filed and the application includes the necessary components for a filing date (see 37 CFR 1.53(b)-(d) and MPEP 506), a Filing Receipt (37 CFR 1.54) will be issued in due course and the date shown on this Acknowledgement Receipt will establish the filing date of the application.

National Stage of an International Application under 35 U.S.C. 371
If a timely submission to enter the national stage of an international application is compliant with the conditions of 35 U.S.C. 371 and other applicable requirements a Form PCT/DO/EO/903 indicating acceptance of the application as a national stage submission under 35 U.S.C. 371 will be issued in addition to the Filing Receipt, in due course.

New International Application Filed with the USPTO as a Receiving Office
If a new international application is being filed and the international application includes the necessary components for an international filing date (see PCT Article 11 and MPEP 1810), a Notification of the International Application Number and of the International Filing Date (Form PCT/RO/105) will be issued in due course, subject to prescriptions concerning national security, and the date shown on this Acknowledgement Receipt will establish the international filing date of the application.

PTO/SB/08a (01-10)
Approved for use through 07/31/2012. OMB 0651-0031
U.S. Patent and Trademark Office; U.S. DEPARTMENT OF COMMERCE

Under the Paperwork Reduction Act of 1995, no persons are required to respond to a collection of information unless it contains a valid OMB control number.

INFORMATION DISCLOSURE STATEMENT BY APPLICANT

(Not for submission under 37 CFR 1.99)

Application Number	13222688
Filing Date	2011-08-31
First Named Inventor	Michael B. Nelson et al.
Art Unit	2884
Examiner Name	Not yet known
Attorney Docket Number	SPEC US-4 (027560.0014)

U.S.PATENTS

Examiner Initial*	Cite No	Patent Number	Kind Code[1]	Issue Date	Name of Patentee or Applicant of cited Document	Pages,Columns,Lines where Relevant Passages or Relevant Figures Appear
	1	5089895	A	1992-02-18	Fraker et al.	
	2	6454437	B1	2002-09-24	Kelly	

If you wish to add additional U.S. Patent citation information please click the Add button.

U.S.PATENT APPLICATION PUBLICATIONS

Examiner Initial*	Cite No	Publication Number	Kind Code[1]	Publication Date	Name of Patentee or Applicant of cited Document	Pages,Columns,Lines where Relevant Passages or Relevant Figures Appear
	1	20040121175	A1	2004-06-24	Flexman et al.	
	2	20040247170	A1	2004-12-09	Furze et al.	
	3	20050265024	A1	2005-12-01	Luk	
	4	20090268426	A1	2009-10-29	Pohlert et al.	

If you wish to add additional U.S. Published Application citation information please click the Add button.

FOREIGN PATENT DOCUMENTS

INFORMATION DISCLOSURE STATEMENT BY APPLICANT (Not for submission under 37 CFR 1.99)		
	Application Number	13222688
	Filing Date	2011-08-31
	First Named Inventor	Michael B. Nelson et al.
	Art Unit	2884
	Examiner Name	Not yet known
	Attorney Docket Number	SPEC US-4 (027560.0014)

Examiner Initial*	Cite No	Foreign Document Number[3]	Country Code[2] i	Kind Code[4]	Publication Date	Name of Patentee or Applicant of cited Document	Pages,Columns,Lines where Relevant Passages or Relevant Figures Appear	T[5]
	1	1040330	JP	A	1998-02-13	Nomura		☐

If you wish to add additional Foreign Patent Document citation information please click the Add button

NON-PATENT LITERATURE DOCUMENTS

Examiner Initials*	Cite No	Include name of the author (in CAPITAL LETTERS), title of the article (when appropriate), title of the item (book, magazine, journal, serial, symposium, catalog, etc), date, pages(s), volume-issue number(s), publisher, city and/or country where published.	T[5]
	1	International Search Report and Written Opinion for PCT/US2011/049998, dated December 22, 2011, 10 pages.	☐

If you wish to add additional non-patent literature document citation information please click the Add button

EXAMINER SIGNATURE

Examiner Signature		Date Considered	

*EXAMINER: Initial if reference considered, whether or not citation is in conformance with MPEP 609. Draw line through a citation if not in conformance and not considered. Include copy of this form with next communication to applicant.

[1] See Kind Codes of USPTO Patent Documents at www.USPTO.GOV or MPEP 901.04. [2] Enter office that issued the document, by the two-letter code (WIPO Standard ST.3). [3] For Japanese patent documents, the indication of the year of the reign of the Emperor must precede the serial number of the patent document. [4] Kind of document by the appropriate symbols as indicated on the document under WIPO Standard ST.16 if possible. [5] Applicant is to place a check mark here if English language translation is attached.

INFORMATION DISCLOSURE STATEMENT BY APPLICANT (Not for submission under 37 CFR 1.99)		
	Application Number	13222688
	Filing Date	2011-08-31
	First Named Inventor	Michael B. Nelson et al.
	Art Unit	2884
	Examiner Name	Not yet known
	Attorney Docket Number	SPEC US-4 (027560.0014)

CERTIFICATION STATEMENT

Please see 37 CFR 1.97 and 1.98 to make the appropriate selection(s):

☐ That each item of information contained in the information disclosure statement was first cited in any communication from a foreign patent office in a counterpart foreign application not more than three months prior to the filing of the information disclosure statement. See 37 CFR 1.97(e)(1).

OR

☐ That no item of information contained in the information disclosure statement was cited in a communication from a foreign patent office in a counterpart foreign application, and, to the knowledge of the person signing the certification after making reasonable inquiry, no item of information contained in the information disclosure statement was known to any individual designated in 37 CFR 1.56(c) more than three months prior to the filing of the information disclosure statement. See 37 CFR 1.97(e)(2).

☐ See attached certification statement.

☐ The fee set forth in 37 CFR 1.17 (p) has been submitted herewith.

☒ A certification statement is not submitted herewith.

SIGNATURE

A signature of the applicant or representative is required in accordance with CFR 1.33, 10.18. Please see CFR 1.4(d) for the form of the signature.

Signature	/Bruce E. Dahl/	Date (YYYY-MM-DD)	2012-02-13
Name/Print	Bruce E. Dahl	Registration Number	33670

This collection of information is required by 37 CFR 1.97 and 1.98. The information is required to obtain or retain a benefit by the public which is to file (and by the USPTO to process) an application. Confidentiality is governed by 35 U.S.C. 122 and 37 CFR 1.14. This collection is estimated to take 1 hour to complete, including gathering, preparing and submitting the completed application form to the USPTO. Time will vary depending upon the individual case. Any comments on the amount of time you require to complete this form and/or suggestions for reducing this burden, should be sent to the Chief Information Officer, U.S. Patent and Trademark Office, U.S. Department of Commerce, P.O. Box 1450, Alexandria, VA 22313-1450. DO NOT SEND FEES OR COMPLETED FORMS TO THIS ADDRESS. **SEND TO: Commissioner for Patents, P.O. Box 1450, Alexandria, VA 22313-1450.**

PATENT COOPERATION TREATY

From the INTERNATIONAL SEARCHING AUTHORITY

To: BRUCE DAHL
FENNEMORE CRAIG, P.C.
1700 LINCOLN STREET
SUITE 2900
DENVER, CO 80203

PCT

NOTIFICATION OF TRANSMITTAL OF THE INTERNATIONAL SEARCH REPORT AND THE WRITTEN OPINION OF THE INTERNATIONAL SEARCHING AUTHORITY, OR THE DECLARATION

(PCT Rule 44.1)

Date of mailing *(day/month/year)*	22 DEC 2011
Applicant's or agent's file reference: SPEC-4PCT	**FOR FURTHER ACTION** See paragraphs 1 and 4 below
International application No.: PCT/US2011/049998	International filing date *(day/month/year)*: 31 August 2011
Applicant: SPECTRAL INSTRUMENTS IMAGING, LLC	

1. ☒ The applicant is hereby notified that the international search report and the written opinion of the International Searching Authority have been established and are transmitted herewith.

   Filing of amendments and statement under Article 19:
   The applicant is entitled, if he so wishes, to amend the claims of the international application (see Rule 46):

   When? The time limit for filing such amendments is normally two months from the date of transmittal of the international search report.

   Where? Directly to the International Bureau of WIPO, 34 chemin des Colombettes 1211 Geneva 20, Switzerland, Facsimile No.: +41 22 338 82 70

   For more detailed instructions, see *PCT Applicant's Guide*, International Phase, paragraphs 9.004 – 9.011.

2. ☐ The applicant is hereby notified that no international search report will be established and that the declaration under Article 17(2)(a) to that effect and the written opinion of the International Searching Authority are transmitted herewith.

3. ☐ **With regard to any protest** against payment of (an) additional fee(s) under Rule 40.2, the applicant is notified that:

   ☐ the protest together with the decision thereon has been transmitted to the International Bureau together with any request to forward the texts of both the protest and the decision thereon to the designated Offices.

   ☐ no decision has been made yet on the protest; the applicant will be notified as soon as a decision is made.

4. **Reminders**

   The applicant may submit comments on an informal basis on the written opinion of the International Searching Authority to the International Bureau. The International Bureau will send a copy of such comments to all designated Offices unless an international preliminary examination report has been or is to be established. Following the expiration of 30 months from the priority date, these comments will also be made available to the public.

   Shortly after the expiration of **18 months** from the priority date, the international application will be published by the International Bureau. If the applicant wishes to avoid or postpone publication, a notice of withdrawal of the international application, or of the priority claim, must reach the International Bureau before the completion of the technical preparations for international publication (Rules 90*bis*.1 and 90*bis*.3).

   Within **19 months** from the priority date, but only in respect of some designated Offices, a demand for international preliminary examination must be filed if the applicant wishes to postpone the entry into the national phase **until 30 months** from the priority date (in some Offices even later); otherwise, the applicant must, **within 20 months** from the priority date, perform the prescribed acts for entry into the national phase before those designated Offices.

   In respect of other designated Offices, the time limit of **30 months** (or later) will apply even if no demand is filed within 19 months.

   For details about the applicable time limits, Office by Office, see www.wipo.int/pct/en/texts/time_limits.html and the *PCT Applicant's Guide*, National Chapters.

Name and mailing address of the ISA/ Mail Stop PCT, Attn: ISA/US Commissioner for Patents P.O. Box 1450, Alexandria, Virginia 22313-1450 Facsimile No. 571-273-3201	Authorized officer Blaine R. Copenheaver PCT Helpdesk: 571-272-4300 PCT OSP: 571-272-7774 Telephone No.

Form PCT/ISA/220 (July 2010)

PATENT COOPERATION TREATY

PCT

INTERNATIONAL SEARCH REPORT

(PCT Article 18 and Rules 43 and 44)

Applicant's or agent's file reference SPEC-4PCT	FOR FURTHER ACTION	see Form PCT/ISA/220 as well as, where applicable, item 5 below.
International application No. PCT/US2011/049998	International filing date *(day/month/year)* 31 August 2011	(Earliest) Priority Date *(day/month/year)* 01 September 2010
Applicant SPECTRAL INSTRUMENTS IMAGING, LLC		

This international search report has been prepared by this International Searching Authority and is transmitted to the applicant according to Article 18. A copy is being transmitted to the International Bureau.

This international search report consists of a total of 7 sheets.

☐ It is also accompanied by a copy of each prior art document cited in this report.

1. **Basis of the report**
   a. With regard to the **language**, the international search was carried out on the basis of:
      ☒ the international application in the language in which it was filed.
      ☐ a translation of the international application into _____ which is the language of a translation furnished for the purposes of international search (Rules 12.3(a) and 23.1(b)).
   b. ☐ This international search report has been established taking into account the **rectification of an obvious mistake** authorized by or notified to this Authority under Rule 91 (Rule 43.6*bis*(a)).
   c. ☐ With regard to any **nucleotide and/or amino acid sequence** disclosed in the international application, see Box No. I.

2. ☐ **Certain claims were found unsearchable** (see Box No. II).

3. ☐ **Unity of invention is lacking** (see Box No. III).

4. With regard to the **title**,
   ☒ the text is approved as submitted by the applicant.
   ☐ the text has been established by this Authority to read as follows:

5. With regard to the **abstract**,
   ☒ the text is approved as submitted by the applicant.
   ☐ the text has been established, according to Rule 38.2, by this Authority as it appears in Box No. IV. The applicant may, within one month from the date of mailing of this international search report, submit comments to this Authority.

6. With regard to the **drawings**,
   a. the figure of the drawings to be published with the abstract is Figure No. 1
      ☒ as suggested by the applicant.
      ☐ as selected by this Authority, because the applicant failed to suggest a figure.
      ☐ as selected by this Authority, because this figure better characterizes the invention.
   b. ☐ none of the figures is to be published with the abstract.

Form PCT/ISA/210 (first sheet) (July 2009)

INTERNATIONAL SEARCH REPORT

International application No.
PCT/US2011/049998

A. CLASSIFICATION OF SUBJECT MATTER
IPC(8) - G03B 15/02 (2011.01)
USPC - 362/11
According to International Patent Classification (IPC) or to both national classification and IPC

B. FIELDS SEARCHED

Minimum documentation searched (classification system followed by classification symbols)
IPC(8) -F21V 1/00, 5/00; G03B 15/02 (2011.01)
USPC - 362/11, 235, 246

Documentation searched other than minimum documentation to the extent that such documents are included in the fields searched

Electronic data base consulted during the international search (name of data base and, where practicable, search terms used)
MicroPatent, Google Scholar

C. DOCUMENTS CONSIDERED TO BE RELEVANT

Category*	Citation of document, with indication, where appropriate, of the relevant passages	Relevant to claim No.
Y	US 2009/0268426 A1 (POHLERT et al) 29 October 2009 (29.10.2009) entire document	1-29
Y	US 6,454,437 B1 (KELLY) 24 September 2002 (24.09.2002) entire document	1-15, 19-29
Y	JP 10-40330 A (NOMURA) 13 February 1998 (13.02.1998) abstract, figures 1, 5	1-29
Y	US 2004/0247170 A1 (FURZE et al) 09 December 2004 (09.12.2004) entire document	5
Y	US 2004/0121175 A1 (FLEXMAN et al) 24 June 2004 (24.06.2004) entire document	27
A	US 5,089,895 A (FRAKER et al) 18 February 1992 (18.02.1992) entire document	1-29
A	US 2005/0265024 A1 (LUK) 01 December 2005 (01.12.2005) entire document	1-29

☐ Further documents are listed in the continuation of Box C. ☐

* Special categories of cited documents:
"A" document defining the general state of the art which is not considered to be of particular relevance
"E" earlier application or patent but published on or after the international filing date
"L" document which may throw doubts on priority claim(s) or which is cited to establish the publication date of another citation or other special reason (as specified)
"O" document referring to an oral disclosure, use, exhibition or other means
"P" document published prior to the international filing date but later than the priority date claimed
"T" later document published after the international filing date or priority date and not in conflict with the application but cited to understand the principle or theory underlying the invention
"X" document of particular relevance; the claimed invention cannot be considered novel or cannot be considered to involve an inventive step when the document is taken alone
"Y" document of particular relevance; the claimed invention cannot be considered to involve an inventive step when the document is combined with one or more other such documents, such combination being obvious to a person skilled in the art
"&" document member of the same patent family

Date of the actual completion of the international search	Date of mailing of the international search report
12 December 2011	22 DEC 2011
Name and mailing address of the ISA/US Mail Stop PCT, Attn: ISA/US, Commissioner for Patents P.O. Box 1450, Alexandria, Virginia 22313-1450 Facsimile No. 571-273-3201	Authorized officer: Blaine R. Copenheaver PCT Helpdesk: 571-272-4300 PCT OSP: 571-272-7774

Form PCT/ISA/210 (second sheet) (July 2009)

SPECTRAL_0000744

PATENT COOPERATION TREATY

From the
INTERNATIONAL SEARCHING AUTHORITY

To: BRUCE DAHL
FENNEMORE CRAIG, P.C.
1700 LINCOLN STREET
SUITE 2900
DENVER, CO 80203

PCT

WRITTEN OPINION OF THE
INTERNATIONAL SEARCHING AUTHORITY

(PCT Rule 43*bis*.1)

Date of mailing *(day/month/year)*	22 DEC 2011
Applicant's or agent's file reference SPEC-4PCT	**FOR FURTHER ACTION** See paragraph 2 below

International application No.	International filing date *(day/month/year)*	Priority date *(day/month/year)*
PCT/US2011/049998	31 August 2011	01 September 2010

International Patent Classification (IPC) or both national classification and IPC
IPC(8) - G03B 15/02 (2011.01)
USPC - 362/11

Applicant SPECTRAL INSTRUMENTS IMAGING, LLC

1. This opinion contains indications relating to the following items:

- [X] Box No. I Basis of the opinion
- [ ] Box No. II Priority
- [ ] Box No. III Non-establishment of opinion with regard to novelty, inventive step and industrial applicability
- [ ] Box No. IV Lack of unity of invention
- [X] Box No. V Reasoned statement under Rule 43*bis*.1(a)(i) with regard to novelty, inventive step or industrial applicability; citations and explanations supporting such statement
- [ ] Box No. VI Certain documents cited
- [ ] Box No. VII Certain defects in the international application
- [ ] Box No. VIII Certain observations on the international application

2. **FURTHER ACTION**

If a demand for international preliminary examination is made, this opinion will be considered to be a written opinion of the International Preliminary Examining Authority ("IPEA") except that this does not apply where the applicant chooses an Authority other than this one to be the IPEA and the chosen IPEA has notified the International Bureau under Rule 66.1*bis*(b) that written opinions of this International Searching Authority will not be so considered.

If this opinion is, as provided above, considered to be a written opinion of the IPEA, the applicant is invited to submit to the IPEA a written reply together, where appropriate, with amendments, before the expiration of 3 months from the date of mailing of Form PCT/ISA/220 or before the expiration of 22 months from the priority date, whichever expires later.

For further options, see Form PCT/ISA/220.

Name and mailing address of the ISA/US	Date of completion of this opinion	Authorized officer:
Mail Stop PCT, Attn: ISA/US Commissioner for Patents P.O. Box 1450, Alexandria, Virginia 22313-1450 Facsimile No. 571-273-3201	12 December 2011	Blaine R. Copenheaver PCT Helpdesk: 571-272-4300 PCT OSP: 571-272-7774

Form PCT/ISA/237 (cover sheet) (July 2011)

WRITTEN OPINION OF THE INTERNATIONAL SEARCHING AUTHORITY

International application No.
PCT/US2011/049998

Box No. I Basis of this opinion

1. With regard to the language, this opinion has been established on the basis of:

   ☒ the international application in the language in which it was filed.

   ☐ a translation of the international application into _____ which is the language of a translation furnished for the purposes of international search (Rules 12.3(a) and 23.1(b)).

2. ☐ This opinion has been established taking into account the rectification of an obvious mistake authorized by or notified to this Authority under Rule 91 (Rule 43*bis*.1(a))

3. With regard to any nucleotide and/or amino acid sequence disclosed in the international application, this opinion has been established on the basis of a sequence listing filed or furnished:

   a. (means)

      ☐ on paper

      ☐ in electronic form

   b. (time)

      ☐ in the international application as filed

      ☐ together with the international application in electronic form

      ☐ subsequently to this Authority for the purposes of search

4. ☐ In addition, in the case that more than one version or copy of a sequence listing has been filed or furnished, the required statements that the information in the subsequent or additional copies is identical to that in the application as filed or does not go beyond the application as filed, as appropriate, were furnished.

5. Additional comments:

WRITTEN OPINION OF THE INTERNATIONAL SEARCHING AUTHORITY

International application No.
PCT/US2011/049998

Box No. V **Reasoned statement under Rule 43*bis*.1(a)(i) with regard to novelty, inventive step or industrial applicability; citations and explanations supporting such statement**

1. Statement

Novelty (N)	Claims	1-29	YES
	Claims	None	NO
Inventive step (IS)	Claims	None	YES
	Claims	1-29	NO
Industrial applicability (IA)	Claims	1-29	YES
	Claims	None	NO

2. Citations and explanations:

Claims 1-4, 6-8, 19-26, 28-29 lack an inventive step under PCT Article 33(3) as being obvious over Pohlert et al., hereinafter referred to as Pohlert, in view of Kelly and further in view of Nomura.

Regarding claim 1, Pohlert teaches a stand-mounted light panel for natural illumination in film, television or video (title) and further teaches a central opening (103, fig. 1; 303 figs. 4-5) having a plurality of lamp receptacles (lamp segment 306, fig. 4; panel frame or frame, abstract, fig. 47a, pars. 0179-0180, receives the LEDs; also see figs. 48a-50b) surrounding the central opening (303, fig 4; 3803, fig. 38A), the structure being mountable to a support structure (330, fig. 3) so that the central opening being aligned with a camera (fig. 1 shows this aspect) also mounted to the support structure (330, fig. 3), so that the field of view of the camera is unobstructed, and a light source (lamps, fig. 2; LEDs or lamps 305, fig. 4; 4705 fig. 47a, para. 0180) positioned within each of the plurality of lamp receptacles (lamp segment 306, fig. 4; panel frame or frame, abstract, fig. 47a, pars. 0179-0180, receives the LEDs; also see figs. 48a-50b), a diffuser (5029, fig. 5a; 1205 fig. 12; 795, 876 in figs 7-8, teach that lens elements spreading the light; this is interpreted as meaning diffusing; paras 0119-0120) positioned adjacent the light source positioned within each of the plurality of lamp receptacles (figs. 4 shows a plurality of lamp segments 306 which contain a plurality of light sources 305; fig. 50a shows the a diffuser 5029 which locate within each lamp panel 4702, 4802, figs. 47a; 50a-50b), each of the diffusers diffusing light produced by each of the light sources (abstract, para. 0023 teaches the diffusion lens being integrated with the lighting panel (receptacle); 795, 876 in figs 7-8, teach that lens elements spreading the light; this is interpreted as meaning diffusing; paras 0119-0120), and a control system (212, fig. 2, para. 0094; and element 1052) operatively connected to each of the light sources (para. 0145, fig. 13, paras. 0091-0092, 0166) positioned within the plurality of lamp receptacles, the control system operating selected ones of the light source to provide a desired illumination to an object within the field of view of the camera (paras. 0091-0092, 0166).
However, Pohlert does not explicitly state a housing defining a central opening which contains the structure which holds a plurality of lamps, for connecting the camera to a central aperture.
Kelly teaches a ring lighting (title) and further teaches a housing (2, figs. 1-2) defining a central opening (3 figs. 1-2) which contains the structure which holds a plurality of lamps (6 figs. 1-2), for connecting the camera to a central aperture (abstract, figs. 1-2).
Therefore, it would have been obvious to one of ordinary skill in the art at the time the invention was made to combine the stand-mounted light panel for natural illumination in film, television or video of Pohlert with the ring lighting of Kelly so as to have a housing defining a central opening which contains the structure which holds a plurality of lamps, for connecting the camera to a central aperture in order to protect the lights and lenses from the environment.
Pohlert also does not explicitly state the apparatus being used as a excitation light source.
Nomura teaches a fluorescent pattern detector and postal matter processor using the detector (title) and further an apparatus comprising a central hole aligned with a camera having a plurality of light sources surrounding the central aperture being used as an excitation light source (abstract, figs. 1, 5).
Therefore, it would have been obvious to one of ordinary skill in the art at the time the invention was made to combine the stand-mounted light panel for natural illumination in film, television or video of Pohlert with the fluorescent pattern detector and postal matter processor using the detector of Nomura so as to have the apparatus used as a excitation light source in order to aid one in recognizing a fluorescent pattern of the object based on a detection signal.

WRITTEN OPINION OF THE INTERNATIONAL SEARCHING AUTHORITY

International application No.
PCT/US2011/049998

Supplemental Box

In case the space in any of the preceding boxes is not sufficient.
Continuation of:

Regarding claim 19, Pohlert teaches a stand-mounted light panel for natural illumination in film, television or video (title) and further teaches a support structure (330, fig. 3) a camera (140, fig. 1) mounted to the support structure (330, para. 0102), a light source assembly (302, figs. 4-5, para. 0102) mounted to the support structure, the light source assembly comprising, a central opening (103, fig. 1; 303 figs. 4-5) having a plurality of lamp receptacles (lamp segment 306, fig. 4; panel frame or frame, abstract, fig. 47a, pars. 0179-0180, receives the LEDs; also see figs. 48a-50b) surrounding the central opening (303, fig 4; 3803, fig. 38A), the structure being mountable to a support structure (330, fig. 3) so that the central opening being aligned with a camera (fig. 1 shows this aspect) also mounted to the support structure (330, fig. 3), so that the field of view of the camera is unobstructed, and a light source (lamps , fig. 2; LEDs or lamps 305, fig. 4; 4705 fig. 47a, para. 0180) positioned within each of the plurality of lamp receptacles (lamp segment 306, fig. 4; panel frame or frame, abstract, fig. 47a, pars. 0179-0180, receives the LEDs; also see figs. 48a-50b), a diffuser (5029, fig. 5a; 1205 fig. 12; 795, 876 in figs 7-8, teach that lens elements spreading the light; this is interpreted as meaning diffusing; paras 0119-0120) positioned adjacent the light source positioned within each of the plurality of lamp receptacles (figs. 4 shows a plurality of lamp segments 306 which contain a plurality of light sources 305; fig. 50a shows the a diffuser 5029 which locate within each lamp panel 4702, 4802, figs. 47a; 50a-50b), each of the diffusers diffusing light produced by each of the light sources (abstract, para. 0023 teaches the diffusion lens being integrated with the lighting panel (receptacle); 795, 876 in figs 7-8, teach that lens elements spreading the light; this is interpreted as meaning diffusing; paras 0119-0120), and a control system (212, fig. 2, para. 0094; and element 1052) operatively connected to each of the light sources (para. 0145, fig. 13, paras. 0091-0092, 0166) positioned within the plurality of lamp receptacles, the control system operating selected ones of the light source to provide a desired illumination to an object within the field of view of the camera (paras. 0091-0092, 0166). Pohlert teaches at least one narrow-band light source positioned within at least one of the plurality of lamp receptacles (blue or green LEDs, paras. 0019, 0118).
However, Pohlert does not explicitly state a housing defining a central opening which contains the structure which holds a plurality of lamps, for connecting the camera to a central aperture.
Kelly teaches a ring lighting (title) and further teaches a housing (2, figs. 1-2) defining a central opening (3 figs. 1-2) which contains the structure which holds a plurality of lamps (6 figs. 1-2), for connecting the camera to a central aperture (abstract, figs. 1-2).
Therefore, it would have been obvious to one of ordinary skill in the art at the time the invention was made to combine the stand-mounted light panel for natural illumination in film, television or video of Pohlert with the ring lighting of Kelly so as to have a housing defining a central opening which contains the structure which holds a plurality of lamps, for connecting the camera to a central aperture in order to protect the lights and lenses from the environment.
Pohlert also does not explicitly state the apparatus being used as a excitation light source.
Nomura teaches a fluorescent pattern detector and postal matter processor using the detector (title) and further an apparatus comprising a central hole aligned with a camera having a plurality of light sources surrounding the central aperture being used as an excitation light source (abstract, figs. 1, 5).
Therefore, it would have been obvious to one of ordinary skill in the art at the time the invention was made to combine the stand-mounted light panel for natural illumination in film, television or video of Pohlert with the fluorescent pattern detector and postal matter processor using the detector of Nomura so as to have the apparatus used as a excitation light source in order to aid one in recognizing a fluorescent pattern of the object based on a detection signal.

Regarding claim 2, Pohlert teaches at least one of the light sources comprising a narrow-band light source (para. 0019) that emits light having a bandwidth (blue or green LEDs, paras. 0019, 0118).
However, Pohlert does not explicitly state the bandwidth of the light source being about 35 nm.
It would have been obvious to one of ordinary skill in the art at the time the invention was made to have the bandwidth of the light source be about 35 nm, since discovering the optimum value of a result effective variable involves only routine skill in the art and in order to produce a narrow-band of light (Pohlert, para. 0019).

Regarding claim 3, Pohlert teaches at least one narrow-band light source comprising a light emitting diode (paras. 0019, 0118-0119).

Regarding claim 4, Pohlert teaches at least one filter (5010, fig. 50a) positioned adjacent at least one diffuser (5029, fig. 50a) in at least one of the lamp receptacles defined by the housing (para. 0187, figs. 50a-50b).

Regarding claim 6, Pohlert teaches at least one of the light sources comprises a broad-band light source (white LEDs, paras. 0098, 0118).

Regarding claim 7, Pohlert teaches at least some of said plurality of lamp receptacles comprise opposed pairs of lamp receptacles on opposite sides of said central opening (different light segments 306 fig. 4), each opposed pair of lamp receptacles producing light of the same color (paras. 0097; para. 0118 teaches that the LEDs can all be the same color).

Regarding claim 8, Pohlert teaches opposing pairs of lamps located in receptacles (lamp segments, figs. 30b-30c) on opposite side the central opening (para. 0097).
However, Pohlert does not explicitly state ten pairs of lamps surrounding the central aperture.
It would have been obvious to one of ordinary skill in the art at the time the invention was made to have ten pairs of lamps surrounding the central aperture, since a mere duplication of essential working parts of device involves only routine skill in the art, and in order to produce the desired amount and display of light.

Regarding claim 20, Pohlert teaches a light filter (5010, fig. 50a) positioned adjacent at each of the diffusers (5029, para. 0187, figs. 50a-50b).

Regarding claim 21, Pohlert teaches each of the lamp receptacles defined by said housing being angled with respect to a central axis of said housing so that light emitted from each of said narrow-band light sources is directed to a desired area within the field of view of said camera (paras. 0166, 0176).

WRITTEN OPINION OF THE INTERNATIONAL SEARCHING AUTHORITY

International application No.
PCT/US2011/049998

Supplemental Box

In case the space in any of the preceding boxes is not sufficient.
Continuation of:

Regarding claim 22, Pohlert teaches each of said narrow-band light sources being selected to provide desired number of illumination bands over a desired spectral range (paras. 0122, 0124).

Regarding claim 23, Pohlert teaches the desired spectral range being from about 430 nm to about 745 nm (paras. 0122, 0124; By teaching the LEDs being red, green, and blue, Pohlert has inferred the spectral range being from about 430 nm to about 745 nm).

Regarding claim 24, Pohlert teaches the use of different color LEDs (paras. 0122, 0124).
However, it does not explicitly state the number of illumination bands being 10.
It would have been obvious to one of ordinary skill in the art at the time the invention was made to have the number of illumination bands being 10, since discovering the optimum number of illumination bands needed to obtain a desired color distribution involves only routine skill in the art.

Regarding claim 25, Pohlert teaches each of the desired illumination bands having a bandwidth ranging from about 30 nm to about 35 nm (paras. 0122, 0124, by teaching the use green and blue LEDs, Pohlert has inferred the that the illumination bandwidth ranges from about 30 nm to about 35 nm).

Regarding claim 26, Pohlert teaches each of the narrow-band light sources comprising a light emitting diode (paras. 0118, 0156).

Regarding claim 28, Pohlert teaches the invention as shown above but lacks the explicit teaching of the desired spectral range being from about 430 nm to about 900 nm.
It would have been obvious to one of ordinary skill in the art at the time the invention was made to have the desired spectral range being from about 430 nm to about 900 nm, since where the general conditions of the claim are disclosed in the prior art, discovering the optimum or workable ranges involves only routine skill in the art, and in order to produce the desired light emitting from the device.

Regarding claim 29, Pohlert teaches the desired spectral range being from about 430 nm to about 800 nm (paras. 0122, 0124; By teaching the LEDs being red, green, and blue, Pohlert has inferred the spectral range being from about 430 nm to about 800 nm).

Claim 5 lacks an inventive step under PCT Article 33(3) as being obvious over Pohlert et al., hereinafter referred to as Pohlert, in view of Kelly, Nomura and further in view of Furze et al., hereinafter referred to as Furze.

Regarding claim 5, Pohlert teaches the invention as shown above but lacks the explicit teaching of at least one filter comprises a notch filter having a wavelength bandpass range of about 30 nm.
Furze teaches the use of patterned structured light to detect and measure surface defects on a golf ball (title) and further teaches at least one filter comprises a notch filter having a wavelength bandpass range of about 30 nm (25 nm is viewed as being about 30 nm, para. 0023).
Therefore, it would have been obvious to one of ordinary skill in the art at the time the invention was made to combine the stand-mounted light panel for natural illumination in film, television or video of Pohlert with the use of patterned structured light to detect and measure surface defects on a golf ball of Furze so as to have at least one filter comprises a notch filter having a wavelength bandpass range in order to allow only a narrow band of wavelengths to pass and thereby allow one to detect the defects in an object/material.

Claim 27 lacks an inventive step under PCT Article 33(3) as being obvious over Pohlert et al., hereinafter referred to as Pohlert, in view of Kelly, Nomura and further in view of Flexman et al., hereinafter referred to as Flexman.

Regarding claim 27, Pohlert as modifed teaches the invention as shown above but lacks the explicit teaching of the housing comprising polyoxymethylene thermoplastic material.
Kelly teaches a ring lighting (title) and further teaches a housing (2, figs. 1-2) defining a central opening (3 figs. 1-2) which contains the structure which holds a plurality of lamps (6 figs. 1-2), for connecting the camera to a central aperture (abstract, figs. 1-2).
Therefore, it would have been obvious to one of ordinary skill in the art at the time the invention was made to combine the stand-mounted light panel for natural illumination in film, television or video of Pohlert with the ring lighting of Kelly so as to have a housing defining a central opening which contains the structure which holds a plurality of lamps, for connecting the camera to a central aperture in order to protect the lights and lenses from the environment.
Pohlert does however teach the lighting frame being made of thermoplastic (para. 0095).
Flexman teaches layered articles having polyoxymethylene blend substrates with enhanced surface properties and at least one layer thereon and process for making the same (title) and further teaches the use of polyoxymethylene thermoplastic material (para. 0033).
Therefore, it would have been obvious to one of ordinary skill in the art at the time the invention was made to combine the stand-mounted light panel for natural illumination in film, television or video of Pohlert with the layered articles having polyoxymethylene blend substrates with enhanced surface properties and at least one layer thereon and process for making the same of Flexman so as to have in order to increase the toughness and durability of the housing so that it is able to withstand the element and occasional drops.

WRITTEN OPINION OF THE INTERNATIONAL SEARCHING AUTHORITY

International application No.
PCT/US2011/049998

Supplemental Box

In case the space in any of the preceding boxes is not sufficient.
Continuation of:

Claims 16-18 lack an inventive step under PCT Article 33(3) as being obvious over Pohlert et al., hereinafter referred to as Pohlert, in view of Nomura.

Regarding claim 16, Pohlert teaches a stand-mounted light panel for natural illumination in film, television or video (title) and further teaches a base member (102, 302, figs. 1, 3-4) defining a central opening therein (103, 303, figs. 1, 3-4), a plurality of first connectors portions (3996 figs. 39-40; screws) mounted to the base member (3802, 3902, 3900 fig. 38a, 39).at positions around the central opening defined by the base member (figs. 38a), a plurality of lamp receptacles (lamp segment 306, fig. 4; panel frame or frame, abstract, fig. 47a, paras. 0179-0180, receives the LEDs; also see figs. 48a-50b), at least some of the plurality of lamp receptacles producing light in different wavelength bands (different color LEDs, paras. 0098, 0118, 0122), a second connector (screw-in bases, para. 0180-0181, figs. 47a-48b, fig. 4) portion mounted to each of the plurality of lamp receptacles (lamp segment 306, fig. 4; panel frame or frame, abstract, fig. 47a, paras. 0179-0180, receives the LEDs; also see figs. 48a-50b), the second connector portion being releasably engagable with a corresponding one of the plurality of first connector portions mounted to the base member (paras. 0164, 0181), the base member being mountable to a support structure (330, fig. 3) so that the central opening is aligned with a camera that is also mounted to the support structure (330, fig. 3), wherein a field of view of the camera is substantially unobstructed by the base member and the lamp receptacles engaged with the base member (figs. 1, 3).
However, Pohlert does not explicitly state the light source assembly being an excitation lighting assembly.
Nomura teaches a fluorescent pattern detector and postal matter processor using the detector (title) and further the light source assembly being an excitation lighting assembly (abstract, figs. 1, 5).
Therefore, it would have been obvious to one of ordinary skill in the art at the time the invention was made to combine the stand-mounted light panel for natural illumination in film, television or video of Pohlert with the fluorescent pattern detector and postal matter processor using the detector of Nomura so as to have the light source assembly being an excitation lighting assembly in order to aid one in recognizing a fluorescent pattern of the object based on a detection signal.

Regarding claim 17, Pohlert teaches a plurality of main body members (1560, 1592 printed circuit board, figs. 15a -15c) each having a main body members being mounted to the base member (1502), each main body member being adapted to mount a corresponding one of the plurality of first connector portions (screws), each main body member having opening therein sized to receive a corresponding one of the plurality of lamp receptacles (para. 0168, the heating rods also facilitate attachment; fig. 4 each light segment or light panel (306) will have a indetentation below it on the base (302) for receiving the light panel; also see fig. 12, 15a-16b).

Regarding claim 18, Pohlert teaches the invention as shown above but lacks the explicit teaching of the base member comprising a C-shaped configuration.
It would have been obvious to one of ordinary skill in the art at the time the invention was made to have the base member comprise a C-shaped configuration, in order to make it easier for one to adjust/align the light assembly on the camera.

Claims 9-15 lack an inventive step under PCT Article 33(3) as being obvious over Pohlert et al., hereinafter referred to as Pohlert, in view of Kelly and further in view of Nomura.

Regarding claim 9, Pohlert teaches a stand-mounted light panel for natural illumination in film, television or video (title) and further teaches a first connector (3996 figs. 39-40; screws) for mounting to a housing, a lamp receptacle (lamp segment 306, fig. 4; panel frame or frame, abstract, fig. 47a, paras. 0179-0180, receives the LEDs; also see figs. 48a-50b) for producing light in a first defined wavelength band (different color LEDs, paras. 0098, 0118, 0122), and a second connector (screw-in bases, para. 0180-0181, figs. 47a-48b, fig. 4) portion mounted to the lamp receptacle (lamp segment 306, fig. 4; panel frame or frame, abstract, fig. 47a, paras. 0179-0180, receives the LEDs; also see figs. 48a-50b), so that the lamp receptacle can be removably engagable with the first connector portion (paras. 0164, 0181), a support structure (330, fig. 3) for mounting the light assembly to the a housing, so that the field of view of the camera that is also mounted to the support structure (330, fig. 3), wherein a field of view of the camera is substantially unobstructed by the lamp receptacles engaged with the base member (figs. 1, 3).
However, Pohlert does not explicitly state a housing defining a central opening being connected to the device.
Kelly teaches a ring lighting (title) and further teaches a housing (2, figs. 1-2) defining a central opening being connected to the device (abstract, figs. 1-2).
Therefore, it would have been obvious to one of ordinary skill in the art at the time the invention was made to combine the stand-mounted light panel for natural illumination in film, television or video of Pohlert with the ring lighting of Kelly so as to have a housing defining a central opening being connected to the device in order to protect the lights and lenses from the environment.
Pohlert also does not explicitly state the apparatus being used as a excitation light source.
Nomura teaches a fluorescent pattern detector and postal matter processor using the detector (title) and further an apparatus comprising a central hole aligned with a camera having a plurality of light sources surrounding the central aperture being used as an excitation light source (abstract, figs. 1, 5).
Therefore, it would have been obvious to one of ordinary skill in the art at the time the invention was made to combine the stand-mounted light panel for natural illumination in film, television or video of Pohlert with the fluorescent pattern detector and postal matter processor using the detector of Nomura so as to have the apparatus used as a excitation light source in order to aid one in recognizing a fluorescent pattern of the object based on a detection signal.

WRITTEN OPINION OF THE INTERNATIONAL SEARCHING AUTHORITY

International application No.
PCT/US2011/049998

Supplemental Box

In case the space in any of the preceding boxes is not sufficient.
Continuation of:

Regarding claim 10, Pohlert teaches the invention as shown above but lacks the explicit teaching of lamp receptacle further comprising a first barrel section adapted to receive said second connector portion, and a second barrel section, and a light source mounted within said second barrel section.
Kelly teaches the lamp receptacle further comprising a first barrel section adapted to receive the second connector portion (fig. 6, this is the section located below elements 5 and 51 in the figure), and a second barrel section (fig. 6 the section located above elements 51 and 5 in the figure), and a light source (6, in fig. 6) mounted within the second barrel section (fig. 2).
Therefore, it would have been obvious to one of ordinary skill in the art at the time the invention was made to combine the stand-mounted light panel for natural illumination in film, television or video of Pohlert with the ring lighting of Kelly so as to have lamp receptacle further comprising a first barrel section adapted to receive said second connector portion, and a second barrel section, and a light source mounted within said second barrel section in order to aid one connecting the light sources to the house so that they may be protected from the environment.

Regarding claim 11, Pohlert teaches the first and second connector portions comprise respective mating electrical connector sections, and wherein said light source electrically connected to the electrical connector section of said second connector portion (fig. 15a-15c, paras. 0102, 0104, the screws for connectors and printed circuit boards, wires and cables for providing the electrical connection).

Regarding claim 12, Pohlert teaches the invention as shown above but lacks the explicit teaching of a diffuser mounted within said second barrel section at a position adjacent said light source.
Kelly teaches a lens (7, fig. 6) being located in the second barrel section at a position adjacent the light source (6, fig. 6). Kelly also teaches the lens diffuses the light (spreads, col. 3 lines 55-60, col. 4 lines 3-10, col. 5 lines 50-62).
Therefore, it would have been obvious to one of ordinary skill in the art at the time the invention was made to combine the stand-mounted light panel for natural illumination in film, television or video of Pohlert with the ring lighting of Kelly so as to have a diffuser mounted within said second barrel section at a position adjacent said light source in order to provide a more uniform illumination of a given area.

Regarding claim 13, Pohlert teaches the invention as shown above but lacks the explicit teaching of a filter mounted within said second barrel section at a position adjacent said light source.
It would have been obvious to one of ordinary skill in the art at the time the invention was made to have a filter mounted within said second barrel section at a position adjacent said light source in order to allow one to illuminate an area with light having a different colors without having to change the actual light source.

Regarding claim 14, Pohlert teaches the invention as shown above but lacks the explicit teaching of the housing comprising a main body portion and a base member portion.
Kelly teaches the housing (2) comprising a main body portion (the shaded area of element 3 in fig. 6) and a base member portion (53, fig. 6).
Therefore, it would have been obvious to one of ordinary skill in the art at the time the invention was made to combine the stand-mounted light panel for natural illumination in film, television or video of Pohlert with the ring lighting of Kelly so as to have the housing comprise a main body portion and a base member portion in order provide a stable and durable housing which will allow protect the light source from the outside environment.

Regarding claim 15, Pohlert teaches the invention as shown above but lacks the explicit teaching of the housing comprises a C-shaped member having a central aperture therein, said central aperture of said C-shaped member being substantially aligned with a lens assembly of the camera, so that the field of view of the camera is substantially unobstructed by said housing and said lamp receptacle.
It would have been obvious to one of ordinary skill in the art at the time the invention was made to havethe housing comprises a C-shaped member having a central aperture therein, said central aperture of said C-shaped member being substantially aligned with a lens assembly of the camera, so that the field of view of the camera is substantially unobstructed by said housing and said lamp receptacle in order to aid one in imaging a an object and make it easier for one to adjust/align the light assembly on the camera.

Claims 1-29 meet the criteria set out in PCT Article 33(4), and thus have industrial applicability because the subject matter claimed can be made or used in industry.

PATENT ABSTRACTS OF JAPAN

(11)Publication number : **10-040330**
(43)Date of publication of application : **13.02.1998**

(51)Int.Cl. G06K 7/10
B07C 3/14
G06K 7/12

(21)Application number : **08-190667**
(22)Date of filing : **19.07.1996**

(71)Applicant : **TOSHIBA CORP**
(72)Inventor : **NOMURA HIROSHI**

(54) FLUORESCENT PATTERN DETECTOR AND POSTAL MATTER PROCESSOR USING THE DETECTOR

(57)Abstract:
PROBLEM TO BE SOLVED: To efficiently detect a fluorescent pattern by detecting light from the fluorescent pattern of an object to be detected which is excited by excitation light with plural wavelengths and recognizing a fluorescent pattern of the object based on a detection signal.
SOLUTION: In the case of detecting the fluorescent pattern of an object 10 to be detected which is moved in an arrow X direction, an ultraviolet lamp 4 is turned on, 1st excitation light La having 1st proper excitation wavelength is emitted and exited from an outgoing window 2, a light emitting member 5 is excited by the excitation light La, and 2nd excitation light Lb with 2nd proper excitation wavelength is emitted and exited from the window 2. Thereby the flurescent pattern 11 of the object 10 is excited by respective excitation light La, Lb and light corresponding to the pattern 11 is made incident upon a camera 6 through the window 2 and an aperture part on the center part of a partition plate 3. Consequently a large signal output and a large SN ratio can be obtained by the photoelectric conversion of the camera 6 to be a light detection element and the fluorescent pattern 11 can be efficiently recognized by a recognition part 7.

DETAILED DESCRIPTION

[Detailed Description of the Invention]
[0001]
[Field of the Invention]This invention relates to the mail processing unit which used the fluorescence pattern detection device and this fluorescence pattern detection device.
[0002]
[Description of the Prior Art]Conventionally, in the mail processing unit which processes much mail, Type accumulation of mail etc. which detected the fluorescence pattern which consists of

HAKODO printed by the print medium of an ink-jet printer (IJP) etc. with the fluorescence pattern detection device are performed.
[0003]The conventional example of such a fluorescence pattern detection device is explained with reference to drawing 5 and drawing 6.
[0004]The case 30 which the fluorescence pattern detection device shown in drawing 5 equipped the end with the radiation window 31, and was provided with the diaphragm 32 in which the center section carried out the opening to the inside, The ultraviolet ray lamp 33 which emits light in the excitation light of the fitness excited wavelengths L1 as shown in drawing 6 of the fluorescence pattern 41 of the detecting object 40 arranged between said radiation window 31 and the diaphragm 32, It is arranged in the side rather than the portion in which said diaphragm 32 carried out the opening inside said case 30, The camera 34 which detects the light from the fluorescence pattern 41 of said detecting object 40 excited by the excitation light emitted through said radiation window 31 from said ultraviolet ray lamp 33, The recognition part 35 which recognizes the fluorescence pattern 41 of said detecting object 40 as text etc. based on the detection result of this camera 34 is provided. The detecting object 40 shall move to an arrow X direction in drawing 5.
[0005]
[Problem to be solved by the invention]However, in the case of the conventional fluorescence pattern detection device mentioned above, it is what is exciting the fluorescence pattern 41 of the detecting object 40 only by the excitation light of the single wavelength L1 from the ultraviolet ray lamp 33, The problem that excitation of the fluorescence pattern of detecting objects, such as mail which had the two fitness excited wavelengths L1 and L2 since the luminosity currently adopted was increased in recent years, could not be performed efficiently occurred.
[0006]In light of the above-mentioned circumstances, this invention is a thing.
The purpose is to provide the mail processing unit using the fluorescence pattern detection device and this fluorescence pattern detection device which can detect efficiently the fluorescence pattern of detecting objects, such as mail with excited wavelengths.

[0007]
[Means for solving problem]The fluorescence pattern detection device of this invention which detects a fluorescence pattern with two or more excited wavelengths given to the detecting object is characterized by that the fluorescence pattern detection device of this invention comprises the following.
The excitation device which emits light in the excitation light of two or more wavelength corresponding to the fluorescence pattern of said detecting object.
The optical system unit which consists of a euphotic means to detect the light from the fluorescence pattern of said detecting object excited by the excitation light of two or more wavelength from this excitation device.
A recognition means to recognize the fluorescence pattern of said detecting object based on the detecting signal of said optical system unit.

[0008]Two or more excited wavelengths of the fluorescence pattern given to said detecting object are the 1st and 2nd fitness excited wavelengths, for example, and the 1st excitation part that emits light in the excitation light of the 1st fitness excited wavelengths, and the 2nd excitation part that emits light in the excitation light of the 2nd fitness excited wavelengths can constitute said excitation device.

[0009]The 1st excitation part can constitute the 2nd excitation part with an ultraviolet ray lamp by the light-emitting member which emits light in the excitation light of said 2nd fitness excited wavelengths by the excitation light from an ultraviolet ray lamp.
[0010]The fluorescence pattern detection device of this invention comprises:
The case which equipped the end with the radiation window and was provided with the diaphragm in which the center section carried out the opening to the inside.
The ultraviolet ray lamp which emits light in the excitation light of the 1st fitness excited wavelengths of the fluorescence pattern of said detecting object arranged between said radiation window and a diaphragm.
The light-emitting member which is arranged at the wall surface by the side of the ultraviolet ray lamp of said diaphragm, and emits light in the excitation light of said 2nd fitness excited wavelengths by the excitation light from this ultraviolet ray lamp.
It is arranged in the side rather than the portion in which said diaphragm carried out the opening inside said case, A recognition means to recognize the fluorescence pattern of said detecting object based on the output signal of the photo detector which detects the light from the fluorescence pattern of said detecting object excited by each excitation light emitted through said radiation window, and this photo detector from said ultraviolet ray lamp and a light-emitting member.

[0011]According to the fluorescence pattern detection device of such composition, detection and recognition of detecting objects, such as mail with two or more fitness excited wavelengths, of a fluorescence pattern are efficiently realizable with the simple composition using the light-emitting member which emits light by the excitation light from an ultraviolet ray lamp and this ultraviolet ray lamp.
[0012]Since the mail processing unit of this invention is provided with the fluorescence pattern detection device of composition of having mentioned above, for example, it is being adopted in recent years, the two fitness excited wavelengths L1 and the fluorescence pattern of mail with L2 can be detected efficiently, and it can recognize them.
[0013]Since it is ** with which the mail rework part which gives the fluorescence pattern for discernment to mail by the read station and this mail processing unit itself of the mail in which the fluorescence pattern detection device of composition of having mentioned above was already given to said fluorescence pattern was equipped according to the mail processing unit of this invention, It becomes possible to process efficiently the mail to which the fluorescence pattern for discernment was newly given with the mail which is fed into this mail processing unit, and to which said fluorescence pattern was already given, and this mail processing unit itself.
[0014]
[Mode for carrying out the invention]Below, an embodiment of the invention is described in detail.
[0015]Drawing 1 is provided with the following.
The case 1 which it is an outline sectional view showing the composition of the fluorescence pattern detection device of an embodiment of the invention, and this fluorescence pattern detection device equipped the end with the radiation window 2, and was provided with the diaphragm 3 in which the center section carried out the opening to the inside.
The ultraviolet ray lamp 4 which emits light in 1st excitation light La of the 1st fitness excited wavelengths L1 in the fluorescence pattern 11 of the detecting objects 10, such as mail arranged between said radiation window 2 and the diaphragm 3.

SPECTRAL_0000754

The light-emitting member 5 which is arranged at the wall surface by the side of the ultraviolet ray lamp 4 of said diaphragm 3, and emits light in the 2nd excitation light Lb of the 2nd fitness excited wavelengths L2 in the fluorescence pattern 11 with 1st excitation light La from this ultraviolet ray lamp 4.
It is arranged in the side (right-hand side) rather than the portion in which said diaphragm 3 carried out the opening inside said case 1, Each excitation light La emitted through said radiation window 2 from said ultraviolet ray lamp 4 and the light-emitting member 5, The optical system unit which consists of the camera (CCD camera) 6 which is a photo detector which receives and detects the light from the fluorescence pattern 11 of said detecting object 10 excited by Lb through the opening part of said radiation window 2 and the center section of the diaphragm 3, The recognition part 7 which recognizes concretely the fluorescence pattern 11 of said detecting object 10 as text etc. based on the output signal of the camera 6 of this optical system unit.
The detecting object 10 shall move to an arrow X direction in drawing 1 (conveyance).
[0016]It faces detecting the fluorescence pattern 11 of the detecting object 10 which moves to an arrow X direction according to the fluorescence pattern detection device of composition of having mentioned above, First, while making 1st excitation light La that turned on said ultraviolet ray lamp 4 and had the 1st fitness excited wavelengths L1 emit light and ejecting this 1st excitation light La from said radiation window 2, Excite the light-emitting member 5 with said 1st excitation light La, the 2nd excitation light Lb of the 2nd fitness excited wavelengths L2 is made to emit light, and this 2nd excitation light Lb is also ejected from said radiation window 2.
[0017]Thereby, the fluorescence pattern 11 of the detecting object 10 is excited by the 1st [said] excitation light La and 2nd excitation light Lb, respectively, and the light corresponding to the fluorescence pattern 11 enters into the camera 6 through the opening part of said radiation window 2 and the center section of the diaphragm 3.
[0018]As a result, a bigger signal output and S/N ratio than a conventional example are obtained by the photoelectric conversion in the camera 6 which is a photo detector, and said fluorescence pattern 11 can be efficiently recognized as text etc. by the recognition part 7.
[0019]Next, with reference to drawing 3 and drawing 4, the outline of the mail processing unit provided with the fluorescence pattern detection device (it gives mark 26 below and shown) of composition of having mentioned above is explained.
[0020]The mail processing unit shown in drawing 3 has the main part 20 of the shape of a large-scale core box, and loads into a left part the postcard 15 grade which is mail in drawing 3 of the main part 20, It had the supply system 21 which it sends out one sheet at a time, and had the Type accumulation system 22 of the long picture which classifies the postcard 15 supplied to the center section of the main part 20 from the supply system 21, and the distribution system 23 of postcard 15 grade and the rework part 24 are formed in the field of the point of the carrying path formed through the Type accumulation system 22 bottom from the supply system 21.
[0021]Said supply system 21 possesses the reading part etc. which read the variety of information of the zip code containing said fluorescence pattern detection device 26 which detects the accumulation part 25 which accumulates postcard 15 grade, and the fluorescence pattern 11 which is given to the postcard 15 grade sent out from this accumulation part 25, and which were described, an address, etc.
[0022]The ink-jet printer 27 which prints the fluorescence pattern 11a with the 1st and 2nd fitness excited wavelengths L1 according to the reading result of a zip code, an address, etc., and L2 on said rework part 24 by the reading part mentioned above, The fluorescence pattern

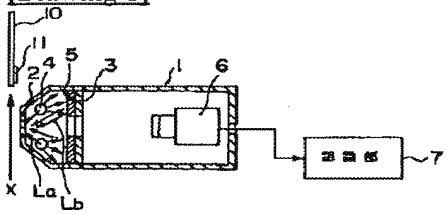
SPECTRAL_0000755

detection device 26 for checking the fluorescence pattern 11a printed by this ink-jet printer 27 is formed.
[0023]Drawing 4 shows an example of the postcard 15 on which the fluorescence pattern 11a was printed by the ink-jet printer 27.
[0024]According to the mail processing unit provided with the fluorescence pattern detection device 26 of composition of having mentioned above, the two fitness excited wavelengths L1 adopted in recent years and the fluorescence pattern 11 of the mail 15 with L2 can be detected efficiently, and can be recognized. According to the mail processing unit provided with the fluorescence pattern detection device 26 of composition of having mentioned above, it becomes possible to process efficiently the mail to which the fluorescence pattern 11a for discernment was newly given with this mail processing unit itself.
[0025]
[Effect of the Invention]According to this invention, the fluorescence pattern detection device which can perform detection and recognition of a detecting object of a fluorescence pattern efficiently with the simple composition of using two or more excitation light can be provided.
[0026]It is possible according to this invention, to detect efficiently the two fitness excited wavelengths L1 and the fluorescence pattern of mail with L2, and to recognize them, for example, it is being adopted in recent years, The mail processing unit which can process efficiently the mail to which the fluorescence pattern for discernment was newly given with the mail processing unit itself can be provided.

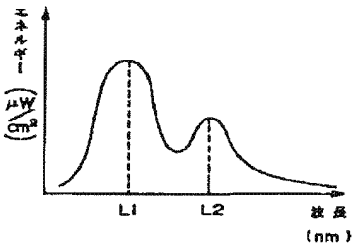
[Translation done.]

DRAWINGS

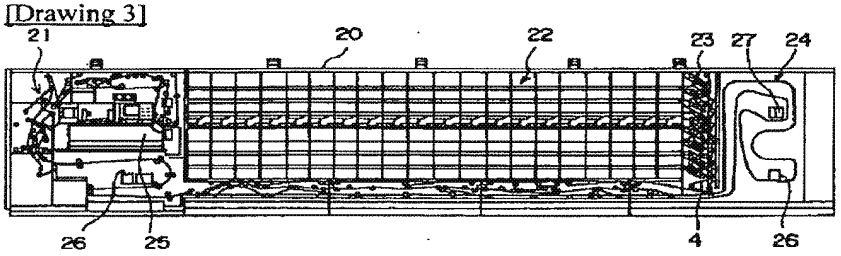
[Drawing 1]



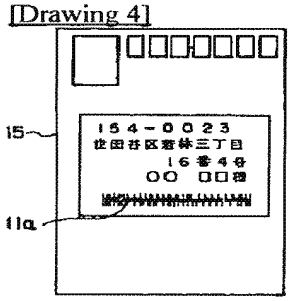
[Drawing 2]



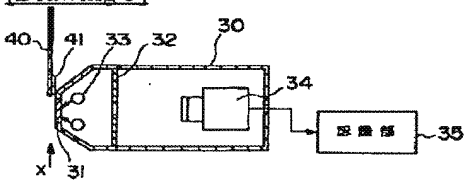
[Drawing 3]



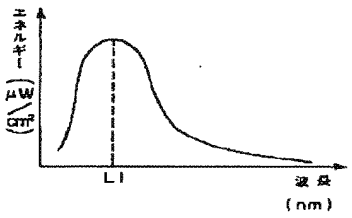
[Drawing 4]



[Drawing 5]



[Drawing 6]



[Translation done.]

[Claim 1]A fluorescence pattern detection device which detects a fluorescence pattern with two or more excited wavelengths given to a detecting object, comprising:
An excitation device which emits light in excitation light of two or more wavelength corresponding to a fluorescence pattern of said detecting object.
A recognition means to recognize a fluorescence pattern of said detecting object based on a detecting signal of an optical system unit which consists of a euphotic means to detect light from a fluorescence pattern of said detecting object excited by excitation light of two or more wavelength from this excitation device, and said optical system unit.

[Claim 2]The 1st given to a detecting object, a fluorescence pattern detection device which detects a fluorescence pattern with the 2nd fitness excited wavelengths characterized by comprising the following.
The 1st excitation part that emits light in excitation light of the 1st fitness excited wavelengths of a fluorescence pattern of said detecting object.
An excitation device which consists of the 2nd excitation part that emits light in excitation light of said 2nd fitness excited wavelengths by excitation light from this 1st excitation part.
An optical system unit which consists of a euphotic means to detect light from a fluorescence pattern of said detecting object excited by excitation light of the 1st [from this excitation device], and 2nd fitness excited wavelengths.
A recognition means to recognize a fluorescence pattern of said detecting object based on a detecting signal of said optical system unit.

[Claim 3]The 1st given to a detecting object, a fluorescence pattern detection device which detects a fluorescence pattern with the 2nd fitness excited wavelengths characterized by comprising the following.
An ultraviolet ray lamp which emits light in excitation light of the 1st fitness excited wavelengths of a fluorescence pattern of said detecting object.
An excitation device which consists of a light-emitting member which emits light in excitation light of said 2nd fitness excited wavelengths by excitation light from this ultraviolet ray lamp.
An optical system unit which consists of a photo detector which detects light from a fluorescence pattern of said detecting object excited by excitation light of the 1st [from this excitation device], and 2nd fitness excited wavelengths.

A recognition means to recognize a fluorescence pattern of said detecting object based on a detecting signal of said optical system unit.

[Claim 4]The 1st given to a detecting object, a fluorescence pattern detection device which detects a fluorescence pattern with the 2nd fitness excited wavelengths characterized by comprising the following.
A case which equipped an end with a radiation window and was provided with a diaphragm in which a center section carried out the opening to an inside.
An ultraviolet ray lamp which emits light in excitation light of the 1st fitness excited wavelengths of a fluorescence pattern of said detecting object arranged between said radiation window and a diaphragm.
A light-emitting member which is arranged at a wall surface by the side of an ultraviolet ray lamp of said diaphragm, and emits light in excitation light of said 2nd fitness excited wavelengths by excitation light from this ultraviolet ray lamp.
It is arranged in the side rather than a portion in which said diaphragm carried out the opening inside said case, A recognition means to recognize a fluorescence pattern of said detecting object based on an output signal of a photo detector which detects light from a fluorescence pattern of said detecting object excited by each excitation light emitted through said radiation window, and this photo detector from said ultraviolet ray lamp and a light-emitting member.

[Claim 5]A mail processing unit which processes mail to which a fluorescence pattern with two or more excited wavelengths was given, comprising:
An excitation device which emits light in excitation light of two or more wavelength corresponding to a fluorescence pattern of mail.
A recognition means to recognize a fluorescence pattern of said mail based on a detecting signal of an optical system unit which consists of a euphotic means to detect light from a fluorescence pattern of said mail excited by excitation light of two or more wavelength from this excitation device, and said optical system unit.

[Claim 6]A mail processing unit which processes mail to which a fluorescence pattern with two or more excited wavelengths was given, comprising:
An excitation device which emits light in excitation light of two or more wavelength corresponding to a fluorescence pattern of mail.
A recognition means to recognize a fluorescence pattern of said mail based on a detecting signal of an optical system unit which consists of a euphotic means to detect light from a fluorescence pattern of said mail excited by excitation light of two or more wavelength from this excitation device, and said optical system unit.

[Translation done.]

SPECTRAL_0000759

Electronic Acknowledgement Receipt

EFS ID:	12058541
Application Number:	13222688
International Application Number:	
Confirmation Number:	5910
Title of Invention:	EXCITATION LIGHT SOURCE ASSEMBLY
First Named Inventor/Applicant Name:	Michael B. Nelson
Customer Number:	27104
Filer:	Bruce E. Dahl/Cynthia Sullivan
Filer Authorized By:	Bruce E. Dahl
Attorney Docket Number:	SPEC US-4 (027560-0014)
Receipt Date:	13-FEB-2012
Filing Date:	31-AUG-2011
Time Stamp:	12:24:51
Application Type:	Utility under 35 USC 111(a)

Payment information:

Submitted with Payment	no

File Listing:

Document Number	Document Description	File Name	File Size(Bytes)/ Message Digest	Multi Part /.zip	Pages (if appl.)
1		SPEC-4-IDS.pdf	604174 c39df43f1218de42d427e91b339ef12ed63dacda	yes	21

	Multipart Description/PDF files in .zip description		
	Document Description	**Start**	**End**
	Information Disclosure Statement (IDS) Form (SB08)	1	3
	Non Patent Literature	4	13
	Foreign Reference	14	21
Warnings:			
Information:			
	Total Files Size (in bytes):	604174	

This Acknowledgement Receipt evidences receipt on the noted date by the USPTO of the indicated documents, characterized by the applicant, and including page counts, where applicable. It serves as evidence of receipt similar to a Post Card, as described in MPEP 503.

New Applications Under 35 U.S.C. 111
If a new application is being filed and the application includes the necessary components for a filing date (see 37 CFR 1.53(b)-(d) and MPEP 506), a Filing Receipt (37 CFR 1.54) will be issued in due course and the date shown on this Acknowledgement Receipt will establish the filing date of the application.

National Stage of an International Application under 35 U.S.C. 371
If a timely submission to enter the national stage of an international application is compliant with the conditions of 35 U.S.C. 371 and other applicable requirements a Form PCT/DO/EO/903 indicating acceptance of the application as a national stage submission under 35 U.S.C. 371 will be issued in addition to the Filing Receipt, in due course.

New International Application Filed with the USPTO as a Receiving Office
If a new international application is being filed and the international application includes the necessary components for an international filing date (see PCT Article 11 and MPEP 1810), a Notification of the International Application Number and of the International Filing Date (Form PCT/RO/105) will be issued in due course, subject to prescriptions concerning national security, and the date shown on this Acknowledgement Receipt will establish the international filing date of the application.

UNITED STATES PATENT AND TRADEMARK OFFICE

UNITED STATES DEPARTMENT OF COMMERCE
United States Patent and Trademark Office
Address: COMMISSIONER FOR PATENTS
P.O. Box 1450
Alexandria, Virginia 22313-1450
www.uspto.gov

APPLICATION NUMBER	FILING OR 371(C) DATE	FIRST NAMED APPLICANT	ATTY. DOCKET NO./TITLE
13/222,688	08/31/2011	Michael B. Nelson	SPEC US-4 (027560-0014)

CONFIRMATION NO. 5910

27104
FENNEMORE CRAIG, P.C.
1700 Lincoln Street
SUITE 2900
DENVER, CO 80203

PUBLICATION NOTICE

OC000000052870803

Title:EXCITATION LIGHT SOURCE ASSEMBLY

Publication No.US-2012-0049089-A1
Publication Date:03/01/2012

NOTICE OF PUBLICATION OF APPLICATION

The above-identified application will be electronically published as a patent application publication pursuant to 37 CFR 1.211, et seq. The patent application publication number and publication date are set forth above.

The publication may be accessed through the USPTO's publically available Searchable Databases via the Internet at www.uspto.gov. The direct link to access the publication is currently http://www.uspto.gov/patft/.

The publication process established by the Office does not provide for mailing a copy of the publication to applicant. A copy of the publication may be obtained from the Office upon payment of the appropriate fee set forth in 37 CFR 1.19(a)(1). Orders for copies of patent application publications are handled by the USPTO's Office of Public Records. The Office of Public Records can be reached by telephone at (703) 308-9726 or (800) 972-6382, by facsimile at (703) 305-8759, by mail addressed to the United States Patent and Trademark Office, Office of Public Records, Alexandria, VA 22313-1450 or via the Internet.

In addition, information on the status of the application, including the mailing date of Office actions and the dates of receipt of correspondence filed in the Office, may also be accessed via the Internet through the Patent Electronic Business Center at www.uspto.gov using the public side of the Patent Application Information and Retrieval (PAIR) system. The direct link to access this status information is currently http://pair.uspto.gov/. Prior to publication, such status information is confidential and may only be obtained by applicant using the private side of PAIR.

Further assistance in electronically accessing the publication, or about PAIR, is available by calling the Patent Electronic Business Center at 1-866-217-9197.

Office of Data Managment, Application Assistance Unit (571) 272-4000, or (571) 272-4200, or 1-888-786-0101

UNITED STATES PATENT AND TRADEMARK OFFICE

UNITED STATES DEPARTMENT OF COMMERCE
United States Patent and Trademark Office
Address: COMMISSIONER FOR PATENTS
P.O. Box 1450
Alexandria, Virginia 22313-1450
www.uspto.gov

APPLICATION NO.	FILING DATE	FIRST NAMED INVENTOR	ATTORNEY DOCKET NO.	CONFIRMATION NO.
13/222,688	08/31/2011	Michael B. Nelson	SPEC US-4 (027560-0014)	5910

27104 7590 11/21/2012

FENNEMORE CRAIG, P.C.
1700 Lincoln Street
SUITE 2900
DENVER, CO 80203

EXAMINER	
TANINGCO, MARCUS H	

ART UNIT	PAPER NUMBER
2884	

MAIL DATE	DELIVERY MODE
11/21/2012	PAPER

Please find below and/or attached an Office communication concerning this application or proceeding.

The time period for reply, if any, is set in the attached communication.

Office Action Summary	Application No.	Applicant(s)	
	13/222,688	NELSON ET AL.	
	Examiner	Art Unit	
	MARCUS TANINGCO	2884	

-- The MAILING DATE of this communication appears on the cover sheet with the correspondence address --

Period for Reply

A SHORTENED STATUTORY PERIOD FOR REPLY IS SET TO EXPIRE 1 MONTH(S) OR THIRTY (30) DAYS, WHICHEVER IS LONGER, FROM THE MAILING DATE OF THIS COMMUNICATION.

- Extensions of time may be available under the provisions of 37 CFR 1.136(a). In no event, however, may a reply be timely filed after SIX (6) MONTHS from the mailing date of this communication.
- If NO period for reply is specified above, the maximum statutory period will apply and will expire SIX (6) MONTHS from the mailing date of this communication.
- Failure to reply within the set or extended period for reply will, by statute, cause the application to become ABANDONED (35 U.S.C. § 133). Any reply received by the Office later than three months after the mailing date of this communication, even if timely filed, may reduce any earned patent term adjustment. See 37 CFR 1.704(b).

Status

1)☐ Responsive to communication(s) filed on _____.

2a)☐ This action is **FINAL**. 2b)☐ This action is non-final.

3)☐ An election was made by the applicant in response to a restriction requirement set forth during the interview on _____; the restriction requirement and election have been incorporated into this action.

4)☐ Since this application is in condition for allowance except for formal matters, prosecution as to the merits is closed in accordance with the practice under *Ex parte Quayle*, 1935 C.D. 11, 453 O.G. 213.

Disposition of Claims

5)☒ Claim(s) 1-29 is/are pending in the application.

5a) Of the above claim(s) _____ is/are withdrawn from consideration.

6)☐ Claim(s) _____ is/are allowed.

7)☐ Claim(s) _____ is/are rejected.

8)☐ Claim(s) _____ is/are objected to.

9)☒ Claim(s) 1-29 are subject to restriction and/or election requirement.

* If any claims have been determined allowable, you may be eligible to benefit from the **Patent Prosecution Highway** program at a participating intellectual property office for the corresponding application. For more information, please see http://www.uspto.gov/patents/init_events/pph/index.jsp or send an inquiry to PPHfeedback@uspto.gov.

Application Papers

10)☐ The specification is objected to by the Examiner.

11)☐ The drawing(s) filed on _____ is/are: a)☐ accepted or b)☐ objected to by the Examiner.

Applicant may not request that any objection to the drawing(s) be held in abeyance. See 37 CFR 1.85(a).

Replacement drawing sheet(s) including the correction is required if the drawing(s) is objected to. See 37 CFR 1.121(d).

12)☐ The oath or declaration is objected to by the Examiner. Note the attached Office Action or form PTO-152.

Priority under 35 U.S.C. § 119

13)☐ Acknowledgment is made of a claim for foreign priority under 35 U.S.C. § 119(a)-(d) or (f).

a)☐ All b)☐ Some * c)☐ None of:

1.☐ Certified copies of the priority documents have been received.

2.☐ Certified copies of the priority documents have been received in Application No. _____.

3.☐ Copies of the certified copies of the priority documents have been received in this National Stage application from the International Bureau (PCT Rule 17.2(a)).

* See the attached detailed Office action for a list of the certified copies not received.

Attachment(s)

1) ☐ Notice of References Cited (PTO-892)
2) ☐ Notice of Draftsperson's Patent Drawing Review (PTO-948)
3) ☐ Information Disclosure Statement(s) (PTO/SB/08) Paper No(s)/Mail Date _____.
4) ☐ Interview Summary (PTO-413) Paper No(s)/Mail Date. _____ .
5) ☐ Notice of Informal Patent Application
6) ☐ Other: _____.

DETAILED ACTION

Election/Restrictions

Restriction to one of the following inventions is required under 35 U.S.C. 121:

I. Claims 1-8 and 19-29, drawn to an excitation light source assembly comprising a housing defining a central opening therein and diffusers, classified in class 250, subclass 458.1.

II. Claims 9-15, drawn to an excitation light source assembly comprising a first and a second connector portion, classified in class 250, subclass 461.2.

III. Claims 16-18, drawn to an excitation light source assembly comprising a plurality of first connector portions, classified in class 250, subclass 461.1.

The inventions are distinct, each from the other because of the following reasons:

Inventions I and II are related as subcombinations disclosed as usable together in a single combination. The subcombinations are distinct if they do not overlap in scope and are not obvious variants, and if it is shown that at least one subcombination is separately usable. In the instant case, subcombination I has separate utility such as an adjustable illumination light source assembly. See MPEP § 806.05(d).

Inventions I and III are related as subcombinations disclosed as usable together in a single combination. The subcombinations are distinct if they do not overlap in scope and are not obvious variants, and if it is shown that at least one subcombination is separately usable. In the instant case, subcombination I has separate utility such as a diffused light source assembly. See MPEP § 806.05(d).

SPECTRAL_0000765

Inventions II and III are related as subcombinations disclosed as usable together in a single combination. The subcombinations are distinct if they do not overlap in scope and are not obvious variants, and if it is shown that at least one subcombination is separately usable. In the instant case, subcombination III has separate utility such as a multi-spectral light source assembly. See MPEP § 806.05(d).

The examiner has required restriction between subcombinations usable together. Where applicant elects a subcombination and claims thereto are subsequently found allowable, any claim(s) depending from or otherwise requiring all the limitations of the allowable subcombination will be examined for patentability in accordance with 37 CFR 1.104. See MPEP § 821.04(a). Applicant is advised that if any claim presented in a continuation or divisional application is anticipated by, or includes all the limitations of, a claim that is allowable in the present application, such claim may be subject to provisional statutory and/or nonstatutory double patenting rejections over the claims of the instant application.

Restriction for examination purposes as indicated is proper because all these inventions listed in this action are independent or distinct for the reasons given above and there would be a serious search and/or examination burden if restriction were not required because at least the following reason(s) apply:

The inventions would require different fields of search.

Applicant is advised that the reply to this requirement to be complete must include (i) an election of a invention to be examined even though the requirement may be traversed (37 CFR 1.143) **and (ii) identification of the claims encompassing the elected invention**.

SPECTRAL_0000766

The election of an invention may be made with or without traverse. To reserve a right to petition, the election must be made with traverse. If the reply does not distinctly and specifically point out supposed errors in the restriction requirement, the election shall be treated as an election without traverse. Traversal must be presented at the time of election in order to be considered timely. Failure to timely traverse the requirement will result in the loss of right to petition under 37 CFR 1.144. If claims are added after the election, applicant must indicate which of these claims are readable upon the elected invention.

Should applicant traverse on the ground that the inventions are not patentably distinct, applicant should submit evidence or identify such evidence now of record showing the inventions to be obvious variants or clearly admit on the record that this is the case. In either instance, if the examiner finds one of the inventions unpatentable over the prior art, the evidence or admission may be used in a rejection under 35 U.S.C. 103(a) of the other invention.

A telephone call was not made request an oral election to the above restriction requirement.

Applicant is reminded that upon the cancellation of claims to a non-elected invention, the inventorship must be amended in compliance with 37 CFR 1.48(b) if one or more of the currently named inventors is no longer an inventor of at least one claim remaining in the application. Any amendment of inventorship must be accompanied by a request under 37 CFR 1.48(b) and by the fee required under 37 CFR 1.17(i).

Any inquiry concerning this communication or earlier communications from the examiner should be directed to MARCUS TANINGCO whose telephone number is (571)272-1848. The examiner can normally be reached on M - F 9:00 - 5:30.

If attempts to reach the examiner by telephone are unsuccessful, the examiner's supervisor, Dave Porta can be reached on (571) 272-2444. The fax phone number for the organization where this application or proceeding is assigned is 571-273-8300.

Information regarding the status of an application may be obtained from the Patent Application Information Retrieval (PAIR) system. Status information for published applications may be obtained from either Private PAIR or Public PAIR. Status information for unpublished applications is available through Private PAIR only. For more information about the PAIR system, see http://pair-direct.uspto.gov. Should you have questions on access to the Private PAIR system, contact the Electronic Business Center (EBC) at 866-217-9197 (toll-free). If you would like assistance from a USPTO Customer Service Representative or access to the automated information system, call 800-786-9199 (IN USA OR CANADA) or 571-272-1000.

/Marcus H Taningco/
Examiner, Art Unit 2884

SPECTRAL_0000768

UNITED STATES PATENT AND TRADEMARK OFFICE

UNITED STATES DEPARTMENT OF COMMERCE
United States Patent and Trademark Office
Address: COMMISSIONER FOR PATENTS
P.O. Box 1450
Alexandria, Virginia 22313-1450
www.uspto.gov

BIB DATA SHEET

CONFIRMATION NO. 5910

SERIAL NUMBER	FILING or 371(c) DATE RULE	CLASS	GROUP ART UNIT	ATTORNEY DOCKET NO.
13/222,688	08/31/2011	250	2884	SPEC US-4 (027560-0014)

APPLICANTS

Michael B. Nelson, Tucson, AZ;
Michael D. Cable, Tucson, AZ;

**** CONTINUING DATA ***************************

This appln claims benefit of 61/379,282 09/01/2010

**** FOREIGN APPLICATIONS ***************************

**** IF REQUIRED, FOREIGN FILING LICENSE GRANTED **** ** SMALL ENTITY **

09/14/2011

Foreign Priority claimed ☐ Yes ☑ No 35 USC 119(a-d) conditions met ☐ Yes ☑ No Verified and Acknowledged /MARCUS H TANINGCO/ Examiner's Signature	☐ Met after Allowance Initials	STATE OR COUNTRY	SHEETS DRAWINGS	TOTAL CLAIMS	INDEPENDENT CLAIMS
		AZ	12	29	4

ADDRESS

FENNEMORE CRAIG, P.C.
1700 Lincoln Street
SUITE 2900
DENVER, CO 80203
UNITED STATES

TITLE

EXCITATION LIGHT SOURCE ASSEMBLY

FILING FEE RECEIVED	FEES: Authority has been given in Paper No._____ to charge/credit DEPOSIT ACCOUNT No._____ for following:	☐ All Fees ☐ 1.16 Fees (Filing) ☐ 1.17 Fees (Processing Ext. of time) ☐ 1.18 Fees (Issue) ☐ Other _____ ☐ Credit
871		

BIB (Rev. 05/07).

Index of Claims	Application/Control No.	Applicant(s)/Patent Under Reexamination
	13222688	NELSON ET AL.
	Examiner	Art Unit
	MARCUS TANINGCO	2884

✓	Rejected	-	Cancelled	N	Non-Elected	A	Appeal
=	Allowed	÷	Restricted	I	Interference	O	Objected

☐ Claims renumbered in the same order as presented by applicant ☐ CPA ☐ T.D. ☐ R.1.47

CLAIM		DATE								
Final	Original	11/18/2012								
	1	÷								
	2	÷								
	3	÷								
	4	÷								
	5	÷								
	6	÷								
	7	÷								
	8	÷								
	9	÷								
	10	÷								
	11	÷								
	12	÷								
	13	÷								
	14	÷								
	15	÷								
	16	÷								
	17	÷								
	18	÷								
	19	÷								
	20	÷								
	21	÷								
	22	÷								
	23	÷								
	24	÷								
	25	÷								
	26	÷								
	27	÷								
	28	÷								
	29	÷								

IN THE UNITED STATES PATENT AND TRADEMARK OFFICE

In Re Application of:	)	
	)	Examiner: Taningco, M.
NELSON, Michael, B., *et al.*	)	
	)	Group Art Unit: 2884
Serial No. 13/222,688	)	
	)	Confirm. No.: 5910
Filing Date: August 31, 2011	)	
	)	Atty. Dkt.: SPEC US-4
For: EXCITATION LIGHT SOURCE ASSEMBLY	)	(027560-0014)
	)	

ELECTION OF INVENTION (Without Traverse)
UNDER 37 C.F.R. §1.142

To: The Commissioner for Patents
P.O. Box 1450
Alexandria, VA 22313-1450

Sir:

In response to the examiner's requirement for restriction in office action, paper no. (unspecified), dated November 21, 2012, applicants hereby elect, without traverse, to prosecute Invention I identified by the examiner. The claims readable on the elected invention are claims 1-8 and 19-29.

R E M A R K S

In the office action dated November 21, 2012, the examiner restricted prosecution to one of three inventions identified by the examiner as Inventions I, II, and III. To meet the examiner's requirement for restriction, applicants have elected, without traverse, the invention classified as Invention I.

SPECTRAL_0000771

If any questions or issues remain to be resolved, the examiner is requested to contact the applicants' attorney at the telephone number listed below.

Respectfully submitted,

FENNEMORE CRAIG, P.C.

/Bruce E. Dahl/
Bruce E. Dahl, Esq.
Attorney for Applicants
PTO Registration No. 33,670
1700 Lincoln Street, Suite 2900
Denver, CO 80203
(303) 291-3200

Date: December 12, 2012

Electronic Acknowledgement Receipt

EFS ID:	14446370
Application Number:	13222688
International Application Number:	
Confirmation Number:	5910
Title of Invention:	EXCITATION LIGHT SOURCE ASSEMBLY
First Named Inventor/Applicant Name:	Michael B. Nelson
Customer Number:	27104
Filer:	Bruce E. Dahl/Cynthia Sullivan
Filer Authorized By:	Bruce E. Dahl
Attorney Docket Number:	SPEC US-4 (027560-0014)
Receipt Date:	12-DEC-2012
Filing Date:	31-AUG-2011
Time Stamp:	12:51:37
Application Type:	Utility under 35 USC 111(a)

Payment information:

Submitted with Payment	no

File Listing:

Document Number	Document Description	File Name	File Size(Bytes)/ Message Digest	Multi Part /.zip	Pages (if appl.)
1	Response to Election / Restriction Filed	Election.pdf	85489 84887def9df0ed534eae1d60091257a3d9553026	no	2
Warnings:					
Information:					

Total Files Size (in bytes):	85489

This Acknowledgement Receipt evidences receipt on the noted date by the USPTO of the indicated documents, characterized by the applicant, and including page counts, where applicable. It serves as evidence of receipt similar to a Post Card, as described in MPEP 503.

New Applications Under 35 U.S.C. 111
If a new application is being filed and the application includes the necessary components for a filing date (see 37 CFR 1.53(b)-(d) and MPEP 506), a Filing Receipt (37 CFR 1.54) will be issued in due course and the date shown on this Acknowledgement Receipt will establish the filing date of the application.

National Stage of an International Application under 35 U.S.C. 371
If a timely submission to enter the national stage of an international application is compliant with the conditions of 35 U.S.C. 371 and other applicable requirements a Form PCT/DO/EO/903 indicating acceptance of the application as a national stage submission under 35 U.S.C. 371 will be issued in addition to the Filing Receipt, in due course.

New International Application Filed with the USPTO as a Receiving Office
If a new international application is being filed and the international application includes the necessary components for an international filing date (see PCT Article 11 and MPEP 1810), a Notification of the International Application Number and of the International Filing Date (Form PCT/RO/105) will be issued in due course, subject to prescriptions concerning national security, and the date shown on this Acknowledgement Receipt will establish the international filing date of the application.

UNITED STATES PATENT AND TRADEMARK OFFICE

UNITED STATES DEPARTMENT OF COMMERCE
United States Patent and Trademark Office
Address: COMMISSIONER FOR PATENTS
P.O. Box 1450
Alexandria, Virginia 22313-1450
www.uspto.gov

APPLICATION NO.	FILING DATE	FIRST NAMED INVENTOR	ATTORNEY DOCKET NO.	CONFIRMATION NO.
13/222,688	08/31/2011	Michael B. Nelson	SPEC US-4 (027560-0014)	5910

27104 7590 01/30/2013

FENNEMORE CRAIG, P.C.
1700 Lincoln Street
SUITE 2900
DENVER, CO 80203

EXAMINER	
TANINGCO, MARCUS H	
ART UNIT	PAPER NUMBER
2884	

MAIL DATE	DELIVERY MODE
01/30/2013	PAPER

Please find below and/or attached an Office communication concerning this application or proceeding.

The time period for reply, if any, is set in the attached communication.

Office Action Summary	Application No.	Applicant(s)	
	13/222,688	NELSON ET AL.	
	Examiner	Art Unit	
	MARCUS TANINGCO	2884	

-- The MAILING DATE of this communication appears on the cover sheet with the correspondence address --

Period for Reply

A SHORTENED STATUTORY PERIOD FOR REPLY IS SET TO EXPIRE *3* MONTH(S) OR THIRTY (30) DAYS, WHICHEVER IS LONGER, FROM THE MAILING DATE OF THIS COMMUNICATION.

- Extensions of time may be available under the provisions of 37 CFR 1.136(a). In no event, however, may a reply be timely filed after SIX (6) MONTHS from the mailing date of this communication.
- If NO period for reply is specified above, the maximum statutory period will apply and will expire SIX (6) MONTHS from the mailing date of this communication.
- Failure to reply within the set or extended period for reply will, by statute, cause the application to become ABANDONED (35 U.S.C. § 133). Any reply received by the Office later than three months after the mailing date of this communication, even if timely filed, may reduce any earned patent term adjustment. See 37 CFR 1.704(b).

Status

1)☐ Responsive to communication(s) filed on _____.

2a)☐ This action is **FINAL**. 2b)☒ This action is non-final.

3)☐ An election was made by the applicant in response to a restriction requirement set forth during the interview on _____; the restriction requirement and election have been incorporated into this action.

4)☐ Since this application is in condition for allowance except for formal matters, prosecution as to the merits is closed in accordance with the practice under *Ex parte Quayle*, 1935 C.D. 11, 453 O.G. 213.

Disposition of Claims

5)☒ Claim(s) *1-29* is/are pending in the application.

5a) Of the above claim(s) *9-18* is/are withdrawn from consideration.

6)☐ Claim(s) _____ is/are allowed.

7)☒ Claim(s) *1-8 and 19-29* is/are rejected.

8)☐ Claim(s) _____ is/are objected to.

9)☐ Claim(s) _____ are subject to restriction and/or election requirement.

* If any claims have been determined allowable, you may be eligible to benefit from the **Patent Prosecution Highway** program at a participating intellectual property office for the corresponding application. For more information, please see http://www.uspto.gov/patents/init_events/pph/index.jsp or send an inquiry to PPHfeedback@uspto.gov.

Application Papers

10)☐ The specification is objected to by the Examiner.

11)☒ The drawing(s) filed on *31 August 2011* is/are: a)☒ accepted or b)☐ objected to by the Examiner.

Applicant may not request that any objection to the drawing(s) be held in abeyance. See 37 CFR 1.85(a).

Replacement drawing sheet(s) including the correction is required if the drawing(s) is objected to. See 37 CFR 1.121(d).

Priority under 35 U.S.C. § 119

12)☐ Acknowledgment is made of a claim for foreign priority under 35 U.S.C. § 119(a)-(d) or (f).

a)☐ All b)☐ Some * c)☐ None of:

1.☐ Certified copies of the priority documents have been received.

2.☐ Certified copies of the priority documents have been received in Application No. _____.

3.☐ Copies of the certified copies of the priority documents have been received in this National Stage application from the International Bureau (PCT Rule 17.2(a)).

* See the attached detailed Office action for a list of the certified copies not received.

Attachment(s)

1) ☒ Notice of References Cited (PTO-892)

2) ☒ Information Disclosure Statement(s) (PTO/SB/08) Paper No(s)/Mail Date *11/11/11, 11/11/11, 2/13/12*.

3) ☐ Interview Summary (PTO-413) Paper No(s)/Mail Date. _____ .

4) ☐ Other: _____.

DETAILED ACTION

Election/Restrictions

Claims 9-18 are withdrawn from further consideration pursuant to 37 CFR 1.142(b) as being drawn to a nonelected invention, there being no allowable generic or linking claim. Election was made **without** traverse in the reply filed on 12/12/12.

Claim Rejections - 35 USC § 103

The following is a quotation of 35 U.S.C. 103(a) which forms the basis for all obviousness rejections set forth in this Office action:

> (a) A patent may not be obtained though the invention is not identically disclosed or described as set forth in section 102 of this title, if the differences between the subject matter sought to be patented and the prior art are such that the subject matter as a whole would have been obvious at the time the invention was made to a person having ordinary skill in the art to which said subject matter pertains. Patentability shall not be negatived by the manner in which the invention was made.

This application currently names joint inventors. In considering patentability of the claims under 35 U.S.C. 103(a), the examiner presumes that the subject matter of the various claims was commonly owned at the time any inventions covered therein were made absent any evidence to the contrary. Applicant is advised of the obligation under 37 CFR 1.56 to point out the inventor and invention dates of each claim that was not commonly owned at the time a later invention was made in order for the examiner to consider the applicability of 35 U.S.C. 103(c) and potential 35 U.S.C. 102(e), (f) or (g) prior art under 35 U.S.C. 103(a).

Claims 1-4, 6-8, 19-26, 28, and 29 are rejected under 35 U.S.C. 103(a) as being unpatentable over Pohlert et al. in view of Kelly and Nomura.

SPECTRAL_0000777

With regards to claim 1, Pohlert teaches a stand-mounted light panel for natural illumination in film, television or video (title) and further teaches a central opening (103, fig. 1; 303 figs. 4-5) having a plurality of lamp receptacles (lamp segment 306, fig. 4; panel frame or frame, abstract, fig. 47a, pars. 0179-0180, receives the LEDs; also see figs. 48a-50b) surrounding the central opening (303, fig 4; 3803, fig. 38A), the structure being mountable to a support structure (330, fig. 3) so that the central opening being aligned with a camera (fig. 1 shows this aspect) also mounted to the support structure (330, fig. 3), so that the field of view of the camera is unobstructed, and a light source (lamps, fig. 2; LEDs or lamps 305, fig. 4; 4705 fig. 47a, para. 0180) positioned within each of the plurality of lamp receptacles (lamp segment 306, fig. 4; panel frame or frame, abstract, fig. 47a, pars. 0179-0180, receives the LEDs; also see figs. 48a-50b), a diffuser (5029, fig. 5a; 1205 fig. 12; 795, 876 in figs 7-8, teach that lens elements spreading the light; this is interpreted as meaning diffusing; paras 0119-0120) positioned adjacent the light source positioned within each of the plurality of lamp receptacles (figs. 4 shows a plurality of lamp segments 306 which contain a plurality of light sources 305; fig. 50a shows the a diffuser 5029 which locate within each lamp panel 4702, 4802, figs. 47a; 50a-50b), each of the diffusers diffusing light produced by each of the light sources (abstract, para. 0023 teaches the diffusion lens being integrated with the lighting panel (receptacle); 795, 876 in figs 7-8, teach that lens elements spreading the light; this is interpreted as meaning diffusing; paras 0119-0120), and a control system (212, fig. 2, para. 0094; and element 1052) operatively connected to each of the light sources (para. 0145, fig. 13, paras. 0091-0092, 0166) positioned within the plurality of lamp receptacles, the control system operating selected ones of the light

source to provide a desired illumination to an object within the field of view of the camera (paras. 0091-0092, 0166).

However, Pohlert does not explicitly state a housing defining a central opening which contains the structure which holds a plurality of lamps, for connecting the camera to a central aperture.

Kelly teaches a ring lighting (title) and further teaches a housing (2, figs. 1-2) defining a central opening (3 figs. 1-2) which contains the structure which holds a plurality of lamps (6 figs. 1-2), for connecting the camera to a central aperture (abstract, figs. 1-2). Therefore, it would have been obvious to one of ordinary skill in the art at the time the invention was made to combine the stand-mounted light panel for natural illumination in film, television or video of Pohlert with the ring lighting of Kelly so as to have a housing defining a central opening which contains the structure which holds a plurality of lamps, for connecting the camera to a central aperture in order to protect the lights and lenses from the environment.

Pohlert also does not explicitly state the apparatus being used as an excitation light source.

Nomura teaches a fluorescent pattern detector and postal matter processor using the detector (title) and further an apparatus comprising a central hole aligned with a camera having a plurality of light sources surrounding the central aperture being used as an excitation light source (abstract, figs. 1, 5). Therefore, it would have been obvious to one of ordinary skill in the art at the time the invention was made to combine the stand-mounted light panel for natural illumination in film, television or video of Pohlert with the fluorescent pattern detector and postal matter processor using the detector of Nomura so as to have the apparatus used as a

excitation light source in order to aid one in recognizing a fluorescent pattern of the object based on a detection signal.

With regards to claim 2, Pohlert teaches at least one of the light sources comprising a narrow-band light source (para. 0019) that emits light having a bandwidth (blue or green LEDs, paras. 0019, 0118). However, Pohlert does not explicitly state the bandwidth of the light source being about 35 nm. It would have been obvious to one of ordinary skill in the art at the time the invention was made to have the bandwidth of the light source be about 35 nm, since discovering the optimum value of a result effective variable involves only routine skill in the art and in order to produce a narrow-band of light (Pohlert, para. 0019).

Regarding claim 3, Pohlert teaches at least one narrow-band light source comprising a light emitting diode (paras. 0019, 0118-0119).

Regarding claim 4, Pohlert teaches at least one filter (5010, fig. 50a) positioned adjacent at least one diffuser (5029, fig. 50a) in at least one of the lamp receptacles defined by the housing (pare. 0187, figs. 50a-50b).

Regarding claim 6, Pohlert teaches at least one of the light sources comprises a broad-band light source (white LEDs, pares. 0098, 0118).

Regarding claim 7, Pohlert teaches at least some of said plurality of lamp receptacles comprise opposed pairs of lamp receptacles on opposite sides of said central opening (different light segments 306 fig. 4), each opposed pair of lamp receptacles producing light of the same color (paras. 0097; para. 0118 teaches that the LEDs can all be the same color).

Regarding claim 8, Pohlert teaches opposing pairs of lamps located in receptacles (lamp segments, figs. 30b-30c) on opposite side the central opening (para. 0097). However, Pohlert

SPECTRAL_0000780

does not explicitly state ten pairs of lamps surrounding the central aperture. It would have been obvious to one of ordinary skill in the art at the time the invention was made to have ten pairs of lamps surrounding the central aperture, since a mere duplication of essential working parts of device involves only routine skill in the art, and in order to produce the desired amount and display of light.

Regarding claim 19, Pohlert teaches a stand-mounted light panel for natural illumination in film, television or video (title) and further teaches a support structure (330, fig. 3) a camera (140, fig. 1) mounted to the support structure (330, para. 0102), a light source assembly (302, figs. 4-5, para. 0102) mounted to the support structure, the light source assembly comprising, a central opening (103, fig. 1; 303 figs. 4-5) having a plurality of lamp receptacles (lamp segment 306, fig. 4; panel frame or frame, abstract, fig. 47a, pars. 0179-0180, receives the LEDs; also see figs. 48a-50b) surrounding the central opening (303, fig 4; 3803, fig. 38A), the structure being mountable to a support structure (330, fig. 3) so that the central opening being aligned with a camera (fig. 1 shows this aspect) also mounted to the support structure (330, fig. 3), so that the field of view of the camera is unobstructed, and a light source (lamps, fig. 2; LEDs or lamps 305, fig. 4; 4705 fig. 47a, para. 0180) positioned within each of the plurality of lamp receptacles (lamp segment 306, fig. 4; panel frame or frame, abstract, fig. 47a, pars. 0179-0180, receives the LEDs; also see figs. 48a-50b), a diffuser (5029, fig. 5a; 1205 fig. 12; 795, 876 in figs 7-8, teach that lens elements spreading the light; this is interpreted as meaning diffusing; paras 0119-0120) positioned adjacent the light source positioned within each of the plurality of lamp receptacles (figs. 4 shows a plurality of lamp segments 306 which contain a plurality of light sources 305; fig. 50a shows the a diffuser 5029 which locate within each lamp panel 4702, 4802, figs. 47a;

SPECTRAL_0000781

50a-50b), each of the diffusers diffusing light produced by each of the light sources (abstract, para. 0023 teaches the diffusion lens being integrated with the lighting panel (receptacle); 795, 876 in figs 7-8, teach that lens elements spreading the light; this is interpreted as meaning diffusing; paras 0119-0120), and a control system (212, fig. 2, para. 0094; and element 1052) operatively connected to each of the light sources (para. 0145, fig. 13, paras. 0091-0092, 0166) positioned within the plurality of lamp receptacles, the control system operating selected ones of the light source to provide a desired illumination to an object within the field of view of the camera (paras. 0091-0092, 0166). Pohlert teaches at least one narrow-band light source positioned within at least one of the plurality of lamp receptacles (blue or green LEDs, paras. 0019, 0118).

However, Pohlert does not explicitly state a housing defining a central opening which contains the structure which holds a plurality of lamps, for connecting the camera to a central aperture.

Kelly teaches a ring lighting (title) and further teaches a housing (2, figs. 1-2) defining a central opening (3 figs. 1-2) which contains the structure which holds a plurality of lamps (6 figs: 1-2), for connecting the camera to a central aperture (abstract, figs. 1-2). Therefore, it would have been obvious to one of ordinary skill in the art at the time the invention was made to combine the stand-mounted light panel for natural illumination in film, television or video of Pohlert with the ring lighting of Kelly so as to have a housing defining a central opening which contains the structure which holds a plurality of lamps, for connecting the camera to a central aperture in order to protect the lights and lenses from the environment.

Pohlert also does not explicitly state the apparatus being used as an excitation light source.

Nomura teaches a fluorescent pattern detector and postal matter processor using the detector (title) and further an apparatus comprising a central hole aligned with a camera having a plurality of light sources surrounding the central aperture being used as an excitation light source (abstract, figs. 1, 5). Therefore, it would have been obvious to one of ordinary skill in the art at the time the invention was made to combine the stand-mounted light panel for natural illumination in film, television or video of Pohlert with the fluorescent pattern detector and postal matter processor using the detector of Nomura so as to have the apparatus used as a excitation light source in order to aid one in recognizing a fluorescent pattern of the object based on a detection signal.

Regarding claim 20, Pohlert teaches a light filter (5010, fig. 50a) positioned adjacent at each of the diffusers (5029, para. 0187, figs. 50a-5Ob).

Regarding claim 21, Pohlert teaches each of the lamp receptacles defined by said housing being angled with respect to a central axis of said housing so that light emitted from each of said narrow-band light sources is directed to a desired area within the field of view of said camera (paras. 0166, 0176).

Regarding claim 22, Pohlert teaches each of said narrow-band light sources being selected to provide desired number of illumination bands over a desired spectral range (paras. 0122, 0124).

SPECTRAL_0000783

Regarding claim 23, Pohlert teaches the desired spectral range being from about 430 nm to about 745 nm (paras. 0122, 0124; By teaching the LEDs being red, green, and blue, Pohlert has inferred the spectral range being from about 430 nm to about 745 nm).

Regarding claim 24, Pohlert teaches the use of different color LEDs (paras. 0122, 0124). However, it does not explicitly state the number of illumination bands being 10. It would have been obvious to one of ordinary skill in the art at the time the invention was made to have the number of illumination bands being 10, since discovering the optimum number of illumination bands needed to obtain a desired color distribution involves only routine skill in the art.

Regarding claim 25, Pohlert teaches each of the desired illumination bands having a bandwidth ranging from about 30 nm to about 35 nm (paras. 0122, 0124, by teaching the use green and blue LEDs, Pohlert has inferred the that the illumination bandwidth ranges from about 30 nm to about 35 nm).

Regarding claim 26, Pohlert teaches each of the narrow-band light sources comprising a light emitting diode (paras. 0118, 0156).

Regarding claim 28, Pohlert teaches the invention as shown above but lacks the explicit teaching of the desired spectral range being from about 430 nm to about 900 nm. It would have been obvious to one of ordinary skill in the art at the time the invention was made to have the desired spectral range being from about 430 nm to about 900 nm, since where the general conditions of the claim are disclosed in the prior art, discovering the optimum or workable ranges involves only routine skill in the art, and in order to produce the desired light emitting from the device.

Regarding claim 29, Pohlert teaches the desired spectral range being from about 430 nm to about 800 nm (paras. 0122, 0124; By teaching the LEDs being red, green, and blue, Pohlert has inferred the spectral range being from about 430 nm to about 800 nm).

Claim 5 is rejected under 35 U.S.C. 103(a) as being unpatentable over Pohlert et al. in view of Kelly, Nomura, and Furze et al.

Regarding claim 5, Pohlert teaches the invention as shown above but lacks the explicit teaching of at least one filter comprises a notch filter having a wavelength bandpass range of about 30 nm. Furze teaches the use of patterned structured light to detect and measure surface defects on a golf ball (title) and further teaches at least one filter comprises a notch filter having a wavelength bandpass range of about 30 nm (25 nm is viewed as being about 30 nm, para. 0023). Therefore, it would have been obvious to one of ordinary skill in the art at the time the invention was made to combine the stand-mounted light panel for natural illumination in film, television or video of Pohlert with the use of patterned structured light to detect and measure surface defects on a golf ball of Furze so as to have at least one filter comprises a notch filter having a wavelength bandpass range in order to allow only a narrow band of wavelengths to pass and thereby allow one to detect the defects in an object/material.

Claim 27 is rejected under 35 U.S.C. 103(a) as being unpatentable over Pohlert et al. in view of Kelly, Nomura, and Flexman et al.

Regarding claim 27, Pohlert as modified teaches the invention as shown above but lacks the explicit teaching of the housing comprising polyoxymethylene thermoplastic material. Kelly

teaches a ring lighting (title) and further teaches a housing (2, figs. 1-2) defining a central opening (3 figs. 1-2) which contains the structure which holds a plurality of lamps (6 figs. 1-2), for connecting the camera to a central aperture (abstract, figs. 1-2). Therefore, it would have been obvious to one of ordinary skill in the art at the time the invention was made to combine the stand-mounted light panel for natural illumination in film, television or video of Pohlert with the ring lighting of Kelly so as to have a housing defining a central opening which contains the structure which holds a plurality of lamps, for connecting the camera to a central aperture in order to protect the lights and lenses from the environment. Pohlert does however teach the lighting frame being made of thermoplastic (para. 0095). Flexman teaches layered articles having polyoxymethylene blend substrates with enhanced surface properties and at least one layer thereon and process for making the same (title) and further teaches the use of polyoxymethylene thermoplastic material (para. 0033). Therefore, it would have been obvious to one of ordinary skill in the art at the time the invention was made to combine the stand-mounted light panel for natural illumination in film, television or video of Pohlert with the layered articles having polyoxymethylene blend substrates with enhanced surface properties and at least one layer thereon and process for making the same of Flexman so as to have in order to increase the toughness and durability of the housing so that it is able to withstand the element and occasional drops.

Conclusion

The prior art made of record and not relied upon is considered pertinent to applicant's disclosure.

SPECTRAL_0000786

Any inquiry concerning this communication or earlier communications from the examiner should be directed to Marcus H. Taningco whose telephone number is (571) 272-1848. The examiner can normally be reached on M - F 9:00 - 5:30.

If attempts to reach the examiner by telephone are unsuccessful, the examiner's supervisor, Dave Porta can be reached on (571) 272-2444. The fax phone number for the organization where this application or proceeding is assigned is 571-273-8300.

Information regarding the status of an application may be obtained from the Patent Application Information Retrieval (PAIR) system. Status information for published applications may be obtained from either Private PAIR or Public PAIR. Status information for unpublished applications is available through Private PAIR only. For more information about the PAIR system, see http://pair-direct.uspto.gov. Should you have questions on access to the Private PAIR system, contact the Electronic Business Center (EBC) at 866-217-9197 (toll-free). If you would like assistance from a USPTO Customer Service Representative or access to the automated information system, call 800-786-9199 (IN USA OR CANADA) or 571-272-1000.

/Marcus H Taningco/
Primary Examiner, Art Unit 2884

SPECTRAL_0000787

Notice of References Cited	Application/Control No. 13/222,688	Applicant(s)/Patent Under Reexamination NELSON ET AL.	
	Examiner MARCUS TANINGCO	Art Unit 2884	Page 1 of 1

U.S. PATENT DOCUMENTS

*		Document Number Country Code-Number-Kind Code	Date MM-YYYY	Name	Classification
*	A	US-2011/0284765 A1	11-2011	Pieper et al.	250/458.1
*	B	US-7,690,801 B2	04-2010	Amphlett, David Richard	362/3
	C	US-			
	D	US-			
	E	US-			
	F	US-			
	G	US-			
	H	US-			
	I	US-			
	J	US-			
	K	US-			
	L	US-			
	M	US-			

FOREIGN PATENT DOCUMENTS

*		Document Number Country Code-Number-Kind Code	Date MM-YYYY	Country	Name	Classification
	N					
	O					
	P					
	Q					
	R					
	S					
	T					

NON-PATENT DOCUMENTS

*		Include as applicable: Author, Title Date, Publisher, Edition or Volume, Pertinent Pages)
	U	
	V	
	W	
	X	

*A copy of this reference is not being furnished with this Office action. (See MPEP § 707.05(a).)
Dates in MM-YYYY format are publication dates. Classifications may be US or foreign.

Index of Claims	Application/Control No.	Applicant(s)/Patent Under Reexamination
	13222688	NELSON ET AL.
	Examiner	Art Unit
	MARCUS TANINGCO	2884

✓	Rejected	-	Cancelled	N	Non-Elected	A	Appeal
=	Allowed	÷	Restricted	I	Interference	O	Objected

☐ Claims renumbered in the same order as presented by applicant ☐ CPA ☐ T.D. ☐ R.1.47

CLAIM		DATE								
Final	Original	11/18/2012								
	1	÷								
	2	÷								
	3	÷								
	4	÷								
	5	÷								
	6	÷								
	7	÷								
	8	÷								
	9	N								
	10	N								
	11	N								
	12	N								
	13	N								
	14	N								
	15	N								
	16	N								
	17	N								
	18	N								
	19	÷								
	20	÷								
	21	÷								
	22	÷								
	23	÷								
	24	÷								
	25	÷								
	26	÷								
	27	÷								
	28	÷								
	29	÷								

Search Notes	Application/Control No.	Applicant(s)/Patent Under Reexamination
	13222688	NELSON ET AL.
	Examiner	Art Unit
	MARCUS TANINGCO	2884

CPC- SEARCHED		
Symbol	Date	Examiner

CPC COMBINATION SETS - SEARCHED		
Symbol	Date	Examiner

US CLASSIFICATION SEARCHED			
Class	Subclass	Date	Examiner
250	461.1	1/27/2013	MT

SEARCH NOTES		
Search Notes	Date	Examiner
Inventor's name searched	1/27/2013	MT
EAST search notes attached	1/27/2013	MT
Text search in 250/458.1, 459.1	1/27/2013	MT
Text search in 362/3	1/27/2013	MT

INTERFERENCE SEARCH			
US Class/ CPC Symbol	US Subclass / CPC Group	Date	Examiner

PTO/SB/08a (01-10)
Approved for use through 07/31/2012. OMB 0651-0031
U.S. Patent and Trademark Office; U.S. DEPARTMENT OF COMMERCE
Under the Paperwork Reduction Act of 1995, no persons are required to respond to a collection of information unless it contains a valid OMB control number.

INFORMATION DISCLOSURE STATEMENT BY APPLICANT

(Not for submission under 37 CFR 1.99)

Application Number	13222688
Filing Date	2011-08-31
First Named Inventor	Michael B. Nelson
Art Unit	2828
Examiner Name	Not yet known
Attorney Docket Number	SPEC US-4 (027560.0014)

U.S.PATENTS Remove

Examiner Initial*	Cite No	Patent Number	Kind Code[1]	Issue Date	Name of Patentee or Applicant of cited Document	Pages,Columns,Lines where Relevant Passages or Relevant Figures Appear
	1					

If you wish to add additional U.S. Patent citation information please click the Add button. Add

U.S.PATENT APPLICATION PUBLICATIONS Remove

Examiner Initial*	Cite No	Publication Number	Kind Code[1]	Publication Date	Name of Patentee or Applicant of cited Document	Pages,Columns,Lines where Relevant Passages or Relevant Figures Appear
	1	20010028510	A1	2001-10-11	Ramm et al.	

If you wish to add additional U.S. Published Application citation information please click the Add button. Add

FOREIGN PATENT DOCUMENTS Remove

Examiner Initial*	Cite No	Foreign Document Number[3]	Country Code[2] i	Kind Code[4]	Publication Date	Name of Patentee or Applicant of cited Document	Pages,Columns,Lines where Relevant Passages or Relevant Figures Appear	T[5]
	1							☐

If you wish to add additional Foreign Patent Document citation information please click the Add button Add

NON-PATENT LITERATURE DOCUMENTS Remove

Examiner Initials*	Cite No	Include name of the author (in CAPITAL LETTERS), title of the article (when appropriate), title of the item (book, magazine, journal, serial, symposium, catalog, etc), date, pages(s), volume-issue number(s), publisher, city and/or country where published.	T[5]

ALL REFERENCES CONSIDERED EXCEPT WHERE LINED THROUGH. /MT/

INFORMATION DISCLOSURE STATEMENT BY APPLICANT (Not for submission under 37 CFR 1.99)		
	Application Number	13222688
	Filing Date	2011-08-31
	First Named Inventor	Michael B. Nelson
	Art Unit	2828
	Examiner Name	Not yet known
	Attorney Docket Number	SPEC US-4 (027560.0014)

	1	HAWORTH, "CCD Image Calibration Using AIP4WIN," http://www.stargazing.net/david, Copyright 2001 David Haworth v. 5.0, pages 1-12.	☐
	2	RODA et al., "Chemiluminescence Imaging Systems for the Analysis of Macrosamples: Microtiter Format, Blot Membrane, and Whole Organs," Methods in Enzymology," Vol. 305, Copyright 2000 by Academic Press, pages 120-132.	☐
	3	STANLEY, "Commercially Available Luminometers and Low-Level Light Imaging Devices," Methods in Enzymology, Vol. 305, Copyright 2000 by Academic Press, pages 96-103.	☐
	4	ROSS et al., "High-speed radiometric imaging with a gated, intensified, digitally-controlled camera[2869-29]," http://ucla.worldcat.org, Proceedings - SPIE the International Society for Optical Engineering, no. 2869, (1996): 386-394, British Library Serials, 2 pages.	☐
	5	RICE et al., "In vivo imaging of light-emitting probes," Journal of Biomedical Optics," Vol. 6, No. 4, October 2001, pages 432-440.	☐
	6	HENGERER et al., "In vivo Procedure for the Measurement Luciferase Reporter Gene Activity with a Low Light Imaging System," Reprint from BIOspektrum 4 (1998), pages 1-3.	☐
	7	BERTHOLD et al., "Luminometer Design and Low Light Detection," Methods in Enzymology, Vol. 305, Copyright 2000 by Academic Press, pages 62-87.	☐
	8	BRAUER et al., "Measuring luminescence with a low light level imaging system using electronic light standards," Siemens AG, Karlsruhe, Germany, Bioluminescence & Chemiluminescence status report," Chichester:Wiley 1993: 13-17, 1 page.	☐
	9	SZALAY et al., "Bioluminescence and chemiluminescence: status report: proceedings of the VIIth Bioluminescence and Chemiluminescence," Banff, March 1993, http://ucla.worldcat.org, 1 page.	☐
	10	FRANCIS et al.,"Monitoring Bioluminescent Staphylococcus aureus Infections in Living Mice Using a Novel luxABCDE Construct," http://iai.asm.org/cgi/content/full/68/6/3594, Xenogen Corporation, Alameda, CA and Division of Neonatal andDevelopmental Medicine, Department of Pediatrics, Stanford University Medical Center, Stanford, CA, Infection and Immunity, Vol. 68, No. 6, June, 2000, cover page and pages 3594-3600.	☐
	11	VOSS et al., "Radiometric and Geometric Calibration of a Visible Spectral Electro-Optic 'Fisheye' Camera Radiance Distribution System," Journal of Atmospheric and Oceanic Technology, Volume 6, (1989), pages 652-662.	☐

ALL REFERENCES CONSIDERED EXCEPT WHERE LINED THROUGH. /MT/

INFORMATION DISCLOSURE STATEMENT BY APPLICANT (Not for submission under 37 CFR 1.99)		
	Application Number	13222688
	Filing Date	2011-08-31
	First Named Inventor	Michael B. Nelson
	Art Unit	2828
	Examiner Name	Not yet known
	Attorney Docket Number	SPEC US-4 (027560.0014)

	12	NILES et al., "Radiometric calibration of a video fluorescence microscope for the quantitative imaging of resonance energy transfer," Rev. Sci, Instrum. 66 (6), June 1995, Copyright 1995 American Institute of Physics, pages 3527-3536.	☐
	13	EDIRISINGHE et al., "Radiometric Callibration of Multispectral Airborne Video Systems," International Journal of Remote Sensing, Vol. 20, No. 14, 1999, cover page and pages 2855-2870.	☐
	14	REHEMTULLA et al.,"Rapid and Quantitative Assessment of Cancer Treatment Response Using In Vivo Bioluminescence Imaging," Neoplasia, Vol. 2, No. 6, 2000, www.nature.com/neo, pages 491-495.	☐
	15	ZHANG et al., "Rapid in vivo funtional analysis of transgenes in mice using whole body imaging of luciferase expression," Transgenic Research 10: 2001 Kluwer Academic Publishers, The Netherlands, pages 423-434.	☐
	16	TSIN et al., "Statistical Calibration of CCD Imaging Process," Appeared in the Proceedings of the IEEE 2001 International Conference on Computer Vision, pages 1-8	☐
	17	CONTAG et al., "Use of Reporter Genes for Optical Measurements of Neoplastic Disease In Vivo," Neoplasia, Vol. 2, Nos. 1-2, January-April 2000, www.nature.com/neo, pages 41-52.	☐
	18	CONTAG et al., "Visualizing Gene Expression in Living Mammals Using a Bioluminescent Reporter," Photochemistry and Photobiology, 1997, 66(4): pages 523-531.	☐

If you wish to add additional non-patent literature document citation information please click the Add button Add

EXAMINER SIGNATURE

Examiner Signature	/Marcus Taningco/	Date Considered	01/27/2013

*EXAMINER: Initial if reference considered, whether or not citation is in conformance with MPEP 609. Draw line through a citation if not in conformance and not considered. Include copy of this form with next communication to applicant.

[1] See Kind Codes of USPTO Patent Documents at www.USPTO.GOV or MPEP 901.04. [2] Enter office that issued the document, by the two-letter code (WIPO Standard ST.3). [3] For Japanese patent documents, the indication of the year of the reign of the Emperor must precede the serial number of the patent document. [4] Kind of document by the appropriate symbols as indicated on the document under WIPO Standard ST.16 if possible. [5] Applicant is to place a check mark here if English language translation is attached.

ALL REFERENCES CONSIDERED EXCEPT WHERE LINED THROUGH. /MT/

Receipt date: 02/13/2012

Doc code: IDS
Doc description: Information Disclosure Statement (IDS) Filed

PTO/SB/08a (01-10)
Approved for use through 07/31/2012. OMB 0651-0031
U.S. Patent and Trademark Office; U.S. DEPARTMENT OF COMMERCE
Under the Paperwork Reduction Act of 1995, no persons are required to respond to a collection of information unless it contains a valid OMB control number.

INFORMATION DISCLOSURE STATEMENT BY APPLICANT
(Not for submission under 37 CFR 1.99)

Application Number	13222688
Filing Date	2011-08-31
First Named Inventor	Michael B. Nelson et al.
Art Unit	2884
Examiner Name	Not yet known
Attorney Docket Number	SPEC US-4 (027560.0014)

U.S.PATENTS

Examiner Initial*	Cite No	Patent Number	Kind Code[1]	Issue Date	Name of Patentee or Applicant of cited Document	Pages,Columns,Lines where Relevant Passages or Relevant Figures Appear
	1	5089895	A	1992-02-18	Fraker et al.	
	2	6454437	B1	2002-09-24	Kelly	

If you wish to add additional U.S. Patent citation information please click the Add button.

U.S.PATENT APPLICATION PUBLICATIONS

Examiner Initial*	Cite No	Publication Number	Kind Code[1]	Publication Date	Name of Patentee or Applicant of cited Document	Pages,Columns,Lines where Relevant Passages or Relevant Figures Appear
	1	20040121175	A1	2004-06-24	Flexman et al.	
	2	20040247170	A1	2004-12-09	Furze et al.	
	3	20050265024	A1	2005-12-01	Luk	
	4	20090268426	A1	2009-10-29	Pohlert et al.	

If you wish to add additional U.S. Published Application citation information please click the Add button.

FOREIGN PATENT DOCUMENTS

EFS Web 2.1.17

ALL REFERENCES CONSIDERED EXCEPT WHERE LINED THROUGH. /MT/

Receipt date: 02/13/2012

INFORMATION DISCLOSURE STATEMENT BY APPLICANT (Not for submission under 37 CFR 1.99)		
	Application Number	13222688
	Filing Date	2011-08-31
	First Named Inventor	Michael B. Nelson et al.
	Art Unit	2884
	Examiner Name	Not yet known
	Attorney Docket Number	SPEC US-4 (027560.0014)

Examiner Initial*	Cite No	Foreign Document Number[3]	Country Code[2]	Kind Code[4]	Publication Date	Name of Patentee or Applicant of cited Document	Pages,Columns,Lines where Relevant Passages or Relevant Figures Appear	T[5]
	1	1040330	JP	A	1998-02-13	Nomura		☐

If you wish to add additional Foreign Patent Document citation information please click the Add button

NON-PATENT LITERATURE DOCUMENTS

Examiner Initials*	Cite No	Include name of the author (in CAPITAL LETTERS), title of the article (when appropriate), title of the item (book, magazine, journal, serial, symposium, catalog, etc), date, pages(s), volume-issue number(s), publisher, city and/or country where published.	T[5]
	1	International Search Report and Written Opinion for PCT/US2011/049998, dated December 22, 2011, 10 pages.	☐

If you wish to add additional non-patent literature document citation information please click the Add button

EXAMINER SIGNATURE

Examiner Signature	/Marcus Taningco/	Date Considered	01/27/2013

*EXAMINER: Initial if reference considered, whether or not citation is in conformance with MPEP 609. Draw line through a citation if not in conformance and not considered. Include copy of this form with next communication to applicant.

[1] See Kind Codes of USPTO Patent Documents at www.USPTO.GOV or MPEP 901.04. [2] Enter office that issued the document, by the two-letter code (WIPO Standard ST.3). [3] For Japanese patent documents, the indication of the year of the reign of the Emperor must precede the serial number of the patent document. [4] Kind of document by the appropriate symbols as indicated on the document under WIPO Standard ST.16 if possible. [5] Applicant is to place a check mark here if English language translation is attached.

EFS Web 2.1.17

ALL REFERENCES CONSIDERED EXCEPT WHERE LINED THROUGH. /MT/

PTO/SB/08a (01-10)
Approved for use through 07/31/2012. OMB 0651-0031
U.S. Patent and Trademark Office; U.S. DEPARTMENT OF COMMERCE
Under the Paperwork Reduction Act of 1995, no persons are required to respond to a collection of information unless it contains a valid OMB control number.

INFORMATION DISCLOSURE STATEMENT BY APPLICANT

(Not for submission under 37 CFR 1.99)

Application Number	13222688
Filing Date	2011-08-31
First Named Inventor	Michael B. Nelson
Art Unit	2828
Examiner Name	Not yet known
Attorney Docket Number	SPEC US-4 (027560.0014)

U.S.PATENTS Remove

Examiner Initial*	Cite No	Patent Number	Kind Code[1]	Issue Date	Name of Patentee or Applicant of cited Document	Pages,Columns,Lines where Relevant Passages or Relevant Figures Appear
	1	3800079		1974-03-26	McNeil et al.	
	2	3871767		1975-03-18	Holm-Hansen et al.	
	3	3949162		1976-04-06	Malueg	
	4	4196994		1980-04-08	de Jesus et al.	
	5	4298887		1981-11-03	Rode	
	6	4343021		1982-08-03	Frame	
	7	4585934		1986-04-29	French et al.	
	8	4593728		1986-06-10	Whitehead et al.	

ALL REFERENCES CONSIDERED EXCEPT WHERE LINED THROUGH. /MT/

Receipt date: 11/11/2011	Application Number	13222688
INFORMATION DISCLOSURE STATEMENT BY APPLICANT	Filing Date	2011-08-31
	First Named Inventor	Michael B. Nelson
	Art Unit	2828
(Not for submission under 37 CFR 1.99)	Examiner Name	Not yet known
	Attorney Docket Number	SPEC US-4 (027560.0014)

	9	4687325		1987-08-18	Corby, Jr.	
	10	4863690		1989-09-05	Berthold et al.	
	11	4885544		1989-12-05	Tago	
	12	4948975		1990-08-14	Erwin et al.	
	13	5008548		1991-04-16	Gat	
	14	5039868		1991-08-13	Kobayashi et al.	
	15	5202091		1993-04-13	Lisenbee	
	16	5401465		1995-03-28	Smethers et al.	
	17	5414258		1995-05-09	Liang	
	18	5515161		1996-05-07	Blumenfeld	
	19	5542012		1996-07-30	Fernandes et al.	

ALL REFERENCES CONSIDERED EXCEPT WHERE LINED THROUGH. /MT/

Receipt date: 11/11/2011	Application Number	13222688
INFORMATION DISCLOSURE STATEMENT BY APPLICANT	Filing Date	2011-08-31
	First Named Inventor	Michael B. Nelson
(Not for submission under 37 CFR 1.99)	Art Unit	2828
	Examiner Name	Not yet known
	Attorney Docket Number	SPEC US-4 (027560.0014)

	20	5587583		1996-12-24	Chin et al.	
	21	5672881		1997-09-30	Striepeke et al.	
	22	5680492		1997-10-21	Hopler et al.	
	23	5689110		1997-11-18	Dietz et al.	
	24	5818977		1998-10-06	Tansley	
	25	5840572		1998-11-24	Copeland et al.	
	26	5865754		1999-02-02	Sevick-Muraca et al.	
	27	5898802		1999-04-27	Chen et al.	
	28	5964220		1999-10-12	Boussignac et al.	
	29	5986271		1999-11-16	Lazarev et al.	
	30	6004767		1999-12-21	Crouch et al.	

ALL REFERENCES CONSIDERED EXCEPT WHERE LINED THROUGH. /MT/

Receipt date: 11/11/2011		
INFORMATION DISCLOSURE STATEMENT BY APPLICANT (**Not for submission under 37 CFR 1.99**)	Application Number	13222688
	Filing Date	2011-08-31
	First Named Inventor	Michael B. Nelson
	Art Unit	2828
	Examiner Name	Not yet known
	Attorney Docket Number	SPEC US-4 (027560.0014)

	31	6038038		2000-03-14	Selby et al.	
	32	6097025		2000-08-01	Modlin et al.	
	33	6154277		2000-11-28	Snelling et al.	
	34	6205244	B1	2001-03-20	Bawolek et al.	
	35	6217847	B1	2001-04-17	Contag et al.	
	36	6377353	B1	2002-04-23	Ellis	
	37	6614452	B1	2003-09-02	Cable	
	38	6642499	B1	2003-11-04	Boni et al.	
	39	6754008	B1	2004-06-22	Wallerstein et al.	
	40	6775567	B2	2004-08-10	Cable et al.	
	41	6894289	B2	2005-05-17	Nilson et al.	

ALL REFERENCES CONSIDERED EXCEPT WHERE LINED THROUGH. /MT/

Receipt date: 11/11/2011	Application Number	13222688
INFORMATION DISCLOSURE STATEMENT BY APPLICANT	Filing Date	2011-08-31
	First Named Inventor	Michael B. Nelson
(Not for submission under 37 CFR 1.99)	Art Unit	2828
	Examiner Name	Not yet known
	Attorney Docket Number	SPEC US-4 (027560.0014)

	42	6901279	B2	2005-05-31	Cable et al.	
	43	6919919	B2	2005-07-19	Nelson et al.	
	44	6922246	B2	2005-07-26	Nilson et al.	
	45	7113217	B2	2006-09-26	Nilson et al.	
	46	7116354	B2	2006-10-03	Rice et al.	
	47	7177024	B2	2007-02-13	Nilson et al.	
	48	7190991	B2	2007-03-13	Cable et al.	
	49	7196190	B2	2007-03-27	Ning et al.	
	50	7255851	B2	2007-08-14	Contag et al.	
	51	7298415	B2	2007-11-20	Nilson et al.	
	52	7299420	B2	2007-11-20	Cable	

ALL REFERENCES CONSIDERED EXCEPT WHERE LINED THROUGH. /MT/

Receipt date: 11/11/2011

INFORMATION DISCLOSURE STATEMENT BY APPLICANT
(Not for submission under 37 CFR 1.99)

Application Number	13222688
Filing Date	2011-08-31
First Named Inventor	Michael B. Nelson
Art Unit	2828
Examiner Name	Not yet known
Attorney Docket Number	SPEC US-4 (027560.0014)

	53	7331341	B2	2008-02-19	Nelson	
	54	7383078	B2	2008-06-03	Cable et al.	
	55	7403812	B2	2008-07-22	Rice et al.	
	56	7449567	B2	2008-11-11	Zhang et al.	
	57	7449615	B2	2008-11-11	Contag et al.	
	58	7461652	B2	2008-12-09	Dalgetty et al.	
	59	7464707	B2	2008-12-16	Dalgetty et al.	
	60	7466418	B2	2008-12-16	Nilson et al.	
	61	7474398	B2	2009-01-06	Nilson et al.	
	62	7474399	B2	2009-01-06	Nilson et al.	
	63	7503323	B2	2009-03-17	Dalgetty et al.	

ALL REFERENCES CONSIDERED EXCEPT WHERE LINED THROUGH. /MT/

Receipt date: 11/11/2011

INFORMATION DISCLOSURE STATEMENT BY APPLICANT
(Not for submission under 37 CFR 1.99)

Application Number	13222688
Filing Date	2011-08-31
First Named Inventor	Michael B. Nelson
Art Unit	2828
Examiner Name	Not yet known
Attorney Docket Number	SPEC US-4 (027560.0014)

	64	7555332	B2	2009-06-30	Rice et al.	
	65	7555334	B2	2009-06-30	Coquoz et al.	
	66	7581191	B2	2009-08-25	Rice et al.	
	67	7589786	B2	2009-09-15	Nilson et al.	
	68	7595838	B2	2009-09-29	Nilson et al.	
	69	7599731	B2	2009-10-06	Rice et al.	
	70	7603167	B2	2009-10-13	Stearns et al.	
	71	7616985	B2	2009-11-10	Stearns et al.	
	72	7663664	B2	2010-02-16	Rice et al.	

If you wish to add additional U.S. Patent citation information please click the Add button. Add

U.S.PATENT APPLICATION PUBLICATIONS Remove

Examiner Initial*	Cite No	Publication Number	Kind Code[1]	Publication Date	Name of Patentee or Applicant of cited Document	Pages,Columns,Lines where Relevant Passages or Relevant Figures Appear

EFS Web 2.1.17

ALL REFERENCES CONSIDERED EXCEPT WHERE LINED THROUGH. /MT/

Receipt date: 11/11/2011

INFORMATION DISCLOSURE STATEMENT BY APPLICANT
(Not for submission under 37 CFR 1.99)

Application Number	13222688
Filing Date	2011-08-31
First Named Inventor	Michael B. Nelson
Art Unit	2828
Examiner Name	Not yet known
Attorney Docket Number	SPEC US-4 (027560.0014)

	1					

If you wish to add additional U.S. Published Application citation information please click the Add button. Add

FOREIGN PATENT DOCUMENTS Remove

Examiner Initial*	Cite No	Foreign Document Number[3]	Country Code[2] i	Kind Code[4]	Publication Date	Name of Patentee or Applicant of cited Document	Pages,Columns,Lines where Relevant Passages or Relevant Figures Appear	T[5]
	1	0097060	EP	A2	1983-12-28	Electronic Pneumatic Apparatus & Controls Ltd.		☐
	2	0228877	EP	A2	1987-07-15	Artel, Inc.		☐
	3	0491131	EP	A1	1992-06-24	Hewlett-Packard Company		☐
	4	0493707	EP	A2	1992-07-08	DiPietro, Matthew, c/o Eastman Kodak Company		☐
	5	0718622	EP	A2	1996-06-26	Biosensor Laboratories Co., Ltd.		☐
	6	1478423	EP	B1	2006-07-26	Dalgetty et al.		☐
	7	1478916	EP	B1	2008-07-09	Nilson et al.		☐
	8	0049938	WO	A1	2000-08-31	Micro Medical Devices, Inc.		☐

ALL REFERENCES CONSIDERED EXCEPT WHERE LINED THROUGH. /MT/

Receipt date: 11/11/2011	Application Number	13222688
INFORMATION DISCLOSURE STATEMENT BY APPLICANT	Filing Date	2011-08-31
	First Named Inventor	Michael B. Nelson
(Not for submission under 37 CFR 1.99)	Art Unit	2828
	Examiner Name	Not yet known
	Attorney Docket Number	SPEC US-4 (027560.0014)

	9	0161324	WO	A1	2001-08-23	The University of Chicago		☐
	10	0163247	WO	A2	2001-08-30	Xenogen Corporation		☐
	11	9908233	WO	A1	1999-02-18	Imaging Research Inc.		☐
	12	9400742	WO	A1	1994-01-06	Holmes et al.		☐

If you wish to add additional Foreign Patent Document citation information please click the Add button Add

NON-PATENT LITERATURE DOCUMENTS Remove

Examiner Initials*	Cite No	Include name of the author (in CAPITAL LETTERS), title of the article (when appropriate), title of the item (book, magazine, journal, serial, symposium, catalog, etc), date, pages(s), volume-issue number(s), publisher, city and/or country where published.	T[5]
	1	O'KANE et al., "Absolute Calibration of Luminometers with Low-Level Light Standards," Methods in Enzymology, Vol. 305, Copyright 2000 by Academic Press, pages 87-96.	☐
	2	BROWN et al., "Absolute Radiometric Calibration of Digital Imaging Systems," IS&T/SPIE Electronic Imaging, San Jose, California, January 2001, 9 pages.	☐
	3	CHEN et al., "Auaomated Calibration of a Zoom Lens CCD Image System for Videogrammetry," International Archives of Photogrammetry and Remote Sensing, Vol. XXXIII, Part B4, Amsterdam, The Netherlands, 2000, pages 180-185.	☐
	4	CAMPBELL et al., "Bioluminescence and Chemiluminescence," Proceedings of the 8th International Symposium of Bioluminescence and Chemiluminescence, Cambridge, September 1994, John Wiley & Sons, 5 pages.	☐
	5	CONTAG et al., "Bioluminescent indicators in living mammals," Nature Medicine, Vol. 4, No. 2, February 1998, http://www.nature.com/naturemedicine, pages 245-247.	☐

ALL REFERENCES CONSIDERED EXCEPT WHERE LINED THROUGH. /MT/

Receipt date: 11/11/2011	Application Number	13222688
INFORMATION DISCLOSURE STATEMENT BY APPLICANT	Filing Date	2011-08-31
	First Named Inventor	Michael B. Nelson
(Not for submission under 37 CFR 1.99)	Art Unit	2828
	Examiner Name	Not yet known
	Attorney Docket Number	SPEC US-4 (027560.0014)

	6	OCHS et al., "Camera Types for Low Level Light Imaging," October 1995, pages 1-6.	☐
	7	GATAN, INC., "CCD Image Acquisition Tutorial," Gatan, Inc., Pleasanton, California, May 2001, cover page and pages 1-7.	☐

If you wish to add additional non-patent literature document citation information please click the Add button **Add**

EXAMINER SIGNATURE

Examiner Signature	/Marcus Taningco/	Date Considered	01/27/2013

*EXAMINER: Initial if reference considered, whether or not citation is in conformance with MPEP 609. Draw line through a citation if not in conformance and not considered. Include copy of this form with next communication to applicant.

[1] See Kind Codes of USPTO Patent Documents at www.USPTO.GOV or MPEP 901.04. [2] Enter office that issued the document, by the two-letter code (WIPO Standard ST.3). [3] For Japanese patent documents, the indication of the year of the reign of the Emperor must precede the serial number of the patent document. [4] Kind of document by the appropriate symbols as indicated on the document under WIPO Standard ST.16 if possible. [5] Applicant is to place a check mark here if English language translation is attached.

ALL REFERENCES CONSIDERED EXCEPT WHERE LINED THROUGH. /MT/

EAST Search History

EAST Search History (Prior Art)

Ref #	Hits	Search Query	DBs	Default Operator	Plurals	Time Stamp
L1	1088	250/461.1.ccls.	US-PGPUB; USPAT; FPRS; EPO; JPO; DERWENT; IBM_TDB	OR	OFF	2013/01/27 14:54
L2	2855	250/458.1.ccls.	US-PGPUB; USPAT; FPRS; EPO; JPO; DERWENT; IBM_TDB	OR	OFF	2013/01/27 14:54
L3	1557	250/459.1.ccls.	US-PGPUB; USPAT; FPRS; EPO; JPO; DERWENT; IBM_TDB	OR	OFF	2013/01/27 14:54
L4	4362	1 2 3	US-PGPUB; USPAT; FPRS; EPO; JPO; DERWENT; IBM_TDB	OR	OFF	2013/01/27 14:54
L5	1	4 and (camera or detect$4 or imager or imaging) with ((multiple or plurality) near2 (receptacle or ight or led or lamp)) with (opening or aperture or hole or fov or (field near view))	US-PGPUB; USPAT; FPRS; EPO; JPO; DERWENT; IBM_TDB	OR	OFF	2013/01/27 14:54
L6	2234	(camera or detect$4 or imager or imaging) with (light or led or lamp) with (halo or ring or surround$4) with (opening or aperture or hole or fov or (field near view))	US-PGPUB; USPAT; FPRS; EPO; JPO; DERWENT; IBM_TDB	OR	OFF	2013/01/27 14:55
L7	3	L6 and ((light or led or lamp) with diffus$4) and 4	US-PGPUB; USPAT; FPRS; EPO; JPO; DERWENT; IBM_TDB	OR	OFF	2013/01/27 14:55
L8	81	("4585934" | "4863690" | "5414258" | "5587583" | "5680492" | "6004767" | "6038038" | "7298415" | "7383078" | "7449615" | "7461652" | "7555334" | "7581191" | "4863690" | "5680492" | "5818977" | "6004767" | "6097025" | "6642499" | "6922246" | "7255851" | "7464707" | "7466418" | "7555332" |	US-PGPUB; USPAT	OR	OFF	2013/01/27 15:00

SPECTRAL_0000806

		"7595838" | "7663664" | "20040121175" | "5672881" | "5689110" | "6901279" | "7116354" | "7177024" | "7555332" | "7589786" | "7595838" | "7599731" | "5039868" | "5202091" | "6775567" | "6919919" | "7474399" | "4885544" | "5515161" | "5542012" | "5840572" | "5964220" | "6205244" | "6922246" | "7255851" | "7299420" | "7331341" | "7616985" | "7449567" | "7461652" | "7555334" | "7589786" | "7603167" | "5454437" | "3800079" | "4687325" | "5008548" | "5898802" | "5986271" | "6377353" | "6614452" | "20010028510" | "4593728" | "4687325" | "4948975" | "5414258" | "5515161" | "6871767" | "7196190" | "7449615" | "7474398" | "7616985" | "5089895" | "3949162" | "5202091" | "6097025" | "6642499" | "7503323" | "3949162" | "4196994" | "4343021" | "4885544" | "5008548" | "5672881" | "5689110" | "5840572" | "5865754" | "5964220" | "5986271" | "6217847" | "7113217" | "7190991" | "7383078" | "7503323" | "7581191" | "7599731" | "20040247170" | "20090268426" | "4196994" | "4343021" | "6217847" | "6754008" | "6894289" | "6919919" | "7196190" | "7449567" | "7464707" | "7474398" | "7603167" | "5587583" | "5898802" | "6377353" | "6754008" | "6901279" | "7177024" | "7299420" | "20050265024" | "3871767" | "4593728" | "4948975" | "5818977" | "6775567" | "7113217" | "7403812" | "7474399" | "7663664" | "0458934" | "5401465" | "5542012" | "6038038" | "6154277" | "6614452" | "7116354" | "7331341" | "4298887" | "5039868" | "5401465" | "5865754" | "6154277" | "7190991" | "7466418" | "3800079" | "4298887" | "6205244" | "6894289" | "7298415" | "7403812").PN.				
L9	8	4 and L8	US-PGPUB; USPAT; FPRS; EPO; JPO; DERWENT; IBM_TDB	OR	OFF	2013/01/27 15:00
L10	280	362/3.ccls.	US-PGPUB; USPAT; FPRS; EPO; JPO; DERWENT; IBM_TDB	OR	OFF	2013/01/27 15:06
L11	4	6 and 10	US-PGPUB; USPAT; FPRS; EPO; JPO; DERWENT; IBM_TDB	OR	OFF	2013/01/27 15:06
S1	1	13/222688	US-PGPUB; USPAT;	OR	OFF	2013/01/25 15:03

			FPRS; EPO; JPO; DERWENT; IBM_TDB			
S2	564	(Nelson near Michael).in.	US-PGPUB; USPAT; FPRS; EPO; JPO; DERWENT; IBM_TDB	OR	OFF	2013/01/25 15:03
S3	38	(Nelson near Michael).in. and fluoresc$4	US-PGPUB; USPAT; FPRS; EPO; JPO; DERWENT; IBM_TDB	OR	OFF	2013/01/25 15:04
S4	4	(Nelson near Michael).in. and fluoresc$4 and ((light near source) same diffus$4)	US-PGPUB; USPAT; FPRS; EPO; JPO; DERWENT; IBM_TDB	OR	OFF	2013/01/25 15:05
S5	81	("4585934" | "4863690" | "5414258" | "5587583" | "5680492" | "6004767" | "6038038" | "7298415" | "7383078" | "7449615" | "7461652" | "7555334" | "7581191" | "4863690" | "5680492" | "5818977" | "6004767" | "6097025" | "6642499" | "6922246" | "7255851" | "7464707" | "7466418" | "7555332" | "7595838" | "7663664" | "20040121175" | "5672881" | "5689110" | "6901279" | "7116354" | "7177024" | "7555332" | "7589786" | "7595838" | "7599731" | "5039868" | "5202091" | "6775567" | "6919919" | "7474399" | "4885544" | "5515161" | "5542012" | "5840572" | "5964220" | "6205244" | "6922246" | "7255851" | "7299420" | "7331341" | "7616985" | "7449567" | "7461652" | "7555334" | "7589786" | "7603167" | "5454437" | "3800079" | "4687325" | "5008548" | "5898802" | "5986271" | "6377353" | "6614452" | "20010028510" | "4593728" | "4687325" | "4948975" | "5414258" | "5515161" | "6871767" | "7196190" | "7449615" | "7474398" | "7616985" | "5089895" | "3949162" | "5202091" | "6097025" | "6642499" | "7503323" | "3949162" | "4196994" | "4343021" | "4885544" | "5008548" | "5672881" | "5689110" | "5840572" | "5865754" | "5964220" | "5986271" | "6217847" | "7113217" | "7190991" | "7383078" | "7503323" | "7581191" | "7599731" | "20040247170" | "20090268426" | "4196994" | "4343021" | "6217847" | "6754008" | "6894289" | "6919919" | "7196190" | "7449567" | "7464707" | "7474398" | "7603167" | "5587583" | "5898802" | "6377353" | "6754008" | "6901279" | "7177024" | "7299420" | "20050265024" | "3871767" |	US-PGPUB; USPAT	OR	OFF	2013/01/25 15:07

		"4593728" | "4948975" | "5818977" | "6775567" | "7113217" | "7403812" | "7474399" | "7663664" | "0458934" | "5401465" | "5542012" | "6038038" | "6154277" | "6614452" | "7116354" | "7331341" | "4298887" | "5039868" | "5401465" | "5865754" | "6154277" | "7190991" | "7466418" | "3800079" | "4298887" | "6205244" | "6894289" | "7298415" | "7403812").PN.				
S6	2234	(camera or detect$4 or imager or imaging) with (light or led or lamp) with (halo or ring or surround$4) with (opening or aperture or hole or fov or (field near view))	US-PGPUB; USPAT; FPRS; EPO; JPO; DERWENT; IBM_TDB	OR	OFF	2013/01/25 15:21
S7	412	S6 and ((light or led or lamp) with diffus$4)	US-PGPUB; USPAT; FPRS; EPO; JPO; DERWENT; IBM_TDB	OR	OFF	2013/01/25 15:21
S8	58	S7 and "250".clas.	US-PGPUB; USPAT; FPRS; EPO; JPO; DERWENT; IBM_TDB	OR	OFF	2013/01/25 15:23
S9	3	(camera or detect$4 or imager or imaging) with ((multiple or plurality) near2 (receptacle or ight or led or lamp)) with (halo or ring or surround$4) with (opening or aperture or hole or fov or (field near view))	US-PGPUB; USPAT; FPRS; EPO; JPO; DERWENT; IBM_TDB	OR	OFF	2013/01/25 21:09
S10	96	(camera or detect$4 or imager or imaging) with ((multiple or plurality) near2 (receptacle or ight or led or lamp)) with (opening or aperture or hole or fov or (field near view))	US-PGPUB; USPAT; FPRS; EPO; JPO; DERWENT; IBM_TDB	OR	OFF	2013/01/25 21:12
S11	4	S10 and "250".clas.	US-PGPUB; USPAT; FPRS; EPO; JPO; DERWENT; IBM_TDB	OR	OFF	2013/01/25 21:13
S12	81	("4585934" | "4863690" | "5414258" | "5587583" | "5680492" | "6004767" | "6038038" | "7298415" | "7383078" | "7449615" | "7461652" | "7555334" | "7581191" | "4863690" | "5680492" | "5818977" | "6004767" | "6097025" | "6642499" | "6922246" | "7255851" | "7464707" | "7466418" | "7555332" | "7595838" | "7663664" | "20040121175" | "5672881" | "5689110" | "6901279" | "7116354" | "7177024" | "7555332" | "7589786" | "7595838" | "7599731" | "5039868" | "5202091" | "6775567" | "6919919" | "7474399" | "4885544" | "5515161" | "5542012" | "5840572" | "5964220" | "6205244" | "6922246" |	US-PGPUB; USPAT	OR	OFF	2013/01/25 21:13

SPECTRAL_0000809

		"7255851" | "7299420" | "7331341" | "7616985" | "7449567" | "7461652" | "7555334" | "7589786" | "7603167" | "5454437" | "3800079" | "4687325" | "5008548" | "5898802" | "5986271" | "6377353" | "6614452" | "20010028510" | "4593728" | "4687325" | "4948975" | "5414258" | "5515161" | "6871767" | "7196190" | "7449615" | "7474398" | "7616985" | "5089895" | "3949162" | "5202091" | "6097025" | "6642499" | "7503323" | "3949162" | "4196994" | "4343021" | "4885544" | "5008548" | "5672881" | "5689110" | "5840572" | "5865754" | "5964220" | "5986271" | "6217847" | "7113217" | "7190991" | "7383078" | "7503323" | "7581191" | "7599731" | "20040247170" | "20090268426" | "4196994" | "4343021" | "6217847" | "6754008" | "6894289" | "6919919" | "7196190" | "7449567" | "7464707" | "7474398" | "7603167" | "5587583" | "5898802" | "6377353" | "6754008" | "6901279" | "7177024" | "7299420" | "20050265024" | "3871767" | "4593728" | "4948975" | "5818977" | "6775567" | "7113217" | "7403812" | "7474399" | "7663664" | "0458934" | "5401465" | "5542012" | "6038038" | "6154277" | "6614452" | "7116354" | "7331341" | "4298887" | "5039868" | "5401465" | "5865754" | "6154277" | "7190991" | "7466418" | "3800079" | "4298887" | "6205244" | "6894289" | "7298415" | "7403812").PN.				
S13	0	S12 and S10	US-PGPUB; USPAT; FPRS; EPO; JPO; DERWENT; IBM_TDB	OR	OFF	2013/01/25 21:13
S14	5	S12 and (camera or detect$4 or imager or imaging) with (light or led or lamp) with (halo or ring or surround$4) with (opening or aperture or hole or fov or (field near view))	US-PGPUB; USPAT; FPRS; EPO; JPO; DERWENT; IBM_TDB	OR	OFF	2013/01/25 21:22
S15	46	S12 and fluoresc$7	US-PGPUB; USPAT; FPRS; EPO; JPO; DERWENT; IBM_TDB	OR	OFF	2013/01/25 21:25
S16	2	("3609451" | "5134277").PN. OR ("6943333").URPN.	US-PGPUB; USPAT; USOCR	OR	OFF	2013/01/25 21:26

EAST Search History (Interference)

< This search history is empty>

1/ 27/ 2013 3:14:40 PM
C:\ Users\ mtaningco\ Documents\ EAST\ Workspaces\ 13222688.wsp

IN THE UNITED STATES PATENT AND TRADEMARK OFFICE

In Re Application of:	)	
	)	Examiner: Taningco, M.
NELSON, Michael, B., *et al.*	)	
	)	Group Art Unit: 2884
Serial No. 13/222,688	)	
	)	Confirm. No.: 5910
Filing Date: August 31, 2011	)	
	)	Atty. Dkt.: SPEC US-4
For: EXCITATION LIGHT SOURCE ASSEMBLY	)	(027560-0014)

AMENDMENT UNDER 37 C.F.R. §§ 1.111 & 1.121

To: The Commissioner for Patents
P.O. Box 1450
Alexandria, VA 22313-1450

Sir:

In response to the office action, dated January 30, 2013, please amend the above-identified patent application as follows:

Amendments to the Specification begin on page 2 of this paper.

Amendments to the Claims are reflected in the listing of claims which begins on page 6 of this paper.

Amendments to the Drawings begin on page 12 of this paper and include both an attached replacement sheet and an annotated sheet showing changes.

Remarks begin on page 13 of this paper.

An **Appendix** including the amended drawing figure is attached beginning on page 25 of this paper.

SPECTRAL_0000812

Amendments to the Specification:

Please replace paragraph [0003] with the following amended paragraph:

[0003] Molecular imaging systems are known in the art and are commonly used to capture various types or modes of images from an object or specimen being analyzed. The objects or specimens that are imaged may comprise any of a wide range of compositions and objects, as is well-known. Primarily, such imaging systems are configured to detect extremely low levels of light emitted by the specimen or object under study. The light emitted by the object or specimen may be generated by a bio-luminescence process, a fluorescence process, or by a combination thereof. Such imaging systems may also be capable of capturing reflected light images, in which light reflected by the object is captured by the imaging system camera. Such a reflected light image is often combined with one or more emitted light images to form a single, composite image. Such a composite image allows a user to more easily correlate features and attributes of the emitted light image(s) with physical locations on the specimen or other characteristics that are contained in the reflected light image.

Please replace paragraph [0041] with the following amended paragraph:

[0041] The various lamp receptacles 18 may be provided at locations on the main body member 14 so as to provide substantially uniform illumination to the object or specimen 42 provided on the imaging platform or stage 60. In the particular embodiment shown and described herein, the main body member 14 is provided with

twenty (20) large diameter lamp receptacles 18, each of which is provided with a plurality of narrow-band light sources 22 and, optionally, diffusers 26, and filters 28. Moreover, and as will be described in further detail below, a given large diameter lamp receptacle 18 (such as receptacle ~~64~~ 68), may be matched with a counterpart large diameter receptacle 18 (such as receptacle ~~64'~~ 68') on the opposite side of central opening 16. See Figure 1. Both the receptacle ~~64~~ 68 and its counterpart receptacle ~~64'~~ 68' may be configured to emit light of the same color or wavelength range. Thus, when energized, each such receptacle ~~64~~ 68 and counterpart receptacle ~~64'~~ 68' will emit light of the same color or wavelength range. Because each such receptacle ~~64~~ 68 and counterpart receptacle ~~64'~~ 68' are located on opposite sides of the central opening 16, the specimen 42 will be more evenly illuminated with this arrangement than would otherwise be the case if the light were emitted only by a single receptacle 18.

Please replace paragraph [0047] with the following amended paragraph:

[0047] In addition, and as was also mentioned above, each of the larger diameter lamp receptacles 18 (e.g., lamp receptacle ~~64~~ 68, Figure 1) may be paired with a counterpart receptacle (e.g., lamp receptacle ~~64'~~ 68') on the opposite side of the central opening 16 in order to provide more even illumination of the specimen 42 provided on the imaging platform or stage 60. For example, if a particular lamp receptacle ~~64~~ 68 is provided with a narrow-band light source 22 that is capable of emitting light having middle or center wavelength of about 465 nm, then its counterpart receptacle ~~64'~~ 68' should also be provided with a narrow-band light source 22 having a middle or center wavelength of about 465 nm.

Please replace paragraph [0048] with the following amended paragraph:

[0048] In the particular embodiment shown and described herein, the excitation light source assembly 10 is capable of emitting excitation light in a plurality of individual bands or colors over a wavelength range from about 430 nm to about 745 nm. Therefore, it will be generally desirable to use for each light source 20 a comparatively narrow-band light source 22 that emits light having wavelengths over a fairly narrow-band. By way of example, narrow-band light sources 22 having bandwidths in the range of about 30-35 nm can be used to advantage in the present invention. If such narrow-band light sources 22 are used, ten (10) such narrow-band light sources 22, properly selected, will be sufficient to cover the exemplary wavelength range. In accordance with this objective, then, the main body member 14 is provided with twenty (20) large diameter receptacles 18 that are arranged in ten pairs of two on opposite sides of the central opening 16. The corresponding receptacle pairs (e.g., ~~64~~ 68 and ~~64'~~ 68', Figure 1) are then provided with narrow-band light sources 22 of the same wavelengths so that the excitation light source assembly 10 is capable of providing illumination in ten different narrow-band wavelength ranges or colors.

Please replace paragraph [0051] with the following amended paragraph:

[0051] Regardless of the particular light source 22 that may be used, it is also generally preferred, but not required, to provide a diffuser 26 within each lamp receptacle 18. ~~the~~ The diffuser 26 may be provided at any convenient position within lamp receptacle

18. In one embodiment, diffuser 26 is located at a position immediately adjacent the light source 20, as best seen in Figure 5. A sleeve 66 provided in the lamp receptacle 18 may be used to support diffuser 26, although other arrangements are possible. As its name implies, the diffuser 26 diffuses or spreads light produced by the light source 20, thereby generally providing for more even illumination than would be provided by the light source 22 alone.

SPECTRAL_0000816

Amendments to the Claims:

This listing of claims will replace all prior versions and listings of claims in the application:

Listing of Claims:

1. (Currently Amended) An excitation light source assembly, comprising:

a housing defining a central opening therein and a plurality of lamp receptacles surrounding the central opening, said housing being mountable to a support structure so that the central opening is aligned with a camera also mounted to the support structure so that a field of view of the camera is unobstructed by said housing;

a light source positioned within each of the plurality of lamp receptacles; and

a diffuser positioned ~~adjacent said light source positioned~~ within ~~each~~ at least some of the plurality of lamp receptacles, each of said diffusers diffusing light produced by each of said light sources; and

a control system operatively connected to each of said light sources ~~positioned within said plurality of lamp receptacles~~, said control system operating selected ones of said light sources to provide a desired excitation illumination to an object within the field of view of said camera, the object fluorescing in response to the excitation illumination provided by said light sources.

2. (Original) The excitation light source assembly of claim 1 wherein at least one of said light sources comprises a narrow-band light source that emits light having a bandwidth of about 35

nm.

3. (Original) The excitation light source assembly of claim 2 wherein said at least one narrow-band light source comprises a light emitting diode.

4. (Original) The excitation light source assembly of claim 1, further comprising at least one filter positioned adjacent at least one diffuser in at least one of the lamp receptacles defined by said housing.

5. (Original) The excitation light source assembly of claim 4, wherein said at least one filter comprises a notch filter having a wavelength bandpass range of about 30 nm.

6. (Original) The excitation light source assembly of claim 1, wherein at least one of the light sources comprises a broad-band light source.

7. (Currently Amended) The excitation light source assembly of claim 1, wherein at least some of said plurality of lamp receptacles comprise opposed pairs of lamp receptacles on opposite sides of said central opening, each opposed pair of lamp receptacles ~~producing~~ receiving light sources that produce light of the same color.

8. (Original) The excitation light source assembly of claim 7, further comprising ten opposed pairs of lamp receptacles on opposite sides of said central opening.

9-18 (Canceled).

SPECTRAL_0000818

19. (Currently Amended) An assembly, comprising:

a support structure;

a camera mounted to said support structure;

an excitation light source assembly mounted to said support structure, said excitation light source assembly comprising:

a housing defining a central opening therein and a plurality of lamp receptacles surrounding the central opening, said housing being mounted to said support structure so that the central opening is aligned with said camera and so that a field of view of said camera is substantially unobstructed by said housing;

at least one narrow-band light source positioned within at least one of the plurality of lamp receptacles; and

a diffuser positioned ~~adjacent said narrow-band light source positioned~~ within ~~each~~ at least some of the plurality of lamp receptacles, each of said diffusers diffusing light produced by each of said narrow-band light sources; and

a control system operatively connected to each of said narrow-band light sources ~~positioned within said plurality of lamp receptacles~~, said control system operating selected ones of said narrow-band light sources to provide a desired excitation illumination to a fluorescent material within the field of view of said camera, the fluorescent material fluorescing in response to the excitation illumination.

20. (Original) The assembly of claim 19, further comprising a light filter positioned adjacent each of the diffusers.

21. (Original) The assembly of claim 19, wherein each of the lamp receptacles defined by said housing are angled with respect to a central axis of said housing so that light emitted from each of said narrow-band light sources is directed to a desired area within the field of view of said camera.

22. (Original) The assembly of claim 19, wherein each of said narrow-band light sources is selected to provide desired number of illumination bands over a desired spectral range.

23. (Original) The assembly of claim 22, wherein the desired spectral range is from about 430 nm to about 745 nm.

24. (Original) The assembly of claim 22, wherein the desired number of illumination bands is 10.

25. (Original) The assembly of claim 22, wherein each desired illumination band has a bandwidth ranging from about 30 nm to about 35 nm.

26. (Original) The assembly of claim 19, wherein each of said narrow-band light sources comprises a light emitting diode.

27. (Original) The assembly of claim 19, wherein said housing comprises a polyoxymethylene thermoplastic material.

28. (Original) The assembly of claim 22, wherein the desired spectral range is from about 430 nm to about 900 nm.

29. (Original) The assembly of claim 22, wherein the desired spectral range is from about 430 nm to about 800 nm.

30. (New) The excitation light source assembly of claim 1, wherein the light source positioned within each of the plurality of lamp receptacles does not extend beyond the lamp receptacle.

31. (New) The excitation light source assembly of claim 1, further comprising a plurality of light sources positioned within at least some of the lamp receptacles so that the plurality of light sources do not extend beyond the lamp receptacles.

32. (New) The excitation light source assembly of claim 31, wherein said plurality of light sources is three light sources.

33. (New) The excitation light source assembly of claim 1, wherein the plurality of light receptacles defined by said housing comprise a plurality of large diameter receptacles and a plurality of small diameter receptacles.

34. (New) The excitation light source assembly of claim 1, wherein the plurality of light receptacles defined by said housing comprise generally cylindrically shaped openings having first and second open ends, said excitation light source assembly further comprising a circuit board mounted to a first side of said housing, said light sources being mounted to said circuit board so that said light sources extend through the first open ends of the generally cylindrically-shaped light receptacles.

35. (New) An excitation light source assembly, comprising:

a housing defining a central opening therein and a plurality of lamp receptacles therein surrounding the central opening, said housing being mountable to a support structure so that the central opening is aligned with a camera also

SPECTRAL_0000821

mounted to the support structure so that a field of view of the camera is unobstructed by said housing;

a light source positioned within each of the plurality of lamp receptacles so that said light sources do not extend beyond the lamp receptacles; and

a control system operatively connected to each of said light sources, said control system operating selected ones of said light sources to provide a desired excitation illumination to an object within the field of view of the camera, th excitation illumination causing fluorescent materials in the object to fluoresce, the camera capturing an image of the fluorescing material in the object.

36. (New) The excitation light source assembly of claim 35, wherein said plurality of lamp receptacles defined by said housing comprise a plurality of large diameter lamp receptacles and a plurality of small diameter lamp receptacles, said large diameter lamp receptacles receiving a plurality of said light sources, said small diameter receptacles receiving a single light source.

37. (New) The excitation light source assembly of claim 35, wherein the plurality of light receptacles defined by said housing comprise generally cylindrically shaped openings having first and second open ends, said excitation light source assembly further comprising a circuit board mounted to a first side of said housing, said light sources being mounted to said circuit board so that said light sources extend through the first open ends of the generally cylindrically shaped light receptacles.

Amendments to the Drawings:

The attached sheet (1/12) of drawings includes changes to Figure 1. This sheet replaces original sheet (1/12). In Figure 1, the elements 64 and 64' are re-numbered as elements 68 and 68', respectively.

Attachment: Replacement Sheet (1/12)
Annotated Sheet Showing Changes

R E M A R K S

Claims 1, 7, and 19 are amended. New claims 30-37 are added. Claims 9-18 are canceled as being drawn to non-elected inventions. Claims 2-6, 8, and 20-29 stand as originally filed. Re-examination and reconsideration are requested.

In the office action, the examiner acknowledged applicants' previous election without traverse of claims 1-8 and 19-29. The examiner rejected claims 1-4, 6-8, 19-26, 28, and 29 under 35 U.S.C. §103(a) as being obvious over Pohlert *et al.*, U.S. Patent Application Publication No. US 2009/0268426 ("Pohlert") in view of Kelly, U.S. Patent No. 6,454,437 ("Kelly") and Nomura, Japanese Patent Application Publication No. JP10-040330 ("Nomura") for the reasons specified on pages 3-10 of the office action. The examiner next rejected claim 5 under Section 103(a) as being unpatentable over Pohlert in view of Kelly, Nomura, and Furze *et al.*, U.S. Patent Application Publication No. US 2004/0247170 ("Furze") for the reasons specified on page 10 of the office action. The examiner also rejected claim 27 under Section 103(a) as being unpatentable over Pohlert in view of Kelly, Nomura, and Flexman *et al.*, U.S. Patent Application Publication No. US 2004/0121175 ("Flexman") for the reasons specified on pages 10 and 11 of the office action.

Re the Specification:

The specification is amended to correct certain minor typographical errors and to change the reference numbers for the larger diameter openings to 68 and 68' from 64 and 64', respectively. In the specification as originally filed, the reference number 64 was also used to identify the circuit board. The change in reference numbers eliminates this duplication. No new matter is added.

Re the Claims:

Claims 1 and 19 are amended to clarify that the diffuser is positioned within at least some of the lamp receptacles. Claims 1 and 19 are also amended to delete certain surplus language, thus clarifying the positional relationships between certain of the elements and to clarify that the excitation light provided by the light sources causes the object to fluoresce.

Support for the amendments to claims 1 and 19 is found, either expressly or inherently, throughout the specification and claims as originally filed and more specifically at, for example, paragraphs [0025], [0030], [0041], and [0051]. No new matter is added.

Claim 7 is amended to clarify that it is the light sources contained within opposed pairs of lamp receptacles that produce light of the same color.

Support for the amendments to claim 7 is found, either expressly or inherently, throughout the specification and claims as originally filed and more specifically at, for example, paragraphs [0028], [0047], and [0048]. No new matter is added.

New claims 30-34 depend from claim 1 and further specify certain details relating to the light source and receptacle structure, as set forth in the new claims. Support for new claims 30-34 is contained throughout the written description and drawings as originally filed and more specifically, at, for example, paragraphs [0030], [0040]-[0042], [0044], and [0045] and Figures 1, 5, 6, 12, and 13. No new matter is added.

New claims 35-37 are directed to an excitation light source assembly having the elements and limitations set forth in the new claims. Support for new claims 35-37 is contained throughout the

written description and claims as originally filed and more specifically, at, for example, paragraphs [0024], [0025], [0030], [0040]-[0042], [0044], [0045], [0051], and [0053], and Figures 1, 5, 6, 12, and 13. No new matter is added.

Re the Drawings:

Figure 1 is amended to change the reference numbers to 68 and 68' from 64 and 64', respectively. The change is made to eliminate a previous duplication of reference numbers. No new matter is added.

Legal Standard For Rejecting Claims Under 35 U.S.C. §103

The examiner has the burden of establishing a prima facie case of obviousness. In re Rouffet, 149 F.3d 1350, 1355 (Fed. Cir. 1998). "If the examination at the initial stage does not produce a prima facie case of unpatentability, then without more the applicant is entitled to grant of the patent." In re Oetiker, 977 F.2d 1443, 1445 (Fed. Cir. 1992). The claims as originally filed are presumptively patentable.

The obviousness determination is controlled by four factors: 1) "the scope and content of the prior art"; 2) the "differences between the claims and the prior art"; 3) "the level of ordinary skill in the pertinent art"; and 4) "objective evidence of non-obviousness." KSR Int'l Co. v. Teleflex, Inc., 127 S. Ct. 1727, 1740-1741 (2007) (quoting Graham v. John Deere Co. of Kansas City, 383 U.S. 1, 17-18 (1966) (internal quotations omitted)).

In considering the scope and content of the prior art, as well as the differences between the claims and the prior art, the fact finder must determine whether all of the claimed elements are present in the prior art, and if so, the fact finder must also

determine "[w]hat the prior art teaches, whether it teaches away from the claimed invention, and whether it motivates a combination of teachings from different references." Dystar Textilfarben GmbH & Co. v. C.H. Patrick Co., 464 F.3d 1356, 1360 (Fed. Cir. 2006).

A claim "composed of several elements is not proved obvious merely by demonstration that each of its elements was, independently, known in the prior art." KSR Int'l Co., 127 S. Ct. at 1741. See also Grain Processing Corp. v. Am. Maize Prods. Co., 840 F.2d 902, 907 (Fed. Cir. 1988): "In determining obviousness, the inquiry is not whether each element existed in the prior art, but whether the prior art made obvious the invention as whole for which patentability is claimed" (citation and internal quotations omitted). The analysis must "guard against slipping into the use of hindsight" and "the temptation to read into the prior art the teachings of the invention at issue." Graham, 383 U.S. at 36.

The Federal Circuit has emphasized that it "is impermissible to use the claimed invention as an instruction manual or 'template' to piece together the teachings of the prior art so that the claimed invention is rendered obvious." In re Fritch, 972 F.2d 1260, 1265 (Fed. Cir. 1992). As a check against hindsight analysis, the examiner must conduct an "explicit" analysis "to determine whether there was an apparent reason to combine the known elements in the fashioned claimed . . . ." KSR Int'l Co., 127 S. Ct. at 1741. As the Supreme Court made clear, "'[R]ejections based on obviousness grounds cannot be sustained by mere conclusory statements; instead, there must be some articulated reasoning with some rational underpinning to support the legal conclusion of obviousness.'" KSR Int'l Co., 127 S. Ct. at 1741 (quoting In re Kahn, 441 F.3d 977, 988 (Fed. Cir. 2006)). Another consideration in the obviousness analysis is "whether the prior art would also have revealed that in so making or carrying out [the claimed

composition or process], those of ordinary skill would have a reasonable expectation of success." In re Vaeck, 947 F.2d 488, 493 (Fed. Cir. 1991). See Takeda Chem. Indus., Ltd. v. Alphapharm Pty, Ltd., 492 F.3d 1350 (Fed. Cir. 2007).

Thus, proving obviousness has three required components: 1) the presence or suggestion of all the claimed elements in the prior art; 2) a reasonable expectation of success from the modification or combination; and 3) an "explicit" analysis of "an apparent reason to combine known elements." MPEP 2143. See In re Vaeck, 947 F.2d at 493.

The fact that a reference "teaches away" from the claimed invention tends to indicate non-obviousness. KSR Int'l Co., 1740. See McGinley v. Franklin Sports, Inc., 262 F.3d 1339, 1354 (Fed. Cir. 2001) ("[R]eferences that teach away cannot serve to create a prima facie case of obviousness"); In re Gurley, 27 F.3d 551, 553 (Fed. Cir. 1994) (citing cases). References "teach away" if they (1) discourage one of skill in the art from following the path laid out in the reference; (2) lead one of skill in the art in a direction different from that taken by the applicant; or (3) suggest that the line of development flowing from the reference's teaching will not achieve the results sought by the inventor. Tec Air, Inc. v. Denso Mfg. Mich. Inc., 192 F.3d 1353, 1360 (Fed. Cir. 1999). "Evidence that supports, rather than negates, patentability must be fairly considered." In re Dow Chem. Co., 837 F.2d 469, 473 (Fed. Cir. 1988).

Re the Rejections of Claims 1-4, 6, 8, 19-26, 28, and 29:

The examiner rejected claims 1-4, 6, 8, 19-26, 28, and 29 as being obvious over Pohlert in view of Kelly and Nomura. The examiner's rejections must be reversed because, even if it were proper to combine Pohlert, Kelly, and Nomura (which is denied, as

explained further below), the resulting combination would still fail to meet at least the limitations of the claims that require the housing 14 to define a plurality of lamp receptacles 18. The combination would also fail to meet the requirement that the light sources 18 be positioned within each of the plurality of lamp receptacles. Because no combination of references would result in a device that would meet these limitations, the examiner has failed to establish the required prima-facie case of obviousness. The rejected claims retain their presumption of patentability.

Independent claim 1 requires that housing 14 define a *plurality* of lamp receptacles 18. Claim 1 also requires at least one light source 20 to be positioned *within* each of the plurality of lamp receptacles 18. These limitations are not met by any of Pohlert, Kelly, and Nomura. For example, while Pohlert discloses several different lighting frame embodiments (e.g., 202, 302, 1101, etc., shown in Figs. 1-4, 11, and 12), none of Pohlert's lighting frames define a plurality of lamp receptacles within which are received the light sources. To the contrary, Pohlert mounts his light sources directly *on* the surfaces of his lighting frames. See, for example, Figures 2, 4, 11, 12, 15c, 30a, 30b, and 30c of Pohlert. Nowhere does Pohlert disclose, or even suggest, an embodiment having a housing that defines both a central opening therein as well as a plurality of lamp receptacles. Pohlert further fails to disclose a lighting system wherein the light sources are positioned *within* each of the receptacles.

The Kelly reference also discloses a ring lighting system. However, Kelly's housing 2 also does not define a plurality of lamp receptacles. Instead, Kelly's housing 2 defines a single annulus (not specifically identified in the Kelly patent). The annulus is sized to receive annular circuit board 5 having a plurality of LEDs 6 mounted thereon as well as an annular lens 7. See Figures 1, 2,

SPECTRAL_0000829

and 6 of Kelly. Kelly does not disclose or suggest an embodiment wherein the housing defines both a central opening and a plurality of lamp receptacles.

Nomura discloses a pattern detector and postal matter processor that uses the detector. Nomura's detector comprises a case 1 that is provided with a radiation window 2 and a diaphragm 3 through which reflected light passes to reach a camera 6. The area defined between the radiation window 2 and diaphragm 3 houses an ultraviolet lamp 4 as well as a light emitting member 5. The light emitting member 5 fluoresces in response to the light from lamp 4, thereby causing Nomura's pattern detector to emit light of two different wavelengths, La (from the lamp 4) and Lb (from the light emitting member 5). Significantly, Nomura's case 1 also does not define a plurality of lamp receptacles. Nomura discloses only one.

In summation, then, no combination of Pohlert, Kelly, and Nomura would result in an excitation light source that meets the claimed limitations that require the housing to define "a plurality of lamp receptacles" therein and further wherein the light sources are "positioned within each of the plurality of lamp receptacles," as specifically required by claim 1. Consequently, independent claim 1, and the claims depending therefrom, i.e., claims 2-8 and new claims 30-34 are prima-facie allowable over Pohlert, Kelly, and Nomura.

Independent claims 19 and 35 are allowable over Pohlert, Kelly, and Nomura for the same reasons expressed above for claim 1. That is, no combination of Pohlert, Kelly, and Nomura would result in an excitation light source that meets the limitations of claims 19 and 35 that require the housing to define "a plurality of lamp receptacles" and further wherein the light sources are "positioned within each of the plurality of lamp receptacles." Claims 19 and

35, as well as the claims depending therefrom (i.e., claims 20-29 and 36-37, respectively), are prima-facie allowable over these references.

Turning now to the question as to whether there would even be a reason to combine the various elements of Pohlert, Kelly, and Nomura in the first place, when considered as a whole, the teachings of the various references do not provide a reason for their combination. To the contrary, Pohlert teaches *against* combining elements of his lighting systems with lighting systems of the type disclosed by Kelly and Nomura. Therefore, there is no rational basis to combine Pohlert with Kelly and/or Nomura.

Pohlert discloses various types of light panels for film, television, or video production. Pohlert's lighting panels are provided with a plurality of light sources, typically LEDs or fluorescent lamps. Pohlert specifically seeks lighting apparatus that produces illumination suitable for "the special needs of the film, commercial, or photographic industries, or with live stage performances...." Pohlert, paragraph [0018]. Significantly, Pohlert states that the illumination needs in this field differ "substantially from what is offered by object inspection lighting apparatus." Pohlert goes on to conclude that lighting systems for such object inspection apparatus are "generally not suitable for the special needs" of the type of lighting systems he discloses. Paragraph [0018].

Kelly and Nomura disclose illumination systems for object inspection apparatus of the type Pohlert characterizes as unsuitable for the types of lighting systems he seeks to use. More specifically, the Kelly reference discloses a ring lighting system for "industrial instrumentation in which it is desired to illuminate an object which is being inspected by a sensor or camera." Col. 1, lines 6-7 of Kelly. Kelly's ring lighting system

SPECTRAL_0000831

uses a plurality of light sources in combination with a ring-shaped or annular lens to provide increased uniformity. See, for example, col. 3, lines 41-49 and lines 54-56 of Kelly. The light sources Kelly uses comprise LED "chips" having very small dimensions (e.g., about 0.25 mm square) (col. 8, line 42) that are positioned very closely together (i.e., about 0.5 mm)(col. 6, line 58).

Nomura also teaches a machine illumination system, but seeks to solve the problem of more efficiently detecting a fluorescent pattern on mail. Nomura solves this problem by providing an additional light emitting member 5 that emits light of a longer wavelength (Lb) after being excited by light of a shorter wavelength (La) from the ultraviolet lamps 4. Light of the two wavelengths is then directed onto the fluorescent pattern to be detected.

The diverse teachings of Pohlert, Kelly, and Nomura preclude their combination in the manner espoused by the examiner. First, Pohlert specifically states that the illumination needs in his field (i.e., film, television, and video production) "differ substantially from what is offered by object inspection lighting apparatus," such as those disclosed by Kelly and Nomura. Pohlert goes on to conclude that "lighting apparatus specially adapted for illumination of objects to be inspected are generally not suitable" for the types of lighting systems he provides. See, for example, paragraph [0018] of Pohlert. Thus, a person having ordinary skill in the art would not seek to combine the teachings of Pohlert with those of Kelly and Nomura because Pohlert specifically counsels against such a combination.

While Pohlert concludes that devices such as Kelly's are "generally not suitable" in Pohlert's field of illumination systems, Kelly also teaches away from Pohlert. That is, Kelly specifically *teaches against* using the individually packaged LEDs

SPECTRAL_0000832

of the type that Pohlert prefers. Kelly decries the use of discrete or individual LEDs, noting that "the pointing accuracy of individual LEDs is poor" which leads to a "lack of uniformity of the illuminated area." See, for example, col. 1, lines 65 and 66 of Kelly. However, such individually packaged LEDs are exactly the type used by Pohlert. See, for example, Figures 4, 7, 8, 32, and 35 of Pohlert.

In summation then, the opposed teachings of Pohlert, Kelly, and Nomura preclude any rational reason for their combination: That which Pohlert embraces, Kelly decries, and vice-versa. Even under KSR, a claim "composed of several elements is not proved obvious merely by demonstration that each of its elements was, independently, known in the prior art." KSR, supra, at 1741. Instead, "in determining obviousness, the inquiry is not whether each element existed in the prior art, but whether the prior art made obvious the invention as whole for which patentability is claimed." Grain Processing, supra, at 907. Because the teachings of Pohlert, Kelly, and Nomura are so divergent that no rational basis can be articulated for their combination, none of the references can be used to establish a prima-facie case of obviousness. The pending claims retain their presumption of patentability.

Re the Rejection of Claim 5:

The examiner rejected claim 5 as being obvious over Pohlert in view of Kelly and Nomura and further in view of Furze. These rejections are improper for the same reasons expressed above for Pohlert, Kelly, and Nomura alone. The disclosure in Furze of narrow-band light filters does nothing to cure those deficiencies.

Furze, like Kelly and Nomura, discloses an object inspection apparatus for golf balls. Thus, the Furze system is of the type

SPECTRAL_0000833

Pohlert finds "not suitable" for the type of video and film production lighting systems that he discloses. Therefore, the proposed combination of Pohlert, Kelly, Nomura, and Furze suffers from the same deficiencies as the combination of Pohlert, Kelly, and Nomura alone. Namely, the divergent teachings of the various references preclude their rational combination.

Still further, even if it were possible to find a rational basis for combining the references, which is denied, the resulting combination would still fail to meet the requirements of the pending claims that require the housing to define a plurality of lamp receptacles and further that the light sources be provided or housed within the lamp receptacles. Claim 5 is therefore patentable over Pohlert, Kelly, Nomura, and Furze.

Re the Rejection of Claim 27:

The examiner rejected claim 27 as being obvious over Pohlert in view of Kelly and Nomura and further in view of Flexman. These rejections are also improper for the same reasons expressed above for the rejections based on Pohlert, Kelly, and Nomura alone. Flexman's disclosure of layered articles made from polyoxymethylene thermoplastic material does not erase the divergent teachings of the various references. There is still no rational basis for combining the various references.

Again, Pohlert specifically states that lighting systems for object inspection systems, such as those disclosed in Kelly and Nomura, are "not suitable" for the types of lighting systems Pohlert is concerned about. If this were not enough, Kelly also specifically teaches away from the types of individual LED illuminators that Pohlert prefers. Flexman is even further afield and relates only to the manufacture of layered plastic articles made from polyoxymethylene. There is nothing in Flexman to

SPECTRAL_0000834

recommend it to any of Pohlert, Kelly, and Nomura for any reason, much less the reasons espoused by the examiner. Claim 27 remains presumptively patentable over these references.

* * *

Applicants believe that all of the claims pending in this patent application are allowable and that all other issues raised by the examiner have been satisfactorily addressed. Applicants respectfully request the examiner to reconsider the rejections and grant an early allowance. If any questions or issues remain to be resolved, the examiner is requested to contact the Applicants' attorney at the telephone number listed below.

The applicants believe that any fees required have been paid. However, if additional fees are required, the applicant authorizes the charge of such fees to Fennemore Craig, P.C., Deposit Account No. 06-0590.

Respectfully submitted,

FENNEMORE CRAIG, P.C.

/Bruce E. Dahl/

Bruce E. Dahl, Esq.
Attorney for Applicants
PTO Registration No. 33,670
1700 Lincoln Street, Suite 2900
Denver, CO 80203-4529
(303) 291-3200

Date: April 30, 2013

APPENDIX

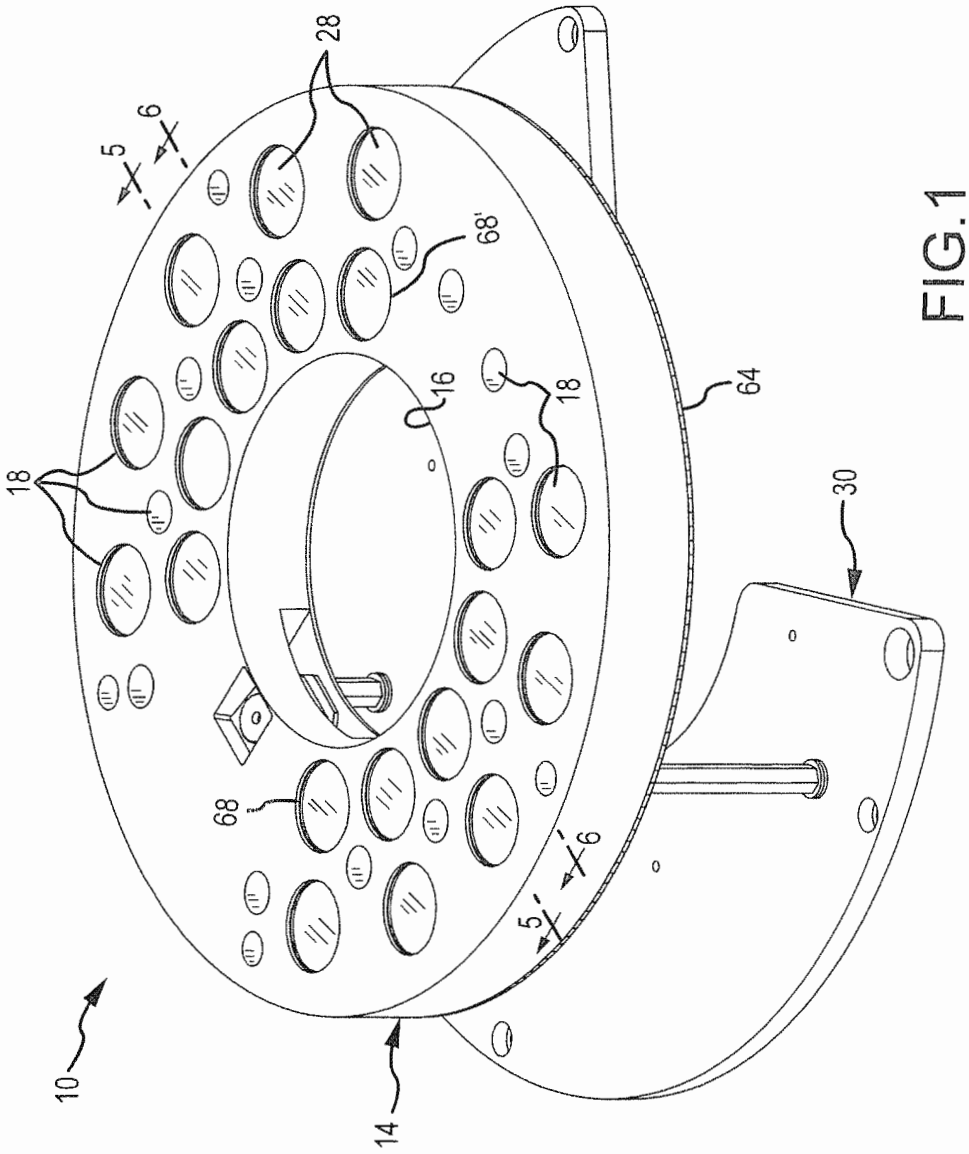


FIG. 1

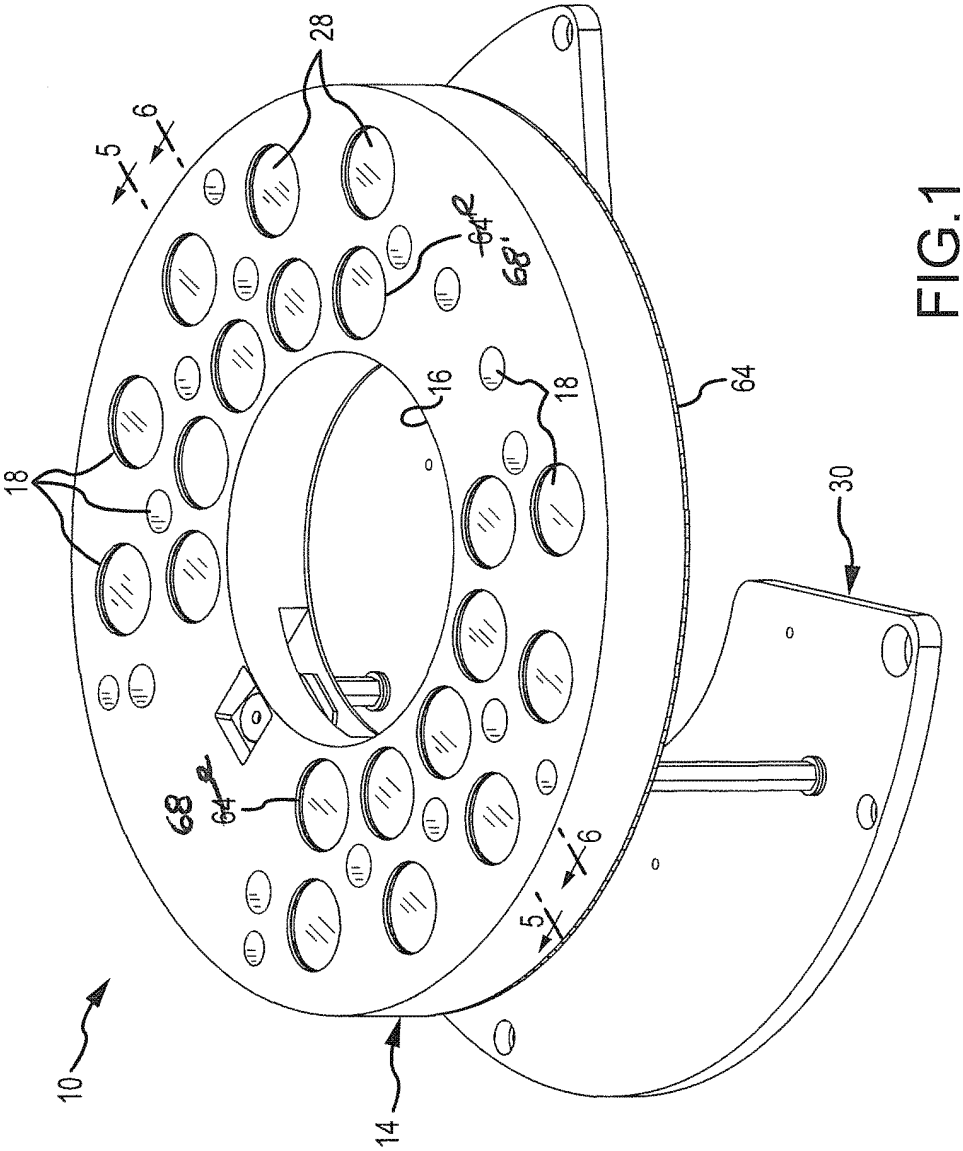


FIG.1

Electronic Acknowledgement Receipt

EFS ID:	15648587
Application Number:	13222688
International Application Number:	
Confirmation Number:	5910
Title of Invention:	EXCITATION LIGHT SOURCE ASSEMBLY
First Named Inventor/Applicant Name:	Michael B. Nelson
Customer Number:	27104
Filer:	Bruce E. Dahl
Filer Authorized By:	
Attorney Docket Number:	SPEC US-4 (027560-0014)
Receipt Date:	30-APR-2013
Filing Date:	31-AUG-2011
Time Stamp:	13:57:22
Application Type:	Utility under 35 USC 111(a)

Payment information:

Submitted with Payment	no

File Listing:

Document Number	Document Description	File Name	File Size(Bytes)/ Message Digest	Multi Part /.zip	Pages (if appl.)
1		Amendment-Replacement_Drawing.pdf	175464 795afcd96988fd8d5a6d3f6fb2688cdeeeb0a9b4	yes	27

	Multipart Description/PDF files in .zip description		
	Document Description	**Start**	**End**
	Amendment/Req. Reconsideration-After Non-Final Reject	1	25
	Drawings-only black and white line drawings	26	27
Warnings:			
Information:			
	Total Files Size (in bytes):	175464	

This Acknowledgement Receipt evidences receipt on the noted date by the USPTO of the indicated documents, characterized by the applicant, and including page counts, where applicable. It serves as evidence of receipt similar to a Post Card, as described in MPEP 503.

New Applications Under 35 U.S.C. 111
If a new application is being filed and the application includes the necessary components for a filing date (see 37 CFR 1.53(b)-(d) and MPEP 506), a Filing Receipt (37 CFR 1.54) will be issued in due course and the date shown on this Acknowledgement Receipt will establish the filing date of the application.

National Stage of an International Application under 35 U.S.C. 371
If a timely submission to enter the national stage of an international application is compliant with the conditions of 35 U.S.C. 371 and other applicable requirements a Form PCT/DO/EO/903 indicating acceptance of the application as a national stage submission under 35 U.S.C. 371 will be issued in addition to the Filing Receipt, in due course.

New International Application Filed with the USPTO as a Receiving Office
If a new international application is being filed and the international application includes the necessary components for an international filing date (see PCT Article 11 and MPEP 1810), a Notification of the International Application Number and of the International Filing Date (Form PCT/RO/105) will be issued in due course, subject to prescriptions concerning national security, and the date shown on this Acknowledgement Receipt will establish the international filing date of the application.

PTO/SB/06 (09-11)
Approved for use through 1/31/2014. OMB 0651-0032
U.S. Patent and Trademark Office; U.S. DEPARTMENT OF COMMERCE
Under the Paperwork Reduction Act of 1995, no persons are required to respond to a collection of information unless it displays a valid OMB control number.

PATENT APPLICATION FEE DETERMINATION RECORD Substitute for Form PTO-875	Application or Docket Number 13/222,688	Filing Date 08/31/2011	☐ To be Mailed

ENTITY: ☐ LARGE ☒ SMALL ☐ MICRO

APPLICATION AS FILED – PART I

	(Column 1)	(Column 2)		
FOR	NUMBER FILED	NUMBER EXTRA	RATE ($)	FEE ($)
☐ BASIC FEE (37 CFR 1.16(a), (b), or (c))	N/A	N/A	N/A	
☐ SEARCH FEE (37 CFR 1.16(k), (i), or (m))	N/A	N/A	N/A	
☐ EXAMINATION FEE (37 CFR 1.16(o), (p), or (q))	N/A	N/A	N/A	
TOTAL CLAIMS (37 CFR 1.16(i))	minus 20 =	*	X $ =	
INDEPENDENT CLAIMS (37 CFR 1.16(h))	minus 3 =	*	X $ =	
☐ APPLICATION SIZE FEE (37 CFR 1.16(s))	If the specification and drawings exceed 100 sheets of paper, the application size fee due is $310 ($155 for small entity) for each additional 50 sheets or fraction thereof. See 35 U.S.C. 41(a)(1)(G) and 37 CFR 1.16(s).			
☐ MULTIPLE DEPENDENT CLAIM PRESENT (37 CFR 1.16(j))				
* If the difference in column 1 is less than zero, enter "0" in column 2.			TOTAL	

APPLICATION AS AMENDED – PART II

		(Column 1)		(Column 2)	(Column 3)		
	04/30/2013	CLAIMS REMAINING AFTER AMENDMENT		HIGHEST NUMBER PREVIOUSLY PAID FOR	PRESENT EXTRA	RATE ($)	ADDITIONAL FEE ($)
AMENDMENT	Total (37 CFR 1.16(i))	* 27	Minus	** 29	= 0	X $40 =	0
	Independent (37 CFR 1.16(h))	* 3	Minus	***4	= 0	X $210 =	0
	☐ Application Size Fee (37 CFR 1.16(s))						
	☐ FIRST PRESENTATION OF MULTIPLE DEPENDENT CLAIM (37 CFR 1.16(j))						
						TOTAL ADD'L FEE	0

		(Column 1)		(Column 2)	(Column 3)		
		CLAIMS REMAINING AFTER AMENDMENT		HIGHEST NUMBER PREVIOUSLY PAID FOR	PRESENT EXTRA	RATE ($)	ADDITIONAL FEE ($)
AMENDMENT	Total (37 CFR 1.16(i))	*	Minus	**	=	X $ =	
	Independent (37 CFR 1.16(h))	*	Minus	***	=	X $ =	
	☐ Application Size Fee (37 CFR 1.16(s))						
	☐ FIRST PRESENTATION OF MULTIPLE DEPENDENT CLAIM (37 CFR 1.16(j))						
						TOTAL ADD'L FEE	

* If the entry in column 1 is less than the entry in column 2, write "0" in column 3.
** If the "Highest Number Previously Paid For" IN THIS SPACE is less than 20, enter "20".
*** If the "Highest Number Previously Paid For" IN THIS SPACE is less than 3, enter "3".
The "Highest Number Previously Paid For" (Total or Independent) is the highest number found in the appropriate box in column 1.

LIE
/DELEACHES YOUNG/

This collection of information is required by 37 CFR 1.16. The information is required to obtain or retain a benefit by the public which is to file (and by the USPTO to process) an application. Confidentiality is governed by 35 U.S.C. 122 and 37 CFR 1.14. This collection is estimated to take 12 minutes to complete, including gathering, preparing, and submitting the completed application form to the USPTO. Time will vary depending upon the individual case. Any comments on the amount of time you require to complete this form and/or suggestions for reducing this burden, should be sent to the Chief Information Officer, U.S. Patent and Trademark Office, U.S. Department of Commerce, P.O. Box 1450, Alexandria, VA 22313-1450. DO NOT SEND FEES OR COMPLETED FORMS TO THIS ADDRESS. **SEND TO: Commissioner for Patents, P.O. Box 1450, Alexandria, VA 22313-1450.**
If you need assistance in completing the form, call 1-800-PTO-9199 and select option 2.

UNITED STATES PATENT AND TRADEMARK OFFICE

UNITED STATES DEPARTMENT OF COMMERCE
United States Patent and Trademark Office
Address: COMMISSIONER FOR PATENTS
P.O. Box 1450
Alexandria, Virginia 22313-1450
www.uspto.gov

APPLICATION NO.	FILING DATE	FIRST NAMED INVENTOR	ATTORNEY DOCKET NO.	CONFIRMATION NO.
13/222,688	08/31/2011	Michael B. Nelson	SPEC US-4 (027560-0014)	5910

27104 7590 07/10/2013

FENNEMORE CRAIG, P.C.
1700 Lincoln Street
SUITE 2900
DENVER, CO 80203

EXAMINER	
TANINGCO, MARCUS H	

ART UNIT	PAPER NUMBER
2884	

MAIL DATE	DELIVERY MODE
07/10/2013	PAPER

Please find below and/or attached an Office communication concerning this application or proceeding.

The time period for reply, if any, is set in the attached communication.

Office Action Summary	Application No. 13/222,688	Applicant(s) NELSON ET AL.	
	Examiner MARCUS TANINGCO	Art Unit 2884	AIA (First Inventor to File) Status No

-- The MAILING DATE of this communication appears on the cover sheet with the correspondence address --

Period for Reply

A SHORTENED STATUTORY PERIOD FOR REPLY IS SET TO EXPIRE 3 MONTH(S) OR THIRTY (30) DAYS, WHICHEVER IS LONGER, FROM THE MAILING DATE OF THIS COMMUNICATION.

- Extensions of time may be available under the provisions of 37 CFR 1.136(a). In no event, however, may a reply be timely filed after SIX (6) MONTHS from the mailing date of this communication.
- If NO period for reply is specified above, the maximum statutory period will apply and will expire SIX (6) MONTHS from the mailing date of this communication.
- Failure to reply within the set or extended period for reply will, by statute, cause the application to become ABANDONED (35 U.S.C. § 133). Any reply received by the Office later than three months after the mailing date of this communication, even if timely filed, may reduce any earned patent term adjustment. See 37 CFR 1.704(b).

Status

1)☒ Responsive to communication(s) filed on *30 April 2013*.

☐ A declaration(s)/affidavit(s) under **37 CFR 1.130(b)** was/were filed on _____.

2a)☐ This action is **FINAL**. 2b)☒ This action is non-final.

3)☐ An election was made by the applicant in response to a restriction requirement set forth during the interview on _____; the restriction requirement and election have been incorporated into this action.

4)☐ Since this application is in condition for allowance except for formal matters, prosecution as to the merits is closed in accordance with the practice under *Ex parte Quayle*, 1935 C.D. 11, 453 O.G. 213.

Disposition of Claims

5)☒ Claim(s) *1-8 and 19-37* is/are pending in the application.

5a) Of the above claim(s) _____ is/are withdrawn from consideration.

6)☐ Claim(s) _____ is/are allowed.

7)☒ Claim(s) *1-8 and 19-37* is/are rejected.

8)☐ Claim(s) _____ is/are objected to.

9)☐ Claim(s) _____ are subject to restriction and/or election requirement.

* If any claims have been determined allowable, you may be eligible to benefit from the **Patent Prosecution Highway** program at a participating intellectual property office for the corresponding application. For more information, please see http://www.uspto.gov/patents/init_events/pph/index.jsp or send an inquiry to PPHfeedback@uspto.gov.

Application Papers

10)☐ The specification is objected to by the Examiner.

11)☒ The drawing(s) filed on *31 August 2011* is/are: a)☒ accepted or b)☐ objected to by the Examiner.

Applicant may not request that any objection to the drawing(s) be held in abeyance. See 37 CFR 1.85(a).

Replacement drawing sheet(s) including the correction is required if the drawing(s) is objected to. See 37 CFR 1.121(d).

Priority under 35 U.S.C. § 119

12)☐ Acknowledgment is made of a claim for foreign priority under 35 U.S.C. § 119(a)-(d) or (f).

Certified copies:

a)☐ All b)☐ Some * c)☐ None of the:

1.☐ Certified copies of the priority documents have been received.

2.☐ Certified copies of the priority documents have been received in Application No. _____.

3.☐ Copies of the certified copies of the priority documents have been received in this National Stage application from the International Bureau (PCT Rule 17.2(a)).

* See the attached detailed Office action for a list of the certified copies not received.

Attachment(s)

1) ☒ Notice of References Cited (PTO-892)

2) ☐ Information Disclosure Statement(s) (PTO/SB/08) Paper No(s)/Mail Date _____.

3) ☐ Interview Summary (PTO-413) Paper No(s)/Mail Date. _____ .

4) ☐ Other: _____.

DETAILED ACTION

Response to Arguments

Applicant's arguments, filed 4/30/2013, with respect to the rejection(s) of claim(s) 1 and 19 under 35 USC § 103 have been fully considered and are persuasive. Therefore, the rejection has been withdrawn. However, upon further consideration, a new ground(s) of rejection is made in view of Chapman et al. In response to applicant's argument that it would not have been obvious to combine the cited references, the fact that applicant has recognized another advantage which would flow naturally from following the suggestion of the prior art cannot be the basis for patentability when the differences would otherwise be obvious. See *Ex parte Obiaya*, 227 USPQ 58, 60 (Bd. Pat. App. & Inter. 1985). Furthermore, although applicant alleges that it would not have been obvious to modify an inspection lighting apparatus to produce the type of lighting apparatus used for film, television, or video production, prior art does not teach away from modifying the type of lighting apparatus used for film, television, or video production to produce an inspection apparatus having known elements. All the claimed elements were known in the prior art and one skilled in the art could have combined the elements as claimed by known methods with no change in their respective functions, and the combination would have yielded predictable results to one of ordinary skill in the art at the time of the invention. Furthermore, the combination of known elements according to known methods is likely to be obvious when it does not more than yield predictable results. When a patent simply arranges old elements with each performing the same function it had been known to perform and yields no more than one

SPECTRAL_0000844

would expect from such an arrangement, the combination is obvious (KSR at 1395-66; citing Sakraida v. AG Pro, Inc., 425 US 273, 282 1976).

Claim Rejections - 35 USC § 103

The following is a quotation of pre-AIA 35 U.S.C. 103(a) which forms the basis for all obviousness rejections set forth in this Office action:

> (a) A patent may not be obtained though the invention is not identically disclosed or described as set forth in section 102 of this title, if the differences between the subject matter sought to be patented and the prior art are such that the subject matter as a whole would have been obvious at the time the invention was made to a person having ordinary skill in the art to which said subject matter pertains. Patentability shall not be negatived by the manner in which the invention was made.

This application currently names joint inventors. In considering patentability of the claims under pre-AIA 35 U.S.C. 103(a), the examiner presumes that the subject matter of the various claims was commonly owned at the time any inventions covered therein were made absent any evidence to the contrary. Applicant is advised of the obligation under 37 CFR 1.56 to point out the inventor and invention dates of each claim that was not commonly owned at the time a later invention was made in order for the examiner to consider the applicability of pre-AIA 35 U.S.C. 103(c) and potential pre-AIA 35 U.S.C. 102(e), (f) or (g) prior art under pre-AIA 35 U.S.C. 103(a).

Claims 1-4, 6-8, 19-26, and 28-37 are rejected under pre-AIA 35 U.S.C. 103(a) as being unpatentable over Pohlert et al. (*Pohlert*, US 2009/0268426) in view of Kelly (US 6,454,437), Nomura (JP10-040330), and Chapman et al. (*Chapman*, US 5,984,494).

With regards to claims 1 and 35, Pohlert teaches a stand-mounted light panel for natural illumination in film, television or video (title) and further teaches a central opening (103, fig. 1; 303 figs. 4-5) having a plurality of lamp segments 306 surrounding the central opening (303, fig 4; 3803, fig. 38A), the structure being mountable to a support structure (330, fig. 3) so that the central opening being aligned with a camera (fig. 1 shows this aspect) also mounted to the support structure (330, fig. 3), so that the field of view of the camera is unobstructed, and a light source 305 positioned on each of the plurality of lamp segments 306, a diffuser (5029, fig. 5a; 1205 fig. 12; 795, 876 in figs 7-8, teach that lens elements spreading the light; this is interpreted as meaning diffusing; paras 0119-0120) positioned adjacent the light source positioned on each of the plurality of lamp segments (figs. 4 shows a plurality of lamp segments 306 which contain a plurality of light sources 305; fig. 50a shows the a diffuser 5029 which locate within each lamp panel 4702, 4802, figs. 47a; 50a-50b), each of the diffusers diffusing light produced by each of the light sources (abstract, para. 0023 teaches the diffusion lens being integrated with the lighting panel; 795, 876 in figs 7-8, teach that lens elements spreading the light; this is interpreted as meaning diffusing; paras 0119-0120), and a control system (212, fig. 2, para. 0094; and element 1052) operatively connected to each of the light sources (para. 0145, fig. 13, paras. 0091-0092, 0166) positioned on the plurality of lamp segments, the control system operating selected ones of the light source to provide a desired illumination to an object within the field of view of the camera (paras. 0091-0092, 0166).

However, Pohlert does not explicitly state a housing defining a central opening which contains the structure which holds a plurality of lamps, for connecting the camera to a central aperture.

Kelly teaches a ring lighting (title) and further teaches a housing (2, figs. 1-2) defining a central opening (3 figs. 1-2) which contains the structure which holds a plurality of lamps (6 figs. 1-2), for connecting the camera to a central aperture (abstract, figs. 1-2). Therefore, it would have been obvious to one of ordinary skill in the art at the time the invention was made to combine the stand-mounted light panel for natural illumination in film, television or video of Pohlert with the ring lighting of Kelly so as to have a housing defining a central opening which contains the structure which holds a plurality of lamps, for connecting the camera to a central aperture in order to protect the lights and lenses from the environment.

Pohlert also fails to explicitly state that said light source is positioned within each of a plurality of lamp receptacles. Nevertheless, those skilled in the art appreciate that such a configuration was known and would have been a matter of design choice since there were a finite number of predictable configurations (i.e. surface mount, recessed receptacle). Chapman teaches an illumination assembly comprising a plurality of LEDs 128, each positioned within a plurality of receptacles 146. Substituting the surface mount configuration taught by Pohlert with the receptacles taught by Chapman would have been obvious since the substitution of one known element for another would have yielded predictable results to one of ordinary skill in the art at the time of the invention.

Pohlert also does not explicitly state the apparatus being used as an excitation light source.

Nomura teaches a fluorescent pattern detector and postal matter processor using the detector (title) and further an apparatus comprising a central hole aligned with a camera having a plurality of light sources surrounding the central aperture being used as an excitation light source

(abstract, figs. 1, 5), said camera capturing an image of the fluorescing material in the pattern (paras. 0015-0018). Therefore, it would have been obvious to one of ordinary skill in the art at the time the invention was made to combine the stand-mounted light panel for natural illumination in film, television or video of Pohlert with the fluorescent pattern detector and postal matter processor using the detector of Nomura so as to have the apparatus used as a excitation light source in order to aid one in recognizing a fluorescent pattern of the object based on a detection signal.

With regards to claim 2, Pohlert teaches at least one of the light sources comprising a narrow-band light source (para. 0019) that emits light having a bandwidth (blue or green LEDs, paras. 0019, 0118). However, Pohlert does not explicitly state the bandwidth of the light source being about 35 nm. It would have been obvious to one of ordinary skill in the art at the time the invention was made to have the bandwidth of the light source be about 35 nm, since discovering the optimum value of a result effective variable involves only routine skill in the art and in order to produce a narrow-band of light (Pohlert, para. 0019).

Regarding claim 3, Pohlert teaches at least one narrow-band light source comprising a light emitting diode (paras. 0019, 0118-0119).

Regarding claim 4, Pohlert, in view of Chapmans teaching of a receptacle, teaches at least one filter (5010, fig. 50a) positioned adjacent at least one diffuser (5029, fig. 50a) in at least one of the lamp receptacles defined by the housing (para. 0187, figs. 50a-50b).

Regarding claim 6, Pohlert teaches at least one of the light sources comprises a broad-band light source (white LEDs, pares. 0098, 0118).

Regarding claim 7, Pohlert, in view of Chapmans teaching of a receptacle, teaches at least some of said plurality of lamp receptacles comprise opposed pairs of lamp receptacles on opposite sides of said central opening (different light segments 306 fig. 4), each opposed pair of lamp receptacles producing light of the same color (paras. 0097; para. 0118 teaches that the LEDs can all be the same color).

Regarding claim 8, Pohlert teaches opposing pairs of lamps located in segments (figs. 30b-30c) on opposite side the central opening (para. 0097). However, Pohlert does not explicitly state ten pairs of lamps surrounding the central aperture. It would have been obvious to one of ordinary skill in the art at the time the invention was made to have ten pairs of lamps surrounding the central aperture, since a mere duplication of essential working parts of device involves only routine skill in the art, and in order to produce the desired amount and display of light.

Regarding claim 19, Pohlert teaches a stand-mounted light panel for natural illumination in film, television or video (title) and further teaches a support structure (330, fig. 3) a camera (140, fig. 1) mounted to the support structure (330, para. 0102), a light source assembly (302, figs. 4-5, para. 0102) mounted to the support structure, the light source assembly comprising, a central opening (103, fig. 1; 303 figs. 4-5) having a plurality of lamp segments 306 surrounding the central opening (303, fig 4; 3803, fig. 38A), the structure being mountable to a support structure (330, fig. 3) so that the central opening being aligned with a camera (fig. 1 shows this aspect) also mounted to the support structure (330, fig. 3), so that the field of view of the camera is unobstructed, and a light source (lamps, fig. 2; LEDs or lamps 305, fig. 4; 4705 fig. 47a, para. 0180) positioned on each of the plurality of lamp segments 306, a diffuser (5029, fig. 5a; 1205 fig. 12; 795, 876 in figs 7-8, teach that lens elements spreading the light; this is interpreted as

meaning diffusing; paras 0119-0120) positioned adjacent the light source positioned on each of the plurality of lamp receptacles (figs. 4 shows a plurality of lamp segments 306 which contain a plurality of light sources 305; fig. 50a shows the a diffuser 5029 which locate within each lamp panel 4702, 4802, figs. 47a; 50a-50b), each of the diffusers diffusing light produced by each of the light sources (abstract, para. 0023 teaches the diffusion lens being integrated with the lighting panel; 795, 876 in figs 7-8, teach that lens elements spreading the light; this is interpreted as meaning diffusing; paras 0119-0120), and a control system (212, fig. 2, para. 0094; and element 1052) operatively connected to each of the light sources (para. 0145, fig. 13, paras. 0091-0092, 0166), the control system operating selected ones of the light source to provide a desired illumination to an object within the field of view of the camera (paras. 0091-0092, 0166). Pohlert teaches at least one narrow-band light source positioned on at least one of the plurality of lamp receptacles (blue or green LEDs, paras. 0019, 0118).

However, Pohlert does not explicitly state a housing defining a central opening which contains the structure which holds a plurality of lamps, for connecting the camera to a central aperture.

Kelly teaches a ring lighting (title) and further teaches a housing (2, figs. 1-2) defining a central opening (3 figs. 1-2) which contains the structure which holds a plurality of lamps (6 figs: 1-2), for connecting the camera to a central aperture (abstract, figs. 1-2). Therefore, it would have been obvious to one of ordinary skill in the art at the time the invention was made to combine the stand-mounted light panel for natural illumination in film, television or video of Pohlert with the ring lighting of Kelly so as to have a housing defining a central opening which

SPECTRAL_0000850

contains the structure which holds a plurality of lamps, for connecting the camera to a central aperture in order to protect the lights and lenses from the environment.

Pohlert also fails to explicitly state that said light source is positioned within each of a plurality of lamp receptacles. Nevertheless, those skilled in the art appreciate that such a configuration was known and would have been a matter of design choice since there were a finite number of predictable configurations (i.e. surface mount, recessed receptacle). Chapman teaches an illumination assembly comprising a plurality of LEDs 128, each positioned within a plurality of receptacles 146. Substituting the surface mount configuration taught by Pohlert with the receptacles taught by Chapman would have been obvious since the substitution of one known element for another would have yielded predictable results to one of ordinary skill in the art at the time of the invention.

Pohlert also does not explicitly state the apparatus being used as an excitation light source.

Nomura teaches a fluorescent pattern detector and postal matter processor using the detector (title) and further an apparatus comprising a central hole aligned with a camera having a plurality of light sources surrounding the central aperture being used as an excitation light source (abstract, figs. 1, 5). Therefore, it would have been obvious to one of ordinary skill in the art at the time the invention was made to combine the stand-mounted light panel for natural illumination in film, television or video of Pohlert with the fluorescent pattern detector and postal matter processor using the detector of Nomura so as to have the apparatus used as a excitation light source in order to aid one in recognizing a fluorescent pattern of the object based on a detection signal.

Regarding claim 20, Pohlert teaches a light filter (5010, fig. 50a) positioned adjacent at each of the diffusers (5029, para. 0187, figs. 50a-5Ob).

Regarding claim 21, Pohlert in view of Chapman teaches each of the lamp receptacles defined by said housing being angled with respect to a central axis of said housing so that light emitted from each of said narrow-band light sources is directed to a desired area within the field of view of said camera (paras. 0166, 0176).

Regarding claim 22, Pohlert teaches each of said narrow-band light sources being selected to provide desired number of illumination bands over a desired spectral range (paras. 0122, 0124).

Regarding claim 23, Pohlert teaches the desired spectral range being from about 430 nm to about 745 nm (paras. 0122, 0124; By teaching the LEDs being red, green, and blue, Pohlert has inferred the spectral range being from about 430 nm to about 745 nm).

Regarding claim 24, Pohlert teaches the use of different color LEDs (paras. 0122, 0124). However, it does not explicitly state the number of illumination bands being 10. It would have been obvious to one of ordinary skill in the art at the time the invention was made to have the number of illumination bands being 10, since discovering the optimum number of illumination bands needed to obtain a desired color distribution involves only routine skill in the art.

Regarding claim 25, Pohlert teaches each of the desired illumination bands having a bandwidth ranging from about 30 nm to about 35 nm (paras. 0122, 0124, by teaching the use green and blue LEDs, Pohlert has inferred the that the illumination bandwidth ranges from about 30 nm to about 35 nm).

Regarding claim 26, Pohlert teaches each of the narrow-band light sources comprising a light emitting diode (paras. 0118, 0156).

Regarding claim 28, Pohlert teaches the invention as shown above but lacks the explicit teaching of the desired spectral range being from about 430 nm to about 900 nm. It would have been obvious to one of ordinary skill in the art at the time the invention was made to have the desired spectral range being from about 430 nm to about 900 nm, since where the general conditions of the claim are disclosed in the prior art, discovering the optimum or workable ranges involves only routine skill in the art, and in order to produce the desired light emitting from the device.

Regarding claim 29, Pohlert teaches the desired spectral range being from about 430 nm to about 800 nm (paras. 0122, 0124; By teaching the LEDs being red, green, and blue, Pohlert has inferred the spectral range being from about 430 nm to about 800 nm).

With regards to claims 30 and 31, Chapman does not explicitly teach wherein the light sources positioned within the receptacles do not extend beyond the lamp receptacles, although such a configuration was known and considered a matter of design choice. Claims 30 and 31 would have been obvious because a person of ordinary skill has good reason to pursue the known options within his or her technical grasp. If this leads to the anticipated success, it is likely the product not of innovation but of ordinary skill.

With regards to claim 32, Pohlert does not explicitly teach three light sources. Nevertheless, providing three light sources was known and would have been obvious in view of adjusting the amount of light.

With regards to claim 33, Chapman discloses receptacles having different diameters 146, 148.

With regards to claims 34 and 37, the combination of Pohlert and Chapman teaches said light sources mounted to a circuit board (Pohlert; para. 0091) and wherein said receptacles comprise the recited shapes (Chapman; Fig. 11).

With regards to claim 36, Chapman discloses receptacles having different diameters 146, 148, but does not explicitly teach wherein the larger diameter receptacles receive a plurality of light sources and the smaller diameter receptacles receive a single light source. Nevertheless, those skilled in the art appreciate that modifying the number of light sources was known and would have been an obvious matter of design choice depending upon the desired light intensity output.

Claim 5 is rejected under 35 U.S.C. 103(a) as being unpatentable over Pohlert et al. in view of Kelly, Nomura, Chapman et al., and Furze et al. (*Furze*, US 2004/0247170).

Regarding claim 5, Pohlert teaches the invention as shown above but lacks the explicit teaching of at least one filter comprises a notch filter having a wavelength bandpass range of about 30 nm. Furze teaches the use of patterned structured light to detect and measure surface defects on a golf ball (title) and further teaches at least one filter comprises a notch filter having a wavelength bandpass range of about 30 nm (25 nm is viewed as being about 30 nm, para. 0023). Therefore, it would have been obvious to one of ordinary skill in the art at the time the invention was made to combine the stand-mounted light panel for natural illumination in film, television or

video of Pohlert with the use of patterned structured light to detect and measure surface defects on a golf ball of Furze so as to have at least one filter comprises a notch filter having a wavelength bandpass range in order to allow only a narrow band of wavelengths to pass and thereby allow one to detect the defects in an object/material.

Claim 27 is rejected under 35 U.S.C. 103(a) as being unpatentable over Pohlert et al. in view of Kelly, Nomura, Chapman et al., and Flexman et al. (*Flexman*, US 2004/0121175).

Regarding claim 27, Pohlert as modified teaches the invention as shown above but lacks the explicit teaching of the housing comprising polyoxymethylene thermoplastic material. Kelly teaches a ring lighting (title) and further teaches a housing (2, figs. 1-2) defining a central opening (3 figs. 1-2) which contains the structure which holds a plurality of lamps (6 figs. 1-2), for connecting the camera to a central aperture (abstract, figs. 1-2). Therefore, it would have been obvious to one of ordinary skill in the art at the time the invention was made to combine the stand-mounted light panel for natural illumination in film, television or video of Pohlert with the ring lighting of Kelly so as to have a housing defining a central opening which contains the structure which holds a plurality of lamps, for connecting the camera to a central aperture in order to protect the lights and lenses from the environment. Pohlert does however teach the lighting frame being made of thermoplastic (para. 0095). Flexman teaches layered articles having polyoxymethylene blend substrates with enhanced surface properties and at least one layer thereon and process for making the same (title) and further teaches the use of polyoxymethylene thermoplastic material (para. 0033). Therefore, it would have been obvious to one of ordinary skill in the art at the time the invention was made to combine the stand-mounted light panel for

SPECTRAL_0000855

natural illumination in film, television or video of Pohlert with the layered articles having polyoxymethylene blend substrates with enhanced surface properties and at least one layer thereon and process for making the same of Flexman so as to have in order to increase the toughness and durability of the housing so that it is able to withstand the element and occasional drops.

Conclusion

The prior art made of record and not relied upon is considered pertinent to applicant's disclosure.

Any inquiry concerning this communication or earlier communications from the examiner should be directed to Marcus H. Taningco whose telephone number is (571) 272-1848. The examiner can normally be reached on M - F 9:00 - 5:30.

If attempts to reach the examiner by telephone are unsuccessful, the examiner's supervisor, Dave Porta can be reached on (571) 272-2444. The fax phone number for the organization where this application or proceeding is assigned is 571-273-8300.

SPECTRAL_0000856

Information regarding the status of an application may be obtained from the Patent Application Information Retrieval (PAIR) system. Status information for published applications may be obtained from either Private PAIR or Public PAIR. Status information for unpublished applications is available through Private PAIR only. For more information about the PAIR system, see http://pair-direct.uspto.gov. Should you have questions on access to the Private PAIR system, contact the Electronic Business Center (EBC) at 866-217-9197 (toll-free). If you would like assistance from a USPTO Customer Service Representative or access to the automated information system, call 800-786-9199 (IN USA OR CANADA) or 571-272-1000.

/Marcus H Taningco/
Primary Examiner, Art Unit 2884

Notice of References Cited	Application/Control No. 13/222,688	Applicant(s)/Patent Under Reexamination NELSON ET AL.	
	Examiner MARCUS TANINGCO	Art Unit 2884	Page 1 of 1

U.S. PATENT DOCUMENTS

*		Document Number Country Code-Number-Kind Code	Date MM-YYYY	Name	Classification
*	A	US-5,984,494 A	11-1999	Chapman et al.	362/470
	B	US-			
	C	US-			
	D	US-			
	E	US-			
	F	US-			
	G	US-			
	H	US-			
	I	US-			
	J	US-			
	K	US-			
	L	US-			
	M	US-			

FOREIGN PATENT DOCUMENTS

*		Document Number Country Code-Number-Kind Code	Date MM-YYYY	Country	Name	Classification
	N					
	O					
	P					
	Q					
	R					
	S					
	T					

NON-PATENT DOCUMENTS

*		Include as applicable: Author, Title Date, Publisher, Edition or Volume, Pertinent Pages)
	U	
	V	
	W	
	X	

*A copy of this reference is not being furnished with this Office action. (See MPEP § 707.05(a).)
Dates in MM-YYYY format are publication dates. Classifications may be US or foreign.

Index of Claims	Application/Control No.	Applicant(s)/Patent Under Reexamination
	13222688	NELSON ET AL.
	Examiner	Art Unit
	MARCUS TANINGCO	2884

✓	Rejected	-	Cancelled	N	Non-Elected	A	Appeal
=	Allowed	÷	Restricted	I	Interference	O	Objected

☐ Claims renumbered in the same order as presented by applicant ☐ CPA ☐ T.D. ☐ R.1.47

CLAIM		DATE								
Final	Original	11/18/2012	07/08/2013							
	1	✓	✓							
	2	✓	✓							
	3	✓	✓							
	4	✓	✓							
	5	✓	✓							
	6	✓	✓							
	7	✓	✓							
	8	✓	✓							
	9	N	-							
	10	N	-							
	11	N	-							
	12	N	-							
	13	N	-							
	14	N	-							
	15	N	-							
	16	N	-							
	17	N	-							
	18	N	-							
	19	✓	✓							
	20	✓	✓							
	21	✓	✓							
	22	✓	✓							
	23	✓	✓							
	24	✓	✓							
	25	✓	✓							
	26	✓	✓							
	27	✓	✓							
	28	✓	✓							
	29	✓	✓							
	30		✓							
	31		✓							
	32		✓							
	33		✓							
	34		✓							
	35		✓							
	36		✓							

Index of Claims	Application/Control No.	Applicant(s)/Patent Under Reexamination
	13222688	NELSON ET AL.
	Examiner	**Art Unit**
	MARCUS TANINGCO	2884

✓	Rejected	-	Cancelled	N	Non-Elected	A	Appeal
=	Allowed	÷	Restricted	I	Interference	O	Objected

☐ Claims renumbered in the same order as presented by applicant ☐ CPA ☐ T.D. ☐ R.1.47

CLAIM		DATE								
Final	Original	11/18/2012	07/08/2013							
	37		✓							

Search Notes	Application/Control No.	Applicant(s)/Patent Under Reexamination
	13222688	NELSON ET AL.
	Examiner	Art Unit
	MARCUS TANINGCO	2884

CPC- SEARCHED		
Symbol	Date	Examiner

CPC COMBINATION SETS - SEARCHED		
Symbol	Date	Examiner

US CLASSIFICATION SEARCHED			
Class	Subclass	Date	Examiner
250	461.1	1/27/2013	MT

SEARCH NOTES		
Search Notes	Date	Examiner
Inventor's name searched	1/27/2013	MT
EAST search notes attached	1/27/2013	MT
Text search in 250/458.1, 459.1	1/27/2013	MT
Text search in 362/3	1/27/2013	MT
Updated EAST search notes attached	7/8/2013	MT

INTERFERENCE SEARCH			
US Class/ CPC Symbol	US Subclass / CPC Group	Date	Examiner

EAST Search History

EAST Search History (Prior Art)

Ref #	Hits	Search Query	DBs	Default Operator	Plurals	Time Stamp
L7	1120	250/461.1.ccls.	US-PGPUB; USPAT; FPRS; EPO; JPO; DERWENT; IBM_TDB	OR	OFF	2013/07/08 10:23
L8	2982	250/458.1.ccls.	US-PGPUB; USPAT; FPRS; EPO; JPO; DERWENT; IBM_TDB	OR	OFF	2013/07/08 10:23
L9	1678	250/459.1.ccls.	US-PGPUB; USPAT; FPRS; EPO; JPO; DERWENT; IBM_TDB	OR	OFF	2013/07/08 10:23
L10	4566	L7 L8 L9	US-PGPUB; USPAT; FPRS; EPO; JPO; DERWENT; IBM_TDB	OR	OFF	2013/07/08 10:23
L11	133	L10 and ((light or led or lamp) near3 (halo or ring or annular))	US-PGPUB; USPAT; FPRS; EPO; JPO; DERWENT; IBM_TDB	OR	OFF	2013/07/08 10:23
L12	56	11 and imag$4.clm.	US-PGPUB; USPAT; FPRS; EPO; JPO; DERWENT; IBM_TDB	OR	OFF	2013/07/08 10:23
L13	19	L10 and ((light or led or lamp) near3 (halo or ring or annular)) same led	US-PGPUB; USPAT; FPRS; EPO; JPO; DERWENT; IBM_TDB	OR	OFF	2013/07/08 10:23
L14	15	L13 and imag$4.clm.	US-PGPUB; USPAT; FPRS; EPO; JPO; DERWENT; IBM_TDB	OR	OFF	2013/07/08 10:23
L15	41	12 not L14	US-PGPUB; USPAT;	OR	OFF	2013/07/08 10:23

			FPRS; EPO; JPO; DERWENT; IBM_TDB			
L16	23	L10 and ((light or led or lamp) near3 (halo or ring or annular)) with excit$6	US-PGPUB; USPAT; FPRS; EPO; JPO; DERWENT; IBM_TDB	OR	OFF	2013/07/08 10:29
L17	4	L10 and (((light or led or lamp) near3 (halo or ring or annular)) with excit$6) same imag$4	US-PGPUB; USPAT; FPRS; EPO; JPO; DERWENT; IBM_TDB	OR	OFF	2013/07/08 10:29
L27	68	(((light or led or lamp) near3 (halo or ring or annular)) same (excit$6 with fluoresc$6)) same imag$4	US-PGPUB; USPAT; FPRS; EPO; JPO; DERWENT; IBM_TDB	OR	OFF	2013/07/08 10:35
L28	68	27 not L14	US-PGPUB; USPAT; FPRS; EPO; JPO; DERWENT; IBM_TDB	OR	OFF	2013/07/08 10:36
L29	2	(((led) near3 (halo or ring or annular)) same (excit$6 with fluoresc$6)) same imag$4	US-PGPUB; USPAT; FPRS; EPO; JPO; DERWENT; IBM_TDB	OR	OFF	2013/07/08 10:41
L30	5	(((light or led or lamp) near3 (halo or ring or annular)) same (excit$6 with fluoresc$6)) same imag$4 same led	US-PGPUB; USPAT; FPRS; EPO; JPO; DERWENT; IBM_TDB	OR	ON	2013/07/08 10:42
S1	1	13/222688	US-PGPUB; USPAT; FPRS; EPO; JPO; DERWENT; IBM_TDB	OR	OFF	2013/01/25 15:03
S2	564	(Nelson near Michael).in.	US-PGPUB; USPAT; FPRS; EPO; JPO; DERWENT; IBM_TDB	OR	OFF	2013/01/25 15:03
S3	38	(Nelson near Michael).in. and fluoresc$4	US-PGPUB; USPAT; FPRS; EPO; JPO; DERWENT; IBM_TDB	OR	OFF	2013/01/25 15:04
S4	4	(Nelson near Michael).in. and fluoresc$4 and ((light near source) same diffus$4)	US-PGPUB; USPAT;	OR	OFF	2013/01/25 15:05

			FPRS; EPO; JPO; DERWENT; IBM_TDB			
S5	81	("4585934" | "4863690" | "5414258" | "5587583" | "5680492" | "6004767" | "6038038" | "7298415" | "7383078" | "7449615" | "7461652" | "7555334" | "7581191" | "4863690" | "5680492" | "5818977" | "6004767" | "6097025" | "6642499" | "6922246" | "7255851" | "7464707" | "7466418" | "7555332" | "7595838" | "7663664" | "20040121175" | "5672881" | "5689110" | "6901279" | "7116354" | "7177024" | "7555332" | "7589786" | "7595838" | "7599731" | "5039868" | "5202091" | "6775567" | "6919919" | "7474399" | "4885544" | "5515161" | "5542012" | "5840572" | "5964220" | "6205244" | "6922246" | "7255851" | "7299420" | "7331341" | "7616985" | "7449567" | "7461652" | "7555334" | "7589786" | "7603167" | "5454437" | "3800079" | "4687325" | "5008548" | "5898802" | "5986271" | "6377353" | "6614452" | "20010028510" | "4593728" | "4687325" | "4948975" | "5414258" | "5515161" | "6871767" | "7196190" | "7449615" | "7474398" | "7616985" | "5089895" | "3949162" | "5202091" | "6097025" | "6642499" | "7503323" | "3949162" | "4196994" | "4343021" | "4885544" | "5008548" | "5672881" | "5689110" | "5840572" | "5865754" | "5964220" | "5986271" | "6217847" | "7113217" | "7190991" | "7383078" | "7503323" | "7581191" | "7599731" | "20040247170" | "20090268426" | "4196994" | "4343021" | "6217847" | "6754008" | "6894289" | "6919919" | "7196190" | "7449567" | "7464707" | "7474398" | "7603167" | "5587583" | "5898802" | "6377353" | "6754008" | "6901279" | "7177024" | "7299420" | "20050265024" | "3871767" | "4593728" | "4948975" | "5818977" | "6775567" | "7113217" | "7403812" | "7474399" | "7663664" | "0458934" | "5401465" | "5542012" | "6038038" | "6154277" | "6614452" | "7116354" | "7331341" | "4298887" | "5039868" | "5401465" | "5865754" | "6154277" | "7190991" | "7466418" | "3800079" | "4298887" | "6205244" | "6894289" | "7298415" | "7403812").PN.	US-PGPUB; USPAT	OR	OFF	2013/01/25 15:07
S6	2234	(camera or detect$4 or imager or imaging) with (light or led or lamp) with (halo or ring or surround$4) with (opening or aperture or hole or fov or (field near view))	US-PGPUB; USPAT; FPRS; EPO; JPO; DERWENT; IBM_TDB	OR	OFF	2013/01/25 15:21
S7	412	S6 and ((light or led or lamp) with diffus$4)	US-PGPUB; USPAT;	OR	OFF	2013/01/25 15:21

			FPRS; EPO; JPO; DERWENT; IBM_TDB			
S8	58	S7 and "250".clas.	US-PGPUB; USPAT; FPRS; EPO; JPO; DERWENT; IBM_TDB	OR	OFF	2013/01/25 15:23
S9	3	(camera or detect$4 or imager or imaging) with ((multiple or plurality) near2 (receptacle or ight or led or lamp)) with (halo or ring or surround$4) with (opening or aperture or hole or fov or (field near view))	US-PGPUB; USPAT; FPRS; EPO; JPO; DERWENT; IBM_TDB	OR	OFF	2013/01/25 21:09
S10	96	(camera or detect$4 or imager or imaging) with ((multiple or plurality) near2 (receptacle or ight or led or lamp)) with (opening or aperture or hole or fov or (field near view))	US-PGPUB; USPAT; FPRS; EPO; JPO; DERWENT; IBM_TDB	OR	OFF	2013/01/25 21:12
S11	4	S10 and "250".clas.	US-PGPUB; USPAT; FPRS; EPO; JPO; DERWENT; IBM_TDB	OR	OFF	2013/01/25 21:13
S12	81	("4585934" | "4863690" | "5414258" | "5587583" | "5680492" | "6004767" | "6038038" | "7298415" | "7383078" | "7449615" | "7461652" | "7555334" | "7581191" | "4863690" | "5680492" | "5818977" | "6004767" | "6097025" | "6642499" | "6922246" | "7255851" | "7464707" | "7466418" | "7555332" | "7595838" | "7663664" | "20040121175" | "5672881" | "5689110" | "6901279" | "7116354" | "7177024" | "7555332" | "7589786" | "7595838" | "7599731" | "5039868" | "5202091" | "6775567" | "6919919" | "7474399" | "4885544" | "5515161" | "5542012" | "5840572" | "5964220" | "6205244" | "6922246" | "7255851" | "7299420" | "7331341" | "7616985" | "7449567" | "7461652" | "7555334" | "7589786" | "7603167" | "5454437" | "3800079" | "4687325" | "5008548" | "5898802" | "5986271" | "6377353" | "6614452" | "20010028510" | "4593728" | "4687325" | "4948975" | "5414258" | "5515161" | "6871767" | "7196190" | "7449615" | "7474398" | "7616985" | "5089895" | "3949162" | "5202091" | "6097025" | "6642499" | "7503323" | "3949162" | "4196994" | "4343021" | "4885544" | "5008548" | "5672881" | "5689110" | "5840572" | "5865754" | "5964220" | "5986271" | "6217847" | "7113217" | "7190991" | "7383078" | "7503323" | "7581191" | "7599731" | "20040247170" |	US-PGPUB; USPAT	OR	OFF	2013/01/25 21:13

		"20090268426" | "4196994" | "4343021" | "6217847" | "6754008" | "6894289" | "6919919" | "7196190" | "7449567" | "7464707" | "7474398" | "7603167" | "5587583" | "5898802" | "6377353" | "6754008" | "6901279" | "7177024" | "7299420" | "20050265024" | "3871767" | "4593728" | "4948975" | "5818977" | "6775567" | "7113217" | "7403812" | "7474399" | "7663664" | "0458934" | "5401465" | "5542012" | "6038038" | "6154277" | "6614452" | "7116354" | "7331341" | "4298887" | "5039868" | "5401465" | "5865754" | "6154277" | "7190991" | "7466418" | "3800079" | "4298887" | "6205244" | "6894289" | "7298415" | "7403812").PN.				
S13	0	S12 and S10	US-PGPUB; USPAT; FPRS; EPO; JPO; DERWENT; IBM_TDB	OR	OFF	2013/01/25 21:13
S14	5	S12 and (camera or detect$4 or imager or imaging) with (light or led or lamp) with (halo or ring or surround$4) with (opening or aperture or hole or fov or (field near view))	US-PGPUB; USPAT; FPRS; EPO; JPO; DERWENT; IBM_TDB	OR	OFF	2013/01/25 21:22
S15	46	S12 and fluoresc$7	US-PGPUB; USPAT; FPRS; EPO; JPO; DERWENT; IBM_TDB	OR	OFF	2013/01/25 21:25
S16	2	("3609451" | "5134277").PN. OR ("6943333").URPN.	US-PGPUB; USPAT; USOCR	OR	OFF	2013/01/25 21:26
S17	1088	250/461.1.ccls.	US-PGPUB; USPAT; FPRS; EPO; JPO; DERWENT; IBM_TDB	OR	OFF	2013/01/27 14:54
S18	2855	250/458.1.ccls.	US-PGPUB; USPAT; FPRS; EPO; JPO; DERWENT; IBM_TDB	OR	OFF	2013/01/27 14:54
S19	1557	250/459.1.ccls.	US-PGPUB; USPAT; FPRS; EPO; JPO; DERWENT; IBM_TDB	OR	OFF	2013/01/27 14:54
S20	4362	S17 S18 S19	US-PGPUB; USPAT; FPRS; EPO; JPO; DERWENT;	OR	OFF	2013/01/27 14:54

			IBM_TDB			
S21	1	S20 and (camera or detect$4 or imager or imaging) with ((multiple or plurality) near2 (receptacle or ight or led or lamp)) with (opening or aperture or hole or fov or (field near view))	US-PGPUB; USPAT; FPRS; EPO; JPO; DERWENT; IBM_TDB	OR	OFF	2013/01/27 14:54
S22	2234	(camera or detect$4 or imager or imaging) with (light or led or lamp) with (halo or ring or surround$4) with (opening or aperture or hole or fov or (field near view))	US-PGPUB; USPAT; FPRS; EPO; JPO; DERWENT; IBM_TDB	OR	OFF	2013/01/27 14:55
S23	3	S22 and ((light or led or lamp) with diffus$4) and S20	US-PGPUB; USPAT; FPRS; EPO; JPO; DERWENT; IBM_TDB	OR	OFF	2013/01/27 14:55
S24	81	("4585934" | "4863690" | "5414258" | "5587583" | "5680492" | "6004767" | "6038038" | "7298415" | "7383078" | "7449615" | "7461652" | "7555334" | "7581191" | "4863690" | "5680492" | "5818977" | "6004767" | "6097025" | "6642499" | "6922246" | "7255851" | "7464707" | "7466418" | "7555332" | "7595838" | "7663664" | "20040121175" | "5672881" | "5689110" | "6901279" | "7116354" | "7177024" | "7555332" | "7589786" | "7595838" | "7599731" | "5039868" | "5202091" | "6775567" | "6919919" | "7474399" | "4885544" | "5515161" | "5542012" | "5840572" | "5964220" | "6205244" | "6922246" | "7255851" | "7299420" | "7331341" | "7616985" | "7449567" | "7461652" | "7555334" | "7589786" | "7603167" | "5454437" | "3800079" | "4687325" | "5008548" | "5898802" | "5986271" | "6377353" | "6614452" | "20010028510" | "4593728" | "4687325" | "4948975" | "5414258" | "5515161" | "6871767" | "7196190" | "7449615" | "7474398" | "7616985" | "5089895" | "3949162" | "5202091" | "6097025" | "6642499" | "7503323" | "3949162" | "4196994" | "4343021" | "4885544" | "5008548" | "5672881" | "5689110" | "5840572" | "5865754" | "5964220" | "5986271" | "6217847" | "7113217" | "7190991" | "7383078" | "7503323" | "7581191" | "7599731" | "20040247170" | "20090268426" | "4196994" | "4343021" | "6217847" | "6754008" | "6894289" | "6919919" | "7196190" | "7449567" | "7464707" | "7474398" | "7603167" | "5587583" | "5898802" | "6377353" | "6754008" | "6901279" | "7177024" | "7299420" | "20050265024" | "3871767" | "4593728" | "4948975" | "5818977" | "6775567" | "7113217" | "7403812" | "7474399" | "7663664" | "0458934" |	US-PGPUB; USPAT	OR	OFF	2013/01/27 15:00

		"5401465" | "5542012" | "6038038" | "6154277" | "6614452" | "7116354" | "7331341" | "4298887" | "5039868" | "5401465" | "5865754" | "6154277" | "7190991" | "7466418" | "3800079" | "4298887" | "6205244" | "6894289" | "7298415" | "7403812").PN.				
S25	8	S20 and S24	US-PGPUB; USPAT; FPRS; EPO; JPO; DERWENT; IBM_TDB	OR	OFF	2013/01/27 15:00
S26	280	362/3.ccls.	US-PGPUB; USPAT; FPRS; EPO; JPO; DERWENT; IBM_TDB	OR	OFF	2013/01/27 15:06
S27	4	S22 and S26	US-PGPUB; USPAT; FPRS; EPO; JPO; DERWENT; IBM_TDB	OR	OFF	2013/01/27 15:06
S28	3	"20090268426"	US-PGPUB; USPAT; FPRS; EPO; JPO; DERWENT; IBM_TDB	OR	OFF	2013/06/24 14:48
S29	2	"6454437".pn.	US-PGPUB; USPAT; FPRS; EPO; JPO; DERWENT; IBM_TDB	OR	OFF	2013/06/24 14:49
S30	746	led near3 receptacle	US-PGPUB; USPAT; FPRS; EPO; JPO; DERWENT; IBM_TDB	OR	OFF	2013/07/05 11:02
S31	14	S30 and "250".clas.	US-PGPUB; USPAT; FPRS; EPO; JPO; DERWENT; IBM_TDB	OR	OFF	2013/07/05 11:03
S32	90	S30 and fluorescen$4	US-PGPUB; USPAT; FPRS; EPO; JPO; DERWENT; IBM_TDB	OR	OFF	2013/07/05 11:05
S33	21	S30 and (fluorescen$4 near3 (excit$4 or detect$4 or sens$4 or illuminat$4))	US-PGPUB; USPAT; FPRS; EPO; JPO; DERWENT; IBM_TDB	OR	OFF	2013/07/05 11:06

S34	1120	250/461.1.ccls.	US-PGPUB; USPAT; FPRS; EPO; JPO; DERWENT; IBM_TDB	OR	OFF	2013/07/05 11:12
S35	2982	250/458.1.ccls.	US-PGPUB; USPAT; FPRS; EPO; JPO; DERWENT; IBM_TDB	OR	OFF	2013/07/05 11:12
S36	1678	250/459.1.ccls.	US-PGPUB; USPAT; FPRS; EPO; JPO; DERWENT; IBM_TDB	OR	OFF	2013/07/05 11:12
S37	4566	S34 S35 S36	US-PGPUB; USPAT; FPRS; EPO; JPO; DERWENT; IBM_TDB	OR	OFF	2013/07/05 11:12
S38	30	S37 and (camera or detect$4 or imager or imaging) with (light or led or lamp) with (halo or ring or surround$4 or annular) with (opening or aperture or hole or fov or (field near view))	US-PGPUB; USPAT; FPRS; EPO; JPO; DERWENT; IBM_TDB	OR	OFF	2013/07/05 11:13
S39	1	S30 and S37	US-PGPUB; USPAT; FPRS; EPO; JPO; DERWENT; IBM_TDB	OR	OFF	2013/07/05 11:48
S40	18	S30 and fluorescen$4.clm.	US-PGPUB; USPAT; FPRS; EPO; JPO; DERWENT; IBM_TDB	OR	OFF	2013/07/05 11:49
S41	40	led near3 ((array or multiple or plural$4) near receptacle)	US-PGPUB; USPAT; FPRS; EPO; JPO; DERWENT; IBM_TDB	OR	ON	2013/07/05 11:51
S42	16	"10040330"	US-PGPUB; USPAT; FPRS; EPO; JPO; DERWENT; IBM_TDB	OR	OFF	2013/07/05 16:26
S43	267	S37 and ((light or led or lamp) near3 (halo or ring or surround$4 or annular))	US-PGPUB; USPAT; FPRS; EPO; JPO; DERWENT; IBM_TDB	OR	OFF	2013/07/05 16:27

S44	78	S43 and imag$4.clm.	US-PGPUB; USPAT; FPRS; EPO; JPO; DERWENT; IBM_TDB	OR	OFF	2013/07/05 16:28
S45	133	S37 and ((light or led or lamp) near3 (halo or ring or annular))	US-PGPUB; USPAT; FPRS; EPO; JPO; DERWENT; IBM_TDB	OR	OFF	2013/07/05 16:28
S46	56	S45 and imag$4.clm.	US-PGPUB; USPAT; FPRS; EPO; JPO; DERWENT; IBM_TDB	OR	OFF	2013/07/05 16:28
S47	19	S37 and ((light or led or lamp) near3 (halo or ring or annular)) same led	US-PGPUB; USPAT; FPRS; EPO; JPO; DERWENT; IBM_TDB	OR	OFF	2013/07/05 16:29
S48	15	S47 and imag$4.clm.	US-PGPUB; USPAT; FPRS; EPO; JPO; DERWENT; IBM_TDB	OR	OFF	2013/07/05 16:29

EAST Search History (Interference)

<This search history is empty>

7/8/2013 11:24:19 AM
C:\Users\mtaningco\Documents\EAST\Workspaces\13222688.wsp

SPECTRAL_0000870

IN THE UNITED STATES PATENT AND TRADEMARK OFFICE

In Re Application of:	)	
	)	Examiner: Taningco, M.
NELSON, Michael, B., *et al.*	)	
	)	Group Art Unit: 2884
Serial No. 13/222,688	)	
	)	Confirm. No.: 5910
Filing Date: August 31, 2011	)	
	)	Atty. Dkt.: SPEC US-4
For: EXCITATION LIGHT SOURCE ASSEMBLY	)	(027560-0014)
	)	

AMENDMENT UNDER 37 C.F.R. §§ 1.111 & 1.121

To: The Commissioner for Patents
P.O. Box 1450
Alexandria, VA 22313-1450

Sir:

In response to the office action, dated July 10, 2013, please amend the above-identified patent application as follows:

A Listing of Claims begins on page 2 of this paper.

Remarks begin on page 9 of this paper.

SPECTRAL_0000871

Listing of Claims:

This listing of claims will replace all prior versions and listings of claims in the application:

Listing of Claims:

1. (Previously Presented) An excitation light source assembly, comprising:

a housing defining a central opening therein and a plurality of lamp receptacles surrounding the central opening, said housing being mountable to a support structure so that the central opening is aligned with a camera also mounted to the support structure so that a field of view of the camera is unobstructed by said housing;

a light source positioned within each of the plurality of lamp receptacles; and

a diffuser positioned within at least some of the plurality of lamp receptacles, each of said diffusers diffusing light produced by each of said light sources; and

a control system operatively connected to each of said light sources, said control system operating selected ones of said light sources to provide a desired excitation illumination to an object within the field of view of said camera, the object fluorescing in response to the excitation illumination provided by said light sources.

2. (Original) The excitation light source assembly of claim 1 wherein at least one of said light sources comprises a narrow-band light source that emits light having a bandwidth of about 35 nm.

3. (Original) The excitation light source assembly of claim 2 wherein said at least one narrow-band light source comprises a light emitting diode.

4. (Original) The excitation light source assembly of claim 1, further comprising at least one filter positioned adjacent at least one diffuser in at least one of the lamp receptacles defined by said housing.

5. (Original) The excitation light source assembly of claim 4, wherein said at least one filter comprises a notch filter having a wavelength bandpass range of about 30 nm.

6. (Original) The excitation light source assembly of claim 1, wherein at least one of the light sources comprises a broad-band light source.

7. (Previously Presented) The excitation light source assembly of claim 1, wherein at least some of said plurality of lamp receptacles comprise opposed pairs of lamp receptacles on opposite sides of said central opening, each opposed pair of lamp receptacles receiving light sources that produce light of the same color.

8. (Original) The excitation light source assembly of claim 7, further comprising ten opposed pairs of lamp receptacles on opposite sides of said central opening.

9-18 (Canceled).

19. (Previously Presented) An assembly, comprising:

a support structure;

a camera mounted to said support structure;

an excitation light source assembly mounted to said support structure, said excitation light source assembly comprising:

a housing defining a central opening therein and a plurality of lamp receptacles surrounding the central opening, said housing being mounted to said support structure so that the central opening is aligned with said camera and so that a field of view of said camera is substantially unobstructed by said housing;

at least one narrow-band light source positioned within at least one of the plurality of lamp receptacles; and

a diffuser positioned within at least some of the plurality of lamp receptacles, each of said diffusers diffusing light produced by each of said narrow-band light sources; and

a control system operatively connected to each of said narrow-band light sources, said control system operating selected ones of said narrow-band light sources to provide a desired excitation illumination to a fluorescent material within the field of view of said camera, the fluorescent material fluorescing in response to the excitation illumination.

20. (Original) The assembly of claim 19, further comprising a light filter positioned adjacent each of the diffusers.

21. (Original) The assembly of claim 19, wherein each of the lamp receptacles defined by said housing are angled with respect to

a central axis of said housing so that light emitted from each of said narrow-band light sources is directed to a desired area within the field of view of said camera.

22. (Original) The assembly of claim 19, wherein each of said narrow-band light sources is selected to provide desired number of illumination bands over a desired spectral range.

23. (Original) The assembly of claim 22, wherein the desired spectral range is from about 430 nm to about 745 nm.

24. (Original) The assembly of claim 22, wherein the desired number of illumination bands is 10.

25. (Original) The assembly of claim 22, wherein each desired illumination band has a bandwidth ranging from about 30 nm to about 35 nm.

26. (Original) The assembly of claim 19, wherein each of said narrow-band light sources comprises a light emitting diode.

27. (Original) The assembly of claim 19, wherein said housing comprises a polyoxymethylene thermoplastic material.

28. (Original) The assembly of claim 22, wherein the desired spectral range is from about 430 nm to about 900 nm.

29. (Original) The assembly of claim 22, wherein the desired spectral range is from about 430 nm to about 800 nm.

30. (Previously Presented) The excitation light source

assembly of claim 1, wherein the light source positioned within each of the plurality of lamp receptacles does not extend beyond the lamp receptacle.

31. (Previously Presented) The excitation light source assembly of claim 1, further comprising a plurality of light sources positioned within at least some of the lamp receptacles so that the plurality of light sources do not extend beyond the lamp receptacles.

32. (Previously Presented) The excitation light source assembly of claim 31, wherein said plurality of light sources is three light sources.

33. (Previously Presented) The excitation light source assembly of claim 1, wherein the plurality of light receptacles defined by said housing comprise a plurality of large diameter receptacles and a plurality of small diameter receptacles.

34. (Previously Presented) The excitation light source assembly of claim 1, wherein the plurality of light receptacles defined by said housing comprise generally cylindrically shaped openings having first and second open ends, said excitation light source assembly further comprising a circuit board mounted to a first side of said housing, said light sources being mounted to said circuit board so that said light sources extend through the first open ends of the generally cylindrically-shaped light receptacles.

35. (Previously Presented) An excitation light source assembly, comprising:

a housing defining a central opening therein and a plurality of lamp receptacles therein surrounding the central opening, said housing being mountable to a support structure so that the central opening is aligned with a camera also mounted to the support structure so that a field of view of the camera is unobstructed by said housing;

a light source positioned within each of the plurality of lamp receptacles so that said light sources do not extend beyond the lamp receptacles; and

a control system operatively connected to each of said light sources, said control system operating selected ones of said light sources to provide a desired excitation illumination to an object within the field of view of the camera, th excitation illumination causing fluorescent materials in the object to fluoresce, the camera capturing an image of the fluorescing material in the object.

36. (Previously Presented) The excitation light source assembly of claim 35, wherein said plurality of lamp receptacles defined by said housing comprise a plurality of large diameter lamp receptacles and a plurality of small diameter lamp receptacles, said large diameter lamp receptacles receiving a plurality of said light sources, said small diameter receptacles receiving a single light source.

37. (Previously Presented) The excitation light source assembly of claim 35, wherein the plurality of light receptacles defined by said housing comprise generally cylindrically shaped openings having first and second open ends, said excitation light source assembly further comprising a circuit board mounted to a first side of said housing, said light sources being mounted to

said circuit board so that said light sources extend through the first open ends of the generally cylindrically shaped light receptacles.

SPECTRAL_0000878

R E M A R K S

Claims 1-8 and 19-37 are pending. Claims 9-18 are canceled as being drawn to non-elected inventions. Claims 1, 7, 19, and 30-37 are previously presented. Claims 2-6, 8, and 20-29 stand as originally filed. Re-examination and reconsideration are requested.

In the office action, dated July 10, 2013, the examiner noted that he found applicants' previous arguments persuasive and withdrew the previous claim rejections. The examiner then made new rejections similar to the old rejections, except that the examiner added a new reference, Chapman *et al.*, U.S. Patent No. 5,984,494 ("Chapman"). In particular, the examiner rejected claims 1-4, 6-8, 19-26, and 28-37 as being unpatentable Pohlert *et al.*, U.S. Patent Application Publication No. US 2009/0268426 ("Pohlert") in view of Kelly, U.S. Patent No. 6,454,437 ("Kelly"), Nomura, Japanese Patent Application Publication No. JP10-040330 ("Nomura") and Chapman for the reasons specified on pages 3-12 of the office action. The examiner rejected claim 5 under Section 103(a) as being unpatentable over Pohlert in view of Kelly, Nomura, Chapman, and Furze *et al.*, U.S. Patent Application Publication No. US 2004/0247170 ("Furze") for the reasons specified on pages 12 and 13 of the office action. The examiner also rejected claim 27 under Section 103(a) as being unpatentable over Pohlert in view of Kelly, Nomura, Chapman, and Flexman *et al.*, U.S. Patent Application Publication No. US 2004/0121175 ("Flexman") for the reasons specified on pages 13 and 14 of the office action.

The Obviousness Rejections

The examiner's rejections are in error because Chapman is non-analogous art, thus cannot be combined with the other references to support the examiner's obviousness rejections. However, even if it

SPECTRAL_0000879

would be permissible to combine Chapman with the other references, the examiner has failed to explain how the divergent, and in some cases contrary, teachings of the references could be reconciled to reach the claimed invention. Consequently, the examiner has failed to establish the required prima-facie case of obviousness. The pending claims thus retain their presumption of patentability and are allowable.

Legal Standard for Determining Whether Prior Art is Analogous

Only analogous prior art can be used as the basis of an obviousness rejection. In re Bigio, 381 F.3d 1320, 1325 (Fed. Cir. 2004); In re Clay, 966 F.2d 656, 658 (Fed. Cir. 1992). Prior art is considered analogous if: (1) it is within the same field of endeavor, regardless of the problem addressed; and (2) if the reference is not within the inventor's field of endeavor, if "the reference is still reasonably pertinent to the particular problem with which the inventor is involved." In re Bigio, 381 F.3d at 1325. The Federal Circuit has held that "[t]his test for analogous art requires the PTO to determine the appropriate field of endeavor by reference to the explanations of the invention's subject matter in the patent application, including the embodiments, function, and structure of the claimed invention." In re Bigio, 381 F.3d at 1325. Further, the Federal Circuit has held that a "reference is reasonably pertinent if, even though it may be in a different field from that of the inventor's endeavor, it is one which, because of the matter with which it deals, logically would have commended itself to an inventor's attention in considering his problems. Thus, the purposes of both the invention and the prior art are important in determining whether the reference is reasonably pertinent to the problem the invention attempts to solve." In re

SPECTRAL_0000880

Clay, 966 F.2d at 659.

The present invention relates to systems for exciting fluorescent materials and more particularly to systems for exciting fluorescent materials in molecular imaging systems. See, for example, paragraph [0002] of the pending application. In one embodiment, the assembly comprises a housing defining a central opening therein and a plurality of lamp receptacles surrounding the central opening. The housing is mountable to a support structure having a camera mounted thereto so that a filed of view of the camera is substantially unobstructed by the housing. A light source is positioned within each of the plurality of lamp receptacles. A diffuser is positioned within at least some of the lamp receptacles. A control system connected to each of the light sources operates selected ones of the light sources to provide a desired excitation illumination to an object within the field of view of the camera. See, for example, pending claim 1. The excitation light source assembly of the present invention may be used to advantage to illuminate an object or specimen with light in multiple narrow bands or colors, thereby allowing a single excitation light source assembly to be used in imaging applications involving a wide range of fluorescent materials that are excited over a wide range of wavelengths. See, for example, paragraph [0032] of the pending application.

The Chapman reference is related to "aircraft landing lights and automobile headlights" (col. 1, lines 14-16). Chapman seeks to solve the problem of providing a landing light system suitable for both covert and conventional aircraft operations (col. 1, lines 51-54). According to Chapman, prior art systems involved the use of multiple incandescent lamps and cold mirrors or filters to block the unwanted wavelengths (col. 1, lines 18-29). However, such systems tended to trap excess heat, which dramatically shortened

bulb life and also involved complex mechanical arrangements (col. 1, lines 22-29). Chapman's aircraft landing light involves a conventional, halogen-type incandescent lamp that is surround by an array of infra-red LEDs. A pilot flying an aircraft provided with Chapman's landing light can illuminate the incandescent lamp for conventional, i.e., visually-based landings. Alternatively, for covert operations, the pilot can illuminate the infra-red LEDs and land with the assistance of a suitable infra-red or "night-vision" system. Clearly, the field of endeavor of Chapman is not the same as that of the present invention.

However, as mentioned above, the Chapman reference still may be analogous if it is "reasonably pertinent" to the problems solved by the present invention. In re Clay, supra, at 1061. The present invention is concerned with the problems of activating or exciting various types of fluorescent materials being imaged by molecular imaging systems. In particular, because such molecular imaging systems are used to image a wide range of fluorescent compositions and materials, many of which must be activated or excited by light of different wavelengths, the present invention seeks an excitation light source assembly that is capable of exciting a wide range of fluorescent materials over a wide range of wavelengths. Chapman, on the other hand, looks to solve the problems associated with vehicle lighting systems (e.g., for automobiles and aircraft), and in particular seeks to provide lighting systems that can be used in both conventional and covert-type situations.

Clearly, the problems addressed by Chapman are not reasonably pertinent to the problems with which the present invention is involved. Chapman is not concerned with exciting fluorescent materials at all, much less exciting different types of fluorescent materials that can only be excited by light of different wavelengths. Of course, Chapman's system does not even involve the

use of a camera, much less a camera that is positioned with respect to the lighting system in a way that allows the camera to be optimally positioned with respect to the object being illuminated, as does the present invention. Accordingly, a person having ordinary skill in the art would not reasonably expect to solve the problems of producing excitation illumination system for molecular imaging systems by considering a reference dealing with vehicle lighting systems that can be used in covert-type operations. Chapman is thus non-analogous art and Chapman cannot be combined with the other references to support an obviousness rejection under Section 103.

Putting aside the fact that Chapman is non-analogous art, even if it would be proper to consider Chapman in combination with the other references, the examiner has failed to explain how the divergent, and in some cases contrary, teachings of the references could be reconciled to reach the claimed invention. Consequently, the examiner has failed to establish the required prima-facie case of obviousness. The pending claims thus retain their presumption of patentability and are allowable.

The Pohlert reference discloses various types of light panels for film, television, or video production. Pohlert's lighting panels are provided with a plurality of light sources, typically LEDs or fluorescent lamps. Pohlert specifically seeks lighting panels that produce illumination suitable for "the special needs of the film, commercial, or photographic industries, or with live stage performances...". See, for example, paragraph [0018] of Pohlert. Significantly, Pohlert states that the illumination needs in this field differ "substantially from what is offered by object inspection lighting apparatus." Pohlert goes on to conclude that lighting systems for such object inspection apparatus are "generally not suitable for the special needs" of the type of

lighting systems he discloses. Paragraph [0018] of Pohlert.

Kelly and Nomura disclose illumination systems for object inspection apparatus of the type Pohlert characterizes as "not suitable" for the types of lighting systems Pohlert uses. The Kelly reference discloses a ring lighting system for "industrial instrumentation in which it is desired to illuminate an object which is being inspected by a sensor or camera." Col. 1, lines 6-7 of Kelly. Kelly's ring lighting system uses a plurality of light sources in combination with a ring-shaped or annular lens to provide increased uniformity. See, for example, col. 3, lines 41-49 and lines 54-56 of Kelly. The light sources Kelly uses comprise LED "chips" having very small dimensions (e.g., about 0.25 mm square) (col. 8, line 42) that are positioned very closely together (i.e., about 0.5 mm)(col. 6, line 58).

Nomura also teaches a machine illumination system, but seeks to solve the problem of more efficiently detecting a fluorescent pattern on mail. Nomura solves this problem by providing an additional light emitting member 5 that emits light of a longer wavelength (of wavelength Lb) after being excited by light of a shorter wavelength (of wavelength La) from the ultraviolet lamps 4. Light of the two different wavelengths is then directed onto the fluorescent pattern to be detected.

As already described, Chapman seeks to solve the problem of vehicle lighting systems, and in particular aircraft landing light systems, that are suitable for both covert and conventional operations.

The diverse teachings and problems addressed by Pohlert, Kelly, Nomura, and Chapman preclude their combination in the manner espoused by the examiner. First, Pohlert specifically states that the illumination needs in his field (i.e., film, television, and video production) "differ substantially from what is offered by

object inspection lighting apparatus," such as those disclosed by Kelly and Nomura. Pohlert goes on to conclude that "lighting apparatus specially adapted for illumination of objects to be inspected are generally not suitable" for the types of lighting systems he provides. See, for example, paragraph [0018] of Pohlert. Thus, a person having ordinary skill in the art would not seek to combine the teachings of Pohlert with those of Kelly and Nomura because Pohlert specifically counsels against such a combination.

While Pohlert concludes that object inspection lighting systems such as Kelly's are "generally not suitable" in studio lighting applications, The Kelly reference also teaches away from aspects of the Pohlert studio lighting system. More specifically, Kelly *teaches against* using the individually packaged LEDs of the type that Pohlert prefers. Kelly decries the use of discrete or individual LEDs, noting that "the pointing accuracy of individual LEDs is poor" which leads to a "lack of uniformity of the illuminated area." See, for example, col. 1, lines 65 and 66 of Kelly. However, such individually packaged LEDs are exactly the type used by Pohlert. See, for example, Figures 4, 7, 8, 32, and 35 of Pohlert.

The teachings of the Chapman reference are similarly unrelated to the teachings of the studio lighting system of Pohlert and the object inspection systems of Kelly and Nomura. Chapman's teachings relate to "aircraft landing lights and automobile headlights" (col. 1, lines 14-16). There is nothing in Chapman that would lead a person having ordinary skill in the art to look to the studio lighting system art (as Pohlert) or to the object inspection art (as Kelly and Nomura) to develop the claimed excitation light source assembly. Similarly, there is nothing in Pohlert, Kelly, and Nomura that would lead a person having ordinary skill in the

art to look to the aircraft landing light art. Even if such a person would look to Chapman, he would certainly not view Chapman as suggesting a modification to his landing light system that would replace the incandescent landing light with a camera, because to do so would make the Chapman system inoperative for its intended purpose. A modification that would make a prior art system inoperative is not obvious.

In adding Chapman to the other references, the examiner has focused solely on finding a reference that discloses a claimed element (i.e., a lighting system with a housing that defines a plurality of lamp receptacles therein) not disclosed by the other references, but without regard to what the various references teach as a whole. As such, the examiner's new rejections amount to nothing more than hindsight reconstruction. That is, rather than considering the references as a whole and how they would be understood by a person having ordinary skill in the art, the examiner's new rejections are based on nothing more than the mere identification in the references of the various elements and limitations of the rejected claims. This type of rationale remains an impermissible basis for rejecting claims, even after KSR: A claim "composed of several elements is not proved obvious merely by demonstration that each of its elements was, independently, known in the prior art." KSR Int'l Co. v. Teleflex, Inc., 127 S.Ct. 1727, 1741 (2007).

In summation then, the unrelated and, in some instances opposed, teachings of Pohlert, Kelly, Nomura, and Chapman precludes any rational reason for their combination: That which Pohlert embraces, Kelly decries, and vice-versa. Chapman's aircraft landing light system isn't even directed to illumination systems for cameras. Consequently, there can be no rational basis to combine Chapman with any of the other references, much less make

Chapman's landing light system inoperable by removing the incandescent landing light so that it can be replaced by a camera. Because the teachings of Pohlert, Kelly, Nomura and Chapman are so divergent, no rational basis can be articulated for their combination. Therefore, they cannot be used to establish a prima-facie case of obviousness. The pending claims retain their presumption of patentability and should be allowed.

Re the Rejection of Claim 5:

The examiner rejected claim 5 as being obvious over Pohlert in view of Kelly, Nomura and Chapman, and further in view of Furze. These rejections are improper for the same reasons expressed above for Pohlert, Kelly, Nomura, and Chapman alone. The disclosure in Furze of narrow-band light filters does nothing to knit together the unrelated teachings of the other references.

Furze discloses an object inspection system for inspecting golf balls. Thus, the Furze system (like the object inspection systems of Kelly and Nomura), is of the type Pohlert finds "not suitable" for the type of video and film production lighting systems that he discloses. Chapman's aircraft landing light system has nothing to do with the object inspection systems of Furze, Nomura, and Kelly and is, of course, unrelated to the studio lighting system of Pohlert. Again, other than to identify where the claimed elements can be found in these various prior art references, the examiner has not explained how a person having ordinary skill in the art would know to pick certain elements from a studio lighting system, combine them with other elements from machine inspection systems for letters and golf balls, and then add features from an aircraft landing light system, all to develop the claimed excitation light source assembly for molecular imaging systems. Absent such an explanation, the examiner has failed to

SPECTRAL_0000887

establish the required prima-facie case of obviousness. Claim 5 is therefore patentable over Pohlert, Kelly, Nomura, Chapman, and Furze.

Re the Rejection of Claim 27:

The examiner rejected claim 27 as being obvious over Pohlert in view of Kelly, Nomura and Chapman, and further in view of Flexman. These rejections are also improper for the same reasons expressed above for the rejections based on Pohlert, Kelly, Nomura, and Chapman alone. Flexman's disclosure of layered articles made from polyoxymethylene thermoplastic material does not unite the divergent teachings of the various references. There is still no rational basis for combining them.

Again, Pohlert specifically states that lighting systems for object inspection systems, such as those disclosed in Kelly and Nomura, are "not suitable" for the types of lighting systems Pohlert is concerned about. If this were not enough, Kelly also specifically teaches away from the types of individual LED illuminators that Pohlert prefers. Chapman's aircraft landing lights are even further afield and would not rationally lead a person having ordinary skill in the art to combine any of the elements of Chapman's landing light with any of the elements from Pohlert, Kelly, and Nomura. Flexman is, of course, unrelated to any of the others because Flexman is concerned with the manufacture of layered plastic articles made from polyoxymethylene. There simply is nothing in Flexman to recommend it to any of Pohlert, Kelly, Nomura, and Chapman for any reason, much less the reasons espoused by the examiner. Claim 27 remains presumptively patentable over these references.

* * *

Applicants believe that all of the claims pending in this patent application are allowable and that all other issues raised by the examiner have been satisfactorily addressed. Applicants respectfully request the examiner to reconsider the rejections and grant an early allowance. If any questions or issues remain to be resolved, the examiner is requested to contact the Applicants' attorney at the telephone number listed below.

The applicants believe that any fees required have been paid. However, if additional fees are required, the applicant authorizes the charge of such fees to Fennemore Craig, P.C., Deposit Account No. 06-0590.

Respectfully submitted,

FENNEMORE CRAIG, P.C.

/Bruce E. Dahl/

Bruce E. Dahl, Esq.
Attorney for Applicants
PTO Registration No. 33,670
1700 Lincoln Street, Suite 2900
Denver, CO 80203-4529
(303) 291-3200

Date: October 10, 2013

Electronic Acknowledgement Receipt

EFS ID:	17090856
Application Number:	13222688
International Application Number:	
Confirmation Number:	5910
Title of Invention:	EXCITATION LIGHT SOURCE ASSEMBLY
First Named Inventor/Applicant Name:	Michael B. Nelson
Customer Number:	27104
Filer:	Bruce E. Dahl
Filer Authorized By:	
Attorney Docket Number:	SPEC US-4 (027560-0014)
Receipt Date:	10-OCT-2013
Filing Date:	31-AUG-2011
Time Stamp:	17:46:28
Application Type:	Utility under 35 USC 111(a)

Payment information:

Submitted with Payment	no

File Listing:

Document Number	Document Description	File Name	File Size(Bytes)/ Message Digest	Multi Part /.zip	Pages (if appl.)
1	Amendment/Req. Reconsideration-After Non-Final Reject	Amendment.pdf	134546 6174b2433694d2d521c748a13ae35d60280342ee	no	19

Warnings:	
Information:	

Total Files Size (in bytes):	134546

This Acknowledgement Receipt evidences receipt on the noted date by the USPTO of the indicated documents, characterized by the applicant, and including page counts, where applicable. It serves as evidence of receipt similar to a Post Card, as described in MPEP 503.

New Applications Under 35 U.S.C. 111
If a new application is being filed and the application includes the necessary components for a filing date (see 37 CFR 1.53(b)-(d) and MPEP 506), a Filing Receipt (37 CFR 1.54) will be issued in due course and the date shown on this Acknowledgement Receipt will establish the filing date of the application.

National Stage of an International Application under 35 U.S.C. 371
If a timely submission to enter the national stage of an international application is compliant with the conditions of 35 U.S.C. 371 and other applicable requirements a Form PCT/DO/EO/903 indicating acceptance of the application as a national stage submission under 35 U.S.C. 371 will be issued in addition to the Filing Receipt, in due course.

New International Application Filed with the USPTO as a Receiving Office
If a new international application is being filed and the international application includes the necessary components for an international filing date (see PCT Article 11 and MPEP 1810), a Notification of the International Application Number and of the International Filing Date (Form PCT/RO/105) will be issued in due course, subject to prescriptions concerning national security, and the date shown on this Acknowledgement Receipt will establish the international filing date of the application.

UNITED STATES PATENT AND TRADEMARK OFFICE

UNITED STATES DEPARTMENT OF COMMERCE
United States Patent and Trademark Office
Address: COMMISSIONER FOR PATENTS
P.O. Box 1450
Alexandria, Virginia 22313-1450
www.uspto.gov

APPLICATION NO.	FILING DATE	FIRST NAMED INVENTOR	ATTORNEY DOCKET NO.	CONFIRMATION NO.
13/222,688	08/31/2011	Michael B. Nelson	SPEC US-4 (027560-0014)	5910

27104 7590 01/09/2014

FENNEMORE CRAIG, P.C.
1700 Lincoln Street
SUITE 2900
DENVER, CO 80203

EXAMINER	
TANINGCO, MARCUS H	

ART UNIT	PAPER NUMBER
2884	

MAIL DATE	DELIVERY MODE
01/09/2014	PAPER

Please find below and/or attached an Office communication concerning this application or proceeding.

The time period for reply, if any, is set in the attached communication.

Office Action Summary	Application No. 13/222,688	Applicant(s) NELSON ET AL.	
	Examiner MARCUS TANINGCO	Art Unit 2884	AIA (First Inventor to File) Status No

-- The MAILING DATE of this communication appears on the cover sheet with the correspondence address --

Period for Reply

A SHORTENED STATUTORY PERIOD FOR REPLY IS SET TO EXPIRE 3 MONTHS FROM THE MAILING DATE OF THIS COMMUNICATION.

- Extensions of time may be available under the provisions of 37 CFR 1.136(a). In no event, however, may a reply be timely filed after SIX (6) MONTHS from the mailing date of this communication.
- If NO period for reply is specified above, the maximum statutory period will apply and will expire SIX (6) MONTHS from the mailing date of this communication.
- Failure to reply within the set or extended period for reply will, by statute, cause the application to become ABANDONED (35 U.S.C. § 133). Any reply received by the Office later than three months after the mailing date of this communication, even if timely filed, may reduce any earned patent term adjustment. See 37 CFR 1.704(b).

Status

1)☒ Responsive to communication(s) filed on *10/10/2013*.

☐ A declaration(s)/affidavit(s) under **37 CFR 1.130(b)** was/were filed on _____.

2a)☐ This action is **FINAL**. 2b)☒ This action is non-final.

3)☐ An election was made by the applicant in response to a restriction requirement set forth during the interview on _____; the restriction requirement and election have been incorporated into this action.

4)☐ Since this application is in condition for allowance except for formal matters, prosecution as to the merits is closed in accordance with the practice under *Ex parte Quayle*, 1935 C.D. 11, 453 O.G. 213.

Disposition of Claims*

5)☒ Claim(s) *1-8 and 19-37* is/are pending in the application.

5a) Of the above claim(s) _____ is/are withdrawn from consideration.

6)☐ Claim(s) _____ is/are allowed.

7)☒ Claim(s) *1-8 and 19-37* is/are rejected.

8)☐ Claim(s) _____ is/are objected to.

9)☐ Claim(s) _____ are subject to restriction and/or election requirement.

* If any claims have been determined allowable, you may be eligible to benefit from the **Patent Prosecution Highway** program at a participating intellectual property office for the corresponding application. For more information, please see http://www.uspto.gov/patents/init_events/pph/index.jsp or send an inquiry to PPHfeedback@uspto.gov.

Application Papers

10)☐ The specification is objected to by the Examiner.

11)☒ The drawing(s) filed on *8/31/2011* is/are: a)☒ accepted or b)☐ objected to by the Examiner.

Applicant may not request that any objection to the drawing(s) be held in abeyance. See 37 CFR 1.85(a).

Replacement drawing sheet(s) including the correction is required if the drawing(s) is objected to. See 37 CFR 1.121(d).

Priority under 35 U.S.C. § 119

12)☐ Acknowledgment is made of a claim for foreign priority under 35 U.S.C. § 119(a)-(d) or (f).

Certified copies:

a)☐ All b)☐ Some** c)☐ None of the:

1.☐ Certified copies of the priority documents have been received.

2.☐ Certified copies of the priority documents have been received in Application No. _____.

3.☐ Copies of the certified copies of the priority documents have been received in this National Stage application from the International Bureau (PCT Rule 17.2(a)).

** See the attached detailed Office action for a list of the certified copies not received.

Attachment(s)

1) ☒ Notice of References Cited (PTO-892)

2) ☐ Information Disclosure Statement(s) (PTO/SB/08a and/or PTO/SB/08b) Paper No(s)/Mail Date _____.

3) ☐ Interview Summary (PTO-413) Paper No(s)/Mail Date. _____ .

4) ☐ Other: _____.

The present application is being examined under the pre-AIA first to invent provisions.

DETAILED ACTION

Response to Arguments

Applicant's arguments, filed 10/10/2013, with respect to the rejection(s) of claim(s) 1-8 and 19-37 under 35 USC § 103 have been fully considered and are persuasive. Therefore, the rejection has been withdrawn. However, upon further consideration, a new ground(s) of rejection is made in view of Nilson et al. and Shozo et al.

Claim Rejections - 35 USC § 103

The following is a quotation of pre-AIA 35 U.S.C. 103(a) which forms the basis for all obviousness rejections set forth in this Office action:

> (a) A patent may not be obtained though the invention is not identically disclosed or described as set forth in section 102 of this title, if the differences between the subject matter sought to be patented and the prior art are such that the subject matter as a whole would have been obvious at the time the invention was made to a person having ordinary skill in the art to which said subject matter pertains. Patentability shall not be negatived by the manner in which the invention was made.

This application currently names joint inventors. In considering patentability of the claims under pre-AIA 35 U.S.C. 103(a), the examiner presumes that the subject matter of the various claims was commonly owned at the time any inventions covered therein were made absent any evidence to the contrary. Applicant is advised of the obligation under 37 CFR 1.56 to point out the inventor and invention dates of each claim that was not commonly owned at the time a later invention was made in order for the examiner to consider the applicability of pre-

SPECTRAL_0000894

AIA 35 U.S.C. 103(c) and potential pre-AIA 35 U.S.C. 102(e), (f) or (g) prior art under pre-AIA 35 U.S.C. 103(a).

Claims 1-8 and 19-37 are rejected under pre-AIA 35 U.S.C. 103(a) as being unpatentable over Nilson et al. (*Nilson*, US 6,894,289) in view of Shozo et al. (*Shozo*, US 6,033,087).

With regards to claims 1, 3, 19, and 26, Nilson discloses a fluorescence illumination assembly (Fig. 2) for an illuminating a sample to excite fluorescence and then capturing an image of the fluorescence comprising: a ring-shaped housing 32 mounted to a support structure 22 defining a central opening 23 and supporting an illumination device 30 surrounding said opening, wherein the opening is aligned with a camera which is also mounted to the support structure such that a field of view of the camera is unobstructed by said housing (column 7, lines 1-7). Nilson fails to specify a plurality of light receptacles, each having a light source positioned therein, a diffuser positioned the receptacles, and a control system for controlling each light source. Shozo discloses an LED illuminating device comprising a housing 2 defining a central opening to accommodate a camera 4, said housing comprising a plurality of receptacles (space defined by the individual openings in said housing) for receiving a plurality of narrow band light sources 11, 12, 13 and a diffuser 8 for diffusing light emitted by said light sources, wherein each light source is controlled by a control unit to optimize illumination (column 6, lines 11-28). It would have been obvious to one with ordinary skill in the art to modify Nilson with the illumination assembly taught by Shozo to provide an illuminating device which uses LED light sources with a simple construction that is free of illumination irregularities, as taught by Shozo. Shozo teaches a single diffuser to diffuse light emitted by said light sources instead of a plurality of diffusers corresponding to each light source. However, it would have been an obvious matter

SPECTRAL_0000895

of design choice to a person of ordinary skill in the art to modify Shozo with a plurality of diffusers because Applicant has not disclosed that a plurality of diffusers provides an advantage, is used for a particular purpose, or solves a stated problem compared to a single diffuser. One of ordinary skill in the art, furthermore, would have expected Applicant's invention to perform equally well with a single diffuser because both configurations would have the same predictable result.

With regards to claim 2, Nilson fails to specify wherein at least on of said light source emits light having a bandwidth of about 35 nm. Nevertheless, the specific bandwidth of each light source would have been obvious to a skilled artisan depending upon the sample being imaged. Therefore, it would have been obvious to one with ordinary skill in the art to modify Nilson with said light source since the recited bandwidth was known in order to produce the desired excitation bandwidth.

With regards to claims 4, 5, and 20, Nilson teaches a filter wheel comprising bandpass filters, long pass filters and shortpass filters (column 9, lines 11-13) for filtering excitation light. Nilson fails to teach wherein said filters are positioned adjacent to the diffuser and wherein the bandpass range is about 30 nm. With respect to the specific location of the filters, Nilson (as modified by Shozo) teaches the recited receptacles and diffuser. As such, positioning said filters adjacent the diffuser within the receptacle would have been, since it has been held that rearranging parts of an invention involves only routine skill in the art. *In re* Japikse, 86 USPQ 70. In addition, the specific bandpass range of the filters would have been obvious to a skilled artisan depending upon the sample being imaged. Therefore, it would have been obvious to one

with ordinary skill in the art to modify Nilson with said bandpass range since the recited range was known in order to produce the desired excitation light.

With regards to claim 6, Nilson disclses a broad band light source (column 8, lines 36-40).

With regards to claims 7 and 8, Shozo discloses said light receptacles comprise opposed receptacles on opposite sides of said opening, each opposed receptacle receiving a light source that produces light of the same color (Fig. 2). Shozo fails to specify said opposed receptacles comprise ten opposed pair of receptacles. Nevertheless, the specific amount of receptacles would have been obvious depending upon the desired light output. Therefore, it would have been obvious to one with ordinary skill in the art at the time the invention was made to modify Nilson and Shozo with the recited amount of receptacles, since it has been held that mere duplication of the essential working parts of a device involves only routine skill in the art.

With regards to claim 21, Nilson and Shozo fail to teach angled receptacles, although they were known. However, Nilson does teach that is was known to change the angle of incident excitation light with respect to a central axis of said housing by using an adjustable reflective surface 116. As such, modifying Nilson and Shozo with the angled receptacles instead of the adjustable reflective surface would have been obvious because the substitution of one known element for another would have yielded predictable results to one of ordinary skill in the art at the time of invention.

With regards to claim 22, Shozo discloses said narrow band light sources emit light in different colors (column 3, lines 34-35).

SPECTRAL_0000897

With regards to claims 23, 28, and 29, Nilson discloses the recited range (column 8, lines 43-44).

With regards to claim 24, Nilson and Shozo fail to teach 10 illumination bands. Nevertheless, the number of illumination bands would have been obvious depending upon the desired output excitation. At the time the invention was made, it would have been an obvious matter of design choice to a person of ordinary skill in the art to modify Nilson and Shozo with 10 illumination bands because Applicant has not disclosed that 10 illumination bands provides an advantage, is used for a particular purpose, or solves a stated problem. One of ordinary skill in the art, furthermore, would have expected Applicant's invention to perform equally well with a different amount of different illumination bands so long as the desired excitation output is produced.

With regards to claim 25, Nilson fails to specify wherein at least on of said light source emits light having a bandwidth of about 35 nm. Nevertheless, the specific bandwidth of each light source would have been obvious to a skilled artisan depending upon the sample being imaged. Therefore, it would have been obvious to one with ordinary skill in the art to modify Nilson with said light source since the recited bandwidth was known in order to produce the desired excitation bandwidth.

With regards to claim 27, Nilson and Shozo fail to teach a housing comprising the recited material. Nevertheless, Nilson discloses the use of Delrin to reduce light reflection (column 11, lines 7-11). As such, it would have been obvious to one with ordinary skill in the art to modify Nilson and Shozo with a housing comprising the material taught by Nilson in order to reduce light reflection within the housing.

With regards to claims 30-33, Shozo does not teach said light sources do not extend beyond the light receptacles. Nevertheless, extending the receptacles such that said light sources do not extend beyond the light receptacles would have been obvious since it was known and further in view of providing directional light. In addition, the number of light sources within each receptacle and the size of each receptacle would have been obvious in view of providing the desired light output.

With regards to claim 34, Shozo discloses said receptacles comprise generally cylindrically shaped openings having a first and second opened ends, a circuit board 3 mounted to a first side of said housing, said light sources mounted to said circuit board so that said light sources extend through the first open ends of the receptacles (Fig. 1).

With regards to claim 35, Nilson discloses a fluorescence illumination assembly (Fig. 2) for an illuminating a sample to excite fluorescence and then capturing an image of the fluorescence comprising: a ring-shaped housing 32 mounted to a support structure 22 defining a central opening 23 and supporting an illumination device 30 surrounding said opening, wherein the opening is aligned with a camera which is also mounted to the support structure such that a field of view of the camera is unobstructed by said housing (column 7, lines 1-7). Nilson fails to specify a plurality of light receptacles, each having a light source positioned therein, a diffuser positioned the receptacles, and a control system for controlling each light source. Shozo discloses an LED illuminating device comprising a housing 2 defining a central opening to accommodate a camera 4, said housing comprising a plurality of receptacles (space defined by the individual openings in said housing) for receiving a plurality of narrow band light sources 11, 12, 13 and a diffuser 8 for diffusing light emitted by said light sources, wherein each light source

SPECTRAL_0000899

is controlled by a control unit to optimize illumination (column 6, lines 11-28). It would have been obvious to one with ordinary skill in the art to modify Nilson with the illumination assembly taught by Shozo to provide an illuminating device which uses LED light sources with a simple construction that is free of illumination irregularities, as taught by Shozo. Shozo does not teach said light sources do not extend beyond the light receptacles. Nevertheless, extending the receptacles such that said light sources do not extend beyond the light receptacles would have been obvious since it was known and further in view of providing directional light.

With regards to claim 36, Shozo does not teach receptacles having different diameters with different number of light sources therein, although it was known to do so. However, the number of light sources within each receptacle and the size of each receptacle would have been obvious in view of providing the desired light output.

With regards to claim 37, Shozo discloses said receptacles comprise generally cylindrically shaped openings having a first and second opened ends, a circuit board 3 mounted to a first side of said housing, said light sources mounted to said circuit board so that said light sources extend through the first open ends of the receptacles (Fig. 1).

Conclusion

The prior art made of record and not relied upon is considered pertinent to applicant's disclosure.

SPECTRAL_0000900

Any inquiry concerning this communication or earlier communications from the examiner should be directed to Marcus H. Taningco whose telephone number is (571) 272-1848. The examiner can normally be reached on M - F 9:00 - 5:30.

If attempts to reach the examiner by telephone are unsuccessful, the examiner's supervisor, Dave Porta can be reached on (571) 272-2444. The fax phone number for the organization where this application or proceeding is assigned is 571-273-8300.

Information regarding the status of an application may be obtained from the Patent Application Information Retrieval (PAIR) system. Status information for published applications may be obtained from either Private PAIR or Public PAIR. Status information for unpublished applications is available through Private PAIR only. For more information about the PAIR system, see http://pair-direct.uspto.gov. Should you have questions on access to the Private PAIR system, contact the Electronic Business Center (EBC) at 866-217-9197 (toll-free). If you would like assistance from a USPTO Customer Service Representative or access to the automated information system, call 800-786-9199 (IN USA OR CANADA) or 571-272-1000.

/Marcus H Taningco/
Primary Examiner, Art Unit 2884

Notice of References Cited	Application/Control No. 13/222,688	Applicant(s)/Patent Under Reexamination NELSON ET AL.	
	Examiner MARCUS TANINGCO	Art Unit 2884	Page 1 of 1

U.S. PATENT DOCUMENTS

*		Document Number Country Code-Number-Kind Code	Date MM-YYYY	Name	Classification
*	A	US-6,033,087 A	03-2000	Shozo et al.	362/244
	B	US-			
	C	US-			
	D	US-			
	E	US-			
	F	US-			
	G	US-			
	H	US-			
	I	US-			
	J	US-			
	K	US-			
	L	US-			
	M	US-			

FOREIGN PATENT DOCUMENTS

*		Document Number Country Code-Number-Kind Code	Date MM-YYYY	Country	Name	Classification
	N					
	O					
	P					
	Q					
	R					
	S					
	T					

NON-PATENT DOCUMENTS

*		Include as applicable: Author, Title Date, Publisher, Edition or Volume, Pertinent Pages)
	U	
	V	
	W	
	X	

*A copy of this reference is not being furnished with this Office action. (See MPEP § 707.05(a).)
Dates in MM-YYYY format are publication dates. Classifications may be US or foreign.

Search Notes	Application/Control No.	Applicant(s)/Patent Under Reexamination
	13222688	NELSON ET AL.
	Examiner	Art Unit
	MARCUS TANINGCO	2884

CPC- SEARCHED		
Symbol	Date	Examiner
G01N21/645, G01N21/6428, G01N2021/7786, G01N21/6458, G01N2021/6463	1/7/2014	MT

CPC COMBINATION SETS - SEARCHED		
Symbol	Date	Examiner

US CLASSIFICATION SEARCHED			
Class	Subclass	Date	Examiner
250	461.1	1/27/2013	MT

SEARCH NOTES		
Search Notes	Date	Examiner
Inventor's name searched	1/27/2013	MT
EAST search notes attached	1/27/2013	MT
Text search in 250/458.1, 459.1	1/27/2013	MT
Text search in 362/3	1/27/2013	MT
Updated EAST search notes attached	7/8/2013	MT
Updated EAST search notes attached	1/7/2014	MT

INTERFERENCE SEARCH			
US Class/ CPC Symbol	US Subclass / CPC Group	Date	Examiner

Index of Claims	Application/Control No.	Applicant(s)/Patent Under Reexamination
	13222688	NELSON ET AL.
	Examiner	Art Unit
	MARCUS TANINGCO	2884

✓	Rejected	-	Cancelled	N	Non-Elected	A	Appeal
=	Allowed	÷	Restricted	I	Interference	O	Objected

☐ Claims renumbered in the same order as presented by applicant ☐ CPA ☐ T.D. ☐ R.1.47

CLAIM		DATE								
Final	Original	11/18/2012	07/08/2013	01/07/2014						
	1	✓	✓	✓						
	2	✓	✓	✓						
	3	✓	✓	✓						
	4	✓	✓	✓						
	5	✓	✓	✓						
	6	✓	✓	✓						
	7	✓	✓	✓						
	8	✓	✓	✓						
	9	N	-	-						
	10	N	-	-						
	11	N	-	-						
	12	N	-	-						
	13	N	-	-						
	14	N	-	-						
	15	N	-	-						
	16	N	-	-						
	17	N	-	-						
	18	N	-	-						
	19	✓	✓	✓						
	20	✓	✓	✓						
	21	✓	✓	✓						
	22	✓	✓	✓						
	23	✓	✓	✓						
	24	✓	✓	✓						
	25	✓	✓	✓						
	26	✓	✓	✓						
	27	✓	✓	✓						
	28	✓	✓	✓						
	29	✓	✓	✓						
	30		✓	✓						
	31		✓	✓						
	32		✓	✓						
	33		✓	✓						
	34		✓	✓						
	35		✓	✓						
	36		✓	✓						

Index of Claims	Application/Control No.	Applicant(s)/Patent Under Reexamination
	13222688	NELSON ET AL.
	Examiner	**Art Unit**
	MARCUS TANINGCO	2884

✓	Rejected	-	Cancelled	N	Non-Elected	A	Appeal
=	Allowed	÷	Restricted	I	Interference	O	Objected

☐ Claims renumbered in the same order as presented by applicant ☐ CPA ☐ T.D. ☐ R.1.47

CLAIM		DATE								
Final	Original	11/18/2012	07/08/2013	01/07/2014						
	37		✓	✓						

EAST Search History

EAST Search History (Prior Art)

Ref #	Hits	Search Query	DBs	Default Operator	Plurals	Time Stamp
L20	2	"20040121175"	US-PGPUB; USPAT; FPRS; EPO; JPO; DERWENT; IBM_TDB	OR	OFF	2014/01/07 11:34
L21	296	polyoxymethylene near thermoplastic	US-PGPUB; USPAT; FPRS; EPO; JPO; DERWENT; IBM_TDB	OR	OFF	2014/01/07 11:36
L22	2	21 and "250".clas.	US-PGPUB; USPAT; FPRS; EPO; JPO; DERWENT; IBM_TDB	OR	OFF	2014/01/07 11:36
L23	0	21 and "356".clas.	US-PGPUB; USPAT; FPRS; EPO; JPO; DERWENT; IBM_TDB	OR	OFF	2014/01/07 11:37
L24	251	delrin and "250".clas.	US-PGPUB; USPAT; FPRS; EPO; JPO; DERWENT; IBM_TDB	OR	OFF	2014/01/07 11:39
L25	0	delrin and "250/4$".clas.	US-PGPUB; USPAT; FPRS; EPO; JPO; DERWENT; IBM_TDB	OR	OFF	2014/01/07 11:39
L26	168	delrin and "356".clas.	US-PGPUB; USPAT; FPRS; EPO; JPO; DERWENT; IBM_TDB	OR	OFF	2014/01/07 11:39
L27	54	24 and 26	US-PGPUB; USPAT; FPRS; EPO; JPO; DERWENT; IBM_TDB	OR	OFF	2014/01/07 11:39
L28	81	("4585934" | "4863690" | "5414258" | "5587583" | "5680492" | "6004767" |	US-PGPUB; USPAT	OR	OFF	2014/01/07 11:40

		"6038038" | "7298415" | "7383078" | "7449615" | "7461652" | "7555334" | "7581191" | "4863690" | "5680492" | "5818977" | "6004767" | "6097025" | "6642499" | "6922246" | "7255851" | "7464707" | "7466418" | "7555332" | "7595838" | "7663664" | "20040121175" | "5672881" | "5689110" | "6901279" | "7116354" | "7177024" | "7555332" | "7589786" | "7595838" | "7599731" | "5039868" | "5202091" | "6775567" | "6919919" | "7474399" | "4885544" | "5515161" | "5542012" | "5840572" | "5964220" | "6205244" | "6922246" | "7255851" | "7299420" | "7331341" | "7616985" | "7449567" | "7461652" | "7555334" | "7589786" | "7603167" | "5454437" | "3800079" | "4687325" | "5008548" | "5898802" | "5986271" | "6377353" | "6614452" | "20010028510" | "4593728" | "4687325" | "4948975" | "5414258" | "5515161" | "6871767" | "7196190" | "7449615" | "7474398" | "7616985" | "5089895" | "3949162" | "5202091" | "6097025" | "6642499" | "7503323" | "3949162" | "4196994" | "4343021" | "4885544" | "5008548" | "5672881" | "5689110" | "5840572" | "5865754" | "5964220" | "5986271" | "6217847" | "7113217" | "7190991" | "7383078" | "7503323" | "7581191" | "7599731" | "20040247170" | "20090268426" | "4196994" | "4343021" | "6217847" | "6754008" | "6894289" | "6919919" | "7196190" | "7449567" | "7464707" | "7474398" | "7603167" | "5587583" | "5898802" | "6377353" | "6754008" | "6901279" | "7177024" | "7299420" | "20050265024" | "3871767" | "4593728" | "4948975" | "5818977" | "6775567" | "7113217" | "7403812" | "7474399" | "7663664" | "0458934" | "5401465" | "5542012" | "6038038" | "6154277" | "6614452" | "7116354" | "7331341" | "4298887" | "5039868" | "5401465" | "5865754" | "6154277" | "7190991" | "7466418" | "3800079" | "4298887" | "6205244" | "6894289" | "7298415" | "7403812").PN.				
L29	6	L28 and delrin	US-PGPUB; USPAT; FPRS; EPO; JPO; DERWENT; IBM_TDB	OR	OFF	2014/01/07 11:40
L30	71	("4947291" | "5039832" | "5400229" | "5580163" | "5685637" | "5690417").PN. OR ("6033087").URPN.	US-PGPUB; USPAT; USOCR	OR	OFF	2014/01/07 11:52
S1	1	13/222688	US-PGPUB; USPAT; FPRS; EPO; JPO; DERWENT;	OR	OFF	2013/01/25 15:03

			IBM_TDB			
S2	564	(Nelson near Michael).in.	US-PGPUB; USPAT; FPRS; EPO; JPO; DERWENT; IBM_TDB	OR	OFF	2013/01/25 15:03
S3	38	(Nelson near Michael).in. and fluoresc$4	US-PGPUB; USPAT; FPRS; EPO; JPO; DERWENT; IBM_TDB	OR	OFF	2013/01/25 15:04
S4	4	(Nelson near Michael).in. and fluoresc$4 and ((light near source) same diffus$4)	US-PGPUB; USPAT; FPRS; EPO; JPO; DERWENT; IBM_TDB	OR	OFF	2013/01/25 15:05
S5	81	("4585934" | "4863690" | "5414258" | "5587583" | "5680492" | "6004767" | "6038038" | "7298415" | "7383078" | "7449615" | "7461652" | "7555334" | "7581191" | "4863690" | "5680492" | "5818977" | "6004767" | "6097025" | "6642499" | "6922246" | "7255851" | "7464707" | "7466418" | "7555332" | "7595838" | "7663664" | "20040121175" | "5672881" | "5689110" | "6901279" | "7116354" | "7177024" | "7555332" | "7589786" | "7595838" | "7599731" | "5039868" | "5202091" | "6775567" | "6919919" | "7474399" | "4885544" | "5515161" | "5542012" | "5840572" | "5964220" | "6205244" | "6922246" | "7255851" | "7299420" | "7331341" | "7616985" | "7449567" | "7461652" | "7555334" | "7589786" | "7603167" | "5454437" | "3800079" | "4687325" | "5008548" | "5898802" | "5986271" | "6377353" | "6614452" | "20010028510" | "4593728" | "4687325" | "4948975" | "5414258" | "5515161" | "6871767" | "7196190" | "7449615" | "7474398" | "7616985" | "5089895" | "3949162" | "5202091" | "6097025" | "6642499" | "7503323" | "3949162" | "4196994" | "4343021" | "4885544" | "5008548" | "5672881" | "5689110" | "5840572" | "5865754" | "5964220" | "5986271" | "6217847" | "7113217" | "7190991" | "7383078" | "7503323" | "7581191" | "7599731" | "20040247170" | "20090268426" | "4196994" | "4343021" | "6217847" | "6754008" | "6894289" | "6919919" | "7196190" | "7449567" | "7464707" | "7474398" | "7603167" | "5587583" | "5898802" | "6377353" | "6754008" | "6901279" | "7177024" | "7299420" | "20050265024" | "3871767" | "4593728" | "4948975" | "5818977" | "6775567" | "7113217" | "7403812" | "7474399" | "7663664" | "0458934" |	US-PGPUB; USPAT	OR	OFF	2013/01/25 15:07

		"5401465" | "5542012" | "6038038" | "6154277" | "6614452" | "7116354" | "7331341" | "4298887" | "5039868" | "5401465" | "5865754" | "6154277" | "7190991" | "7466418" | "3800079" | "4298887" | "6205244" | "6894289" | "7298415" | "7403812").PN.				
S6	2234	(camera or detect$4 or imager or imaging) with (light or led or lamp) with (halo or ring or surround$4) with (opening or aperture or hole or fov or (field near view))	US-PGPUB; USPAT; FPRS; EPO; JPO; DERWENT; IBM_TDB	OR	OFF	2013/01/25 15:21
S7	412	S6 and ((light or led or lamp) with diffus$4)	US-PGPUB; USPAT; FPRS; EPO; JPO; DERWENT; IBM_TDB	OR	OFF	2013/01/25 15:21
S8	58	S7 and "250".clas.	US-PGPUB; USPAT; FPRS; EPO; JPO; DERWENT; IBM_TDB	OR	OFF	2013/01/25 15:23
S9	3	(camera or detect$4 or imager or imaging) with ((multiple or plurality) near2 (receptacle or ight or led or lamp)) with (halo or ring or surround$4) with (opening or aperture or hole or fov or (field near view))	US-PGPUB; USPAT; FPRS; EPO; JPO; DERWENT; IBM_TDB	OR	OFF	2013/01/25 21:09
S10	96	(camera or detect$4 or imager or imaging) with ((multiple or plurality) near2 (receptacle or ight or led or lamp)) with (opening or aperture or hole or fov or (field near view))	US-PGPUB; USPAT; FPRS; EPO; JPO; DERWENT; IBM_TDB	OR	OFF	2013/01/25 21:12
S11	4	S10 and "250".clas.	US-PGPUB; USPAT; FPRS; EPO; JPO; DERWENT; IBM_TDB	OR	OFF	2013/01/25 21:13
S12	81	("4585934" | "4863690" | "5414258" | "5587583" | "5680492" | "6004767" | "6038038" | "7298415" | "7383078" | "7449615" | "7461652" | "7555334" | "7581191" | "4863690" | "5680492" | "5818977" | "6004767" | "6097025" | "6642499" | "6922246" | "7255851" | "7464707" | "7466418" | "7555332" | "7595838" | "7663664" | "20040121175" | "5672881" | "5689110" | "6901279" | "7116354" | "7177024" | "7555332" | "7589786" | "7595838" | "7599731" | "5039868" | "5202091" | "6775567" | "6919919" | "7474399" | "4885544" | "5515161" | "5542012" | "5840572" | "5964220" | "6205244" | "6922246" | "7255851" | "7299420" | "7331341" | "7616985" | "7449567" | "7461652" | "7555334" | "7589786" | "7603167" |	US-PGPUB; USPAT	OR	OFF	2013/01/25 21:13

		"5454437" | "3800079" | "4687325" | "5008548" | "5898802" | "5986271" | "6377353" | "6614452" | "20010028510" | "4593728" | "4687325" | "4948975" | "5414258" | "5515161" | "6871767" | "7196190" | "7449615" | "7474398" | "7616985" | "5089895" | "3949162" | "5202091" | "6097025" | "6642499" | "7503323" | "3949162" | "4196994" | "4343021" | "4885544" | "5008548" | "5672881" | "5689110" | "5840572" | "5865754" | "5964220" | "5986271" | "6217847" | "7113217" | "7190991" | "7383078" | "7503323" | "7581191" | "7599731" | "20040247170" | "20090268426" | "4196994" | "4343021" | "6217847" | "6754008" | "6894289" | "6919919" | "7196190" | "7449567" | "7464707" | "7474398" | "7603167" | "5587583" | "5898802" | "6377353" | "6754008" | "6901279" | "7177024" | "7299420" | "20050265024" | "3871767" | "4593728" | "4948975" | "5818977" | "6775567" | "7113217" | "7403812" | "7474399" | "7663664" | "0458934" | "5401465" | "5542012" | "6038038" | "6154277" | "6614452" | "7116354" | "7331341" | "4298887" | "5039868" | "5401465" | "5865754" | "6154277" | "7190991" | "7466418" | "3800079" | "4298887" | "6205244" | "6894289" | "7298415" | "7403812").PN.				
S13	0	S12 and S10	US-PGPUB; USPAT; FPRS; EPO; JPO; DERWENT; IBM_TDB	OR	OFF	2013/01/25 21:13
S14	5	S12 and (camera or detect$4 or imager or imaging) with (light or led or lamp) with (halo or ring or surround$4) with (opening or aperture or hole or fov or (field near view))	US-PGPUB; USPAT; FPRS; EPO; JPO; DERWENT; IBM_TDB	OR	OFF	2013/01/25 21:22
S15	46	S12 and fluoresc$7	US-PGPUB; USPAT; FPRS; EPO; JPO; DERWENT; IBM_TDB	OR	OFF	2013/01/25 21:25
S16	2	("3609451" | "5134277").PN. OR ("6943333").URPN.	US-PGPUB; USPAT; USOCR	OR	OFF	2013/01/25 21:26
S17	1088	250/461.1.ccls.	US-PGPUB; USPAT; FPRS; EPO; JPO; DERWENT; IBM_TDB	OR	OFF	2013/01/27 14:54
S18	2855	250/458.1.ccls.	US-PGPUB; USPAT; FPRS;	OR	OFF	2013/01/27 14:54

			EPO; JPO; DERWENT; IBM_TDB			
S19	1557	250/459.1.ccls.	US-PGPUB; USPAT; FPRS; EPO; JPO; DERWENT; IBM_TDB	OR	OFF	2013/01/27 14:54
S20	4362	S17 S18 S19	US-PGPUB; USPAT; FPRS; EPO; JPO; DERWENT; IBM_TDB	OR	OFF	2013/01/27 14:54
S21	1	S20 and (camera or detect$4 or imager or imaging) with ((multiple or plurality) near2 (receptacle or ight or led or lamp)) with (opening or aperture or hole or fov or (field near view))	US-PGPUB; USPAT; FPRS; EPO; JPO; DERWENT; IBM_TDB	OR	OFF	2013/01/27 14:54
S22	2234	(camera or detect$4 or imager or imaging) with (light or led or lamp) with (halo or ring or surround$4) with (opening or aperture or hole or fov or (field near view))	US-PGPUB; USPAT; FPRS; EPO; JPO; DERWENT; IBM_TDB	OR	OFF	2013/01/27 14:55
S23	3	S22 and ((light or led or lamp) with diffus$4) and S20	US-PGPUB; USPAT; FPRS; EPO; JPO; DERWENT; IBM_TDB	OR	OFF	2013/01/27 14:55
S24	81	("4585934" | "4863690" | "5414258" | "5587583" | "5680492" | "6004767" | "6038038" | "7298415" | "7383078" | "7449615" | "7461652" | "7555334" | "7581191" | "4863690" | "5680492" | "5818977" | "6004767" | "6097025" | "6642499" | "6922246" | "7255851" | "7464707" | "7466418" | "7555332" | "7595838" | "7663664" | "20040121175" | "5672881" | "5689110" | "6901279" | "7116354" | "7177024" | "7555332" | "7589786" | "7595838" | "7599731" | "5039868" | "5202091" | "6775567" | "6919919" | "7474399" | "4885544" | "5515161" | "5542012" | "5840572" | "5964220" | "6205244" | "6922246" | "7255851" | "7299420" | "7331341" | "7616985" | "7449567" | "7461652" | "7555334" | "7589786" | "7603167" | "5454437" | "3800079" | "4687325" | "5008548" | "5898802" | "5986271" | "6377353" | "6614452" | "20010028510" | "4593728" | "4687325" | "4948975" | "5414258" | "5515161" | "6871767" | "7196190" | "7449615" | "7474398" | "7616985" | "5089895" | "3949162" | "5202091" | "6097025" | "6642499" | "7503323" | "3949162" | "4196994" | "4343021" | "4885544" | "5008548" |	US-PGPUB; USPAT	OR	OFF	2013/01/27 15:00

		"5672881" | "5689110" | "5840572" | "5865754" | "5964220" | "5986271" | "6217847" | "7113217" | "7190991" | "7383078" | "7503323" | "7581191" | "7599731" | "20040247170" | "20090268426" | "4196994" | "4343021" | "6217847" | "6754008" | "6894289" | "6919919" | "7196190" | "7449567" | "7464707" | "7474398" | "7603167" | "5587583" | "5898802" | "6377353" | "6754008" | "6901279" | "7177024" | "7299420" | "20050265024" | "3871767" | "4593728" | "4948975" | "5818977" | "6775567" | "7113217" | "7403812" | "7474399" | "7663664" | "0458934" | "5401465" | "5542012" | "6038038" | "6154277" | "6614452" | "7116354" | "7331341" | "4298887" | "5039868" | "5401465" | "5865754" | "6154277" | "7190991" | "7466418" | "3800079" | "4298887" | "6205244" | "6894289" | "7298415" | "7403812").PN.				
S25	8	S20 and S24	US-PGPUB; USPAT; FPRS; EPO; JPO; DERWENT; IBM_TDB	OR	OFF	2013/01/27 15:00
S26	280	362/3.ccls.	US-PGPUB; USPAT; FPRS; EPO; JPO; DERWENT; IBM_TDB	OR	OFF	2013/01/27 15:06
S27	4	S22 and S26	US-PGPUB; USPAT; FPRS; EPO; JPO; DERWENT; IBM_TDB	OR	OFF	2013/01/27 15:06
S28	3	"20090268426"	US-PGPUB; USPAT; FPRS; EPO; JPO; DERWENT; IBM_TDB	OR	OFF	2013/06/24 14:48
S29	2	"6454437".pn.	US-PGPUB; USPAT; FPRS; EPO; JPO; DERWENT; IBM_TDB	OR	OFF	2013/06/24 14:49
S30	746	led near3 receptacle	US-PGPUB; USPAT; FPRS; EPO; JPO; DERWENT; IBM_TDB	OR	OFF	2013/07/05 11:02
S31	14	S30 and "250".clas.	US-PGPUB; USPAT; FPRS; EPO; JPO;	OR	OFF	2013/07/05 11:03

			DERWENT; IBM_TDB			
S32	90	S30 and fluorescen$4	US-PGPUB; USPAT; FPRS; EPO; JPO; DERWENT; IBM_TDB	OR	OFF	2013/07/05 11:05
S33	21	S30 and (fluorescen$4 near3 (excit$4 or detect$4 or sens$4 or illuminat$4))	US-PGPUB; USPAT; FPRS; EPO; JPO; DERWENT; IBM_TDB	OR	OFF	2013/07/05 11:06
S34	1120	250/461.1.ccls.	US-PGPUB; USPAT; FPRS; EPO; JPO; DERWENT; IBM_TDB	OR	OFF	2013/07/05 11:12
S35	2982	250/458.1.ccls.	US-PGPUB; USPAT; FPRS; EPO; JPO; DERWENT; IBM_TDB	OR	OFF	2013/07/05 11:12
S36	1678	250/459.1.ccls.	US-PGPUB; USPAT; FPRS; EPO; JPO; DERWENT; IBM_TDB	OR	OFF	2013/07/05 11:12
S37	4566	S34 S35 S36	US-PGPUB; USPAT; FPRS; EPO; JPO; DERWENT; IBM_TDB	OR	OFF	2013/07/05 11:12
S38	30	S37 and (camera or detect$4 or imager or imaging) with (light or led or lamp) with (halo or ring or surround$4 or annular) with (opening or aperture or hole or fov or (field near view))	US-PGPUB; USPAT; FPRS; EPO; JPO; DERWENT; IBM_TDB	OR	OFF	2013/07/05 11:13
S39	1	S30 and S37	US-PGPUB; USPAT; FPRS; EPO; JPO; DERWENT; IBM_TDB	OR	OFF	2013/07/05 11:48
S40	18	S30 and fluorescen$4.clm.	US-PGPUB; USPAT; FPRS; EPO; JPO; DERWENT; IBM_TDB	OR	OFF	2013/07/05 11:49
S41	40	led near3 ((array or multiple or plural$4) near receptacle)	US-PGPUB; USPAT; FPRS; EPO; JPO;	OR	ON	2013/07/05 11:51

			DERWENT; IBM_TDB			
S42	16	"10040330"	US-PGPUB; USPAT; FPRS; EPO; JPO; DERWENT; IBM_TDB	OR	OFF	2013/07/05 16:26
S43	267	S37 and ((light or led or lamp) near3 (halo or ring or surround$4 or annular))	US-PGPUB; USPAT; FPRS; EPO; JPO; DERWENT; IBM_TDB	OR	OFF	2013/07/05 16:27
S44	78	S43 and imag$4.clm.	US-PGPUB; USPAT; FPRS; EPO; JPO; DERWENT; IBM_TDB	OR	OFF	2013/07/05 16:28
S45	133	S37 and ((light or led or lamp) near3 (halo or ring or annular))	US-PGPUB; USPAT; FPRS; EPO; JPO; DERWENT; IBM_TDB	OR	OFF	2013/07/05 16:28
S46	56	S45 and imag$4.clm.	US-PGPUB; USPAT; FPRS; EPO; JPO; DERWENT; IBM_TDB	OR	OFF	2013/07/05 16:28
S47	19	S37 and ((light or led or lamp) near3 (halo or ring or annular)) same led	US-PGPUB; USPAT; FPRS; EPO; JPO; DERWENT; IBM_TDB	OR	OFF	2013/07/05 16:29
S48	15	S47 and imag$4.clm.	US-PGPUB; USPAT; FPRS; EPO; JPO; DERWENT; IBM_TDB	OR	OFF	2013/07/05 16:29
S49	1120	250/461.1.ccls.	US-PGPUB; USPAT; FPRS; EPO; JPO; DERWENT; IBM_TDB	OR	OFF	2013/07/08 10:23
S50	2982	250/458.1.ccls.	US-PGPUB; USPAT; FPRS; EPO; JPO; DERWENT; IBM_TDB	OR	OFF	2013/07/08 10:23
S51	1678	250/459.1.ccls.	US-PGPUB; USPAT; FPRS; EPO; JPO;	OR	OFF	2013/07/08 10:23

			DERWENT; IBM_TDB			
S52	4566	S49 S50 S51	US-PGPUB; USPAT; FPRS; EPO; JPO; DERWENT; IBM_TDB	OR	OFF	2013/07/08 10:23
S53	133	S52 and ((light or led or lamp) near3 (halo or ring or annular))	US-PGPUB; USPAT; FPRS; EPO; JPO; DERWENT; IBM_TDB	OR	OFF	2013/07/08 10:23
S54	56	S53 and imag$4.clm.	US-PGPUB; USPAT; FPRS; EPO; JPO; DERWENT; IBM_TDB	OR	OFF	2013/07/08 10:23
S55	19	S52 and ((light or led or lamp) near3 (halo or ring or annular)) same led	US-PGPUB; USPAT; FPRS; EPO; JPO; DERWENT; IBM_TDB	OR	OFF	2013/07/08 10:23
S56	15	S55 and imag$4.clm.	US-PGPUB; USPAT; FPRS; EPO; JPO; DERWENT; IBM_TDB	OR	OFF	2013/07/08 10:23
S57	41	S54 not S56	US-PGPUB; USPAT; FPRS; EPO; JPO; DERWENT; IBM_TDB	OR	OFF	2013/07/08 10:23
S58	23	S52 and ((light or led or lamp) near3 (halo or ring or annular)) with excit$6	US-PGPUB; USPAT; FPRS; EPO; JPO; DERWENT; IBM_TDB	OR	OFF	2013/07/08 10:29
S59	4	S52 and (((light or led or lamp) near3 (halo or ring or annular)) with excit$6) same imag$4	US-PGPUB; USPAT; FPRS; EPO; JPO; DERWENT; IBM_TDB	OR	OFF	2013/07/08 10:29
S60	68	(((light or led or lamp) near3 (halo or ring or annular)) same (excit$6 with fluoresc$6)) same imag$4	US-PGPUB; USPAT; FPRS; EPO; JPO; DERWENT; IBM_TDB	OR	OFF	2013/07/08 10:35
S61	68	S60 not S56	US-PGPUB; USPAT; FPRS; EPO; JPO;	OR	OFF	2013/07/08 10:36

			DERWENT; IBM_TDB			
S62	2	(((led) near3 (halo or ring or annular)) same (excit$6 with fluoresc$6)) same imag$4	US-PGPUB; USPAT; FPRS; EPO; JPO; DERWENT; IBM_TDB	OR	OFF	2013/07/08 10:41
S63	5	(((light or led or lamp) near3 (halo or ring or annular)) same (excit$6 with fluoresc$6)) same imag$4 same led	US-PGPUB; USPAT; FPRS; EPO; JPO; DERWENT; IBM_TDB	OR	ON	2013/07/08 10:42
S64	221	((light or led or lamp) near3 (halo or ring or annular)) same ((sens$4 or detect$4 or determin$4 or measur$4 or excit$6) near3 fluoresc$6)	US-PGPUB; USPAT; FPRS; EPO; JPO; DERWENT; IBM_TDB	OR	OFF	2014/01/06 19:33
S65	188	S64 and @ad<"20110831"	US-PGPUB; USPAT; FPRS; EPO; JPO; DERWENT; IBM_TDB	OR	OFF	2014/01/06 19:33
S66	117	S65 and (fluoresc$6 with (imag$4 or camera))	US-PGPUB; USPAT; FPRS; EPO; JPO; DERWENT; IBM_TDB	OR	OFF	2014/01/06 19:35
S67	81	("4585934" | "4863690" | "5414258" | "5587583" | "5680492" | "6004767" | "6038038" | "7298415" | "7383078" | "7449615" | "7461652" | "7555334" | "7581191" | "4863690" | "5680492" | "5818977" | "6004767" | "6097025" | "6642499" | "6922246" | "7255851" | "7464707" | "7466418" | "7555332" | "7595838" | "7663664" | "20040121175" | "5672881" | "5689110" | "6901279" | "7116354" | "7177024" | "7555332" | "7589786" | "7595838" | "7599731" | "5039868" | "5202091" | "6775567" | "6919919" | "7474399" | "4885544" | "5515161" | "5542012" | "5840572" | "5964220" | "6205244" | "6922246" | "7255851" | "7299420" | "7331341" | "7616985" | "7449567" | "7461652" | "7555334" | "7589786" | "7603167" | "5454437" | "3800079" | "4687325" | "5008548" | "5898802" | "5986271" | "6377353" | "6614452" | "20010028510" | "4593728" | "4687325" | "4948975" | "5414258" | "5515161" | "6871767" | "7196190" | "7449615" | "7474398" | "7616985" | "5089895" | "3949162" | "5202091" | "6097025" | "6642499" | "7503323" | "3949162" | "4196994" | "4343021" | "4885544" | "5008548" | "5672881" | "5689110" | "5840572" |	US-PGPUB; USPAT	OR	OFF	2014/01/06 19:49

		"5865754" | "5964220" | "5986271" | "6217847" | "7113217" | "7190991" | "7383078" | "7503323" | "7581191" | "7599731" | "20040247170" | "20090268426" | "4196994" | "4343021" | "6217847" | "6754008" | "6894289" | "6919919" | "7196190" | "7449567" | "7464707" | "7474398" | "7603167" | "5587583" | "5898802" | "6377353" | "6754008" | "6901279" | "7177024" | "7299420" | "20050265024" | "3871767" | "4593728" | "4948975" | "5818977" | "6775567" | "7113217" | "7403812" | "7474399" | "7663664" | "0458934" | "5401465" | "5542012" | "6038038" | "6154277" | "6614452" | "7116354" | "7331341" | "4298887" | "5039868" | "5401465" | "5865754" | "6154277" | "7190991" | "7466418" | "3800079" | "4298887" | "6205244" | "6894289" | "7298415" | "7403812").PN.				
S68	1	("7918557").PN.	US-PGPUB; USPAT	OR	OFF	2014/01/06 19:50
S69	8	("20020016533" | "20030018271" | "20050033145" | "6021344" | "6032070" | "6230046" | "6439715" | "7006861").PN. OR ("7406347").URPN.	US-PGPUB; USPAT; USOCR	OR	OFF	2014/01/06 19:55
S70	55	("20010028510" | "20050201614" | "20050237423" | "3871767" | "4076420" | "4582406" | "4593728" | "4708475" | "4863690" | "5039868" | "5202091" | "5319209" | "5414258" | "5542012" | "5636299" | "5637874" | "5650135" | "5672881" | "5680492" | "5705807" | "5738101" | "5840572" | "5867250" | "5898802" | "5916160" | "5943129" | "5970164" | "5986271" | "6036920" | "6043506" | "6071748" | "6084680" | "6097025" | "6217847" | "6242743" | "6321111" | "6364829" | "6373568" | "6381058" | "6403947" | "6510281" | "6597864" | "6615063" | "6665072" | "6690466" | "6693710" | "6750964" | "6775567" | "6894289" | "6901279" | "6922246" | "6924893" | "7177024").PN. OR ("7474399").URPN.	US-PGPUB; USPAT; USOCR	OR	OFF	2014/01/06 19:59
S71	55	("20010028510" | "20050201614" | "20050237423" | "3871767" | "4076420" | "4582406" | "4593728" | "4708475" | "4863690" | "5039868" | "5202091" | "5319209" | "5414258" | "5542012" | "5636299" | "5637874" | "5650135" | "5672881" | "5680492" | "5705807" | "5738101" | "5840572" | "5867250" | "5898802" | "5916160" | "5943129" | "5970164" | "5986271" | "6036920" | "6043506" | "6071748" | "6084680" | "6097025" | "6217847" | "6242743" | "6321111" | "6364829" | "6373568" | "6381058" | "6403947" | "6510281" | "6597864" | "6615063" | "6665072" | "6690466" | "6693710" | "6750964" | "6775567" | "6894289" | "6901279" |	US-PGPUB; USPAT; USOCR	OR	OFF	2014/01/06 19:59

SPECTRAL_0000917

		"6922246" | "6924893" | "7177024").PN. OR ("7474398").URPN.				
S72	55	S70 or S71	US-PGPUB; USPAT; FPRS; EPO; JPO; DERWENT; IBM_TDB	OR	OFF	2014/01/06 19:59
S73	24	S72 and ring	US-PGPUB; USPAT; FPRS; EPO; JPO; DERWENT; IBM_TDB	OR	OFF	2014/01/06 19:59
S74	46	("20010028510" | "3871767" | "4076420" | "4582406" | "4593728" | "4708475" | "4863690" | "5039868" | "5202091" | "5319209" | "5414258" | "5542012" | "5636299" | "5637874" | "5650135" | "5672881" | "5680492" | "5705807" | "5738101" | "5840572" | "5867250" | "5898802" | "5916160" | "5970164" | "5986271" | "6036920" | "6043506" | "6071748" | "6084680" | "6097025" | "6217847" | "6242743" | "6321111" | "6364829" | "6510281" | "6597864" | "6615063" | "6775567" | "6894289" | "6901279" | "6922246").PN. OR ("7177024").URPN.	US-PGPUB; USPAT; USOCR	OR	OFF	2014/01/06 20:03
S75	593	(((light or led or lamp or illuminat$4) near3 (halo or ring or annular)) same (multiple or plurality or array)) and ((sens$4 or detect$4 or determin$4 or measur$4 or excit$6 or imag$4) near3 fluoresc$6)	US-PGPUB; USPAT; FPRS; EPO; JPO; DERWENT; IBM_TDB	OR	OFF	2014/01/06 20:11
S76	612	(((light or led or lamp or illuminat$4 or excit$6) near3 (halo or ring or annular)) same (multiple or plurality or array)) and ((sens$4 or detect$4 or determin$4 or measur$4 or excit$6 or imag$4) near3 fluoresc$6)	US-PGPUB; USPAT; FPRS; EPO; JPO; DERWENT; IBM_TDB	OR	OFF	2014/01/06 20:12
S77	565	S76 and (light or led or lamp or illuminat$4 or excit$6) with (camera or imaging or detect$4 or sens$4)	US-PGPUB; USPAT; FPRS; EPO; JPO; DERWENT; IBM_TDB	OR	OFF	2014/01/06 20:13
S78	530	S77 and @ad<"20110831"	US-PGPUB; USPAT; FPRS; EPO; JPO; DERWENT; IBM_TDB	OR	OFF	2014/01/06 20:13
S79	221	S78 and ("250".clas. or "356".clas.)	US-PGPUB; USPAT; FPRS; EPO; JPO; DERWENT; IBM_TDB	OR	OFF	2014/01/06 20:15
S80	34	S64 AND ((G01N21/645 OR G01N21/6428 OR G01N2021/7786 OR	US-PGPUB; USPAT;	OR	OFF	2014/01/06 20:18

		G01N21/6458 OR G01N2021/6463).CPC.)	FPRS; EPO; JPO; DERWENT; IBM_TDB			
S81	217	S79 not S73	US-PGPUB; USPAT; FPRS; EPO; JPO; DERWENT; IBM_TDB	OR	OFF	2014/01/06 20:18
S82	186	S81 and (light or led or lamp or illuminat$4 or excit$6) with (hold$4or contain$4 or cavit$4 or receiv$4 or receptacle)	US-PGPUB; USPAT; FPRS; EPO; JPO; DERWENT; IBM_TDB	OR	OFF	2014/01/06 20:19
S83	74	S79 not (fiber near optic$4)	US-PGPUB; USPAT; FPRS; EPO; JPO; DERWENT; IBM_TDB	OR	OFF	2014/01/06 20:21
S84	55	S83 and (light or led or lamp or illuminat$4 or excit$6) with (hold$4or contain$4 or cavit$4 or receiv$4 or receptacle)	US-PGPUB; USPAT; FPRS; EPO; JPO; DERWENT; IBM_TDB	OR	OFF	2014/01/06 20:23
S85	60	S83 and (light or led or lamp or illuminat$4 or excit$6) with (hold$4 or contain$4 or cavit$4 or receiv$4 or receptacle)	US-PGPUB; USPAT; FPRS; EPO; JPO; DERWENT; IBM_TDB	OR	OFF	2014/01/06 20:23
S86	19667	(light or led or lamp or illuminat$4) with receptacle	US-PGPUB; USPAT; FPRS; EPO; JPO; DERWENT; IBM_TDB	OR	OFF	2014/01/06 20:42
S87	8	S76 and S86	US-PGPUB; USPAT; FPRS; EPO; JPO; DERWENT; IBM_TDB	OR	OFF	2014/01/06 20:42
S88	2	"5690417".pn.	US-PGPUB; USPAT; FPRS; EPO; JPO; DERWENT; IBM_TDB	OR	OFF	2014/01/06 20:46
S89	89	("4567551" | "4893223" | "5038258").PN. OR ("5690417").URPN.	US-PGPUB; USPAT; USOCR	OR	OFF	2014/01/06 20:47
S90	13	S89 and receptacle	US-PGPUB; USPAT; FPRS; EPO; JPO; DERWENT;	OR	OFF	2014/01/06 20:51

			IBM_TDB			
S91	1303	((Nelson or cable) near Michael).in.	US-PGPUB; USPAT; FPRS; EPO; JPO; DERWENT; IBM_TDB	OR	OFF	2014/01/06 21:25
S92	77	S91 and fluoresc$4	US-PGPUB; USPAT; FPRS; EPO; JPO; DERWENT; IBM_TDB	OR	OFF	2014/01/06 21:26
S93	0	S91 and fluoresc$4 and recetacle	US-PGPUB; USPAT; FPRS; EPO; JPO; DERWENT; IBM_TDB	OR	OFF	2014/01/06 21:26
S94	6	S91 and fluoresc$4 and receptacle	US-PGPUB; USPAT; FPRS; EPO; JPO; DERWENT; IBM_TDB	OR	OFF	2014/01/06 21:26

EAST Search History (Interference)

<This search history is empty>

1/7/2014 1:10:53 PM
C:\Users\mtaningco\Documents\EAST\Workspaces\13222688.wsp

IN THE UNITED STATES PATENT AND TRADEMARK OFFICE

In Re Application of:	
	Examiner: Taningco, M.
NELSON, Michael, B., *et al.*	
	Group Art Unit: 2884
Serial No. 13/222,688	
	Confirm. No.: 5910
Filing Date: August 31, 2011	
	Atty. Dkt.: SPEC US-4
For: EXCITATION LIGHT SOURCE ASSEMBLY	(027560-0014)

RESPONSE UNDER 37 C.F.R. §§ 1.111 & 1.121

To: The Commissioner for Patents
P.O. Box 1450
Alexandria, VA 22313-1450

Sir:

In response to the office action, dated January 9, 2014, please amend the above-identified patent application as follows:

Amendments to the Claims are reflected in the listing of claims which begins on page 2 of this paper.

Remarks begin on page 9 of this paper.

SPECTRAL_0000921

Listing of Claims:

This listing of claims will replace all prior versions and listings of claims in the application:

Listing of Claims:

1. (Currently Amended) An excitation light source assembly, comprising:

a housing defining a central opening therein and a plurality of lamp receptacles surrounding the central opening, said housing being mountable to a support structure so that the central opening is aligned with a camera also mounted to the support structure so that a field of view of the camera is unobstructed by said housing;

a light source positioned within each of the plurality of lamp receptacles, wherein at least one of said light sources comprises a narrow-band light source; and

a diffuser positioned within at least some of the plurality of lamp receptacles, each of said diffusers diffusing light produced by each of said light sources; and

a control system operatively connected to each of said light sources, said control system operating selected ones of said light sources to provide a desired excitation illumination to an object within the field of view of said camera, the object fluorescing in response to the excitation illumination provided by said light sources.

2. (Currently Amended) The excitation light source assembly of claim 1 wherein ~~at least one of~~ said ~~light sources comprises a~~ narrow-band light source ~~that~~ emits light having a bandwidth of about 35 nm.

SPECTRAL_0000922

3. (Original) The excitation light source assembly of claim 2 wherein said at least one narrow-band light source comprises a light emitting diode.

4. (Original) The excitation light source assembly of claim 1, further comprising at least one filter positioned adjacent at least one diffuser in at least one of the lamp receptacles defined by said housing.

5. (Original) The excitation light source assembly of claim 4, wherein said at least one filter comprises a notch filter having a wavelength bandpass range of about 30 nm.

6. (Original) The excitation light source assembly of claim 1, wherein at least one of the light sources comprises a broad-band light source.

7. (Previously Presented) The excitation light source assembly of claim 1, wherein at least some of said plurality of lamp receptacles comprise opposed pairs of lamp receptacles on opposite sides of said central opening, each opposed pair of lamp receptacles receiving light sources that produce light of the same color.

8. (Original) The excitation light source assembly of claim 7, further comprising ten opposed pairs of lamp receptacles on opposite sides of said central opening.

9-18 (Canceled).

19. (Previously Presented) An assembly, comprising:

a support structure;

a camera mounted to said support structure;

an excitation light source assembly mounted to said support structure, said excitation light source assembly comprising:

a housing defining a central opening therein and a plurality of lamp receptacles surrounding the central opening, said housing being mounted to said support structure so that the central opening is aligned with said camera and so that a field of view of said camera is substantially unobstructed by said housing;

at least one narrow-band light source positioned within at least one of the plurality of lamp receptacles; and

a diffuser positioned within at least some of the plurality of lamp receptacles, each of said diffusers diffusing light produced by each of said narrow-band light sources; and

a control system operatively connected to each of said narrow-band light sources, said control system operating selected ones of said narrow-band light sources to provide a desired excitation illumination to a fluorescent material within the field of view of said camera, the fluorescent material fluorescing in response to the excitation illumination.

20. (Original) The assembly of claim 19, further comprising a light filter positioned adjacent each of the diffusers.

21. (Original) The assembly of claim 19, wherein each of the lamp receptacles defined by said housing are angled with respect to

SPECTRAL_0000924

a central axis of said housing so that light emitted from each of said narrow-band light sources is directed to a desired area within the field of view of said camera.

22. (Original) The assembly of claim 19, wherein each of said narrow-band light sources is selected to provide desired number of illumination bands over a desired spectral range.

23. (Original) The assembly of claim 22, wherein the desired spectral range is from about 430 nm to about 745 nm.

24. (Original) The assembly of claim 22, wherein the desired number of illumination bands is 10.

25. (Original) The assembly of claim 22, wherein each desired illumination band has a bandwidth ranging from about 30 nm to about 35 nm.

26. (Original) The assembly of claim 19, wherein each of said narrow-band light sources comprises a light emitting diode.

27. (Original) The assembly of claim 19, wherein said housing comprises a polyoxymethylene thermoplastic material.

28. (Original) The assembly of claim 22, wherein the desired spectral range is from about 430 nm to about 900 nm.

29. (Original) The assembly of claim 22, wherein the desired spectral range is from about 430 nm to about 800 nm.

30. (Previously Presented) The excitation light source

assembly of claim 1, wherein the light source positioned within each of the plurality of lamp receptacles does not extend beyond the lamp receptacle.

31. (Previously Presented) The excitation light source assembly of claim 1, further comprising a plurality of light sources positioned within at least some of the lamp receptacles so that the plurality of light sources do not extend beyond the lamp receptacles.

32. (Previously Presented) The excitation light source assembly of claim 31, wherein said plurality of light sources is three light sources.

33. (Previously Presented) The excitation light source assembly of claim 1, wherein the plurality of light receptacles defined by said housing comprise a plurality of large diameter receptacles and a plurality of small diameter receptacles.

34. (Previously Presented) The excitation light source assembly of claim 1, wherein the plurality of light receptacles defined by said housing comprise generally cylindrically shaped openings having first and second open ends, said excitation light source assembly further comprising a circuit board mounted to a first side of said housing, said light sources being mounted to said circuit board so that said light sources extend through the first open ends of the generally cylindrically-shaped light receptacles.

35. (Currently Amended) An excitation light source assembly, comprising:

SPECTRAL_0000926

a housing defining a central opening therein and a plurality of lamp receptacles therein surrounding the central opening, said housing being mountable to a support structure so that the central opening is aligned with a camera also mounted to the support structure so that a field of view of the camera is unobstructed by said housing;

a light source positioned within each of the plurality of lamp receptacles so that said light sources do not extend beyond the lamp receptacles, wherein at least one of said light sources comprises a narrow-band light source; and

a control system operatively connected to each of said light sources, said control system operating selected ones of said light sources to provide a desired excitation illumination to an object within the field of view of the camera, th excitation illumination causing fluorescent materials in the object to fluoresce, the camera capturing an image of the fluorescing material in the object.

36. (Previously Presented) The excitation light source assembly of claim 35, wherein said plurality of lamp receptacles defined by said housing comprise a plurality of large diameter lamp receptacles and a plurality of small diameter lamp receptacles, said large diameter lamp receptacles receiving a plurality of said light sources, said small diameter receptacles receiving a single light source.

37. (Previously Presented) The excitation light source assembly of claim 35, wherein the plurality of light receptacles defined by said housing comprise generally cylindrically shaped openings having first and second open ends, said excitation light source assembly further comprising a circuit board mounted to a

first side of said housing, said light sources being mounted to said circuit board so that said light sources extend through the first open ends of the generally cylindrically shaped light receptacles.

SPECTRAL_0000928

R E M A R K S

Claims 1-8 and 19-37 are pending. Claims 9-18 are canceled as being drawn to non-elected inventions. Claims 1, 2, and 35 are amended. Claims 7, 19, and 30-34, 36, and 37 are previously presented. Claims 2-6, 8, and 20-29 stand as originally filed. Re-examination and reconsideration are requested.

In the office action, dated January 9, 2014, the examiner noted that he found applicants' previous arguments persuasive and withdrew the previous claim rejections. The examiner then made new rejections based on two newly applied references. Specifically, the examiner rejected claims 1-8 and 19-37 under (pre-AIA) 35 U.S.C. §103(a) as being unpatentable Nilson *et al.*, U.S. Patent No. 6,894,289 ("Nilson") in view of Shozo *et al.*, U.S. Patent No. 6,033,087 ("Shozo") for the reasons specified on pages 3-8 of the office action.

Re the Claims:

Claim 1 is amended incorporate a limitation from claim 2 that at least one of the light sources comprises a narrow-band light source. No new matter is added.

Claim 2 is amended to make it consistent with the amendments to claim 1.

Claim 35 is amended to require that at least one of the light sources comprises narrow-band light source. No new matter is added.

Re the Obviousness Rejections:

The examiner's rejections are in error because Nilson's requirement for a broadband light source that is external to the imaging compartment would not motivate, and indeed would discourage, a person having ordinary skill in the art from

replacing various elements of the Nilson system with certain of those from Shozo to reach the claimed invention. Even more significantly, the fact that neither Nilson nor Shozo even *recognize* the problems associated with using broadband light sources to provide excitation illumination, much less propose solutions to those problems, means that neither reference can support a prima-facie case of obviousness. The pending claims thus retain their presumption of patentability and are allowable.

The legal standards for rejecting claims under 35 U.S.C. §103 are set forth in the prior office action response dated April 30, 2013. Applicants specifically incorporate those legal standards herein by reference as if they were repeated herein.

The Present Invention:

The present invention relates to systems for exciting fluorescent materials and more particularly to systems for exciting fluorescent materials in molecular imaging systems. See, for example, paragraph [0002] of the pending application. In one embodiment, the assembly comprises a housing defining a central opening therein and a plurality of lamp receptacles surrounding the central opening. The housing is mountable to a support structure having a camera mounted thereto so that a field of view of the camera is substantially unobstructed by the housing. A light source is positioned within each of the plurality of lamp receptacles, at least one of which is a narrowband light source. A diffuser is positioned within at least some of the lamp receptacles. A control system connected to each of the light sources operates selected ones of the light sources to provide a desired excitation illumination to an object within the field of view of the camera. See, for example, pending claim 1.

The excitation light source assembly of the present invention

may be used to advantage to illuminate an object or specimen with light in selected narrow bands or colors, thereby allowing a single excitation light source assembly to be used in imaging applications involving a wide range of fluorescent materials that are excited over a wide range of wavelengths. See, for example, paragraph [0032] of the pending application.

Moreover, and as further detailed in the attached Rule 132 declaration of Michael Nelson, the excitation light source of a molecular imaging system typically remains illuminated while the camera system is collecting light from the fluorescing object. Accordingly, light from the excitation light source that is outside the desired wavelength range represents undesired background noise that will degrade the quality of the image data captured by the camera system. Moreover, the presence in the imaging chamber of excitation light having undesired wavelengths also may induce fluorescence in other materials in the object being imaged, thus potentially further degrading the quality of the image data produced by the camera system. The present invention solves these problems by providing an excitation light source assembly that produces excitation light in the desired wavelength range only.

The Nilson Reference:

The Nilson reference discloses a molecular imaging system that also utilizes an excitation light source 37. However, in Nilson, the excitation light source 37 is a broadband light source that is mounted outside the imaging compartment 25. A filter wheel 47 filters or removes the undesired wavelengths from the broadband light source in order to produce excitation light within the desired wavelength range. In one embodiment, Nilson uses a fiber optic bundle 35 to bring the filtered or excitation light into the imaging compartment 25, whereupon it exits via a ring-shaped frame

32. In another embodiment, Nilson uses a plurality of reflectors 122 provided on brackets 118 to direct light from individual branches of the fiber optic bundle to the desired imaging area. However, Nilson still utilizes a broadband light source 37 and filter wheel assembly that is mounted outside the imaging compartment 21.

The Shozo Reference:

The Shozo reference discloses an LED-based illuminating device for visual inspection purposes. The illuminating device comprises a cylindrical main body having a plurality of LEDs 1 of different colors disposed therein. The device further comprises a ring-shaped diffusing element 8, a lens 6 and a ring-shaped polarizing prism 5 for directing light from the LEDs 1 to the desired area. While Shozo teaches that his illuminating devices may be used in optical inspection apparatus, nowhere does Shozo ever mention, or even suggest, that his illumination system could be used as an *excitation* light source to excite fluorescent materials, as required in molecular imaging systems.

No Reason to Combine:

The examiner's rejections are improper because his proposed combination of the references runs counter to the teachings of the Nilson reference and fails to recognize the differences between a system for simply illuminating an object to be inspected, as in Shozo, versus systems for exciting fluorescent materials, as in Nilson. The differences between the Shozo and Nilson systems would preclude their combination in the manner espoused by the patent examiner.

Referring now to the Nilson reference, Nilson specifically *requires* a broadband light source. The broadband light source is

SPECTRAL_0000932

also required to be external to the imaging chamber and Nilson goes to great lengths to accommodate that arrangement. First, Nilson's external broadband light source must be provided with a variety of filters and collimation systems to select only those narrow wavelengths required to excite the particular fluorescent materials involved and to direct the filtered light into the fiber optic bundle. The fiber optic bundle then carries the filtered, collimated light into the imaging compartment, whereupon it exits via the ring-shaped illuminator.

Because of the extremely low light levels involved with such imaging systems, Nilson also goes to great lengths to ensure that stray light does not enter the imaging chamber and to avoid the use of materials that would auto-fluoresce, which would interfere with the imaging process. See, for example, col. 8, lines 1-24 of Nilson. To these ends, Nilson is careful to require that the fiber optic bundle be sheathed in materials (e.g., metal and a black PVC material) to prevent stray light from entering the bundle (col. 8, lines 1-8). Similarly, Nilson requires that the fiber optic bundle itself be fabricated from materials containing minimal amounts of materials that might auto-fluoresce. See, for example, col. 7, lines 11-34 of Nilson. Still further, Nilson requires the use of special light baffles in the external light source assembly to prevent stray, un-filtered light from entering the fiber optic bundle. See, for example, col. 10, line 23 - col. 11, line 11 of Nilson. Significantly, Nilson recognizes (and teaches) that the requirements for fluorescent imaging require special design features, such as the use of his light baffle:

> "While the collective optical arrangement of a conventional filter wheel assembly is applicable for most optical applications, **this set-up is not suitable for fluorescent imaging.**" Col. 10, lines 23-25 of Nilson

SPECTRAL_0000933

(emphasis added).

In contrast to Nilson, Shozo provides a simple illumination system for producing a uniform light spot for object inspection systems. While Shozo mentions that his illumination system could be used in a wide range of applications, nowhere does Shozo mention, nor even suggest, that his illumination system could be used as an excitation light source in the type of low-level fluorescent type imaging systems of Nilson and the present invention. To the contrary, rather than seeking to produce narrow band illumination, as does Nilson, Shozo seeks to provide a broadband illumination system by *combining* the light produced by various red, green, and blue LEDs. See for example, col. 3, lines 33-45 of Shozo. Indeed, Shozo even teaches that more green LEDs must be provided (due to their lower light output) in order to provide "white" light illumination. Col. 3, lines 40-45.

Considering now the question of obviousness, a person having ordinary skill in the art (and with no knowledge of the present invention), would not conclude from Nilson and Shozo that they could be combined. First, such a person would conclude form Nilson that the issues involved with providing excitation light sources for fluorescent imaging applications are considerably different than the issues associated with simple object illumination systems of the type with which Shozo is concerned. Namely, excitation systems must provide light within a narrow band and at specific wavelengths. In contrast, Shozo seeks to provide broadband light (e.g., by using individual red, green, and blue LEDs and aiming them so that they converge). Indeed, Shozo explains in great length how a control unit may be used to achieve the desired brightness and chromaticity of the superimposed light beams. See, for example, col. 6, lines 11-32. Nowhere does Shozo ever suggest,

much less describe an embodiment that could be used to provide excitation light to fluorescent materials, as in Nilson.

Stated simply, the teachings of Nilson and Shozo are opposed: While Nilson starts with white light and uses a filter wheel to *remove* undesired wavelengths, Shozo *combines* wavelengths from various colored LEDs to produce white light. These opposed teachings would discourage a person having ordinary skill in the art from combining any features or elements of Nilson and Shozo.

Still further, because the Nilson arrangement is presumed to be effective for its intended purpose, namely to provide narrowband excitation light to excite selected fluorescent materials, there would be no need, thus no suggestion or incentive, to modify Nilson to include any elements from Shozo's broadband illumination system. Indeed, to do so would make Nilson's system inoperative. That is, the use of Shozo's broadband or white light illumination system would excite a wide range of fluorescent materials in the object, the opposite of what Nilson desires.

Moreover, while Shozo discloses a ring-shaped illumination system with a camera in the central aperture, that arrangement is already disclosed in Nilson, by means of his ring-shaped illuminator. Here again, a person having ordinary skill in the art would not be motivated to use these features from Shozo because Nilson already uses them.

In combining the Nilson and Shozo references, the examiner has focused solely on finding references that disclose claimed elements (i.e., a lighting system with a housing that defines a plurality of lamp receptacles therein as in Shozo), but without regard to what the various references would teach or suggest to a person having ordinary skill in the art and with no knowledge of the present invention. As such, the examiner's new rejections amount to nothing more than hindsight reconstruction. That is, rather than

considering the references as a whole and how they would be understood by a person having ordinary skill in the art, the examiner's new rejections are based on nothing more than the mere identification in the references of the various elements and limitations of the rejected claims. This type of rationale remains an impermissible basis for rejecting claims, even after KSR:

> A claim "composed of several elements **is not proved obvious** merely by demonstration that each of its elements was, independently, known in the prior art." (emphasis added).

KSR Int'l Co. v. Teleflex, Inc., 127 S.Ct. 1727, 1741 (2007).

Prior Art Failed to Recognize the Problem:

"An invention can often be the recognition of a problem itself." Leo Pharmaceutical Products, Ltd. v Rea, 726 F.3d 1346, 1353 (Fed. Cir. 2013). See also Cardiac Pacemakers, Inc. v. St. Jude Med., Inc., 381 F.3d 1271, 1377 (Fed. Cir. 2004): "There can of course arise situations wherein identification of the problem itself is the invention."

As discussed in the attached Rule 132 Declaration of Michael Nelson, the excitation light source of a molecular imaging system typically remains illuminated while the camera system is collecting light from the fluorescing object. Accordingly, light from the excitation light source that is outside the desired wavelength range represents undesired background noise that will degrade the quality of the image data captured by the camera system. Furthermore, the presence in the imaging chamber of light having undesired wavelengths may induce fluorescence in other (undesired) materials in the object being imaged, thus potentially further

SPECTRAL_0000936

degrading the quality of the image data produced by the camera system.

While the illumination system of Nilson seeks to provide excitation light in the desired narrow band or wavelength range, the filters used by Nilson are not perfect filters and will always allow some light to pass that is outside the desired wavelength range. As set forth in the attached Rule 132 declaration of Michael Nelson, even the best optical filters, i.e., those having optical densities of 5 or 6, allow significant amounts of light to pass that is outside the desired wavelength range. The presence in the imaging chamber of such out-of-band light represents a significant source of background light or "noise" that will degrade the quality of the image data captured by the camera system, particularly at the extremely low light levels involved in such imaging systems. Moreover, the presence of such undesired background light may also excite (or cause to fluoresce) other materials in the object that are not desired to be imaged.

Nowhere does Nilson ever discuss the problems associated with such filter systems, much less propose solutions to them. Shozo is also silent as to such problems. To the contrary, Shozo specifically seeks to provide an illumination system that simultaneously provides light over as large a wavelength range as possible.

Therefore, the present invention is not simply a combination of elements found in the prior art. Rather, it is a unique combination of elements specifically configured to solve a problem that the prior art did not even recognize, much less address. Because neither Nilson or Shozo recognized or disclosed the background problem, there would be no reason for a person having ordinary skill in the art to improve upon either reference, much less attempt to combine them in the manner required by the pending

claims. The pending claims are therefore patentable because they represent a solution to problems not recognized by the prior art. See, for example, Leo Pharmaceuticals, supra, and Cardiac Pacemakers, supra.

In summation then, the unrelated and, in some instances opposed, teachings of Nilson and Shozo would preclude any rational reason for their combination: A person having ordinary skill in the art would not seek to combine Nilson and Shozo because they disclose two very different types of lighting systems for two very different purposes. Therefore, they cannot be used to establish a prima-facie case of obviousness. Moreover, neither reference even recognizes the background problem, much less attempts to solve it. The pending claims retain their presumption of patentability and should be allowed.

* * *

Applicants believe that all of the claims pending in this patent application are allowable and that all other issues raised by the examiner have been satisfactorily addressed. Applicants respectfully request the examiner to reconsider the rejections and grant an early allowance. If any questions or issues remain to be resolved, the examiner is requested to contact the Applicants' attorney at the telephone number listed below.

The applicants believe that any fees required have been paid. However, if additional fees are required, the applicant authorizes

the charge of such fees to Fennemore Craig, P.C., Deposit Account No. 06-0590.

Respectfully submitted,

FENNEMORE CRAIG, P.C.

Bruce E. Dahl, Esq.
Attorney for Applicants
PTO Registration No. 33,670
1700 Lincoln Street, Suite 2900
Denver, CO 80203-4529
(303) 291-3200

Date: 9 May 2014

IN THE UNITED STATES PATENT AND TRADEMARK OFFICE

In Re Application of:	)	
	)	Examiner: Taningco, M.
NELSON, Michael, B., *et al.*	)	
	)	Group Art Unit: 2884
Serial No. 13/222,688	)	
	)	Confirm. No.: 5910
Filing Date: August 31, 2011	)	
	)	Atty. Dkt.: SPEC US-4
For: EXCITATION LIGHT SOURCE ASSEMBLY	)	(027560-0014)
	)	

DECLARATION OF MICHAEL B. NELSON
UNDER 37 C.F.R. §§ 1.132 and 1.68

To: Commissioner for Patents
P.O. Box 1450
Alexandria, VA 22313-1450

Sir:

I, Michael B. Nelson, declare and state that:

1. I am over twenty-one (21) years old, a resident of Tucson, Arizona, and a United States citizen.

2. I am making this declaration in support of United States patent application serial no. 13/222,688 and the prosecution thereof in the United States Patent and Trademark Office.

3. I have been employed by Spectral Instruments Imaging, Inc., since September of 2009. My current title is Chief Technology Officer.

4. I am the co-inventor of the patent application and an employee of Spectral Instruments Imaging, Inc., the assignee of the

subject patent application. However, in spite of my interest in the patent application, the statements I make herein are true, factual, and accurate to the best of my ability.

5. My background qualifications, experience, and credentials for making this declaration are set forth below:

6. In 1988, I received a Bachelor of Science Degree in Physics from San Jose State University.

7. I have 12 years of experience in the design and manufacture of molecular imaging systems and am the named inventor or co-inventor on numerous United States and foreign patents for such systems. I have 9 years of experience in detector and diagnostic systems for laser-based plasma physics experiments at Lawrence Livermore National Laboratory.

8. My job responsibilities at Spectral Instruments Imaging, Inc., include new product development, particularly as it relates to the design and manufacture of molecular imaging systems and in the design and manufacture of excitation light source assemblies for such molecular imaging systems.

9. Additional information regarding my background qualifications, experience, and credentials for making this declaration are set forth in Exhibit A.

10. The system described in U.S. Patent No. 6,894,289 to Nilson *et al.*, ("Nilson") uses a broadband or 'white' light source that produces light across a wide range of wavelengths.

11. Nilson uses a filter wheel assembly to remove or filter

the undesired wavelengths from the broadband source to produce excitation light in the desired wavelength range, typically with a width of about 20 nm, as specified in col. 9, line 27 of the Nilson patent.

12. While light filters are available for removing such undesired wavelengths, none are 'perfect' filters and will also pass some percentage of light in other wavelengths.

13. The measure of the ability of a given light filter to block light in undesired wavelength ranges is referred to as 'optical density' (OD). As is known, the optical density of a filter material is a logarithmic ratio (typically the common log) of the radiation falling upon the filter material to the radiation transmitted through the filter material. Expressed mathematically:

$$OD_{\lambda} = -\log_{10}(I_1/I_0)$$

where:

OD_{λ} = the optical density at a certain wavelength λ;

I_1 = the intensity of the light that has passed through the filter material;

I_0 = the intensity of the light before it passes through the filter material.

14. Most commercially available optical filter materials have out-of-band optical densities of 5 or 6. Nilson states that the filters he uses have a rejection of $>10^6$ (col. 9, line 30), which corresponds to an optical density of 6.

15. Even a filter with an out-of-band OD of 6 will essentially allow through 1 photon out of 1,000,000. Given that a light source that is still invisible to the unaided eye produces

about 1 billion (10^9) photons per second, a filter with an out-of-band OD of 6 will still be a significant source of unwanted "background" at the low light levels typically associated with the use of molecular imaging systems.

16. A vast majority of the imaging performed by molecular imaging systems is done with the excitation light sources illuminated during the image capture process.

17. The presence in the imaging chamber of light outside of the desired excitation wavelengths (and not resulting from the fluorescence of the desired materials) represents undesired background light or noise. Because a significant amount of the undesired background light is captured by the camera system during the image capture process, the presence of undesired background light will degrade the overall quality of the image data captured by the camera system.

18. The presence in the imaging chamber of such undesired background light may also excite other fluorescent materials in the object being imaged. The inadvertent excitation of such other fluorescent materials is typically undesirable and represents another source of degradation of the image data captured by the camera system.

19. The narrow band light sources used in the invention described in the subject patent application do not produce significant amounts of out-of-band light. Therefore, the excitation light sources of the subject patent application will not introduce into the imaging chamber significant amounts of unwanted background light.

20. I hereby declare that all statements made herein of my own knowledge are true and that all statements made on information and belief are believed to be true; and further that these statements are made with the knowledge that willful false statements and the like so made are punishable by fine or imprisonment, or both, under Section 1001 of Title 18 of the United States Code, and that such willful false statements may jeopardize the validity of my application or any patent issued thereon.

Michael B. Nelson

Date: 5/9/14

EXHIBIT A

SPECTRAL_0000945

MICHAEL B. NELSON

PROFESSIONAL EXPERIENCE

SPECTRAL INSTRUMENTS IMAGING, Sept 2009 to present
CHIEF TECHNOLOGY OFFICER

Design, test and manufacture molecular imaging systems. Manage research and development, testing, new product development, software development and maintenance, field service programs and customer training. Brought to market two new molecular imaging systems based on modern and novel concepts to compete with older systems already on the market. Responsible for sales program with two full time salesmen in North American and distributors abroad. Managing a team of engineers, technicians and consultants.

GENERAL ATOMICS, La Jolla, CA, Jan 2008 to Sept 2009
PRODUCTION OPERATIONS

Introduced industrial production practices to a very academic minded organization producing first-of-a-kind targets to the US laser fusion laboratory community (Lawrence Livermore National Laboratory, Los Alamos National Laboratory, Sandia National Laboratory and the Laboratory for Laser Energetics at the University of Rochester). 80% of this work is make-to-order while the remainder is essentially R&D/developmental. Interface with external principle investigators (physicists) and designers (engineers) to ascertain experimental target requirements then assemble appropriate internal team of scientists, engineers and technicians to develop a production plan including R&D gates if required. As part of General Atomics' responsibility to the National Laser User Facility (via DOE funding), assisted university (MIT) professors in design of experiments and targets to be shot at OMEGA laser at the Laboratory for Laser Energetics. Redesigned lab space for better equipment utilization, work station cleanliness and safety. Consolidated scheduling and database software for the many groups. Directly responsible for Capsules, Plastic Coating, Foams, and Micro-Assembly groups.

CONSULTANT, 2005 to Jan 2008
Wide-ranging consulting practice that includes manufacturing, nuclear instrumentation, animal imaging, instrumentation training, and fisheries science (catch rate data and economic impact analysis). Customers include Diablo Technologies, Xenogen Corporation and Caliper Life Sciences.

XENOGEN CORPORATION, Alameda, CA, 1998 to 2005
Rapid progression through the following increasingly responsible positions

DIVISIONAL VP, MANUFACTURING OPERATIONS, 2004 to 2005
INSTRUMENTATION DIVISION DIRECTOR, 2001 to 2004
BIOIMAGING LAP MANAGER, 1998 to 2001
Managed all facets of production and operation for a global scientific device manufacturer: purchasing, receiving, inventory, floor planning, manufacturing, calibration, testing/quality assurance, packaging, international shipping and documentation (including VAT and carnet issues), equipment installations, customer training, and field service. Selected and qualified vendors; led new product introduction from concept and design to production development (production beta units, life time studies, cost reduction, reliability/performance improvements, and CE verification). Worked closely with business, sales, and marketing groups; served as key technical liaison with

customers in large pharmaceutical companies, biotech firms, and universities. Managed four direct reports with overall responsibility for 35-person staff.

Key accomplishments:

- Steadily increased production of new Xenogen instrument, from design, prototype, introduction at 20 units in 2001 to 130 units and sales of $20M+ in 2005.
- Established and led Instrumentation Division, which ultimately included 35 engineers, physicists, technicians, and support personnel.
- Won IR&D award in 2001 for IVIS 100.
- Spearheaded introduction of four new instruments and five accessories.
- Led design of Xenogen's gas anesthesia machine for small animals (XGI-8); device balanced gas flow to up to five mice while reducing personnel exposure by a factor of 10.
- Produced products featuring absolute calibrations.
- Designed two new adaptable manufacturing facilities.
- Identified, championed, and produced a lower-priced, higher-margin instrument that now accounts for 25% of revenue.
- Negotiated supply agreements with two key vendors that saved nearly $1M in 2003 alone..
- Implemented materials management and procurement system (SysPro).
- Introduced systems installation and designed user training programs handled by cross-trained QA and calibration engineers.
- Personally installed instruments and trained users worldwide for major pharmaceutical customers who licensed Xenogen's bio-technology.

LeCroy Corporation, Oakland, CA, 1996 to 1998
Physicist / Western Region Manager

Managed product sales and support for western North America and Hawaii for leading provider of state-of-the-art instrumentation for the Nuclear and Elementary Particle Physics Research Community. Worked closely with customers in the high energy physics, military, medical research and imaging, RADAR, LIDAR, LADAR, isotope production, astronomy, laser, atmospheric research, and automotive industries. Designed acquisition systems to customer's experimental needs and recommended detector selection; demonstrated products; facilitated purchasing, delivery, and technical support.

Key accomplishments:

- Exceeded LeCroy FY98 quota by 31% with total sales of nearly $1.6M.
- Second in company sales in 1998.

Lawrence Livermore National Laboratory, Livermore, CA, 1985 to 1996
Physicist, 1988 to 1996
Student Researcher, 1985 to 1988

Lawrence Livermore National Laboratory (LLNL) is an applied science laboratory that is part of the National Nuclear Security Administration (NNSA), within the Department of Energy (DOE). Managed a 4000 square foot laboratory housing a neutron generator and a Heavy Ion Fusion recirculator prototype with associated control room and data acquisition systems.

Key accomplishments:

- Managed all Environmental, Safety and Health (ES&H) issues for this lab from 1993 to 1996 including over 80 radioactive sources.
- Heavily involved in design, construction, calibration, and operation of a 960-channel neutron time-of-flight detector and data acquisition system (LaNSA).

- Used a neutron generator with computerized data acquisition system to design an automated system to calibrate individual detector modules offline.
- Represented LLNL on experiments conducted in England in 1995 and 1996.

EDUCATION

Significant graduate work in physics, San Jose State University, San Jose, CA

B.S. in Physics (minors in Chemistry and Math), San Jose State University, San Jose, CA

A.S. in Electronics Technology

948

SPECTRAL_0000948

Electronic Patent Application Fee Transmittal

Application Number:	13222688
Filing Date:	31-Aug-2011
Title of Invention:	EXCITATION LIGHT SOURCE ASSEMBLY
First Named Inventor/Applicant Name:	Michael B. Nelson
Filer:	Bruce E. Dahl/Cynthia Sullivan
Attorney Docket Number:	SPEC US-4 (027560-0014)

Filed as Small Entity

Utility under 35 USC 111(a) Filing Fees

Description	Fee Code	Quantity	Amount	Sub-Total in USD($)
Basic Filing:				
Pages:				
Claims:				
Miscellaneous-Filing:				
Petition:				
Patent-Appeals-and-Interference:				
Post-Allowance-and-Post-Issuance:				
Extension-of-Time:				
Extension - 1 month with $0 paid	2251	1	100	100

Description	Fee Code	Quantity	Amount	Sub-Total in USD($)
Miscellaneous:				
			Total in USD ($)	**100**

Electronic Acknowledgement Receipt

EFS ID:	18992185
Application Number:	13222688
International Application Number:	
Confirmation Number:	5910
Title of Invention:	EXCITATION LIGHT SOURCE ASSEMBLY
First Named Inventor/Applicant Name:	Michael B. Nelson
Customer Number:	27104
Filer:	Bruce E. Dahl
Filer Authorized By:	
Attorney Docket Number:	SPEC US-4 (027560-0014)
Receipt Date:	09-MAY-2014
Filing Date:	31-AUG-2011
Time Stamp:	16:25:31
Application Type:	Utility under 35 USC 111(a)

Payment information:

Submitted with Payment	yes
Payment Type	Deposit Account
Payment was successfully received in RAM	$100
RAM confirmation Number	2741
Deposit Account	060590
Authorized User	
The Director of the USPTO is hereby authorized to charge indicated fees and credit any overpayment as follows: Charge any Additional Fees required under 37 C.F.R. Section 1.16 (National application filing, search, and examination fees) Charge any Additional Fees required under 37 C.F.R. Section 1.17 (Patent application and reexamination processing fees)	

Charge any Additional Fees required under 37 C.F.R. Section 1.19 (Document supply fees)

Charge any Additional Fees required under 37 C.F.R. Section 1.20 (Post Issuance fees)

Charge any Additional Fees required under 37 C.F.R. Section 1.21 (Miscellaneous fees and charges)

File Listing:

Document Number	Document Description	File Name	File Size(Bytes)/ Message Digest	Multi Part /.zip	Pages (if appl.)
1		Ext-Resp-Decl.pdf	793903 ae42295591493de2d78b2693a23bc25454e3f8be	yes	29

	Multipart Description/PDF files in .zip description		
	Document Description	Start	End
	Extension of Time	1	1
	Amendment/Req. Reconsideration-After Non-Final Reject	2	29

Warnings:

Information:

2	Fee Worksheet (SB06)	fee-info.pdf	30648 2e66e63a25c6051aa7d7d979d7ac154ea6515728	no	2

Warnings:

Information:

Total Files Size (in bytes):	824551

This Acknowledgement Receipt evidences receipt on the noted date by the USPTO of the indicated documents, characterized by the applicant, and including page counts, where applicable. It serves as evidence of receipt similar to a Post Card, as described in MPEP 503.

New Applications Under 35 U.S.C. 111

If a new application is being filed and the application includes the necessary components for a filing date (see 37 CFR 1.53(b)-(d) and MPEP 506), a Filing Receipt (37 CFR 1.54) will be issued in due course and the date shown on this Acknowledgement Receipt will establish the filing date of the application.

National Stage of an International Application under 35 U.S.C. 371

If a timely submission to enter the national stage of an international application is compliant with the conditions of 35 U.S.C. 371 and other applicable requirements a Form PCT/DO/EO/903 indicating acceptance of the application as a national stage submission under 35 U.S.C. 371 will be issued in addition to the Filing Receipt, in due course.

New International Application Filed with the USPTO as a Receiving Office

If a new international application is being filed and the international application includes the necessary components for an international filing date (see PCT Article 11 and MPEP 1810), a Notification of the International Application Number and of the International Filing Date (Form PCT/RO/105) will be issued in due course, subject to prescriptions concerning national security, and the date shown on this Acknowledgement Receipt will establish the international filing date of the application.

PTO/AIA/22 (03-13)
Approved for use through 7/31/2016. OMB 0651-0031
U.S. Patent and Trademark Office; U.S. DEPARTMENT OF COMMERCE
Under the Paperwork Reduction Act of 1995, no persons are required to respond to a collection of information unless it displays a valid OMB control number.

PETITION FOR EXTENSION OF TIME UNDER 37 CFR 1.136(a)

Docket Number (Optional): SPEC US-4 (027353.0014)

Application Number: 13/222,688

Filed: August 31, 2011

For: EXCITATION LIGHT SOURCE ASSEMBLY

Art Unit: 2884

Examiner: Taningco, M.

This is a request under the provisions of 37 CFR 1.136(a) to extend the period for filing a reply in the above-identified application.

The requested extension and fee are as follows (check time period desired and enter the appropriate fee below):

		Fee	Small Entity Fee	Micro Entity Fee	
☑	One month (37 CFR 1.17(a)(1))	$200	$100	$50	$ 100
☐	Two months (37 CFR 1.17(a)(2))	$600	$300	$150	$
☐	Three months (37 CFR 1.17(a)(3))	$1,400	$700	$350	$
☐	Four months (37 CFR 1.17(a)(4))	$2,200	$1,100	$550	$
☐	Five months (37 CFR 1.17(a)(5))	$3,000	$1,500	$750	$

☐ Applicant asserts small entity status. See 37 CFR 1.27.

☐ Applicant certifies micro entity status. See 37 CFR 1.29.
Form PTO/SB/15A or B or equivalent must either be enclosed or have been submitted previously.

☐ A check in the amount of the fee is enclosed.

☐ Payment by credit card. Form PTO-2038 is attached.

☐ The Director has already been authorized to charge fees in this application to a Deposit Account.

☑ The Director is hereby authorized to charge any fees which may be required, or credit any overpayment, to Deposit Account Number 06-0590.

☑ Payment made via EFS-Web.

WARNING: Information on this form may become public. Credit card information should not be included on this form. Provide credit card information and authorization on PTO-2038.

I am the

☐ applicant.

☑ attorney or agent of record. Registration number 33,670.

☐ attorney or agent acting under 37 CFR 1.34. Registration number _____.

/Bruce E. Dahl/ — Signature

May 9, 2014 — Date

Bruce E. Dahl — Typed or printed name

(303) 291-3200 — Telephone Number

NOTE: This form must be signed in accordance with 37 CFR 1.33. See 37 CFR 1.4 for signature requirements and certifications. Submit multiple forms if more than one signature is required, see below*.

☑ * Total of 1 forms are submitted.

This collection of information is required by 37 CFR 1.136(a). The information is required to obtain or retain a benefit by the public, which is to file (and by the USPTO to process) an application. Confidentiality is governed by 35 U.S.C. 122 and 37 CFR 1.11 and 1.14. This collection is estimated to take 6 minutes to complete, including gathering, preparing, and submitting the completed application form to the USPTO. Time will vary depending upon the individual case. Any comments on the amount of time you require to complete this form and/or suggestions for reducing this burden should be sent to the Chief Information Officer, U.S. Patent and Trademark Office, U.S. Department of Commerce, P.O. Box 1450, Alexandria, VA 22313-1450. DO NOT SEND FEES OR COMPLETED FORMS TO THIS ADDRESS. SEND TO: Mail Stop PCT, Commissioner for Patents, P.O. Box 1450, Alexandria, VA 22313-1450.

PTO/SB/06 (09-11)
Approved for use through 1/31/2014. OMB 0651-0032
U.S. Patent and Trademark Office; U.S. DEPARTMENT OF COMMERCE
Under the Paperwork Reduction Act of 1995, no persons are required to respond to a collection of information unless it displays a valid OMB control number.

PATENT APPLICATION FEE DETERMINATION RECORD Substitute for Form PTO-875	Application or Docket Number 13/222,688	Filing Date 08/31/2011	☐ To be Mailed

ENTITY: ☐ LARGE ☒ SMALL ☐ MICRO

APPLICATION AS FILED – PART I

	(Column 1)	(Column 2)		
FOR	NUMBER FILED	NUMBER EXTRA	RATE ($)	FEE ($)
☐ BASIC FEE (37 CFR 1.16(a), (b), or (c))	N/A	N/A	N/A	
☐ SEARCH FEE (37 CFR 1.16(k), (i), or (m))	N/A	N/A	N/A	
☐ EXAMINATION FEE (37 CFR 1.16(o), (p), or (q))	N/A	N/A	N/A	
TOTAL CLAIMS (37 CFR 1.16(i))	minus 20 =	*	X $ =	
INDEPENDENT CLAIMS (37 CFR 1.16(h))	minus 3 =	*	X $ =	
☐ APPLICATION SIZE FEE (37 CFR 1.16(s))	If the specification and drawings exceed 100 sheets of paper, the application size fee due is $310 ($155 for small entity) for each additional 50 sheets or fraction thereof. See 35 U.S.C. 41(a)(1)(G) and 37 CFR 1.16(s).			
☐ MULTIPLE DEPENDENT CLAIM PRESENT (37 CFR 1.16(j))				
* If the difference in column 1 is less than zero, enter "0" in column 2.			TOTAL	

APPLICATION AS AMENDED – PART II

		(Column 1)		(Column 2)	(Column 3)		
AMENDMENT	05/09/2014	CLAIMS REMAINING AFTER AMENDMENT		HIGHEST NUMBER PREVIOUSLY PAID FOR	PRESENT EXTRA	RATE ($)	ADDITIONAL FEE ($)
	Total (37 CFR 1.16(i))	* 27	Minus	** 29	= 0	X $40 =	0
	Independent (37 CFR 1.16(h))	* 3	Minus	***4	= 0	X $210 =	0
	☐ Application Size Fee (37 CFR 1.16(s))						
	☐ FIRST PRESENTATION OF MULTIPLE DEPENDENT CLAIM (37 CFR 1.16(j))						
						TOTAL ADD'L FEE	0

		(Column 1)		(Column 2)	(Column 3)		
AMENDMENT		CLAIMS REMAINING AFTER AMENDMENT		HIGHEST NUMBER PREVIOUSLY PAID FOR	PRESENT EXTRA	RATE ($)	ADDITIONAL FEE ($)
	Total (37 CFR 1.16(i))	*	Minus	**	=	X $ =	
	Independent (37 CFR 1.16(h))	*	Minus	***	=	X $ =	
	☐ Application Size Fee (37 CFR 1.16(s))						
	☐ FIRST PRESENTATION OF MULTIPLE DEPENDENT CLAIM (37 CFR 1.16(j))						
						TOTAL ADD'L FEE	

* If the entry in column 1 is less than the entry in column 2, write "0" in column 3.
** If the "Highest Number Previously Paid For" IN THIS SPACE is less than 20, enter "20".
*** If the "Highest Number Previously Paid For" IN THIS SPACE is less than 3, enter "3".
The "Highest Number Previously Paid For" (Total or Independent) is the highest number found in the appropriate box in column 1.

LIE
/JONYA SMALLS/

This collection of information is required by 37 CFR 1.16. The information is required to obtain or retain a benefit by the public which is to file (and by the USPTO to process) an application. Confidentiality is governed by 35 U.S.C. 122 and 37 CFR 1.14. This collection is estimated to take 12 minutes to complete, including gathering, preparing, and submitting the completed application form to the USPTO. Time will vary depending upon the individual case. Any comments on the amount of time you require to complete this form and/or suggestions for reducing this burden, should be sent to the Chief Information Officer, U.S. Patent and Trademark Office, U.S. Department of Commerce, P.O. Box 1450, Alexandria, VA 22313-1450. DO NOT SEND FEES OR COMPLETED FORMS TO THIS ADDRESS. **SEND TO: Commissioner for Patents, P.O. Box 1450, Alexandria, VA 22313-1450.**
If you need assistance in completing the form, call 1-800-PTO-9199 and select option 2.

UNITED STATES PATENT AND TRADEMARK OFFICE

UNITED STATES DEPARTMENT OF COMMERCE
United States Patent and Trademark Office
Address: COMMISSIONER FOR PATENTS
P.O. Box 1450
Alexandria, Virginia 22313-1450
www.uspto.gov

NOTICE OF ALLOWANCE AND FEE(S) DUE

27104 7590 08/29/2014

FENNEMORE CRAIG, P.C.
1700 Lincoln Street
SUITE 2900
DENVER, CO 80203

EXAMINER	
TANINGCO, MARCUS H	
ART UNIT	PAPER NUMBER
2884	

DATE MAILED: 08/29/2014

APPLICATION NO.	FILING DATE	FIRST NAMED INVENTOR	ATTORNEY DOCKET NO.	CONFIRMATION NO.
13/222,688	08/31/2011	Michael B. Nelson	SPEC US-4 (027560-0014)	5910

TITLE OF INVENTION: EXCITATION LIGHT SOURCE ASSEMBLY

APPLN. TYPE	ENTITY STATUS	ISSUE FEE DUE	PUBLICATION FEE DUE	PREV. PAID ISSUE FEE	TOTAL FEE(S) DUE	DATE DUE
nonprovisional	SMALL	$480	$0	$0	$480	12/01/2014

THE APPLICATION IDENTIFIED ABOVE HAS BEEN EXAMINED AND IS ALLOWED FOR ISSUANCE AS A PATENT. PROSECUTION ON THE MERITS IS CLOSED. THIS NOTICE OF ALLOWANCE IS NOT A GRANT OF PATENT RIGHTS. THIS APPLICATION IS SUBJECT TO WITHDRAWAL FROM ISSUE AT THE INITIATIVE OF THE OFFICE OR UPON PETITION BY THE APPLICANT. SEE 37 CFR 1.313 AND MPEP 1308.

THE ISSUE FEE AND PUBLICATION FEE (IF REQUIRED) MUST BE PAID WITHIN THREE MONTHS FROM THE MAILING DATE OF THIS NOTICE OR THIS APPLICATION SHALL BE REGARDED AS ABANDONED. THIS STATUTORY PERIOD CANNOT BE EXTENDED. SEE 35 U.S.C. 151. THE ISSUE FEE DUE INDICATED ABOVE DOES NOT REFLECT A CREDIT FOR ANY PREVIOUSLY PAID ISSUE FEE IN THIS APPLICATION. IF AN ISSUE FEE HAS PREVIOUSLY BEEN PAID IN THIS APPLICATION (AS SHOWN ABOVE), THE RETURN OF PART B OF THIS FORM WILL BE CONSIDERED A REQUEST TO REAPPLY THE PREVIOUSLY PAID ISSUE FEE TOWARD THE ISSUE FEE NOW DUE.

HOW TO REPLY TO THIS NOTICE:

I. Review the ENTITY STATUS shown above. If the ENTITY STATUS is shown as SMALL or MICRO, verify whether entitlement to that entity status still applies.

If the ENTITY STATUS is the same as shown above, pay the TOTAL FEE(S) DUE shown above.

If the ENTITY STATUS is changed from that shown above, on PART B - FEE(S) TRANSMITTAL, complete section number 5 titled "Change in Entity Status (from status indicated above)".

For purposes of this notice, small entity fees are 1/2 the amount of undiscounted fees, and micro entity fees are 1/2 the amount of small entity fees.

II. PART B - FEE(S) TRANSMITTAL, or its equivalent, must be completed and returned to the United States Patent and Trademark Office (USPTO) with your ISSUE FEE and PUBLICATION FEE (if required). If you are charging the fee(s) to your deposit account, section "4b" of Part B - Fee(s) Transmittal should be completed and an extra copy of the form should be submitted. If an equivalent of Part B is filed, a request to reapply a previously paid issue fee must be clearly made, and delays in processing may occur due to the difficulty in recognizing the paper as an equivalent of Part B.

III. All communications regarding this application must give the application number. Please direct all communications prior to issuance to Mail Stop ISSUE FEE unless advised to the contrary.

IMPORTANT REMINDER: Utility patents issuing on applications filed on or after Dec. 12, 1980 may require payment of maintenance fees. It is patentee's responsibility to ensure timely payment of maintenance fees when due.

PART B - FEE(S) TRANSMITTAL

Complete and send this form, together with applicable fee(s), to: Mail **Mail Stop ISSUE FEE**
Commissioner for Patents
P.O. Box 1450
Alexandria, Virginia 22313-1450
or Fax (571)-273-2885

INSTRUCTIONS: This form should be used for transmitting the ISSUE FEE and PUBLICATION FEE (if required). Blocks 1 through 5 should be completed where appropriate. All further correspondence including the Patent, advance orders and notification of maintenance fees will be mailed to the current correspondence address as indicated unless corrected below or directed otherwise in Block 1, by (a) specifying a new correspondence address; and/or (b) indicating a separate "FEE ADDRESS" for maintenance fee notifications.

CURRENT CORRESPONDENCE ADDRESS (Note: Use Block 1 for any change of address)

27104 7590 08/29/2014
FENNEMORE CRAIG, P.C.
1700 Lincoln Street
SUITE 2900
DENVER, CO 80203

Note: A certificate of mailing can only be used for domestic mailings of the Fee(s) Transmittal. This certificate cannot be used for any other accompanying papers. Each additional paper, such as an assignment or formal drawing, must have its own certificate of mailing or transmission.

Certificate of Mailing or Transmission
I hereby certify that this Fee(s) Transmittal is being deposited with the United States Postal Service with sufficient postage for first class mail in an envelope addressed to the Mail Stop ISSUE FEE address above, or being facsimile transmitted to the USPTO (571) 273-2885, on the date indicated below.

(Depositor's name)
(Signature)
(Date)

APPLICATION NO.	FILING DATE	FIRST NAMED INVENTOR	ATTORNEY DOCKET NO.	CONFIRMATION NO.
13/222,688	08/31/2011	Michael B. Nelson	SPEC US-4 (027560-0014)	5910

TITLE OF INVENTION: EXCITATION LIGHT SOURCE ASSEMBLY

APPLN. TYPE	ENTITY STATUS	ISSUE FEE DUE	PUBLICATION FEE DUE	PREV. PAID ISSUE FEE	TOTAL FEE(S) DUE	DATE DUE
nonprovisional	SMALL	$480	$0	$0	$480	12/01/2014

EXAMINER	ART UNIT	CLASS-SUBCLASS
TANINGCO, MARCUS H	2884	250-461100

1. Change of correspondence address or indication of "Fee Address" (37 CFR 1.363).
- ☐ Change of correspondence address (or Change of Correspondence Address form PTO/SB/122) attached.
- ☐ "Fee Address" indication (or "Fee Address" Indication form PTO/SB/47; Rev 03-02 or more recent) attached. **Use of a Customer Number is required.**

2. For printing on the patent front page, list
(1) The names of up to 3 registered patent attorneys or agents OR, alternatively,
(2) The name of a single firm (having as a member a registered attorney or agent) and the names of up to 2 registered patent attorneys or agents. If no name is listed, no name will be printed.
1 _____
2 _____
3 _____

3. ASSIGNEE NAME AND RESIDENCE DATA TO BE PRINTED ON THE PATENT (print or type)

PLEASE NOTE: Unless an assignee is identified below, no assignee data will appear on the patent. If an assignee is identified below, the document has been filed for recordation as set forth in 37 CFR 3.11. Completion of this form is NOT a substitute for filing an assignment.

(A) NAME OF ASSIGNEE (B) RESIDENCE: (CITY and STATE OR COUNTRY)

Please check the appropriate assignee category or categories (will not be printed on the patent) : ☐ Individual ☐ Corporation or other private group entity ☐ Government

4a. The following fee(s) are submitted:
- ☐ Issue Fee
- ☐ Publication Fee (No small entity discount permitted)
- ☐ Advance Order - # of Copies _____

4b. Payment of Fee(s): **(Please first reapply any previously paid issue fee shown above)**
- ☐ A check is enclosed.
- ☐ Payment by credit card. Form PTO-2038 is attached.
- ☐ The Director is hereby authorized to charge the required fee(s), any deficiency, or credits any overpayment, to Deposit Account Number _____ (enclose an extra copy of this form).

5. **Change in Entity Status** (from status indicated above)
- ☐ Applicant certifying micro entity status. See 37 CFR 1.29 — NOTE: Absent a valid certification of Micro Entity Status (see forms PTO/SB/15A and 15B), issue fee payment in the micro entity amount will not be accepted at the risk of application abandonment.
- ☐ Applicant asserting small entity status. See 37 CFR 1.27 — NOTE: If the application was previously under micro entity status, checking this box will be taken to be a notification of loss of entitlement to micro entity status.
- ☐ Applicant changing to regular undiscounted fee status. — NOTE: Checking this box will be taken to be a notification of loss of entitlement to small or micro entity status, as applicable.

NOTE: This form must be signed in accordance with 37 CFR 1.31 and 1.33. See 37 CFR 1.4 for signature requirements and certifications.

Authorized Signature _____ Date _____

Typed or printed name _____ Registration No. _____

PTOL-85 Part B (10-13) Approved for use through 10/31/2013. OMB 0651-0033 U.S. Patent and Trademark Office; U.S. DEPARTMENT OF COMMERCE

UNITED STATES PATENT AND TRADEMARK OFFICE

UNITED STATES DEPARTMENT OF COMMERCE
United States Patent and Trademark Office
Address: COMMISSIONER FOR PATENTS
P.O. Box 1450
Alexandria, Virginia 22313-1450
www.uspto.gov

APPLICATION NO.	FILING DATE	FIRST NAMED INVENTOR	ATTORNEY DOCKET NO.	CONFIRMATION NO.
13/222,688	08/31/2011	Michael B. Nelson	SPEC US-4 (027560-0014)	5910

27104 7590 08/29/2014

FENNEMORE CRAIG, P.C.
1700 Lincoln Street
SUITE 2900
DENVER, CO 80203

EXAMINER	
TANINGCO, MARCUS H	

ART UNIT	PAPER NUMBER
2884	

DATE MAILED: 08/29/2014

Determination of Patent Term Adjustment under 35 U.S.C. 154 (b)
(Applications filed on or after May 29, 2000)

The Office has discontinued providing a Patent Term Adjustment (PTA) calculation with the Notice of Allowance.

Section 1(h)(2) of the AIA Technical Corrections Act amended 35 U.S.C. 154(b)(3)(B)(i) to eliminate the requirement that the Office provide a patent term adjustment determination with the notice of allowance. See Revisions to Patent Term Adjustment, 78 Fed. Reg. 19416, 19417 (Apr. 1, 2013). Therefore, the Office is no longer providing an initial patent term adjustment determination with the notice of allowance. The Office will continue to provide a patent term adjustment determination with the Issue Notification Letter that is mailed to applicant approximately three weeks prior to the issue date of the patent, and will include the patent term adjustment on the patent. Any request for reconsideration of the patent term adjustment determination (or reinstatement of patent term adjustment) should follow the process outlined in 37 CFR 1.705.

Any questions regarding the Patent Term Extension or Adjustment determination should be directed to the Office of Patent Legal Administration at (571)-272-7702. Questions relating to issue and publication fee payments should be directed to the Customer Service Center of the Office of Patent Publication at 1-(888)-786-0101 or (571)-272-4200.

OMB Clearance and PRA Burden Statement for PTOL-85 Part B

The Paperwork Reduction Act (PRA) of 1995 requires Federal agencies to obtain Office of Management and Budget approval before requesting most types of information from the public. When OMB approves an agency request to collect information from the public, OMB (i) provides a valid OMB Control Number and expiration date for the agency to display on the instrument that will be used to collect the information and (ii) requires the agency to inform the public about the OMB Control Number's legal significance in accordance with 5 CFR 1320.5(b).

The information collected by PTOL-85 Part B is required by 37 CFR 1.311. The information is required to obtain or retain a benefit by the public which is to file (and by the USPTO to process) an application. Confidentiality is governed by 35 U.S.C. 122 and 37 CFR 1.14. This collection is estimated to take 12 minutes to complete, including gathering, preparing, and submitting the completed application form to the USPTO. Time will vary depending upon the individual case. Any comments on the amount of time you require to complete this form and/or suggestions for reducing this burden, should be sent to the Chief Information Officer, U.S. Patent and Trademark Office, U.S. Department of Commerce, P.O. Box 1450, Alexandria, Virginia 22313-1450. DO NOT SEND FEES OR COMPLETED FORMS TO THIS ADDRESS. SEND TO: Commissioner for Patents, P.O. Box 1450, Alexandria, Virginia 22313-1450. Under the Paperwork Reduction Act of 1995, no persons are required to respond to a collection of information unless it displays a valid OMB control number.

Privacy Act Statement

The Privacy Act of 1974 (P.L. 93-579) requires that you be given certain information in connection with your submission of the attached form related to a patent application or patent. Accordingly, pursuant to the requirements of the Act, please be advised that: (1) the general authority for the collection of this information is 35 U.S.C. 2(b)(2); (2) furnishing of the information solicited is voluntary; and (3) the principal purpose for which the information is used by the U.S. Patent and Trademark Office is to process and/or examine your submission related to a patent application or patent. If you do not furnish the requested information, the U.S. Patent and Trademark Office may not be able to process and/or examine your submission, which may result in termination of proceedings or abandonment of the application or expiration of the patent.

The information provided by you in this form will be subject to the following routine uses:

1. The information on this form will be treated confidentially to the extent allowed under the Freedom of Information Act (5 U.S.C. 552) and the Privacy Act (5 U.S.C 552a). Records from this system of records may be disclosed to the Department of Justice to determine whether disclosure of these records is required by the Freedom of Information Act.
2. A record from this system of records may be disclosed, as a routine use, in the course of presenting evidence to a court, magistrate, or administrative tribunal, including disclosures to opposing counsel in the course of settlement negotiations.
3. A record in this system of records may be disclosed, as a routine use, to a Member of Congress submitting a request involving an individual, to whom the record pertains, when the individual has requested assistance from the Member with respect to the subject matter of the record.
4. A record in this system of records may be disclosed, as a routine use, to a contractor of the Agency having need for the information in order to perform a contract. Recipients of information shall be required to comply with the requirements of the Privacy Act of 1974, as amended, pursuant to 5 U.S.C. 552a(m).
5. A record related to an International Application filed under the Patent Cooperation Treaty in this system of records may be disclosed, as a routine use, to the International Bureau of the World Intellectual Property Organization, pursuant to the Patent Cooperation Treaty.
6. A record in this system of records may be disclosed, as a routine use, to another federal agency for purposes of National Security review (35 U.S.C. 181) and for review pursuant to the Atomic Energy Act (42 U.S.C. 218(c)).
7. A record from this system of records may be disclosed, as a routine use, to the Administrator, General Services, or his/her designee, during an inspection of records conducted by GSA as part of that agency's responsibility to recommend improvements in records management practices and programs, under authority of 44 U.S.C. 2904 and 2906. Such disclosure shall be made in accordance with the GSA regulations governing inspection of records for this purpose, and any other relevant (i.e., GSA or Commerce) directive. Such disclosure shall not be used to make determinations about individuals.
8. A record from this system of records may be disclosed, as a routine use, to the public after either publication of the application pursuant to 35 U.S.C. 122(b) or issuance of a patent pursuant to 35 U.S.C. 151. Further, a record may be disclosed, subject to the limitations of 37 CFR 1.14, as a routine use, to the public if the record was filed in an application which became abandoned or in which the proceedings were terminated and which application is referenced by either a published application, an application open to public inspection or an issued patent.
9. A record from this system of records may be disclosed, as a routine use, to a Federal, State, or local law enforcement agency, if the USPTO becomes aware of a violation or potential violation of law or regulation.

Notice of Allowability	Application No. 13/222,688	Applicant(s) NELSON ET AL.	
	Examiner MARCUS TANINGCO	Art Unit 2884	AIA (First Inventor to File) Status No

-- The MAILING DATE of this communication appears on the cover sheet with the correspondence address--

All claims being allowable, PROSECUTION ON THE MERITS IS (OR REMAINS) CLOSED in this application. If not included herewith (or previously mailed), a Notice of Allowance (PTOL-85) or other appropriate communication will be mailed in due course. **THIS NOTICE OF ALLOWABILITY IS NOT A GRANT OF PATENT RIGHTS.** This application is subject to withdrawal from issue at the initiative of the Office or upon petition by the applicant. See 37 CFR 1.313 and MPEP 1308.

1. ☒ This communication is responsive to *5/09/2014*.
   ☐ A declaration(s)/affidavit(s) under **37 CFR 1.130(b)** was/were filed on_____.
2. ☐ An election was made by the applicant in response to a restriction requirement set forth during the interview on _____; the restriction requirement and election have been incorporated into this action.
3. ☒ The allowed claim(s) is/are *1-8 and 19-37*. As a result of the allowed claim(s), you may be eligible to benefit from the **Patent Prosecution Highway** program at a participating intellectual property office for the corresponding application. For more information, please see http://www.uspto.gov/patents/init_events/pph/index.jsp or send an inquiry to PPHfeedback@uspto.gov .
4. ☐ Acknowledgment is made of a claim for foreign priority under 35 U.S.C. § 119(a)-(d) or (f).

   Certified copies:

   a) ☐ All b) ☐ Some *c) ☐ None of the:
   1. ☐ Certified copies of the priority documents have been received.
   2. ☐ Certified copies of the priority documents have been received in Application No. _____ .
   3. ☐ Copies of the certified copies of the priority documents have been received in this national stage application from the International Bureau (PCT Rule 17.2(a)).

   * Certified copies not received: _____.

Applicant has THREE MONTHS FROM THE "MAILING DATE" of this communication to file a reply complying with the requirements noted below. Failure to timely comply will result in ABANDONMENT of this application.
THIS THREE-MONTH PERIOD IS NOT EXTENDABLE.

5. ☐ CORRECTED DRAWINGS (as "replacement sheets") must be submitted.
   ☐ including changes required by the attached Examiner's Amendment / Comment or in the Office action of Paper No./Mail Date _____.

   Identifying indicia such as the application number (see 37 CFR 1.84(c)) should be written on the drawings in the front (not the back) of each sheet. Replacement sheet(s) should be labeled as such in the header according to 37 CFR 1.121(d).
6. ☐ DEPOSIT OF and/or INFORMATION about the deposit of BIOLOGICAL MATERIAL must be submitted. Note the attached Examiner's comment regarding REQUIREMENT FOR THE DEPOSIT OF BIOLOGICAL MATERIAL.

Attachment(s)

1. ☐ Notice of References Cited (PTO-892)
2. ☐ Information Disclosure Statements (PTO/SB/08), Paper No./Mail Date _____
3. ☐ Examiner's Comment Regarding Requirement for Deposit of Biological Material
4. ☐ Interview Summary (PTO-413), Paper No./Mail Date _____ .
5. ☐ Examiner's Amendment/Comment
6. ☒ Examiner's Statement of Reasons for Allowance
7. ☐ Other _____.

/MARCUS TANINGCO/
Primary Examiner, Art Unit 2884

The present application is being examined under the pre-AIA first to invent provisions.

DETAILED ACTION

Allowable Subject Matter

Claims 1-8 and 19-37 are allowed.

The following is an examiner's statement of reasons for allowance:

With regards to claims 1, 19, and 35, applicant's persuasive arguments presented overcome the rejections to the claims as well as the amendments to more clearly define the invention

Any comments considered necessary by applicant must be submitted no later than the payment of the issue fee and, to avoid processing delays, should preferably accompany the issue fee. Such submissions should be clearly labeled "Comments on Statement of Reasons for Allowance."

Conclusion

Any inquiry concerning this communication or earlier communications from the examiner should be directed to Marcus H. Taningco whose telephone number is (571) 272-1848. The examiner can normally be reached on M - F 9:00 - 5:30.

If attempts to reach the examiner by telephone are unsuccessful, the examiner's supervisor, Dave Porta can be reached on (571) 272-2444. The fax phone number for the organization where this application or proceeding is assigned is 571-273-8300.

SPECTRAL_0000960

Information regarding the status of an application may be obtained from the Patent Application Information Retrieval (PAIR) system. Status information for published applications may be obtained from either Private PAIR or Public PAIR. Status information for unpublished applications is available through Private PAIR only. For more information about the PAIR system, see http://pair-direct.uspto.gov. Should you have questions on access to the Private PAIR system, contact the Electronic Business Center (EBC) at 866-217-9197 (toll-free). If you would like assistance from a USPTO Customer Service Representative or access to the automated information system, call 800-786-9199 (IN USA OR CANADA) or 571-272-1000.

/Marcus H Taningco/
Examiner, Art Unit 2884

Search Notes	Application/Control No.	Applicant(s)/Patent Under Reexamination
	13222688	NELSON ET AL.
	Examiner	Art Unit
	MARCUS TANINGCO	2884

CPC- SEARCHED		
Symbol	Date	Examiner
G01N21/645, G01N21/6428, G01N2021/7786, G01N21/6458, G01N2021/6463	1/7/2014	MT

CPC COMBINATION SETS - SEARCHED		
Symbol	Date	Examiner

US CLASSIFICATION SEARCHED			
Class	Subclass	Date	Examiner
250	461.1	1/27/2013	MT

SEARCH NOTES		
Search Notes	Date	Examiner
Inventor's name searched	1/27/2013	MT
EAST search notes attached	1/27/2013	MT
Text search in 250/458.1, 459.1	1/27/2013	MT
Text search in 362/3	1/27/2013	MT
Updated EAST search notes attached	7/8/2013	MT
Updated EAST search notes attached	8/21/2014	MT

INTERFERENCE SEARCH			
US Class/ CPC Symbol	US Subclass / CPC Group	Date	Examiner
	Interference search notes attached	8/21/2014	MT

EAST Search History

EAST Search History (Prior Art)

Ref #	Hits	Search Query	DBs	Default Operator	Plurals	Time Stamp
L10	621	(((light or led or lamp or illuminat$4) near3 (halo or ring or annular)) same (multiple or plurality or array)) and ((sens$4 or detect$4 or determin$4 or measur$4 or excit$6 or imag$4) near3 fluoresc$6)	US-PGPUB; USPAT; FPRS; EPO; JPO; DERWENT; IBM_TDB	OR	OFF	2014/08/21 13:33
L11	2850	(molecul$4 near imag$4) same fluoresc$6	US-PGPUB; USPAT; FPRS; EPO; JPO; DERWENT; IBM_TDB	OR	OFF	2014/08/21 13:34
L12	33	10 and 11	US-PGPUB; USPAT; FPRS; EPO; JPO; DERWENT; IBM_TDB	OR	OFF	2014/08/21 13:35
L13	29	12 and @ad<"20100901"	US-PGPUB; USPAT; FPRS; EPO; JPO; DERWENT; IBM_TDB	OR	OFF	2014/08/21 13:35
L14	0	13 and (diode or LED) with ((narrow near band) or nm)	US-PGPUB; USPAT; FPRS; EPO; JPO; DERWENT; IBM_TDB	OR	OFF	2014/08/21 13:36
L15	87	11 and ((light adj2 diode) or LED) with ((narrow near band) or nm)	US-PGPUB; USPAT; FPRS; EPO; JPO; DERWENT; IBM_TDB	OR	OFF	2014/08/21 13:36
L16	0	(((light or led or lamp or illuminat$4) near3 (halo or ring or annular)) same (multiple or plurality or array)) and 15	US-PGPUB; USPAT; FPRS; EPO; JPO; DERWENT; IBM_TDB	OR	OFF	2014/08/21 13:37
L17	2	(((light or led or lamp or illuminat$4 diode) near3 (surround or circ$4 or halo or ring or annular)) same (multiple or plurality or array)) and 15	US-PGPUB; USPAT; FPRS; EPO; JPO; DERWENT; IBM_TDB	OR	OFF	2014/08/21 13:37
L18	641	(((light or led or lamp or illuminat$4 or excit$6) near3 (halo or ring or annular))	US-PGPUB; USPAT;	OR	OFF	2014/08/21 13:40

		same (multiple or plurality or array)) and ((sens$4 or detect$4 or determin$4 or measur$4 or excit$6 or imag$4) near3 fluoresc$6)	FPRS; EPO; JPO; DERWENT; IBM_TDB			
L19	589	L18 and (light or led or lamp or illuminat$4 or excit$6) with (camera or imaging or detect$4 or sens$4)	US-PGPUB; USPAT; FPRS; EPO; JPO; DERWENT; IBM_TDB	OR	OFF	2014/08/21 13:40
L20	541	L19 and @ad<"20110831"	US-PGPUB; USPAT; FPRS; EPO; JPO; DERWENT; IBM_TDB	OR	OFF	2014/08/21 13:40
L21	226	L20 and ("250".clas. or "356".clas.)	US-PGPUB; USPAT; FPRS; EPO; JPO; DERWENT; IBM_TDB	OR	OFF	2014/08/21 13:40
S1	1	13/222688	US-PGPUB; USPAT; FPRS; EPO; JPO; DERWENT; IBM_TDB	OR	OFF	2013/01/25 15:03
S2	564	(Nelson near Michael).in.	US-PGPUB; USPAT; FPRS; EPO; JPO; DERWENT; IBM_TDB	OR	OFF	2013/01/25 15:03
S3	38	(Nelson near Michael).in. and fluoresc$4	US-PGPUB; USPAT; FPRS; EPO; JPO; DERWENT; IBM_TDB	OR	OFF	2013/01/25 15:04
S4	4	(Nelson near Michael).in. and fluoresc$4 and ((light near source) same diffus$4)	US-PGPUB; USPAT; FPRS; EPO; JPO; DERWENT; IBM_TDB	OR	OFF	2013/01/25 15:05
S5	81	("4585934" | "4863690" | "5414258" | "5587583" | "5680492" | "6004767" | "6038038" | "7298415" | "7383078" | "7449615" | "7461652" | "7555334" | "7581191" | "4863690" | "5680492" | "5818977" | "6004767" | "6097025" | "6642499" | "6922246" | "7255851" | "7464707" | "7466418" | "7555332" | "7595838" | "7663664" | "20040121175" | "5672881" | "5689110" | "6901279" | "7116354" | "7177024" | "7555332" | "7589786" | "7595838" | "7599731" | "5039868" | "5202091" | "6775567" | "6919919" | "7474399" | "4885544" | "5515161" | "5542012" | "5840572" |	US-PGPUB; USPAT	OR	OFF	2013/01/25 15:07

SPECTRAL_0000964

		"5964220" | "6205244" | "6922246" | "7255851" | "7299420" | "7331341" | "7616985" | "7449567" | "7461652" | "7555334" | "7589786" | "7603167" | "5454437" | "3800079" | "4687325" | "5008548" | "5898802" | "5986271" | "6377353" | "6614452" | "20010028510" | "4593728" | "4687325" | "4948975" | "5414258" | "5515161" | "6871767" | "7196190" | "7449615" | "7474398" | "7616985" | "5089895" | "3949162" | "5202091" | "6097025" | "6642499" | "7503323" | "3949162" | "4196994" | "4343021" | "4885544" | "5008548" | "5672881" | "5689110" | "5840572" | "5865754" | "5964220" | "5986271" | "6217847" | "7113217" | "7190991" | "7383078" | "7503323" | "7581191" | "7599731" | "20040247170" | "20090268426" | "4196994" | "4343021" | "6217847" | "6754008" | "6894289" | "6919919" | "7196190" | "7449567" | "7464707" | "7474398" | "7603167" | "5587583" | "5898802" | "6377353" | "6754008" | "6901279" | "7177024" | "7299420" | "20050265024" | "3871767" | "4593728" | "4948975" | "5818977" | "6775567" | "7113217" | "7403812" | "7474399" | "7663664" | "0458934" | "5401465" | "5542012" | "6038038" | "6154277" | "6614452" | "7116354" | "7331341" | "4298887" | "5039868" | "5401465" | "5865754" | "6154277" | "7190991" | "7466418" | "3800079" | "4298887" | "6205244" | "6894289" | "7298415" | "7403812").PN.				
S6	2234	(camera or detect$4 or imager or imaging) with (light or led or lamp) with (halo or ring or surround$4) with (opening or aperture or hole or fov or (field near view))	US-PGPUB; USPAT; FPRS; EPO; JPO; DERWENT; IBM_TDB	OR	OFF	2013/01/25 15:21
S7	412	S6 and ((light or led or lamp) with diffus$4)	US-PGPUB; USPAT; FPRS; EPO; JPO; DERWENT; IBM_TDB	OR	OFF	2013/01/25 15:21
S8	58	S7 and "250".clas.	US-PGPUB; USPAT; FPRS; EPO; JPO; DERWENT; IBM_TDB	OR	OFF	2013/01/25 15:23
S9	3	(camera or detect$4 or imager or imaging) with ((multiple or plurality) near2 (receptacle or ight or led or lamp)) with (halo or ring or surround$4) with (opening or aperture or hole or fov or (field near view))	US-PGPUB; USPAT; FPRS; EPO; JPO; DERWENT; IBM_TDB	OR	OFF	2013/01/25 21:09
S10	96	(camera or detect$4 or imager or imaging) with ((multiple or plurality)	US-PGPUB; USPAT;	OR	OFF	2013/01/25 21:12

		near2 (receptacle or ight or led or lamp)) with (opening or aperture or hole or fov or (field near view))	FPRS; EPO; JPO; DERWENT; IBM_TDB			
S11	4	S10 and "250".clas.	US-PGPUB; USPAT; FPRS; EPO; JPO; DERWENT; IBM_TDB	OR	OFF	2013/01/25 21:13
S12	81	("4585934" | "4863690" | "5414258" | "5587583" | "5680492" | "6004767" | "6038038" | "7298415" | "7383078" | "7449615" | "7461652" | "7555334" | "7581191" | "4863690" | "5680492" | "5818977" | "6004767" | "6097025" | "6642499" | "6922246" | "7255851" | "7464707" | "7466418" | "7555332" | "7595838" | "7663664" | "20040121175" | "5672881" | "5689110" | "6901279" | "7116354" | "7177024" | "7555332" | "7589786" | "7595838" | "7599731" | "5039868" | "5202091" | "6775567" | "6919919" | "7474399" | "4885544" | "5515161" | "5542012" | "5840572" | "5964220" | "6205244" | "6922246" | "7255851" | "7299420" | "7331341" | "7616985" | "7449567" | "7461652" | "7555334" | "7589786" | "7603167" | "5454437" | "3800079" | "4687325" | "5008548" | "5898802" | "5986271" | "6377353" | "6614452" | "20010028510" | "4593728" | "4687325" | "4948975" | "5414258" | "5515161" | "6871767" | "7196190" | "7449615" | "7474398" | "7616985" | "5089895" | "3949162" | "5202091" | "6097025" | "6642499" | "7503323" | "3949162" | "4196994" | "4343021" | "4885544" | "5008548" | "5672881" | "5689110" | "5840572" | "5865754" | "5964220" | "5986271" | "6217847" | "7113217" | "7190991" | "7383078" | "7503323" | "7581191" | "7599731" | "20040247170" | "20090268426" | "4196994" | "4343021" | "6217847" | "6754008" | "6894289" | "6919919" | "7196190" | "7449567" | "7464707" | "7474398" | "7603167" | "5587583" | "5898802" | "6377353" | "6754008" | "6901279" | "7177024" | "7299420" | "20050265024" | "3871767" | "4593728" | "4948975" | "5818977" | "6775567" | "7113217" | "7403812" | "7474399" | "7663664" | "0458934" | "5401465" | "5542012" | "6038038" | "6154277" | "6614452" | "7116354" | "7331341" | "4298887" | "5039868" | "5401465" | "5865754" | "6154277" | "7190991" | "7466418" | "3800079" | "4298887" | "6205244" | "6894289" | "7298415" | "7403812").PN.	US-PGPUB; USPAT	OR	OFF	2013/01/25 21:13
S13	0	S12 and S10	US-PGPUB; USPAT;	OR	OFF	2013/01/25 21:13

			FPRS; EPO; JPO; DERWENT; IBM_TDB			
S14	5	S12 and (camera or detect$4 or imager or imaging) with (light or led or lamp) with (halo or ring or surround$4) with (opening or aperture or hole or fov or (field near view))	US-PGPUB; USPAT; FPRS; EPO; JPO; DERWENT; IBM_TDB	OR	OFF	2013/01/25 21:22
S15	46	S12 and fluoresc$7	US-PGPUB; USPAT; FPRS; EPO; JPO; DERWENT; IBM_TDB	OR	OFF	2013/01/25 21:25
S16	2	("3609451" | "5134277").PN. OR ("6943333").URPN.	US-PGPUB; USPAT; USOCR	OR	OFF	2013/01/25 21:26
S17	1088	250/461.1.ccls.	US-PGPUB; USPAT; FPRS; EPO; JPO; DERWENT; IBM_TDB	OR	OFF	2013/01/27 14:54
S18	2855	250/458.1.ccls.	US-PGPUB; USPAT; FPRS; EPO; JPO; DERWENT; IBM_TDB	OR	OFF	2013/01/27 14:54
S19	1557	250/459.1.ccls.	US-PGPUB; USPAT; FPRS; EPO; JPO; DERWENT; IBM_TDB	OR	OFF	2013/01/27 14:54
S20	4362	S17 S18 S19	US-PGPUB; USPAT; FPRS; EPO; JPO; DERWENT; IBM_TDB	OR	OFF	2013/01/27 14:54
S21	1	S20 and (camera or detect$4 or imager or imaging) with ((multiple or plurality) near2 (receptacle or ight or led or lamp)) with (opening or aperture or hole or fov or (field near view))	US-PGPUB; USPAT; FPRS; EPO; JPO; DERWENT; IBM_TDB	OR	OFF	2013/01/27 14:54
S22	2234	(camera or detect$4 or imager or imaging) with (light or led or lamp) with (halo or ring or surround$4) with (opening or aperture or hole or fov or (field near view))	US-PGPUB; USPAT; FPRS; EPO; JPO; DERWENT; IBM_TDB	OR	OFF	2013/01/27 14:55
S23	3	S22 and ((light or led or lamp) with diffus$4) and S20	US-PGPUB; USPAT; FPRS; EPO; JPO; DERWENT;	OR	OFF	2013/01/27 14:55

			IBM_TDB			
S24	81	("4585934" | "4863690" | "5414258" | "5587583" | "5680492" | "6004767" | "6038038" | "7298415" | "7383078" | "7449615" | "7461652" | "7555334" | "7581191" | "4863690" | "5680492" | "5818977" | "6004767" | "6097025" | "6642499" | "6922246" | "7255851" | "7464707" | "7466418" | "7555332" | "7595838" | "7663664" | "20040121175" | "5672881" | "5689110" | "6901279" | "7116354" | "7177024" | "7555332" | "7589786" | "7595838" | "7599731" | "5039868" | "5202091" | "6775567" | "6919919" | "7474399" | "4885544" | "5515161" | "5542012" | "5840572" | "5964220" | "6205244" | "6922246" | "7255851" | "7299420" | "7331341" | "7616985" | "7449567" | "7461652" | "7555334" | "7589786" | "7603167" | "5454437" | "3800079" | "4687325" | "5008548" | "5898802" | "5986271" | "6377353" | "6614452" | "20010028510" | "4593728" | "4687325" | "4948975" | "5414258" | "5515161" | "6871767" | "7196190" | "7449615" | "7474398" | "7616985" | "5089895" | "3949162" | "5202091" | "6097025" | "6642499" | "7503323" | "3949162" | "4196994" | "4343021" | "4885544" | "5008548" | "5672881" | "5689110" | "5840572" | "5865754" | "5964220" | "5986271" | "6217847" | "7113217" | "7190991" | "7383078" | "7503323" | "7581191" | "7599731" | "20040247170" | "20090268426" | "4196994" | "4343021" | "6217847" | "6754008" | "6894289" | "6919919" | "7196190" | "7449567" | "7464707" | "7474398" | "7603167" | "5587583" | "5898802" | "6377353" | "6754008" | "6901279" | "7177024" | "7299420" | "20050265024" | "3871767" | "4593728" | "4948975" | "5818977" | "6775567" | "7113217" | "7403812" | "7474399" | "7663664" | "0458934" | "5401465" | "5542012" | "6038038" | "6154277" | "6614452" | "7116354" | "7331341" | "4298887" | "5039868" | "5401465" | "5865754" | "6154277" | "7190991" | "7466418" | "3800079" | "4298887" | "6205244" | "6894289" | "7298415" | "7403812").PN.	US-PGPUB; USPAT	OR	OFF	2013/01/27 15:00
S25	8	S20 and S24	US-PGPUB; USPAT; FPRS; EPO; JPO; DERWENT; IBM_TDB	OR	OFF	2013/01/27 15:00
S26	280	362/3.ccls.	US-PGPUB; USPAT; FPRS; EPO; JPO; DERWENT;	OR	OFF	2013/01/27 15:06

			IBM_TDB			
S27	4	S22 and S26	US-PGPUB; USPAT; FPRS; EPO; JPO; DERWENT; IBM_TDB	OR	OFF	2013/01/27 15:06
S28	3	"20090268426"	US-PGPUB; USPAT; FPRS; EPO; JPO; DERWENT; IBM_TDB	OR	OFF	2013/06/24 14:48
S29	2	"6454437".pn.	US-PGPUB; USPAT; FPRS; EPO; JPO; DERWENT; IBM_TDB	OR	OFF	2013/06/24 14:49
S30	746	led near3 receptacle	US-PGPUB; USPAT; FPRS; EPO; JPO; DERWENT; IBM_TDB	OR	OFF	2013/07/05 11:02
S31	14	S30 and "250".clas.	US-PGPUB; USPAT; FPRS; EPO; JPO; DERWENT; IBM_TDB	OR	OFF	2013/07/05 11:03
S32	90	S30 and fluorescen$4	US-PGPUB; USPAT; FPRS; EPO; JPO; DERWENT; IBM_TDB	OR	OFF	2013/07/05 11:05
S33	21	S30 and (fluorescen$4 near3 (excit$4 or detect$4 or sens$4 or illuminat$4))	US-PGPUB; USPAT; FPRS; EPO; JPO; DERWENT; IBM_TDB	OR	OFF	2013/07/05 11:06
S34	1120	250/461.1.ccls.	US-PGPUB; USPAT; FPRS; EPO; JPO; DERWENT; IBM_TDB	OR	OFF	2013/07/05 11:12
S35	2982	250/458.1.ccls.	US-PGPUB; USPAT; FPRS; EPO; JPO; DERWENT; IBM_TDB	OR	OFF	2013/07/05 11:12
S36	1678	250/459.1.ccls.	US-PGPUB; USPAT; FPRS; EPO; JPO; DERWENT;	OR	OFF	2013/07/05 11:12

			IBM_TDB			
S37	4566	S34 S35 S36	US-PGPUB; USPAT; FPRS; EPO; JPO; DERWENT; IBM_TDB	OR	OFF	2013/07/05 11:12
S38	30	S37 and (camera or detect$4 or imager or imaging) with (light or led or lamp) with (halo or ring or surround$4 or annular) with (opening or aperture or hole or fov or (field near view))	US-PGPUB; USPAT; FPRS; EPO; JPO; DERWENT; IBM_TDB	OR	OFF	2013/07/05 11:13
S39	1	S30 and S37	US-PGPUB; USPAT; FPRS; EPO; JPO; DERWENT; IBM_TDB	OR	OFF	2013/07/05 11:48
S40	18	S30 and fluorescen$4.clm.	US-PGPUB; USPAT; FPRS; EPO; JPO; DERWENT; IBM_TDB	OR	OFF	2013/07/05 11:49
S41	40	led near3 ((array or multiple or plural$4) near receptacle)	US-PGPUB; USPAT; FPRS; EPO; JPO; DERWENT; IBM_TDB	OR	ON	2013/07/05 11:51
S42	16	"10040330"	US-PGPUB; USPAT; FPRS; EPO; JPO; DERWENT; IBM_TDB	OR	OFF	2013/07/05 16:26
S43	267	S37 and ((light or led or lamp) near3 (halo or ring or surround$4 or annular))	US-PGPUB; USPAT; FPRS; EPO; JPO; DERWENT; IBM_TDB	OR	OFF	2013/07/05 16:27
S44	78	S43 and imag$4.clm.	US-PGPUB; USPAT; FPRS; EPO; JPO; DERWENT; IBM_TDB	OR	OFF	2013/07/05 16:28
S45	133	S37 and ((light or led or lamp) near3 (halo or ring or annular))	US-PGPUB; USPAT; FPRS; EPO; JPO; DERWENT; IBM_TDB	OR	OFF	2013/07/05 16:28
S46	56	S45 and imag$4.clm.	US-PGPUB; USPAT; FPRS; EPO; JPO; DERWENT;	OR	OFF	2013/07/05 16:28

			IBM_TDB			
S47	19	S37 and ((light or led or lamp) near3 (halo or ring or annular)) same led	US-PGPUB; USPAT; FPRS; EPO; JPO; DERWENT; IBM_TDB	OR	OFF	2013/07/05 16:29
S48	15	S47 and imag$4.clm.	US-PGPUB; USPAT; FPRS; EPO; JPO; DERWENT; IBM_TDB	OR	OFF	2013/07/05 16:29
S49	1120	250/461.1.ccls.	US-PGPUB; USPAT; FPRS; EPO; JPO; DERWENT; IBM_TDB	OR	OFF	2013/07/08 10:23
S50	2982	250/458.1.ccls.	US-PGPUB; USPAT; FPRS; EPO; JPO; DERWENT; IBM_TDB	OR	OFF	2013/07/08 10:23
S51	1678	250/459.1.ccls.	US-PGPUB; USPAT; FPRS; EPO; JPO; DERWENT; IBM_TDB	OR	OFF	2013/07/08 10:23
S52	4566	S49 S50 S51	US-PGPUB; USPAT; FPRS; EPO; JPO; DERWENT; IBM_TDB	OR	OFF	2013/07/08 10:23
S53	133	S52 and ((light or led or lamp) near3 (halo or ring or annular))	US-PGPUB; USPAT; FPRS; EPO; JPO; DERWENT; IBM_TDB	OR	OFF	2013/07/08 10:23
S54	56	S53 and imag$4.clm.	US-PGPUB; USPAT; FPRS; EPO; JPO; DERWENT; IBM_TDB	OR	OFF	2013/07/08 10:23
S55	19	S52 and ((light or led or lamp) near3 (halo or ring or annular)) same led	US-PGPUB; USPAT; FPRS; EPO; JPO; DERWENT; IBM_TDB	OR	OFF	2013/07/08 10:23
S56	15	S55 and imag$4.clm.	US-PGPUB; USPAT; FPRS; EPO; JPO; DERWENT;	OR	OFF	2013/07/08 10:23

			IBM_TDB			
S57	41	S54 not S56	US-PGPUB; USPAT; FPRS; EPO; JPO; DERWENT; IBM_TDB	OR	OFF	2013/07/08 10:23
S58	23	S52 and ((light or led or lamp) near3 (halo or ring or annular)) with excit$6	US-PGPUB; USPAT; FPRS; EPO; JPO; DERWENT; IBM_TDB	OR	OFF	2013/07/08 10:29
S59	4	S52 and (((light or led or lamp) near3 (halo or ring or annular)) with excit$6) same imag$4	US-PGPUB; USPAT; FPRS; EPO; JPO; DERWENT; IBM_TDB	OR	OFF	2013/07/08 10:29
S60	68	(((light or led or lamp) near3 (halo or ring or annular)) same (excit$6 with fluoresc$6)) same imag$4	US-PGPUB; USPAT; FPRS; EPO; JPO; DERWENT; IBM_TDB	OR	OFF	2013/07/08 10:35
S61	68	S60 not S56	US-PGPUB; USPAT; FPRS; EPO; JPO; DERWENT; IBM_TDB	OR	OFF	2013/07/08 10:36
S62	2	(((led) near3 (halo or ring or annular)) same (excit$6 with fluoresc$6)) same imag$4	US-PGPUB; USPAT; FPRS; EPO; JPO; DERWENT; IBM_TDB	OR	OFF	2013/07/08 10:41
S63	5	(((light or led or lamp) near3 (halo or ring or annular)) same (excit$6 with fluoresc$6)) same imag$4 same led	US-PGPUB; USPAT; FPRS; EPO; JPO; DERWENT; IBM_TDB	OR	ON	2013/07/08 10:42
S64	221	((light or led or lamp) near3 (halo or ring or annular)) same ((sens$4 or detect$4 or determin$4 or measur$4 or excit$6) near3 fluoresc$6)	US-PGPUB; USPAT; FPRS; EPO; JPO; DERWENT; IBM_TDB	OR	OFF	2014/01/06 19:33
S65	188	S64 and @ad<"20110831"	US-PGPUB; USPAT; FPRS; EPO; JPO; DERWENT; IBM_TDB	OR	OFF	2014/01/06 19:33
S66	117	S65 and (fluoresc$6 with (imag$4 or camera))	US-PGPUB; USPAT; FPRS; EPO; JPO; DERWENT;	OR	OFF	2014/01/06 19:35

			IBM_TDB			
S67	81	("4585934" | "4863690" | "5414258" | "5587583" | "5680492" | "6004767" | "6038038" | "7298415" | "7383078" | "7449615" | "7461652" | "7555334" | "7581191" | "4863690" | "5680492" | "5818977" | "6004767" | "6097025" | "6642499" | "6922246" | "7255851" | "7464707" | "7466418" | "7555332" | "7595838" | "7663664" | "20040121175" | "5672881" | "5689110" | "6901279" | "7116354" | "7177024" | "7555332" | "7589786" | "7595838" | "7599731" | "5039868" | "5202091" | "6775567" | "6919919" | "7474399" | "4885544" | "5515161" | "5542012" | "5840572" | "5964220" | "6205244" | "6922246" | "7255851" | "7299420" | "7331341" | "7616985" | "7449567" | "7461652" | "7555334" | "7589786" | "7603167" | "5454437" | "3800079" | "4687325" | "5008548" | "5898802" | "5986271" | "6377353" | "6614452" | "20010028510" | "4593728" | "4687325" | "4948975" | "5414258" | "5515161" | "6871767" | "7196190" | "7449615" | "7474398" | "7616985" | "5089895" | "3949162" | "5202091" | "6097025" | "6642499" | "7503323" | "3949162" | "4196994" | "4343021" | "4885544" | "5008548" | "5672881" | "5689110" | "5840572" | "5865754" | "5964220" | "5986271" | "6217847" | "7113217" | "7190991" | "7383078" | "7503323" | "7581191" | "7599731" | "20040247170" | "20090268426" | "4196994" | "4343021" | "6217847" | "6754008" | "6894289" | "6919919" | "7196190" | "7449567" | "7464707" | "7474398" | "7603167" | "5587583" | "5898802" | "6377353" | "6754008" | "6901279" | "7177024" | "7299420" | "20050265024" | "3871767" | "4593728" | "4948975" | "5818977" | "6775567" | "7113217" | "7403812" | "7474399" | "7663664" | "0458934" | "5401465" | "5542012" | "6038038" | "6154277" | "6614452" | "7116354" | "7331341" | "4298887" | "5039868" | "5401465" | "5865754" | "6154277" | "7190991" | "7466418" | "3800079" | "4298887" | "6205244" | "6894289" | "7298415" | "7403812").PN.	US-PGPUB; USPAT	OR	OFF	2014/01/06 19:49
S68	1	("7918557").PN.	US-PGPUB; USPAT	OR	OFF	2014/01/06 19:50
S69	8	("20020016533" | "20030018271" | "20050033145" | "6021344" | "6032070" | "6230046" | "6439715" | "7006861").PN. OR ("7406347").URPN.	US-PGPUB; USPAT; USOCR	OR	OFF	2014/01/06 19:55
S70	55	("20010028510" | "20050201614" | "20050237423" | "3871767" | "4076420" | "4582406" | "4593728" | "4708475" | "4863690" | "5039868" | "5202091" | "5319209" | "5414258" | "5542012" |	US-PGPUB; USPAT; USOCR	OR	OFF	2014/01/06 19:59

		"5636299" | "5637874" | "5650135" | "5672881" | "5680492" | "5705807" | "5738101" | "5840572" | "5867250" | "5898802" | "5916160" | "5943129" | "5970164" | "5986271" | "6036920" | "6043506" | "6071748" | "6084680" | "6097025" | "6217847" | "6242743" | "6321111" | "6364829" | "6373568" | "6381058" | "6403947" | "6510281" | "6597864" | "6615063" | "6665072" | "6690466" | "6693710" | "6750964" | "6775567" | "6894289" | "6901279" | "6922246" | "6924893" | "7177024").PN. OR ("7474399").URPN.				
S71	55	("20010028510" | "20050201614" | "20050237423" | "3871767" | "4076420" | "4582406" | "4593728" | "4708475" | "4863690" | "5039868" | "5202091" | "5319209" | "5414258" | "5542012" | "5636299" | "5637874" | "5650135" | "5672881" | "5680492" | "5705807" | "5738101" | "5840572" | "5867250" | "5898802" | "5916160" | "5943129" | "5970164" | "5986271" | "6036920" | "6043506" | "6071748" | "6084680" | "6097025" | "6217847" | "6242743" | "6321111" | "6364829" | "6373568" | "6381058" | "6403947" | "6510281" | "6597864" | "6615063" | "6665072" | "6690466" | "6693710" | "6750964" | "6775567" | "6894289" | "6901279" | "6922246" | "6924893" | "7177024").PN. OR ("7474398").URPN.	US-PGPUB; USPAT; USOCR	OR	OFF	2014/01/06 19:59
S72	55	S70 or S71	US-PGPUB; USPAT; FPRS; EPO; JPO; DERWENT; IBM_TDB	OR	OFF	2014/01/06 19:59
S73	24	S72 and ring	US-PGPUB; USPAT; FPRS; EPO; JPO; DERWENT; IBM_TDB	OR	OFF	2014/01/06 19:59
S74	46	("20010028510" | "3871767" | "4076420" | "4582406" | "4593728" | "4708475" | "4863690" | "5039868" | "5202091" | "5319209" | "5414258" | "5542012" | "5636299" | "5637874" | "5650135" | "5672881" | "5680492" | "5705807" | "5738101" | "5840572" | "5867250" | "5898802" | "5916160" | "5970164" | "5986271" | "6036920" | "6043506" | "6071748" | "6084680" | "6097025" | "6217847" | "6242743" | "6321111" | "6364829" | "6510281" | "6597864" | "6615063" | "6775567" | "6894289" | "6901279" | "6922246").PN. OR ("7177024").URPN.	US-PGPUB; USPAT; USOCR	OR	OFF	2014/01/06 20:03
S75	593	(((light or led or lamp or illuminat$4) near3 (halo or ring or annular)) same	US-PGPUB; USPAT;	OR	OFF	2014/01/06 20:11

		(multiple or plurality or array)) and ((sens$4 or detect$4 or determin$4 or measur$4 or excit$6 or imag$4) near3 fluoresc$6)	FPRS; EPO; JPO; DERWENT; IBM_TDB			
S76	612	(((light or led or lamp or illuminat$4 or excit$6) near3 (halo or ring or annular)) same (multiple or plurality or array)) and ((sens$4 or detect$4 or determin$4 or measur$4 or excit$6 or imag$4) near3 fluoresc$6)	US-PGPUB; USPAT; FPRS; EPO; JPO; DERWENT; IBM_TDB	OR	OFF	2014/01/06 20:12
S77	565	S76 and (light or led or lamp or illuminat$4 or excit$6) with (camera or imaging or detect$4 or sens$4)	US-PGPUB; USPAT; FPRS; EPO; JPO; DERWENT; IBM_TDB	OR	OFF	2014/01/06 20:13
S78	530	S77 and @ad<"20110831"	US-PGPUB; USPAT; FPRS; EPO; JPO; DERWENT; IBM_TDB	OR	OFF	2014/01/06 20:13
S79	221	S78 and ("250".clas. or "356".clas.)	US-PGPUB; USPAT; FPRS; EPO; JPO; DERWENT; IBM_TDB	OR	OFF	2014/01/06 20:15
S80	34	S64 AND ((G01N21/645 OR G01N21/6428 OR G01N2021/7786 OR G01N21/6458 OR G01N2021/6463).CPC.)	US-PGPUB; USPAT; FPRS; EPO; JPO; DERWENT; IBM_TDB	OR	OFF	2014/01/06 20:18
S81	217	S79 not S73	US-PGPUB; USPAT; FPRS; EPO; JPO; DERWENT; IBM_TDB	OR	OFF	2014/01/06 20:18
S82	186	S81 and (light or led or lamp or illuminat$4 or excit$6) with (hold$4or contain$4 or cavit$4 or receiv$4 or receptacle)	US-PGPUB; USPAT; FPRS; EPO; JPO; DERWENT; IBM_TDB	OR	OFF	2014/01/06 20:19
S83	74	S79 not (fiber near optic$4)	US-PGPUB; USPAT; FPRS; EPO; JPO; DERWENT; IBM_TDB	OR	OFF	2014/01/06 20:21
S84	55	S83 and (light or led or lamp or illuminat$4 or excit$6) with (hold$4or contain$4 or cavit$4 or receiv$4 or receptacle)	US-PGPUB; USPAT; FPRS; EPO; JPO; DERWENT; IBM_TDB	OR	OFF	2014/01/06 20:23
S85	60	S83 and (light or led or lamp or illuminat$4 or excit$6) with (hold$4 or	US-PGPUB; USPAT;	OR	OFF	2014/01/06 20:23

		contain$4 or cavit$4 or receiv$4 or receptacle)	FPRS; EPO; JPO; DERWENT; IBM_TDB			
S86	19667	(light or led or lamp or illuminat$4) with receptacle	US-PGPUB; USPAT; FPRS; EPO; JPO; DERWENT; IBM_TDB	OR	OFF	2014/01/06 20:42
S87	8	S76 and S86	US-PGPUB; USPAT; FPRS; EPO; JPO; DERWENT; IBM_TDB	OR	OFF	2014/01/06 20:42
S88	2	"5690417".pn.	US-PGPUB; USPAT; FPRS; EPO; JPO; DERWENT; IBM_TDB	OR	OFF	2014/01/06 20:46
S89	89	("4567551" | "4893223" | "5038258").PN. OR ("5690417").URPN.	US-PGPUB; USPAT; USOCR	OR	OFF	2014/01/06 20:47
S90	13	S89 and receptacle	US-PGPUB; USPAT; FPRS; EPO; JPO; DERWENT; IBM_TDB	OR	OFF	2014/01/06 20:51
S91	1303	((Nelson or cable) near Michael).in.	US-PGPUB; USPAT; FPRS; EPO; JPO; DERWENT; IBM_TDB	OR	OFF	2014/01/06 21:25
S92	77	S91 and fluoresc$4	US-PGPUB; USPAT; FPRS; EPO; JPO; DERWENT; IBM_TDB	OR	OFF	2014/01/06 21:26
S93	0	S91 and fluoresc$4 and recetacle	US-PGPUB; USPAT; FPRS; EPO; JPO; DERWENT; IBM_TDB	OR	OFF	2014/01/06 21:26
S94	6	S91 and fluoresc$4 and receptacle	US-PGPUB; USPAT; FPRS; EPO; JPO; DERWENT; IBM_TDB	OR	OFF	2014/01/06 21:26
S95	2	"20040121175"	US-PGPUB; USPAT; FPRS; EPO; JPO; DERWENT;	OR	OFF	2014/01/07 11:34

			IBM_TDB			
S96	296	polyoxymethylene near thermoplastic	US-PGPUB; USPAT; FPRS; EPO; JPO; DERWENT; IBM_TDB	OR	OFF	2014/01/07 11:36
S97	2	S96 and "250".clas.	US-PGPUB; USPAT; FPRS; EPO; JPO; DERWENT; IBM_TDB	OR	OFF	2014/01/07 11:36
S98	0	S96 and "356".clas.	US-PGPUB; USPAT; FPRS; EPO; JPO; DERWENT; IBM_TDB	OR	OFF	2014/01/07 11:37
S99	251	delrin and "250".clas.	US-PGPUB; USPAT; FPRS; EPO; JPO; DERWENT; IBM_TDB	OR	OFF	2014/01/07 11:39
S100	0	delrin and "250/4$".clas.	US-PGPUB; USPAT; FPRS; EPO; JPO; DERWENT; IBM_TDB	OR	OFF	2014/01/07 11:39
S101	168	delrin and "356".clas.	US-PGPUB; USPAT; FPRS; EPO; JPO; DERWENT; IBM_TDB	OR	OFF	2014/01/07 11:39
S102	54	S99 and S101	US-PGPUB; USPAT; FPRS; EPO; JPO; DERWENT; IBM_TDB	OR	OFF	2014/01/07 11:39
S103	81	("4585934" | "4863690" | "5414258" | "5587583" | "5680492" | "6004767" | "6038038" | "7298415" | "7383078" | "7449615" | "7461652" | "7555334" | "7581191" | "4863690" | "5680492" | "5818977" | "6004767" | "6097025" | "6642499" | "6922246" | "7255851" | "7464707" | "7466418" | "7555332" | "7595838" | "7663664" | "20040121175" | "5672881" | "5689110" | "6901279" | "7116354" | "7177024" | "7555332" | "7589786" | "7595838" | "7599731" | "5039868" | "5202091" | "6775567" | "6919919" | "7474399" | "4885544" | "5515161" | "5542012" | "5840572" | "5964220" | "6205244" | "6922246" | "7255851" | "7299420" | "7331341" | "7616985" | "7449567" | "7461652" |	US-PGPUB; USPAT	OR	OFF	2014/01/07 11:40

		"7555334" | "7589786" | "7603167" | "5454437" | "3800079" | "4687325" | "5008548" | "5898802" | "5986271" | "6377353" | "6614452" | "20010028510" | "4593728" | "4687325" | "4948975" | "5414258" | "5515161" | "6871767" | "7196190" | "7449615" | "7474398" | "7616985" | "5089895" | "3949162" | "5202091" | "6097025" | "6642499" | "7503323" | "3949162" | "4196994" | "4343021" | "4885544" | "5008548" | "5672881" | "5689110" | "5840572" | "5865754" | "5964220" | "5986271" | "6217847" | "7113217" | "7190991" | "7383078" | "7503323" | "7581191" | "7599731" | "20040247170" | "20090268426" | "4196994" | "4343021" | "6217847" | "6754008" | "6894289" | "6919919" | "7196190" | "7449567" | "7464707" | "7474398" | "7603167" | "5587583" | "5898802" | "6377353" | "6754008" | "6901279" | "7177024" | "7299420" | "20050265024" | "3871767" | "4593728" | "4948975" | "5818977" | "6775567" | "7113217" | "7403812" | "7474399" | "7663664" | "0458934" | "5401465" | "5542012" | "6038038" | "6154277" | "6614452" | "7116354" | "7331341" | "4298887" | "5039868" | "5401465" | "5865754" | "6154277" | "7190991" | "7466418" | "3800079" | "4298887" | "6205244" | "6894289" | "7298415" | "7403812").PN.				
S104	6	S103 and delrin	US-PGPUB; USPAT; FPRS; EPO; JPO; DERWENT; IBM_TDB	OR	OFF	2014/01/07 11:40
S105	71	("4947291" | "5039832" | "5400229" | "5580163" | "5685637" | "5690417").PN. OR ("6033087").URPN.	US-PGPUB; USPAT; USOCR	OR	OFF	2014/01/07 11:52

EAST Search History (Interference)

Ref #	Hits	Search Query	DBs	Default Operator	Plurals	Time Stamp
L22	11	((((light or led or lamp or illuminat$4) near3 (halo or ring or annular)) same (multiple or plurality or array)) and ((sens$4 or detect$4 or determin$4 or measur$4 or excit$6 or imag$4) near3 fluoresc$6)).clm.	USPAT; UPAD	OR	OFF	2014/08/21 13:55
L23	0	22 and (diffus$4 and camera and (narrow near band)).clm.	USPAT; UPAD	OR	OFF	2014/08/21 13:56

8/ 21/ 2014 2:03:37 PM
C:\ Users\ mtaningco\ Documents\ EAST\ Workspaces\ 13222688.wsp

Issue Classification	Application/Control No.	Applicant(s)/Patent Under Reexamination
	13222688	NELSON ET AL.
	Examiner	**Art Unit**
	MARCUS TANINGCO	2884

CPC						
Symbol					**Type**	**Version**
G01N		21	/	645	F	2013-01-01
G01N		21	/	6456	I	2013-01-01
G03B		15	/	05	I	2013-01-01
G01N		2021	/	6419	A	2013-01-01
G01N		2021	/	6421	A	2013-01-01
G01N		2021	/	6423	A	2013-01-01
G01N		2021	/	6471	A	2013-01-01
			/			
			/			
			/			
			/			
			/			
			/			
			/			
			/			

CPC Combination Sets							
Symbol				**Type**	**Set**	**Ranking**	**Version**
			/				
			/				

NONE		**Total Claims Allowed:**	
(Assistant Examiner)	(Date)	27	
/MARCUS TANINGCO/ Primary Examiner.Art Unit 2884	08/21/2014	O.G. Print Claim(s)	O.G. Print Figure
(Primary Examiner)	(Date)	1	12

U.S. Patent and Trademark Office — Part of Paper No. 20140821

Issue Classification	Application/Control No.	Applicant(s)/Patent Under Reexamination
	13222688	NELSON ET AL.
	Examiner	**Art Unit**
	MARCUS TANINGCO	2884

US ORIGINAL CLASSIFICATION		INTERNATIONAL CLASSIFICATION	
CLASS	SUBCLASS	CLAIMED	NON-CLAIMED
250	461.1	G 0 1 N 21 / 64 (2006.0)	

CROSS REFERENCE(S)					
CLASS	SUBCLASS (ONE SUBCLASS PER BLOCK)				

NONE		**Total Claims Allowed:**	
(Assistant Examiner)	(Date)	27	
/MARCUS TANINGCO/ Primary Examiner.Art Unit 2884	08/21/2014	O.G. Print Claim(s)	O.G. Print Figure
(Primary Examiner)	(Date)	1	12

Issue Classification	Application/Control No.	Applicant(s)/Patent Under Reexamination
	13222688	NELSON ET AL.
	Examiner	**Art Unit**
	MARCUS TANINGCO	2884

☐ Claims renumbered in the same order as presented by applicant ☐ CPA ☐ T.D. ☐ R.1.47

Final	Original	Final	Original	Final	Original	Final	Original	Final	Original	Final	Original	Final	Original	Final	Original
1	1		17	12	33										
2	2		18	13	34										
3	3	14	19	25	35										
4	4	15	20	26	36										
5	5	16	21	27	37										
6	6	17	22												
7	7	18	23												
8	8	19	24												
	9	20	25												
	10	23	26												
	11	24	27												
	12	21	28												
	13	22	29												
	14	9	30												
	15	10	31												
	16	11	32												

NONE (Assistant Examiner)	(Date)	**Total Claims Allowed:** 27	
/MARCUS TANINGCO/ Primary Examiner.Art Unit 2884 (Primary Examiner)	08/21/2014 (Date)	O.G. Print Claim(s) 1	O.G. Print Figure 12

U.S. Patent and Trademark Office Part of Paper No. 20140821

PART B - FEE(S) TRANSMITTAL

Complete and send this form, together with applicable fee(s), to: Mail **Mail Stop ISSUE FEE**
Commissioner for Patents
P.O. Box 1450
Alexandria, Virginia 22313-1450
or Fax (571)-273-2885

INSTRUCTIONS: This form should be used for transmitting the ISSUE FEE and PUBLICATION FEE (if required). Blocks 1 through 5 should be completed where appropriate. All further correspondence including the Patent, advance orders and notification of maintenance fees will be mailed to the current correspondence address as indicated unless corrected below or directed otherwise in Block 1, by (a) specifying a new correspondence address; and/or (b) indicating a separate "FEE ADDRESS" for maintenance fee notifications.

CURRENT CORRESPONDENCE ADDRESS (Note: Use Block 1 for any change of address)

27104 7590 08/29/2014
FENNEMORE CRAIG, P.C.
1700 Lincoln Street
SUITE 2900
DENVER, CO 80203

Note: A certificate of mailing can only be used for domestic mailings of the Fee(s) Transmittal. This certificate cannot be used for any other accompanying papers. Each additional paper, such as an assignment or formal drawing, must have its own certificate of mailing or transmission.

Certificate of Mailing or Transmission
I hereby certify that this Fee(s) Transmittal is being deposited with the United States Postal Service with sufficient postage for first class mail in an envelope addressed to the Mail Stop ISSUE FEE address above, or being facsimile transmitted to the USPTO (571) 273-2885, on the date indicated below.

(Depositor's name)
(Signature)
(Date)

APPLICATION NO.	FILING DATE	FIRST NAMED INVENTOR	ATTORNEY DOCKET NO.	CONFIRMATION NO.
13/222,688	08/31/2011	Michael B. Nelson	SPEC US-4 (027560-0014)	5910

TITLE OF INVENTION: EXCITATION LIGHT SOURCE ASSEMBLY

APPLN. TYPE	ENTITY STATUS	ISSUE FEE DUE	PUBLICATION FEE DUE	PREV. PAID ISSUE FEE	TOTAL FEE(S) DUE	DATE DUE
nonprovisional	SMALL	$480	$0	$0	$480	12/01/2014

EXAMINER	ART UNIT	CLASS-SUBCLASS
TANINGCO, MARCUS H	2884	250-461100

1. Change of correspondence address or indication of "Fee Address" (37 CFR 1.363).
☐ Change of correspondence address (or Change of Correspondence Address form PTO/SB/122) attached.
☐ "Fee Address" indication (or "Fee Address" Indication form PTO/SB/47; Rev 03-02 or more recent) attached. **Use of a Customer Number is required.**

2. For printing on the patent front page, list
(1) The names of up to 3 registered patent attorneys or agents OR, alternatively,
(2) The name of a single firm (having as a member a registered attorney or agent) and the names of up to 2 registered patent attorneys or agents. If no name is listed, no name will be printed.

1 FENNEMORE CRAIG, P.C.
2 _____
3 _____

3. ASSIGNEE NAME AND RESIDENCE DATA TO BE PRINTED ON THE PATENT (print or type)

PLEASE NOTE: Unless an assignee is identified below, no assignee data will appear on the patent. If an assignee is identified below, the document has been filed for recordation as set forth in 37 CFR 3.11. Completion of this form is NOT a substitute for filing an assignment.

(A) NAME OF ASSIGNEE: Spectral Instruments Imaging, LLC
(B) RESIDENCE: (CITY and STATE OR COUNTRY): Tuscon, Arizona

Please check the appropriate assignee category or categories (will not be printed on the patent) : ☐ Individual ☒ Corporation or other private group entity ☐ Government

4a. The following fee(s) are submitted:
☒ Issue Fee
☐ Publication Fee (No small entity discount permitted)
☐ Advance Order - # of Copies _____

4b. Payment of Fee(s): **(Please first reapply any previously paid issue fee shown above)**
☐ A check is enclosed.
☐ Payment by credit card. Form PTO-2038 is attached.
☒ The Director is hereby authorized to charge the required fee(s), any deficiency, or credits any overpayment, to Deposit Account Number 060590 (enclose an extra copy of this form).

5. **Change in Entity Status** (from status indicated above)
☐ Applicant certifying micro entity status. See 37 CFR 1.29
NOTE: Absent a valid certification of Micro Entity Status (see forms PTO/SB/15A and 15B), issue fee payment in the micro entity amount will not be accepted at the risk of application abandonment.
☐ Applicant asserting small entity status. See 37 CFR 1.27
NOTE: If the application was previously under micro entity status, checking this box will be taken to be a notification of loss of entitlement to micro entity status.
☐ Applicant changing to regular undiscounted fee status.
NOTE: Checking this box will be taken to be a notification of loss of entitlement to small or micro entity status, as applicable.

NOTE: This form must be signed in accordance with 37 CFR 1.31 and 1.33. See 37 CFR 1.4 for signature requirements and certifications.

Authorized Signature /Bruce E. Dahl/ Date October 31, 2014
Typed or printed name Bruce E. Dahl Registration No. 33,670

PTOL-85 Part B (10-13) Approved for use through 10/31/2013. OMB 0651-0033 U.S. Patent and Trademark Office; U.S. DEPARTMENT OF COMMERCE

Electronic Patent Application Fee Transmittal

Application Number:	13222688
Filing Date:	31-Aug-2011
Title of Invention:	EXCITATION LIGHT SOURCE ASSEMBLY
First Named Inventor/Applicant Name:	Michael B. Nelson
Filer:	Bruce E. Dahl/Cynthia Sullivan
Attorney Docket Number:	SPEC US-4 (027560-0014)

Filed as Small Entity

Utility under 35 USC 111(a) Filing Fees

Description	Fee Code	Quantity	Amount	Sub-Total in USD($)
Basic Filing:				
Pages:				
Claims:				
Miscellaneous-Filing:				
Petition:				
Patent-Appeals-and-Interference:				
Post-Allowance-and-Post-Issuance:				
Utility Appl Issue Fee	2501	1	480	480
Extension-of-Time:				

Description	Fee Code	Quantity	Amount	Sub-Total in USD($)
Miscellaneous:				
			Total in USD ($)	**480**

SPECTRAL_0000984

Electronic Acknowledgement Receipt

EFS ID:	20572636
Application Number:	13222688
International Application Number:	
Confirmation Number:	5910
Title of Invention:	EXCITATION LIGHT SOURCE ASSEMBLY
First Named Inventor/Applicant Name:	Michael B. Nelson
Customer Number:	27104
Filer:	Bruce E. Dahl
Filer Authorized By:	
Attorney Docket Number:	SPEC US-4 (027560-0014)
Receipt Date:	31-OCT-2014
Filing Date:	31-AUG-2011
Time Stamp:	12:15:10
Application Type:	Utility under 35 USC 111(a)

Payment information:

Submitted with Payment	yes
Payment Type	Deposit Account
Payment was successfully received in RAM	$480
RAM confirmation Number	9485
Deposit Account	060590
Authorized User	
The Director of the USPTO is hereby authorized to charge indicated fees and credit any overpayment as follows: Charge any Additional Fees required under 37 C.F.R. Section 1.16 (National application filing, search, and examination fees) Charge any Additional Fees required under 37 C.F.R. Section 1.17 (Patent application and reexamination processing fees)	

Charge any Additional Fees required under 37 C.F.R. Section 1.19 (Document supply fees) Charge any Additional Fees required under 37 C.F.R. Section 1.20 (Post Issuance fees) Charge any Additional Fees required under 37 C.F.R. Section 1.21 (Miscellaneous fees and charges)

File Listing:

Document Number	Document Description	File Name	File Size(Bytes)/ Message Digest	Multi Part /.zip	Pages (if appl.)
1	Issue Fee Payment (PTO-85B)	IssueFee-SPEC_US-4.pdf	72951 09001f4e4b11b25a857e65f1b48bcf88ff3ead5f	no	1
Warnings:					
Information:					
2	Fee Worksheet (SB06)	fee-info.pdf	30546 980a2fa514b24749f2ea5850fef430e373f6453e	no	2
Warnings:					
Information:					
		Total Files Size (in bytes):	103497		

This Acknowledgement Receipt evidences receipt on the noted date by the USPTO of the indicated documents, characterized by the applicant, and including page counts, where applicable. It serves as evidence of receipt similar to a Post Card, as described in MPEP 503.

New Applications Under 35 U.S.C. 111
If a new application is being filed and the application includes the necessary components for a filing date (see 37 CFR 1.53(b)-(d) and MPEP 506), a Filing Receipt (37 CFR 1.54) will be issued in due course and the date shown on this Acknowledgement Receipt will establish the filing date of the application.

National Stage of an International Application under 35 U.S.C. 371
If a timely submission to enter the national stage of an international application is compliant with the conditions of 35 U.S.C. 371 and other applicable requirements a Form PCT/DO/EO/903 indicating acceptance of the application as a national stage submission under 35 U.S.C. 371 will be issued in addition to the Filing Receipt, in due course.

New International Application Filed with the USPTO as a Receiving Office
If a new international application is being filed and the international application includes the necessary components for an international filing date (see PCT Article 11 and MPEP 1810), a Notification of the International Application Number and of the International Filing Date (Form PCT/RO/105) will be issued in due course, subject to prescriptions concerning national security, and the date shown on this Acknowledgement Receipt will establish the international filing date of the application.

UNITED STATES PATENT AND TRADEMARK OFFICE

UNITED STATES DEPARTMENT OF COMMERCE
United States Patent and Trademark Office
Address: COMMISSIONER FOR PATENTS
P.O. Box 1450
Alexandria, Virginia 22313-1450
www.uspto.gov

APPLICATION NO.	ISSUE DATE	PATENT NO.	ATTORNEY DOCKET NO.	CONFIRMATION NO.
13/222,688	12/02/2014	8901516	SPEC US-4 (027560-0014)	5910

27104 7590 11/12/2014

FENNEMORE CRAIG, P.C.
1700 Lincoln Street
SUITE 2900
DENVER, CO 80203

ISSUE NOTIFICATION

The projected patent number and issue date are specified above.

Determination of Patent Term Adjustment under 35 U.S.C. 154 (b)
(application filed on or after May 29, 2000)

The Patent Term Adjustment is 84 day(s). Any patent to issue from the above-identified application will include an indication of the adjustment on the front page.

If a Continued Prosecution Application (CPA) was filed in the above-identified application, the filing date that determines Patent Term Adjustment is the filing date of the most recent CPA.

Applicant will be able to obtain more detailed information by accessing the Patent Application Information Retrieval (PAIR) WEB site (http://pair.uspto.gov).

Any questions regarding the Patent Term Extension or Adjustment determination should be directed to the Office of Patent Legal Administration at (571)-272-7702. Questions relating to issue and publication fee payments should be directed to the Application Assistance Unit (AAU) of the Office of Data Management (ODM) at (571)-272-4200.

APPLICANT(s) (Please see PAIR WEB site http://pair.uspto.gov for additional applicants):

Michael B. Nelson, Tucson, AZ;
Michael D. Cable, Tucson, AZ;

The United States represents the largest, most dynamic marketplace in the world and is an unparalleled location for business investment, innovation, and commercialization of new technologies. The USA offers tremendous resources and advantages for those who invest and manufacture goods here. Through SelectUSA, our nation works to encourage and facilitate business investment. To learn more about why the USA is the best country in the world to develop technology, manufacture products, and grow your business, visit SelectUSA.gov.

13/222,688	EXCITATION LIGHT SOURCE ASSEMBLY	SPEC US-4 (027560-0014)	07-10-2022::08:22:23

Patent Assignment Abstract of Title

Total Assignments: 1

Application #: 13222688 **Filing Dt:** 08/31/2011 **Patent #:** 8901516 **Issue Dt:** 12/02/2014

PCT #: NONE **Intl Reg #:** **Publication #:** US20120049089 **Pub Dt:** 03/01/2012

Inventors: Michael B. Nelson, Michael D. Cable

Title: EXCITATION LIGHT SOURCE ASSEMBLY

Assignment: 1

Reel/Frame: 027156 / 0495 **Received:** 11/01/2011 **Recorded:** 11/01/2011 **Mailed:** 11/01/2011 **Pages:** 4

Conveyance: ASSIGNMENT OF ASSIGNORS INTEREST (SEE DOCUMENT FOR DETAILS).

Assignors: NELSON, MICHAEL B. **Exec Dt:** 10/05/2011

CABLE, MICHAEL D. **Exec Dt:** 10/20/2011

Assignee: SPECTRAL INSTRUMENTS IMAGING, LLC
420 BONITA AVENUE
TUCSON, ARIZONA 85745

Correspondent: FENNEMORE CRAIG, P.C.
1700 LINCOLN STREET
SUITE 2900
DENVER, CO 80203

Search Results as of: 07/10/2022 08:22:19 AM

Disclaimer:
Assignment information on the assignment database reflects assignment documents that have been actually recorded.
If the assignment for a patent was not recorded, the name of the assignee on the patent application publication or patent may be different.
If you have any comments or questions concerning the data displayed, contact OPR / Assignments at 571-272-3350

Close Window

> Archives of Past Meetings

WMIC

WMIC 2019 Highlights

WMIC 2018 Highlights: 'Molecular Imaging – Visualizing Biology to Improve Medicine'

WMIC 2017 Highlights: 'IMAGinING the Future: From Molecules to Medicine'

WMIC 2016 Highlights: Imaging Biology... Improving Therapy

WMIC 2015 Highlights: Precision Medicine... Visualized

Highlights from WMIC 2014: Propelling Discoveries with Molecular Imaging

WMIC 2013 Award Winners

WMIC 2012 Award Winners

WMIC 2010 Exhibitors and Sponsors

The WMIC thanks the 2010 Sponsors and Supporters:

Platinum Level Support: Caliper Life Sciences, GE Healthcare, Siemens Healthcare

Silver Level Support: Bruker, FujiFilm

Bronze Level Support: SCETI, Carestream Molecular Imaging

The WMIC gratefully acknowledges the following companies for their contributions:

Carestream Molecular Imaging for Internet access, (WiFi & Internet Cafe) within the Congress

Bayer Schering Pharma AG for sponsorship of the Young Investigator's Award

Bracco for sponsorship of the Jorge Barrio Award

Caliper for sponsorship of the lanyards

Spectral Instruments for sponsorship of the pens

Celsense Inc. for sponsorship of the USB drive

WMIC 2010 Exhibitors

ABT Molecular Imaging, Inc.

ABX Advanced Biochemical Compounds

ABX-CRO Advanced Pharmaceutical Services GmbH

Advanced Cyclotron Systems Inc.

ART – Advanced Research Technologies Inc.

Aspect Magnet Technologies Ltd.

Berthold Japan K.K.

Best Cyclotron Ltd.

BioActs

Bioscan Inc., Sowa Trading Co. Inc., Philips

Biospace Lab

Bruker BioSpin, Bruker Daltonics

Caliper Life Sciences

Capintec, Inc.

Carestream Molecular Imaging

Charles River Discovery & Imaging Services

Comecer

Cyanine Technologies S.p.A

DS Pharma Biomedical Co. Ltd.

Eckert & Ziegler Eurotope

Endra, Inc.

Fluoptics

GE Healthcare

Huayi Isotopes Co.

ImaginAb, Inc.

INDEC BioSystems

Inter Medical Co., Ltd.

ISMRM – International Society for Magnetic Resonance in Medicine

kibero GmbH

Kurabo Industries Ltd. , CRi – Cambridge Research & Instrumentation, Inc.

LI-COR Biosciences

Mediso Medical Imaging Systems

MICAD – Molecular Imaging & Contrast Agent Database

MILabs

Miltenyi Biotec GmbH

MR Solutions Ltd

NCI – National Cancer Institute

PET Technology Supplies Inc.

Primetech Corporation

Quidd

RAPID Biomedical GmbH

Rigaku Corporation

SA Instruments, Inc.

SCETI K.K

Schooner Investments

Shimadzu Corporation

Siemens Healthcare/Molecular Imaging Group

SkyScan NV

SNM – Society for Nuclear Medicine

Sofie Biosciences

Solve Corporation

Springer

TAIYO NIPPON SANSO Corporation

Tema Sinergie S.r.l.

UVP, LLC

Varian, Inc. – now Agilent Technologies

VisEn Medical

VisualSonics

Copyright 2015 World Molecular Imaging Society. All rights reserved.